

5101-287
Flat-Plate Solar
Array Project

DOE/JPL--1012-122
DE87 005426

DOE/JPL-1012-122
Distribution Category UC-63b

CONF-8510405-

Proceedings of the Flat-Plate Solar Array Project Workshop on Low-Cost Polysilicon for Terrestrial Photovoltaic Solar-Cell Applications

(October 28-30, 1985, at Las Vegas, Nevada)

DISCLAIMER

This report was prepared as an account of work sponsored by an agency of the United States Government. Neither the United States Government nor any agency thereof, nor any of their employees, makes any warranty, express or implied, or assumes any legal liability or responsibility for the accuracy, completeness, or usefulness of any information, apparatus, product, or process disclosed, or represents that its use would not infringe privately owned rights. Reference herein to any specific commercial product, process, or service by trade name, trademark, manufacturer, or otherwise does not necessarily constitute or imply its endorsement, recommendation, or favoring by the United States Government or any agency thereof. The views and opinions of authors expressed herein do not necessarily state or reflect those of the United States Government or any agency thereof.

February 1986

Prepared for
U.S. Department of Energy
Through an Agreement with
National Aeronautics and Space Administration
by
Jet Propulsion Laboratory
California Institute of Technology
Pasadena, California

JPL Publication 86-11

MASTER

DISTRIBUTION OF THIS DOCUMENT IS UNLIMITED

Prepared by the Jet Propulsion Laboratory, California Institute of Technology,
for the U.S. Department of Energy through an agreement with the National
Aeronautics and Space Administration.

The JPL Flat-Plate Solar Array Project is sponsored by the U.S. Department of
Energy and is part of the National Photovoltaics Program to initiate a major
effort toward the development of cost-competitive solar arrays.

This report was prepared as an account of work sponsored by an agency of the
United States Government. Neither the United States Government nor any
agency thereof, nor any of their employees, makes any warranty, express or
implied, or assumes any legal liability or responsibility for the accuracy, com-
pleteness, or usefulness of any information, apparatus, product, or process
disclosed, or represents that its use would not infringe privately owned rights.

Reference herein to any specific commercial product, process, or service by trade
name, trademark, manufacturer, or otherwise, does not necessarily constitute or
imply its endorsement, recommendation, or favoring by the United States
Government or any agency thereof. The views and opinions of authors expressed
herein do not necessarily state or reflect those of the United States Government
or any agency thereof.

This document reports on work done under NASA Task RE-152, Amendment
419, DOE/NASA IAA No. DE-AI01-85CE89008.

DISCLAIMER

This report was prepared as an account of work sponsored by an agency of the United States Government. Neither the United States Government nor any agency Thereof, nor any of their employees, makes any warranty, express or implied, or assumes any legal liability or responsibility for the accuracy, completeness, or usefulness of any information, apparatus, product, or process disclosed, or represents that its use would not infringe privately owned rights. Reference herein to any specific commercial product, process, or service by trade name, trademark, manufacturer, or otherwise does not necessarily constitute or imply its endorsement, recommendation, or favoring by the United States Government or any agency thereof. The views and opinions of authors expressed herein do not necessarily state or reflect those of the United States Government or any agency thereof.

DISCLAIMER

Portions of this document may be illegible in electronic image products. Images are produced from the best available original document.

ABSTRACT

The Workshop on Low-Cost Polysilicon for Terrestrial Photovoltaic Solar-Cell Applications was held October 28, 29, and 30, 1985, at the Sahara Hotel, Las Vegas, Nevada. It was sponsored by the Flat-Plate Solar Array (FSA) Project of the Jet Propulsion Laboratory (JPL). The sessions were: Polysilicon Material Requirements; Economics; Process Developments in the USA; Process Developments, International; and Polysilicon Market and Forecasts. There were two forums dealing with polysilicon process technology and polysilicon markets. Twenty-one invited papers were presented and discussion periods followed the papers. This report contains a record of the papers, the forums, and the discussions.

FOREWORD

The Workshop on Low-Cost Polysilicon for Terrestrial Photovoltaic Solar-Cell Applications was intended to provide a forum for descriptions and discussions of polysilicon processes that are being used commercially or are being developed, of polysilicon process economics, and of the polysilicon market for the semiconductor and photovoltaic solar-cell industries. These areas, which are interrelated in a complex manner, are of interest and concern to both the producers and the users of polysilicon. The agenda was comprised of: Polysilicon Material Requirements; Economics; Process Developments in the USA; Process Developments, International; and Polysilicon Market and Forecasts. Two forums dealing with polysilicon process technology and polysilicon markets were also held. All of the papers were invited and were selected to present comprehensive views of each area. The invited speakers are well recognized in their fields of expertise. The attendees took the opportunity of this Workshop for exchanges of information and discussions of technical and economic problems.

The Proceedings contain the papers submitted by the authors before the Workshop; hence, the actual presentations may have differed somewhat from the papers. The Proceedings also contain transcriptions of tapes of the discussions. These were edited, as necessary, to enhance clarity of expression.

R. Lutwack
Chairman

ACKNOWLEDGMENT

The Chairman is grateful to the guest speakers for making the considerable effort necessary for the preparation of the papers and for their participation in the discussion periods. The audience was very active in raising questions, in presenting additional information, and in discussing areas of uncertainty. The interchanges made the Workshop successful.

The efforts of Mary Phillips, Conference Coordinator, and Joyce Murry, who provided editorial support, are also gratefully acknowledged.

The workshop was funded by the U.S. Department of Energy through the Flat-Plate Solar Array Project at the Jet Propulsion Laboratory.

CONTENTS

WORKSHOP INTRODUCTION

R. Lutwack, Chairman (Jet Propulsion Laboratory)	1
--	---

SILICON MATERIAL TASK OF THE DOE/FSA PROJECT

R. Lutwack (Jet Propulsion Laboratory)	3
--	---

SESSION I: POLYSILICON MATERIAL REQUIREMENTS

Chairman: J. McCormick (Hemlock Semiconductor Corp.)

Effects of Impurities on Silicon Solar-Cell Performance

R. Hopkins (Westinghouse R&D Center)	15
Discussion	35

Requirements for High-Efficiency Solar Cells

C.T. Sah (University of Illinois)	37
Discussion	53

SESSION II: ECONOMICS

Chairman: R. Pellin (Consultant)

Economics of the Polysilicon Process: A View from Japan

Y. Shimizu (Osaka Titanium Co., Ltd.)	57
Discussion	78

Economics of Polysilicon Processes

C. Yaws (Lamar University)	79
Discussion	122

Sensitivity Analysis for Solar Panels

R. Aster (Jet Propulsion Laboratory)	123
Discussion	131

SESSION III: PROCESS DEVELOPMENTS IN THE USA

Chairman: P. Maycock (PV Energy Systems)

Development of the Silane Process for the Production of Low-Cost Polysilicon

S. Iya (Union Carbide Corp.)	135
Discussion	144

Fluidized-Bed Development at Jet Propulsion Laboratory

G. Hsu (Jet Propulsion Laboratory)	147
Discussion	166

Fluidized-Bed Reactor Modeling for Production of Silicon by Silane Pyrolysis	
M. Dudukovic (Washington University at St. Louis)	167
Discussion	185
Silicon Production in an Aerosol Reactor	
R. Flagan (California Institute of Technology)	187
Discussion	209

SESSION IV: PROCESS DEVELOPMENTS, INTERNATIONAL
Chairman: R. Lutwack (Jet Propulsion Laboratory)

Processes and Process Developments in Japan	
T. Noda (Osaka Titanium Co., Ltd.)	213
Discussion	231
Processes and Process Developments in Taiwan	
H-L. Hwang (National Tsing Hua University)	233
Discussion	249
Refining of Metallurgical-Grade Silicon	
J. Dietl (Heliotronics GmbH)	251
Discussion	266
Solar-Grade Silicon Prepared by Carbothermic Reduction of Silica	
H. Aulich (Siemens AG)	267
Discussion	276
A Metallurgical Route to Solar-Grade Silicon	
A. Schei (Elkem a/s, R&D Center)	279
Discussion	295
Solar Silicon from Directional Solidification of MG Silicon Produced via the Silicon Carbide Route	
M. Rustioni (Enichimica)	297
Discussion	321

SESSION V: PROCESS DEVELOPMENTS IN THE USA
(Continuation of Session III)
Chairman: A. Briglio (Jet Propulsion Laboratory)

Characterization of Solar-Grade Silicon Produced by the SiF₄-Na Process	
A. Sanjurjo (SRI International)	325
Discussion	344
A Silane-Based Polysilicon Process	
P. Grayson (Eagle-Picher Industries, Inc.)	347
Discussion	366

Silicon Purification Using a Cu-Si Alloy Source	
R. Powell (Solar Energy Research Institute)	367
FORUM: Polysilicon Process Technology	
Chairman: H. Aulich (Siemens AG)	
Discussion	381
SESSION VI: POLYSILICON MARKET AND FORECASTS	
Chairman: M. Prince (U.S. Department of Energy)	
Semiconductor Market	
R. Pellin (Consultant)	397
Discussion	415
Silicon Requirements of the Photovoltaic Solar Cell Market	
P. Maycock (PV Energy Systems)	417
Discussion	423
FORUM: Polysilicon Markets	
Chairman: J. Lorenz (Consultant)	
Discussion	429
CLOSING COMMENTS	
R. Lutwack, Chairman	433
APPENDIX: PARTICIPANT LIST	A-1

WORKSHOP INTRODUCTION

Ralph Lutwack

I am pleased to welcome you to the Workshop on Low-Cost Silicon for Terrestrial Photovoltaic Solar Cell-Applications. It is a special pleasure to welcome the invited speakers from Taiwan, Norway, Japan, Italy, and Germany, and to also extend a special welcome to attendees from these and other countries.

This Workshop is intended to provide a forum for the exchange of information. The agenda consists of invited papers describing polysilicon material requirements for photovoltaic solar cells, innovative processes for preparing silicon, special reactor studies, the economics of various polysilicon processes, and views of the present and future markets for silicon use in the photovoltaic solar cell and semiconductor industries.

The Workshop will be successful if we exchange information by asking questions, by presenting problems, and by offering comments and information. Participation will be especially important for the success of the two forums: one on Tuesday afternoon on polysilicon process technology and the other on Wednesday morning dealing with polysilicon markets.

There are some program changes. Please note that Dr. Jain is unable to attend and present his paper. Also, Dr. Aulich has graciously offered to be the chairman of the Tuesday afternoon forum replacing Dr. Wald, who cannot be here because of illness.

SILICON MATERIAL TASK OF THE DOE/FSA PROJECT

Ralph Lutwack
Jet Propulsion Laboratory
Pasadena, California

The Silicon Material Task of the FSA Project has been described through the reports of the contractors, through JPL reports, and through presentations by JPL and the contractors at various meetings. In fact, eight papers to be presented at this Workshop deal with investigations carried out entirely or in part under the Task. This morning, I want to present an insight into the Task program from its inception in 1974.

The concept of a low-cost, single-crystal silicon (Si) solar array project to develop the technology and establish the capability for producing arrays for terrestrial applications was first outlined in a letter of interest from JPL to the National Science Foundation (NSF) in April 1973. The Cherry Hill, NJ Conference on Photovoltaic (PV) Conversion of Solar Energy (SE) for Terrestrial Applications, held in October 1973, was organized and conducted by JPL as part of an NSF contract for \$69K. Two of the general conclusions of the conference were: 1) a 10-year government-funded program to establish the commercial practicality of PV for terrestrial applications should be started as soon as possible, and 2) the primary candidate for development should be the single-crystal Si array. The recommendations of the conference workshop on single-crystal Si solar cells were that the objective should be to achieve a cell price of \$0.50/peak W and a cell production capacity of 500 peak MW/year by 1985 with a goal of \$0.10/peak W cell and 50,000 peak MW by 2000; a large-scale polySi plant was earmarked for on-stream production in FY'83. These recommendations from the Cherry Hill conference formed the basis for several PV solar energy plans.

In June 1974, JPL submitted a proposal to NSF/Research Applied to National Needs to conduct a program to develop the technical and industrial capability for producing 500 MW of single-crystal PV solar arrays at a cost of < \$500/peak kW by 1984. The contract started in August 1974. The program limits of the Si Material Task were set by material and price goals: the Si needed to be suitable for the fabrication of 10% conversion-efficient arrays at < \$35/kg. The first Task plan had five phases: (1) for the evaluation and selection of the process developments; (2) for experimental studies of chemical kinetics and yields, chemical engineering, energy use, reactor design, and preliminary economic estimates; (3) for continued experiments in scaled-up reactors to obtain data data for steady-state operation and for optimization analyses; (4) for pilot plants to characterize major equipment and process designs; and (5) for large-scale plants. It was assumed that the pilot plants and large-scale plants would be government-funded and operated under government licenses (Figure 1).

The last four phases were fitted into a Task structure which also included subtasks for support investigations for the process developments

(Figure 1, where pilot plants are called Experimental Process System Development Units). Consultants (Figure 2) were used throughout the program to analyze problems and to critique technical developments. Professor Friedlander, Professor Levenspiel, and Dr. Roberts were involved in a review and analysis of the problem of the collection of Si from the gas phase in the Westinghouse arc heater process, for example; and Dr. Fitzgerald and Professor Levenspiel were engaged from the early stages of the program in critically examining the problems and progress of the chemical engineering R&D of several contracts, especially and most intensely of the SiH_4 fluidized bed development. Professor Sah prepared in-depth reviews and analyses which pertained to the impurity-effects area.

The first major problem faced in constructing a plan for the Si Material Task was how to deal with the words "solar-grade Si" and "Si suitable for the fabrication of 10% solar arrays." Although the terminology had been used before and seemed to be a reasonable basis for forming program objectives, it could not be used as a definition. We realized that quantitative information relating the effects of concentration levels of specific elements on the performance of cells was needed for the process developments. It would be required to determine reactor efficiency; to assess the requirements for purification units; to construct process designs; and, of course, to estimate process economics. Therefore, the effort for studies of impurity effects on cell performance was given a major position in the program. The results of these studies will be described in Workshop papers by Dr. Hopkins of Westinghouse and Professor Sah of the University of Illinois. Complementary investigations to measure impurity concentrations and lifetime/diffusion lengths, to develop analytical procedures, and to evaluate impurity-doped cells were also employed (Figure 3).

Several program plans were constructed to meet varying requirements of the government sponsor. One of the first long-term plans established a schedule culminating in a 6000 MT/yr plant being on-stream in June 1986 (Figure 4). However, as early as the NSF grantee review in Maine in August of 1976 we were requested to prepare plans for obtaining small quantities of Si from the development units of the processes in 1980. Then, in the fall of 1977 plans were prepared in response to a proposed major change in the Task program (Figure 5). The change introduced an intermediate 1982 objective to obtain polySi for the Project program. Several options of development schedules and budgets were devised to meet this new goal. To determine the response to accelerated schedules by process development contractors, a meeting was held in Washington, D.C. involving managers of four of the contracts, JPL, and the DOE. Production capacities of 500 and 1500 MT/yr before 1986 were suggested as goals for discussion; this was the so-called Marvin plan. Proposed plans ranged from purchases of Si to meet needs in the near-term years to the use of nonoptimized production plants to be on-stream in 1983; but, it was emphasized that accelerated schedules which would enable large-production plants to be on-stream in 1983 would be higher risk as a result of the sacrifice of a conservative data base for process designs. The probable consequence would be production from plants less efficient in material and energy use as well as operating with lower product yield and higher process cost.

The Task incorporated some of the recommendations into proposed Task budgets and schedules to meet the intermediate production requirements.

All of these Task plans still stressed the necessity for maintaining the basic 1986 plan intact without decreasing the resources for the 1986 program in order to accomplish any 1982-1983 production needs.

Task plans were also formulated to fit the requirements of the congressional McCormack bill in which the array production was to be doubled each year through 1988, reaching 2000 MW in 1988. The demands in this case were not as severe for the 1982-1983 period, but more extensive planning was involved to take care of the very large increases in production following 1983. The resulting plans assumed a linear increase in the efficiency of using polySi so that the MT/MW decreased from 12/1 to 6/1. In each of the plans the near-term demand was to be met with Si purchases, the intermediate demand by production from large Experimental Process System Development Units (EPSDUs), and the demand beyond 1985 by two 6000 MT/yr plants based on the assumption of increased efficiency in Si-use or two 12,000 MT/yr plants based on a constant 40% efficiency use of Si. For comparison, the basic low-cost solar array project/DOE program goals were for two 3000 MT/yr plants in 1986.

While the discussions and the planning were under way to meet the series of increased demands with the associated more drastic schedules, the Task proceeded on its basic track with modifications caused by the difficulties some contractors had in reaching the goal of establishing process feasibility; five processes were still under contract in early 1980 (Figure 6).

In FY'80 the Task program was limited to two EPSDUs by a budget reduction. The Silane Process developed by Union Carbide was selected for one EPSDU. The contending processes for the second EPSDU were the SiH_2Cl_2 -Siemens process of Hemlock Semiconductor and the Zn-SiCl_4 -FBR process of Battelle. The supporting program efforts in 1980 were for the Silane Process. These were the study of the hydrochlorination reactor by Dr. Mui first at MIT and then at Solar-electronics; the research at JPL on the free space reactor (FSR) and fluidized bed reactor (FBR); and starting late in 1980, the research by Professor Flagan of Caltech on the growth of fine particles in a SiH_4 pyrolysis system (Figure 7).

Further budget reductions at the start of FY'81 forced the Task to a limit of one EPSDU; the choice was the Silane Process. Only the SiH_2Cl_2 -Siemens development by Hemlock Semiconductor was continued beyond early 1981 as a potential competitor should more funds become available later in the program.

Since the development of the SiH_4 process by Union Carbide can be considered as the primary success of the Si Material Task program--notwithstanding the fact that the deposition reactors in the pilot plant and commercial plant are Siemens-type CVD reactors designed by Komatsu and that hence the process is still not a low-cost process in the context of the Task goal--I would like to describe this contractual development from the Task management viewpoint. Dr. Iya will present a paper at this workshop which will deal with many of the technical development aspects.

After a critical review of the process design for the EPSDU, which served to emphasize the very large scope of the EPSDU phase of the Silane Process development, JPL instituted a contractual program control called

a Work Breakdown Structure (WBS) to perform its obligations of managing the EPSDU phase (Figure 8). This WBS was divided into sections for design/procurement, equipment fabrication/delivery, EPSDU installation and checkout, EPSDU operation, economic analysis of a commercial process, support R&D (which in this case was for FBR technology), and management and deliverables. The primary divisions were broken down further for assignments to every task of the EPSDU (Figures 9 and 10). To manage the Union Carbide contract through the WBS, the Task made other assignments in addition to the contract technical manager and the procurement representative. The assignments were to provide quality assurance of the equipment; to control the delivery schedules of many items of equipment; to carefully monitor the construction; and to monitor and match the expenditures to the estimates. The WBS structure seemed at first to be cumbersome, but both the Task and Union Carbide used it enthusiastically after the capability of the WBS to control the EPSDU project was demonstrated.

When all of the major equipment, including the distillation columns, had been fabricated or purchased and were on the construction site and after a large part of the structure was in place, the other budget-shoe was dropped and the Flat Plate Solar Array Project was informed of a budget reduction so severe that the Task had to inform Union Carbide that the EPSDU could not be completed without an extended stretch-out of the contract or substantial cost sharing by Union Carbide. Extended negotiations led to an agreement by which the title to the EPSDU equipment would be transferred to Union Carbide in return for the completion of the EPSDU installation and its operation by Union Carbide. Union Carbide then made the decision to move the equipment and to install the EPSDU at Washougal, WA, where it has been in operation since 1983.

As I have cited, several investigations supported the Silane Process development. For example, the investigation of the hydrochlorination reactor conducted by Dr. Mui was continued to April 1983. In this work, he determined the thermodynamic constants, the reaction rates, the operating conditions for high yield and rate, the catalyst characteristics, and the suitability of various reactor materials.

Another supporting study has been the research at Caltech by Professor Flagan on fine particle growth. This will continue until the end of 1985. (Professor Flagan will present a paper on this research at this workshop.)

After the technology for SiH_4 preparation was demonstrated, the development of the FBR became the crucial technology area in the development of the low-cost SiH_4 process. This R&D has been carried out at Union Carbide and at JPL. (Dr. Iya and Dr. Hsu will present papers describing these studies.) Supporting investigations for the FBR endeavors have been carried out by Professor Levenspiel at Oregon State University on the radiantly heated FBR and by Professor Duduković of Washington University at St. Louis on modeling the SiH_4 -FBR system. (Professor Duduković will summarize his results in a paper at this workshop.)

The technical output as well as the effect of the program of the Si Material Task can also be measured by the number of process developments which were initiated in the Task and then were carried further under non-government funding. In the papers at this workshop by Dr. Schei of Elkem

and by Dr. Sanjurjo of SRI International, some aspects of two of these processes will be described. Dr. Schei will present the extensive development by Elkem based on the concept of the carbothermic reduction of quartz in a direct arc furnace, which was investigated by Dow Corning in the Task program. Dr. Sanjurjo will describe the advances made in the process involving the Na reduction of SiF_4 . Other Task developments carried further under private funding are those by the J. C. Schumacher Corp. for the process using bromosilane chemistry and by AeroChem Research Laboratories and Universal Silicon Corp. for the process based on the gas phase Na- SiCl_4 reaction, first studied by AeroChem in the Task program. Although considerable success was obtained by Hemlock Semiconductor in the studies of the SiH_2Cl_2 -Siemens process in the Task program, there is no information of further work or of the commercial use of this process.

The Si Material Task will be over at the end of 1985. Although the primary objective of establishing the practicality of a low-cost process for $< \$10/\text{kg Si}$ was not fully achieved (it now seems to depend on the full development of SiH_4 -FBR technology), I believe that we should be allowed to put in the win-column the Silane Process development, the study of the effects of impurities on cell performance, and the four process developments which were started in the Task program and were then continued under private funding. On behalf of the Task, I wish to acknowledge the diligent efforts of the contractors of the program and of the Task staff.



SILICON MATERIAL TASK TASK STRUCTURE

- PROCESS DEVELOPMENTS
 - PHASE I – TECHNICAL FEASIBILITY
 - PHASE II – SCALE-UP EXPERIMENTS
 - PHASE III – EXPERIMENTAL PROCESS SYSTEM DEVELOPMENT UNITS
 - PHASE IV – LARGE SCALE PRODUCTION PLANTS

- PROCESS DEVELOPMENTS – SUPPORTING SUBTASKS
 - EFFECTS OF IMPURITIES
 - MATERIALS OF CONSTRUCTION
 - COMPOSITION ANALYSES
 - ECONOMIC ANALYSES
 - IN-HOUSE EXPERIMENTAL PROGRAM
 - JPL ANALYSTS
 - CONSULTANTS
 - CHEMICAL PROCESSING
 - CHEMICAL ENGINEERING
 - SOLID STATE PHYSICS

FIGURE 1

SILICON MATERIAL TASK SUPPORT PROGRAMS CONSULTANTS

CHLOROSILANE AND SILANE CHEMISTRY

DR. DONALD BAILEY

CONSULTANT

CHEMICAL ENGINEERING

DR. THOMAS FITZGERALD

OREGON STATE UNIVERSITY (CONSULTANT)

PROFESSOR SHELDON FRIEDLANDER

CALIFORNIA INSTITUTE OF TECHNOLOGY
(UNIVERSITY OF CALIFORNIA AT LOS ANGELES)

DR. DARYL ROBERTS

CALIFORNIA INSTITUTE OF TECHNOLOGY
(SRI INTERNATIONAL)

PROFESSOR OCTAVE LEVENSPIEL

OREGON STATE UNIVERSITY

PROFESSOR CARL YAWS

LAMAR UNIVERSITY

SOLID STATE PHYSICS

PROFESSOR C.T. SAH

UNIVERSITY OF ILLINOIS

FIGURE 2

**SILICON MATERIAL TASK
SUPPORT PROGRAMS
IMPURITY EFFECTS**

<u>CONTRACT TITLE</u>	<u>CONTRACTOR</u>	<u>START</u>	<u>END</u>
DETERMINATION OF DEFINITION OF SOLAR GRADE Si	MONSANTO	10/75	9/76
EFFECTS OF IMPURITIES AND PROCESSING ON Si SOLAR CELLS	WESTINGHOUSE RESEARCH CENTER	10/75	2/82
LIFETIME AND DIFFUSION LENGTH MEASUREMENTS	NORTHROP RESEARCH CENTER	12/76	11/77
ANALYSIS OF EFFECTS OF IMPURITIES	SPECTROLAB	2/77	12/77
EFFECTS OF IMPURITIES ON Si SOLAR CELL PERFORMANCE	C.T. SAH ASSOCIATES	2/77	--
ANALYSES OF DOPED Si	NATIONAL BUREAU OF STANDARDS	4/77	1/79
COMPOSITION MEASUREMENTS BY PHOTON CATALYSIS	AEROSPACE	10/78	9/79
ANALYSIS OF EFFECTS OF IMPURITIES	SOLAREX	1/79	1/80
NAA OF DOPED Si	LAWRENCE LIVERMORE LAB.	8/83	9/85

FIGURE 3



LOW-COST SILICON SOLAR ARRAY PROJECT
SILICON MATERIAL TASK
SILICON MATERIAL TASK SCHEDULE

- 10/75 – INITIATION FIRST CONTRACTS (10/75)
- 10/76 – FIRST DEMONSTRATIONS OF PRACTICAL FEASIBILITY (12/78)*
- 10/76 – PRELIMINARY RESULTS OF EFFECTS OF IMPURITIES (7/78 – 2/82)
- 10/77 – DECISION-REVIEWS OF ALL PROCESS DEVELOPMENTS
- 6/78 – COMPLETION OF DESIGNS FOR EXPERIMENTAL PRODUCTION FACILITIES (6/80)*
- 1/81 – EXPERIMENTAL PRODUCTION FACILITIES ON-STREAM (1/83)*
- 6/82 – SELECTION OF PROCESSES FOR FULL SCALE PRODUCTION PLANTS (FSPP)
- 6/82 – INITIATION OF DESIGNS FSPP
- 6/86 – FULL SCALE PRODUCTION PLANTS ON-STREAM (EARLY 1985)*

*SILANE PROCESS (UNION CARBIDE)

FIGURE 4



SILICON MATERIAL TASK PROJECTED REQUIREMENTS FOR Si (MT/YR)

FY	78	79	80	81	82	83	84	85	86	87	88
TASK PLAN*	3.6	7.8	12.	14.	36.	48.			6000.		
ACCELERATED PLAN*	18.	48.	96.	180.	300.						
MARVIN PLAN*			240.	480.	900.	1500.					
McCORMACK BILL**		47.	89.	167.	312.	583.	1080.	2000.	3665.	6670.	12000.

*CALCULATED ON THE BASIS OF 12% ENERGY CONVERSION EFFICIENCY, 0.025 CM THICK CELLS, 0.1 W/CM² INCIDENT POWER, AND 40% Si UTILIZATION

**CALCULATED USING A LINEAR DECREASE IN MT/MW FROM 12/1 TO 6/1 FROM FY 79 THROUGH FY 88. Si PRODUCTION IN FY 88 TO MEET 2,000 MW PRODUCED IN FY 88. ARRAY PRODUCTION DOUBLED EACH YEAR THROUGH FY 88.

FIGURE 5



SILICON MATERIAL TASK PROCESS DEVELOPMENT CONTRACTORS

<u>PROCESS</u>	<u>CONTRACTOR</u>	<u>START</u>	<u>END</u>
Zn/SiCl ₄ FLUIDIZED BED	BATELLE COLUMBUS LABORATORY	10/75	1/81
SiH ₄	UNION CARBIDE	10/75	1/86
Na/SiF ₄ CHEMICAL VAPOR TRANSPORT	MOTOROLA	2/76	10/79
SiO ₂ /C THERMAL PLASMA	TEXAS INSTRUMENTS	2/76	1/77
Na/SiF ₄ GAS PHASE REACTION	SRI INTERNATIONAL	6/76	2/80
NON-EQUILIBRIUM PLASMA JET	AERO CHEM RESEARCH LAB	7/76	10/78
SiO ₂ mg/C DIRECT ARC FURNACE	DOW CORNING	7/76	10/78
Na/SiCl ₄ ARC HEATER	WESTINGHOUSE ELECTRIC	10/76	12/79
Na/SiCl ₄ FLAME	AERO CHEM RESEARCH LAB	5/77	2/81
BROMOSILANE FLUIDIZED BED	J.C. SCHUMACHER	10/77	11/78
SiH ₂ Cl ₂ SIEMENS	HEMLOCK SEMICONDUCTOR	10/79	5/83

FIGURE 6

**SILICON MATERIAL TASK
SUPPORT PROGRAMS
PROCESS DEVELOPMENTS**

<u>CONTRACT TITLE</u>	<u>CONTRACTOR</u>	<u>START</u>	<u>END</u>
PROCESS FEASIBILITY STUDIES	LAMAR UNIVERSITY	10/75	2/81
HYDROCHLORINATION OF SiCl ₄	MASSACHUSETTS INSTITUTE OF TECHNOLOGY	3/79	4/81
PARTICLE GROWTH FROM SiH ₄ IN A FREE SPACE REACTOR	CALIFORNIA INSTITUTE OF TECHNOLOGY	9/80	1/86
SILICON PRODUCTION PROCESS EVALUATIONS	TEXAS RESEARCH AND ENG. INSTITUTE	5/81	7/82
HYDROCHLORINATION OF SiCl ₄	SOLARELECTRONICS	7/81	4/83
MODEL OF SiH ₄ – FLUIDIZED BED REACTOR	WASHINGTON UNIVERSITY AT ST. LOUIS	12/83	12/84
RADIANTLY HEATED FLUIDIZED BED	OREGON STATE UNIVERSITY	9/82	8/83

FIGURE 7

**JPL SILICON MATERIAL TASK
SILANE PROCESS (UNION CARBIDE)
EPSDU WORK BREAKDOWN STRUCTURE (WBS)**

- 1.1 EPSDU – DESIGN/PROCUREMENT
- 1.2 EPSDU – EQUIPMENT FABRICATION/DELIVERY
- 1.3 EPSDU – INSTALLATION AND CHECKOUT
- 1.4 EPSDU – OPERATION
- 1.5 COMMERCIAL PROCESS ECONOMIC ANALYSIS
- 1.6 PROCESS SUPPORT R&D
- 1.7 MANAGEMENT AND DELIVERABLES

FIGURE 8



- 1.1 EPSSU — DESIGN / PROCUREMENT**
 - 1.1.1 PROCESS DESIGN
 - 1.1.2 ENGINEERING DESIGN
 - 1.1.3 EQUIPMENT SPECIFICATIONS / PROCUREMENT
 - 1.1.4 INSTALLATION DRAWINGS
 - 1.1.5 ENVIRONMENTAL
 - 1.1.6 COST ESTIMATE
- 1.2 EPSSU — EQUIPMENT FABRICATION / DELIVERY**
 - 1.2.1 MECHANICAL
 - 1.2.2 ELECTRICAL
 - 1.2.3 INSTRUMENTS AND CONTROLS
 - 1.2.4 OTHER EQUIPMENT
- 1.3 EPSSU — INSTALLATION AND CHECKOUT**
 - 1.3.1 SITE EVALUATIONS
 - 1.3.2 INSTALLATION
 - 1.3.3 CHECKOUT

FIGURE 9



**SILICON MATERIAL TASK
SILANE PROCESS (UNION CARBIDE)
EPSSU WORK BREAKDOWN STRUCTURE
(WBS) (Cont'd)**

- 1.4 EPSSU — OPERATION**
 - 1.4.1 PREPARATION
 - 1.4.2 START-UP
 - 1.4.3 MODIFICATION
 - 1.4.4 INITIAL FEASIBILITY DEMONSTRATION
 - 1.4.5 DATA GENERATION AND ANALYSIS
 - 1.4.6 SILICON CONSOLIDATION R&D, 1986 LSA GOALS
 - 1.4.7 OFF-SITE QC ANALYSIS
 - 1.4.8 FINAL PERFORMANCE RUN
 - 1.4.9 EQUIPMENT DURABILITY ASSESSMENT
 - 1.4.10 SHUTDOWN
- 1.5 COMMERCIAL PROCESS ECONOMIC ANALYSIS**
 - 1.5.1 PROCESS DESIGN
 - 1.5.2 ENGINEERING DESIGN
 - 1.5.3 COST ESTIMATING
 - 1.5.4 ASSESSMENT AND REPORTING
- 1.6 PROCESS SUPPORT R&D**
 - 1.6.1 FREE-SPACE REACTOR DEVELOPMENT
 - 1.6.2 MELTING / CONSOLIDATION DEVELOPMENT
 - 1.6.3 FLUIDIZED BED REACTOR DEVELOPMENT
 - 1.6.4 QUALITY CONTROL
- 1.7 MANAGEMENT AND DELIVERABLES**
 - 1.7.1 PROJECT MANAGEMENT
 - 1.7.2 PROGRAM MANAGEMENT
 - 1.7.3 DELIVERABLES

FIGURE 10

SESSION I

POLYSILICON MATERIAL REQUIREMENTS

J. McCormick, Chairman

EFFECTS OF IMPURITIES ON SILICON SOLAR-CELL PERFORMANCE

R. H. Hopkins
Westinghouse R&D Center
Pittsburgh, PA 15235

ABSTRACT

Model analyses indicate that sophisticated solar cell designs including, e.g., back surface fields, optical reflectors, surface passivation, and double layer antireflective coatings can produce devices with conversion efficiencies above 20% (AM1). To realize this potential, the quality of the silicon from which the cells are made must be improved; and these excellent electrical properties must be maintained during device processing.

As the cell efficiency rises, the sensitivity to trace contaminants also increases. For example, the threshold Ti impurity concentration at which cell performance degrades is more than an order of magnitude lower for an 18% cell than for a 16% cell. Similar behavior occurs for numerous other metal species which introduce deep level traps that stimulate the recombination of photogenerated carriers in silicon.

Purification via crystal growth in conjunction with gettering steps to preserve the large diffusion length of the as-grown material can lead to the production of devices with efficiencies above 18%, as we have verified experimentally.

1. INTRODUCTION

For photovoltaic (PV) power generation to compete on a large scale with other forms of energy production, the price of solar cell modules must be substantially reduced. Because area-related costs, such as land, support structures, encapsulation, etc., become significant in large systems, it is now recognized that reduced system costs require much more efficient modules and cells than are currently manufactured.^(1,2)

For this reason, a major thrust of recent photovoltaic research has been to raise solar cell efficiency by innovative cell design and careful device processing coupled with improvements in the quality of the silicon material from which the cells are made. In this paper, some basic considerations for cell efficiency improvement are examined, the performance-limiting mechanisms due to impurities are described, and techniques to minimize impurity effects are outlined.

2. APPROACHES TO CELL EFFICIENCY IMPROVEMENT

When light shines on a solar cell, photogenerated carriers (hole-electron pairs) are produced which diffuse to, and are separated by, the high field region at the junction of the device. A photovoltage is produced, and a current flows in the external circuit connected to the cell⁽³⁻⁵⁾. If the carriers recombine before reaching the junction, they do not contribute to voltage and current; and cell efficiency is reduced. Thus the carrier diffusion length L or the recombination lifetime τ to which it is related ($L = \sqrt{D\tau}$ where D is the carrier diffusivity) must be made as large as possible. For example, L should be at least equal to the cell thickness, to maximize efficiency.

Diffusion length is a strong function of impurities and defects in the silicon which act as centers for recombination. In addition, carrier recombination at surfaces and in the heavily doped regions of the cell can also limit performance. By controlling these performance limiting factors, we increase solar cell efficiency which is given by

$$\eta = \frac{V_{oc} \times I_{sc} \times FF}{P_{IN}} \quad (1)$$

where: V_{oc} is the open circuit cell voltage

I_{sc} is the short circuit current

FF is a curve ideality factor, and

P_{IN} is the incident solar power.

Advanced cell designs and increases in the quality of the silicon material are the two main methods to improve solar cell efficiency. Such features as oxide passivation to reduce carrier recombination at surfaces, double layer antireflection coatings, back surface reflectors, back surface fields, and improved emitter designs fall in the first category⁽³⁾. Controlling the defect content and purity of the bulk material to increase diffusion length are important aspects of material quality. Impurity effects and their control are the subjects of this paper.

Mathematical models of the solar cell can be used effectively to analyze how parameters like carrier diffusion length control device performance, and how they can be manipulated to gain efficiency improvement. We have used two types of models to evaluate device performance and impurity effects: one-dimensional analytic models which relate the overall material and design parameters to cell efficiency^(4,5), and a semi-empirical impurity effects model which connects the concentration of specific impurities to diffusion length and cell performance⁽⁶⁾.

In the one-dimensional model, the solar cell is divided into several elements, and the surface recombination velocity (S_0), the base diffusion length, the cell width, and the doping density are input variables. The internal recombination velocity is calculated iteratively from the device surfaces toward the junction using the relation

$$S_2 = \frac{N_2}{N_1} \frac{D}{L} \exp(\Delta V_{G2} - \Delta V_{G1}) \frac{S_1 \frac{L}{D} + \tanh\left(\frac{W}{L}\right)}{1 + S_1 \frac{L}{D} \tanh\left(\frac{W}{L}\right)} \quad (2)$$

where W is the width of the element; $(S_1, N_1, \Delta V_{G1})$ and $(S_2, N_2, \Delta V_{G2})$ are the recombination velocity, doping density, and the bandgap narrowing at the two boundaries of the element. (Here D and L are the diffusivity and diffusion length of the minority carriers within the element.) With this approach V_{oc} is calculated which, when coupled with measured or estimated values of I_{sc} , gives the expected cell efficiency⁽⁴⁾.

Figure 1 for example, illustrates the internal recombination velocities calculated for a cell made from a 250 μm thick 4 Ωcm resistivity silicon having a base diffusion length of 400 μm and various degrees of surface passivation^(4,5).

Passivation of the front and back surfaces is assumed to reduce surface recombination rates from 10^6 to 500 cm/sec in the model with resultant reduced recombination throughout the device. For the passivated device in the figure, cell efficiency is increased from 15.2% to 17% by the passivation step alone, a prediction which has been experimentally verified⁽⁷⁾. Improvements to the model⁽⁵⁾ permit direct calculation of I_{sc} and finally the cell efficiency.

If we make no assumptions regarding the mechanisms limiting the bulk material quality, we can employ the one-dimensional model to estimate how changes in the base material properties affect cell performance. The key parameter is the carrier diffusion length. We want L to be comparable to, or larger than the cell thickness to maximize efficiency. Defects such as dislocations, grain boundaries, impurity-induced recombination centers and to some extent the doping concentration all affect the value of L .

High cell efficiency can be reached by different combinations of resistivity and diffusion length as illustrated by the calculations listed in Table 1. In these specific passivated devices ($S_{on}^+ = 500$, $S_{op}^+ = 500$ cm/sec), 17.5% efficient cells required a 467 μm diffusion length when the base doping level corresponded to 4 Ωcm , but only a 125 μm diffusion length when base resistivity was 0.2 Ωcm . Increases in V_{oc} more than offset the reduction in I_{sc} due to the shorter diffusion length in the low resistivity cells. If the diffusion length of the low resistivity material is raised to 300 μm (coupled with a reduction in emitter doping to 1×10^{19} cm^{-3}), cell efficiencies over 20% are predicted.

The important point to recognize is that once cell design and resistivity are fixed, the base material diffusion length becomes the controlling parameter for efficiency improvement. Each doubling of minority carrier lifetime τ produces an absolute efficiency improvement of about 0.5%.

3. IMPURITY EFFECTS

3.1 Diffusion Length

Detailed analyses of impurities in silicon solar cells^(6,8) indicate that most metal impurities form carrier recombination centers in the bandgap and thus degrade solar cell performance dominantly by reducing diffusion length and device short circuit current. For example, Figure 2 depicts the energy levels of centers measured by deep level transient spectroscopy (DLTS) on silicon single crystals grown from melts purposely contaminated with impurities. The DLTS method is unique in its ability to detect minute amounts of active impurities⁽⁸⁾. The DLTS detection limit is about four orders of magnitude below the doping density, so concentrations as low as 10^{10} cm^{-3} (0.5 parts per trillion) can be detected in high resistivity silicon. Each impurity exhibits a particular energy level or levels which are characterized by an energy, a density, and a capture cross-section for holes or electrons.

By comparing the concentration of electrically-active (deep level) impurities in a crystal with the total metallurgical impurity content (determined by neutron activation analysis or mass spectroscopy), we discovered that the fraction of impurity that remains electrically active, and thus affects device performance, varies with the metal species, viz, Figure 3. For example all the Mo in a crystal is active following growth while only about 23% of the Cr atoms contribute to cell performance reduction. This is an indication that material thermal history strongly influences final cell efficiency, a point we will return to later.

The DLTS data on impurity recombination effects are supported by detailed dark IV measurements like those for Ti in Figure 4. The position of the upper segment of the IV curve directly relates to the bulk diffusion length of the base material^(6,9). The upward shift of the curve corresponds to an increase in I_0 , the current intercept at $V = 0$ indicating reduction in the bulk diffusion length^(6,10). The reduction in L correlates directly with the electrically active concentration (N_T) of impurities measured in the silicon by DLTS: $I_0 \propto \frac{1}{L} \propto \sqrt{N_T}$. Data for Ti were typical of most impurities studied; a few like Cu and Ni produce no apparent diffusion length reduction but degrade solar cell junctions by forming precipitates which act as electrical short circuits⁽⁶⁾.

3.2 Impurity Effects Model

The DLTS and dark IV analyses provide the foundation for an impurity effects model which gives a relationship between silicon impurity concentration and the conversion efficiency in high performance devices^(6,10). Briefly, the assumptions of the model are that the device performance is base controlled, that impurities primarily degrade diffusion length and that the number of recombination centers produced is a linear function of the metallurgical concentration of the contaminating species present.

From these assumptions, we showed that the bulk diffusion length is related to L_{no} , the diffusion length in the uncontaminated solar cell, by $\frac{1}{L^2} = \frac{1}{L_{no}^2} + K_x N_x + K_y N_y + \dots + K_z N_z$ where the K 's are constants and N is the metallurgical concentration of a given species⁽⁶⁾. For this case I_n , the

short circuit current of the contaminated devices normalized by the value for the metal-free baseline cells is given by

$$\left[\frac{I_{n\infty}}{I_n} - 1 \right]^2 = C_{2x} (N_{ox} + N_x) \quad (3)$$

in which $I_{n\infty}$ (a constant related to device geometry) = 1.11, N_x is the metallurgical impurity concentration and C_{2x} and N_{ox} are model constants determined by fitting the equation to experimental data^(6,10). N_{ox} can be interpreted as a threshold concentration for the onset of cell degradation; at $N_x = N_{ox}$, $I_n = 0.97$ and the normalized efficiency $\eta/\eta_0 = 0.92$.

We showed further that this equation can be coupled with an empirical approximation to the relationship between normalized efficiency and I_n so that cell efficiency as a function of impurity content is given by

$$\eta/\eta_0 = 0.8721 I_n^{1.128} + 0.1279 I_n^{12} \quad (4)$$

A least squares fit of equation (3) to the short circuit current data for Mo-doped cells yields $C_{2x} = 2.0 \times 10^{-14}$ and $N_{ox} = 6.08 \times 10^{11} \text{ cm}^{-3}$. The fit of the model to the efficiency data for Mo is illustrated in Figure 5. The threshold values obtained in similar fashion for over twenty metal impurities are tabulated in Reference 6. Figure 6 illustrates how the threshold for cell degradation, N_{ox} , varies with the position of the metal element in the periodic table. With these values of N_{ox} , equations (3) and (4) can be used to obtain the cell efficiency as a function of impurity type and content. The projected curves resemble Figure 5 and describe the experimentally observed behavior of 26 metals very well⁽⁶⁾ reinforcing the conclusion that the primary effect of the impurity is to degrade bulk lifetime by carrier recombination at a trapping center.

The model predicts well the behavior of both singly and multiply-contaminated solar cells made using either conventional diffused n^+ or p^+ junction designs lacking a back surface field, surface passivation, or other refinements. The average cell efficiency of this "standard efficiency" (SE) device made on silicon containing no purposely added contaminants was $14.1 \pm 0.7\%$ ^(6,10).

3.3 High Efficiency Cells

Using data for our conventional (SE) devices a qualitative understanding of how material properties influence the performance of cells with higher efficiencies can be attained by extension of the impurity effects model. A convenient way to do this is to determine the threshold impurity concentration N_{ox} for a higher efficiency (H) device and then to compare it to the value of N_{ox} deduced for our 4 Ωcm SE cells.

The relationship between the two types of devices was derived by Davis et al^(6,10):

$$N_{\text{ox}}(\text{H}) = N_{\text{ox}}(\text{SE}) \left[\frac{L_{\text{no}}(\text{SE})}{L_{\text{no}}(\text{H})} \right]^2 \left(\frac{D_n(\text{H})}{D_n(\text{SE})} \right) \quad (5)$$

$$\text{which reduces to } N_{\text{ox}}(\text{H}) = N_{\text{ox}}(\text{SE}) \left[\frac{L_{\text{no}}(\text{SE})}{L_{\text{no}}(\text{H})} \right] \quad (6)$$

when both devices have the same base resistivity.

This relationship, plotted in Figure 7 for several impurities, indicates that the sensitivity of solar cells to impurities, measured by the degradation threshold, decreases as the quality of the material denoted by L_{no} increases. For example, raising L_{no} to 600 μm from 175 μm lowers the impurity concentration at which cell performance just begins to degrade to 2.2×10^{11} Ti atoms cm^{-3} from 2.5×10^{12} Ti atoms cm^{-3} . That is, as the performance of a device is increased by material quality improvements, the sensitivity of the device to trace contamination increases.

We can place this phenomena in the context of cell efficiency with the aid of Figure 8 in which the normalized solar cell efficiency is plotted versus Ti concentration for silicon base material whose uncontaminated diffusion lengths are 175, 450, and 600 μm , respectively. The baseline (uncontaminated) devices made using this SE design would have efficiencies of 14, 14.5, and 15%, respectively. In each case once the threshold value is exceeded the cell efficiency value falls monotonically with impurity concentration. However, for the higher efficiency devices the onset of efficiency reduction occurs at succeedingly lower Ti concentrations (lower N_{ox}) as forecast by equation (6).

With the addition of $2.6 \times 10^{12} \text{ cm}^{-3}$ of Ti, the efficiency of the device with $L_{\text{no}} = 175 \mu\text{m}$ would fall from 14% to 12.6% in absolute terms. The same relative efficiency reduction, 15% to 13.5% ($\eta/\eta_0 = 0.91$), would take place at a Ti concentration of only $2.2 \times 10^{11} \text{ cm}^{-3}$ in the device with $L_{\text{no}} = 600 \mu\text{m}$. Similar calculations can be made for other impurities using the values of N_{ox} for SE cells taken from Figure 6 or from Reference 6. Compared to Ti the onset of impurity degradation would occur at a lower concentration for impurities like Mo and at higher concentrations for impurities like Cr, viz Figure 6.

Sophisticated techniques like surface passivation, back surface fields, and special emitter designs should produce cell efficiencies of 20% or better, e.g., Table 1. To analyze impurity effects on these high efficiency (HE) designs, we need to make use of the more detailed one dimensional analytic model coupled with the established linkage between diffusion length and impurity content outlined above^(6,10). Using Ti as a typical impurity, we assume an HE device design with front and back surface passivation, a back surface field, a double layer antireflective coating and a cell thickness of 275 μm equal to that of the SE cells. Again, the assumed diffusion lengths of the uncontaminated baseline cells are 175, 450, and 600 μm , producing calculated cell efficiencies of 16.1, 18, and 18.5% AML. As noted, the efficiency of the SE cell chosen for comparison is 14% when $L_{\text{no}} = 175 \mu\text{m}$.

The effect of Ti additions on HE cell performance, Figure 9, is qualitatively similar to that for the SE design: as the cell efficiency increases, the Ti concentration at which performance reduction begins is reduced. That is, higher efficiency devices are more impurity sensitive (quantitative comparisons of Figures 8 and 9 are difficult due to minor differences in the model assumptions for the two cases).

Taken together, the data indicate that small amounts of metal contaminants may be tolerated when cell efficiencies are low to moderate, 12 to 15%, but that impurities must be limited to very low levels if very high efficiencies are to be achieved (a Ti concentration of about 10^{11} cm⁻³, 2 parts per trillion, is sufficient to reduce cell efficiency from 18.5% to about 16.8%). The harmfulness of a specific impurity depends on its value of N_{OX} , Figure 9. In addition, other defects which reduce bulk lifetime must also be minimized.

4. IMPURITY CONTROL

Currently there are two approaches to control the electrically-active impurity concentration in silicon solar cells: (1) minimize contamination of the base material by purification to provide the highest value of L possible in the wafers from which cells are made, and (2) maintain or improve the initial diffusion length by chemical or thermochemical "getting" techniques during the cell processing itself^(11,12). In the first method, impurities are eliminated; in the second, they may be removed or made electrically inactive by precipitation or chemical complexing to eliminate carrier recombination sites.

4.1 Purification

Silicon for solar cells is produced in two steps - decomposition of highly-purified trichlorosilane or silicon tetrachloride to form polycrystalline silicon⁽¹³⁾ and the subsequent transformation of polysilicon to a single crystal ingot by Czochralski pulling (CZ) or float zone (FZ) refining,^(14,15) or to sheet by newer ribbon growing processes⁽¹⁶⁾. The crystal growth step is an integral part of the purification since most impurities tend to accumulate preferentially in the liquid during growth leaving the solid proportionately purer. The degree of purification for a given contaminant is measured by its effective segregation coefficient k_e , the ratio of the crystal impurity content to the impurity content of the feedstock from which the crystal grew⁽¹⁵⁾.

Our measurements, Table 2, confirm that the segregation coefficients of metal contaminants grown into silicon crystals during Czochralski pulling^(6,10) are in general extremely small, ranging from 3×10^{-2} for Al to 1.7×10^{-8} for W. (k values for ribbon growing by the dendritic web process are comparably small⁽¹⁶⁾). Perhaps one of the most striking and useful features of metal impurity segregation in silicon is the relationship between the cell degradation threshold concentration and the effective segregation coefficient, viz Figure 10. Those impurities most effective at reducing bulk diffusion length, e.g., Ta, Mo, and Zr, have the smallest segregation coefficients and are therefore the most easy to eliminate during the crystal growth step.

Although there is no clear-cut theoretical explanation for the observed relationship, we expect impurities with the largest atom size and chemical character disparities to silicon to exhibit the smallest value of k , a fact consistent with experiment, viz Figure 11 (see also reference 10). These are the same impurities whose electronic structure favor the formation of deep levels with large carrier capture cross-sections⁽¹⁷⁾. The general sloping of the threshold values from the upper right to lower left in Figure 6 though not completely understood, suggests an increase in effective carrier recombination cross-section.

To take fullest advantage of the segregation behavior of metal contaminants, we can employ zone refining to purify the silicon from which cells are made. For example, after two zone passes our model Ti impurity could be reduced below 10^{10} cm^{-3} from an assumed feedstock concentration of 10^{16} cm^{-3} . The purification effect would be somewhat less for CZ pulling and web growth, but it is still significant. Experimentally, the most efficient solar cells have been produced on Wacker float zoned silicon substrates. Data for cells made in our laboratory on FZ material, Table 3, show the obvious advantages of increased purification. Comparable cells made on Czochralski and web material typically exhibited efficiencies lower by as much as 1 to 2% absolute. The purity of these materials is high enough that no deep levels can be measured even by DLTS; total heavy metal impurity concentrations of less than 0.01 ppba (5×10^{11} cm^{-3}) for float zone silicon and less than 1 ppba (5×10^{13} cm^{-3}) for Czochralski material are typical⁽¹²⁾.

4.2 Post Growth Impurity Control

Despite the fact that crystals of extremely high purity can be produced, contaminants introduced during subsequent device processing may significantly degrade bulk material properties. Wafer preparation, handling, and high temperature process steps are common entry points for metal species into the silicon⁽¹⁸⁾. Besides cleaner processing, one way to minimize the effects of contamination and to enhance bulk material properties is by impurity gettering^(11, 12).

We found that volatilization of impurities as chlorides by heat treatment in Cl-bearing ambients, migration of contaminants to regions of enhanced solubility such as diffused junctions, and precipitation at deliberately induced defects all can be used to electrically deactivate impurities in silicon solar cells and to raise cell efficiency^(10, 19). However, the effectiveness of each technique appears highly species and process history dependent.

A key step in most gettering processes is the diffusion of impurity atoms to a sink where the electrical activity of the metal is ultimately neutralized by precipitation or complexing. To test the response of various species to gettering, we diffused metal-doped wafers at 825°C in POCl_3 , a treatment which also mimics the solar cell junction formation step. The diffused layer was dissolved, and a series of steps was etched from the wafer surface into the bulk silicon. Schottky diodes formed on the steps permitted us to measure by DLTS the impurity concentration as a function of depth into the wafer, Figure 12. The starting wafer concentrations were 4×10^{14} cm^{-3} V, 2×10^{14} cm^{-3} Ti, 10^{15} cm^{-3} Cr, and 4×10^{12} Mo cm^{-3} , respectively.

The variation in impurity response to the thermochemical process is striking. Following gettering, the electrically active Ti and V concentrations exhibited a profile with decreasing concentration toward the surface indicating diffusion of the metals to the junction region and electrical deactivation. The electrically active Cr concentration which was about 10^{14} before heat treatment fell below the DLTS detection limit of $3.5 \times 10^{11} \text{ cm}^{-3}$ at all locations in the sample. No change in the Mo concentration could be detected. A more detailed study of Ti gettering, Figure 13, indicated that the process was diffusion controlled and could be modeled closely by assuming an activation energy of 1.66 eV⁽¹³⁾. In general, the effectiveness of POCl_3 gettering depended directly on the diffusion coefficient of the species ($D_{\text{Cr}} > D_{\text{Ti}} > D_{\text{V}} > D_{\text{Mo}}$) and so the process cycle must be tailored to some extent for each impurity or class of impurity (Fe, Cr, Co, Cu).

For example, the data in Table 4 indicate how solar cell efficiency and silicon impurity concentration vary with the gettering treatment for silicon which initially contained $8 \times 10^{13} \text{ cm}^{-3}$ of electrically active Ti. Higher temperatures and longer times decrease the Ti concentration near the surface and increase the cell efficiency. For the starting concentration chosen in these experiments, no process tested completely deactivated all the Ti, so the cell efficiency recovered to only about 70% of the uncontaminated baseline value of 14%. For rapidly diffusing species like Cr and Fe, full recovery of the baseline cell efficiency was achieved^(10,19). For impurities like Mo, almost no improvement in cell efficiency was obtained even after several hours POCl_3 gettering at 1200°C.

HCl treatments at temperatures between 825 and 1200°C provided qualitatively similar results but appeared to be somewhat more effective than the POCl_3 treatment. Shorter times or lower temperatures diminished the impurity effects to the same level as for POCl_3 . Backside damage and argon implant-induced damage reduced the electrical activity of most contaminants studied but were most effective when used in combination with HCl treatments⁽¹⁰⁾.

The data on gettering are encouraging as a means to improve cell efficiency, but we know of no systematic studies in which the method has been employed to produce higher efficiency devices than those attained by conventional methods.

Coupled with float zoning, gettering may provide material quality enhancements permitting the full exploitation of device design improvements suggested from the model studies.

5. CONCLUSION

Economic analyses indicate that high efficiency (> 18%) solar cells and modules will be required if photovoltaic power generation systems are to achieve widespread application, especially in utility networks. While clever cell design can produce significant efficiency improvements, the quality of the silicon from which the cells are made must be increased and its bulk properties maintained during cell processing if these design improvements are to be fully realized.

Cell efficiency, particularly in high efficiency devices, is strongly degraded by metal contaminants which reduce bulk diffusion length. For example, as few as 10^{11} cm⁻³ Ti atoms cm⁻³ can reduce the efficiency of an 18.5% to 16.8%, a significant depreciation. Elements to the left of the periodic table like W and Mo are more harmful per unit concentration than are elements to the right like Cr and Fe. Low base resistivity permits lower diffusion lengths for a given efficiency so that such devices are more impurity tolerant.

Raising bulk diffusion length can be achieved mainly by starting with high purity silicon then employing zone refining. The segregation coefficients for all metal contaminants are small, typically 10^{-5} or less so that several zone passes lower the impurity concentration well below the detection limits of even the most sensitive analytical techniques. To preserve diffusion length during silicon handling is more difficult and requires extremely clean procedures to guard against unwanted contamination. A gettering step to maintain diffusion length during processing ultimately may be required to provide the highest efficiency devices.

ACKNOWLEDGEMENTS

We acknowledge the major contributions to this work by our colleagues at the Westinghouse R&D Center and Advanced Energy Systems Division including the late J. R. Davis, D. L. Meier, P. G. McMullin, M. H. Hanes, P. D. Blais, P. Rai-Choudhury, R. G. Seidensticker, and R. B. Campbell. We also thank Dr. Martin Wolf, U. of Pennsylvania for use of the program SPCOLAY to model solar cell performance.

The work was supported by the DOE/JPL Flat Plate Solar Array Project.

REFERENCES

1. A. Rohatgi and E. F. Federman, *J. Solar Energy* (1985).
2. D. L. Bowler and M. Wolf, *IEEE Transactions Compon. Hybrid Manufact. Tech.*, V3, p. 464, (1980).
3. M. Wolf, *Proc. 14th IEEE Photovoltaic Specialists Conference*, p. 674, (1980).
4. J. R. Davis and A. Rohatgi, *Proceedings 14th IEEE Photovoltaic Specialists Conference*, p. 569 (1980).
5. M. Wolf, *IEEE Transactions on Electron Devices*, V ED-28, p. 566, (1981).
6. J. R. Davis et al, *IEEE Transaction on Electron Devices*, V ED-27, p. 677, (1980).
7. A. Rohatgi and P. Rai-Choudhury, *IEEE Transactions on Electron Devices*, ED-31, p. 596 (1984).
8. A. Rohatgi, J. R. Davis, R. H. Hopkins, and P. G. McMullin, *Solid State Electronics*, V26, pl. 1039, (1983).
9. A. Rohatgi, R. H. Hopkins, J. R. Davis, and R. B. Campbell, *Solid State Electronics*, V. 23, p. 1185, (1980).
10. R. H. Hopkins et al, *Final Report, Impurity Effects in Silicon Solar Cells*, DOE/JPL 954331, (1982).
11. L. E. Katz, P. F. Schmidt, and C. W. Pearce, *J. Electrochem. Soc.*, V 128, p. 620, (1981).
12. J. R. Monkowski, *Solid State Technology*, p. 44 (1981).
13. See e.g., J. Dietl, D. Helmreich, and E. Sirtl, *Crystals: Growth Properties and Applications*, V 5, p. 43, (1981).
14. W. Zulehner and D. Huber, *Crystals: Growth Properties and Applications*, V 8, p. 3, (1982).
15. B. Chalmers, *Principles of Solidification* (J. Wiley & Sons, NY), p. 3, (1964).
16. R. G. Seidensticker, *Crystals: Growth, Properties and Applications*, V 8, p. (1982).
17. L. A. Hemstreet, *Phys. Rev. B*, V 15, p. 834 (1977).
18. P. F. Schmidt and C. W. Pearce, *J. Electrochem Soc.*, V 128, p. 630 (1981).
19. A. Rohatgi et al., *Proceedings 14th IEEE Photovoltaic Specialists Conf.*, p. 908, (1980).

LIST OF FIGURES

1. Model Calculations and Internal Recombination Velocity Plots for 4-ohm-cm Base Cells with a Base Diffusion Length of 400.
2. Measured Deep Levels for Impurities Grown into Silicon Single Crystals.
3. Measured Electrically Active Deep-Level Concentrations versus the Metallurgical Concentrations for Several Metal Impurities.
4. Transferred Dark IV Curves for Ti-Doped Solar Cells.
5. Calculated and Measured Cell Performance for Mo-Contaminated Devices.
6. Threshold Impurity Concentrations for Cell Performance Reduction.
7. Variation in Degradation Threshold with Diffusion Length of Baseline SE Cell.
8. Cell Efficiency Variation with Ti Concentration for Various Initial Base Diffusion Lengths.
9. Variation in Cell Performance with Ti Concentration: HE Cell Design.
10. Relation of Cell Degradation Threshold to Impurity Segregation Coefficient.
11. Variation of Segregation Coefficient with Impurity Bond Radius.
12. Electrically Active Impurity Profiles for Several Species after an 825°C, 50-min POCl_3 Treatment.
13. Electrically Active Ti Concentration Profiles Following 50-min POCl_3 Gettering at Several Temperatures.

TABLE 1

RESISTIVITY AND DIFFUSION LENGTH REOUIREMENTS
FOR HIGH EFFICIENCY SOLAR CELLS

$W = 150 \mu\text{m}$ (cell thickness)

$N_{xj} = 3 \times 10^{17} \text{ cm}^{-3}$ (emitter junction edge doping concentration)

$S_{op}^+ = S_{on}^+ = 500 \text{ cm/sec}$ (surface recombination velocities)

$N_s = 2 \times 10^{20} \text{ cm}^{-3}$ (emitter surface coping concentration)

ρ <u>$\Omega\text{-cm}$</u>	L <u>(μm)</u>	J_{sc} <u>(ma/cm^2)</u>	V_{oc} <u>(volts)</u>	η <u>$(\%)$</u>
4.0	467	35.2	.597	17.5
0.2	125	33.2	.634	17.5
*0.2	300	35.0	.687	20.3

* $N_s = 1 \times 10^{19} \text{ cm}^{-3}$

TABLE 2

EFFECTIVE SEGREGATION COEFFICIENTS IN SILICON

<u>Element</u>	<u>Segregation Coefficient</u>
Ag	1.7×10^{-5}
Al	3×10^{-2}
Au	2.5×10^{-5}
Co	2×10^{-5}
Cr	1.1×10^{-5}
Cu	8.0×10^{-4}
Fe	6.4×10^{-6}
Mn	1.3×10^{-5}
Mo	4.5×10^{-8}
Nb	4.4×10^{-7}
Ni	1.3×10^{-4}
Pd	5×10^{-5}
Sn	3.2×10^{-2}
Ta	2.1×10^{-8}
Ti	2.0×10^{-6}
V	4×10^{-6}
W	1.7×10^{-8}
Zr	1.6×10^{-8}

TABLE 3

OXIDE-PASSIVATED SOLAR CELLS WITH DOUBLE-LAYER ANTIREFLECTIVE
COATING PRODUCED ON 0.25 Ω -cm FLOAT ZONED SILICON

<u>Cell ID*</u>	<u>Area</u> <u>cm²</u>	<u>J_{sc}</u> <u>mA/cm²</u>	<u>V_{oc}</u> <u>mV</u>	<u>FF</u>	<u>η</u> <u>%</u>
25-1	1.0	37.5	614	0.791	18.2
25-2	1.0	37.1	617	0.784	18.0
9-1	1.0	36.8	617	0.797	18.1
9-2	1.0	36.3	617	0.806	18.0
4-1	1.0	35.9	623	0.809	18.1
4-2	1.0	36.2	622	0.809	18.2
4-3	1.0	36.1	623	0.815	18.3
4-4	1.0	36.0	622	0.809	18.1

TABLE 4

VARIATION IN CELL EFFICIENCY AND TRAP CONCENTRATION (N_T) AS A FUNCTION OF
GETTERING TREATMENT FOR SILICON CONTAINING A METALLURGICAL TI

<u>Gettering Condition</u>	<u>Cell Efficiency</u> <u>(%)</u>	<u>Concentration</u> <u>(N_T) of $E_V + 0.30$</u> <u>eV TRAP (cm⁻³)</u>
None (starting wafer)	---	8.0×10^{13}
None (solar cell)	5.88	1.76×10^{13}
950°C/1 hr.	6.58	6.35×10^{12}
1000°C/1 hr.	7.14	3.94×10^{12}
1100°C/1 hr.	7.42	2.99×10^{12}
1100°C/2 hr.	7.76	2.50×10^{12}
1100°C/3 hr.	8.27	2.39×10^{12}
1100°C/5 hr.	9.27	1.49×10^{12}

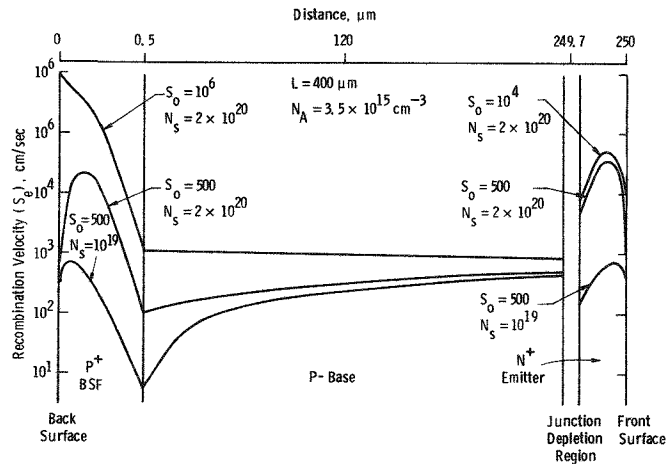


Figure 1 Model Calculations and Internal Recombination Velocity Plots for 4-ohm-cm Base Cells with a Base Diffusion Length of 400 μm

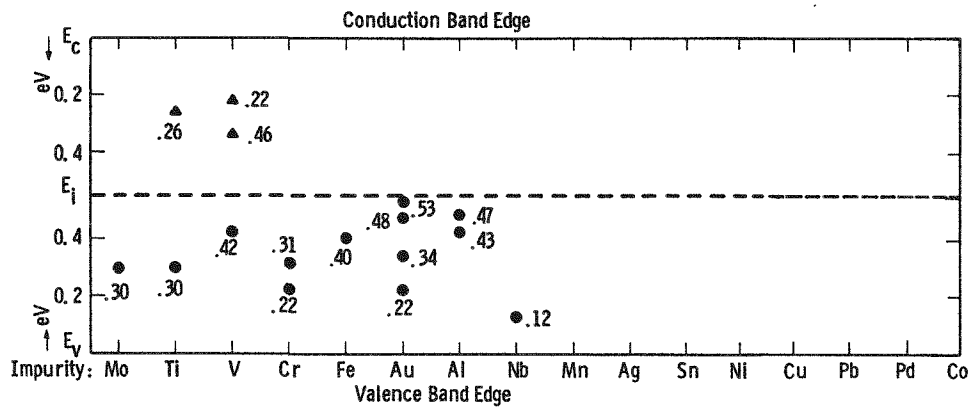


Figure 2 Measured Deep Levels for Impurities Grown into Silicon Single Crystals.

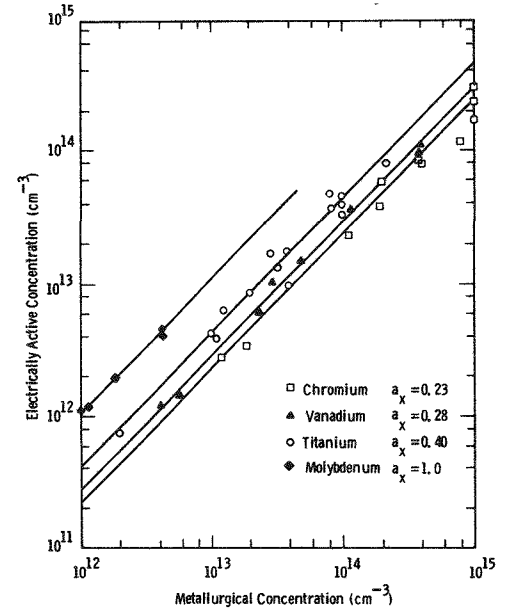


Figure 3 Measured Electrically Active Deep-Level Concentrations versus the Metallurgical Concentrations for Several Metal Impurities.

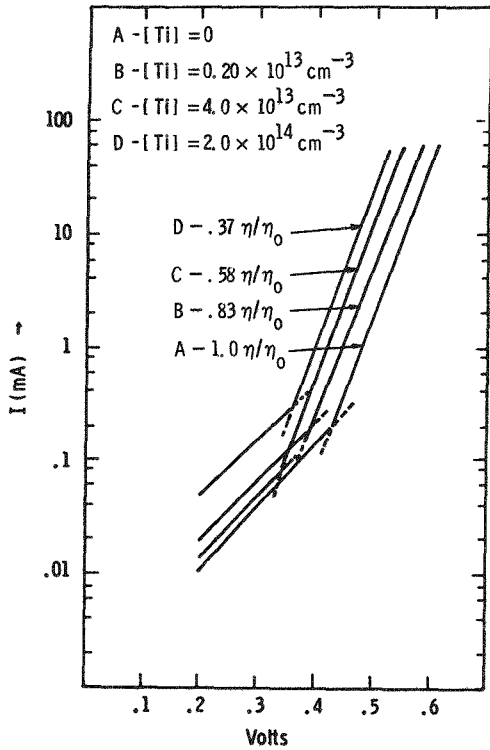


Figure 4 Transformed Dark IV Curves for Ti-Doped Solar Cells.

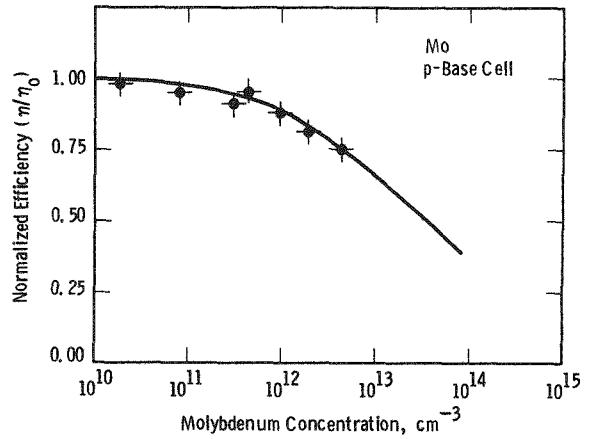


Figure 5 Calculated and Measured Cell Performance for Mo-Contaminated Devices.

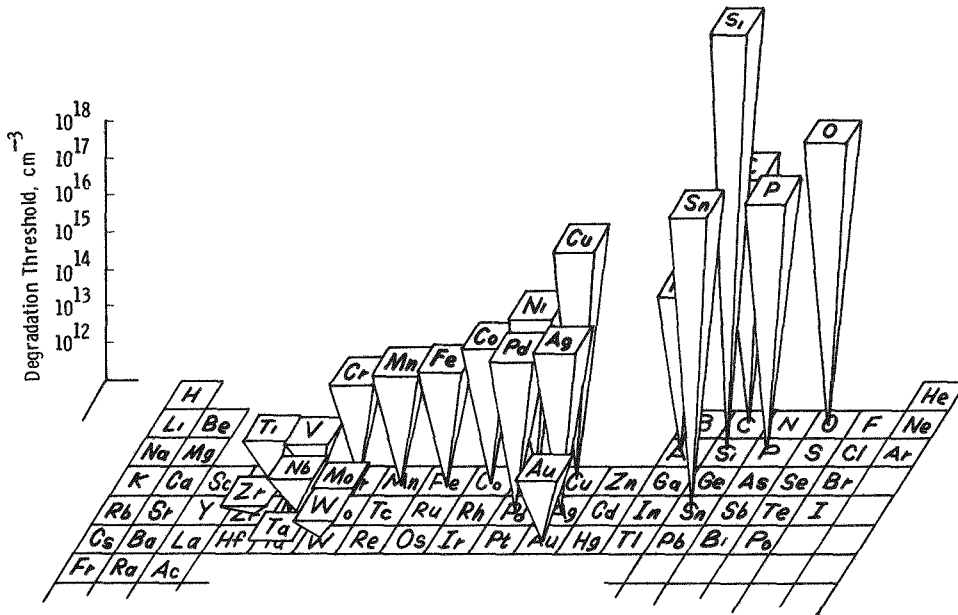


Figure 6 Threshold Impurity Concentrations for Cell Performance Reduction.

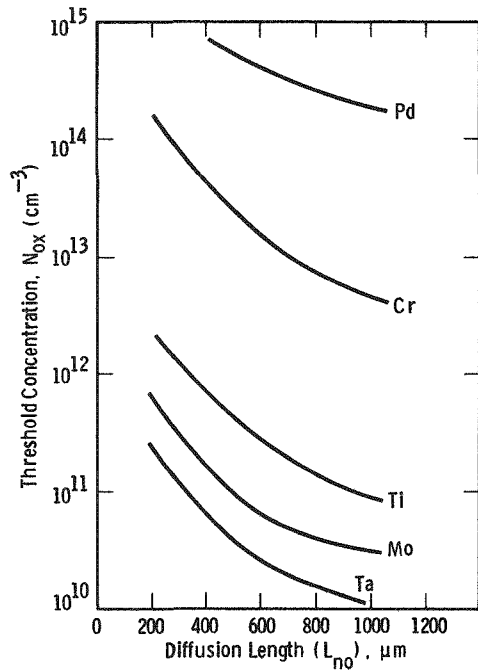


Figure 7 Variation in Degradation Threshold with Diffusion Length of Baseline SE Cell.

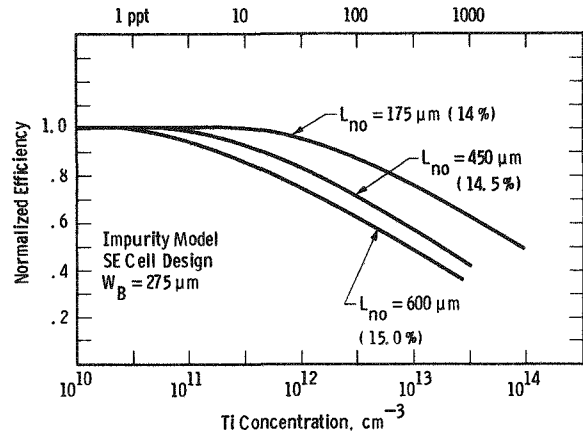


Figure 8 Cell Efficiency Variation with Ti Concentration for Various Initial Base Diffusion Lengths.

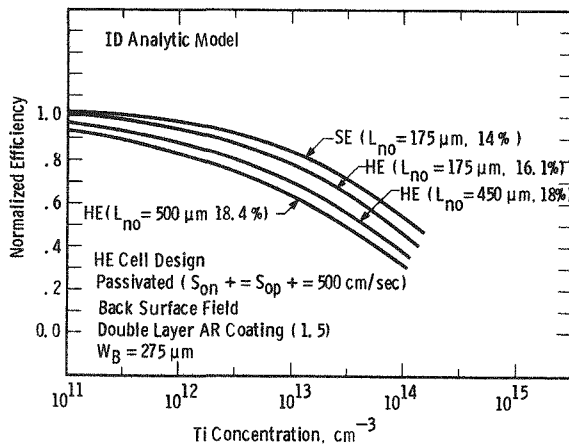


Figure 9 Variation in Cell Performance with Ti Concentration: HE Cell Design.

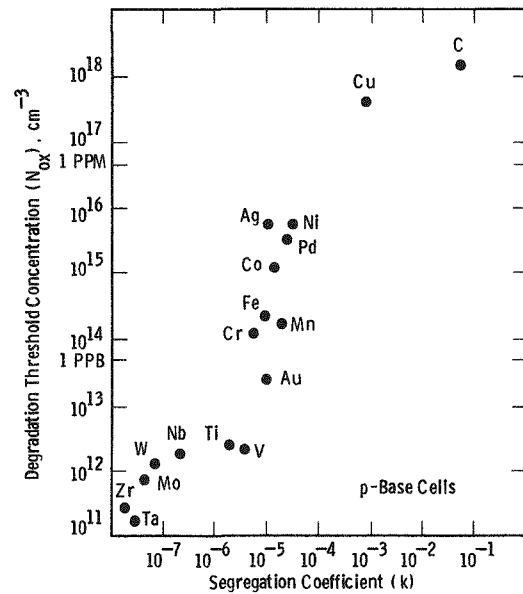


Figure 10 Relation of Cell Degradation Threshold to Impurity Segregation Coefficient.

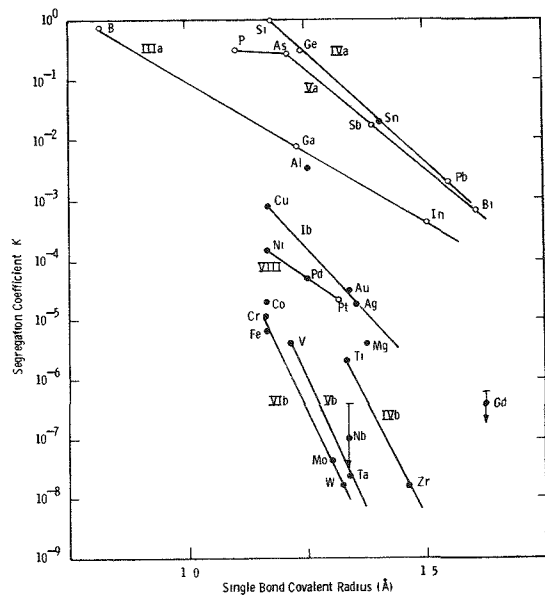


Figure 11 Variation of Segregation Coefficient with Impurity Bond Radius.

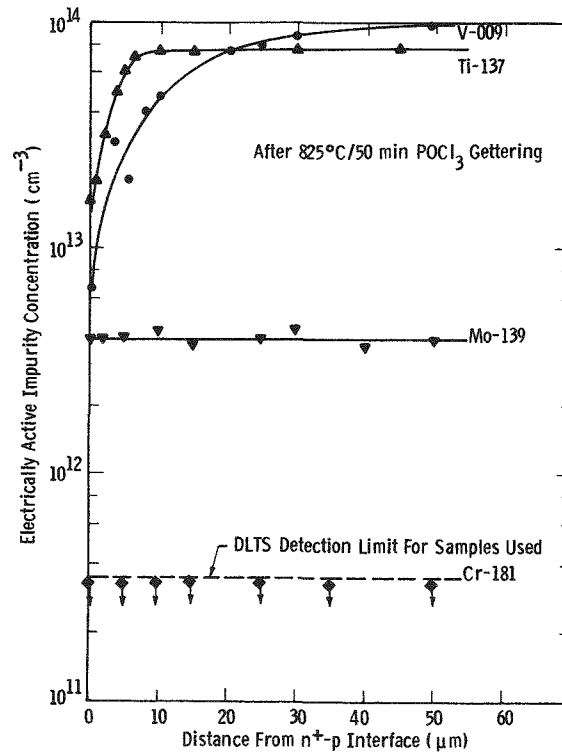


Figure 12 Electrically Active Impurity Profiles for Several Species after an 825°C, 50-min POCl_3 Treatment.

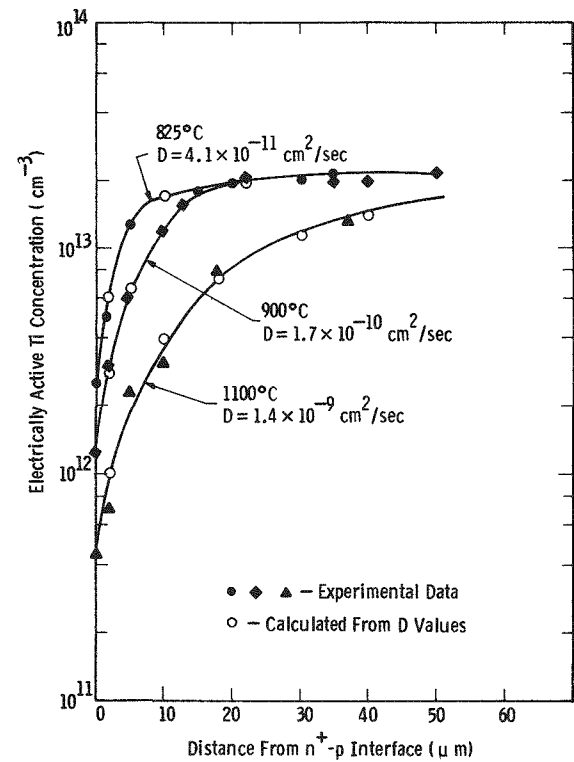


Figure 13 Electrically Active Ti Concentration Profiles Following 50-min POCl_3 Gettering at Several Temperatures.

DISCUSSION

AULICH: Did you look at the effects of boron, phosphorus, and carbon on the impurity relationships?

HOPKINS: We did a very small amount of work with carbon. We had a great deal of difficulty getting structurally good ingots. Jim McCormick (Hemlock Semiconductor) is more familiar with the ingot-growing problems and could answer questions about that part better than I can. We really didn't investigate carbon extensively. We did some work with phosphorus. I can't remember the concentration levels, but they were fairly high. There does seem to be a turnover for phosphorus. Ranny Davis believed that this was largely due to a reduction in mobility due to ionized impurity scattering. We did not do a significant study using boron.

AULICH: If an impurity level is detrimental, can anything be done during cell processing to inactivate the impurity? In other words, is there a chance of converting an impure, bad material into a good efficiency material?

HOPKINS: Our experience wouldn't lead to a claim that this could be done. However, in some of our systematic studies of gettering using conventional back-surface damage (or phosphorus oxychloride or HCL as gettering agents, or in some cases using ion implantation damage to stimulate gettering), we found that the electrically active concentrations of a number of the impurities could be deactivated or reduced. If the impurities behaved like chromium and iron, which have relatively high diffusion coefficients, the electrically active concentrations were reduced to essentially zero. The concentrations of impurities having diffusion properties similar to titanium and vanadium could be reduced, but not eliminated. Thus, the efficiencies of devices containing titanium or vanadium, for example, could be improved by one or maybe two points over the range of temperatures and times we used experimentally, but the uncontaminated baseline values could not be reached. Some benefits can be obtained from gettering. We didn't do enough to really define the total spectrum of conditions needed to render all impurities harmless, but I think there is a limit to how much can be done if the initial impurity concentrations are very high.

HWANG: In a recent report describing silicon solar cells with efficiencies exceeding 18%, the materials used (with very few exceptions) were float-zone crystals with resistivities of 0.2 to 0.3 ohm-cm. This seems to indicate that phosphorus and boron might have a larger effect than the metal content. In these cases, the diffusion lengths were just a few tenths of a micrometer. Would you kindly comment on these data?

HOPKINS: What you said is true. In fact, the data that I showed for the 18% cells were for cells made from a seemingly unique piece of low-resistivity float-zone material. It doesn't seem to be unique anymore. The diffusion length was low, but it was still up in the hundreds of micrometers. I think the metal contamination levels must be kept very low to achieve these high-efficiency values. In fact, in our modeling of the 18%

devices, it became clear that the diffusion length must be high, which it was, even though the resistivity was low. Our conclusion was that the impurity concentrations must be kept at very low levels to get high-efficiency cells.

SCHMID: It seems that oxygen and carbon would be very significant elements in influencing the levels of impurities. I guess most of the work you did was with high-quality silicon. What were the levels of oxygen and carbon?

HOPKINS: Levels of oxygen were typically those found in most Czochralski-grown ingots, on the order of 10^{18} , and the level of carbon was about an order of magnitude lower. We did some work with float-zone crystals, and we found that the oxygen and carbon were reduced and there were lower levels of the metal impurities, although it wasn't dramatic. However, we only looked at three or four ingots out of a total of 200 or more.

SCHMID: You mentioned that you did some work in higher carbon content and you did see some breakdown. At what level did you see the breakdown as a factor of just increasing carbon concentration?

HOPKINS: I wish I could answer. It's been quite awhile, and the amount of work we did with carbon was relatively low. I don't think I can characterize the effects. I think the people who work with castings could describe the levels of carbon concentration which cause problems. As I said, we used Czochralski ingots for most of our work, and the main issue was to maintain the oxygen and carbon concentrations nearly the same from crystal to crystal to provide a valid method of comparison for determining the effects of impurities. I would like to look at that problem. If our program had not ended in 1982, we would have.

REQUIREMENTS FOR HIGH-EFFICIENCY SOLAR CELLS

C. Tang Sah
University of Illinois
Urbana, Illinois 61801

Minimum recombination and low injection level are essential for high efficiency. Twenty percent AM1 efficiency requires a dark recombination current density of $2 \times 10^{-13} \text{ A/cm}^2$ and a recombination center density of less than about 10^{10} cm^{-3} . Recombination mechanisms at thirteen locations in a conventional single-crystalline silicon cell design are reviewed. Three additional recombination locations are described at grain boundaries in polycrystalline cells. Material perfection and fabrication process optimization requirements for high efficiency are outlined. Innovative device designs to reduce recombination in the bulk and interfaces of single-crystalline cells and in the grain boundary of poly-crystalline cells are reviewed.

I. INTRODUCTION

Increasing efficiency and lowering cost have been the main objectives of solar cell research to achieve cost parity with other electrical power generation methods. Single-crystalline silicon cell efficiency approaching 18% (AM1) has been attained under production environment, moving the current research target to 20% or beyond [1]. Poly-crystalline silicon cell approach may lower the manufacturing cost further to a competitive level.

This paper will provide a review of the requirements for achieving high efficiencies. The next section, II, will review the dark d.c. current-voltage characteristics of a cell. Section III describes the dominant recombination mechanisms at thirteen locations in single-crystalline and three additional grain boundary locations in poly-crystalline cells. Section IV outlines the material requirements for minimizing recombination. Section V gives a discussion of process optimizations for high efficiency. Device design optimizations for high efficiency are reviewed in section VI. Section VII gives a summary.

II. D. C. CURRENT-VOLTAGE CHARACTERISTICS

The d.c. current-voltage characteristics of a solar cell in the dark provides a clear indication of its performance under sun light. It can be expressed generally by the diode equation

$$J = J_r [\exp(qV/rkT) - 1] \quad (1)$$

where J is the dark current density (A/cm^2), J_r is the recombination current density coefficient (A/cm^2) which will be called recombination current, q is the charge of the electron, V is the voltage across the cell with p-side positive and n-side negative in the p/n junction cell, r is the recombination law or junction ideality factor, k is the Boltzmann constant and T is the cell temperature.

The highest efficiency is achieved when both J_r and r are small. The dependence on r is illustrated by the illuminated current-voltage characteristic of a solar cell in Fig.1 whose equivalent circuit is also given in this figure. It is evident that the smallest r gives the largest area under the illuminated I-V curve and hence the highest power deliverable to the load. In a practical cell whose efficiency loss comes from electron-hole recombination at traps due to crystalline imperfections, the lowest recombination factor is $r=1$. This corresponds to low level injection, that is, the photogenerated electron and hole concentration levels are much less than the dark equilibrium majority carrier (electron in n-type or hole in p-type silicon) concentration. The limiting recombination is via imperfection located in the base layer of the cell under the low level condition in a properly designed high efficiency cell.

The other I-V curves in Fig. 1 are from different recombination and conduction mechanisms. The ideal zero recombination case, $r=0$, is also known as the threshold diode. The $r=2/3$ case comes from zero imperfection so that the residual recombination is due to the direct recombination of an electron with a hole during which another electron or hole carries away the recombination energy. This is known as the interband Auger recombination. The factor $2/3$ arises from the high injection level condition in an interband Auger recombination-limited cell since electron and hole densities are increasing with the terminal voltage V as $\exp(qV/2kT)$ while the recombination rate or current is increasing with the product of concentration of two electrons and one hole or one electron and two holes, N^2P or NP^2 . Additional discussions and references are given by this author in a recent review article [2]. The $r=2$ case comes from high-level recombination at the imperfection centers. The SCL curve has the current limited by the space charge of the photogenerated electrons and holes, known as the space-charge-limited case. It is the worse efficiency case and was a limitation of some earlier amorphous silicon cells [3] whose base layer has a rather high resistivity.

Thus, the highest efficiency for the current technology in which electron-hole recombination at the traps due to imperfections dominates is a cell whose r should be made to approach one and whose recombination current density, J_r or J_1 , be reduced to as small a value as possible.

In Table I, the theoretical results that relate J_1 to the AM1 efficiency are given. They show that in order to reach a 20% AM1 efficiency given in the column labeled EFF, the recombination current density, J_1 , must be less than 0.2 pico-ampere per square centimeter. They also show that for each 2% increase of the efficiency, the recombination current density must decrease by one order of magnitude. It lowers to 0.2 femto-ampere per square centimeter in order for the efficiency to reach 26%. At this low recombination loss level, the recombination events are dominated by the interband Auger mechanism instead of the trap mechanism and the former limits the intrinsic or ultimate efficiency to about 25% for silicon solar cell at AM1 illumination on the earth surface [2].

The figures in the table are obtained by a simple calculation to maximize the output power to the load, $P=IV$, using Eq.(1) with $r=1$. The short circuit current, J_{SC} , is taken to be a constant 36.0 mA/cm^2 while the cell temperature is assumed to be at 297.15K or 24C. V_{OC} is the open circuit voltage. FF is the fill factor, sometimes called the curve factor (CF) and it is defined by $FF=P_{MAX}/(J_{SC}V_{OC})$ where P_{MAX} is the maximum available power.

III. RECOMBINATION LOCATIONS AND MECHANISMS

In order to reduce and eliminate recombination losses, a review of the recombination locations and dominant recombination mechanisms is given in this section. The single-crystalline cell will be discussed first followed by an extension to poly-crystalline cells.

A. SINGLE-CRYSTALLINE CELL

A conventional single-crystalline cell structure is used whose cross-sectional view is given in Fig. 2. Thirteen recombination locations are identified and numerically labeled. These are now described by deviding the cell into four electrically active layers in the four-layer model.

EMITTER QUASI-NEUTRAL LAYER *****

1. Contact Metal to Silicon Emitter Interface

Thermal recombination dominates at the interface traps, especially when the interfacial contact layer is imbedded with oxide islands which can give rise to silicon and oxygen dangling bonds that are efficient electron-hole recombination sites. These are similar to the interface traps which also degrade the performance of metal-oxide-silicon field-effect transistors. This recombination is also known as the Shockley-Read-Hall (SRH) thermal recombination mechanisms in which the recombination energy is dissipated by lattice vibration or phonon emission.

2. Anti-Reflection Coated Oxide to Silicon Emitter Interface

SRH thermal as well as the interband- and bound-Auger recombination mechanisms can be important, the former at the oxide/silicon interface traps due to dangling silicon and oxygen bonds and the latter due to the high concentration of majority carrier or dopant impurity at the silicon surface under the oxide/silicon interface.

3. Bulk Emitter Layer

SRH thermal and the interband- and bound-Auger recombination mechanisms can be important due to the high dopant impurity density which can result in high density of traps in the emitter layer.

4. Emitter Perimeter

Saw damage and exposed chemically-etched surface at the emitter perimeter will have both high density of dangling silicon bonds and non-dopant impurities which may be electron-hole recombination traps.

EMITTER SPACE CHARGE LAYER

5. Emitter Bulk Space Charge Layer

Dominant recombination in this layer is mainly through the thermal SRH mechanism at traps due to residual non-dopant impurities. A $r=2$ value can be expected for the most dominant traps with bound state energy level at the midgap position of the silicon energy gap. Generally, $1 < r < 2$ has been observed.

6. Emitter Perimeter Space Charge Layer

The dominant recombination is also the thermal SRH mechanism at the traps due to dangling silicon bonds at the exposed surface and silicon and oxygen dangling bonds at partially oxide-covered silicon surface.

BASE QUASI-NEUTRAL LAYER

7. Bulk Base Layer

The 20% efficiency is limited by the extrinsic recombination mechanism due to thermal SRH recombination at residual non-dopant impurity traps and at physical defects or dangling silicon bonds. The ultimate efficiency of 25 to 26% is limited by the intrinsic recombination mechanisms of interband Auger recombination and interband radiative recombination of electrons with holes directly.

8. Back Contact Metal to Silicon Interface

This is similar to the front contact metal to silicon interface described for location 1 previously. However, its recombination rate could be higher due to the lower dopant impurity concentration than that of the diffused front surface, the latter may have a potential barrier repulsive to minority carriers. The thermal SRH mechanism dominates. Two device designs have been employed to reduce this loss. One is the use of a very thick silicon wafer. The other is the use of a built-in electric field from the dopant impurity concentration gradient to repulse the photo-generated minority carriers. This is known as the back surface field cell and discussed in the following subsection with location numbers 10 to 13.

9. Base Layer Perimeter

Thermal SRH recombination dominates at the traps due to dangling silicon bonds at the exposed and saw damaged surface and silicon and oxygen dangling bonds at the partially oxide-covered surface from etching residuals.

BACK-SURFACE-FIELD LAYER

The cross-sectional view of the Back-Surface-Field (BSF) solar cell structure is shown in Fig. 3. The BSF layer can be fabricated either by alloying aluminum into a p-type silicon bulk since aluminum is a dopant acceptor impurity with solubility above 10^{18} Al/cm³, or it can be fabricated by solid state diffusion of either boron into a p-type substrate or phosphorus, arsenic or antimony into a n-type substrate. The aluminum alloying is an earlier technique which is not as effective due to deep and less controlled penetration of the alloy layer into the silicon base [4] while the diffused BSF layer in 18% silicon cells has been demonstrated more recently but is less reproducible due to the imperfections introduced during high temperature diffusion.

10. Bulk N+ (or P+) Layer

This is a highly doped layer where the recombination losses are mainly due to the thermal SRH mechanism at traps arisen from the heavy doping.

11. Back Contact Metal to Silicon Interface

Recombination at this interface is identical to that at the similar front interface. However, its effect on efficiency is less since it is away from the region where electrons and holes are generated by light.

12. Back Oxide to Silicon Interface

Recombination at interface traps on the back interface here is similar to that at the front interface discussed for location 2 above. The effect on efficiency is again smaller than that from the front interface. However, recombination losses at both locations 11 and 12 cannot be neglected in high efficiency cell designs.

13. Back Surface Field Perimeter

Recombination in this layer is dominated mainly by the thermal SRH mechanism due to the presence of surface and interface traps similar to those present at the other part of the perimeter surface, such as locations 4, 6 and 9. However, a high interfacial recombination loss can seriously offset the effect of shielding the back contact/ and oxide/silicon interface recombination sites from the photogenerated minority carriers [4].

B. POLY-CRYSTALLINE CELLS

All of the above recombination locations and mechanisms are important in poly-crystalline cells. Most are emphasized since there are more non-dopant impurity traps and more physical defects in the polycrystalline silicon material. In addition to these, an important and frequently dominating loss of photogenerated electrons and holes is recombination at the grain boundaries separating the single-crystalline grains in the poly-crystalline materials. We envision three grain boundary locations which have somewhat different recom-

ination mechanisms and rates. These are discussed using Fig. 4.

14. Grain Boundary in the Bulk Film

Grain boundary has high density of dangling silicon bonds which are recombination sites for electrons and holes. Grain boundaries penetrate through the entire poly-crystalline silicon film passing through the four layers: the N+ emitter layer, the N+/P emitter junction space charge layer, the P quasi-neutral base and the P/P+ BSF layer. In each layer, the recombination rate at the grain boundary traps is different although all with the same thermal SRH recombination mechanism.

15. Grain Boundary Intersect at the Oxide/Silicon-Emitter Interface

Again the thermal SRH mechanism and the interband- and bound-Auger mechanism may dominate the electron-hole recombination. However, the high density of dangling bond traps at the grain boundary would further increase the recombination loss at this intersection.

16. Grain Boundary Intersect at Contact-Metal/Silicon-Emitter Interface

The high density of traps in the grain boundary would also increase the recombination loss at this contact.

IV. MATERIAL IMPERFECTIONS

If quantum mechanical electron bound states are present at an imperfection in a crystal, it will trap or bound an electron and effecting the recombination of a hole with the trapped electron. A similar electron-hole recombination can occur at an imperfection which has a hole bound state or can trap a hole. Such an electronically active imperfection is commonly known as an electronic (either electron or hole) trap. Imperfections can also act as atomic traps which can trap and release other atoms or ions, for example the hydrogen trapping property of the group-III acceptors (B, Al, Ga and In) recently discovered by us [6]. An imperfection in a crystal can be an electronic trap, an atomic trap, either an electronic trap or an atomic trap differing in atomic configuration, both an electronic trap and an atomic trap, and neither an electronic nor an atomic trap. It is evident that a combination of these properties to eliminate the electronic trapping property or the electronic bound state would be the goal for improving efficiency. The oxygen and silicon dangling bond type of imperfection at the oxide/silicon interface is an example in which its electronic trap or electron-hole recombination properties can be eliminated by atomic or hydrogen trapping which is known as hydrogenation of the dangling bonds. In addition, imperfections may also aggregate to form extended conduction paths or insulating regions which may seriously reduce the cell efficiency by distorting the ideal current-voltage characteristics of the solar cell junction.

Material imperfections can be divided into two groups, the chemical impurities and the physical defects. These are briefly discussed below.

A. CHEMICAL IMPURITIES

1. Recombination Sites

Metals (Au, Ti, V, Mo, W, Zn, Ag and others) and non-metals (S, Se, Te and others) are known electronic traps in silicon. Au is a dominant residual trap in unprocessed single crystal silicon and after high temperature integrated circuit processing. Ti, Mo and W were shown to be among the dominant residual impurities in solar cell grade single crystal and these metals cannot be easily and completely gettered out of the cell layers during cell fabrication.

2. Low Resistance Paths

Copper segregates onto dislocations to form resistance paths which may parallel the p/n junction of the cell, causing shorts or low resistive shunts that reduce the cell efficiency.

3. Carrier Fluctuation

Random clusters of dopant impurities (B, Ga, Al, P, As and Sb) may occur at high concentrations which could cause large spatial fluctuation of the electron and hole concentrations. Such fluctuations could significantly degrade the ideal current-voltage characteristics of a high-efficiency cell.

4. Insulating Clusters

Oxygen and nitrogen in silicon may form silicon-oxide and silicon-nitride clusters of random sizes. They are insulating or having a large energy gap and hence high potential barrier that prevent the transport of electrons and holes. These insulating layers will also degrade the current-voltage characteristics and reduce efficiency. There were indications that they may also serve as sinks for the recombination impurities to reduce the trap density in the active region of a integrated circuit transistor. This property is less effective since the thickness of the electronically active layer in solar cell is much larger (about 100 micro-meters) than that in integrated circuits (a few micro-meters or less).

5. Electronic Trap Passivation

It has been known that atomic hydrogen is very effective in passivation of electronic traps at non-dopant impurities and grain-boundary. The former is a result of hydrogen-impurity bond formation known as hydrogenation of the impurity which renders the impurity electronically inactive or causes its electronic bound state to disappear. Grain boundary passivation by hydrogen has been known for many years and is presumably due to the hydrogen bond formation with the dangling silicon bonds in the grain boundary.

B. PHYSICAL DEFECTS

Physical defects are missing host atoms and extra host atoms in interstitial sites. Most of the missing host defects are known electronic traps which can be readily deactivated by hydrogenation electrically. Some of these are the vacancy, divacancy and vacancy clusters, vacancy-impurity clusters, grain boundaries and perimeter damages.

V. PROCESS OPTIMIZATION

There are various ways to reduce the imperfection density and the recombination losses via selection of fabrication processes. A few possibilities are reviewed.

A. CLEAN PROCESS

A major part of the recombination impurity may be introduced during wafer handling prior to high temperature processing. Clean handling is critical to reduce the residual recombination impurity to less than about 10^{10} cm^{-3} which would give a lifetime of about 300 microseconds and a recombination current density of about $2 \times 10^{-13} \text{ A/cm}^2$ needed to reach 20% AM1 efficiency. The density was based on a electron trapping diameter of 10A and base doping density of 10^{16} cm^{-3} .

B. LOW TEMPERATURE

Recombination losses at physical defects and defect-impurity complexes are important limiting factor in high efficiency cells due to the very low density requirement we just indicated on the recombination impurities. Silicon dangling bonds and other physical defects are less likely to form at lower processing temperatures. The current silicon solar cell processing temperature of 800 to 900C may already be in the optimum range.

C. PASSIVATION

Passivation of the impurity and defect recombination centers by atomic hydrogen is a distinct possibility to further reduce the residual electrically active recombination centers. Hydrogenation of the residual dangling bonds at the oxide/silicon interface and some metallic recombination impurities and silicon vacancy clusters in the silicon bulk have been demonstrated in silicon single crystals but yet to be in silicon device or solar cells. Hydrogen passivation of the silicon dangling bonds at grain boundary and in amorphous silicon has been well known for many years. In view of the very low density requirement of the high efficiency cells, the dangling bond density in the starting silicon and in the finished cell before passivation must be very low and then a nearly complete passivation by hydrogen of the residual bonds may be attained which is necessary for the very high efficiency cells. Passivation by hydrogen may be a viable process for solar cells whose active layers are thick (tens to hundreds of micrometers) since the diffusion and migration rate of atomic hydrogen is very high at temperatures slightly above room temperature. This high mobility, although an advantage for deactivating the dangling bonds of the recombination traps, may also be a limiting factor on the

cell reliability such as the goal of 20-year or the more recent 30-year operating life.

D. GETTERING

Gettering of the recombination impurities to reduce recombination or J_1 has been successfully demonstrated in the laboratory and gettering has sometimes been employed in the production of silicon transistors and integrated circuits. The sink for the recombination impurities during a high temperature gettering procedure is usually a surface oxide glass, a damaged surface layer, a high concentration diffused surface layer or even a polysilicon surface layer. The last has been the most effective. Gettering relies on the high mobility or diffusivity of the recombination impurities in silicon at the gettering temperatures, usually nearly the diffusion or the oxidation temperature. It also relies on the assumption that the sink has a much higher solubility than silicon at the gettering temperature and the gettering volume or layer thickness is sufficiently large so that it is not saturated by the gettered impurity. Gettering can be made effective in many silicon transistor and integrated circuit fabrication processes since the active silicon layers are usually very thin so that a relatively short gettering time and low gettering temperature are adequate. Gettering may not be as effective in solar cell, especially for improving the efficiency to beyond 20% since the active layer in solar cell is very thick and may be ten or more times larger than diffusion length of the to-be-gettered recombination impurities for a one-hour high temperature gettering. Considerable research efforts have been spent to show that the important recombination impurities, Ti, Mo, and W, in silicon solar cell only diffuses toward the surface sinks by a small amount, up to about five microns, in the cell fabrication temperature range of 800 to 1000C. This is highly inadequate for gettering these impurities by a surface sink in a 100-micrometer active layer of a high efficiency silicon solar cell.

VI. DEVICE DESIGNS

Innovative device designs have been proposed and demonstrated by a number of silicon solar cell researchers to reduce recombination losses in order to improve the efficiency to 20% and beyond. Some of these are described below. More detailed descriptions of these cell structures and the experimental results can be found in the articles of the special issue of Solar Cell [1] and in references cited in [2].

A. REDUCTION OF INTERFACE RECOMBINATION LOSSES

Polysilicon emitter and polysilicon base contacts have been proposed and demonstrated to reduce the interfacial recombination losses at these contacts which were discussed as recombination locations 1 and 11.

The polysilicon emitter concept may be thought of as an extension of the thin-oxide-barrier between the emitter metal contact and the silicon emitter used by Green to attain 19% AM1 efficiency. The reliability and reproducibility of the thin tunneling oxide barrier are yet to be demonstrated for the very large area cells while the polysilicon emitter is expected to be much superior due to the higher temperature of formation and the thicker film of the polysilicon emitter.

Oxidized front and back silicon surfaces have also been employed to reduce the interfacial recombination losses at the exposed front surface (location 2) and a major part of the back surface (location 12) just described. The improvement is especially dramatic for the front surface which was demonstrated by removing the front oxide, resulting in a large rise of the dark recombination current, J_1 , and a noticeable lowering of the efficiency. The oxide passivation concept has been extended and implemented to the back surface with observable improvement but the effect is less due to shielding by the BSF layer.

The high/low junction shield concept was first employed for the back surface by the NASA-Lewis group [see references in [4]]. This was extended to the front emitter layer by us [7] and included some innovative high efficiency cell designs by others supported by the JPL/DOE program. It is probable that the nearly 20% cell of Green had such a high/low emitter junction which is inevitably present in a doubly diffused emitter that consists of a first low-concentration and deeper (0.2 micron) diffusion and a second high-concentration shallower diffusion (0.1 micron or less).

B. REDUCTION OF BULK RECOMBINATION LOSSES

Thin [8] and graded [9] base, especially using epitaxial layers on highly doped substrate, should be effective in reducing the base recombination losses which are thought to be the main remaining loss after emitter recombination losses are eliminated in high efficiency (20%) to very high efficiency (>20%) cells. Design demonstrations were given by us recently [8] which showed that 20% cells can be attained by reducing the active base to about 50 microns even for a not-too-high minority carrier lifetime, 20 microseconds, or a base recombination impurity density of 10^{12} cm^{-3} . This recombination impurity concentration requirement is 100 times less severe than 10^{10} cm^{-3} quoted in the early part of this paper for a thick base cell. It dramatically illustrates one attractive cell design concept for high efficiency, the thin graded base, which has yet to be fully explored experimentally.

C. REDUCTION OF PERIMETER RECOMBINATION LOSSES

Perimeter recombination losses (locations 4, 6, 9 and 13) can drastically reduce the cell efficiency [5]. Dicing the cell by chemical etch instead saw cut could reduce the recombination trap density on the perimeter surface. Etched groove which is subsequently oxidized can further reduce perimeter recombination losses. Diffusion isolation of the cell edge may be most effective at the expense of a small reduction of the effective cell area. The main point is that to reach efficiencies of more than 20%, the perimeter recombination loss, previously unimportant in 17% or less cells, may become a limiting factor.

D. GRAIN BOUNDARY PASSIVATION IN POLYSILICON CELLS

In poly-crystalline silicon solar cells, high efficiency cell structures may be fabricated using the high diffusivity of phosphorus and hydrogen along the grain boundary plane. Fig. 5 shows a P+/N/N+ cell structure where use is made of the fast phosphorus diffusion along the grain boundary from the back

surface during the N+ BSF diffusion. Fig. 6 shows the opposite of Fig. 5 in which the phosphorus diffusion down the grain boundary is from the front surface during the N+ emitter diffusion in an N+/P/P+ cell structure. For ease of illustration, the grain boundaries are shown perpendicular to the film plane and equally spaced. Grain size and boundary are randomly distributed in realistic situations. For both of these two structures, the grain boundary diffusion of phosphorus has helped to form a high/low junction shield labeled 1 on these figures (N+/N in the P+/N/N+ cell in Fig. 5 and P+/P in the N+/P/P+ cell in Fig. 6). These high/low junction potential barriers shield the photo-generated minority carriers from reaching the grain boundary which contains a high density of recombination centers. The region labeled 2 in Fig. 6 is a N/P junction which shields the grain boundary from the minority carriers. The intersection at the oxide surface, labeled 3, could allowed enhanced hydrogen diffusion down to the grain boundary in order to passivate the grain boundary traps by hydrogenation, which would be futher enhanced if the oxide on the end of the grain boundary can be removed by a preferential etchant.

VII. SUMMARY

The requirements for high-efficiency silicon solar cells are: (1) low resistivity bulk to maintain low injection level in the base in order to have the $r=1$ ideal Shockley dark diode law, (2) low recombination center density in the base, after emitter and interface recombination losses are reduced or eliminated, and low recombination center density in grain boundaries of polysilicon cells such as by phosphorus and hydrogen diffusion passivation, (3) low temperature and clean fabrication processing to reduce impurity and physical defect recombination sites, and (4) innovative cell designs to shield the high trap density sites from photo-generated minority carriers by potential barriers of high/low junctions and polysilicon/silicon contacts barriers.

ACKNOWLEDGMENT

We would like to thank Dr. Ralph Lutwack for inviting us to this workshop as well as for earlier supports which started our solar cell effort. This work was made possible by the supports from the Jet Propulsion Laboratory and the U.S. Department of Energy during the past ten years. We would also like to thank Professor Fredrik A. Lindholm of the University of Florida for continued interaction and collaboration in the last ten years on solar cell studies.

REFERENCES

- [1] See the February 1986 special issue of the journal, Solar Cells, on High Efficiency Crystalline Solar Cells.
- [2] C. T. Sah, "High Efficiency Crystalline Solar Cells," Solar Cells, February, 1986.
- [3] C. T. Sah, "Prospects of amorphous silicon solar cells," JPL Publication JPL/DOE 660411-78/01, 87pp. 31 July 1978.
- [4] C. T. Sah, K. A. Yamakawa and R. Lutwack, "Reduction of solar cell efficiency by bulk defects across the back-surface-field junction," J.Appl.Phys. 53(4), pp.3278-3290, April 1982.
- [5] C. T. Sah, K. A. Yamakawa and R. Lutwack, "Reduction of solar cell efficiency by edge defects across the back-surface-field junction: - a developed perimeter model," Solid-State Electronics, 25(9), pp.851-858, September 1982.
- [6] C. T. Sah, Sam Pan and Charles Hsu, "Hydrogenation and annealing kinetics of group-III acceptors in oxidized silicon," J. Appl. Phys. 57(12), 5148-5161, 15 June 1985.
- [7] C. T. Sah, F. A. Lindholm and J. G. Fossum, "A high-low junction emitter structure for improving silicon solar cell efficiency," IEEE Trans. on Electron Devices, ED-25(1), 66-67, January 1978.
- [8] C. T. Sah, K. A. Yamakawa and R. Lutwack, "Effect of thickness on silicon solar cell efficiency," IEEE Trans. Electron Devices, ED-29(5), 903-908, May, 1982.
- [9] C. T. Sah and F. A. Lindholm, "Performance improvements from penetrating back surface field in a very high efficiency terrestrial thin-film crystalline silicon solar cells," J. Appl. Phys. 55(4), 1174-1182, 15 February 1984.

*

TABLE I High efficiency requirements from theory of an ideal Shockley diode dark current-voltage characteristics.

HIGH EFFICIENCY REQUIREMENTS

SOURCE	J_1 (A)	J_{SC} (mA)	V_{OC} (mV)	FF	EFF (%)
Theory	2.0×10^{-16}	36.0	840	0.8664	26.0
Theory	2.0×10^{-15}	36.0	780	0.8588	24.0
Theory	2.0×10^{-14}	36.0	720	0.8501	22.0
Theory	2.0×10^{-13}	36.0	660	0.8402	20.0

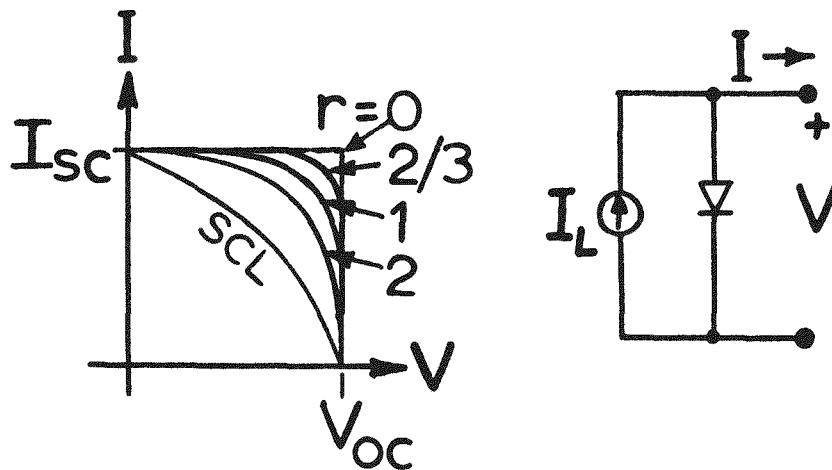


Figure 1 Current-Voltage characteristics of five illuminated diodes with different recombination mechanisms and their equivalent circuit diagram.

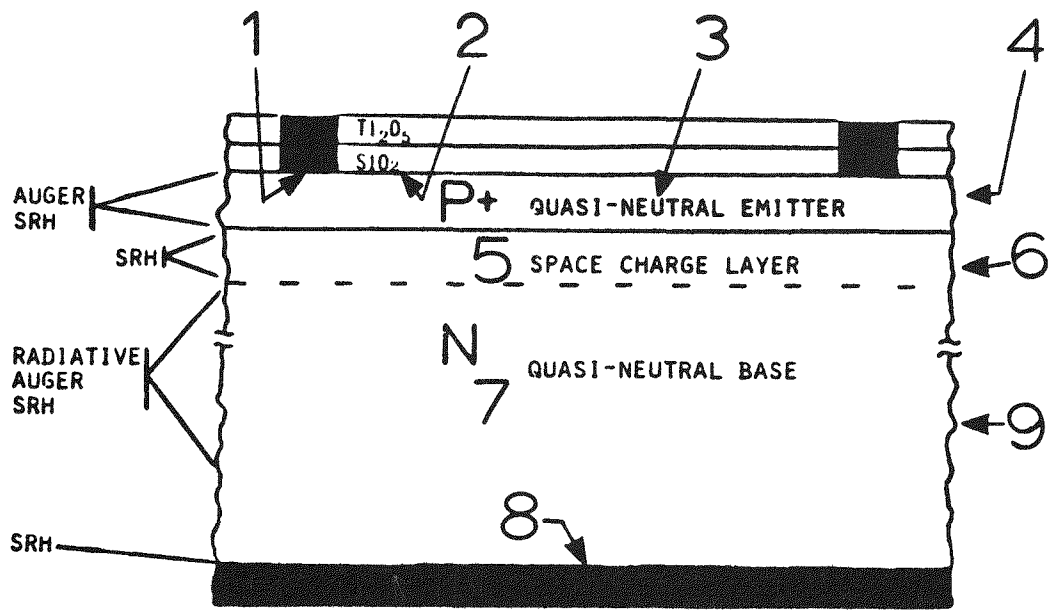


Figure 2 Nine important recombination locations and dominant mechanisms in a typical single-crystalline solar cell.

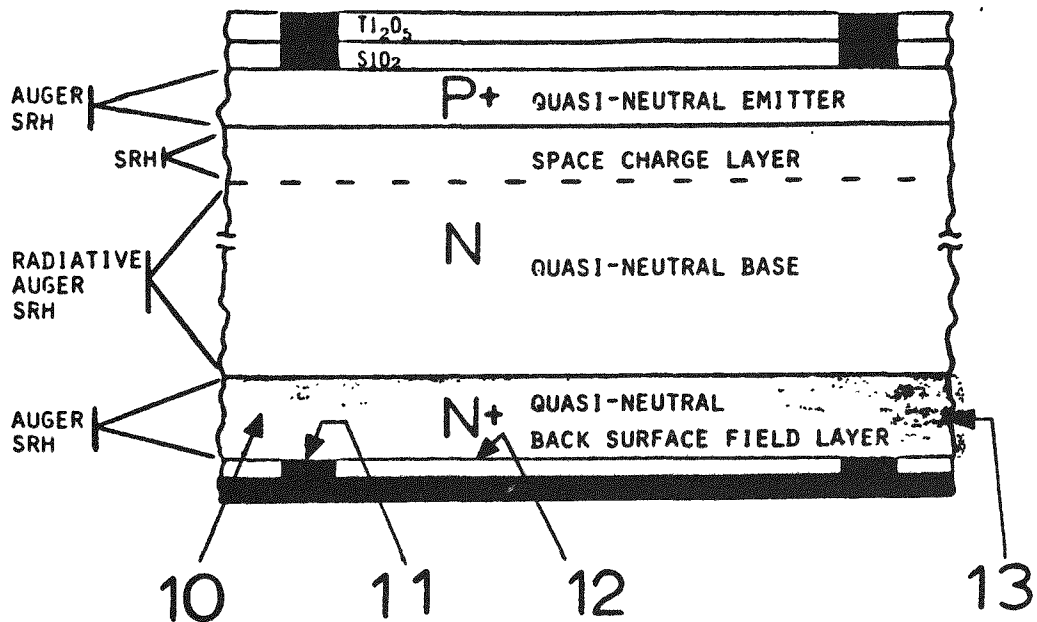


Figure 3 Four recombination locations in the back surface field layer of a single-crystalline solar cell.

POLY CRYSTALLINE CELLS

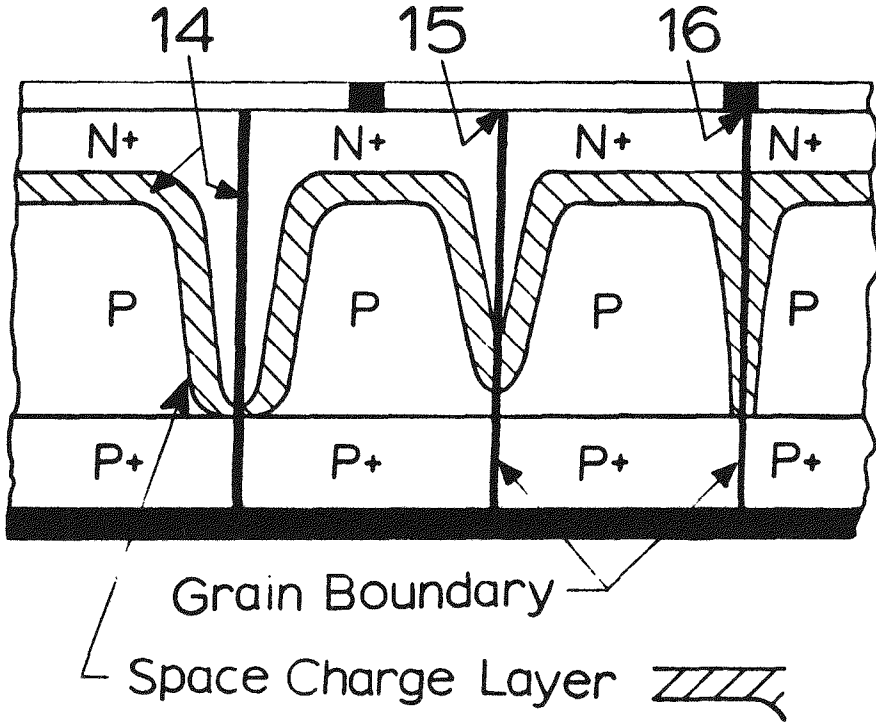


Figure 4 Recombination locations in the grain boundaries of a poly-crystalline solar cell.

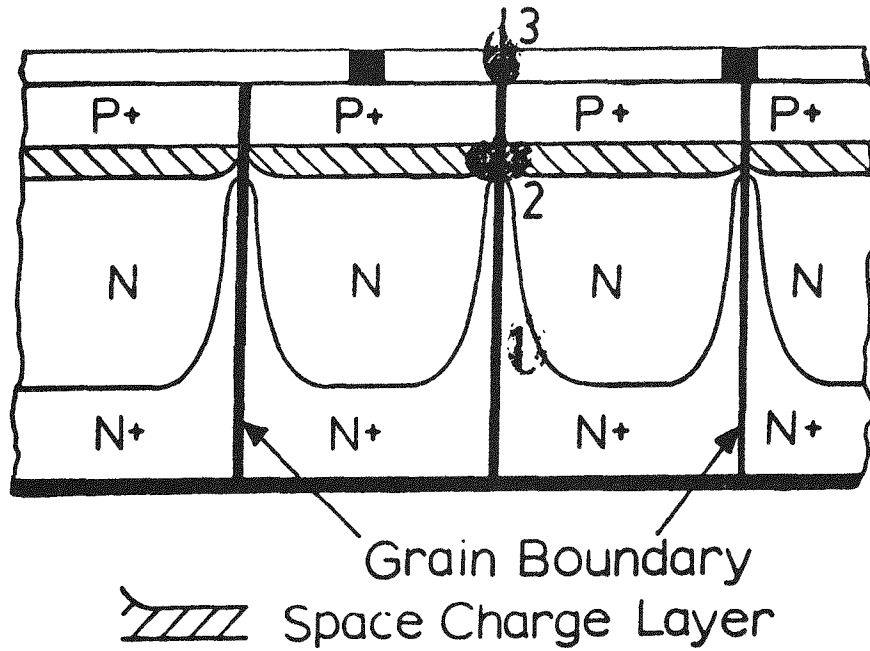


Figure 5 Passivation or shielding of the grain boundaries by phosphorus and hydrogen diffusion in a n-type polysilicon solar cell.

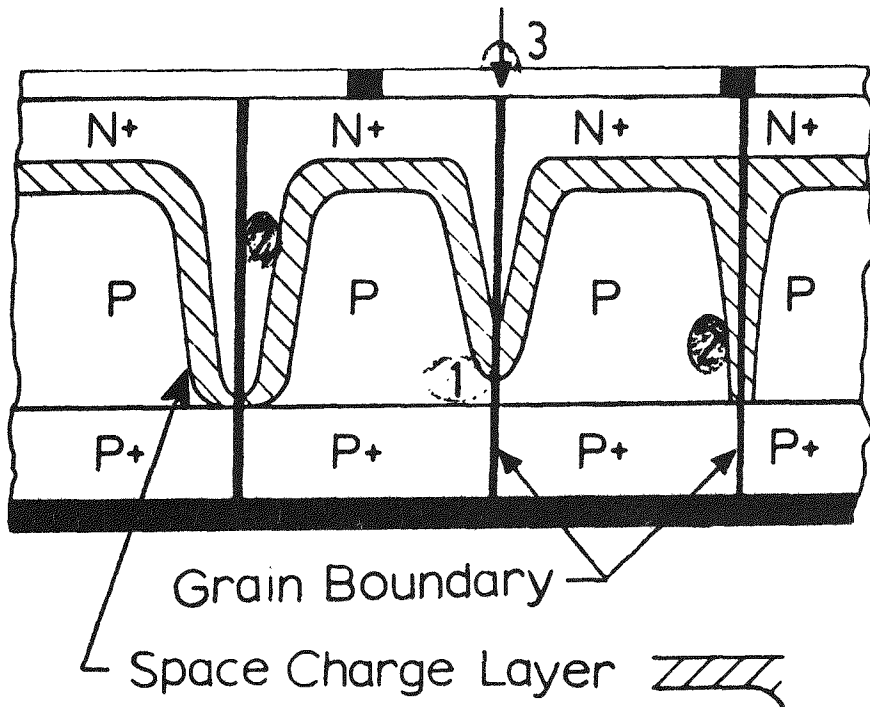


Figure 6 Passivation or shielding of the grain boundaries by phosphorus and hydrogen diffusion in a p-type poly-silicon solar cell.

DISCUSSION

PRINCE: You gave us a very thorough discussion of the various recombination processes, 13 in single-crystal and 16 in polycrystal. Have you ordered these in some way to tell us which are the most important ones that must be eliminated, or are you going to have that information in your paper, or can you reference some papers that have this information?

SAH: I think for single-crystal material, the impurity recombination in the base would be the remaining one. After most of the impurity recombination in the base is removed, then a limit will be reached that will not be possible to reduce much further due to the radiative intra-band Auger recombination. At that point, cells with efficiencies of 23 to 24% or more will be obtained. In the polycrystalline cells, the grain boundary is the most serious problem. One needs to eliminate the recombinations in the grain boundary by, perhaps, specially designed devices, structure design, or by hydrogenation. I think that if the dangling bonds in the grain boundary were tied up with hydrogen, they will not be electrically active as recombination sites.

SESSION II

ECONOMICS

R. Pellin, Chairman

Economics of Polysilicon Process--A view from Japan

Yasuhiro Shimizu
Osaka Titanium Co., Ltd.
Amagasaki, Hyogo, Japan

Abstract

Osaka Titanium Co., Ltd. and Shin-etsu Chemical Co., Ltd. have researched the production process of solar-grade Silicon (SOG-Si) through trichlorosilane (TCS) in a program sponsored by New Energy Development Organization (NEDO). The NEDO process consists of the following two steps:

- (1) TCS production from by-product silicon tetrachloride (STC)
- (2) SOG-Si formation from TCS using a fluidized-bed reactor (FBR)

Based on the data obtained during the research program, the manufacturing cost of the NEDO process and other polysilicon manufacturing processes listed below were compared.

- (1) TCS processes; Conventional Siemens, NEDO FBR and Recycle-filament processes
- (2) Dichlorosilane (DCS) process; Hemlock filament process
- (3) Monosilane (MS) processes; UCC filament and UCC-JPL FBR processes.

The manufacturing cost was calculated on the basis of 1000 tons/year production, using data and information in reports issued by the Subcommittee on Silicon Metal and Resources, Japan Electronic Industry Development Association ("the Subcommittee Reports") and in other data in published reports, magazines, newspapers, etc.

Actual manufacturing costs are difficult to compare because of differences in local conditions, production scale, contents of direct and indirect costs and reliability of published data. To reduce these differences, the published data was modified according to a certain estimate method prior to manufacturing cost calculation.

Our cost estimate showed that the cost of producing silicon by all of new processes is less than the cost by the conventional Siemens process. Using a new process, the cost of producing semiconductor-grade silicon (SEG-Si) was found to be virtually the same with any of the TCS, DCS and MS processes when by-products are recycled.

The SOG-Si manufacturing processes using FBR, (the NEDO and UCC-JPL FBR processes,) which need further development for practical application, have a greater probability of cost reduction than the filament processes.

1. INTRODUCTION

Research and development of various processes for manufacturing low cost SOG-Si are under way worldwide. One approach is the solid purification process, in which SOG-Si is produced directly from the reduction of silica in solid state. A substantial cost reduction can be expected, but the impurity removal technique has not yet been established. In this process it would be difficult to upgrade the present SOG-Si to SEG-Si in the future. Another approach to cost reduction uses gas purification based on the current SEG-Si manufacturing process. This refinement of the gaseous silicon compounds satisfies the quality required for as SOG-Si.

This report compares manufacturing costs of gas purification processes whose developments are reaching completion.

Sponsored by NEDO, the Japan Electronic Industry Development Association investigated demand, processing technologies, and future tasks regarding silica, metallurgical silicon (MG-Si) and polysilicon, necessary for solar cell manufacture. The summary of this investigation was reported in the Journal of Electronics Industry (1). Manufacturing cost were estimated on the basis of the data in the Subcommittee Reports and the final reports of Hemlock and UCC (2, 3) as well as data published in newspapers, magazines, etc.

2. MANUFACTURING PROCESSES AND MATERIAL FLOW

2-1. TCS: Conventional Siemens Process

In this most common SEG-Si manufacturing process, polysilicon deposits from TCS onto silicon slim rods (filaments) in a bell jar reactor. Figs. 1 and 2 show the process diagram and the material flow of this process (2).

HCl is produced via a H_2-Cl_2 reaction; additional H_2 is used to ensure 100% Cl_2 consumption in the reaction. Passing through absorption, stripper and drying towers, HCl is introduced into MG-Si FBR at around $300^\circ C$ to produce TCS. A reaction gas roughly of 90 % TCS and 10 % STC is cooled and condensed. Impurities such as B, P and carbon compounds are removed by distillation. A purity of around 11 N is required to obtain the material gas for SEG-Si. Distillation columns are designed to be operated with a high reflux ratio and equipped with many trays. This process requires a large amount of energy per unit weight of product.

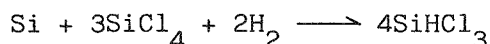
Polysilicon deposits on silicon filaments heated to $1050 - 1150^\circ C$. The conversion yield of TCS into silicon is as low as 10 to 20 %. Unreacted TCS and by-product STC in decomposition reactor are then cooled, condensed, collected and distilled. The distilled TCS is reused as materials, whereas STC is removed from the process and used as raw material for silica powder, etc. The major problems of this conventional Siemens process are; 1) the amount of by-product STC over ten times or more than that of polysilicon, and 2) a large amount of energy required for unit weight of product.

2-2. TCS: NEDO Process

This process in which MG-Si is converted into SOG-Si by supplying energy only, ideally requires no other raw material than MG-Si. The process diagram and material flow are shown in Figs. 3 and 4.

Distillated TCS is diluted with H₂ and introduced to a FBR filled with silicon seeds. SOG-Si deposits on the seeds, growing into larger granules. As in the conventional Siemens process, unreacted TCS and by-product STC are condensed and recovered. After distillation, TCS then being reused as material, and by-product STC is used as raw material of TCS in the recycle system.

The TCS reproduction process is the same as that used in Hemlock and UCC processes, i.e.,



In the NEDO process, the reaction takes place at a lower-pressure and higher H₂/STC molar ratio than in the Hemlock and UCC processes. The relative advantages as compared with high-pressure, low-molar ratio operation depend on the equipment and operation costs required for safety and legal regulations.

A pilot plant of 10 tons/year of silicon granules has already been operated for 2000 to 3000 hours, resulting in a power requirement of 30 kwh/Si-kg for decomposition. The basic operation technology has been established, and the quality of Si in this process has already been demonstrated. Future tasks are to develop large scale FBR and establish technology for a long-term continuous operation.

2-3. TCS Recycle-Filament Process

SEG-Si is currently produced and consumed at approx. 5000 tons a year worldwide. Considering the expected increase in the consumption of semiconductors, the demand for SEG-Si is very likely to grow steadily to 10,000 to 15,000 tons in 1990. In the conventional Siemens process, where a large amount of STC is by-produced, the recycling system of STC would be necessary in a large-scale polysilicon plant.

A process, which combines filament decomposition with the recycle of by-product STC, would be one of the leading processes for manufacturing SEG-Si. In this combined process, by-product STC is fed with hydrogen into MG-Si FBR, hydrogenated and recycled as TCS.

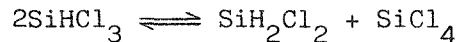
The filament reactor used for the reduction of TCS should be made of metal. A large reactor is necessary to decrease power consumption. The process diagram and material flow of this Recycle-Filament process are shown in Figs. 5 and 6.

The calculation was done on the basis of energy and material required for the reduction in the conventional Siemens process and for the hydrogenation in the NEDO process. Fig. 6 suggests that, approaching complete recycle, the required amounts of STC and hydrogen decrease, and MG-Si is converted through

TCS and STC into SEG-Si. The key points of this process are; 1) recycling of by-product STC via hydrogenation into TCS, and 2) complete recycling of vent gases generated in reduction and other stages.

2-4. DCS: Hemlock Process

The high cost of the conventional Siemens process is mostly due to high power consumption for the reduction of TCS. Hemlock used DCS instead of TCS as material, which may lead to a lower power requirement for the reduction and to higher productivity. Figs. 7 and 8 show the process diagram and material flow of the Hemlock process. This process is characterized by; 1) DCS synthesis by TCS redistribution,



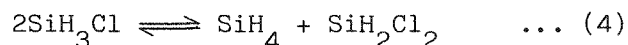
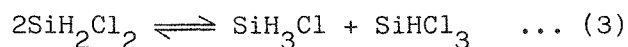
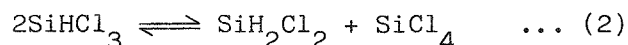
2) polysilicon formation by DCS reduction in an improved Siemens reactor, and 3) hydrogenation of by-product STC in FBR, as in the UCC process.

Conversion efficiency of DCS into Si is higher than that of TCS, therefore less amount of DCS is required. Figs. 2 and 8 show, however, nearly the same amount of TCS is necessary as in the conventional Siemens process. Nearly the same capacity is required for TCS distillation as in the conventional Siemens process, and additionally to purify DCS suitable for SEG-Si, the boron removal column or the DCS distillation columns need to be highly efficient since the boiling points of DCS (8.2°C) and BCl₃ (12.5°C) are quite close.

In the DCS reduction stage, the decomposition rate, yield and temperature are more favorable than in TCS. However, to prevent metal fog generation (i.e., homogeneous decomposition), high H₂/DCS molar ratio operation is necessary, which reduces the advantage of DCS high reactivity. Another drawback is larger energy requirement for the reaction gas recovery. The energy requirement for refrigerator is larger than in TCS because of the low DCS concentration in the reaction gases and the low-boiling point materials involved in this process.

2-5. UCC-JPL FBR Process

Basic research into this process began in the early 1970's by UCC, followed by DOE-supported development (3).



TCS is synthesized by hydrogenation of STC as expressed in equation (1) above, then MS is synthesized, followed by redistribution reaction (2) through (4) above.

The UCC final report proposed decomposition of MS in a free space reactor and then producing lump SOG-Si via silicon powder consolidation or casting. UCC and JPL are now conducting research for practical application of granule Si formation using FBR. The process diagram and material flow of UCC-JPL FBR process are shown in Figs. 9 and 10.

The wide boiling-point difference between MS (b.p. -112°C) and the other impurities such as B or P compounds permits easy separation of impurities from MS during the distillation. As a result, distillation is simple and energy per unit distillate costs low.

In the manufacture of Si granules from MS with FBR, product/seed weight ratio should be 100 or higher (as in the filament processes) from the viewpoint of cost. MS must be substantially diluted with H_2 to achieve higher gas flow velocity in FBR. Since decomposition temperature of MS is lower than that of TCS, the design and operating conditions of FBR are easier and simpler than those in the NEDO process.

2-6. UCC Filament Process

This section discusses a process producing polysilicon with filaments from MS synthesized. MS reduction occurs at a lower temperature and at a faster rate with higher conversion yield to Si than TCS and DCS. It should be noted that MS reduction begins at 400°C , rapidly increasing its rate at 600°C and above, and reaches the full reduction level at 800°C (3). To depress decomposition in free space of reactor, its temperature is maintained low providing steep temperature gradient along distance from the filaments. It would be difficult to produce large diameter polysilicon rods in a large reactor with multiple filaments, therefore the high reactivity of MS cannot be made full use of.

3. COST COMPARISON

Since actual manufacturing cost varies with local conditions, production scale, utilization ratio, reserve funds, contents of direct and indirect costs, etc., emphasis in this report is placed on relative comparison using a fixed unit cost basis. Calculation was based on the Subcommittee Reports, with production scale fixed at 1000 tons a year and the yen-dollar exchange rate at ¥250/\$.

For the conventional Siemens and NEDO processes, figures were used without modification.

3-1. Equipment Cost

To estimate equipment and construction cost, the amounts of liquids/gases processed are figured at each manufacturing stage and shown in Table 1. For the construction cost for SEG-Si manufacture, data published in newspapers and magazines are used.

(1) TCS: Recycle-Filament Process

Wacker's expansion plan data in Electronic Business News of January 1, 1985, were used for estimation.

(2) DCS: Hemlock Process

The amounts of liquids/gases in Table 1 were compared with those for the NEDO process, and the estimated capital costs in the Subcommittee Report were used.

(3) MS: UCC Filament Process

The amounts of liquids/gases processed at each manufacturing stage are shown in table 1. Equipment cost for this process is taken from an article on UCC in the Nikkei Sangyo Newspaper of February 7, 1985.

(4) MS: UCC-JPL FBR Process

Since this process has many similarities to the NEDO process, the estimated figures in the Subcommittee Reports were used.

3-2. Material Cost

The amounts of materials required for manufacturing one kg of product Si were calculated on the basis of material chemical reaction. Materials unit prices are ¥300/kg for MG-Si, ¥250/kg for STC when purchased, ¥120/kg for STC when sold, ¥100/m³ for H₂, ¥60/kg for Cl₂ and ¥70/kg for NaOH. Material costs also include cost of Si seeds, catalyst and other gases.

3-3. Electric Power Cost

For the TCS process, 100 - 150 kwh/Si-kg was reported using the most advanced equipment (4). Based on these figures, the average value of 125 kwh/Si-kg was adopted for the Recycle-Filament process.

For the DCS process, the experimental data at Hemlock CVD reactors ranged from 90 to 130 kwh/Si-kg. However, the 60 kwh/Si-kg target was considered attainable in comparison with the TCS process. When the power for other than decomposition was added, 90 kwh/Si-kg was adopted.

In the UCC filament process, power requirements in the reduction reactor were estimated approximately 40 kwh/Si-kg, considering heat transfer to cooling water via thermal radiation and gas conduction, and the operation temperature in TCS and in MS decomposition being 1050 to 1150°C and 700 to 1000°C, respectively. For the UCC-JPL FBR process, power requirements in the reduction reactor were estimated to be approximately 10 kwh/Si-kg and the total power consumption was estimated to be 40 kwh/Si-kg.

The power cost heating the STC hydrogenation reactor was also included. The power cost for one kwh was fixed at ¥15 in Japan.

3-4. Steam and Fuel Costs

Energy for heating was calculated on the basis of the amounts of liquids/gases and shown in Table 1.

3-5. Other Operating Cost

Although other operating costs, including repair cost, vary with different manufacturing processes, the fixed values given in the Subcommittee Reports were used.

3-6. Labor Cost

SEG-Si is manufactured by the filament processes and SOG-Si by the FBR processes. Considering the characteristics of these manufacturing processes and the data from the Subcommittee Reports, a 75-worker operation was assumed for the filament processes and 50-worker operation for the FBR processes.

3-7. Other Cost

Depreciation, interest, indirect and general administrative costs were calculated by the same rule as used in the Subcommittee reports.

3-8. Results

Our calculation results are shown in Table 2 and Fig. 11. For those processes in which STC is recycled via hydrogenation into TCS, manufacturing costs are virtually the same for all filament processes regardless of material gas. The manufacturing cost of SEG-Si can be reduced to 80 % of that in the conventional Siemens process.

SOG-Si manufacturing costs by the FBR processes are almost the same, at the ¥5000/Si-kg level, about 50 % of conventional Siemens-process manufacturing cost.

This study focusing on relative comparisons under fixed conditions, the resultant estimates differ from actual manufacturing costs. According to the NEDO's interim report, SOG-Si manufacturing costs with the NEDO process will be approximately ¥4300/Si-kg at a commercialized plant.

4. CONCLUSION

The manufacturing costs for various processes were estimated on the basis of SOG-Si production research sponsored by the NEDO.

When the by-products are recycled, all processes for SEG-Si will result in similar manufacturing costs. The TCS processes with filaments will be more firmly established if electric power for polysilicon formation can be lowered. The DCS process can save silicon deposition power consumption, but entails a large amount of energy for the distillation and redistribution. Moreover, the advantage of high DCS reactivity may not be fully utilized since reduction

must be kept at low DCS concentration to prevent metal fog. Whereas, in the MS process, the material gas can be produced at lower cost, but the total manufacturing cost is virtually the same as those of other processes since the advantage of high MS reactivity cannot be fully utilized for the silicon formation.

The Si-granule production by FBR cost approx. ¥5000/kg. The MS process, in particular, permits low temperature operation, compared to the TCS process, and facilitates the design and development of equipment: future advances are fully hoped for.

ACKNOWLEDGMENT

The author wishes to express his appreciation to the New Energy Development Organization, and Electronic Industry Development Association for permission to publish the data. Thanks are also due to Mr. K. Isogaya of Mitsui Toatsu Chemicals, Inc., for many fruitful discussions during the course of preparing this report.

References

1. H. Koinuma and T. Ozawa: Journal of Electronics Industry, 26, (5), 37-51 (1984) (Japanese)
2. Hemlock Semiconductor Corp.: DOE/JPL 955533-83 (1983)
3. Low Cost Solar Array Project, DOE/JPL 954334-10 (1979)
4. Rare Metal News, No. 1279 (1984) (Japanese)

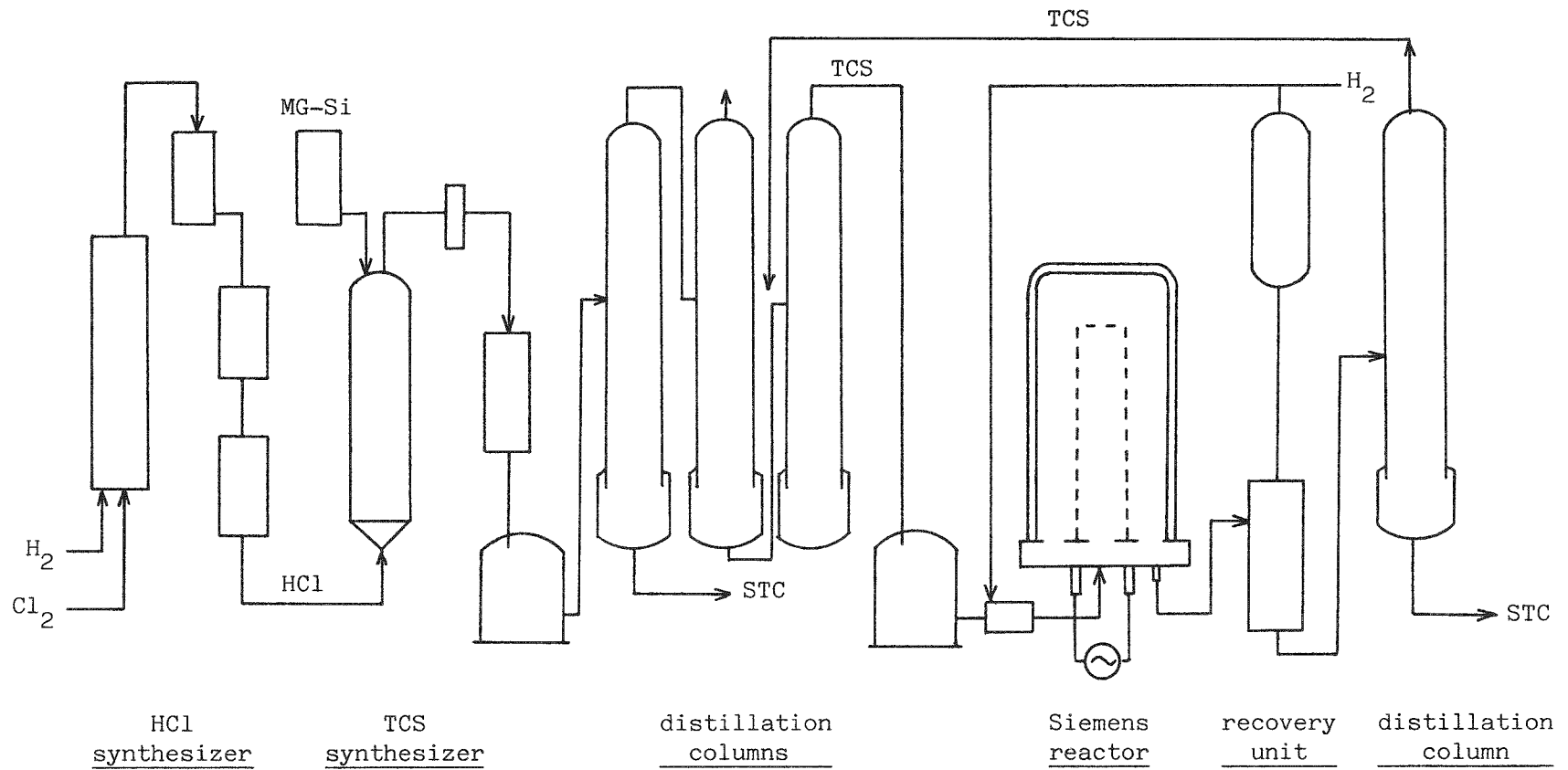


Fig. 1. Conventional Siemens Process

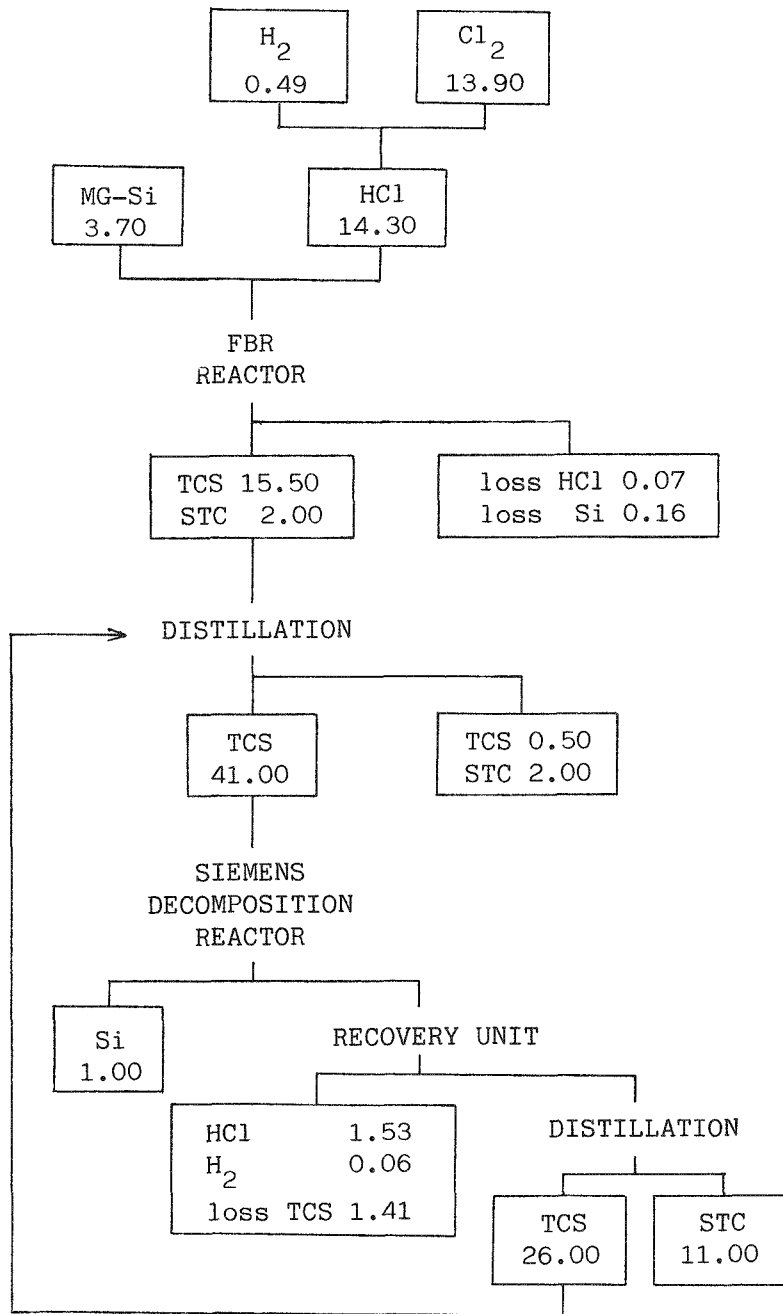


Fig. 2. Conventional Siemens Process (kg/kg-Si)

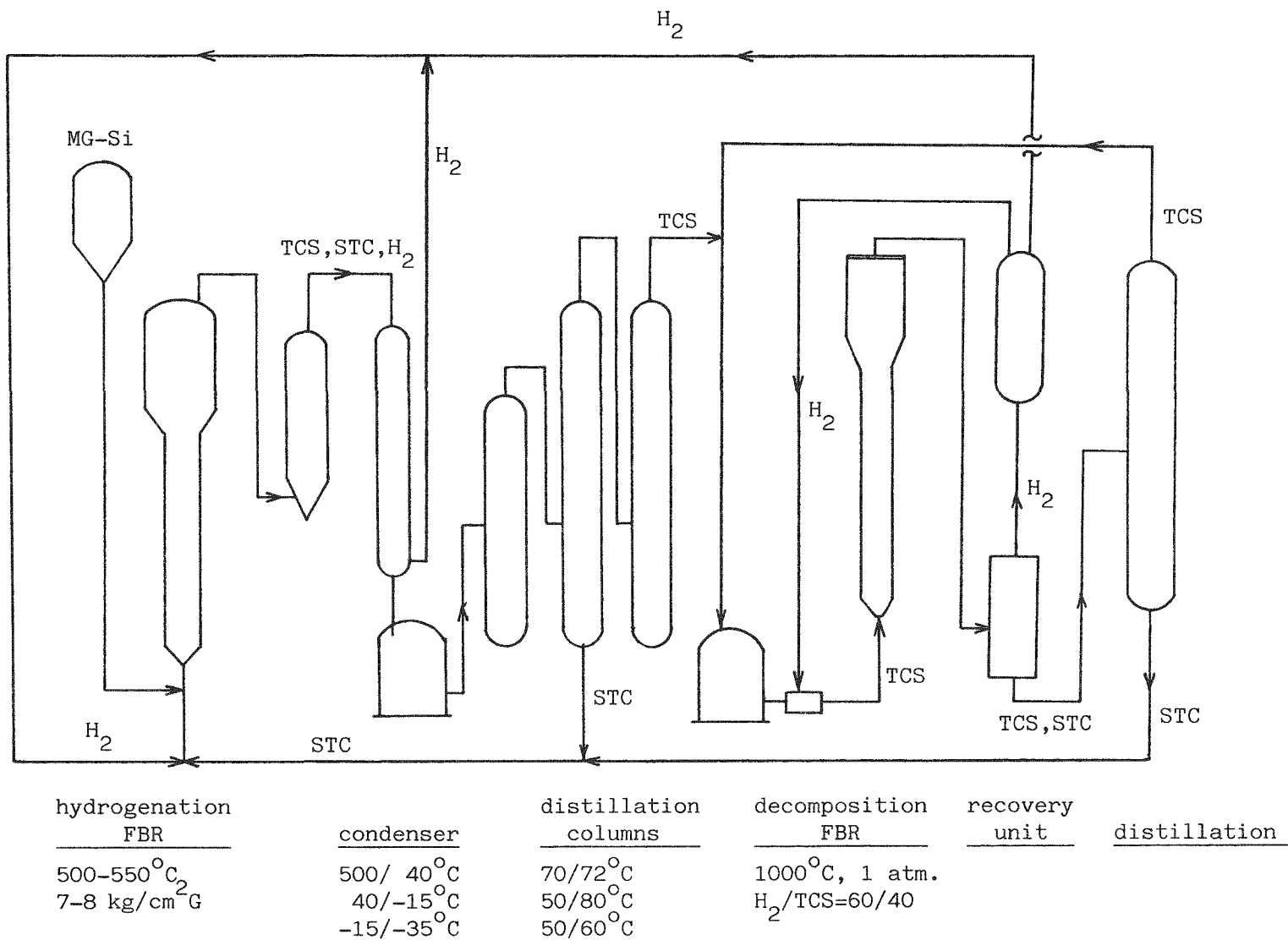


Fig. 3. TCS-Based NEDO FBR Process

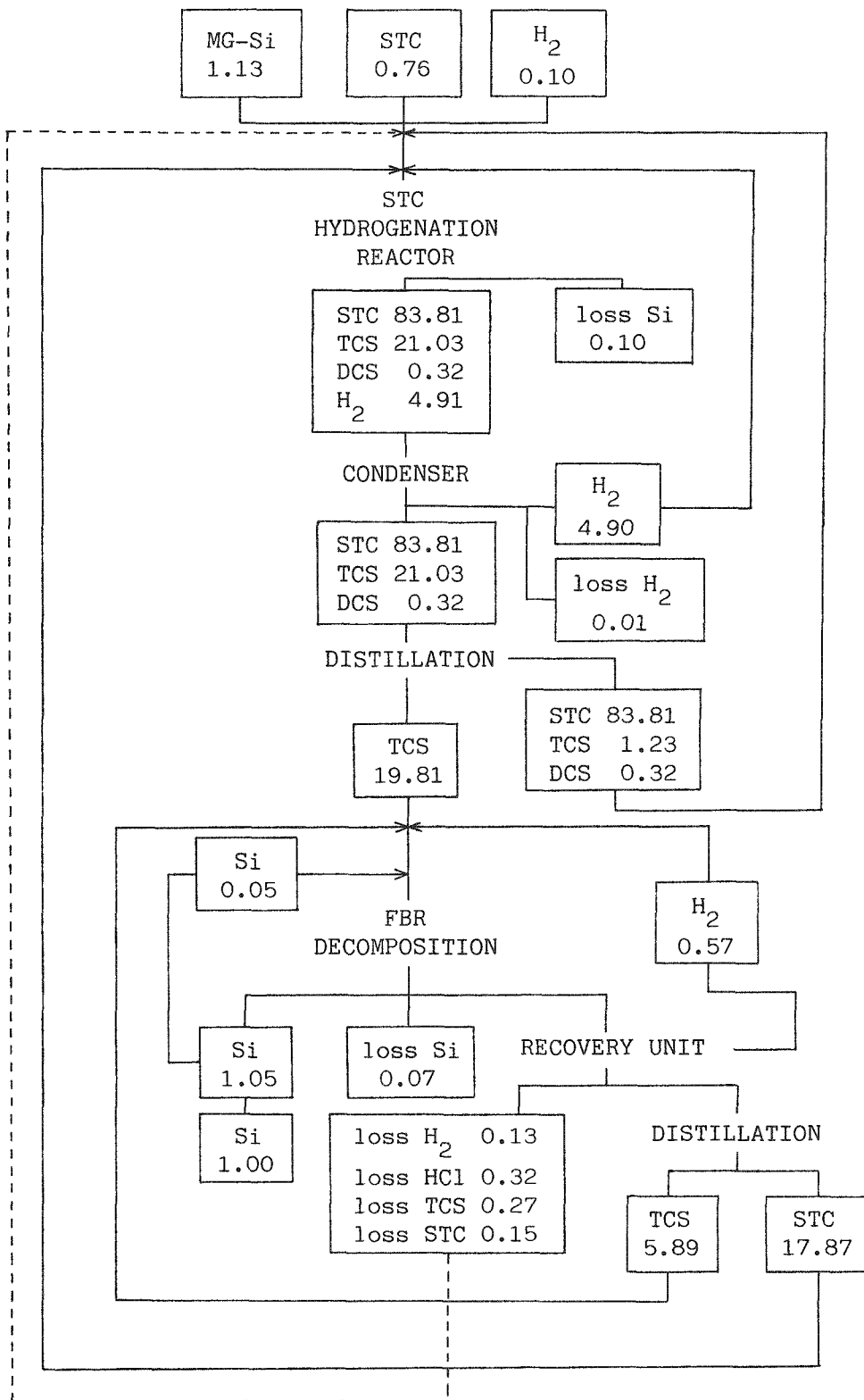


Fig. 4. TCS-Based NEDO FBR Process (kg/kg-Si)

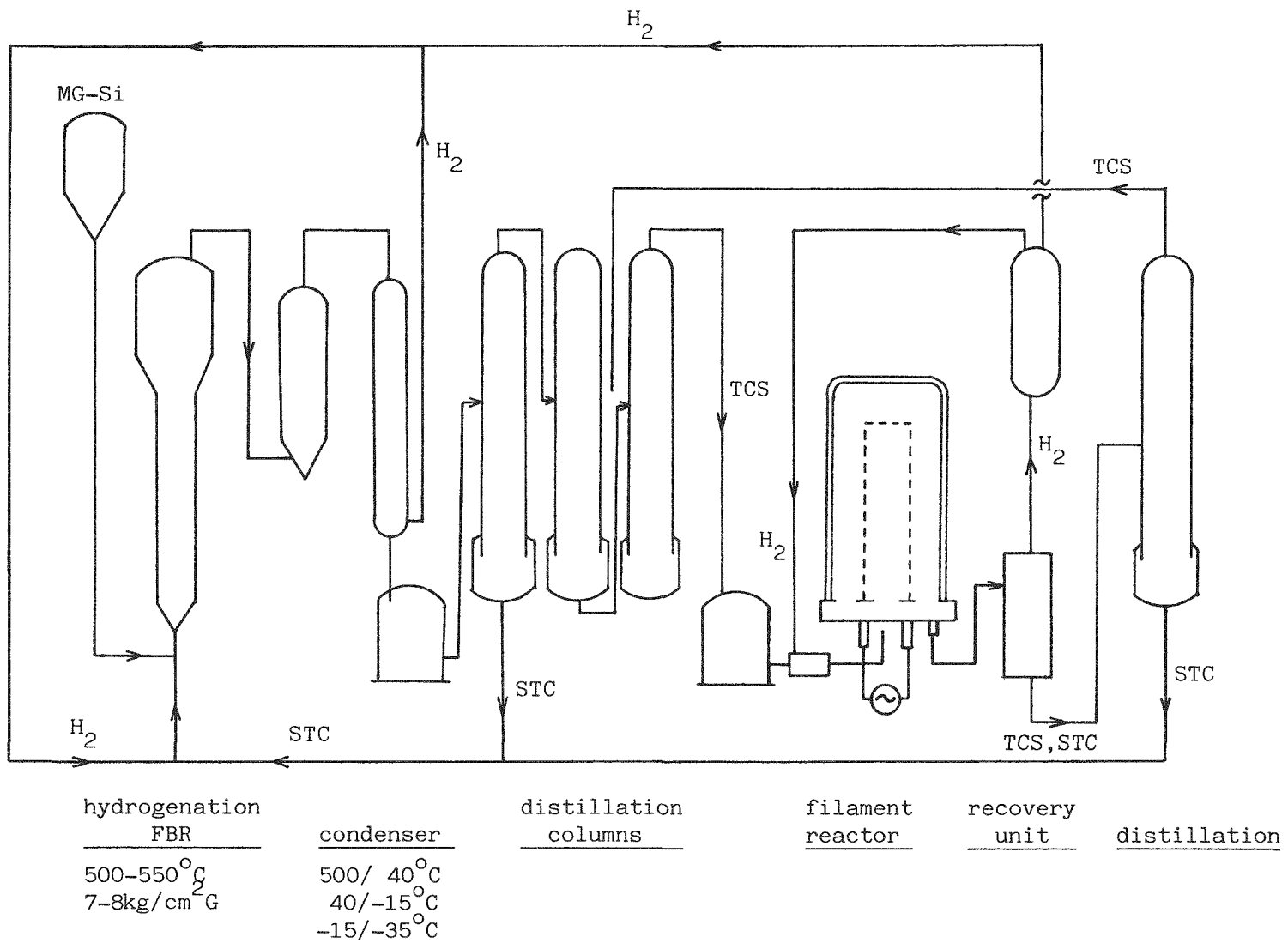


Fig. 5. TCS-Based Recycle Filament Process

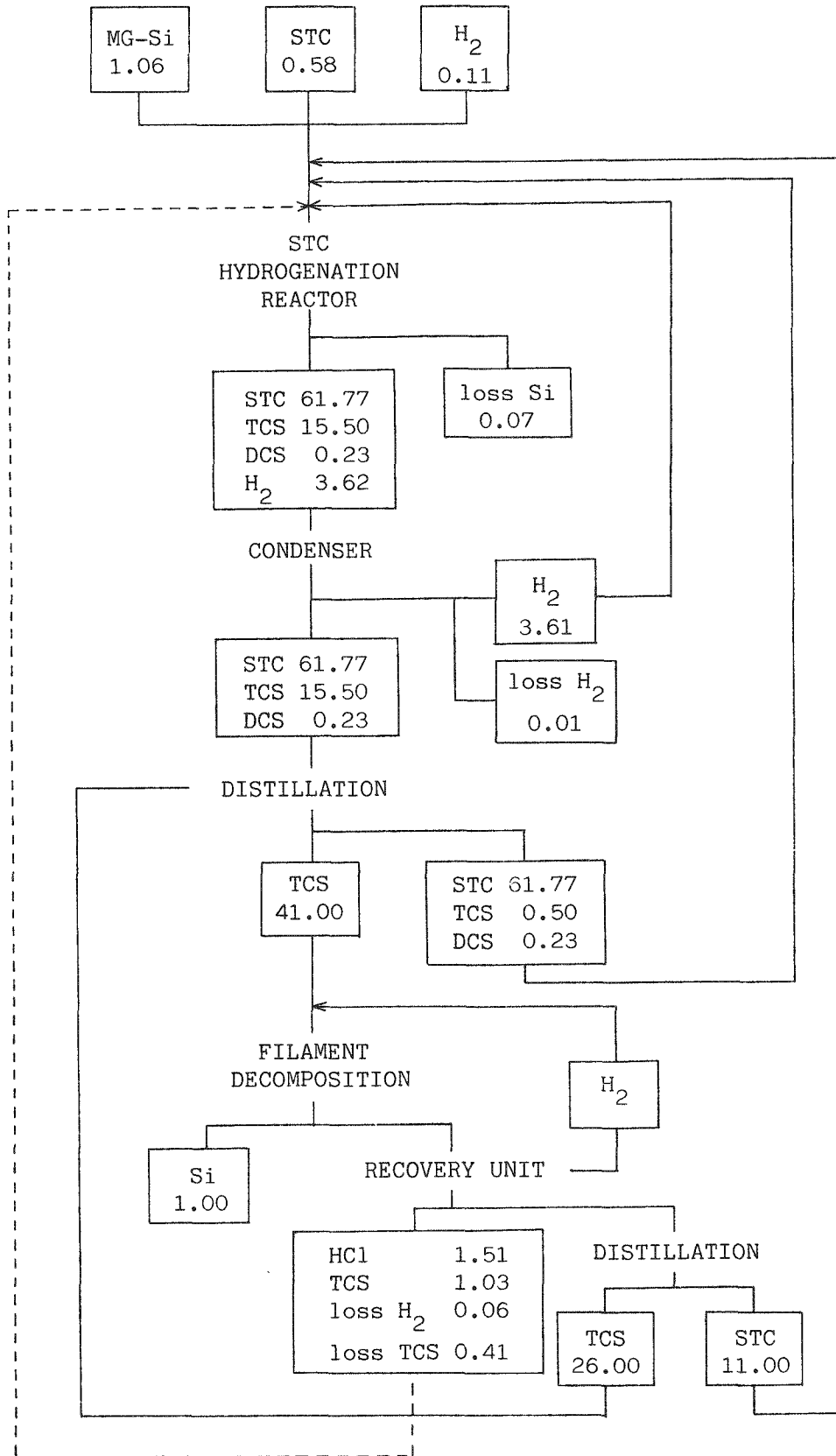
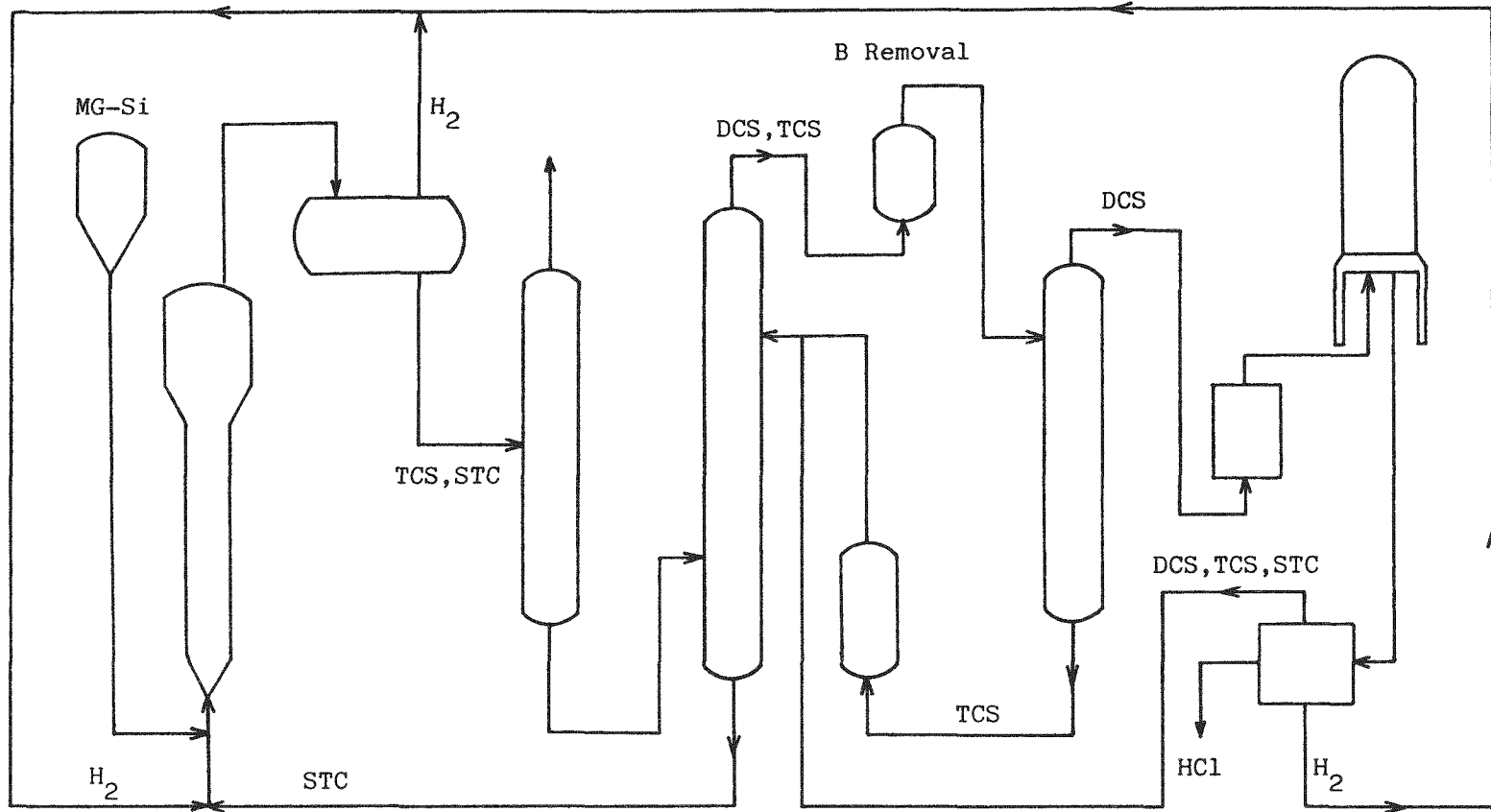


Fig. 6. TCS-Based Recycle Filament Process (kg/kg-Si)



hydrogenation FBR	condenser	stripper	TCS distillation column	DCS distillation column	recovery unit	filament reactor
500°C, 35kg/cm ² G H ₂ /STC=1/1 yield=24%		-29/117°C rr=1.9	91/126°C rr=2.0	52/97°C rr=1.5		
			redistribution reactor			
			80°C, 5kg/cm ² G yield=20%			

Fig. 7. DCS-Based Hemlock Filament Process

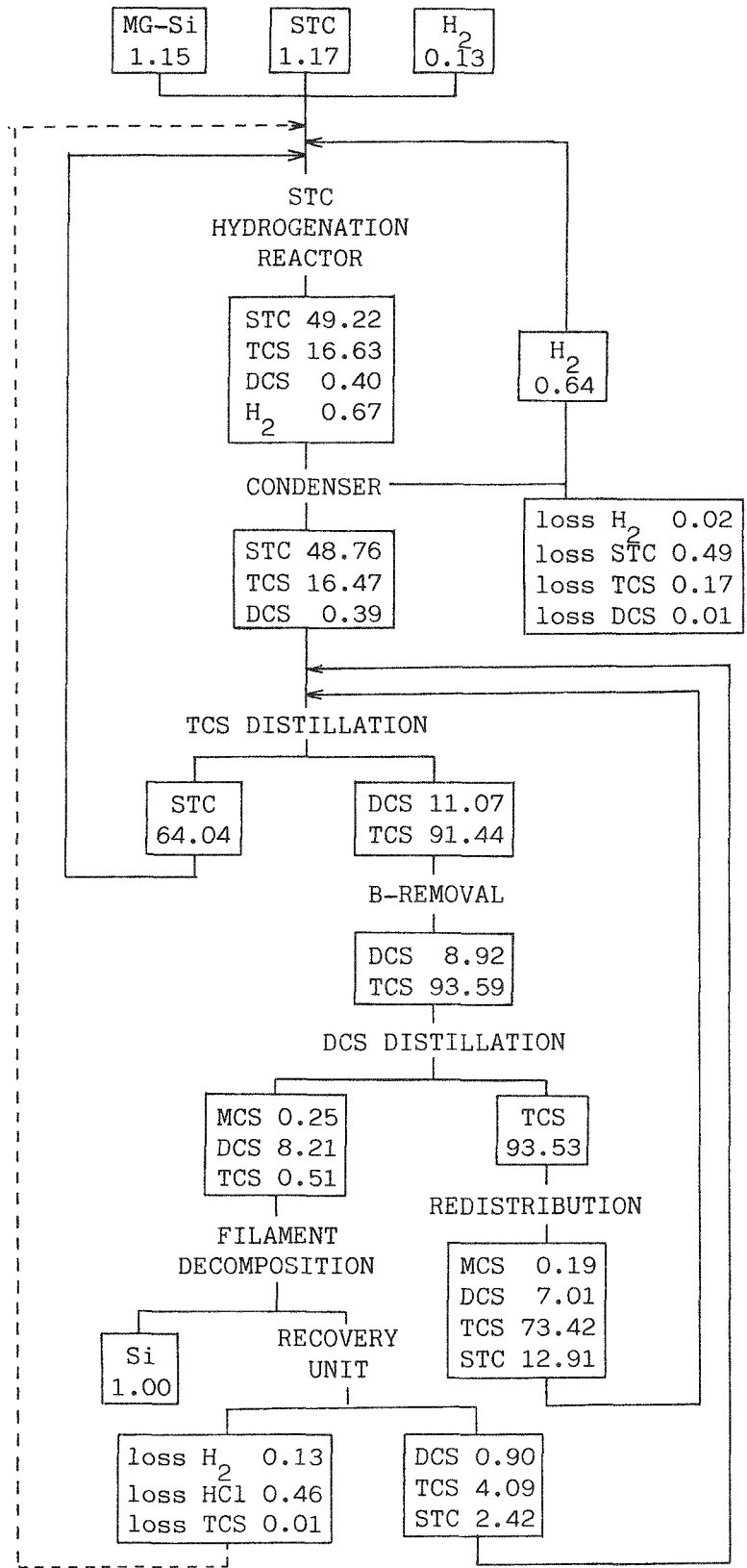


Fig. 8. DCS-Based Filament Process (kg/kg-Si)

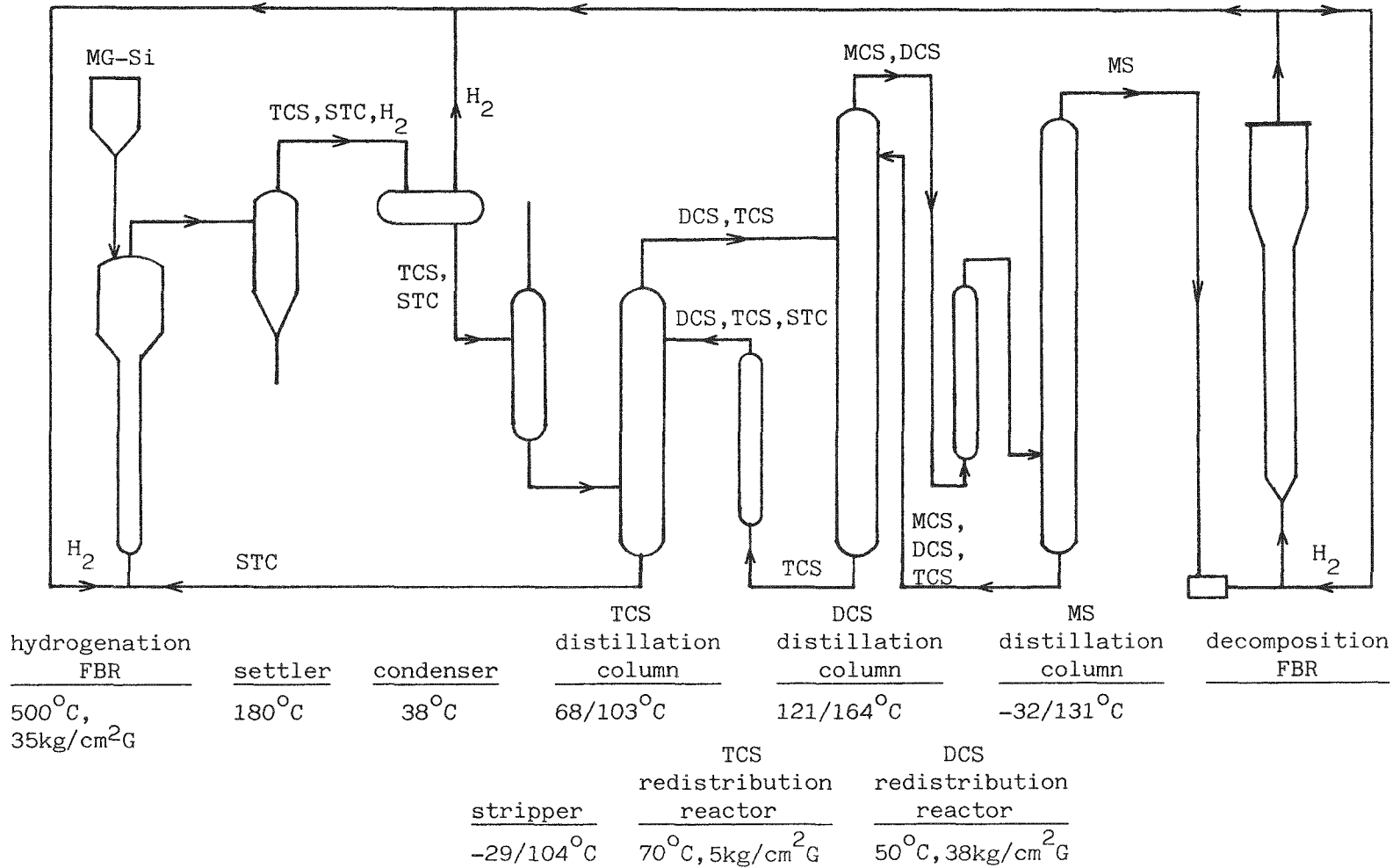


Fig. 9. MS-Based UCC FBR Process

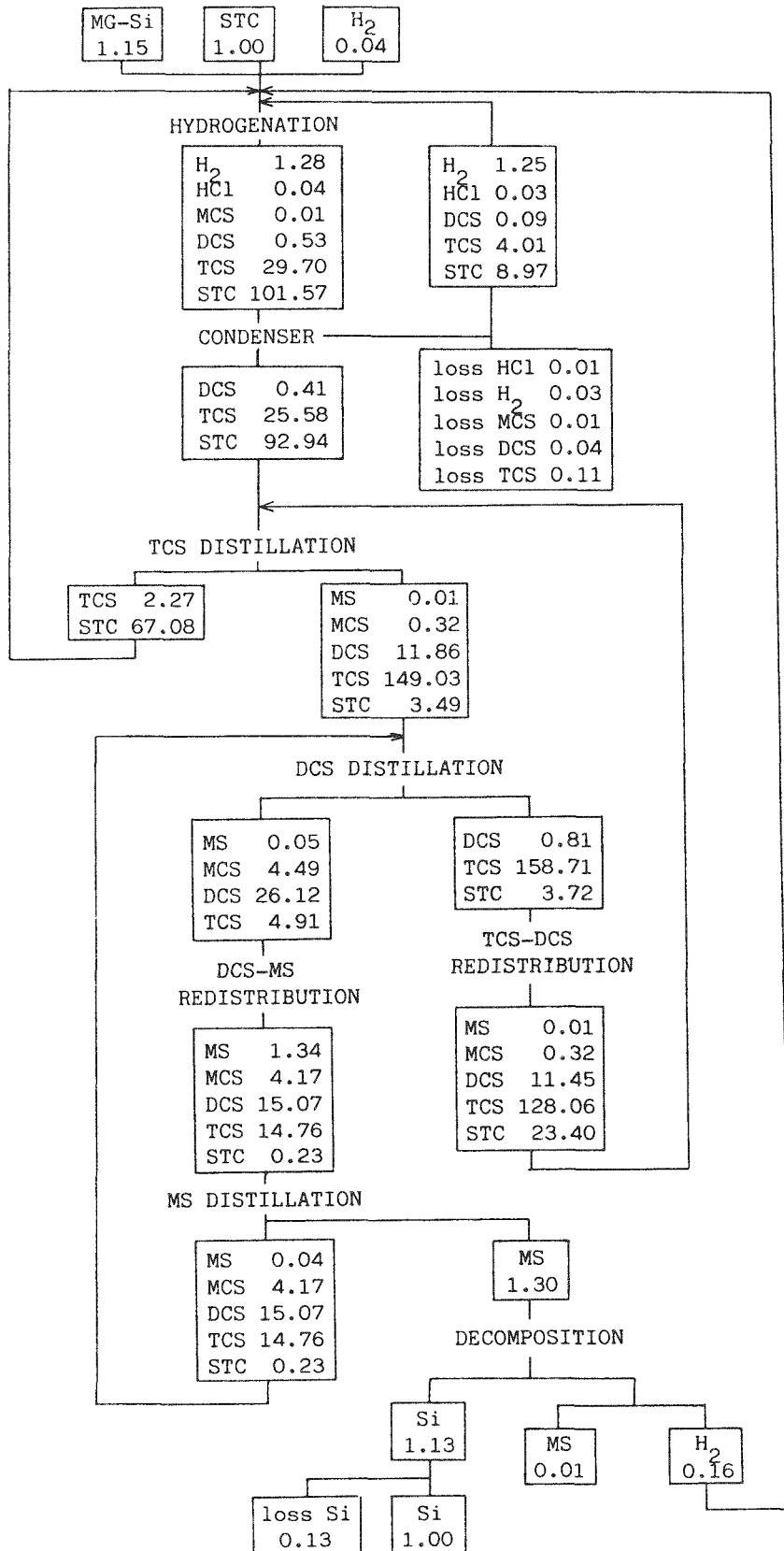


Fig. 10. MS-Based UCC FBR Process (kg/kg-Si)

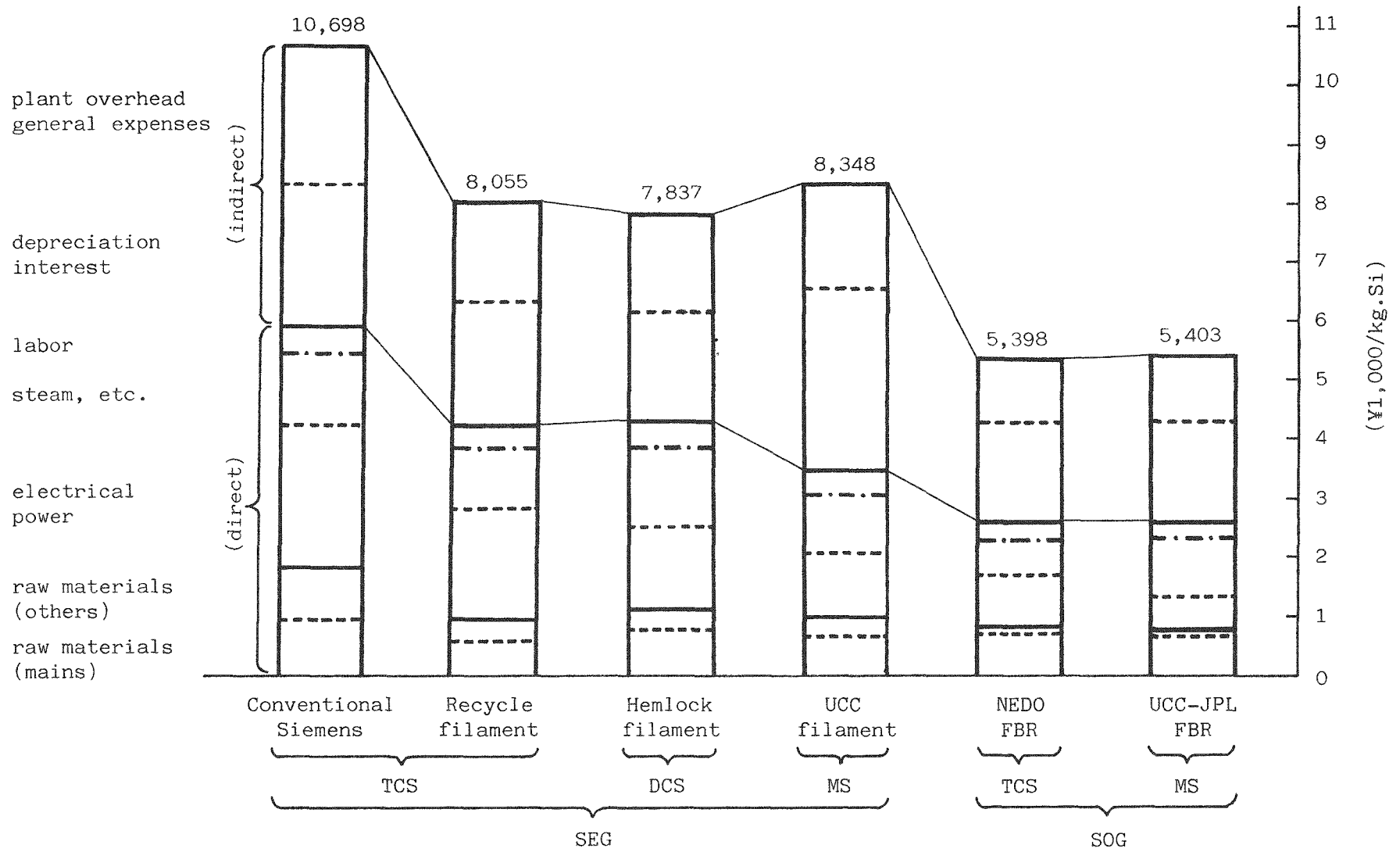


Fig. 11. Production Cost of SEG and SOG-Si (yen/kg-Si) (¥250/\$)

Table 1. Process Gases/Liquids in Each Process

(kg/kg-Si)

Material gas		T C S			DCS	MS	
Process		Siemens Filament	NEDO FBR	Recycle, Filament	Hemlock Filament	UCC-JPL FBR	UCC Filament
Process		chlorination	STC→TCS	STC→TCS	STC→TCS	STC→TCS	STC→TCS
TCS Synthesis	Feed	17.50	105.16	77.50	66.24	131.81	131.81
	Product	15.50	21.03	15.50	16.63	29.70	29.70
	Feed	---	---	---	93.53	163.24	163.24
DCS redistribution	Feed	---	---	---	---	35.57	35.57
TCS distillation	Crude	17.50	105.16	77.50	159.15	282.17	282.17
	Recovery	37.00	23.75	37.00	7.40	---	---
	Distillate	41.00	25.69	41.00	102.51	164.70	164.70
DCS distillation	Feed	---	---	---	102.51	198.97	198.97
	Distillate	---	---	---	8.97	35.57	35.57
MS distillation	Feed	---	---	---	---	35.57	35.57
	Distillate	---	---	---	---	1.30	1.30
Decomposition	Feed	41.00	25.69	41.00	8.97	1.30	1.30
	H ₂ /Mat. ratio	5~10	1.5	5~10	15~24	0~4	---
Recovery	Chlorosilanes	38.44	24.17	38.44	7.41	---	---
	Concentration	6~10 %	32 %	6~10 %	1.5~3 %	---	---
Waste	Loss	3.01	0.73	0.41	0.67	0.01	0.01
	Treatment	neutralization	←	←	←	combustion	←
	NaOH	3.00	0.72	0.36	0.63	---	---

Table 2. Manufacturing Cost Estimate for Polycrystalline Silicon (¥/kg)

basis: 1,000t/y

Quality	SEG						SOG				Remarks	
	TCS				DCS		MS		TCS			MS
Material gas	Siemens Filament		Recycle-Filament		Hemlock Filament		UCC Filament		NEDO FBR		UCC-JPL FBR	
Process	requirement		requirement		requirement		requirement		requirement		requirement	
Raw Materials												
MG-Si (¥300/kg)	3.70kg	1,110	1.06kg	318	1.15kg	345	1.15kg	345	1.13kg	339	1.15kg	345
STC (¥250(Δ¥120)/kg)	Δ13.00kg	Δ1,560	0.58kg	145	1.17kg	293	1.00kg	250	0.76kg	190	1.00kg	250
H ₂ (¥100/m ³)	5.40m ³	540	1.19m ³	119	1.41m ³	141	0.39m ³	39	1.13m ³	113	0.39m ³	39
Others		1,744		350		350		350		76		70
Sub total		1,834		932		1,129		984		759		704
Utilities												
Power (¥15/kwh)	160kwh	2,400	125kwh	1,875	90kwh	1,350	70kwh	1,050	61kwh	915	40kwh	600
Steam, etc.		1,020		800		1,200		800		404		800
Others										22		
Sub total		3,420		2,675		2,550		1,850		1,341		1,400
Other directs		180		180		180		180		180		180
Labor, 6 M-¥/man.y	75men	450	75men	450	75men	450	75men	450	50men	300	50men	300
Direct cost total		5,884		4,237		4,309		3,464		2,580		2,584 B
Depreciation, Interest		2,400		2,000		1,760		3,000		1,600		1,600 A × 0.2 = C
Plant overhead		1,019		767		746		795		514		514 (B + C) × 0.123
Indirect cost total		3,419		2,767		2,506		3,795		2,114		2,114
Total manuf. cost		9,303		7,004		6,815		7,259		4,694		4,698 D
General expenses		1,395		1,051		1,022		1,089		704		705 D × 0.15
Product cost		10,698		8,055		7,837		8,348		5,398		5,403
Plant investment (M-¥)		12,000		10,000		8,800		15,000		8,000		8,000 A

Note : ¥250/¢

DISCUSSION

MAYCOCK: When you use the 15 yen/kWh for the electricity cost, is that your estimate of the average or the actual cost in Japan?

SHIMIZU: That is the industrial cost.

MAYCOCK: I wondered, because there is a factor of two in that number in the world now.

SHIMIZU: It is much cheaper in the United States. In general, other cost estimates can still vary from my estimate.

LEIPOLD: You mentioned that the quality of the silicon from the NEDO fluidized-bed reactor process is proven. Can you define the word "proven" further with any analyses?

SHIMIZU: This silicon granular material is now being used in the casting process.

PELLIN: Can you give concentration levels of boron and phosphorus?

SHIMIZU: The resistivity is about 10 ohm-cm.

AULICH: What are the next goals in your project? You said that 10 MT/year is being produced. What are the future plans?

SHIMIZU: I'm not sure I can answer. This question is best asked of Dr. Noda.

ECONOMICS OF POLYSILICON PROCESSES

Carl L. Yaws, K. Y. Li and S. M. Chou
Lamar University
Beaumont, Texas 77710, U.S.A.

ABSTRACT

New technologies are being developed to provide lower cost polysilicon material for solar cells. Existing technology which normally provides semiconductor industry polysilicon material is undergoing changes and also being used to provide polysilicon material for solar cells.

Economics of new and existing technologies are presented for producing polysilicon. The economics are primarily based on the preliminary process design of a plant to produce 1,000 metric tons/year of silicon. The polysilicon processes include: Siemens process (hydrogen reduction of trichlorosilane); Union Carbide process (silane decomposition) and Hemlock Semiconductor process (hydrogen reduction of dichlorosilane). The economics include cost estimates of capital investment and product cost to produce the polysilicon via the technology. Sensitivity analysis results are also presented to disclose the effect of major parameters such as utilities, labor, raw materials and capital investment.

1. INTRODUCTION

A typical sequence for process selection is presented in Figure 1. The process evaluation activities are shown in relation to their usefulness in the comparison of processes and in the selection for scale-up to pilot plant and large scale plant. The process evaluation activities which primarily involve chemical engineering and economic analyses are useful in the evaluation of alternate processes under consideration for the production of polysilicon. Specifically, the process evaluation provides technical and economic data which may be used for the identification of those processes having good potential for producing polysilicon within the cost goals of the project.

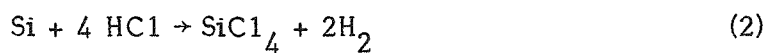
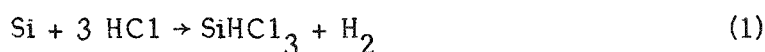
The objective of the present work is to provide initial economics for several processes for the production of polysilicon. The results are intended to be semi-quantitative and useful in initial project studies.

2. SIEMENS PROCESS

Process Description And Design

The flowsheet (1, 2, 33, 34, 36, 39, 41-43, 45) for the Siemens process, consisting of several major processing operations of hydrochlorination, condensation, distillation and chemical vapor deposition, is shown in Figure 2.

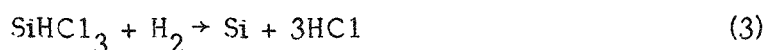
Initially, metallurgical grade silicon (MGSi) is reacted with anhydrous hydrogen chloride (HCl) in a fluidized bed (300-350°C) to produce a mixture of chlorosilanes. The mixture is primarily trichlorosilane (TCS) and silicon tetrachloride (TET) which are produced via the representative reactions:



Since the reactions are highly exothermic, heat transfer for removal of heat of reaction is required to maintain reaction temperature control.

The mixture of chlorosilanes from the reaction is condensed and subjected to several distillations to separate by-products and remove impurities. Representative results for boron impurity removal from TCS are shown in Figure 2A. Figure 2B presents representative results for phosphorous impurity removal.

The purified TCS is reacted with hydrogen (H_2) in a rod reactor to obtain polysilicon deposition via the representative reaction:



The deposition reaction occurs on the surface of a hot rod (1000-1100°C) which is heated by passage of electrical current through the rod. Large electrical energy requirements are necessary because of the endothermic reaction, radiation heat

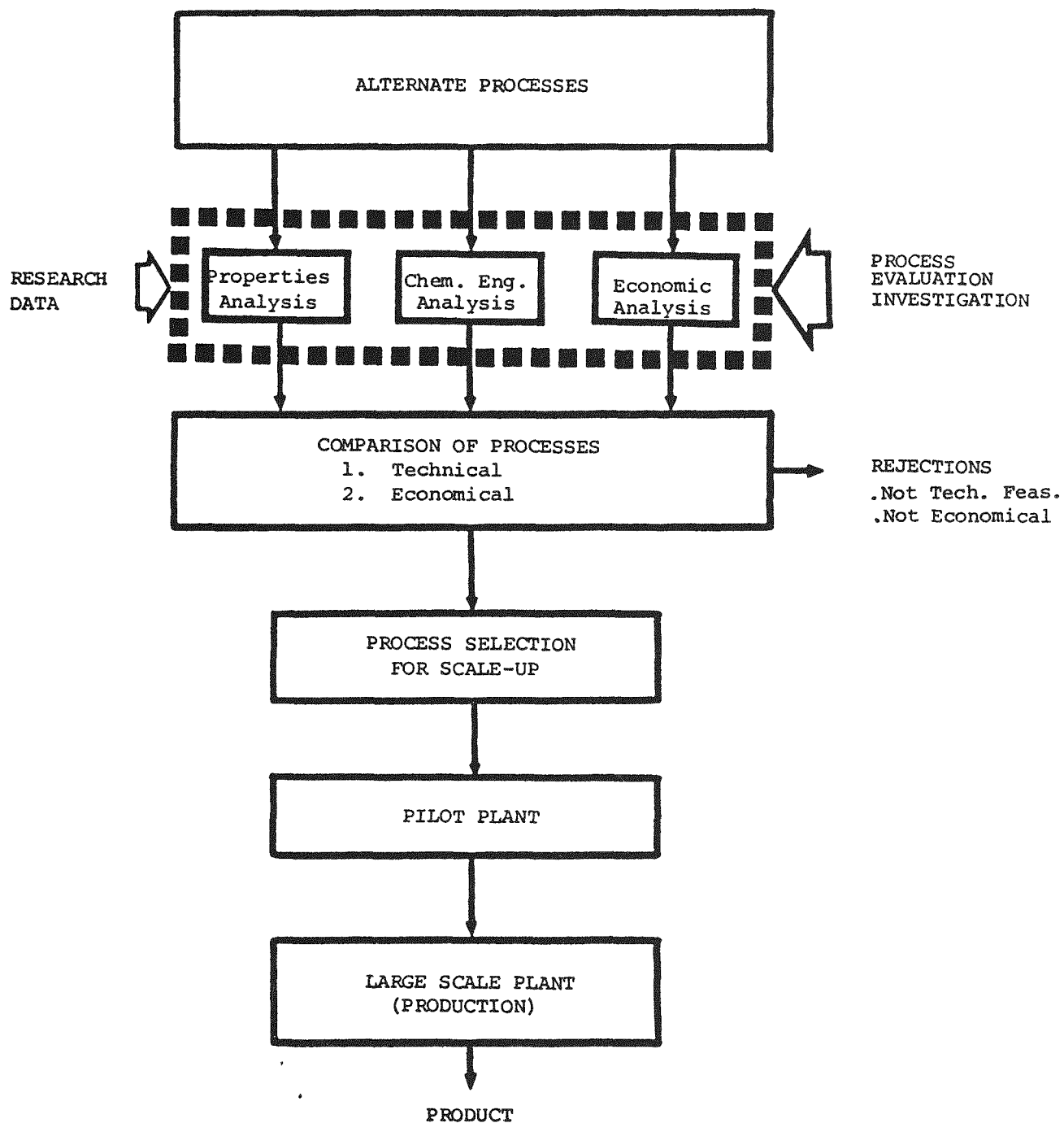


FIGURE 1. TYPICAL SEQUENCE FOR PROCESS SELECTION

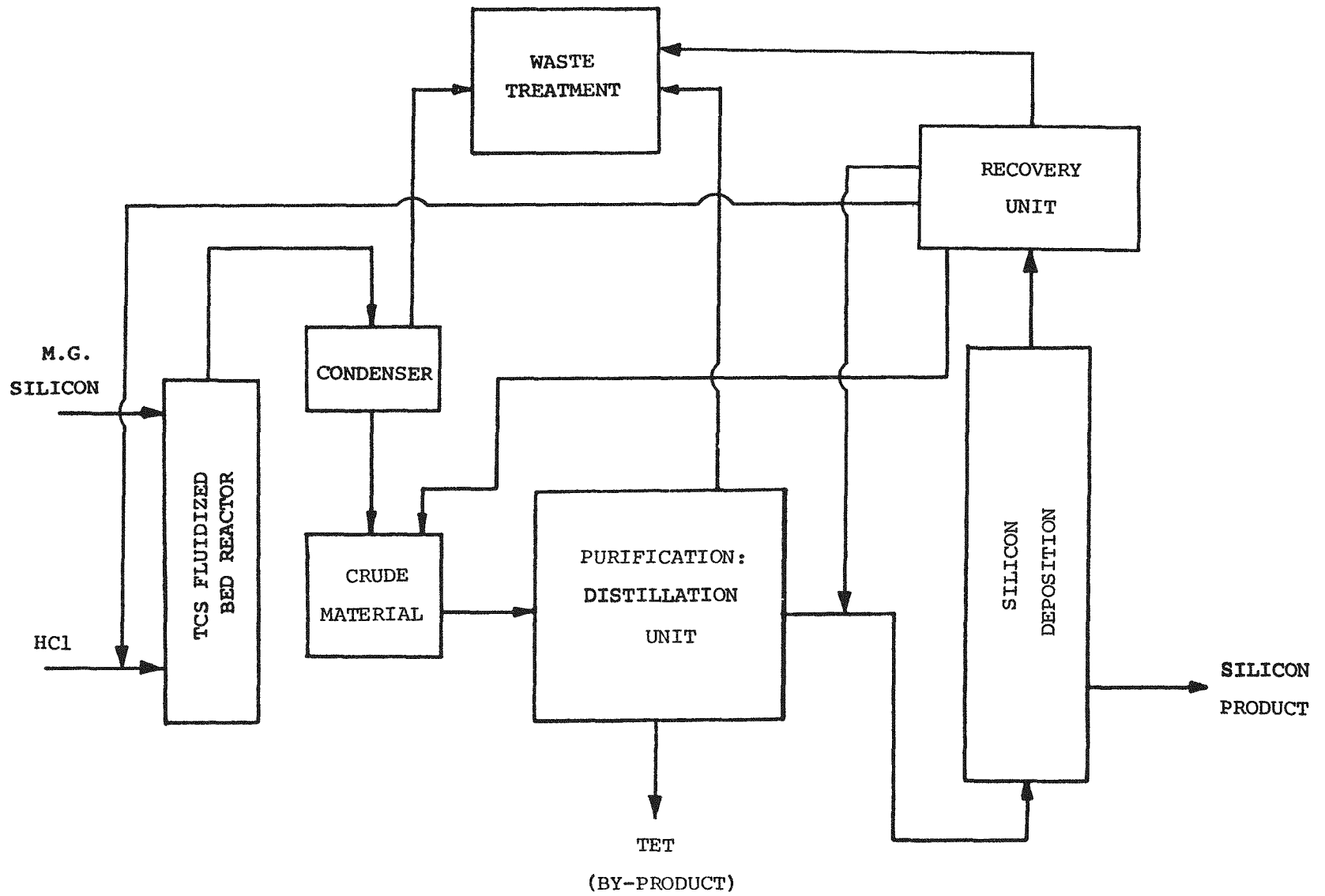


FIGURE 2. FLOWSHEET FOR SIEMENS PROCESS

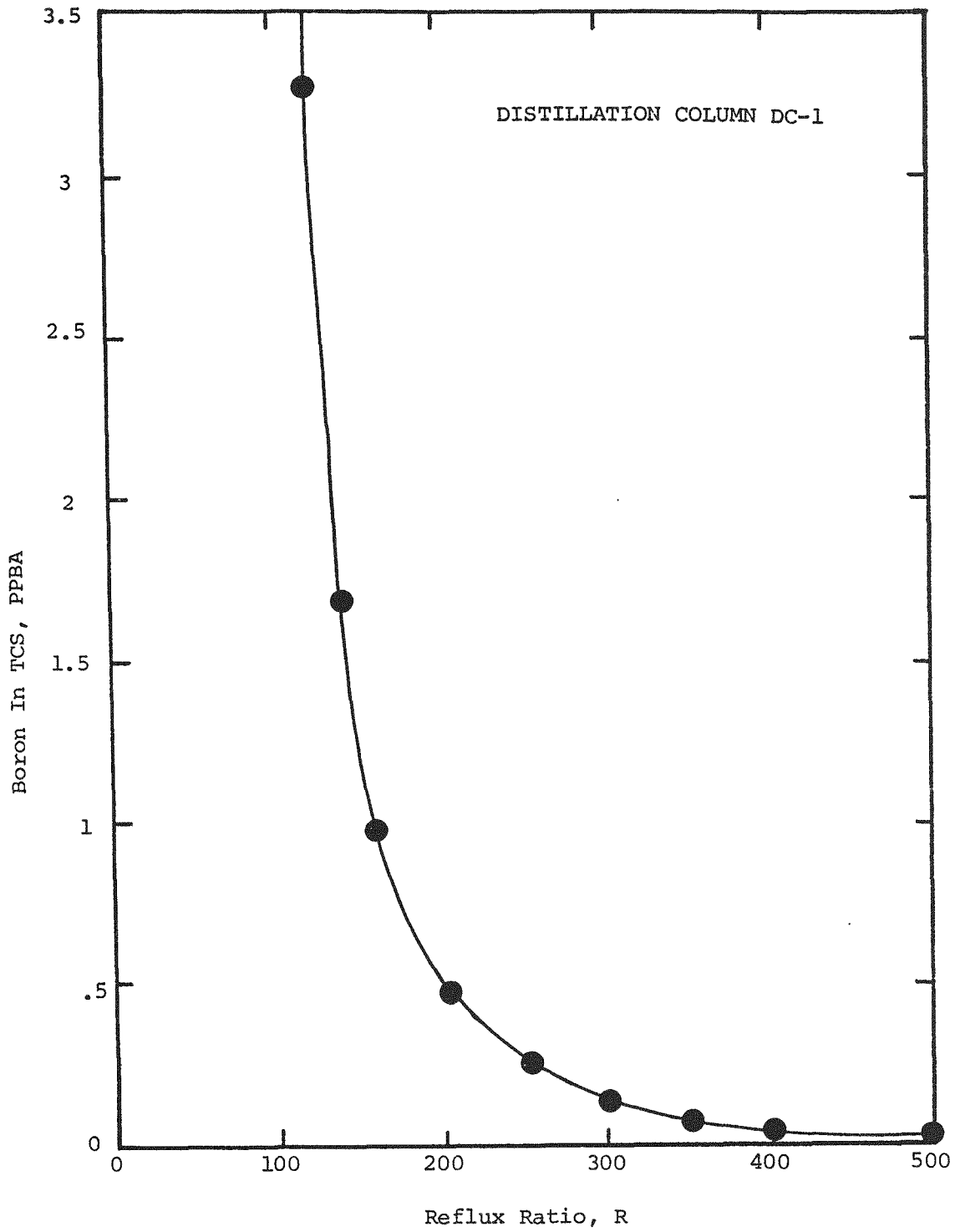


FIGURE 2A. REPRESENTATIVE RESULTS FOR BORON IMPURITY REMOVAL

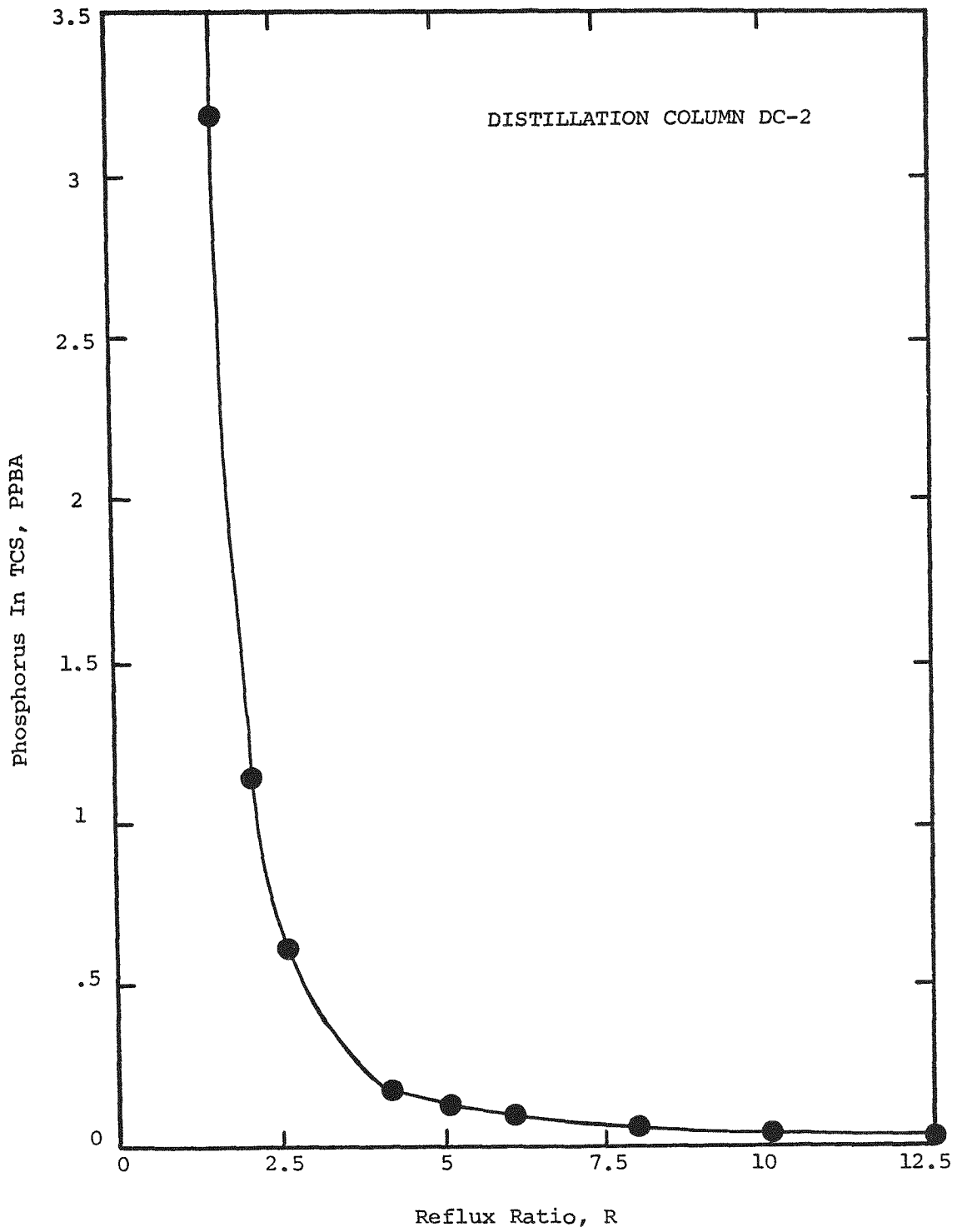


FIGURE 2B. REPRESENTATIVE RESULTS FOR PHOSPHORUS IMPURITY REMOVAL

losses and incomplete conversion of the TCS. Unreacted chlorosilanes, hydrogen chloride and hydrogen are separated and recycled.

A representative polysilicon deposition reactor using trichlorosilane as the silicon source material is shown in Figure 3.

In the chemical engineering analysis of the process, a process design was performed to obtain data for the cost analysis. The design was based on a plant for the production of 1,000 metric tons/yr of polysilicon via the Siemens process. The detailed design included TCS production in a fluidized bed; TCS purification by distillation; silicon production by chemical vapor deposition in a Siemens type rod reactor; recycle of chlorosilanes, hydrogen chloride, and hydrogen; waste treatment provisions to meet environmental quality; and storage considerations for feed, in-process and product materials.

The process design provided detailed data for raw materials, utilities, major process equipment and production labor requirements which are necessary for polysilicon production.

Cost Analysis

The cost analysis results for producing silicon by this technology are presented in Table 1 including costs for raw materials, labor, utilities and other items composing the product cost (total cost of producing silicon). The tabulation summarizes all of these items to give a total product cost without profit of 29.49 \$/kg Si (1985 dollars). This product cost without profit includes direct manufacturing cost, indirect manufacturing cost, plant overhead and general expenses.

The economic summary for the process is given in Table 2. Results for process, plant size, plant product, plant investment, profitability analysis and sensitivity analysis are displayed in the tabulation.

A sensitivity analysis was performed to determine the influence of cost parameters on the economics of producing silicon by this technology. The cost sensitivity results are given in Figure 4 in which product cost (\$/kg Si) is plotted vs variation (-100 to 0 to +100 percent) of the primary cost parameters (raw materials, labor and utilities). The 0 per cent variation represents the base case. The -100 per cent variation corresponds to the case of no costs for the parameter; and the +100 per cent represents the case for a doubling of cost for each parameter. The plot illustrates that product cost is greatly influenced by utilities (electrical energy).

The variation of product cost (\$/kg Si) with electrical energy requirements (kw-hr/kg Si) is shown in Figure 5. The present study which is based on electrical energy requirements of 120 kw-hr/kg of Si and 5 ¢/kw-hr is shown as the darkened circle in the figure. If electrical energy requirements are increased from 120 to 220 kw-hr, the product cost increases from \$29.5 to \$34.5 per kg of Si. The increase is even more pronounced at 7.5 ¢/kw-hr electricity.

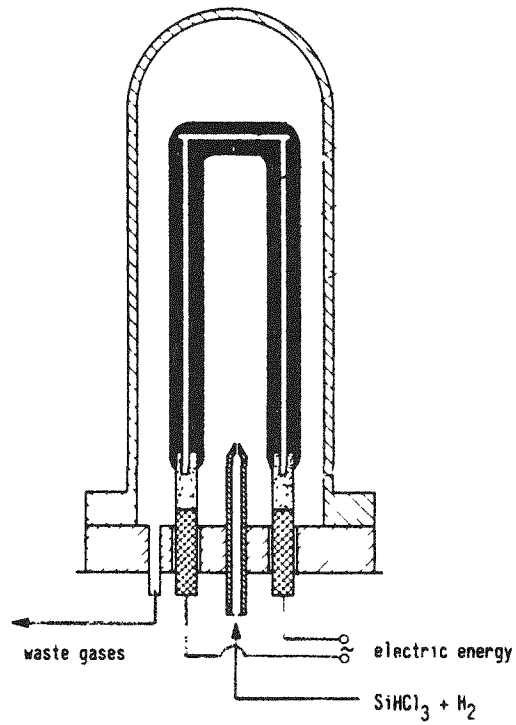


FIGURE 3. REPRESENTATIVE POLYCRYSTALLINE DEPOSITION REACTION FOR TRICHLOROSILANE
(GOVERNMENT REPORT: CISZEK (2))

TABLE 1

ESTIMATION OF PRODUCT COST FOR SIEMENS PROCESS

	COST \$/kg of Si

1. Direct Manufacturing Cost.....	16.09
Raw Materials	
Direct Operating Labor	
Utilities	
Supervision and Clerical	
Maintenance and Repairs	
Operating Supplies	
Laboratory Charge	
2. Indirect Manufacturing Cost.....	7.80
Depreciation	
Local Taxes	
Insurance	
3. Plant Overhead.....	1.76
4. General Expenses.....	3.85
Administration	
Distribution and Sales	
Research and Development	

5. Product Cost without Profit.....	29.49

Note: 1985 Dollars

TABLE 2

ECONOMIC SUMMARY: COST ANALYSIS FOR SIEMENS PROCESS

1. Process -----	SIEMENS PROCESS
2. Plant Size -----	1000 MT/yr
3. Plant Product -----	POLYSILICON
4. Plant Investment -----	\$ 69.00 Million

Fixed Capital ----	\$ 60.00 Million
Working Capital --	\$ 9.00 Million
Total Capital ----	\$ 69.00 Million

5. Profitability Analysis

Return on Original Investment after Taxes (% ROI)
Discounted Cash Flow Rate of Return after Taxes (% DCF)

Return	Sales Price \$/kg of Si	Return	Sales Price \$/kg of Si
0 % ROI	29.49	0 % DCF	29.49
10 % ROI	42.27	10 % DCF	38.13
20 % ROI	55.05	20 % DCF	48.22
30 % ROI	67.83	30 % DCF	59.32
40 % ROI	80.60	40 % DCF	71.08
50 % ROI	93.38	50 % DCF	83.25
60 % ROI	106.16	60 % DCF	95.66
70 % ROI	118.94	70 % DCF	108.21
80 % ROI	131.71	80 % DCF	120.85
90 % ROI	144.49	90 % DCF	133.54
100 % ROI	157.27	100 % DCF	146.27

Based on 10 year project life and 10 year straight
line depreciation. Tax rate (federal) of 46 %.

6. Sensitivity Analysis

	Product Cost, \$/kg of Si					DELTA
	-100%	-50%	BASE	+50%	+100%	
Raw Materials	25.40	27.45	29.49	31.54	33.58	4.09
Labor	27.60	28.54	29.49	30.44	31.39	1.90
Utilities	21.76	25.63	29.49	33.36	37.22	7.73
Plant Investment (Fixed Capital)	17.93	23.71	29.49	35.27	41.05	11.56

Note: 1985 Dollars

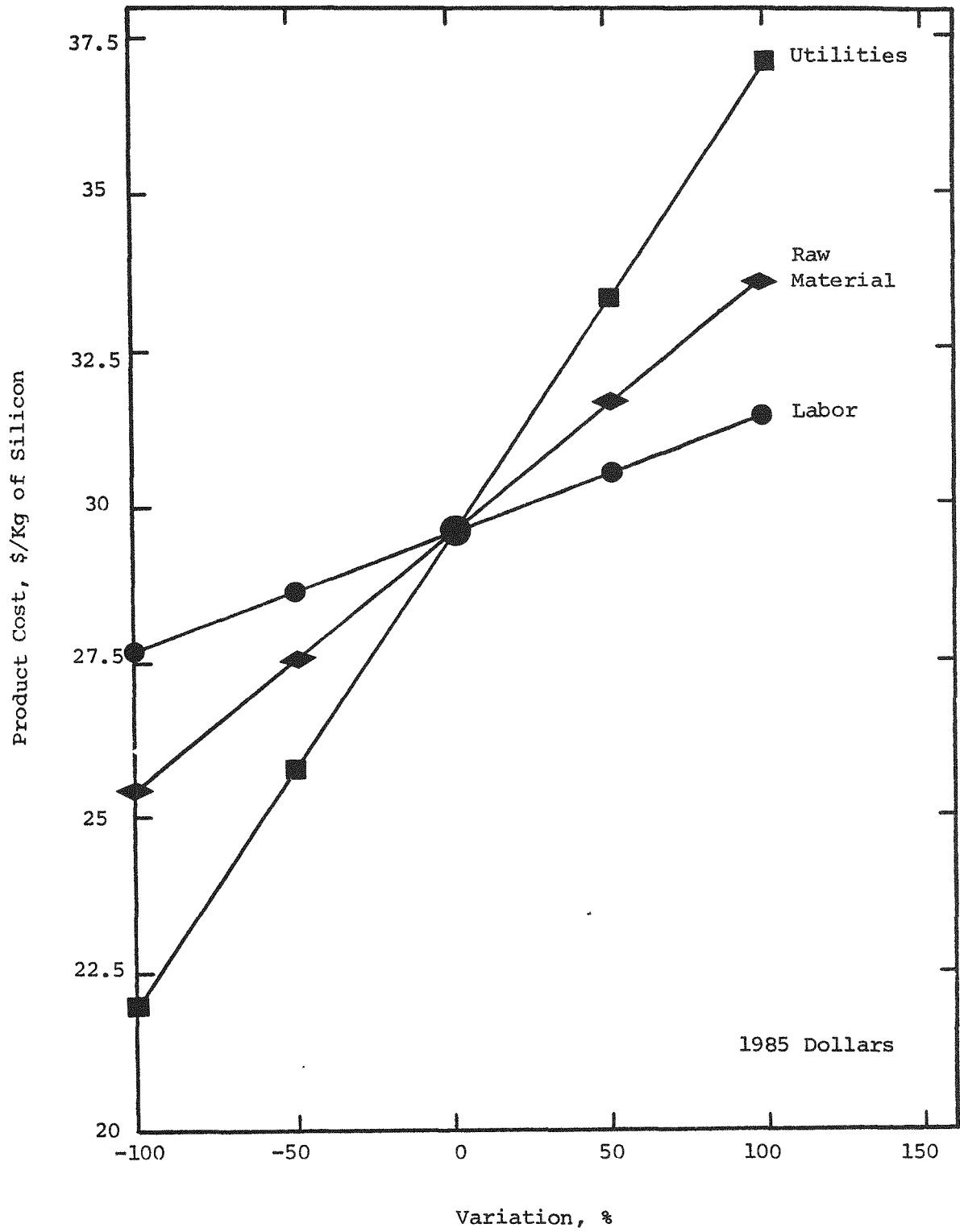


FIGURE 4. SENSITIVITY PLOT FOR SIEMEN S PROCESS

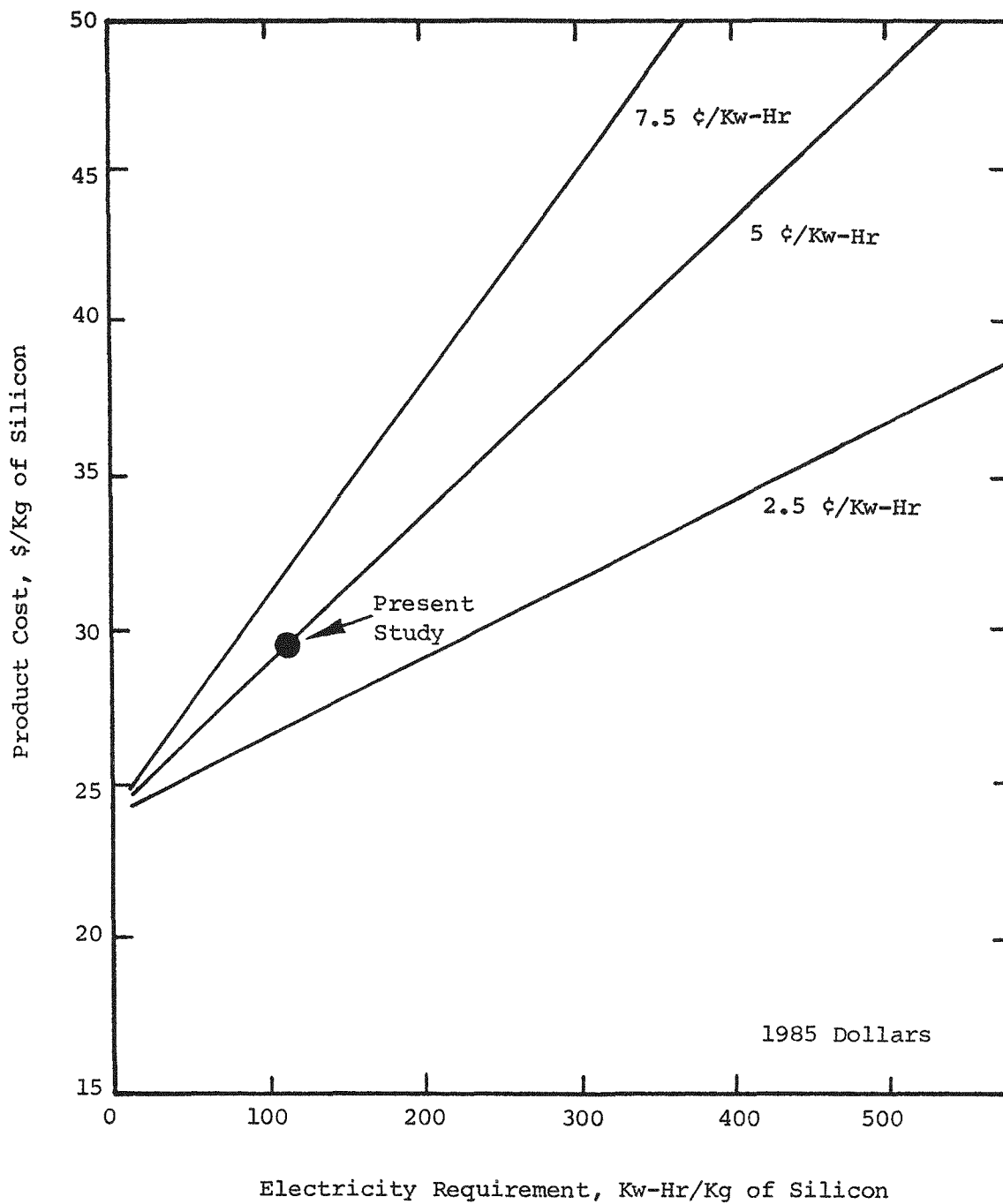


FIGURE 5. PRODUCT COST VS. ELECTRICITY REQUIREMENTS FOR SIEMENS PROCESS

2. UNION CARBIDE PROCESS

Process Description And Design

The Union Carbide process (7-9, 27, 36, 39) for silicon involves several processing operations of hydrogenation-hydrochlorination reaction, stripping, distillation, redistribution reaction, silane purification, and silicon deposition. The process flowsheet is shown in Figure 6.

Hydrogen, silicon tetrachloride, and metallurgical grade silicon are fed to the hydrogenation reactor (fluidized bed, 500C, 515 psia, copper catalyst) to produce a mixture of chlorosilanes. The mixture of chlorosilanes from the hydrogenation reaction is condensed and subjected to several distillations to separate components and remove impurities.

Initially, the condensed liquid mixture is sent to D-01 stripper (90 psia) to remove inert gases and volatile impurities. The stripper bottoms go to D-02 distillation (55 psia) which separates TCS (trichlorosilane) and TET (silicon tetrachloride). The TCS redistribution reactor (liquid phase, 85 psia, 140°F catalyst) is used to produce DCS (dichlorosilane). The separation of DCS and TCS is achieved in D-03 distillation (320 psia). The overhead goes to DCS redistribution reactor (liquid phase, 510 psia, 140°F, catalyst) to produce silane (SiH₄). The silane is purified by separation from trace impurities (such as B₂H₆) by D-04 distillation (355 psia). Representative results for diborane impurity removal are shown in Figure 6A.

The purified silane is mixed with hydrogen and then introduced into the deposition reactor (Komatsu license, 7) to produce silicon via the representative reaction:



The reaction occurs in a deposition reactor which is heated by passage of electrical current through the silicon rods to attain a temperature in the 800-900C range (21, 22). Deposition rates of 4-8 micrometers/min of silicon on the rod surface are reported in the Komatsu patents.

For the deposition reactor, the homogeneous decomposition reaction resulting in silicon dust formation is not desirable. The heterogeneous decomposition reaction resulting in silicon deposition on the rod surface is desirable. The temperature dependence of critical silane concentration for homogeneous and heterogeneous decomposition regions has been studied by Iya (20) and others (28). Results from the recent report of Dudukovic (5) are shown in Figure 7. At 800C, the heterogeneous decomposition region appears to be in the 1-2% concentration range for silane in hydrogen.

A representative polysilicon deposition reactor for silane is shown in Figure 8 (Komatsu patent: 21, 22). The thermal insulator in the reaction chamber is obvious in both the side and top views. The thermal insulators provide for radiation benefits (individual silicon rods from radiation from the other red-heated silicon rods) and for temperature control benefits for reduction of homogeneous reaction in the gas phase.

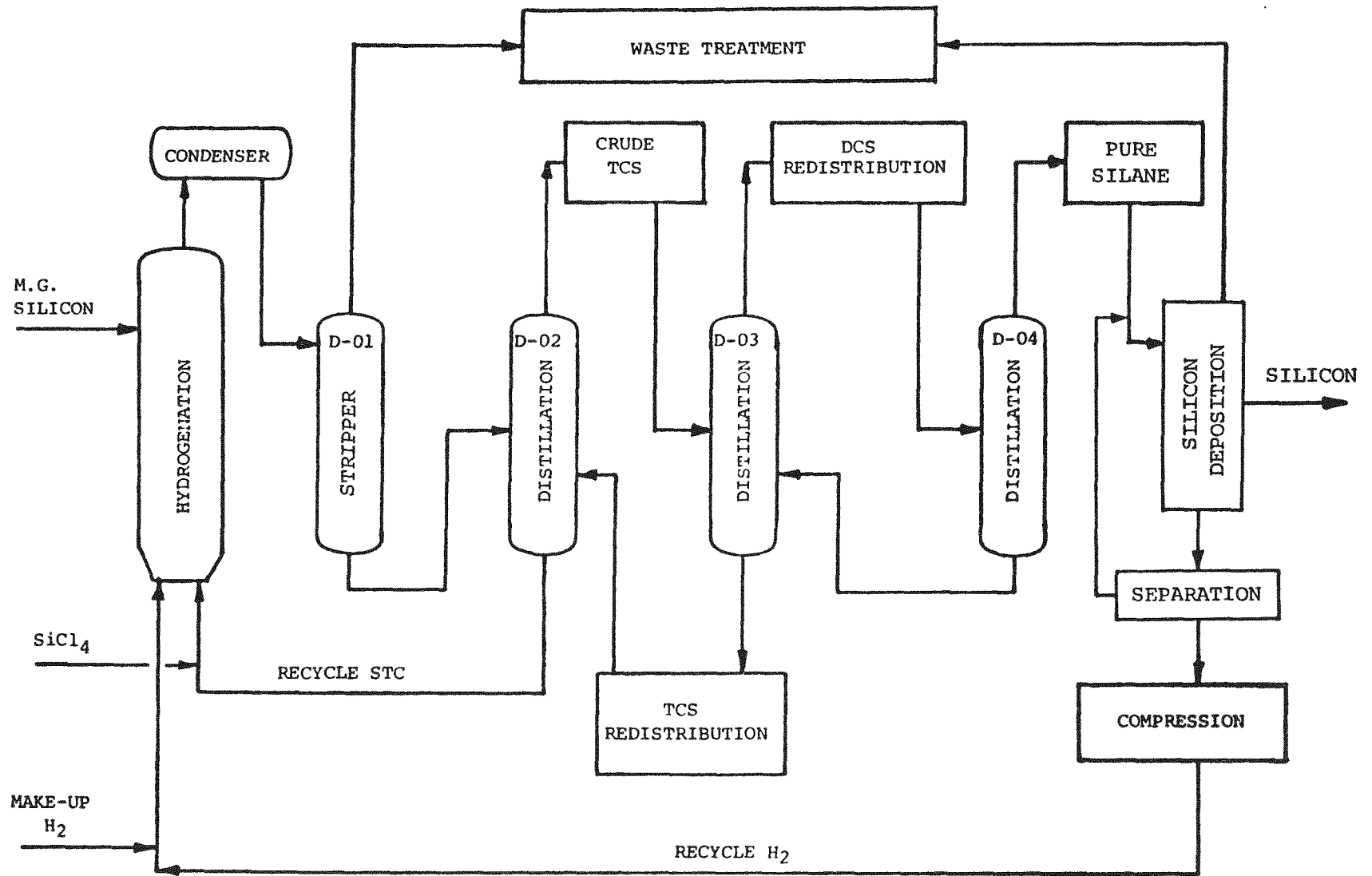


FIGURE 6. FLOWSHEET FOR UNION CARBIDE PROCESS

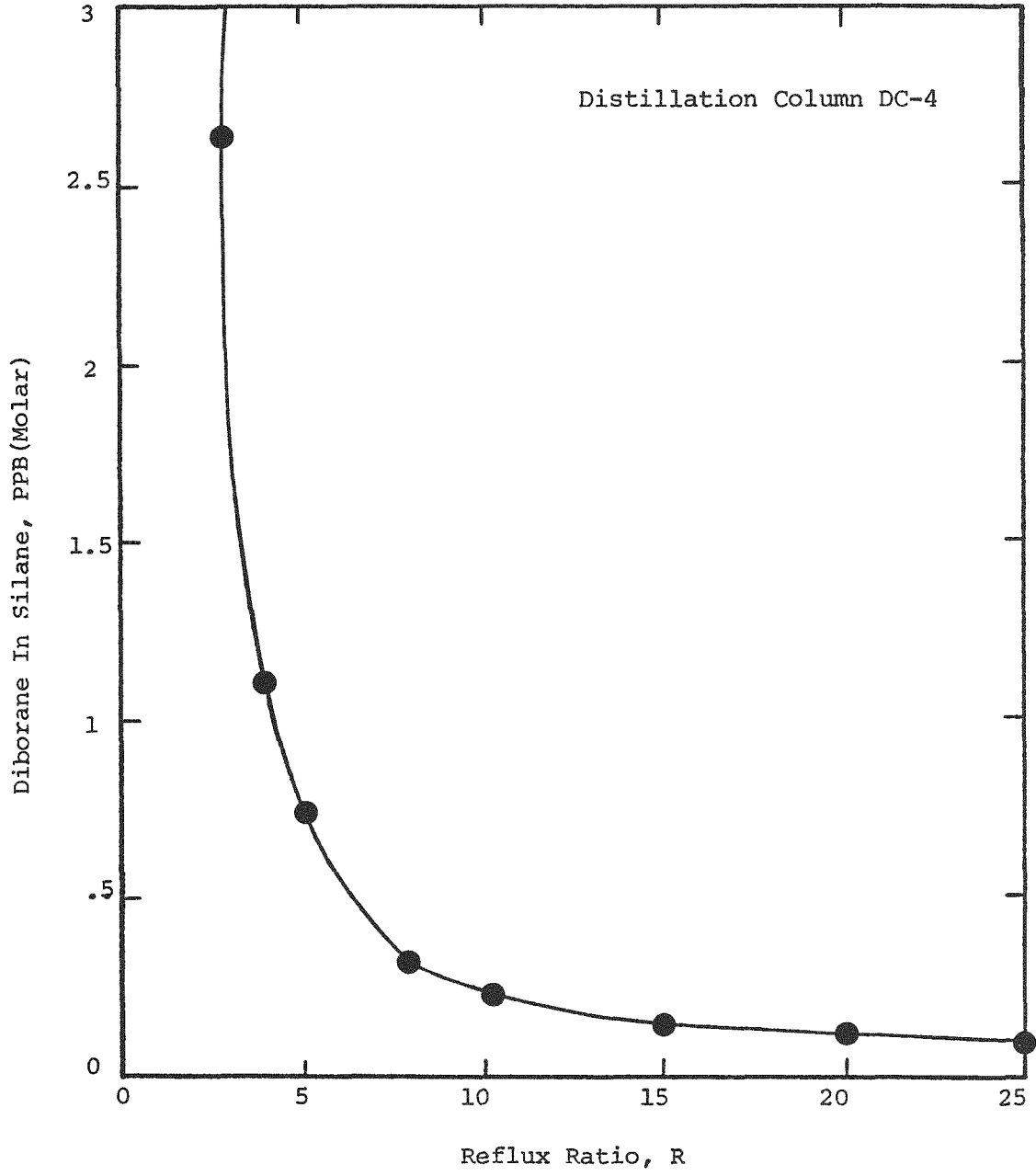


FIGURE 6A REPRESENTATIVE RESULTS FOR DIBORANE IMPURITY REMOVAL

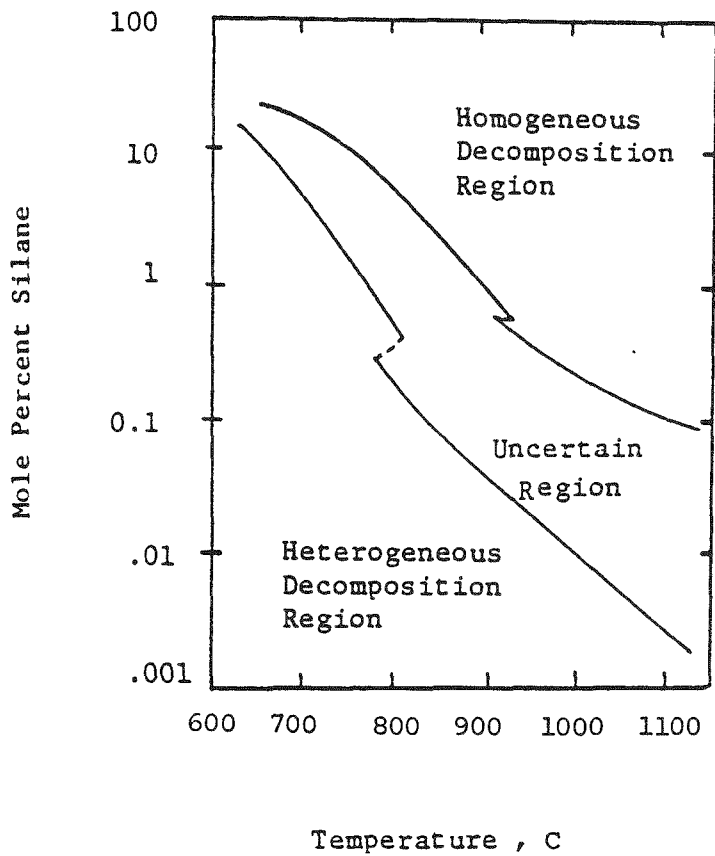
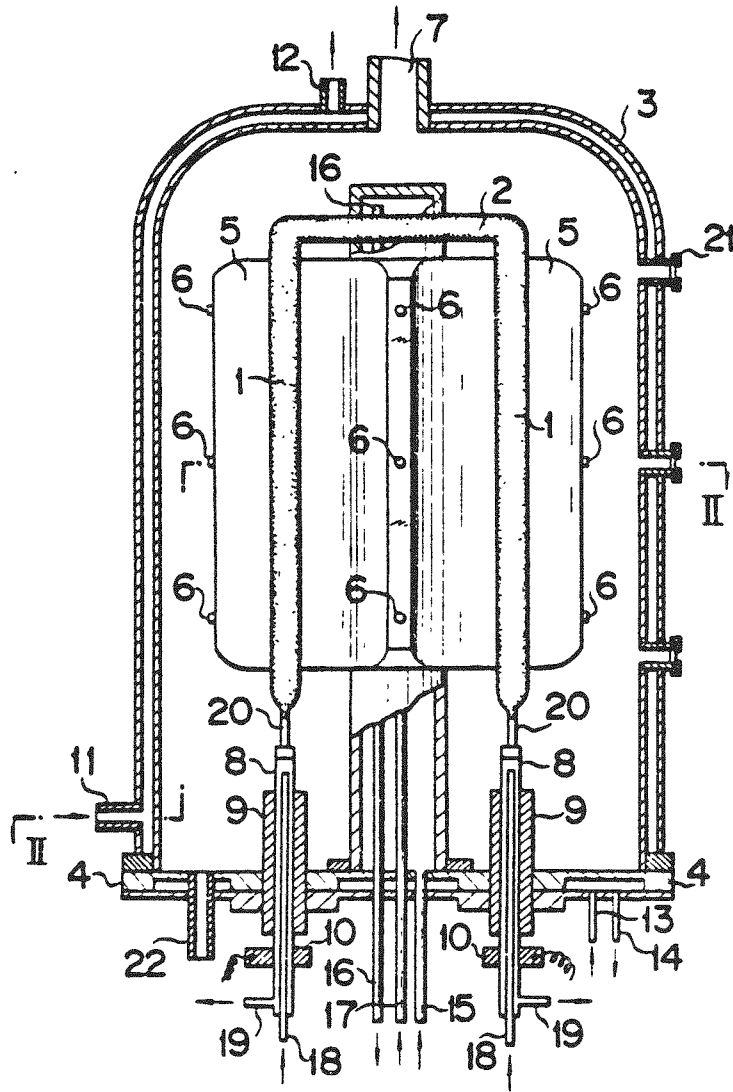
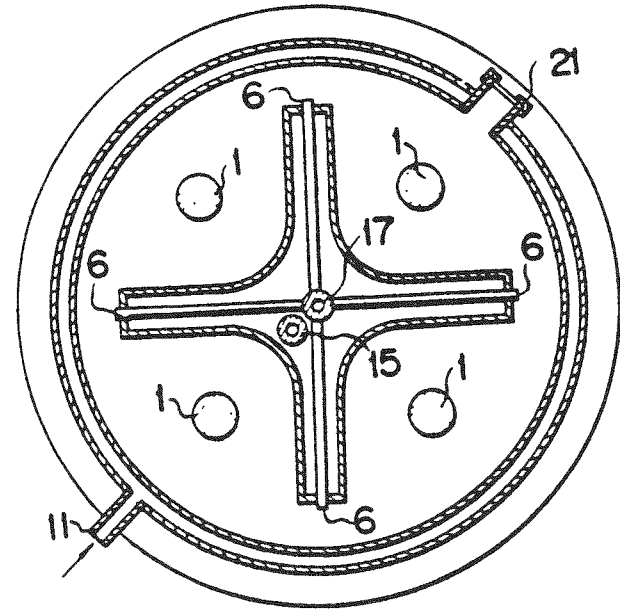


FIGURE 7. TEMPERATURE DEPENDENCE OF CRITICAL SILANE CONCENTRATION
 (GOVERNMENT REPORT: IYA (20), DUDUKOVIC (5))



(A) SIDE VIEW



(B) TOP VIEW

FIGURE 8. REPRESENTATIVE POLYCILICON DEPOSITION REACTOR FOR SILANE
 (KOMATSU: U.S. PATENT 4,150,168 (REF. 22))

In the chemical engineering analysis of the Union Carbide process, a process design was performed for a plant to produce 1,000 metric tons/yr of polysilicon.

Cost Analysis

Cost analysis results for producing polysilicon via the Union Carbide process with chemical vapor deposition reactors are given in Table 3. The results indicate a product cost without profit of 24.65 \$/kg Si (1985 dollars).

Table 4 presents the economic summary of results for process, plant size, plant product, plant investment, profitability analysis and sensitivity analysis. The capital investment of \$74.75 million of the present study for 1,000 metric ton plant is in the range of the \$85 million for a 1,500 metric ton plant reported by Union Carbide in a news release (9) and \$90 million reported for a doubling of capacity to 2,400 metric tons (8).

The sensitivity analysis plot is shown in Figure 9. The product cost is influenced most by utilities (electrical energy).

4. HEMLOCK SEMICONDUCTOR PROCESS

Process Description and Design

The process flowsheet for Hemlock Semiconductor process for polysilicon is shown in Figure 10. The process involves major processing operations of hydrochlorination, separation, several distillation units, redistribution, boron removal, silicon deposition, recovery unit and waste treatment.

Metallurgical grade silicon is hydrochlorinated in the presence of hydrogen and silicon tetrachloride in a fluidized bed reactor (500C, 515 psia). In the process, the reaction product issuing from the hydrochlorination reactor (hydrochlorination-hydrogenation reaction) is cooled and undergoes a vapor-liquid flash separation. The vapor fraction containing the hydrogen from the flash is recycled back to the hydrochlorination reactor. The liquid fraction containing the chlorosilanes and dissolved gases is fed to the initial distillation column.

The function of the initial distillation column (D-01, stripper column, 90 psia) in the process is to remove volatile gases (such as hydrogen and nitrogen) which are dissolved in liquid chlorosilanes. For the engineering design, TCS (trichlorosilane) was selected as the heavy key component for the separation.

The second distillation column (D-02, TCS column, 90 psia) in the process separates TCS (trichlorosilane) and TET (silicon tetrachloride). The distillation column has three feeds (bottoms from the third distillation, chlorosilanes from the recovery unit and bottoms from the initial distillation). The TET from the distillation is recycled to the hydrochlorination reactor for additional conversion.

TABLE 3

ESTIMATION OF PRODUCT COST FOR UNION CARBIDE PROCESS

	COST \$/kg of Si

1. Direct Manufacturing Cost.....	11.19
Raw Materials	
Direct Operating Labor	
Utilities	
Supervision and Clerical	
Maintenance and Repairs	
Operating Supplies	
Laboratory Charge	
2. Indirect Manufacturing Cost.....	8.45
Depreciation	
Local Taxes	
Insurance	
3. Plant Overhead.....	1.80
4. General Expenses.....	3.21
Administration	
Distribution and Sales	
Research and Development	

5. Product Cost without Profit.....	24.65

Note: 1985 Dollars

TABLE 4

ECONOMIC SUMMARY: COST ANALYSIS FOR UNION CARBIDE PROCESS

1. Process -----	UNION CARBIDE PROCESS
2. Plant Size -----	1000 MT/yr
3. Plant Product -----	POLYSILICON
4. Plant Investment -----	\$ 74.75 Million

Fixed Capital ----	\$ 65.00 Million
Working Capital --	\$ 9.75 Million
Total Capital ----	\$ 74.75 Million

5. Profitability Analysis

Return on Original Investment after Taxes (% ROI)
Discounted Cash Flow Rate of Return after Taxes (% DCF)

Return	Sales Price \$/kg of Si	Return	Sales Price \$/kg of Si
0 % ROI	24.65	0 % DCF	24.65
10 % ROI	38.49	10 % DCF	34.00
20 % ROI	52.33	20 % DCF	44.93
30 % ROI	66.17	30 % DCF	56.96
40 % ROI	80.02	40 % DCF	69.70
50 % ROI	93.86	50 % DCF	82.88
60 % ROI	107.70	60 % DCF	96.33
70 % ROI	121.54	70 % DCF	109.93
80 % ROI	135.39	80 % DCF	123.62
90 % ROI	149.23	90 % DCF	137.37
100 % ROI	163.07	100 % DCF	151.15

Based on 10 year project life and 10 year straight line depreciation. Tax rate (federal) of 46 %.

6. Sensitivity Analysis

	Product Cost, \$/kg of Si					DELTA
	-100%	-50%	BASE	+50%	+100%	
Raw Materials	21.74	23.19	24.65	26.10	27.55	2.91
Labor	22.75	23.70	24.65	25.59	26.54	1.90
Utilities	20.78	22.71	24.65	26.58	28.51	3.87
Plant Investment (Fixed Capital)	12.13	18.39	24.65	30.91	37.17	12.52

Note: 1985 Dollars

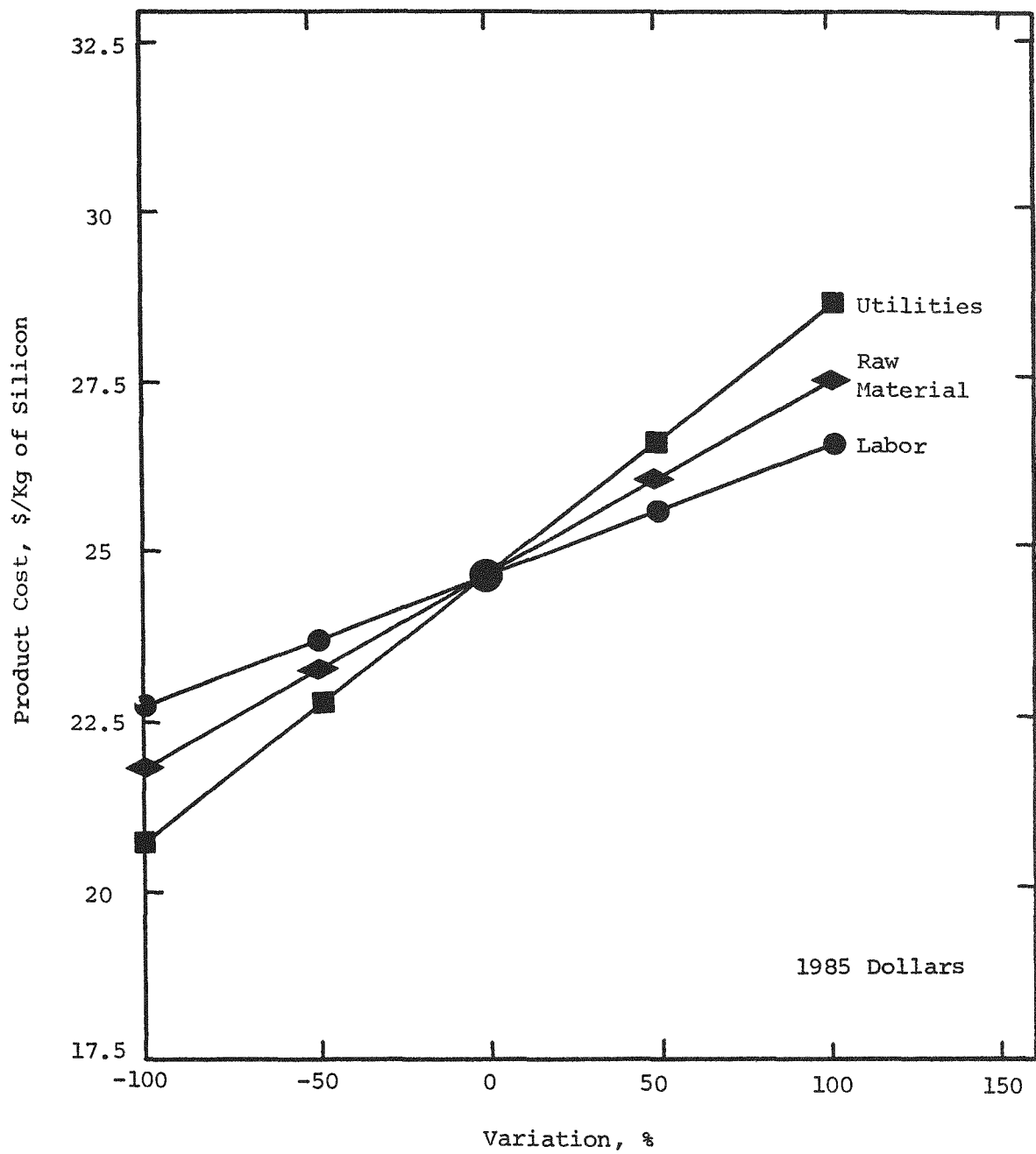


FIGURE 9. SENSITIVITY PLOT FOR UNION CARBIDE PROCESS

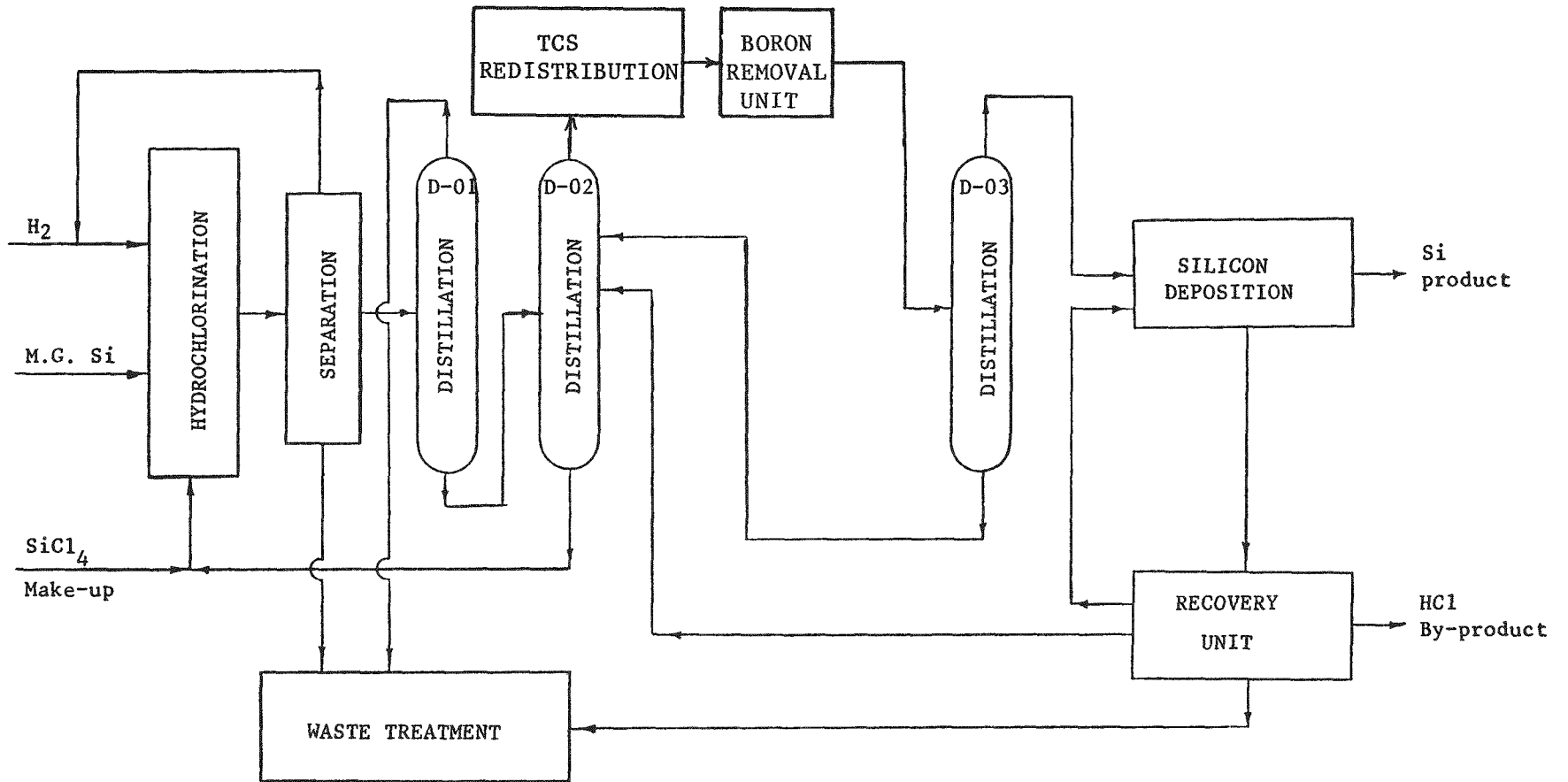
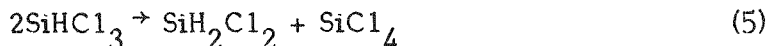


FIGURE 10. FLOWSHEET FOR HEMLOCK SEMICONDUCTOR PROCESS

The TCS from the second distillation is sent to the redistribution reactor (liquid phase, 80 psia, 80C) where TCS is redistributed to DCS and TET according to the representative chemical reaction equation:



The conversion from pure TCS is about 10.5% to DCS.

After redistribution the stream is sent to the boron removal unit and the third distillation. The third distillation column (D-03, DCS column, 90 psia) in the process separates DCS (dichlorosilane) and TCS (trichlorosilane). DCS from the distillation is sent to the silicon deposition reactors.

The purified DCS is reacted with hydrogen (H_2) in a rod reactor to obtain polysilicon deposition via the following representative chemical reaction equation:



The above reaction equation may include several reaction steps. Chemical equilibrium is involved and in reality, several chlorosilanes (such as SiH_2Cl_2 , SiHCl_3 and SiCl_4) are also present in the gas phase by-products.

The chemical vapor deposition reaction with DCS is very fast and occurs on the surface of a hot rod (1000-1200C) which is heated by passage of electrical current through the rod. Deposition rates and conversions for dichlorosilane are approximately twice (2X) those for the usual trichlorosilane process. Other benefits include higher molar silicon conversion and lower power consumption (25, 26).

In this process using dichlorosilane as the silicon source material, wall deposits resulting from the dichlorosilane deposition reaction are not desirable. Representative bell jar silicon deposition is shown in Figure 11. The homogeneous gas phase reaction resulting in the formation of solid silicon particles (not on the rod surface) is also not desirable. The reduction of wall deposits has been investigated by Hemlock Semiconductor (26). One approach involved an advanced decomposition reactor with a cool bell jar temperature (300C) as compared with hot bell jar reactor (750C). The study also encompassed screening of lower cost materials of construction such as stainless steels and other metallic alloys.

A process design was performed to obtain data for a cost analysis of a process plant to produce 1,000 metric tons/yr of polysilicon via the Hemlock Semiconductor process.

Cost Analysis

Cost analysis results for producing polysilicon by the Hemlock Semiconductor process are displayed in Table 5 including raw materials, labor, utilities and other items. A total product cost without profit of 19.48 \$/kg Si (1985 dollars) is indicated.

The economic summary for the process is provided in Table 6 including plant investment, profitability analysis and sensitivity analysis.

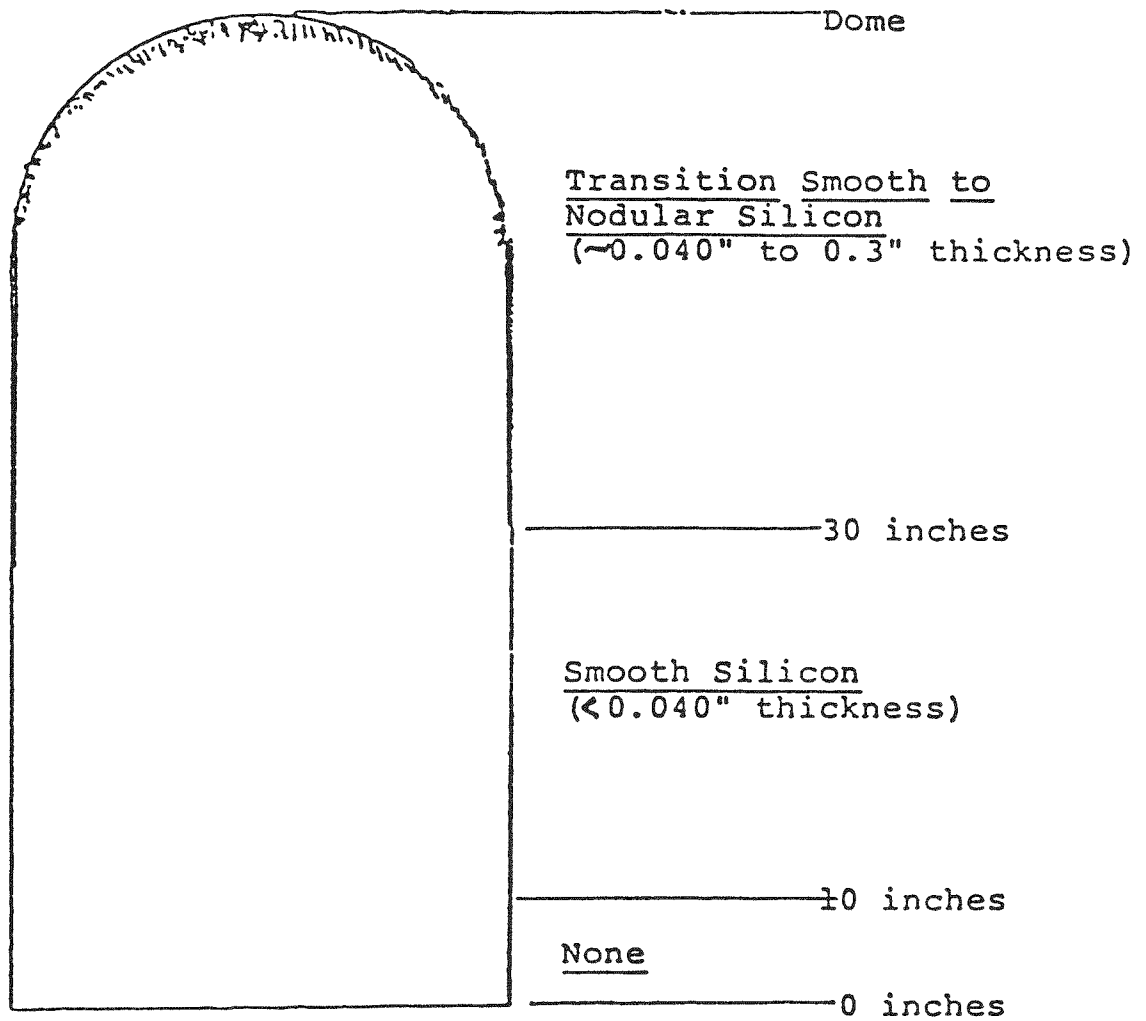


FIGURE 11. REPRESENTATIVE BELL JAR SILICON DEPOSITION (GOVERNMENT REPORT:HEMLOCK SEMICONDUCTOR, REF.25, PAGE 79)

TABLE 5

ESTIMATION OF PRODUCT COST FOR HEMLOCK SEMICONDUCTOR PROCESS

	COST \$/kg of Si -----
1. Direct Manufacturing Cost.....	11.05
Raw Materials	
Direct Operating Labor	
Utilities	
Supervision and Clerical	
Maintenance and Repairs	
Operating Supplies	
Laboratory Charge	
2. Indirect Manufacturing Cost.....	4.68
Depreciation	
Local Taxes	
Insurance	
3. Plant Overhead.....	1.21
4. General Expenses.....	2.54
Administration	
Distribution and Sales	
Research and Development	

5. Product Cost without Profit.....	19.48

Note: 1985 Dollars

TABLE 6

ECONOMIC SUMMARY: COST ANALYSIS FOR HEMLOCK SEMICONDUCTOR PROCESS

1. Process -----	HEMLOCK SEMICONDUCTOR PROCESS
2. Plant Size -----	1000 MT/yr
3. Plant Product -----	POLYSILICON
4. Plant Investment -----	\$ 41.40 Million

Fixed Capital ----	\$ 36.00 Million
Working Capital --	\$ 5.40 Million
Total Capital ----	\$ 41.40 Million

5. Profitability Analysis

Return on Original Investment after Taxes (% ROI)
Discounted Cash Flow Rate of Return after Taxes (% DCF)

Return	Sales Price \$/kg of Si	Return	Sales Price \$/kg of Si
0 % ROI	19.48	0 % DCF	19.48
10 % ROI	27.15	10 % DCF	24.67
20 % ROI	34.82	20 % DCF	30.72
30 % ROI	42.48	30 % DCF	37.38
40 % ROI	50.15	40 % DCF	44.44
50 % ROI	57.82	50 % DCF	51.74
60 % ROI	65.48	60 % DCF	59.18
70 % ROI	73.15	70 % DCF	66.72
80 % ROI	80.82	80 % DCF	74.30
90 % ROI	88.48	90 % DCF	81.91
100 % ROI	96.15	100 % DCF	89.55

Based on 10 year project life and 10 year straight line depreciation. Tax rate (federal) of 46 %.

6. Sensitivity Analysis

	Product Cost, \$/kg of Si					DELTA
	-100%	-50%	BASE	+50%	+100%	
Raw Materials	16.15	17.81	19.48	21.15	22.82	3.34
Labor	18.11	18.80	19.48	20.17	20.85	1.37
Utilities	14.63	17.06	19.48	21.91	24.34	4.85
Plant Investment (Fixed Capital)	12.55	16.02	19.48	22.95	26.42	6.93

Note: 1985 Dollars

The sensitivity analysis results for primary cost parameters is displayed in Figure 12. The product cost is influenced much by utilities (electrical energy).

5. COST COMPARISON

A cursory cost comparison for capital investment is made in Figure 13 for the Siemens process. In 1980, Wacker (12) announced a \$13 million capital investment for a 500 MT/yr polysilicon plant expansion (1,200–1,300 to 1,800 MT/yr). The first block in the figure shows this data. The second block with a capital investment of \$31.2 million represents this data adjusted to 1,000 MT/yr expansion and 1985 dollars. The third block presents the present study. The capital investment of \$69 million (complete plant) of the present study is higher than the \$31.2 million (plant expansion).

Results for capital investment for the Union Carbide process are displayed in Figures 14 and 15. In 1984, Union Carbide (9) announced its plans to start silane production in its \$85 million polysilicon facility (Moses Lake, Washington) capable of producing 1,500 MT/yr. The first block in Figure 14 presents this data. The second block shows the adjusted data of \$56.7 million (1,000 MT/yr, 1985 dollars). The result of \$74.8 million (1,000 MT/yr, 1985 dollars) for the present study is higher. In 1985, capital investment of \$90 million was reported (8) to double the capacity of the polysilicon facility to 2,400 MT annually. The adjusted value for a 1,000 MT/hr is about \$75 million (plant expansion). The adjusted value is about the same as the result of \$74.75 (complete plant) of the present study.

Capital investment results for the Hemlock Semiconductor process are presented in Figure 16. A capital investment of \$25.21 million (1980 dollars) for 1,000 MT/yr polysilicon plant using dichlorosilane as the silicon source material is given in the Hemlock Semiconductor report (25). The adjusted value is \$30.25 million (1985 dollars). The results of \$41.40 million (1985 dollars) of the present study are higher.

The results for product cost are shown in Figure 17 for the Hemlock Semiconductor process. A product cost for polysilicon of 15.60 \$/kg (1980 dollars) is presented in the Hemlock semiconductor report (25). The adjusted value is about 18.72 \$/kg (1985 dollars). The product cost of 19.48 \$/kg (1985 dollars) of the present study is slightly higher. Both results suggest product cost without profit is in the 20 \$/kg range.

Results for capital investment are shown in Figure 18 for Siemens, Union Carbide and Hemlock Semiconductor processes. The cursory comparison suggests that capital investment of \$41.4 million for the Hemlock Semiconductor process is lower than the \$69 million and \$74.75 million for Siemens and Union Carbide processes.

The results for product cost are given in Figure 19. The product cost per kg of polysilicon of \$29.49 for Siemens process appears to be the highest. The \$24.65 for Union Carbide process appears to be intermediate. The \$19.49 for Hemlock Semiconductor process appears to be lowest.

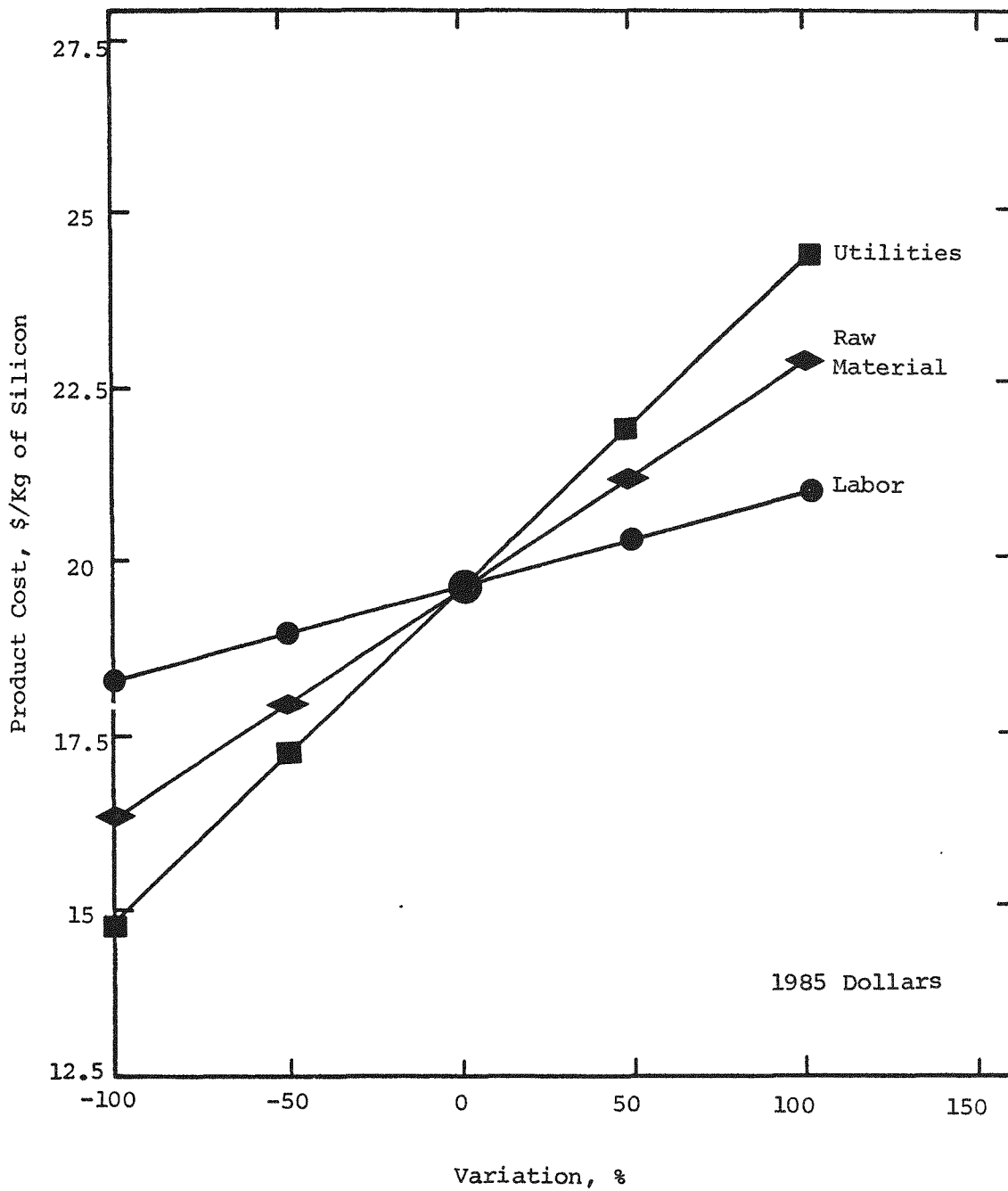


FIGURE 12. SENSITIVITY PLOT FOR HEMLOCK SEMICONDUCTOR PROCESS

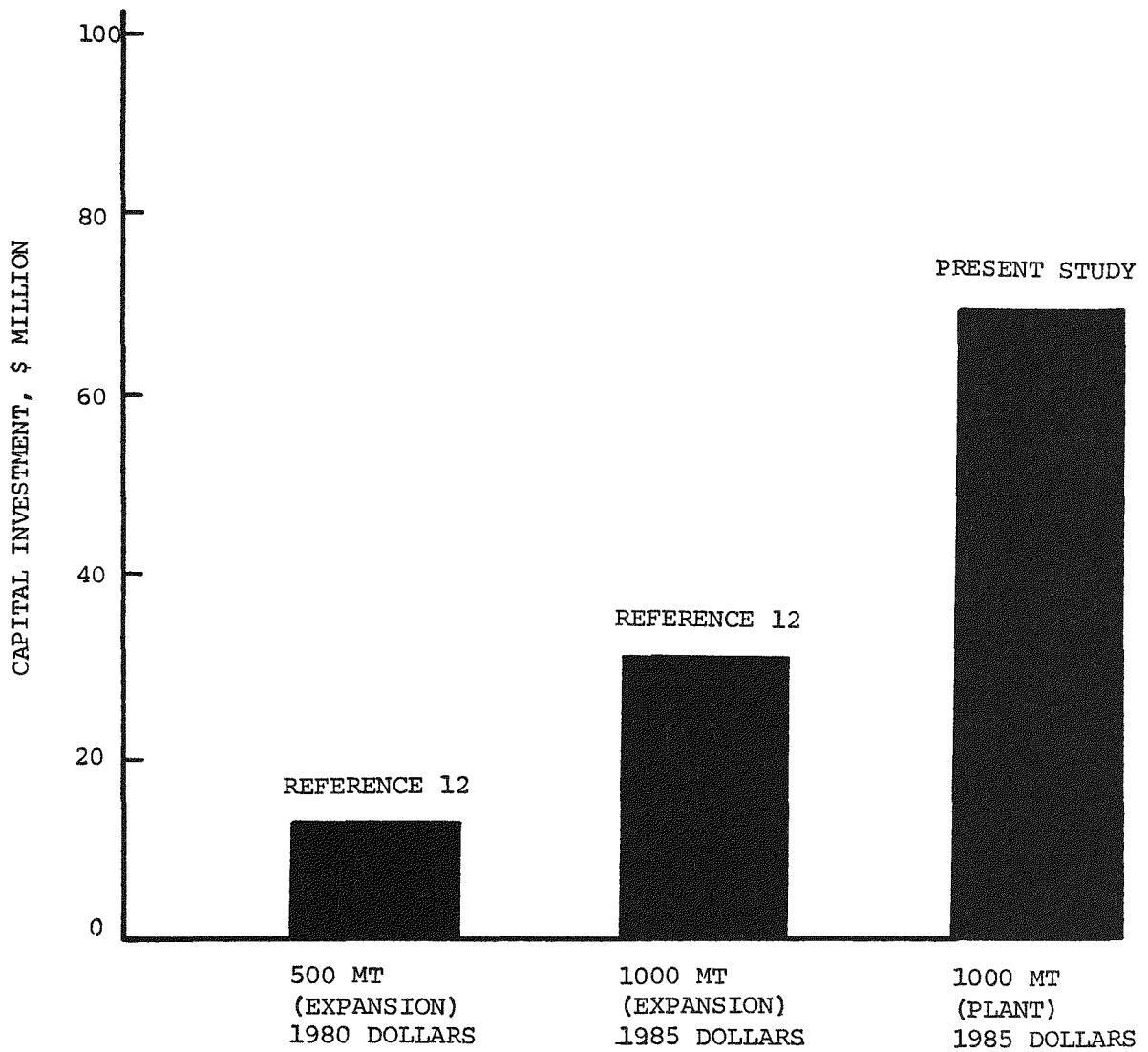


FIGURE 13 RESULTS FOR CAPITAL INVESTMENT: SIEMENS PROCESS

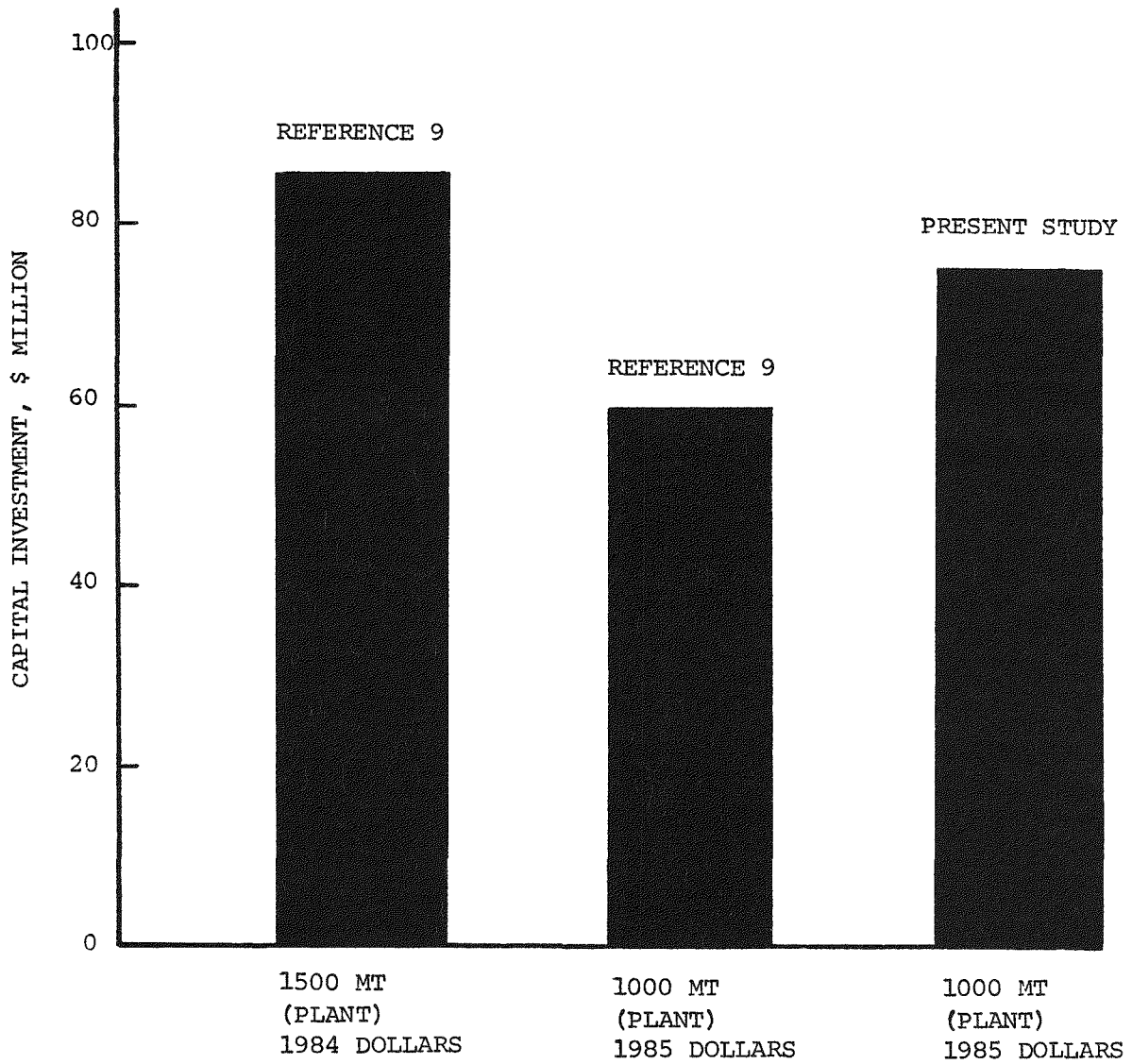


FIGURE 14 RESULTS FOR CAPITAL INVESTMENT: UNION CARBIDE PROCESS

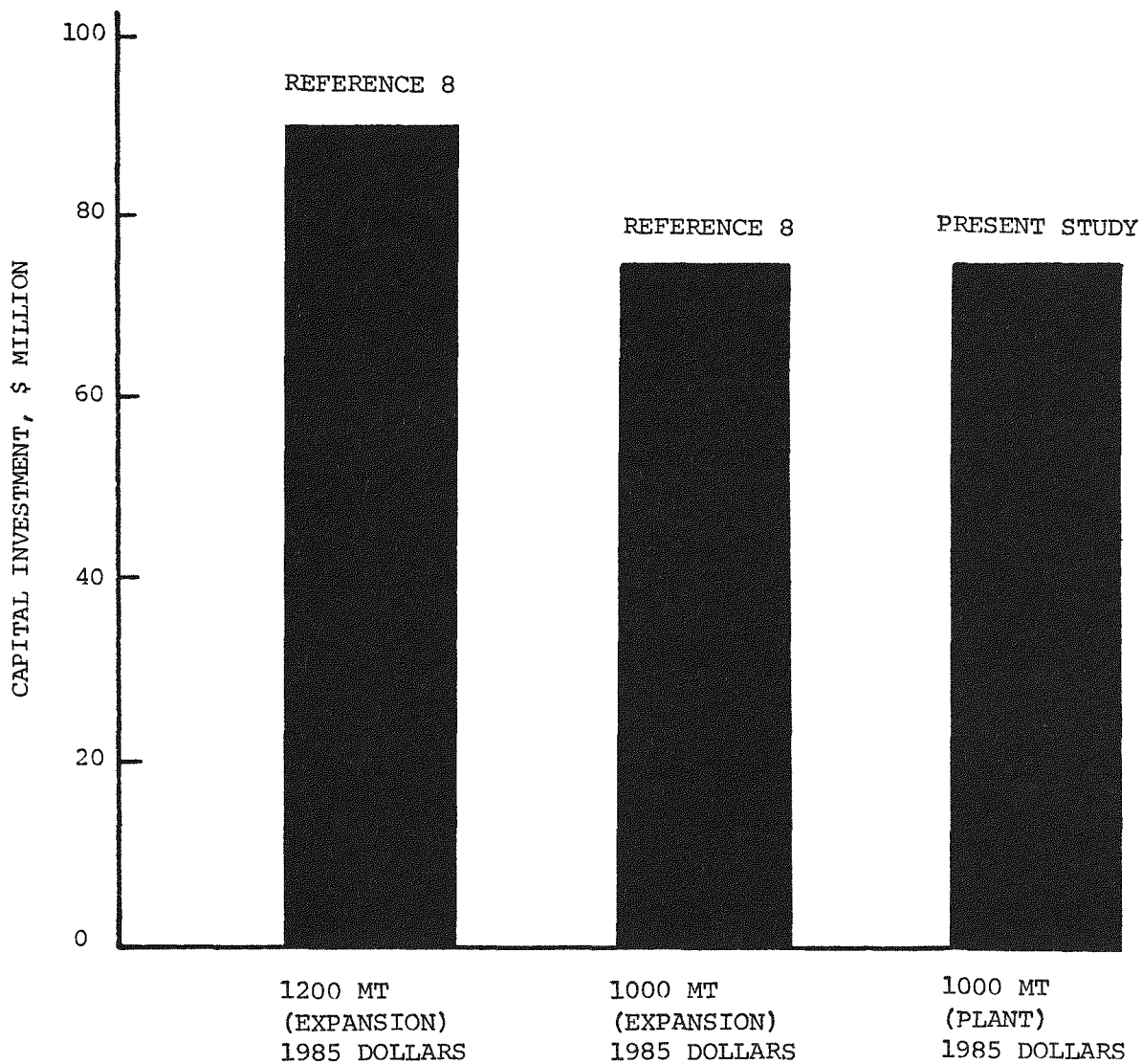


FIGURE 15 RESULTS FOR CAPITAL INVESTMENT: UNION CARBIDE PROCESS

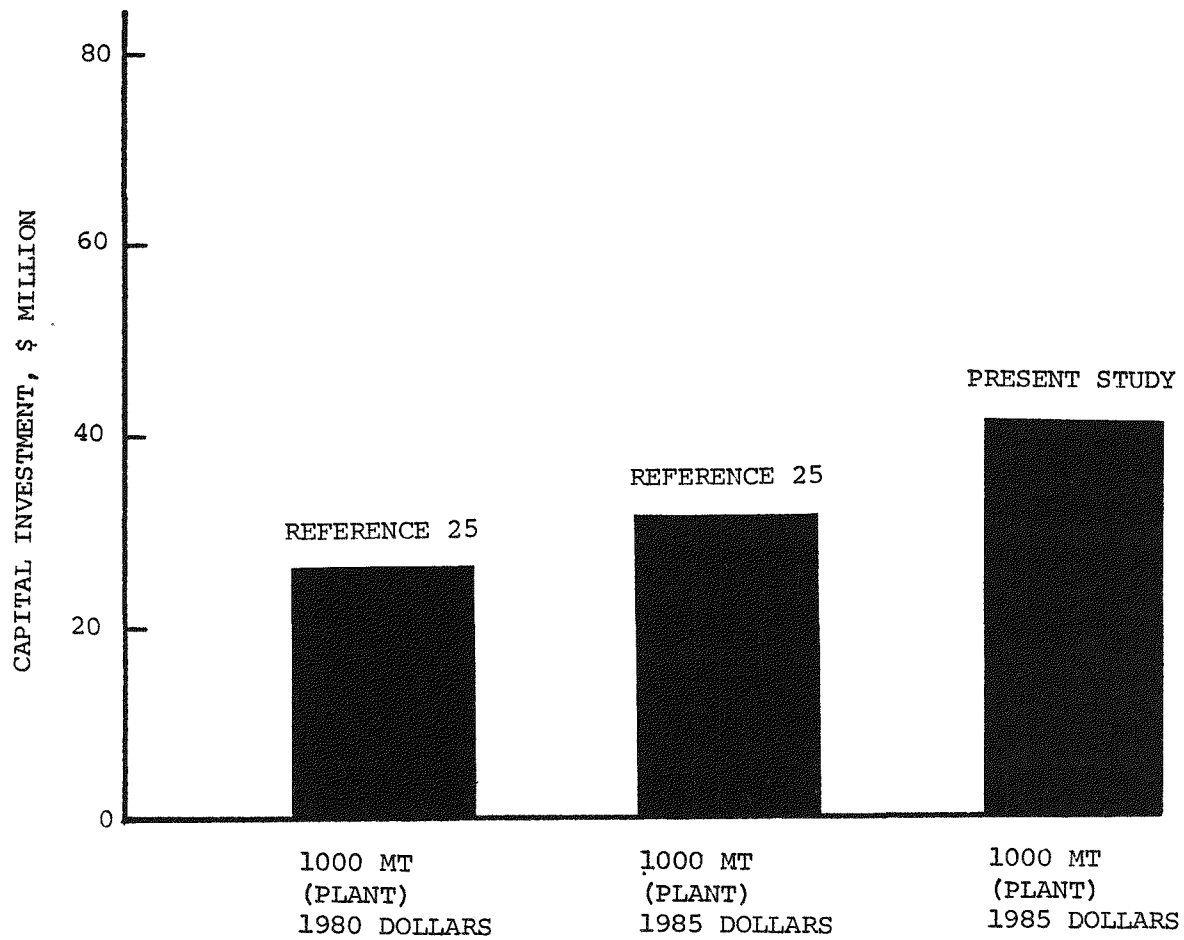


FIGURE 16 RESULTS FOR CAPITAL INVESTMENT: HEMLOCK SEMICONDUCTOR PROCESS

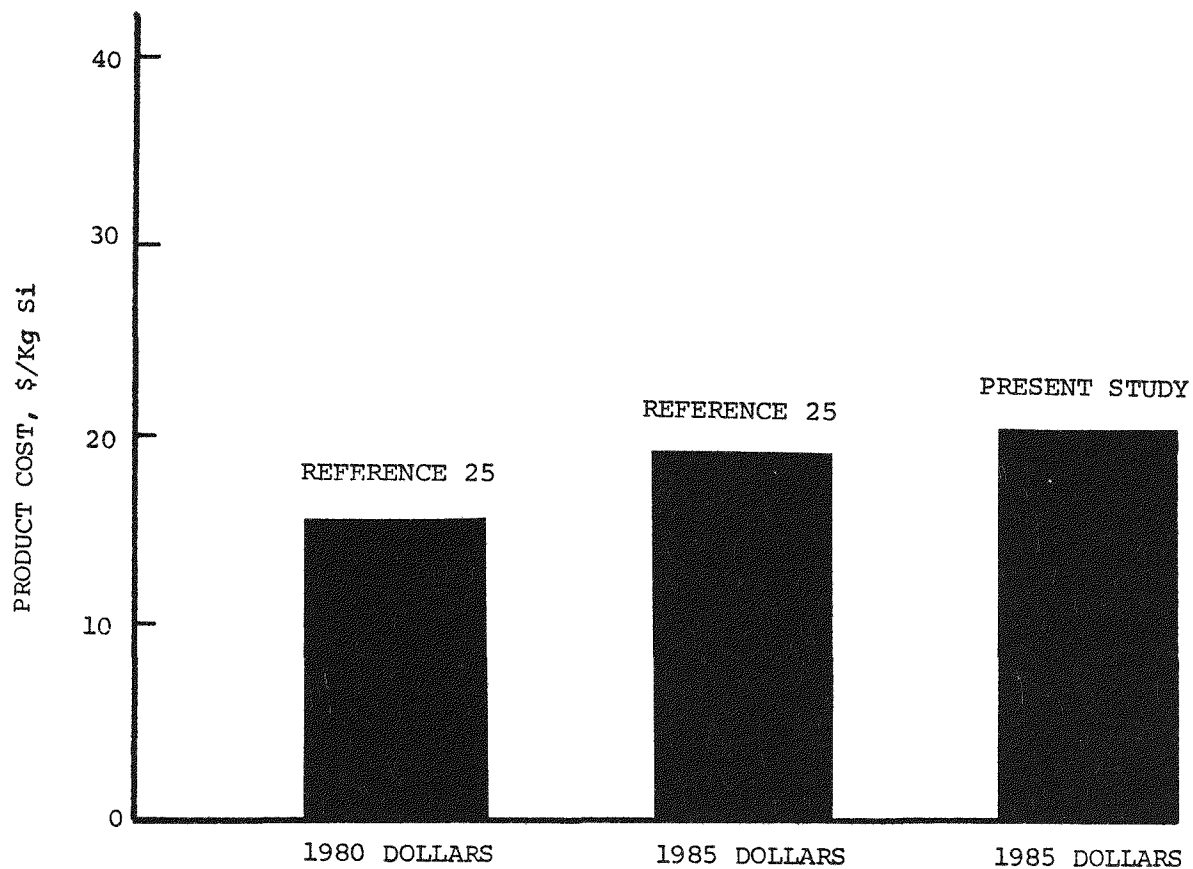


FIGURE 17 RESULTS FOR PRODUCT COST: HEMLOCK SEMICONDUCTOR PROCESS

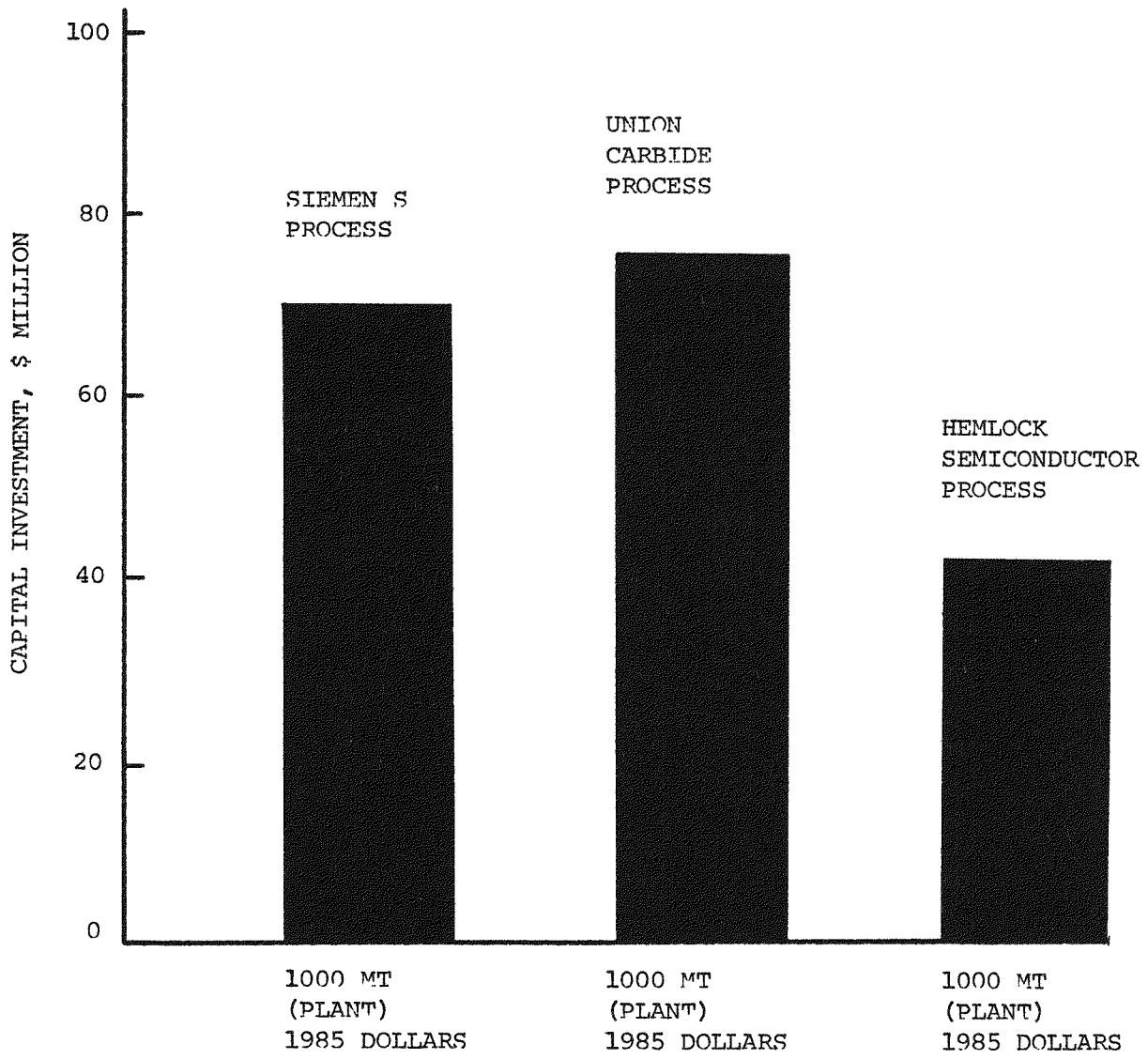


FIGURE 18 RESULTS FOR CAPITAL INVESTMENT

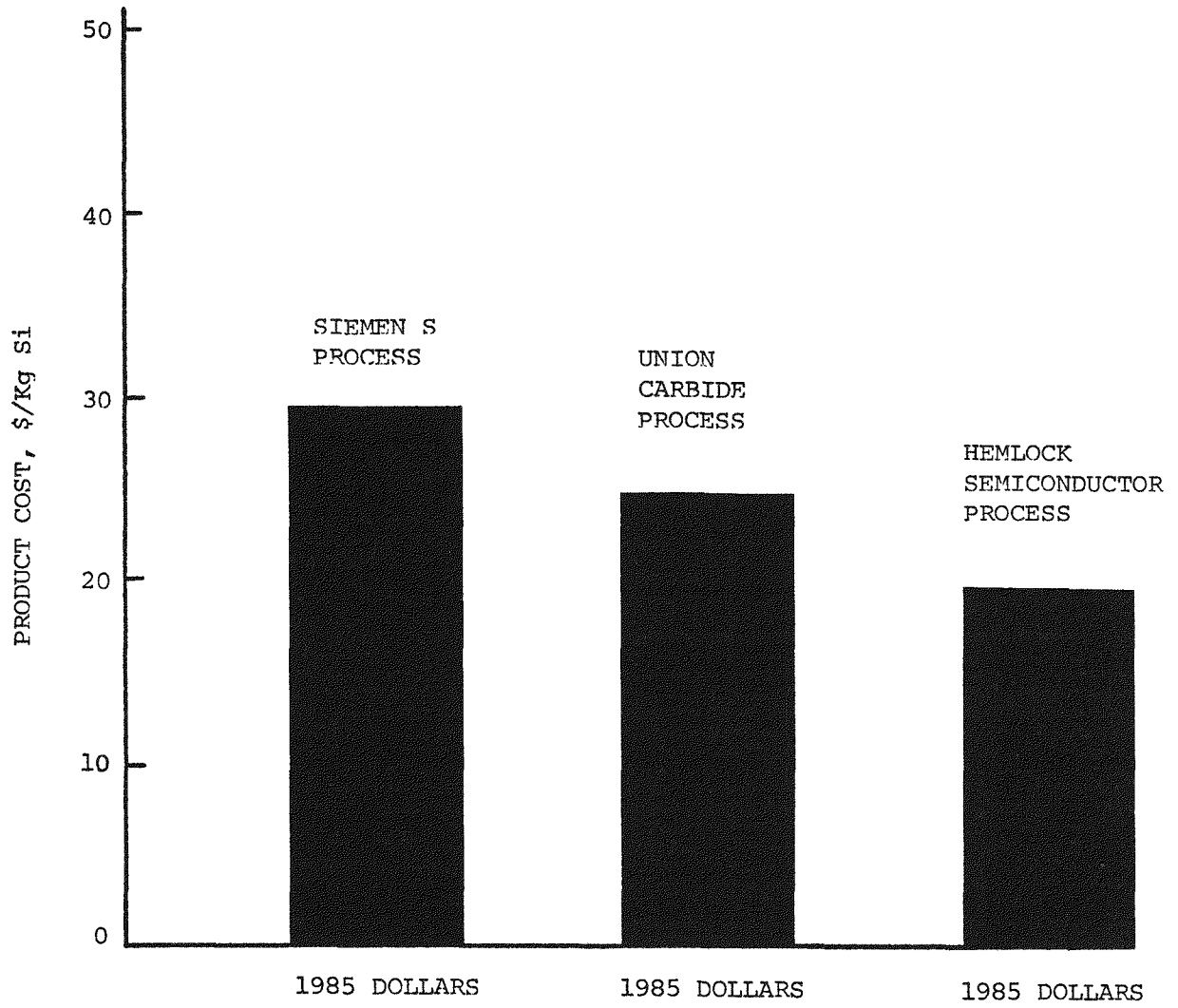


FIGURE 19 RESULTS FOR PRODUCT COST

6. OTHER PROCESSES

Other processes that depart from conventional technology are also under consideration for the production of polysilicon:

1. Zinc Reduction of Silicon Tetrachloride (Batelle Columbus Laboratories)
2. Bromosilane Process (J. C. Schumacher Co.)
3. Sodium Reduction of Silicon Tetrafluoride (SRI International, Inc.)
4. Sodium Reduction of Silicon Tetrachloride (AeroChem Research Laboratories, Inc., and Universal Silicon, Inc.).
5. Direct-Arc Furnace Process (Dow Corning Corporation)
6. Silicon Difluoride Transport Process (Motorola Inc.)
7. Carbothermic Reduction of Silicon Dioxide (Texas Instruments, Inc.)
8. Rotary Chamber Reactor for Use in a Closed-Cycle Process (Texas Instruments, Inc.)
9. High-Capacity Arc Heater Process (Westinghouse Electric Corporation)
10. Gaseous Melt Replenishment System (Energy Materials Corporation)
11. FBR Process (Osaka Titanium Co.)
12. Refining of Metallurgical-Grade Silicon (Heliotronic, GmbH)
13. Solar Cell Grade Silicon Prepared By Carbothermic Reduction of Silica (Siemens Research Laboratories)
14. A Metallurgical Route to Solar Grade Silicon (Elkem)
15. Solar Silicon From Directional Solidification of MG Silicon Produced Via The Silicon Carbide Route (Enichmico)
16. Silane Based Polysilicon Process (Eagle-Picher Industries, Inc.)
17. Silicon Purification Using A Cu-Si Alloy Source (Solar Energy Research Institute)

Initial economics of process 1 are given by Yaws (38, 39). Several recent news releases (16-18) relate to process 2. A good summary of processes 1-9 is provided by Lutwack (24). Process 10 is reported by Jewett, Bates and Hill (47). The remaining processes 11-17 are discussed in the proceedings of this meeting.

7. SUMMARY AND CONCLUSIONS

The following summary and conclusions are made as a result of the present study:

1. The economics of producing polysilicon in a 1,000 MT/yr plant are presented for the Siemens process (hydrogen reduction of trichlorosilane), Union Carbide process (silane decomposition) and Hemlock Semiconductor process (hydrogen reduction of dichlorosilane). The economics include estimates of capital investment and product cost to produce the polysilicon.
2. For the Siemens process using trichlorosilane, the product cost without profit is estimated to be 29.49 \$/kg Si (1985 dollars). This product cost includes provisions for hydrogen recycle, hydrogen chloride recycle and chlorosilane recycle. Without such raw material recycle, the product cost will be higher. The product cost also includes low electrical usage (120 kw-hr/kg Si). If higher

electrical usage is required, the product cost will be higher.

3. For the Union Carbide process using silane in a hot rod reactor (Komatsu), the product cost without profit is estimated to be 24.65 \$/kg Si (1985 dollars). This product cost assumes reasonable resolution of homogeneous gas phase decomposition reaction. Electrical usage is estimated at 62.4 kw-hr/kg Si.

4. For the Hemlock Semiconductor process using dichlorosilane, the product cost without profit is estimated at 19.48 \$/kg Si. This product cost assumes reasonable resolution of wall deposits and homogeneous reaction. An overall electrical power consumption of 82 kw-hr/kg Si is used.

5. A cursory cost comparison is made for capital investment cost. For the Siemens process, the comparison suggests that the capital investment of \$69 million of the present study may be high. For the Union Carbide process, the comparison indicates that the capital investment of the present study may be slightly high or equivalent. For the Hemlock semiconductor process, the comparison suggests that the capital investment of the present study may be slightly high.

6. The polysilicon economics (capital investment, product cost) presented in the present study are intended for use in initial project studies.

Acknowledgement

The JPL Low-Cost Solar Array Project is sponsored by the U. S. Department of Energy and forms part of the Solar Photovoltaic Conversion Program to initiate a major effort toward the development of low-cost solar arrays. A portion of this work was performed for the Jet Propulsion Laboratory, California Institute of Technology by agreement between NASA and DOE.

REFERENCES

1. Bawa, M. S., R. C. Goodman and J. K. Truitt, "Kinetics and Mechanism of Deposition of Silicon by Reduction of Chlorosilanes with Hydrogen", Chem. Vap. Dep. 4th Int. Conf., Electro. Chem. Soc., Princeton, N. J., pgs. 63-73, (1973).
2. Ciszek, T. F., "Silicon for Solar Cells", Government Report, SERI/TR-212-2084, DE 84004503, Solar Energy Research Institute (April, 1984).
3. Costogue, E. N., R. R. Ferber and R. Lutwack, "Polycrystalline Silicon Study", Government Report, DOE/ET/20356-17, DE 85000327, Jet Propulsion Laboratory (May, 1984).
4. Costogue, E. N. and R. Pellin, "Polycrystalline Silicon Material Availability and Market Pricing Outlook Study for 1980 to 88", Government Report, DOE/JPL-1012-79A, DE 84001226, Jet Propulsion Laboratory (February, 1983).
5. Dudukovic, M. P., P. A. Ramachandran and S. Lai, "Modeling of Fluidized-Bed Reactors for Manufacture of Silicon from Silane", Government Report, DOE/JPL-956737-8517, Distribution Category UC-63, Washington University (September, 1985).
6. Ecco High Frequency Corp., Personal Communication, North Bergen, N.J. (1977)
7. Electronic News, "Carbide Gets Silane License (Komatsu)", 58 (May 11, 1981).
8. Electronic News, "UC to Double Moses Lake Capacity", \$90 million for double capacity to 2,400 tons annually, 71 (January 28, 1985)
9. Electronic News, "Carbide to Start Silane Production", \$85 million for 1,500 tons per year, 15 (December 24, 1984)
10. Electronic News, "Mitsubishi Buys 12.25% Hemlock Stake", \$47 million for plant expansion of 1,000-1,200 tons annually, 15 (December 24, 1984).
11. Electronic News, "Say Poly Shortage Possible by 1987", \$47 million to increase production by 1,000 tons annually, 47 (January 7, 1985).
12. Electronic News, "Wacker in \$13M Poly Plant Expansion", \$13 million for increase of capacity from 1,200-1,300 to 1,800 metric tons per year, 69 (October 20, 1980).
13. Electronic News, "Siltronic (Wacker) to Build \$80 M Polysilicon Plant", \$80 million for polysilicon plant to be capable of manufacturing 5,000 metric tons per year, 70 (October 6, 1984).

14. Electronic News, "Toxic Substances Delay Building of Wacker Poly Plant", 63 (June 24, 1985).
15. Electronic News, "GE to Sell Poly Plant to NKK, Exit Market", \$16 million for poly plant with reported 200 metric tons capacity, 62 (October 7, 1985).
16. Electronic News, "Schumacher Names Materials Mgnt.", process of choosing sites for 1,000 tons/year polysilicon facility, 61 (January 21, 1985).
17. Electronic News, "Schumacher Breaks Out Chemical Div.", Semiconductor Materials Division for capital intensive polysilicon plants, 41 (April 15, 1985).
18. Electronic News, "Schumacher Plans Wafer Mfg. Facilities", company expects to start up pilot poly plant (50-75 metric tons), 54 (September 30, 1985).
19. Electronic News, "Site Selection", 3 (September 23, 1985).
20. Iya, S. K., R. N. Flagella and F. S. DiPaolo, J. Electrochem. Soc., 129 (7), 1531 (July, 1982).
21. Komatsu (Assignee, Japan), Yatsurgi, Y., A. Yusa and N. Takahashi (Inventors), U.S. Patent 4, 147, 814 (April 3, 1979).
22. Komatsu (Assignee, Japan), Yatsurgi Y., A. Yusa and N. Takahashi (Inventors), U.S. Patent 4, 150, 168 (April 17, 1979).
23. Levenspiel, O., et. al., "Preliminary Study of a Radiantly Heated Fluidized Bed for the Production of High Purity Silicon", Government Report, DOE/JPL-956133-83-1, DE 83016569, Oregon State University (August, 1983).
24. Lutwack, R., "A Review of the Silicon Material Task", Government Report, DOE/JPL-1012-96, DE 84014599, Jet Propulsion Laboratory (February, 1984).
25. McCormick, J. R., et. al., "Development of a Polysilicon Process Based on Chemical Vapor Deposition (Phase 1 and Phase 2)", Government Report, DOE/JPL-955533-83/7, DE 84004975, Hemlock Semiconductor Corporation (August, 1982).
26. McCormick, J. R., et. al., "Development of a Polysilicon Process Based on Chemical Vapor Deposition of Dichlorosilane in an Advanced Siemens Reactor", Government Report, DOE/JPL-955533-83, DE 84017155, Hemlock Semiconductor Corporation (July, 1983).
27. Mui, J.Y.P., "Investigation of the Hydrochlorination of SiCl_4 ", Government

- Report, DOE/JPL-956061-7, DE 83015173, Solarelectronics (April, 1973).
28. Murthy, T.U.M.S., N. Miyamoto, M. Shimbo and J. Nishiyawa, J. of Crystal Growth, 33, 1 (1976).
 29. Reiter, L. J., "A Probabilistic Analysis of Silicon Cost", Government Report, DOE/JPL/1012-93, DE 84005741, Jet Propulsion Laboratory (November, 1983).
 30. Rogers, Leo, "Polycrystalline Silicon Plants", News Release, Polycrystalline Silicon Technology Corporation (P.S.T.), Mesa, Arizona (June 15, 1985).
 31. Smiel, "Silicon for the Semiconductor Industry", Company Brochure, MONTEDISON Group (May, 1979).
 32. TREI, "Silicon Production Process Evaluations", Government Report, DOE/JPL-956045-82/5, Distribution Category UC-63 (July, 1982).
 33. Wacker (Assignee, Germany), Koppl, F. and H. Hamster (inventors), U.S. Patent 4,173,944 (Nov., 1979).
 34. Yaws, C.L., T. G. Digges, Jr., M. A. Drews and B. J. Boggs, "High Purity Silicon Manufacturing Facility", Government Report AFRL-TR-71-130, Texas Instruments (July 1971).
 35. Yaws, C. L., J. W. Miller, Jr., R. Lutwack and G. Hsu, "Electricity from Sunlight: Low Cost Silicon for Solar Cells", Energy and the Environment-Proceedings of the Fifth National Conference, A.I.Ch.E.-A.P.C.A., p. 329, Cincinnati, Ohio (Oct. 31-Nov. 3, 1977).
 36. Yaws, C. L., J. W. Miller, Jr., R. Lutwack, and G. Hsu, Solid State Technology, 63 (January, 1979).
 37. Yaws, C. L., F. C. Jelen, K. Y. Li, P. M. Patel and C. S. Fang, Solar Energy, 22 (No. 6), 547 (1979).
 38. Yaws, C. L., K. Y. Li, C. S. Fang, R. Lutwack, S. Hsu and H. Leven, Solar Energy, 24 (No. 6), 359 (1980).
 39. Yaws, C. L., et. al., "Process Feasibility Study in Support of Silicon Material Task I", Government Report, Jet Propulsion Laboratory, Contract No. 954343, DOE/JPL-954343-81, Distribution Category UC-63, Lamar University (February, 1981).
 40. Yaws, C. L., K. Y. Li, T. C. T. Chu, C. S. Fang, R. Lutwack and A. Briglio, Solar Energy, 27 (No.6), 539 (1981).
 41. Chen, C.C., M. M. Chang, F. R. Shu and C. S. Liu, J. Ch. I. Ch. E., 5, 93 (1974).

42. Chen, C.C., M. M. Chang, C. S. Liu, C. T. Chang and F. R. Shu, J. Ch. I. Ch. E., 5, 99 (1974).
43. Chen, C.C., M. M. Chang, F. R. Shu and C. S. Liu, J. Ch. I. Ch. E., 5, 107 (1974).
44. Peters, M. S., and K. D. Timmerhaus, "Plant Design and Economics for Chemical Engineers," 3rd edition, McGraw-Hill Book Co., N.Y. (1980).
45. Ingle, W. M. and R. D. Darnell, J. Electrochem. Soc., 1236 (May, 1985)
46. Ingle, W. M. and R. D. Darnell, J. Electrochem. Soc., 1240 (May, 1985).
47. Jewett, D. N., H. E. Bates and D. M. Hill, "Gaseous Melt Replenishment System," Government Report, DOE/JPL-955269-80/1, Distribution Category VC-63, Energy Materials Corporation (April, 1980).

APPENDIX A

COSTS USED IN ECONOMIC ANALYSIS

1. Raw Material Costs

	<u>Raw Material</u>	<u>Raw Material Cost</u>
1.	M. G. Silicon	.763 \$/lb
2.	Silicon Tetrachloride	.227 \$/lb
3.	Liquid Hydrogen	9 \$/1000 ft ³
4.	Copper Catalyst	1.548 \$/lb
5.	Hydrate Lime	.0252 \$/lb
6.	Hydrogen Chloride	.168 \$/lb
7.	Nitrogen	4.08 \$/1000 ft ³

Source: Hemlock Semiconductor (ref. 25), page 129, adjusted to 1985 dollars

2. Utility Costs

	<u>Utility</u>	<u>Cost of Utility</u>
1.	Electricity	5 /kw-hr
2.	Steam	1.89 \$/mmBTU
3.	Hot Oil	1.89 \$/mmBTU
4.	Cooling Water	.144 \$/mgal
5.	Process Water	.680 \$/mgal
6.	Refrigerant (-40°F)	18.68 \$/mmBTU
7.	Refrigerant (34°F)	3.75 \$/mmBTU
	m = 1,000	
	mm = 1,000,000	

Source: Hemlock Semiconductor (ref. 25), page 128, and Peters and Timmerhaus (ref 43), page 881, adjusted to 1985 dollars

3. Labor Cost 12.00 \$/hr

Source: Electronic News (ref. 19)

APPENDIX B

CHECKLIST FOR CHEMICAL ENGINEERING ANALYSIS

121

<u>Prel. Process Design Activity</u>	<u>Status</u>	<u>Prel. Process Design Activity</u>	<u>Status</u>
1. Specify Base Case Conditions	●	7. Equipment Design Calculations	●
1. Plant Size	●	1. Storage Vessels	●
2. Product Specifics	●	2. Unit Operations Equipment	●
3. Additional Conditions	●	3. Process Data (P, T, rate, etc.)	●
		4. Additional	●
2. Define Reaction Chemistry	●	8. List of Major Process Equipment	●
1. Reactants, Products	●	1. Size	●
2. Equilibrium	●	2. Type	●
3. Process Flow Diagram	●	3. Materials of Construction	●
1. Flow Sequence, Unit Operations	●	8a. Major Technical Factors	●
2. Process Conditions (T, P, etc.)	●	(Potential Problem Areas)	●
3. Environmental	●	1. Materials Compatibility	●
4. Company Interaction	●	2. Process Condition Limitations	●
(Technology Exchange)		3. Additional	●
4. Material Balance Calculations	●	9. Production Labor Requirements	●
1. Raw Materials	●	1. Process Technology	●
2. Products	●	2. Production Volume	●
3. By-Products	●	10. Forward for Economic Analysis	●
5. Energy Balance Calculations	●		
1. Heating	●	○ Plan	
2. Cooling	●	● In Progress	
3. Additional	●	● Complete	
6. Property Data	●		
1. Physical	●		
2. Thermodynamic	●		
3. Additional	●		

DISCUSSION

SHIMIZU: This morning, I presented a paper about the same subject and I obtained quite different conclusions. Would you comment on my paper?

YAWS: Although I didn't write down complete notes on your paper, the order in which the processes was placed is about the same as in my analysis. I think you had the Hemlock Semiconductor process lower than the Union Carbide process with the Komatsu reactor, and you had the conventional Siemens process at a higher cost than Union Carbide.

SHIMIZU: Also, this morning, I compared those processes and others. In the case of silane, I compared two processes. One was the fluidized-bed reactor process, and the other was the Komatsu reactor.

YAWS: The comparison showed that the Union Carbide process with the Komatsu reactor had a lower production cost than the Siemens process.

SHIMIZU: In my estimate, the cost is about 80% that of the conventional Siemens process.

YAWS: Your table showed that the Siemens process is the most expensive. Union Carbide, using the Komatsu reactor, is second. The third is Hemlock using dichlorosilane. Those are the same results that I got. Now the numbers may be a little different, but I think our ranking orders are the same. I didn't look at as many processes as you did.

WRIGHT: You used a scaling factor for production levels from about 1500 MT/year down to 1000 MT/year. Was that a linear scaling factor? What was your justification for using that particular scaling factor?

YAWS: For normal chemical industry equipment, the factor is about 0.6, or a scaling factor which has been determined to be best for a specific type of equipment can be used. I assumed that the major cost was in reactors so that a linear factor was used for additional reactors.

PRINCE: Did you make the calculations for the Union Carbide process with the fluidized-bed reactor?

YAWS: No. That was not part of this study. The calculations were for the Union Carbide process operating with Komatsu deposition reactors.

AULICH: Your calculations were for 1000 MT/year. Since 1000 MT/year capacity plants are not needed now for the photovoltaic industry, what is the analysis of the cost of these processes if smaller units of about 200 MT/year are used?

YAWS: Smaller plants would result in higher costs. Someone would have to do a study to get the answers. I can't respond to your question now, because I haven't done the analysis, but it can be done.

SENSITIVITY ANALYSIS FOR SOLAR PANELS

Robert W. Aster
Jet Propulsion Laboratory
Pasadena, California

The Project Analysis and Integration (PA&I) task of the Flat-Plate Solar Array (FSA) project has prepared economic evaluation methods and analyses of emerging photovoltaic (PV) technology since 1976. The purpose of this paper is to apply this type of analysis to the silicon research portion of the PV Program in order to determine the importance of this research effort in relationship to the successful development of commercial PV systems.

This analysis addresses all four of the generic types of PV that use silicon. The first generic type of PV is the one that uses the most silicon, where crystalline silicon ingots are grown either by the Czochralski method or by some sort of ingot casting method. The second type of PV uses ribbons that are pulled directly from molten silicon, thus avoiding material losses associated with sawing wafers from an ingot. The third type of PV device is an amorphous silicon thin film, which attempts to achieve low cost by minimizing silicon material utilization. A fourth type of PV device is the concentrator system, which can use high concentration lenses (500x to 1000x) to minimize silicon material utilization. This last type of PV technology can be analyzed very simply because the amount of silicon used will be roughly 500 to 1000 times less per unit of PV energy produced than would be the case with the first generic type of PV.

SILICON COST RANGE

In order to show the value of the silicon research program, it is first necessary to construct a hypothetical range of silicon prices that would occur if there had been no program. In 1975, at the start of the program, the price of semiconductor grade polycrystalline silicon was \$50/kg. In order to standardize financial units, this cost figure (and all subsequent cost figures in this paper) will be inflated to 1982 dollars. Inflation over that period was a factor of 1.68, thus if the price of silicon had increased with inflation it would now be \$84/kg in 1982 dollars. However, the market price of silicon fluctuates due to changes in supply and demand, so that a price range of \$50/kg to \$120/kg in 1982 would be appropriate.

However, a silicon manufacturing research program has been conducted since 1975, which is expected to have a significant impact on future silicon price. L. Reiter (Ref. 1) conducted a study where PV prices were projected for the 1990s. In this study, price was defined as the revenue required to meet all direct and indirect costs, including the after-tax return on investment that is normally obtained by the chemical industry. Three technologies were analyzed: the Union Carbide fluidized bed reactor process,

the Hemlock process, and the Union Carbide Komatsu process. The major components of each process were assessed in terms of the costs of capital equipment, labor, materials, and utilities. These assessments were encoded as the probabilities assigned by experts for achieving various cost values or production rates. The result was a combined probability curve of silicon cost. This is a reasonable approach because of the uncertainties inherent in a research program and in projections of the future. The 1st and 99th percentiles of the resulting probability curve were approximately \$10/kg and \$30/kg (in 1982 dollars), respectively. These values are used in this analysis as the range of silicon prices that may be found in the industry in the 1990s, due to the silicon research program.

The impact of silicon research on PV costs is determined not only on the two cost ranges described above, but also on the amount of silicon needed to construct a PV device. This amount will vary with different types of PV technology.

INGOT AND RIBBON PHOTOVOLTAICS

Ingots require the greatest amount of silicon per square meter of PV cell. The thickness of the wafer must be increased by the size of the kerf loss, which varies with different types of saws. Silicon utilization is also reduced by ingot growth losses, slicing losses, and cell manufacturing yields. Table 1 provides representative values for each of these parameters, and shows that between 1.6 and 2.8 kilograms of silicon are required for every square meter of PV cell area.

Table 1. Ingot PV Silicon Mass per Square Meter of Cell

Thickness (mils)	Saw Type	Representative Yields (%)				Kilograms of Silicon per Square Meter of Cell
		Growth	Slice	Cells	Cumulative	
16	Wire	95	70	85	57	1.68
20		95	90	85	73	1.63
24	ID MBS	95	95	85	77	1.85
28		95	95	85	77	2.16
32		95	95	85	77	2.47
36		95	95	85	77	2.78

One of the major reasons for the development of ribbon technology is to reduce the amount of silicon that must be utilized to manufacture PV cells. Table 2 shows the thickness associated with four types of ribbon. Typically these range from 4 mils to 14 mils of crystal thickness, with no kerf loss. As a result, the number of kilograms of silicon per square meter of cell is reduced significantly.

Table 2. Ribbon PV Silicon Mass per Square Meter of Cell

Thickness (mils)	Ribbon Type	Representative Yields (%)			Kilograms of Silicon per Square Meter of Cell
		Growth	Cells	Cumulative	
4	Web	90	85	77	0.31
6		90	85	77	0.46
8	EFG	95	85	81	0.59
10		95	85	81	0.73
12	ESP	95	85	81	0.88
14		95	85	81	1.03

The results of Tables 1 and 2 can be combined with the silicon cost ranges developed previously to show the contribution of silicon to PV module cost. This is done in Table 3, where the contribution to PV module cost is expressed in 1982 \$/sqm. In these units it is possible to compare those results with the DOE Program goal for modules, which is \$90/sqm. It can be seen immediately that without a silicon research program that ingot PV would have no chance of meeting the DOE goal, particularly when it is realized that part of that goal must be allocated to the costs of ingot growth and slicing, cell fabrication, and module encapsulation (Ref. 2,3). In the latest published set of Allocation Guidelines (pg 502, Ref. 3), the allocation for silicon and sheet fabrication (including costs associated with labor, investment, and utilities, as well as for materials) for an advanced, 15% efficient module is \$31 per square meter in 1982 dollars. Because of the silicon research program, ingot technology may have some chance of meeting the DOE energy cost goal, particularly if cell efficiencies can be increased above 15%, but only if silicon utilization rates are minimized and silicon price comes in at the low end of the probability range, and reductions in the other costs of sheet production (ingot growth and slicing) are realized.

Ribbon technology has what appears to be a more realistic chance of achieving the DOE energy cost goal because it uses less silicon. The silicon cost reduction research program still plays an important role in the development of this technology, however, because it provides potential cost reductions that range from \$14/sqm to \$106/sqm of cell.

Table 3. Silicon Contribution to Ingot PV cost

Sheet Type	Kilograms of Silicon per Square Meter Cell	Silicon Cost (1982 \$/kg)					
		10	20	30	50	84	120
Ribbon	0.30	3	7	10	17	28	41
	0.45	5	10	15	25	43	61
	0.60	7	14	20	34	57	81
	0.75	8	17	25	42	71	102
	0.90	10	20	30	51	85	122
	1.05	12	24	36	59	99	142
Ingot	1.60	18	36	54	90	152	217
	2.00	23	45	68	113	190	271
	2.40	27	54	81	135	227	325
	2.80	32	63	95	158	265	379

A burden rate of 20% and a cell-to-module area ratio of 0.94 are assumed.

AMORPHOUS SILICON PHOTOVOLTAICS

Amorphous silicon is grown from silane. High efficiency is required, and in order to obtain high efficiency, it is likely that only very pure (device grade) silane can be used. At this time, device grade silane costs from \$500/kg to \$2000/kg. In industrial quantities this cost range might go down to \$200 to \$500/kg. However, a spinoff from the silicon research program is a Union Carbide method to produce very pure silane at a cost of \$5/kg to \$10/kg.

An important feature of thin film photovoltaics is the fact that very little material is used. Material requirements will be proportional to device thickness, silane utilization rates, and module yield. In this analysis, a nominal thickness of 0.7 microns is used, along with a range of silane utilization rates of 2% to 40%. Module yield is not known at this time, but for purposes of this analysis a range of 50% to 100% is used. The 50% figure was selected as a lower bound because it is unlikely that amorphous silicon would be commercially viable at lower yields, due to the costs of module encapsulation materials and processing (Ref. 4).

Table 4 shows the amount of silane used per square meter of cell area, based on the figures described above. It can be seen that material utilization is indeed lower for this technology. The worst case amorphous silicon material requirement is a factor of 2 less than the lowest silicon material requirements for ribbon technology, and in most cases it is a great deal lower.

Table 4. Amorphous Silicon Silane Mass per Square Meter of Cell

Kilogram Silane per Square Meter of Cell	Silane Cost (\$/kg)			
	5	10	200	500
0.005	0.03	0.06	1.13	2.82
0.010	0.06	0.11	2.26	5.64
0.020	0.11	0.23	4.51	11.28
0.030	0.17	0.34	6.77	16.92
0.040	0.23	0.45	9.02	22.56
0.050	0.28	0.56	11.28	28.20
0.100	0.56	1.13	22.56	56.40
0.150	0.85	1.69	33.84	84.60

A burden rate of 20% and a cell-to-module area ratio of 0.94 are assumed.

These low silane material requirements are combined with the rather large silane cost range in Table 5, to obtain silane contribution to the cost of an amorphous PV module, in 1982 dollars per square meter of module. It can be seen immediately that the lower silane costs that may result from the silicon research program significantly reduces the sensitivity of silane utilization rate on module cost, and thus may simplify the development of this technology considerably. If silane cost were to remain at \$500/kg, then material utilization rates would be a critical parameter which might conceivably compromise the achievement of other targets that must be met in order to commercialize this form of PV.

Table 5. Silane Contribution to Module Cost (1982 \$/sqm)

Utilization Rate	Module Yields					
	50	60	70	80	90	100
0.02	0.143	0.119	0.102	0.089	0.079	0.071
0.05	0.057	0.048	0.041	0.036	0.032	0.029
0.10	0.029	0.024	0.020	0.018	0.016	0.014
0.15	0.019	0.016	0.014	0.012	0.011	0.010
0.20	0.014	0.012	0.010	0.009	0.008	0.007
0.25	0.011	0.010	0.008	0.007	0.006	0.006
0.30	0.010	0.008	0.007	0.006	0.005	0.005
0.35	0.008	0.007	0.006	0.005	0.005	0.004
0.40	0.007	0.006	0.005	0.004	0.004	0.004

IMPACT ON PHOTOVOLTAIC ENERGY COST

There are a number of ways that PV energy cost can be derived from module cost and other factors that need to be considered. The standard approach of the DOE PV research program is described in the Five Year Photovoltaic Research Plan (Ref. 5), and a discussion of how to best implement that approach can be found in JPL's sensitivity analysis of central station photovoltaic systems (Ref. 6). While there are many factors to be considered such as insolation levels, tracking options, and system lifetime; two very important factors are module cost and module efficiency (page 2, Ref. 6).

The DOE energy cost goal is \$0.15/kWh. Using the DOE energy cost equation and JPL's recommended parameter values for a fixed flat plate system a rough rule of thumb can be calculated to determine the sensitivity of energy cost to changes in module cost. If the module is 15% efficient, then a \$10/sqm change in module cost will result in a \$0.01/kWh change in system energy cost. This rule of thumb can be used for both ingot and ribbon technology. If the module is 10% efficient, then a \$6.6/sqm change in module cost will result in a \$0.01/kWh change in system energy cost. This rule of thumb can be applied to future thin films or to low efficiency (e.g., cast ingots using lower grade silicon) types of PV modules.

Successful silicon research and commercialization will reduce the cost of energy from ingot PV by about \$0.15/kWh. This represents critical progress towards viability for this type of PV module. Without silicon research, the energy cost from this type of PV approach would be at least double the DOE goal.

Energy cost from ribbon PV is reduced by about \$0.03/kWh for the thinner ribbons (web), and by about \$0.05/kWh for the thicker ribbons (EFG, ESP). Successful silicon research has been very important for this type of PV approach. Without that research, energy costs would be at least 20% to 30% above the DOE goal.

Energy cost from amorphous silicon systems will be reduced by about \$0.01/kWh to \$0.04/kWh if silane utilization is on the order of 10% to 2%, respectively. Successful silane R&D will make it unnecessary to achieve high material utilization rates, and thus is an important step in the development of viable commercial amorphous silicon PV.

Energy cost from concentrating systems is 2 to 3 orders of magnitude less sensitive to the cost of silicon than flat plate ingot technology, and therefore this research program will not be a factor in the successful commercialization of this particular technology. However, all of the flat plate varieties of PV that use silicon have benefited greatly by the success of this part of the DOE PV research Program.

CONCLUSION

A successful silicon research program will play a major role in the effort to reduce the cost of energy derived from photovoltaic systems. This is particularly true for today's commercial technology, which is ingot-based, and will remain true for the major flat plate PV options of the foreseeable future.

References

1. Reiter, L. J., A Probabilistic Analysis of Silicon Cost, DOE/JPL 1012-93, November 15, 1983.
2. Aster, R. W., Price Allocation Guidelines, DOE/JPL-1012-47, January 15, 1980.
3. Aster, R. W., "New Allocation Guidelines", published in FSA Project Progress Report 21, DOE/JPL-1012-88, January, 1983.
4. Aster, R. W., "Thin-Film Encapsulating Costs," published in FSA Project Progress Report 21, DOE/JPL-1012-88, January, 1983.
5. U. S. Department of Energy, National Photovoltaics Program, Five-Year Research Plan 1984-1988: Photovoltaics: Electricity from Sunlight, DOE/CE-0072, May, 1983.
6. Crosetti, M. R., et. al., A Sensitivity Analysis of Central Station Flat-Plate Photovoltaic Systems and Implications for National Photovoltaics Program Planning, DOE/JPL-1012-114, August 30, 1985.

DISCUSSION

SCHMIDT: You used a comparison between ingot and ribbon, and I would like to comment on that. Typically, there isn't a lot of segregation in ribbon processes and, therefore, the quality of the silicon material used for ribbon should be much higher than for an ingot process. There is very effective segregation using a good ingot process and lower quality material could be used, and the overall cost would be about the same or maybe even less.

ASTER: Thank you for that comment. There are a lot of tradeoffs between material use and efficiency. It's difficult to predict what the ultimate answer is for that comparison.

HUANG: You presented data for ribbon and amorphous-silicon technologies. What is the position in your calculations for the combination of solar-grade silicon with a casting process?

ASTER: I'm not sure what solar-grade silicon is. If metallurgical-grade silicon is used, the module efficiencies are too low to be commercially useful.

HWANG: I don't mean metallurgical-grade silicon. I mean solar-grade silicon as it is conventionally defined.

ASTER: Well, when the FSA Project started, there was a belief that a solar-grade silicon could be produced that would be significantly less costly than semiconductor-grade silicon, and part of the Project had a goal of developing those processes. I used the data for the Union Carbide and Hemlock Semiconductor processes in my calculations. I assumed \$10 to \$30/kg for those processes. There may be other, less expensive processes producing silicon adequate for cells. Please comment on them, if you will.

HWANG: This morning, the NEDO processes for semiconductor-grade silicon and solar-grade silicon were described. Where would be the position of that type of solar-grade material coupled with a casting process in your calculations on the assumption of 10% module efficiency?

ASTER: I would use the same technology as I used for semiconductor-grade silicon, since it applies to casting as well as for Czochralski ingots. Then, I would use the \$7/m² of module cost which is equivalent to \$0.01/kWh; I think this percentage/kilowatt hour is appropriate. Of course, usefulness of the solar-grade silicon for 10% cells would have to be demonstrated.

PELLIN: Amorphous silicon requires a substrate, whether it be plastic, glass, or stainless steel. How would the amorphous silicon compare when the cost of the substrate is included?

ASTER: Well, the best way to compare the cost of rather different photovoltaic technologies is on the basis of energy cost. There have been attempts to

do it in many other ways. The basis of dollars/square meter is probably not appropriate, because efficiency is important. We do know the cost of the substrate, the metallization of amorphous silicon, and so forth, will probably be about $\$3/\text{m}^2$ in any event, even if the photovoltaic system is free. The comparisons have to be made on a common basis to be valid. The best common basis is energy cost, and I believe the program goal of about $\$50/\text{m}^2$ for 10% amorphous-silicon modules is roughly equivalent to $\$90/\text{m}^2$ for a 15% module in terms of energy cost.

LEIPOLD: I have a comment rather than a question. When considering other elements of amorphous-silicon cost (for example, the silane utilization of 2 to 5%), the need to dispose of the other 95 to 98% of the unutilized silane may, in fact, cost more than the product that is put in.

ASTER: I think that, eventually, the maturity of research in that area will allow us to look at the effluent cost and other aspects of the cost, and then we can do a complete cost analysis of that technology. I think it's too early to do that at this point.

WRIGHT: We are in the process of completing a paper for the Electric Power Research Institute that will be published some time in December or January. In the paper, we go over the four technology areas that you have commented on. Effluent disposal in amorphous-silicon production was accounted for in our cost model. I'm not prepared to present our results at this time, but I feel you might be interested in looking at the published paper.

SESSION III

PROCESS DEVELOPMENTS IN THE USA

P. Maycock, Chairman

**DEVELOPMENT OF THE SILANE PROCESS
FOR THE PRODUCTION OF LOW-COST POLYSILICON**

Sridhar K. Iya
Union Carbide Corporation
Washougal, Washington

INTRODUCTION

Union Carbide Corporation (UCC) has been a major participant in the Jet Propulsion Laboratory (JPL)/Department of Energy (DOE) Flat-Plate Solar Array (FSA) Project to develop the technology for producing low-cost polysilicon for terrestrial photovoltaic solar cell applications. Based on its technology developed over many years of research activities, UCC responded to a request for proposal from JPL to conduct process feasibility studies aimed at producing polycrystalline silicon in accordance with stringent economic goals of the Solar Array Project, and was awarded a contract in late 1975. This contractual work progressed through several phases, culminating with the final design of a 100 metric tons per year Experimental Process System Development Unit (EPSDU). This pilot plant was originally to be installed on the site of a UCC facility in East Chicago, Indiana. However, shortly after the start of its construction, the activity was stopped because of contract-funding reductions. By mutual agreement between UCC and DOE, it was decided to relocate EPSDU to Washougal, Washington, and continue the pilot plant program using UCC funds as a first step in the commercialization of the silane to silicon process. A licensing agreement was arranged with Komatsu Electronic Metals of Japan to obtain commercially proven technology for decomposing silane to produce polycrystalline silicon.

Construction of the silane to silicon EPSDU was completed in 1982, and it was operated successfully to produce silane and polysilicon of exceptionally high purity for the electronics industry. Based on the original design data base developed under the JPL/DOE program, UCC constructed a 1200 metric tons per year capacity commercial plant in Moses Lake, Washington. This plant was brought on stream in early 1985, and is currently supplying high purity polysilicon to the industry.

Early in the JPL/DOE program, it was recognized that the traditional "hot rod" type deposition process for decomposing silane is energy intensive, and a different approach for converting silane to silicon was required to address the low-cost goals. A fluidized bed process was chosen to be the most promising method for this purpose, and its development was pursued with a laboratory process development unit (PDU). Several encouraging test runs have been conducted to date on the fluid

bed PDU and this technology continues to be a very promising one for producing low-cost polysilicon.

This paper will discuss the UCC silane process and the research and development (R&D) work on fluidized bed silane decomposition conducted under JPL/DOE sponsorship.

SILANE PROCESS

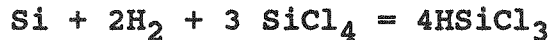
The UCC silane process is based on many technical innovations in proven chlorosilane chemistry to achieve very high purity levels in the product. The use of silane as a single reactant instead of a binary trichlorosilane-hydrogen mixture as in the traditional Siemens Process has the following significant advantages:

- The boiling point of silane is lower than that of all the chlorosilanes and impurities such as the chlorides and hydrides of boron, phosphorus, and arsenic. Consequently, it is easier to purify silane and it can be purified to higher levels than any of the chlorosilanes.
- Silane can be totally decomposed to produce high-purity silicon and hydrogen in a single pass. Since silane is converted to silicon in single-pass operation, the possibility of contamination is minimized.
- The byproduct hydrogen can be readily separated from the solid silicon product, and is electrically inactive.
- The absence of corrosive chlorine compounds in the product stream minimizes the chances of contamination, and simplifies material selection.

The silane to silicon process starts with metallurgical grade (m.g.) silicon and refines it to semiconductor grade product in a series of reaction and purification steps. The process consists of three major steps:

- Hydrogenation, where silicon, silicon tetrachloride (STC), and hydrogen react at high temperature and pressure to form trichlorosilane (TCS),
- Redistribution, where the hydrogen and chlorine atoms are redistributed within the chlorosilane molecules, eventually yielding high-purity silane, and
- Decomposition, where purified silane is thermally decomposed to yield semiconductor grade polycrystalline silicon.

The process is described by the flow diagram shown in Figure 1. M. G. silicon, STC and hydrogen are reacted at high pressure and temperature in the hydrogenation reactor to yield TCS:

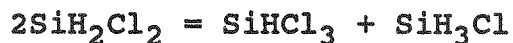


This reaction is carried out in a fluidized bed consisting of fine silicon particles. The hot product gases leaving the reactor are quenched to their dew point in a venturi contactor. The quenched two-phase mixture enters a waste settler tank where many of the metal contaminants form insoluble complexes with one another and settle to the bottom. Vapors from the settler are cooled in a quench condenser which condenses the chlorosilanes. The condensed 'crude' TCS is sent to a storage tank, and the uncondensed hydrogen is recycled to the hydrogenation reactor. The heavy non-volatile impurities and elutriated silicon fines are periodically purged out of the settler to the waste treatment area.

The next major processing area is distillation/redistribution. In this section, TCS is redistributed eventually forming silane, and the impurities are rejected from the process streams. The redistribution reactions take place in two packed-bed liquid phase reactors containing an ion-exchange resin which serves as a catalyst for the reactions. In the TCS redistribution reactor, dichlorosilane (DCS) and STC are produced according to the reaction,



In the DCS redistribution reactor, DCS is redistributed to form monochlorosilane (MCS) which rapidly redistributes to form silane,



The remainder of the purification train consists of four distillation columns which provide the required feed composition for the reactors and reject the impurities.

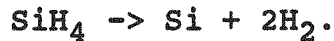
The first distillation column is a light-gas stripper. It receives the crude TCS product from the hydrogenation reactor and removes dissolved gases such as residual hydrogen from hydrogenation and inert gases from process purges.

The TCS column separates TCS and DCS from STC. It receives the stripped crude TCS from the stripper and the product from the TCS redistribution reactor. The distilled TCS-DCS mixture is fed to the DCS distillation column, and the STC bottoms product is recycled to hydrogenation.

The DCS column provides proper feeds to the redistribution reactors. It receives the TCS-DCS mixture from the overhead of the TCS column and the bottoms stream from the silane column. The bottoms product from the DCS column (primarily TCS) is fed to the TCS redistribution reactor, and the distillate, which is DCS with some MCS, is fed to the DCS redistribution reactor.

The silane column is designed to produce very high-purity silane while rejecting all chlorosilanes and any other contaminants. The feed stream to this column is the product from the DCS redistribution reactor. Silane is removed as the overhead product and is sent to storage tanks, while the bottoms stream containing the remaining chlorosilanes is returned to the DCS column. The silane column is keyed for separating silane from diborane which is the most volatile electronic contaminant in the system.

Silane thus produced is decomposed utilizing the technology acquired from Komatsu Electronic Metals of Japan,



Heterogeneous decomposition of silane is accomplished on electrically heated seed rods which grow from an initial diameter of 7.5 mm to final diameters in the range of 80 to 100 mm. The byproduct hydrogen is recycled to hydrogenation.

POLYSILICON PURITY EVALUATION

Purity evaluation of polycrystalline silicon is accomplished by taking core samples from the polysilicon rod product, and zone-refining into small single crystal rods. Wafers sliced from the seed and tang ends of the single crystal rod are analyzed by Fourier transform photoluminescence (FTPL) spectroscopy at liquid helium temperature to obtain donor/acceptor impurity concentrations in the material. Carbon and oxygen impurity levels are measured by Fourier transform infrared (FTIR) spectroscopy at liquid helium temperature. Resistivity values are obtained with a high-impedance four-point probe. Resistivity profiling of the sample single crystal ingot is done by a high impedance two point probe. The sample ingot is also analyzed for minority carrier lifetime.

Typical purity evaluation data for the present production grade silicon material are as shown below:

Boron	<0.06 ppba
Phosphorus	<0.30 ppba
Aluminum	Not Detected

Arsenic	Not Detected
Antimony	Not Detected
Carbon	<0.5 ppma
Lifetime	5 milliseconds
Resistivity	>1,000 ohm-cm

The above material is ideally suited for single crystallization by Czochralski or Float Zone method for semiconductor applications.

FLUID BED SILANE DECOMPOSITION

Fluid bed pyrolysis of silane involves heterogeneous decomposition of silane gas on hot silicon seeds to produce free-flowing particles of silicon. The method offers the potential for converting high-purity silane into pure silicon product at a cost which is consistent with the overall goals of the FSA program. Furthermore, since the fluid bed product consists of free-flowing particles, it can be directly processed in a Czochralski furnace where continuous growth by melt replenishment may be feasible.

Under the JPL/DOE program, UCC has been engaged in R&D work on deposition of silicon in a fluidized bed reactor. The goals of this program are to demonstrate the process feasibility, determine a suitable operating window for the fluid bed reactor, conduct long-duration tests, and demonstrate silicon purity.

Several experimental runs have been conducted to date using a 6 inch diameter quartz-lined reactor and product samples have been produced for purity evaluation. A schematic of the fluid bed PDU is shown in Figure 2. The reactor assembly consists of a stainless steel shell with an internal high-purity liner. The reactor contains a bed of silicon seed particles which grow in size due to heterogeneous decomposition of silane. The reactor wall is heated with multi-zone resistance heaters which maintain the bed in the temperature range 600 to 700°C. The product is cooled and collected in bags.

Silane and hydrogen are pre-mixed in desired concentrations, and the mixture is fed to the reactor through a water-cooled gas distributor assembly. The gas velocity at the bottom of the fluid bed is approximately 3.5 times the minimum fluidization velocity. The effluent hydrogen in the PDU is cooled and vented after taking a small sample stream to a gas chromatograph which monitors the silane conversion in the fluid bed.

A number of long-duration test runs have been conducted, the longest single continuous run to date being of 66 hours duration. In these runs, the feed silane concentration was typically in the range of 25 to 30% in hydrogen, although concentrations up to 50% have been tested for short durations. The average silicon deposition rate was in the range 1 to 2 kg per hour. Seed particles of initial mean size 300 microns were grown to approximately 600 microns. The growth of larger particles, up to 1000 microns, is considered feasible.

Samples of seed and product particles were studied by scanning electron microscope and optical micrographs. The starting seed particles have an irregular shape with sharp edges. The product particles display a smooth rounded exterior surface with a ring-like, layered structure. The product particles have a dense and uniform deposition morphology with a bulk density of approximately 1.6 gm/cc.

The seed and product samples were analyzed for heavy metals by spark source mass spectrometry. The results are shown below for a typical test run H-02:

<u>ELEMENT</u>	<u>SEED, PPMA</u>	<u>PRODUCT, PPMA</u>
Fe	3	1
Al	10	2
Cr	0.05	0.03
Mn	0.3	0.1
Ni	< 0.5	< 0.5
Cu	≤ 0.02	≤ 0.02

It is clear that the product has less metallic contamination than the seed, indicating that the deposited growth layer is of higher purity. These data also support the use of a liner as an impurity barrier from the reactor walls since earlier results without a liner had shown metallic contaminant levels of over 100 ppm in the product samples.

Samples of seed and product from the fluid bed reactor (run H-02) were melted in a Czochralski furnace in an attempt to single crystallize them in two successive runs. The seed material yielded a polycrystalline ingot while the product sample resulted in a 3" diameter 21" long dislocation-free crystal, followed by 7" of dislocated single crystal and 4" of polycrystalline ingot. Wafers sliced from the top and bottom ends of the single crystal from the product sample were analyzed for donor/acceptor concentrations by Fourier Transform Infrared Spectroscopy (FTIR) at liquid helium temperature. The wafers were also analyzed for electrical resistivity. The results are shown below:

	<u>TOP END</u>	<u>BOTTOM END</u>
Phosphorus, ppba	4.2	8.5
Boron, ppba	8.5	10.0
Arsenic, ppba	0.1	0.28
Aluminium, ppba	1.2	4.6
Antimony, ppba	< 0.02	0.07
Carbon, ppma	4.99	22.0
Oxygen, ppma	14.0	18.0
Calculated Resistivity, ohm-cm	50 P type	40 P type
Measured Resistivity, ohm-cm (average of 10 points)	87 P type	87.6 P type

It is clear that the donor and acceptor concentrations are in the parts per billion range. The results so far have indicated that the starting seed material is not of high purity, and is a major source of contamination. R&D work currently in progress aims at minimizing this contamination by preparing high purity seed material. Additional test runs using improved seed material will be conducted to establish fluid bed product purity.

CONCLUSIONS

The UCC silane to silicon process has produced both silane and polysilicon of exceptionally high purity. The silane technology developed under the JPL/DOE sponsorship has been successfully commercialized.

The fluid bed process for silane decomposition shows an excellent promise for producing high purity silicon material, consistent with the cost goals of the FSA project.

ACKNOWLEDGEMENTS

The active support received from the U.S. Department of Energy and the Jet Propulsion Laboratory is gratefully acknowledged. Several other individuals at Union Carbide have also contributed to the development work described in this paper, the most notable among whom are Messrs. W.C. Breneman, L.M. Coleman, and R.N. Flagella.

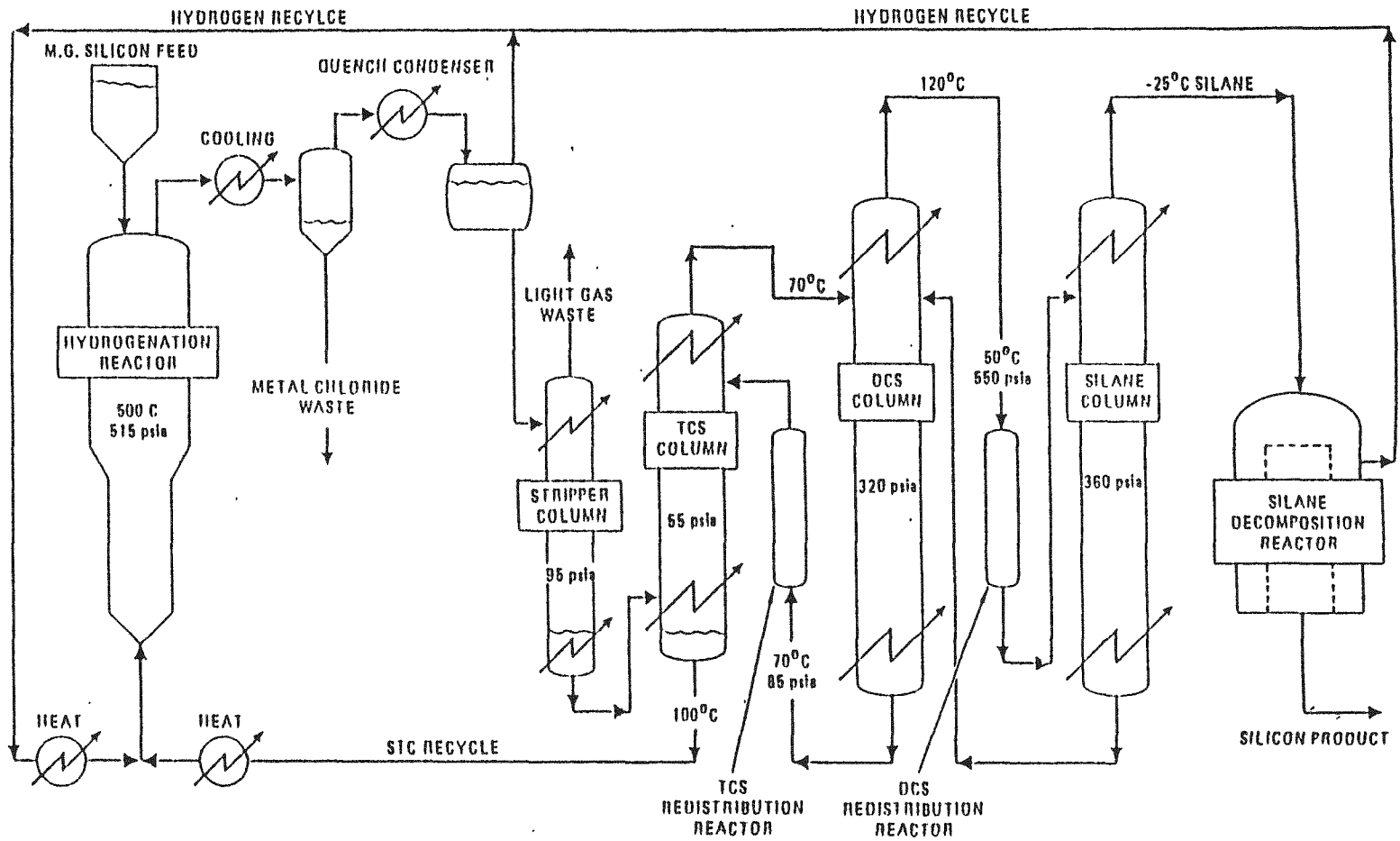


FIGURE 1: FLOW SCHEMATIC OF SILANE TO SILICON PROCESS

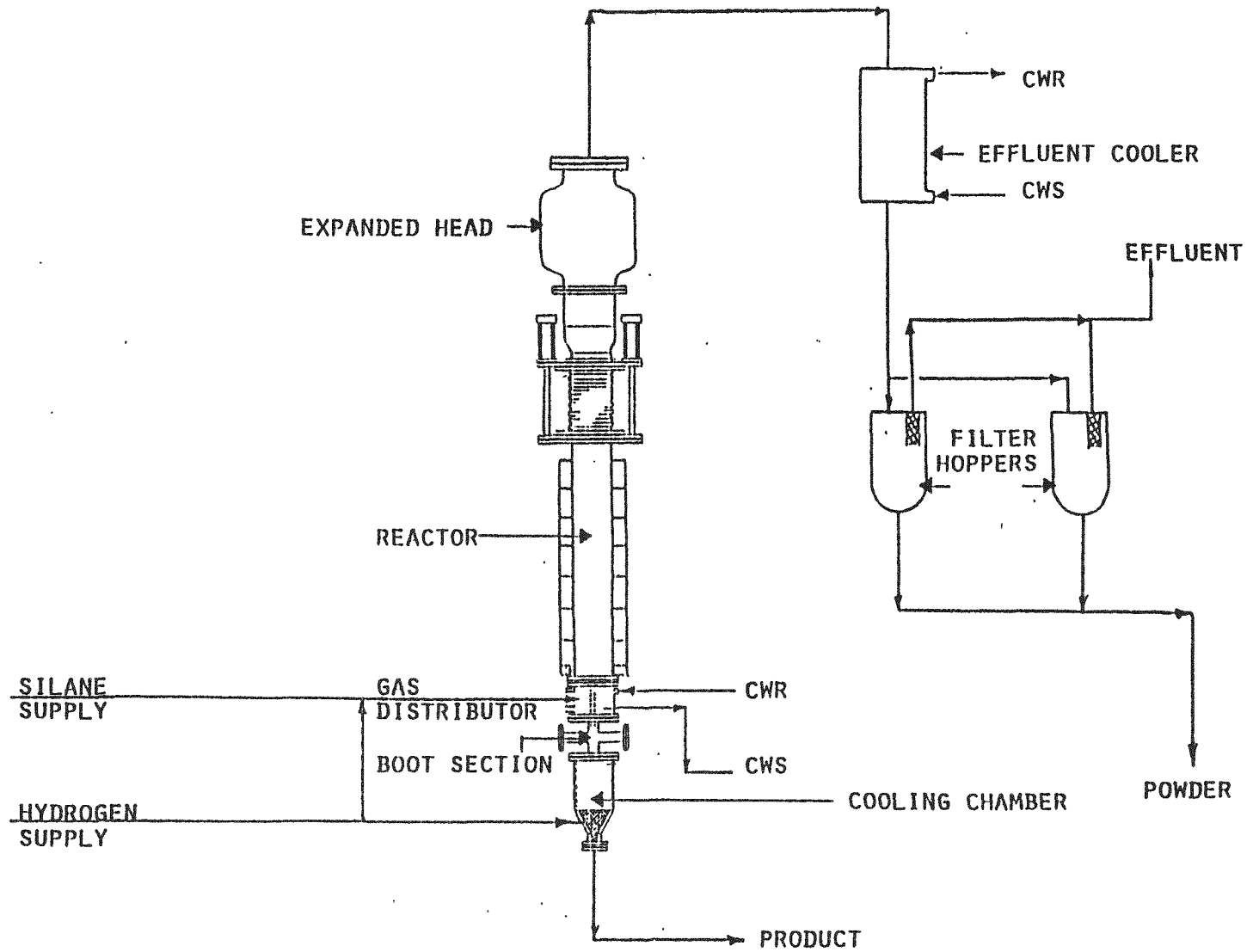


FIGURE 2: FLUID BED PROCESS DEVELOPMENT UNIT

DISCUSSION

SANJURJO: Professor Carl Yaws has just addressed the problem of homogeneous nucleation in the Komatsu reactor. Would you describe the nucleation problem further? What is its impact on production?

IYA: Well, I'm not prepared to discuss the Komatsu reactor, per se. Professor Yaws referred to a paper which was published in the Journal of the Electrochemical Society that describes the conditions under which silane can be decomposed either homogeneously or heterogeneously, and I refer you to that paper.

SCHWUTTKE: Do I understand correctly that Union Carbide plans to have a 1998 production capacity of 5500 MT/year? If I'm correct, this corresponds approximately to the total world capacity today. Is this correct?

MAYCOCK: Dr. Pellin is going to discuss this in depth later. The answer is essentially yes.

SCHWUTTKE: I'm somewhat confused by your presentation of the data for the purity of the silicon produced in the Union Carbide silane process. Would you describe more carefully the silicon products from the Komatsu reactors and the fluidized-bed reactor?

IYA: The data I gave for the silicon from the EPSDU and from the Moses Lake commercial plant showed that these products are very high-purity, semiconductor-grade materials. Union Carbide is marketing the commercial product throughout the world. On the other hand, the data for the silicon granules from the experimental fluidized-bed reactor show that the purity is not semiconductor grade. In our experimental program, we also intend to work toward meeting the semiconductor-grade purity levels for the fluidized-bed product.

AULICH: You mention that your process yields electronic-grade silicon. We already have an electronic-grade silicon produced by the Siemens process which is too expensive. Do you have any plans of offering so-called solar-grade silicon at a considerably lower price, or are you only looking at the electronic market?

IYA: This is a question that should be answered by our marketing people. I'm certainly not in a position to do that.

KOINUMA: What are the main reasons preventing you from extending the duration of the fluidized-bed reactor operation and also growing particles larger than 800 μm ?

IYA: We have been conducting essentially research and development work using a laboratory unit, and there are time limitations for conducting these experiments. But, aside from that fact, I think we will probably run into some inherent limitation on the particle size as we grow larger particles. Some of the experts in fluidization point out that

fluidization will become difficult. We don't know what the limit is. So far, the particles have been grown to about 800 μm size.

KOINUMA: Could you also tell me how you collected the fine particles? I think you mentioned that about 5.5 to 6% of the product is fine particles. How do you collect these fine particles?

IYA: We have filters located downstream of the process, and at the end of the run we collect the particles. We then weigh the mass to determine the fines content.

FUJII: What improvement do you seek in the preparation of seed particles?

IYA: We are trying to implement a cleaning method that involves acid cleaning and handling the seed material so that it remains in a fairly pure state.

MAYCOCK: I think that we should notice the location of their plant. Our Japanese paper showed electricity cost 15 yen/kWh which is approximately 6¢. Dr. Yaws used 5¢ in his economic analysis, and I would guess that the Union Carbide, Washougal plant, is about 2¢. Is that correct? It used to be 9 mills. Before the energy crisis, it was 9 mills, and then it went up to almost 30 mills during the shortage of water. Now, with water running over the dams and power to burn, I think they are probably back to something around 20 mills cost. Those of you doing economics on Union Carbide need to find out what that cost is.

FLUIDIZED-BED DEVELOPMENT AT JPL

G. Hsu
Jet Propulsion Laboratory
Pasadena, California

ABSTRACT

Silicon deposition on silicon seed particles by silane pyrolysis in a fluidized bed reactor (FBR) has been under investigation as a low-cost, high throughput method to produce high purity polysilicon for solar cell applications. The emphasis of the research at JPL is fundamental understanding of fluidized bed silicon deposition. The mechanisms involved were modeled as a six-path process: (1) Heterogeneous deposition; (2) Homogeneous decomposition; (3) Coalescence; (4) Coagulation; (5) Scavenging; and (6) Chemical vapor deposition growth on fines.

INTRODUCTION

The Flat-Plate Solar Array (FSA) Project was initiated in 1975 by the Department of Energy (DOE, then ERDA) to develop the technology for low-cost terrestrial photovoltaic arrays. In silicon material area, the Project was assigned a responsibility to develop the capability of producing polycrystalline silicon of semiconductor grade purity, suitable for the manufacture of terrestrial solar cells, at a price of less than \$14/Kg (in 1980 \$)(ref.1,2). In 1976, the Silicon Material Task of FSA initiated the fluidized bed silicon deposition in-house work parallel to the contractual development work by Union Carbide Corporation via silane decomposition and by Battelle via zinc reduction of silicon tetrachloride.(ref.3) Initially, the JPL in-house work was primarily installed to keep the contract management on top of the cutting-edge technologies that JPL/FSA was managing for DOE. Over the years, the emphasis has been redirected to fundamental understanding of silicon production in the advanced reactors and to identify critical research areas in order to complement the industrial process development efforts. Based on the simple chemistry of silane decomposition, the reactor technology studies at JPL in-house included: free space reactor, direct conversion to molten silicon, and fluidized bed silicon deposition. Constrained by funding situation in the contractual development work, FSA/Si Material Task decided to concentrate on the fluidized bed reactor (FBR) for low-cost production of silicon. Complemented by the JPL FBR research, Union Carbide Corporation has developed the essential parts of this technology in a R&D scale under a FSA contract. Currently, DOE considers the R&D of FBR technology mature enough to

*This paper presents the results of research carried out at the Jet Propulsion Laboratory, California Institute of Technology, sponsored by the U.S. Department of Energy, through an agreement with the National Aeronautics and Space Administration.

be pursued by the industry for final pilot plant development leading to commercialization. Consequently, the JPL in-house FBR development was concluded in June 1985, whereas the overall FSA silicon material work was completed in December 1985. This paper summarizes the fluidized bed development at JPL, and reports the engineering and scientific status of JPL FBR with a brief recommendation for the remaining R&D.

REACTION MECHANISM

The mechanisms involved were modeled as a six-path process (ref. 4):

Deposition and Decomposition: In a FBR, silane is thermally decomposed and silicon is formed via two major paths (see Figure 1); 1) heterogeneous chemical vapor deposition on the surface of seed particles in the emulsion phase of the bed, and 2) homogeneous gas phase pyrolysis forming condensable Si species in the bubble phase of the bed leading to formation of nuclei.

Coalescence: The tiny silicon nuclei move about within the bubble by Brownian motion and fuse by the action of Van der Waals forces - the path (3) in Figure 1. The growth rate of a nucleus with a radius r is found to be

$$\frac{dr}{dt} = \left(\frac{2kTf_s}{3\pi\mu} \right) \frac{1}{r^2} \quad (1)$$

where k is the Boltzmann constant

μ is the viscosity of nucleus in the gas stream

f_s is the volume fraction of solids in the gas-solids mixture

T is temperature in $^{\circ}\text{K}$.

By the time nuclei grow to $0.3 \mu\text{m}$ size, they are so few and far between that the growth rate drops by a factor of 10^{-4} . The resulting fine particle from this stage of nuclei coalescence is called coccal silicon. As a result of bubble distortion and kneading of fluid eddies in the fluidization medium, these coccal silicon fines may come out of the gas bubble into the emulsion phase.

Coagulation: Within the bubbles the coccal silicon fines coagulate into clusters. The size of a cluster grows as the residence time of the bubble in the bed increases. The resulting cluster is light in density, and travels with the gas bubble. At the top of the bed, bubbles burst and typically $<10\%$ of the silicon input in the forms of clusters and residual coccal silicon fines are elutriated and collected in the exit filter. Limited by the terminal velocity of the operation of fluidized bed, the maximum size of elutriated clusters is about $10 \mu\text{m}$ under the experimental conditions.

Scavenging: In the emulsion phase, the seeds sweep up the fine particles, which are coccal silicon and initial clusters released from the bubbles. This phenomenon is called scavenging.

Based on the data, it appears that in order to incorporate fines, the following criteria must be met:

- 1) The temperature of the scavenging region must be higher than the Tammann temperature* of silicon - defined as $0.52 \times$ (the melting point of silicon in $^{\circ}\text{K}$).

This threshold temperature is about 610°C . In the FBR case, it represents the minimum seed particle surface temperature required to incorporate fines. As shown by SEM pictures in earlier work^(ref.5), scavenging of fines at temperature below the Tammann temperature leads only to loose adhesion.

- 2) Chemical vapor deposition (CVD) reaction serves to cement the homogeneous fines into the growth. This surface adsorption of homogeneously nucleated particles and simultaneous heterogeneous deposition is similar to the model proposed in the carbon deposition literature.^(ref.6.7)

Heterogeneous Growth of Fines: Fines, mostly coccal silicon, grow by heterogeneous chemical vapor deposition in the emulsion phase - i.e. the path (6) in Figure 1.

REACTOR DESIGN

The fluidized bed reactor is depicted in Figure 2. It is constructed from a 6-inch schedule 40 stainless steel 316 pipe and has dimensions of 6.065 inch inside diameter x 48 inch high. It has an expanded head of 24 inch x 24 inch to allow entrained particles to drop back into the bed.

Gas Distributor:

Five different types of gas distributors were investigated at JPL^(ref.8) namely, a porous carbon unit with nine spouts, a nozzle with 1/4-inch diameter opening, a multi-layer screen (trade name - DYNAPORE) distributor and two-distributors fabricated from either one or two layers of No. 325 mesh stainless steel screen supported by a 1/20 inch thick plate perforated with 1/8 inch diameter holes. All these gas distributors were able to provide a bubbling fluidized bed with the exception of the nozzle-type distributor. Although a spouting distributor creates vigorous mixing of solids, it is difficult to ensure a firm contact of the metallic cooling coil underneath the porous carbon material. Distributors with one or two layers of No. 325 mesh screens were found most effective because of the simplicity in design to provide external water cooling.

A distributor temperature about 350°C will cause partial decomposition of silane at the distributor followed by clogging of the particles in the bed. Three distributor cooling systems were investigated: (1) Water cooling at the periphery of the distributor and a 1/2 inch thick cooling ring located

*Tammann temperature is an index for surface mobility or the minimum temperature at which a solid undergoes solid-solid interactions such as a transformation from a non-wetting to a wetting condition.

between the distributor and the reactor flange; (2) The same cooling system supplemented with internal water cooling tubes within the fluidized bed, located 1/4 inch above the distributor screen; and (3) water cooling at the periphery of the distributor in addition to a water cooling coil located beneath the distributor. A copper cooling coil was silver soldered to a 1/20 inch thick plate with multiple holes. The distributor screen is spot welded to the support plate to ensure firm contact. The first two cooling systems were inadequate to keep the distributor temperature below 350°C. The water cooling tubes located within the fluidized bed not only increased the load on the heaters, but also caused an excessive temperature gradient between the fluidized bed and the reactor wall resulting in silicon deposits on the wall. The third cooling system was found most satisfactory, both to keep the distributor temperature below 350°C and to eliminate wall deposits.

Heaters: The reactor was externally heated by a two-zone fast response, 12 inch high silicon carbide heater with a total output of 9 kw. Both zones are independently controlled in order to achieve an isothermal condition in the bed with 3 inches from the distributor. On the top of silicon carbide heater there is a single-zone independently controlled 18 inches high ceramic clam-shell heater with a heating element made of an alloy of iron, chromium, cobalt, and aluminum with a total power output of 9 kw. The main purpose of this heater is to provide a thermal insulation around the reactor and distribute the heat input throughout the bed height.

Product Withdrawal System

The fluidized bed is equipped with a continuous silicon withdrawal system to maintain a constant bed height.(ref.9) This system is depicted in Figure 3. It consists of an externally water-cooled silicon withdrawal tube, 15 inches long x 0.87 inches I.D. The particles in the withdrawal tube were fluidized at around minimal fluidization velocity in order to: (1) keep silane out of the withdrawal tube, (2) permit accumulation of large particles in the tube, and (3) cool the tube more effectively by preventing a sudden drop of hot bed particles within the tube.

At the bottom of the tube, an electronically controlled pinch valve (trade name - RED VALVE) is located. This valve is opened at a predetermined frequency (10-15 second intervals) for a duration of one second to allow particles to drop into a tee. The tube is water-cooled and provides cooling for the particles. The particles in the tee are pneumatically transported to a cyclone separator and collected in a silicon holding tank.

Reactor Liner System

The quartz liner design is depicted in Figure 4. It consists of a 5.75-in. outside diameter x 4 feet long quartz tube with 1/8-in. wall thickness. The top end of quartz liner is supported against a ring with 1/4-in. groove and a graphoil gasket. The bottom end of the quartz liner stands on a piston-gas distributor assembly with 1/4-in. groove and a quartz sleeve used as a gasket. The outside surface of piston consists of a pneumatic cylinder. The interface is vacuum and pressure sealed with a viton o-ring. The entire assembly is water cooled to maintain integrity of the o-ring. The pneumatic cylinder is mounted against the reactor flange.

Initially, the reactor containing quartz liner is filled with silicon particles. The reactor is closed and evacuated to remove oxygen prior to heating. The particles are fluidized with nitrogen or helium. A pressure of 200 psig. is applied at the pneumatic cylinder to mechanically seal the top end of quartz liner against the graphoil gasket. The pressure at the pneumatic cylinder compensates the differential thermal expansion between the stainless steel reactor wall and the quartz liner in axial direction. The bottom end of the quartz liner is not completely sealed and hydrogen is permitted to flow at a rate of less than 1 SLPM. During entire heating cycle, as well as silicon deposition experiment, a differential positive pressure of 20-in. water column is maintained between annular space and inlet port for silane/hydrogen gas mixture. This procedure assures that hydrogen can leak into the reactor but under these conditions silane/hydrogen mixture cannot leak into the annular space and cause wall deposits.

Seed Generation Device

A jet milling technique to grind silicon by impinging jets has been studied in this work for FBR seed particle generation. This device involves grinding of silicon particles by impingement of two opposing nitrogen jets carrying silicon particles. It is lined with high-density polypropylene and polyurethane to avoid exposure of silicon to metallic surfaces. It has an impact chamber of 0.75 in. diameter x 2 in. long. It is equipped with two opposing nitrogen jets with orifice diameter of 0.078 inches.

Silicon Cleaning Device

In the silicon cleaning device (ref.10), silicon particles are fluidized by the cleaning solution. The entire system in contact with either silicon or acid is constructed out of polyethylene and polypropylene. It consists of three plastic bottles of 3.5 inches diameter x 8 inches high. Each bottle holds up 500 grams of silicon. The bottom of the bottle is equipped with a 50 μm pore diameter plastic screen and distributor to provide a tangential flow of cleaning solution for good mixing. The top of the bottle is equipped with another 75 μm pore diameter screen to retain the particles within the bottles. All these three bottles are installed in a plastic tank which is filled with up to 2 gallons of cleaning solution. The cleaning solution is circulated through the system via a plastic pump. The flow rate of cleaning solution is adjusted by a plastic needle valve to obtain desired fluidization of silicon particles.

The cleaning of silicon seed obtained from grinding of silicon chunks includes the following steps:

- (1) Deionized water wash in a liquid-solid fluidized bed mode to remove fine silicon particles of less than 75 μm in diameter.
- (2) Seed cleaning in a mixture of two parts of 12N HCl and one part of 16N HNO₃ in fluidized bed mode for 20 minutes.
- (3) Acids are drained and particles are washed with deionized water in a fluidized bed mode until the effluent water is neutral.
- (4) Etching of silicon particles with 48% HF in a fluidized bed mode for 20 minutes.

- (5) HF is drained and particles are washed with deionized water in a fluidized bed mode until effluent water is neutral and has a resistivity of 16 mega-ohms.
- (6) The wet particles are dried in a diffusion furnace at 150°C under nitrogen blanket.
- (7) After drying, particles are transferred into a plastic bag and sealed.

REACTOR PERFORMANCE

The overall mass balance data indicate that more than 90% of the total silicon fed into the reactor is deposited on the silicon seed particles and the remaining 10% ends up as elutriated fines. The rate of silicon production is a function of silane concentration, seed particle size and U/U_{mf} . Figure 5 shows that in the 6 inch FBR, a silicon production rate of 1.5 Kg/hr at 30% silane concentration or 3.5 Kg/hr at 80% silane concentration is achievable without formation of excessive fines. Most of the experiments conducted at JPL of the 6 inch FBR were of short duration (~4 hrs).

Silicon Particle Growth

The large seed particles (e.g., more than 200 μm diameter) in a FBR sweep up and collect the homogeneously nucleated fines (e.g., smaller than 1 μm) onto the particle surfaces, followed by sealing of the simultaneous heterogeneous deposition. Consider a seed particle of radius r and density ρ travelling up and down in a fluidized bed. The surrounding environment contains homogeneously nucleated fines of weight concentration ω_f travelling at a velocity U' of the fluidizing gas. The mass balance around a particle due to the scavenging and incorporation of homogeneously nucleated fines is (Ref. 11).

$$\rho 4\pi r^2 \frac{dr}{dt} = \pi r^2 (\Delta U) \omega_f \quad (2)$$

where ΔU can be approximated by the actual fluidized gas velocity U' . ω_f can be approximated from the silane concentration and the subsequent concentration reduction in the coalescence step leading to the fines.

$$\omega_f = C_{Ao} \times M_{Si} \times \frac{Kg}{K_S + Kg} \times \frac{1}{1 + X_A} \times 0.5 \times \left(\frac{25 \times 10^{-10}}{0.15 \times 10^{-6}} \right)^2 \quad (3)$$

silane feed conc.	Si mol. weight	homo reaction fraction	dilution factor due to hydrogen formation	Average in the bed	Number of fines reduced from collisions of nuclei (50Å) to fines (0.3 μm)
-------------------------	-------------------	------------------------------	---	--------------------------	--

where X_A is the fraction of silane concentration in the feed.

K_g is the first order rate constant for homogeneous decomposition of silane, 10.4 sec^{-1} at 650°C . (ref.12)

K_s is first order rate constant for heterogeneous decomposition of silane, 3.1 sec^{-1} at 650°C . (ref.13)

On the other hand, the seed particle growth due to heterogeneous deposition can be described by the following mass balance:

$$N \cdot 4\pi r^2 \frac{dr}{dt} = \frac{K_s}{K_s + K_g} C_{Ao} M_{Si} uA \quad (4)$$

where:

$$N = \frac{\omega_0}{\frac{4}{3} \pi r_0^3 \rho} \quad (5)$$

N is the number of particles in the bed,

ω_0 is the initial bed weight

r_0 is radius of initial seed particle

u is the superficial velocity of the gas, $\epsilon U'$

The total growth rate of a particle equals the sum of equations (2) and (4).

Based on equations (2) and (4), the theoretical particle growth can be estimated as shown in Table 1. The actual particle growth (averaged) can be obtained from a mass balance over the experiment, together with the measured particle size distribution of the product. It can be seen that the calculated values agree nicely with the experimentally measured sizes.

Combining equations (4) and (5), the following relationship holds:

$$\frac{dr}{dt} = p \frac{r_0 F}{\omega_0} C_{Ao} \quad (6)$$

where p is a constant, $\frac{1}{3} \left(\frac{K_s}{K_s + K_g} \right) \rho M_{Si}$

F is the total flow rate, uA .

This means that the deposition rate is linearly proportional to C_{AO} , r_o and F , and is inversely proportional to ω_o . If r_o , and F and ω_o are held constant, a simple correlation of deposition rate (dr/dt) versus silane feed concentration (C_{AO}) is obtained. This can be shown by normalizing the deposition rate data, $\mu\text{m/hr}$, from Table 1 versus initial particle size of $227 \mu\text{m}$, initial bed weight of 400.2 moles of silicon and total flow rate of 3.0 moles/min. These rate data (dr/dt) are plotted against percentage feed silane concentration in hydrogen (X_A) in Figure 6. This results in a straight line correlation. In this way, the rate constant of the overall growth model, K , is obtained as $13 \mu\text{m/hr}$ for the 6-in. JPL FBR design.

$$\left. \frac{dr}{dt} \right|_{r_o, \omega_o, F} = K X_A \quad (7)$$

PRODUCT PURITY

The purity of FBR product was determined for two cases: (1) the FBR was operated without a liner and silicon particles were exposed to hot stainless steel reactor wall, and (2) the FBR was operated with a quartz liner to isolate the silicon particles from stainless steel reactor wall.

For the first case, the metallic impurities in FBR product is shown in Table 2. It indicates that silicon product in that case is heavily contaminated with metallic impurities. The iron, chromium and nickel impurities are approximately 70%, 17% and 12% of total identified impurities which are similar to the composition of stainless steel 316 material. Thus, it is evident that hot silicon particles erode the stainless steel wall material and incorporate metallic impurities on top of the seed particles.

For the second case, the metallic impurities in FBR product are shown in Table 3 (ref. 10). Within the accuracy limit of the analytical method, e.g., in this case, spark source mass spectroscopy is selected as the best analytical method for most of metallic impurities. The results suggest that the FBR processing does not introduce contamination into the product, and the quartz liner is effective to preserve the seed particle purity.

RECOMMENDATIONS

Although the JPL in-house research program has contributed over the years towards a fundamental understanding of fluidized bed silicon deposition, the following problems are still left to be solved.

- Demonstrate that FBR product particles are of semiconductor-grade purity (i.e., The particulate form of product makes the current analytical techniques difficult to reach to less than ppb for some of the impurities).
- Eliminate the problem of small particle accumulation in the FBR.

- Develop fluid jet milling to generate FBR seeds in a continuous loop with the FBR process.
- Demonstrate the operation of FBR in a steady state long-duration fashion.

CONCLUSION

This paper summarizes the fluidized-bed development at JPL, and characterizes the JPL FBR in terms of engineering design parameters such as gas distributor, cooling systems, heaters, product withdrawal, and a quartz liner with support. Also, the operation support systems including silicon seed generation and seed cleaning device are described. The overall mass-balance data indicate that more than 90% of the total silicon fed into the reactor is deposited on seed particles and the remaining less-than 10% of the total silicon bed ends up as the fines elutriants. A six-inch diameter FBR was demonstrated to be capable of producing 3.5 Kg/hr of silicon using 80% silane feed concentration, with a first order linear growth rate constant at 650°C of 13 $\mu\text{m/hr}$. The benefit of a quartz liner in avoiding the erosion contamination from fluidizing silicon particles against the metallic reactor wall was demonstrated with product purity experiments.

REFERENCES

1. DOE/JPL Low-Cost Solar Array Project Annual Operating Plan for Fiscal Year 1980, JPL Report No. 5101-127, August 31, 1979.
2. "National Photovoltaics Program Five Year Research Plan" - 1984-1988; Photovoltaic Energy Technology Division, U.S. Department of Energy, May, 1983.
3. Lutwack, R., "A Review of the Silicon Material Task", JL Report No. 5101-244, Feb. 1, 1984.
4. Hsu, G., Morrison, A., Rohatgi, N., Lutwack, R., and MacConnell, T., Proceedings of the 17th IEEE PV Specialists Conference, May 1-4, 1984.
5. Hsu, G., Hogle, R., Rohatgi, N., and Morrison, A., J. Electrochem. Soc.: 131, No. 3, p. 660, March 1984.
6. Bokros, J.C., Chapter of "Deposition, Structure and Properties of Pyrolytic Carbon", Vol. 5, a series of advances on "Chemistry and Physics of Carbon", ed. by P.L. Walker, Jr., Marcel Dekker Inc., N.Y. 1969.
7. Kaae, J.L., Gulden, T.D. and Liang, S., Carbon 10, 701, 1972.
8. Hsu, G., Rohatgi, N., and Houseman, J., proceeding of AIChE Annual Meeting, San Francisco, November, 1985.
9. Rohatgi, N., and Hsu, G., "Silicon Production in a Fluidized Bed Reactor: A Parameter Study", JPL Report No. 5101-129, October 1983.

10. Rohatgi, N., "Silicon Production in a Fluidized Bed Reactor: Final Report", JPL Report in preparation, 1985.
11. Hsu, G., Rohatgi, N., and Houseman, J., "Silicon Particle Growth in a Fluidized Bed Reactor" submitted to AIChEJl.
12. Hogness, T., et. al., Jl. Amer. Chem. Soc., 58, 108, 1936.
13. Iya, S., et. al., Jl. Electrochem. Soc., 129, No. 7, p. 1531, 1982.

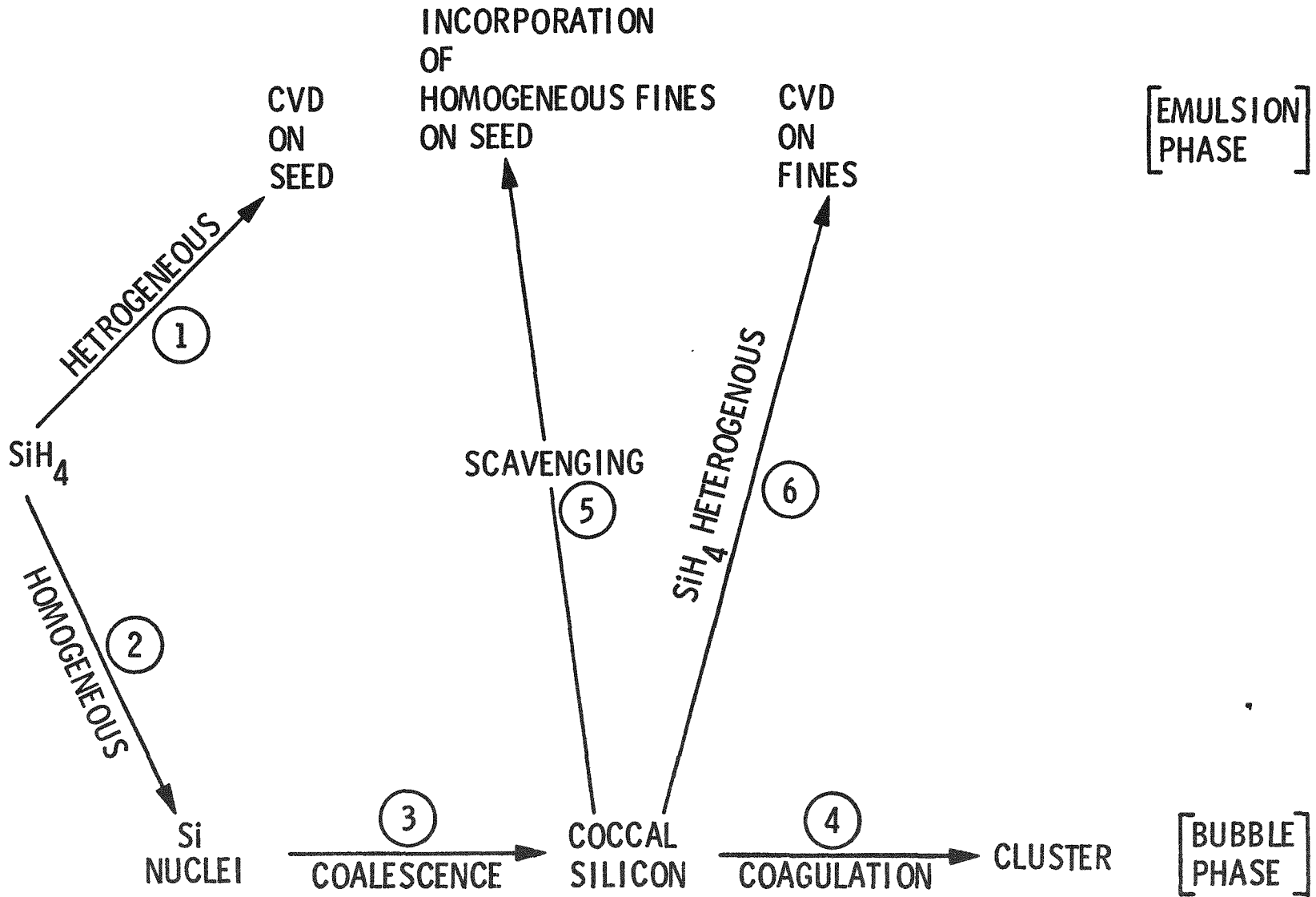
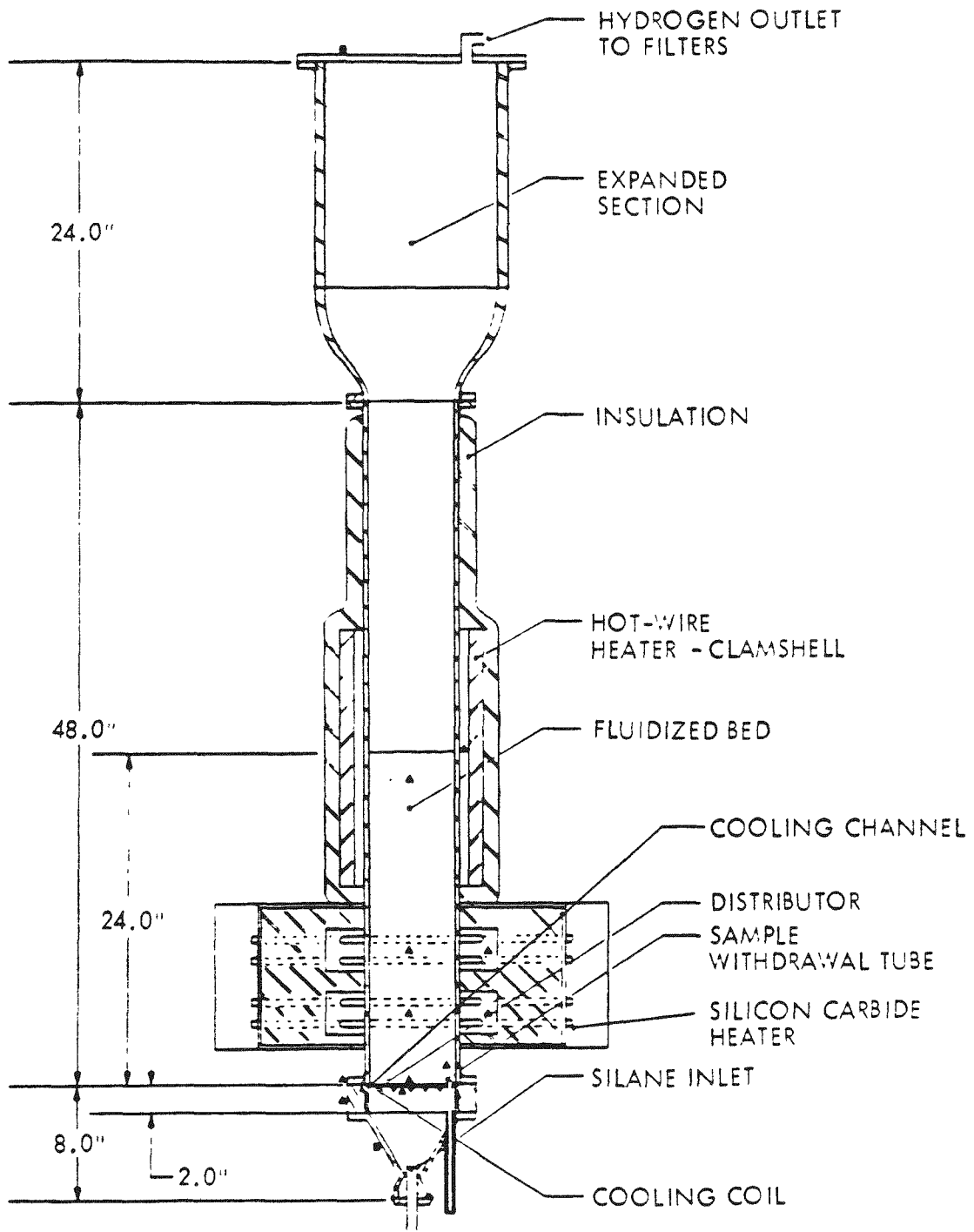


Figure 1. Reaction Paths for Silane Pyrolysis in a FBR



- ▲ THERMOCOUPLE
- DIFFERENTIAL PRESSURE PORT

Figure 2. Six-inch Diameter Fluidized Bed Reactor

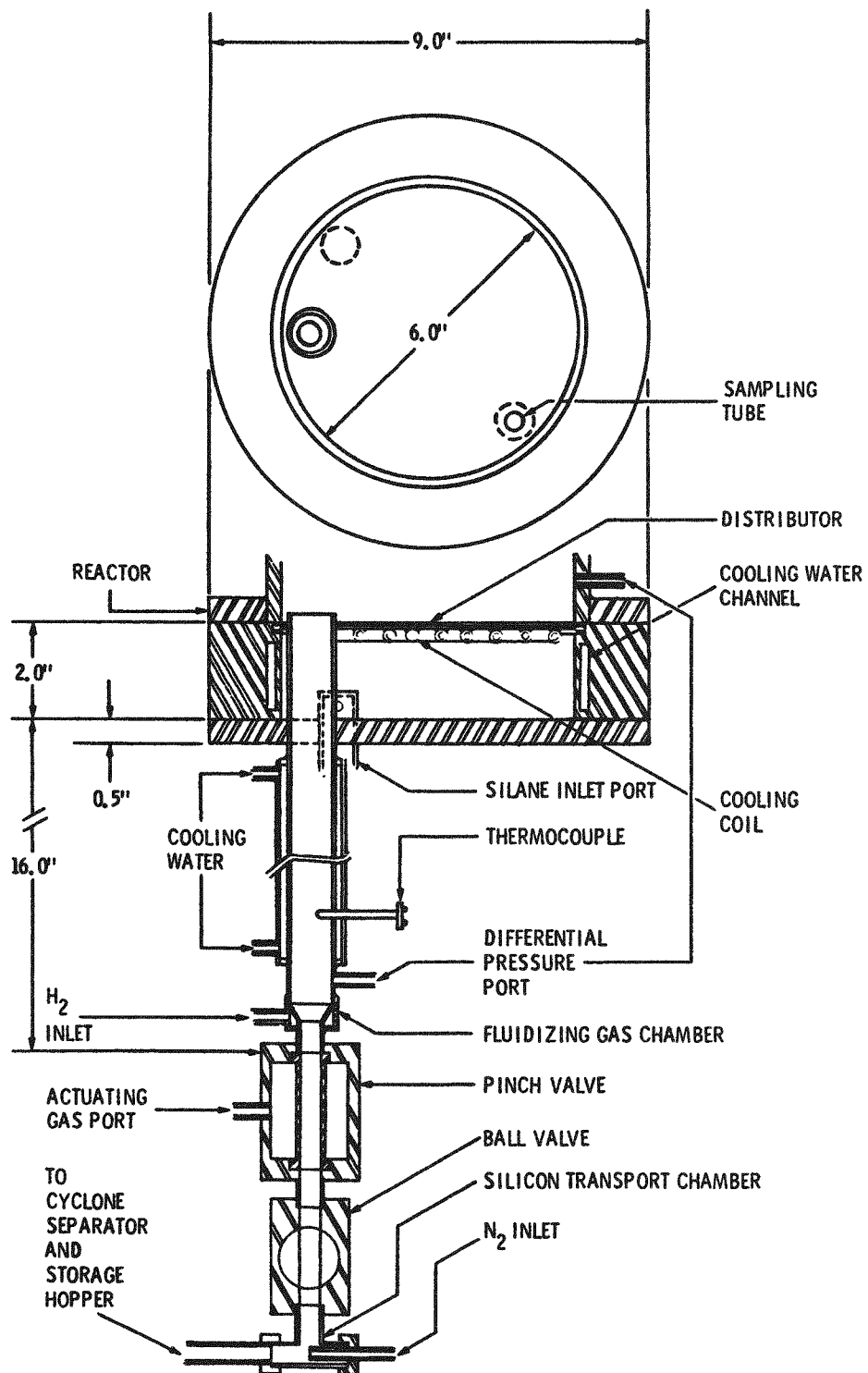
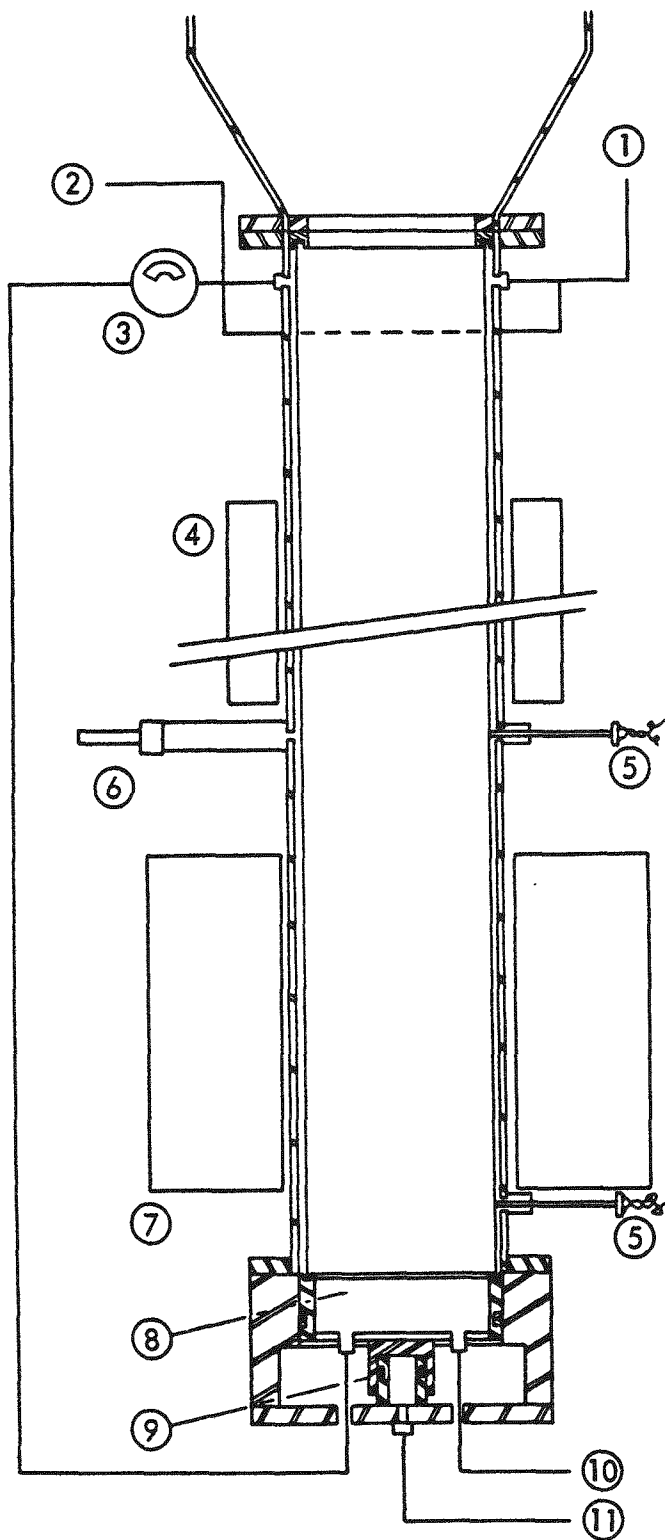


Figure 3. Product Withdrawal System



- ① HYDROGEN EXHAUST
- ② HYDROGEN INLET
- ③ DIFFERENTIAL PRESSURE GAGE
- ④ CLAMSHELL HEATER
- ⑤ THERMOCOUPLE
- ⑥ PYROMETER
- ⑦ SILICON CARBIDE HEATER
- ⑧ PISTON
- ⑨ PNEUMATIC CYLINDER
- ⑩ SILANE INLET
- ⑪ NITROGEN INLET

Figure 4. Quartz Liner for FBR

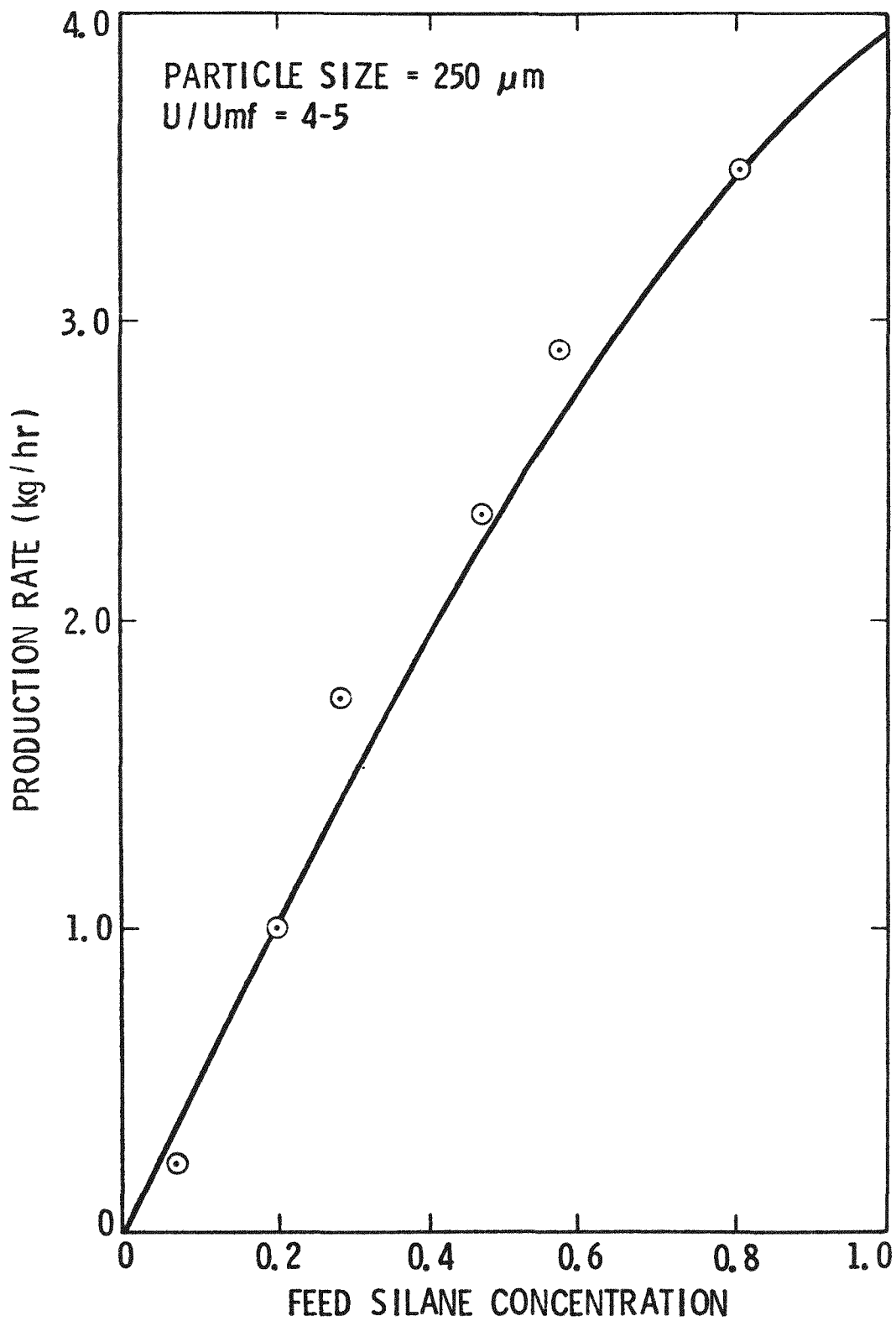


Figure 5. Experimental Production Rate vs. Silane Concentration

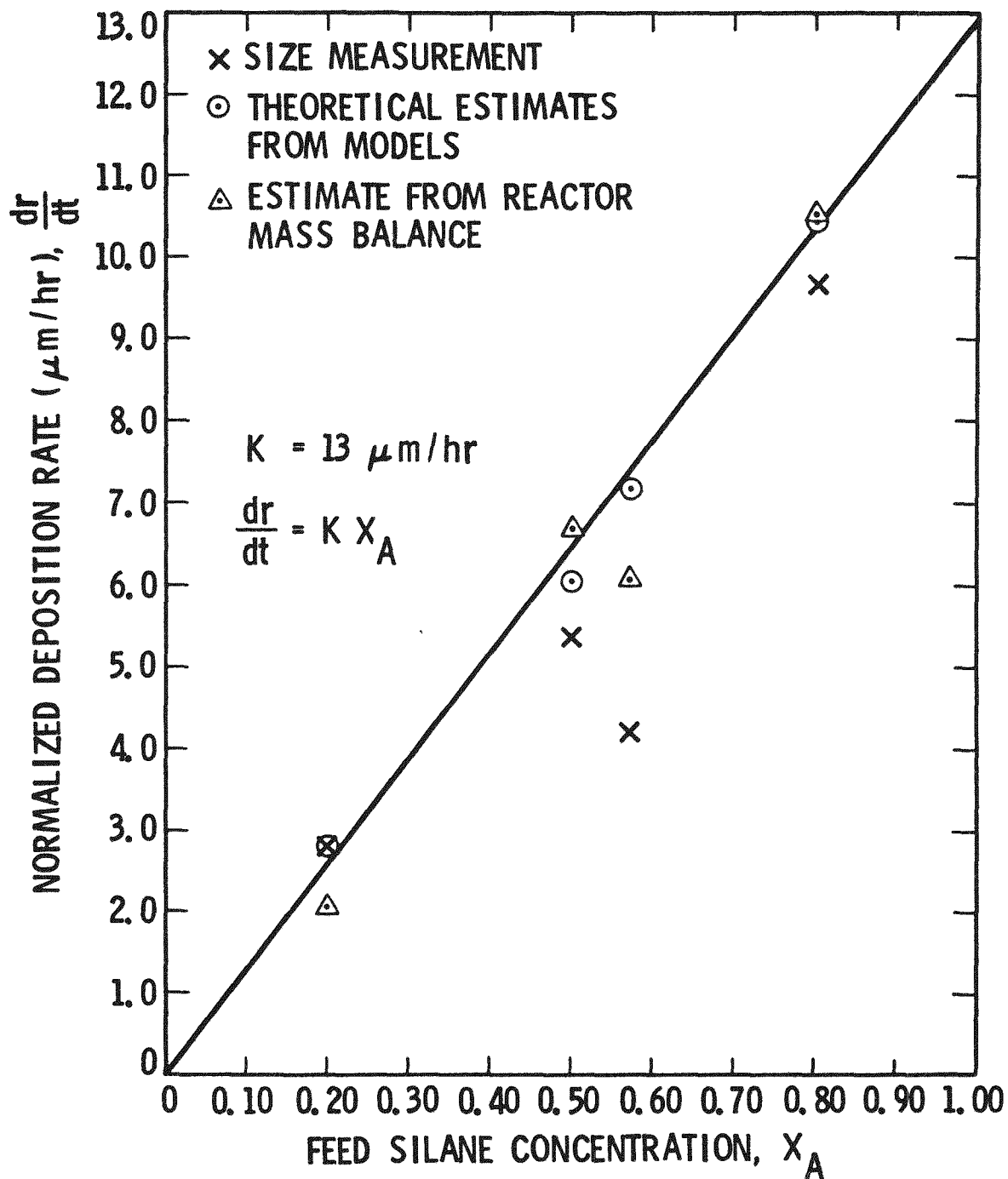


Figure 6. Normalized Deposition Rate vs. Feed Silane Concentration

Table 1. Silicon Particle Growth

SILANE CONCENTRATION (VOL %)	RUN DURATION (MIN.)	INITIAL DIAMETER OF PARTICLE (μm)	THEORETICAL ESTIMATE FOR DEPOSITION DUE TO SCAVENGING* (μm)	THEORETICAL ESTIMATE FOR HETEROGENEOUS DEPOSITION** (μm)	THEORETICAL FROM MODELS		MEASURED FINAL DIAMETER SIZE ANALYSIS (μm)	ESTIMATED FROM MASS BALANCE	
					DIAM. (μm)	% DEV. FROM MEAS.		DIAM. (μm)	% DEV. FROM MEAS.
20	90	227	5.4	3.0	235.4	0%	235.5	233.2	-1%
50	120	268	17.4	16.0	301.4	+1.3%	297.6	305.1	+2.5%
57	120	236	17.0	10.0	263.0	+4.4%	251.9	259.0	+2.8%
80	173	212	18.0	14.0	244.0	+1.0%	241.5	244.2	+1.1%

AVERAGE INITIAL BED WEIGHT: 10 KG; T = 650°C, U/U_{MF} = 5

* EQUATION (2)

** EQUATION (3)

Table 2. Purity of FBR Product without a Liner (PPmw), (Neutron Activation Analysis - Lawrence Livermore Lab)

<u>JPL RUN No.</u>	<u>Cr</u>	<u>Fe</u>	<u>Ni</u>	<u>Co</u>	<u>Mo</u>	<u>W</u>	<u>Na</u>	<u>TOTAL IDENTIFIED</u>
111 (SEED)	4		1		0.05	0.04	1.3	
111-4P*	16 (15%)	77 (72%)	11 (11%)	0.16	0.76 (0.7%)	0.1	2	107
111-8P**	45 (17%)	185 (70%)	31 (12%)	0.36	3.8 (1.4%)	0.15	1.3	266
115P***	46 (17%)	197 (71%)	30 (11%)	0.4	1 (0.4%)	0.1	1.1	275
115 INGOT - BOTTOM	0.7						1.3	
115 INGOT - MIDDLE	0.2						4.2	
115 INGOT - TOP	0.3						1.2	

REACTOR WALL MATERIAL S.S.316: Cr 17%, Fe 70%, Ni 12%, Mo 2.5%, Mn 2%, Si 1%
EXPERIMENTAL CONDITIONS FOR RUN #111 AND 115, REFER TO REPORT (26).

* 4P IS PRODUCT OBTAINED AFTER 4 hrs.

** 8P IS PRODUCT OBTAINED AFTER 8 hrs.

*** P IS FINAL SILICON PRODUCT

Table 3. Purity of FBR Product with Quartz Liner (PPma)

ELEMENTS	JET MILLED AND ACID CLEANED SEED FOR FBR	FBR PRODUCT*
	SSMS**	SSMS
P	0.2	0.1
Fe	≤0.6	≤0.6
Cr	0.03	<0.02
Ni	<0.5	<0.5
Cu	≤0.02	<0.02
Zn	≤0.04	<0.04
Co	≤0.1	≤0.1
Mn	≤0.02	<0.02
Na	≤0.1	≤0.1
Mg	<1	<1
Al	0.05	0.05
S	<1	<1
K	<0.1	<0.1
Ca	0.1	0.1

* RUN NOS. 502 AND 503

** SPARK SOURCE MASS SPECTROSCOPY CONDUCTED BY THE NORTHERN ANALYTICAL LAB

DISCUSSION

SANJURJO: Perhaps I missed it, but I didn't see any boron concentration data in the analysis of the silicon obtained with the jetmill process. Can you comment on this?

HSU: I'm sorry, but we don't have those results.

FLUIDIZED-BED REACTOR MODELING FOR PRODUCTION OF SILICON BY SILANE PYROLYSIS

M. P. Duduković, P. A. Ramachandran and S. Lai
Washington University
St. Louis, Missouri 63130, USA

INTRODUCTION

Traditionally high purity silicon for solar and electronic applications has been produced in Siemens decomposers by hydrogen reduction of chlorosilanes [1]. The yield in the Siemens process is poor. The new cheap routes to silane offer an attractive alternative for silicon production via silane pyrolysis. The thermodynamic yield of this process is 100%. However, higher feed concentrations of silane (a few percent) in Siemens decomposers lead to formation of fines via homogeneous nucleation. In order to realize the potential of silane pyrolysis the formation of fines must be prevented or at least kept below a certain acceptable minimum level. Fluidized beds offer an attractive possibility, and extensive experimental studies have been conducted [2,3]. Modeling efforts have lagged far behind the experimental activities.

The objective of this paper is to develop a mathematical model for fluidized bed pyrolysis of silane that relates production rate and product silicon properties (such as size, size distribution, presence and absence of fines) with fluidized-bed size and operating parameters (such as wall temperature, feed concentration, gas flow rate, seed size, etc.) and with bed grid design. Upon model verification it is desired to expand the model to account for product morphology, *i.e.* porous versus nonporous particles, etc. While fluidized-bed models for catalytic processes are abundant (e.g. see reviews by Grace or Yates [4,5,6]) and models for gas-solid reactions with changing solids have been well established by Kunii and Levenspiel [7,8], a comprehensive model needed for simultaneous chemical vapor deposition (CVD) and nucleation reactions has not been reported.

MODEL DEVELOPMENT

A suitable mathematical model for silane pyrolysis in fluidized-bed reactors should consider various reaction pathways, the problem of "smoke" (fines) formation, the suppression of "smoke" formation and its capture by large particles. We approach these problems on two levels. First, we attempt to identify a plausible description of the key chemical and physical rate determining steps in reaction pathways from silane to silicon. Then we address the question of flow and gas-solid contacting in fluidized-beds, and develop a model for the reactor. We treat here only batch growth of solids because data are readily available only for this model of operation.

Reaction Pathways from Silane to Solid Silicon

The mechanism of silane pyrolysis is not completely understood [1]. Active

work is in progress in addressing this question [9,10]. We do not know for certain which intermediate species is the first to nucleate. Based on the current understanding of the system we arrive at the picture presented in Figure 1 for the various pathways from silane to silicon. We assign the rate of the rate limiting step to each pathway. In doing so we have assumed that silane can decompose by two independent pathways. One is the homogeneous decomposition (pathway 3) into a gaseous precursor that can nucleate a new solid phase of silicon. We use the form reported by Hogness et. al. [11] with the variations suggested by either Purnell and Walsh [12] or O'Neal and Ring [13] to describe it. The other route for silane decomposition is the heterogeneous chemical vapor decomposition (CVD) of silane on the existing silicon seed particles (pathway 1) or on the formed nuclei (pathway 2). For this rate we use the first-order form reported by Iya et. al. [14]. It can readily be shown that in fluidized beds, due to rapid particle-gas transfer, CVD would control the growth rate of large particles rather than mass transfer. Since the molecular bombardment rate of small particles (fines) is larger than the CVD rate at the temperature of interest (500 to 750°C) then CVD also controls the silane loss to fines (pathway 2).

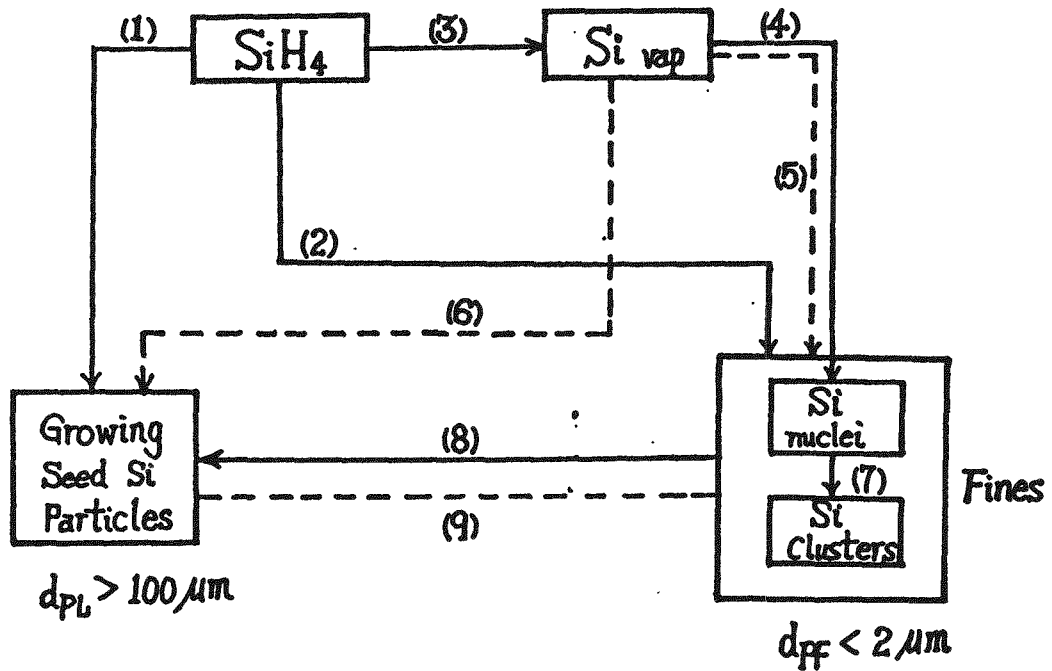
The intermediate which leads to the nucleation of the new phase is assumed to be the silicon vapor. The concentration of this intermediate formed by homogeneous pathway 3 is always very small. By pathway 4 nucleation of critical size nuclei, r^* , occurs whenever supersaturation $S = 1$ is exceeded. The concentration of silicon vapor can be suppressed by diffusion and condensation on large particles (pathway 6) and by molecular bombardment of fines (pathway 5). We assume here that nucleation occurs by the homogeneous nucleation theory [15]. The molecular bombardment rate of small particles (pathway 5) is calculated by the classical expression of kinetic theory [16] while the diffusion rate to large particles (pathway 6) is readily obtained from film theory of mass transfer [16]. This concludes the description of those pathways in Figure 1 that include gaseous and solid species. The rate forms used are indicated on the figure.

Population Balance for Fines

In order to describe the size of fines and the ability of large particles to scavenge them, we need a population balance for fines. We define $n_v(v)dv$ to be the number of fines having volumes in the range v to $v + dv$ per unit volume of the gas. The population balance, based on a well mixed gas volume, yields the following equation:

$$\begin{aligned} \frac{q_e}{V_I} n_v(v) + \frac{\partial}{\partial v} [R_G(v) n_v(v)] &= \frac{1}{2} \int_{v^*}^{v-v^*} \beta(v-\tilde{v}, \tilde{v}) n_v(v-\tilde{v}) n_v(\tilde{v}) d\tilde{v} \\ - \int_{v^*}^{\infty} \beta(v, \tilde{v}) n_v(v) n_v(\tilde{v}) d\tilde{v} - \alpha(v, v_L) n_v(v) &+ r_{HN} N_A \delta(v-v^*) \end{aligned} \quad (1)$$

The LHS terms of Eq. (1) are the elutriation rate and growth rate into size range by CVD of silane and molecular bombardment of Si vapor. The RHS terms are growth rate into size range by coagulation of fines, rate of loss in size range by coagulation, rate of loss in size range by scavenging by large particles (seeds) and the nucleation rate of the critical size. The pseudo-state approximation is used here since we are interested in observing the system at the time



- (1) CVD growth on seed particles } $r_{HT} = 2.79 \times 10^8 \exp(-19530/T) C_{SiH_4}$
- (2) CVD growth on fines } Heterogeneous decomposition
- (3) Homogeneous silane decomposition $r_{HD} = 2 \times 10^{13} \exp(-26,000/T) C_{SiH_4}$
- (4) Homogeneous nucleation $r_{HN} = (N_A \frac{\alpha_c}{\rho_{Si}} (\frac{2\sigma_m}{\pi})^{1/2}) \exp(-\frac{4\pi r^* \alpha_{NA}}{3R_g T}) C_{Si}^{*2}$
- (5) Molecular bombardment of fines } Si diffusion $r_{DF} = \phi_s \sqrt{R_g T / 2\pi M_{Si}} (C_{Si} - C_{Si_0})$
- (6) Diffusion to growing seeds } $r_{DL} = (2\phi_s D / d_{PL}) (C_{Si} - C_{Si_0})$
- (7) Coagulation and coalescence of fines - eq. (4)
- (8) Scavenging by seed particles on fines - eq. (10)
- (9) Attrition of large particles (not included)

Figure 1. Schematic of Various Pathways for Conversion of Silane to Silicon.

scale for growth of large particles which is very long compared to other time scales.

It should be kept in mind that we are not interested in a precise description of the size distribution of fines. We mainly need to establish if their formation can be suppressed and if not, what their mean size might be. We, therefore, solve the population balance approximately by using the method of moments. We define:

$$M_0 = \int_{v^*}^{\infty} n_v(v) dv = (\text{total number of particles per unit volume of gas}) \quad (2)$$

$$M_1 = \int_{v^*}^{\infty} v n_v(v) dv = (\text{total volume of particles per unit volume of gas}) \quad (3)$$

The number average mean volume of fines is then obtained by the ratio of the first and zeroth moment $\bar{v} = M_1/M_0$. In order to reduce eq. (1) to a set of equations for the moments we need to make a set of assumptions. These are:

i) The coagulation coefficient is assumed to be a constant which only depends on the average size of fines. This approach is often used in the continuum regime where the problem is thus reduced to a Smoluchowski type equation [16,17]. We use the same approach for the free molecular regime and take the following value of the coagulation coefficient β_0

$$\beta_0 = \begin{cases} \frac{8kT}{3\mu} & \text{continuum region} \\ 2^{5/2} \left(\frac{3}{4\pi}\right)^{1/6} \left(\frac{6kT}{\rho}\right)^{-1/6} \bar{v}^{-1/6} & \text{free molecular regime} \end{cases} \quad (4a)$$

$$\quad (4b)$$

ii) The scavenging coefficient is assumed to be dependent only on the mean size (diameter) of the large seed particles and of the fines. Following the work of Doganoglu et. al. [18] and Peters et. al. [19] we represent the scavenging coefficient of fines by large particles in a fluidized bed by:

$$\alpha(\bar{v}_L, \bar{v}_F) = E u_{mf} \frac{3(1-\epsilon_{mf})}{2\bar{d}_{PL} \epsilon_{mf}} \quad (5)$$

where ϵ_{mf} , u_{mf} are bed voidage and superficial gas velocity at minimum fluidization, α is the scavenging coefficient, \bar{d}_{PL} is the mean diameter of large particles (seeds) and E is the single large particle collection efficiency. It is well established [16,17] that single body collection efficiency can be approximately represented as a sum of efficiency for impaction, interception, diffusion, and diffusion with interception. The diffusional mechanism dominates under the conditions prevailing in a fluidized bed reactor and

$$E = 2 Pe^{-2/3} \quad (6)$$

where $Pe = \bar{d}_{PL} u_{mf}/D$ and $D = kT/3\pi\mu \bar{d}_{PF}$. The mean particle diameter for small and large particles is estimated.

iii) The growth rate of fines, which is due to the combined effect of CVD growth from silane and molecular bombardment of gaseous silicon, is assumed to be given as a function of the average size of fines, i.e.

$$\int_{v^*}^{\infty} v \frac{\partial}{\partial v} [R_G(v)n_v(v)]dv = -\sigma v^{-2/3}M_0 = -\sigma v^{-1/3}M_1 = -\sigma M_0^{1/3}M_1^{2/3} \quad (7)$$

where $\sigma = (M_{Si}/\phi_s \rho_{Si})(4)^{1/3} 3^{2/3}(r_{HT} + r_{DF})$.

With the above three assumptions the population balance, eq. (1), is reduced to the following two equations for the moments:

$$-\frac{1}{2} \beta_0 M_0 - \left(\alpha + \frac{q_e}{V_I}\right) M_0 - r_{HN} N_A = 0 \quad (8)$$

$$\sigma M_0^{1/3} M_1^{2/3} - \left(\alpha + \frac{q_e}{V_I}\right) M_1 + r_{HN} N_A v^* = 0 \quad (9)$$

The scavenging rate of fines by large particles is now given by:

$$m_{Sca} = \frac{Si}{N_L} \int_{v_L \min}^{v_L \max} \int_{v_F \min}^{v_F \max} v_F \alpha(v_L, v_F) n_L(v_L) n_F(v_F) dv_L dv_F \quad (10)$$

with the scavenging coefficient α given by eq. (5).

This completes the description of various pathways of Figure 1, namely pathway 7, by which a population of fines with a certain average size is established, and of pathway 8 for scavenging (filtering) of fines by large particles.

Backmixed Reactor (CSTR) Model

The hydrodynamics of a fluidized bed and gas-particle contacting are complex and not entirely understood. It is useful, however, to develop models that characterize the limiting behavior of the system which can only be approached in practice. Here we deal with the competitive homogeneous and heterogeneous reaction. Intimate gas-solid contacting, high solids to gas ratio and no gas bypassing will favor the heterogeneous route. Homogeneous nucleation is to be prevented compared to CVD growth and diffusion of Si vapor. The former can be regarded as a reaction of high order and, hence, will be suppressed the most by complete micromixing such as found in an ideal CSTR. Therefore, both suppression of homogeneous decomposition and of homogeneous nucleation will be favored in a CSTR, i.e. in an ideally backmixed reactor. This situation can be approached in fluidized beds when bubble formation is suppressed while good solids mixing is maintained.

We formulated the CSTR model based on the following assumptions: i) no wall deposition, i.e. negligible wall to particles area, ii) no temperature gradients between the gas and particles, iii) uniform composition and temperature in the reactor. In addition, for the results presented in this paper, we assumed that all seed particles have the same initial size and grow at the same rate.

The equations to be solved are:

- i) The mass balance on silane:

$$q_f C_{S,f} - q_e C_{S,e} = A_{TL} r_{HT} + A_{TF} r_{HT} + V r_{HD} \quad (11)$$

ii) The mass balance on silicon vapor:

$$0 - q_e C_{Si,e} + V r_{HD} = V r_{HN} + A_{TL} r_{DL} + A_{TF} r_{DF} \quad (12)$$

iii) The balance on fines given by eqs. (8-9):

iv) The energy balance which can be shown to readily simplify to the following equation for temperature:

$$T_e = \frac{h_D A_D / h_w A_w}{1 + h_D A_D / h_w A_w} T_D + \frac{1}{1 + h_D A_D / h_w A_w} T_w \quad (13)$$

v) The growth rate of large seed particles

$$\frac{dR_L}{dt} = \frac{M_{Si}}{\rho_{Si}} \frac{(r_{HT} + r_{DL})}{\phi_s} + \frac{m_{Sca}}{4 \pi R_L^2 N_L \rho_{Si}} \quad (14)$$

The total surface area of large and small particles A_{TL} , A_{TF} , respectively, are estimated from their average size.

A computer program was developed for solution of eqs. (11-14) and eqs. (8-9). In addition to the quantities already discussed many parameters of the fluidized bed such as bed height at minimum fluidization, the elutriation constant, heat transfer coefficients, etc. are estimated from the literature [7,20, 21]. It should be noted that the distributor must be cooled to keep its temperature below 350° to prevent silane CVD in the nozzles. When the distributor and wall temperatures are known bed temperature is given by eq. (13). When bed temperature is known eq. (13) is bypassed in the program.

The required input variables for the CSTR model are bed diameter, initial weight of solids, initial size of solids, gas flow rate, inlet gas temperature, inlet gas composition and pressure. Equations (8-9), (11) and (12) are solved for the initial seed size and the RHS of eq. (14) is then evaluated. The process is repeated for various selected values of seed size. This generates the set of pairs of values of R_L vs dR_L/dt which is numerically integrated to establish the relationship between time and particle (seed) radius. It should be noted that the CSTR as presented here has no adjustable parameters. Given the input quantities, the rate forms and transport properties are calculated by the appropriate subroutines and reactor performance is predicted, *i.e.* the growth rate of seeds, amounts of fines elutriated and silane conversion are calculated.

The fraction of silane that ended in the form of free fines, F_f , is calculated at each set of conditions from

$$F_f = 1 - \frac{\text{growth rate of large particles}}{\text{total rate of silane deposition}} = 1 - \frac{A_{TL} (r_{HT} + r_{DL}) M_{Si} + m_{Sca}}{(A_{TL} r_{HT} + A_{TF} r_{HT} + V r_{HD}) M_{Si}} \quad (15)$$

Bubbling Fluidized Bed (FBBR) Model

A large diameter fluidized bed of silicon particles operated at three to ten times the minimum fluidization velocity will behave like a bubbling bed provided bed diameter is large enough. However, since the information regarding the kinetics of the system under study is not very refined, a sophisticated bubbling bed model is not necessary. Only the key features of the bubbling bed need to be incorporated in the model. These are the existence of three distinct regions: the grid region, emulsion region (including the cloud) and the bubble region. We assume that in beds of large particles jets form in the grid region. We assume gas to be in plug flow in the jets, and jet penetration height is calculated from the Yang and Keairns' [22] formulas. When jets break up, gas is assumed to pass through the emulsion phase at minimum fluidization velocity. There are no gradients between gas and particles in the emulsion phase which is assumed well mixed. The excess gas, $u - u_{mf}$, forms bubbles which rise in plug flow. Average bubble diameter, average bubble volume fraction, bubble rise velocity, etc. are calculated from the available correlations. The overall mass and heat transfer coefficients between bubbles and emulsion are evaluated based on the approach suggested by Kunii and Levenspiel [7]. The mass and heat transfer exchange coefficients between jets and emulsion are calculated as a multiple of bubble-emulsion exchange coefficients as suggested by Weimer and Clough [23]. This multiplicative factor f_{jb} defined by

$$K_{je} = f_{jb} (K_{be})_b \quad (16)$$

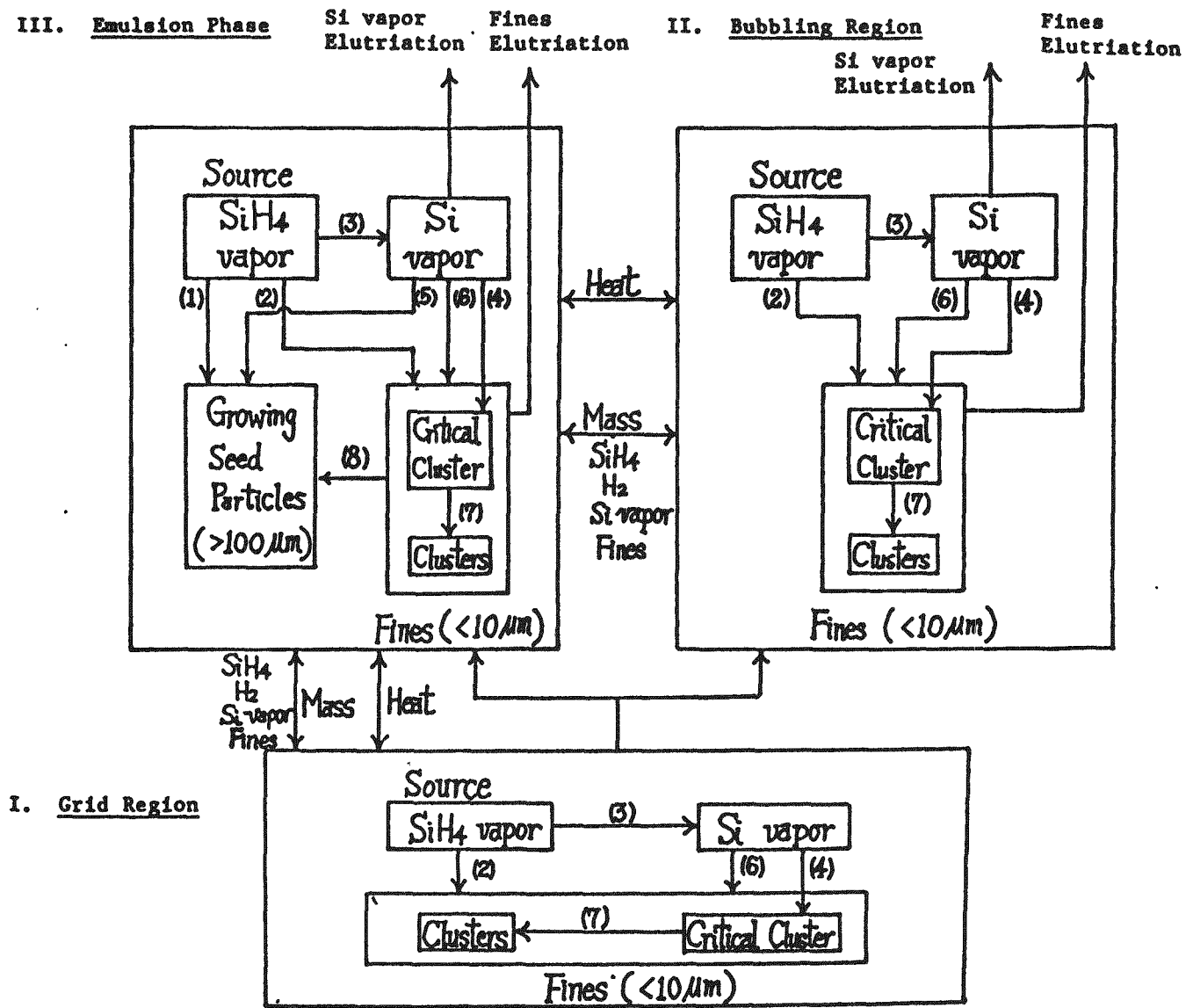
is the only adjustable parameter for the bubbling bed model. It is also assumed that no large particles are present in the jets and bubbles.

The schematic of the bubbling bed model is shown in Figure 2. The various pathways described in Figure 1 can take place now in each of the three regions: jets, bubbles and emulsion. In addition, one must account for the interchange between the various regions. The equations for the mass balance on silane, silicon vapor and fines and for the energy balance in each of the three regions are lengthy and will be omitted here but are given elsewhere [24].

The input parameters besides those required by the CSTR model include the specification of the distributor, *i.e.* number or orifice holes, hole diameter, etc. The details of the computer algorithm are reported elsewhere [24]. Given all input parameters the program calculates silane conversion, fraction of silane in form of fines and growth rate of large particles. Repeated calculations at various particle sizes lead to desired time on stream-particle size relationship.

RESULTS AND DISCUSSION

Model predicted results are compared with two JPL experimental runs in Table 1. Both models predict reasonably well the production rate and final particle size. However, model discrimination is impossible because the experimental runs were of insufficient duration so that the actual final particle size could not be determined accurately. This also leads to problems in the mass balance for the experimental runs and slight discrepancies in reported production rates and final particle size.



- | | |
|--|--|
| (1) CVD Growth on seed particles | (6) Molecular bombardment of Si vapor to fines |
| (2) CVD growth on fines | (7) Coagulation of fines |
| (3) Homogeneous SiH ₄ decomposition | (8) Scavenging of fines by seed particles |
| (4) Homogeneous nucleation | |
| (5) Brownian diffusion of Si Vapor into seed particles | |

Figure 2. Schematic of the Fluidized Bubbling Bed Reactor (FBBR) Model for Silane Pyrolysis.

Table 1. Comparison of the CSTR and FBBR Model Predictions and Experimental Results for Two JPL Runs

Silicon Seed		Experimental Conditions			
Weight (Kg)	\bar{d}_p (μm)	Silane Feed Conc. (%)	Bed temp. ($^{\circ}\text{C}$)	Total gas flow rate (moles/min)	Duration (min)
10.50	227	20	650	3.0	90
11.34	212	80	650	2.5	173

PRODUCT COMPARISON

Experimental Data		Model Predicted (CSTR)		Model Predicted (FBBR)	
Production rate	\bar{d}_p (μm)	Production rate (Kg/hr)	\bar{d}_p (μm)	Production rate	\bar{d}_p (μm)
0.87	235.5	1.00	237.4	0.93	236.6
3.50	241.5	3.30	260.3	3.16	257.7

Reactor Specifications: Bed diameter 15.4 cm (6.065" I.D.); Number of orifice holes in distributor: 4,500.

Orifice area: 0.02 cm^2 ; Distributor temperature: 200°C ; Entering gas temperature: 200°C .

In order to illustrate the dominant pathways in silane conversion to silicon the modeling results for the two runs of Table 1 are presented schematically in Figure 3 for the CSTR model. It is clear that in an ideal CSTR gas-solid contacting is very efficient, micromixing is excellent and homogeneous nucleation and fines formation can be effectively suppressed. For example even at 80% SiH_4 in the feed (Figure 3b) 84% of decomposed silane (2.82 kg/h) reacts by CVD on the growing seed particles, 15% (0.49 kg/h) decomposes homogeneously and 1% (0.035 kg/h) reacts by CVD on the fines. Silane conversion is over 99%. The Si vapor is formed at a rate of 0.49 kg/h, but 75% of it (0.36 kg/h) is effectively scavenged by diffusion to and condensation on seed particles, while only 25% (0.12 kg/h) contributes to the mass generation of fines. The nucleation rate is kept at a very low level of $4 \times 10^{-5} \text{ kg/h}$. The nucleated fines gain 78% of their mass (0.12 kg/h) by molecular bombardment of silicon vapor and 22% (0.035 kg/h) by CVD of silane on fines. Most importantly due to excellent contacting 70% (0.11 kg/h) of the fines formed are scavenged by large particles and only 30% (0.04 kg/h) are elutriated. This means that in an ideal CSTR at 650°C bed temperature and at a high production rate of 3.3 kg/h only 1.5% of silane would end in the undesirable form of fines at the reactor exit even at 80% SiH_4 in the feed.

Figure 4 illustrates the FBBR model predictions for the JPL run listed as example 1 in Table 1 at 20% SiH_4 in the feed. The values computed in Figure 4 are based on the assumption that the exchange between jets and emulsion is fifty times faster than between bubbles and emulsion, *i.e.* $f_{jb} = 50$. Homogeneous decomposition is favored over CVD on seeds in the jet region due to poor gas-

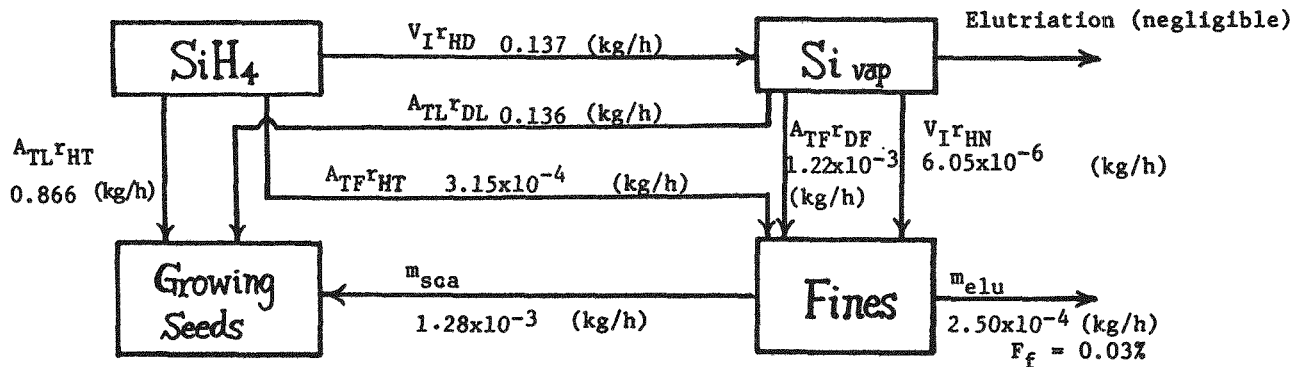


Figure 3a. Net growth rate: 1.00 (kg/h)
 Backmixed (CSTR) Reactor: 20% SiH₄ in the Feed

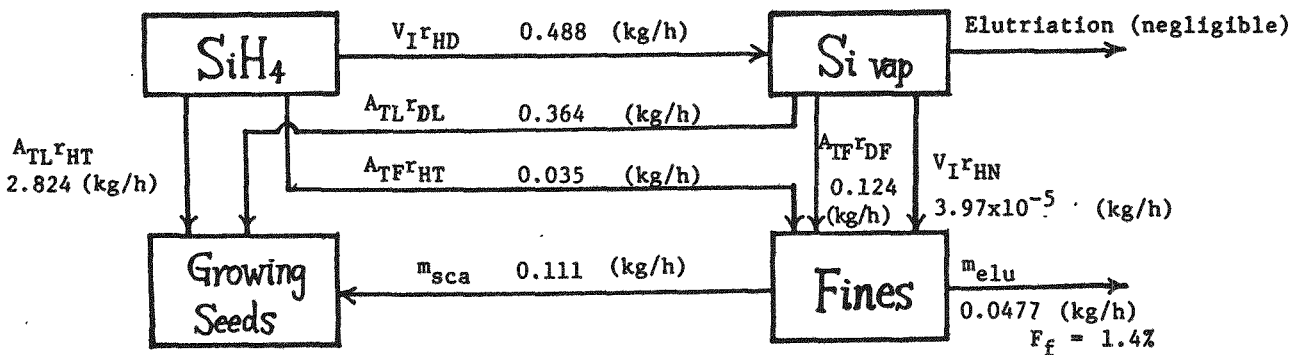


Figure 3b. Net growth rate: 3.30 (kg/h)
 Backmixed (CSTR) Reactor: 80% SiH₄ in the Feed

Figure 3. Rates of Various Pathways for Silane Decomposition as Calculated by the CSTR Model for Bed Temperature of 650°C

3a. 20% SiH₄ in the feed

3b. 80% SiH₄ in the feed

III. Emulsion Phase

II. Bubbling Region

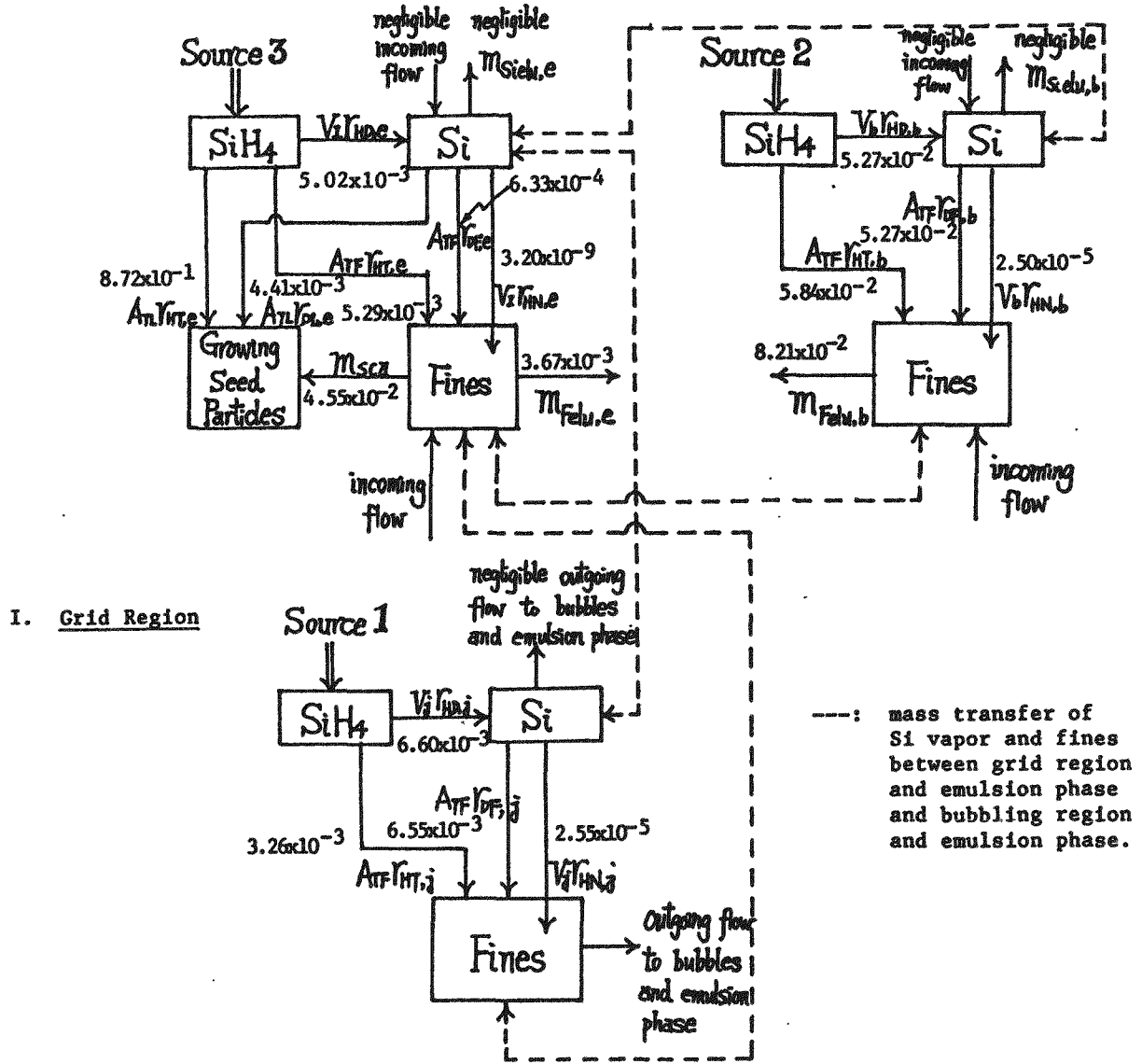


Figure 4. Rates of Various Pathways for Silane Decomposition as Calculated by the FBBR Model (Run 1, $T_e = 650^\circ\text{C}$, $f_{jb} = 50$).

solid contacting in spite of the high exchange coefficients. Most of the homogeneous nucleation takes place in the jets (grid region) (2.6×10^{-5} kg/h) followed up by nucleation in the bubbles (2.5×10^{-5} kg/h) while little occurs in the emulsion phase (3.2×10^{-9} kg/h). The fines gain the most mass in the bubbles at a rate of 0.11 kg/h, followed by the grid region with the rate of 0.010 kg/h and the emulsion region with the rate of 0.0059 kg/h. Bubbles are the main culprit in formation of fines since 88% of the mass of fines is generated there. The predicted fraction of silane that is elutriated as silicon fines is 8.1% which exceeds the experimental value of 3%. However, in the run of such short duration the mass balance is difficult to close and it is questionable whether all the fines have been detected in the experimental run. There are reasons to believe that actual elutriation rate of fines is higher than reported values.

The comparison of CSTR and FBBR ($f_{jb} = 50$) predictions for deposition rate with 20% SiH_4 in the feed and as a function of bed temperature and gas flow rate is illustrated in Figure 5. At low bed temperatures and at low gas flow rate (i.e. close to minimum fluidization conditions) CSTR and FBBR predictions are close. While mathematically this is to be expected, it is doubtful that CSTR behavior can be achieved in practice since solids circulation would not be vigorous enough at close to minimum fluidization conditions. It is clear that the CSTR model gives an upper bound on deposition rate as argued earlier. At higher temperatures FBBR predictions can deviate significantly from CSTR behavior due to increased production of fines. This is to be expected for two reasons. The homogeneous decomposition has a higher activation energy than the CVD reaction and is favored at higher temperatures. At the same time bubble expansion is more drastic at higher temperatures and the gas bypassing problem is aggravated.

A limited parametric sensitivity study of the model was performed. The changes in deposition rate, silane conversion and formation of fines were determined as a function of the following quantities: (i) the kinetic form for homogeneous decomposition [11,12,13], (ii) the jet-emulsion exchange coefficient, i.e. variation in f_{jb} values, (iii) grid design, (iv) method of treatment of the population balance. It was shown [24] that the variations in the kinetic forms and method of treatment of the population balance for fines have a limited effect on production rate and fines elutriation. The model is, however, most sensitive to the jet-emulsion exchange coefficient. Table 2 illustrates that an increase in the jet-emulsion exchange coefficient in the limit leads to CSTR behavior. Unfortunately, there is no reliable model for the grid region based on which the exchange coefficients could be tied intimately to grid design. Therefore, two different assumptions are made in order to estimate the effects of grid design on reactor performance. In the first case, it is assumed that jet emulsion exchange is governed mainly by bed dynamics which is primarily affected by bed diameter, height and total gas flow. the ratio of jet-emulsion and bubble-emulsion exchange was set a $f_{jb} = 50$ for all grids. The effect of grid design is illustrated in Table 3. Clearly, silane overall conversion is hardly affected by grid design. Higher deposition rates (and lower formation and elutriation of fines) are obtained at lower jet velocities. Higher jet penetration at the same gas velocity also favors improved deposition rate. Yang and Keairns [22] indicate that the jet penetration length is proportional to $d_o^{0.8} u_o^{0.36}$ where d_o is orifice

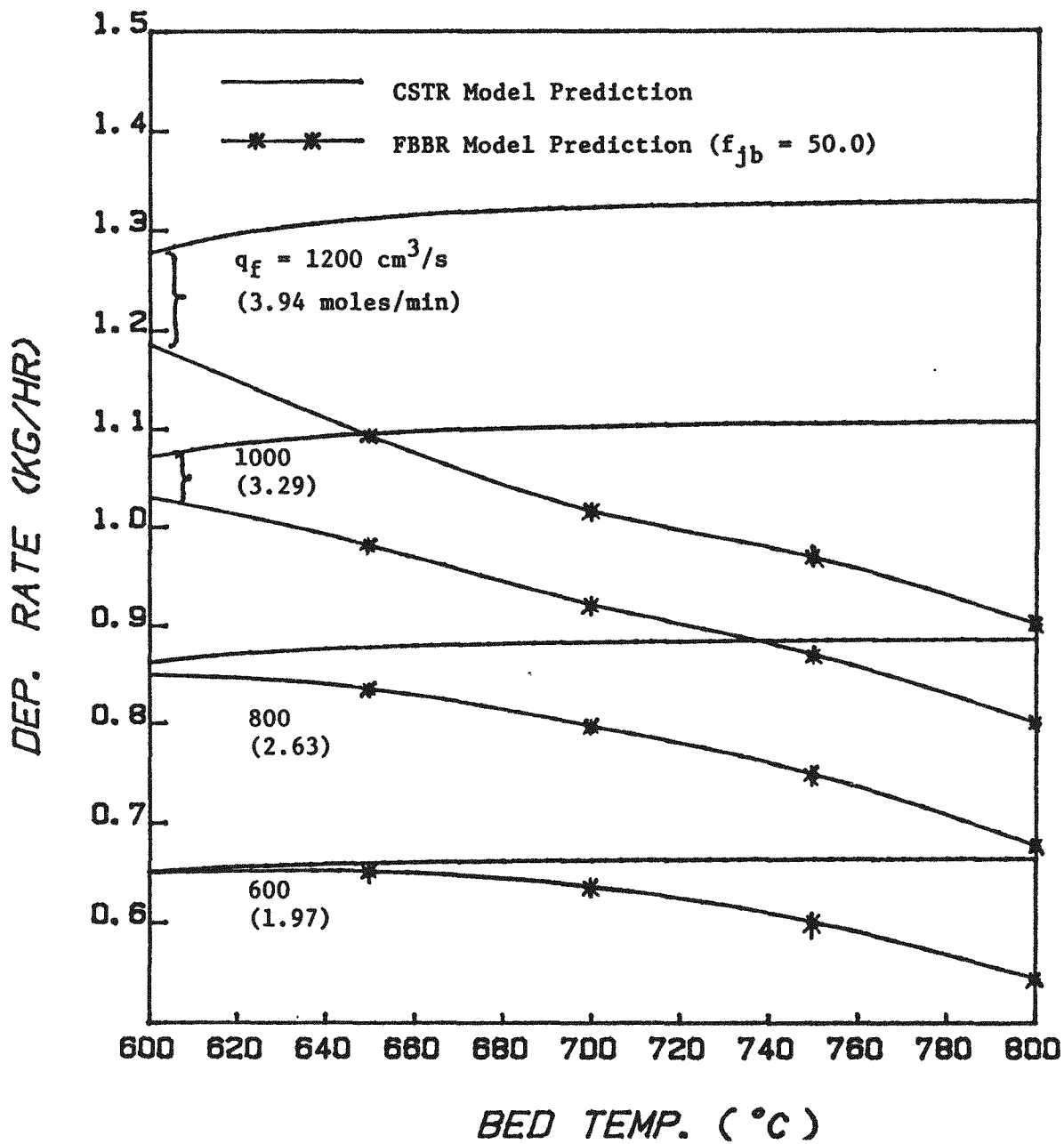


Figure 5. Comparison of CSTR and FBBR Model Predictions for Deposition Rate (Run 1).

Table 2. Comparison of the FBBR Model at Different Levels of Jet-Emulsion Exchange and the CSTR Model (Conditions of Run 1, Table 1.)

	FBBR			CSTR
	$f_{jb} = 10$	$f_{jb} = 50$	$f_{jb} = 100$	-
Silane Conversion (%)	99.50	99.21	99.15	99.04
Fines Elutriation (%)	30.9	9.1	1.6	0.0
Deposition Rate (kg/h)	0.696	0.922	0.986	1.002

Table 3. Effect of Grid Design (Constant $f_{jb} = 50$)

	Grid 1	Grid 2	Grid 3	Grid 4	Grid 5
	$A_{ro}=0.002\text{cm}^2$	$A_{ro}=0.02\text{cm}^2$	$A_{ro}=0.02\text{cm}^2$	$A_{ro}=0.2\text{cm}^2$	$A_{ro}=2.0\text{cm}^2$
	$N_t=4,500$	$N_t=450$	$N_t=45$	$N_t=45$	$N_t=45$
Jetting height(cm)	0.35	0.83	1.97	2.12	2.29
Jetting velocity (cm/s)	10.1-29.5	101-256	1014-1680	101-284	10.1-34.3
Silane Conversion (%)	99.2	99.5	99.7	99.3	99.3
Fines Elutriation (%)	8.1	30.7	47.8	21.0	0.9
Deposition Rate (kg/h)	0.92	0.70	0.53	0.79	1.00
$N_t^{0.64}A_{ro}(\text{cm}^2)$	4.4	1.0	0.23	2.3	23

diameter and u_o is the velocity at the orifice. At fixed total gas flow rate it can then be shown that the gas residence time in the jetting region is proportional to $N_t^{0.64}d_o^{2.08} = N_t^{0.64}A_{ro}$ where N_t is the total number of orifice holes and A_{ro} is the surface area of an individual orifice. Last row of Table 3 gives the value of this group for each grid. It is apparent that deposition rate correlates at least qualitatively with the residence time in the jetting region.

On the other hand one can assume that the jet-emulsion exchange is dominated by the grid hydrodynamics and that f_{jb} increases proportionately with jet velocity. The deposition rate for grids 2, 3 and 4 which now have $f_{jb} = 150, 450, 150$, respectively, is increased compared to values in Table 3, but not sufficiently to approach the superior performance of grid 5. However, grid 4 would yield now a deposition rate of 0.97 (kg/h) and fines elutriation of 3.1% which is better than the grid 1 performance. This indicates, as expected, that $N_t^{0.64}A_{ro}$ is not the only measure of grid performance. The exchange coefficient is another key variable. Its a priori predictions at present are not possible. Grid 5 design is also unrealistic.

The above results indicate the importance of grid design and gas-solids contacting in the grid region on reactor performance. Good jet penetration, high gas residence time in the jetting region and excellent jet-emulsion

exchange are necessary for suppression of formation of fines. The current models for the grid region are insufficient to fully quantify reactor performance and can benefit from further improvements. It should be noted that the current FBBR model is capable of predicting temperature gradients in the grid region and that such gradients have been observed experimentally.

CONCLUSIONS

An ideal backmixed reactor model (CSTR) and a fluidized-bed bubbling reactor model (FBBR) have been developed for silane pyrolysis. Silane decomposition is assumed to occur via two pathways: homogeneous decomposition and heterogeneous CVD. Both models account for homogeneous and heterogeneous silane decomposition, homogeneous nucleation, coagulation and growth by diffusion of fines, scavenging of fines by large particles, elutriation of fines and CVD growth of large seed particles. At present the models do not account for attrition.

The preliminary comparison of model predictions with JPL experimental results shows reasonable agreement. The CSTR model with no adjustable parameter yields a lower bound on fines formed and upper estimate on production rate. The FBBR model overpredicts the formation of fines but could be matched to experimental data by adjusting the unknown jet-emulsion exchange coefficients. In the limit of low gas flow-rate and large exchange coefficients the FBBR model is reduced to the CSTR model provided the jet region becomes negligibly small.

The models indicate clearly that in order to suppress formation of fines (smoke) one must achieve good gas-solid contacting in the grid region and eliminate or suppress the formation of bubbles.

ACKNOWLEDGEMENT

The authors are indebted to JPL for financial support and to Dr. R. Lutwack and Dr. G. Hsu for their valuable input and information.

NOMENCLATURE

A_D	- area of the distributor excluding orifice holes, cm^2
A_{TF}	- total surface area of fines in the reactor, cm^2
A_{TL}	- total surface area of seed particles in the reactor, cm^2
A_w	- area of vessel wall, cm^2
C_{SiH_4}	- concentration of SiH_4 , mol/cm^3
$C_{S,f}, C_{S,e}$	- concentration of SiH_4 in the feed gas and in the backmixed reactor, respectively, mol/cm^3
$C_{\text{Si},e}, C_{\text{Si}}$	- concentration of Si vapor, mol/cm^3
C_{Si^0}	- equilibrium Si vapor concentration, mol/cm^3
C_{Si}^*	- the supersaturated concentration of silicon in the gas phase from homogeneous decomposition, mol/cm^3
d_{PL}	- diameter of seed particle, cm

$\bar{d}_{PL}, \bar{d}_{PF}$	- average diameter of seed particles and fines, respectively, cm
D	- particle diffusion coefficient, cm^2/s
E	- single seed particle collection efficiency, Eq. (13)
f_{jb}	- ratio relating jetting-emulsion interchange to bubble-emulsion interchange
F_f	- fraction of silane decomposed into fines
h_D	- heat transfer coefficient between bed and distributor, $\text{J}/\text{cm}^2\text{sK}$
h_w	- heat transfer coefficient between bed and surface, $\text{J}/\text{cm}^2\text{sK}$
k	- Boltzman constant, $1.38066 \times 10^{-23} \text{ J}/\text{molecule K}$
K_{je}	- interchange coefficient between jets and emulsion per unit volume of jets, s^{-1}
$(K_{be})_b$	- interchange coefficient between bubbles and emulsion phase based on volume of bubbles, s^{-1}
m	- mass of molecule, g/molecule
m_{Sca}	- total amount of fines captured by seed particles, g/s
M_0	- total number of particles per unit volume of gas, cm^{-3}
M_1	- total volume of particles per unit volume of gas, cm^3/cm^3
M_{Si}	- molecular weight of silicon, g/mol
$n_v(v, t)$	- size distribution density function of fines per unit volume of fluid, $\text{cm}^{-3}\text{cm}^{-3}$
N_A	- Avogadro's number, $6.02 \times 10^{23} \text{ molecules}/\text{mol}$
N_L	- total number of seed particles in the reactor
Pe	- Peclet number
P_{Si}	- partial pressure of Si vapor, atm
P_{Si}^o	- equilibrium Si vapor pressure, atm
q_e	- volumetric flow rate of gas in the backmixed reactor, cm^2/s
q_f	- inlet volumetric flow rate of gas, cm^3/s
r^*	- radius of the critical nucleus, cm
r_{DF}	- rate of molecular bombardment of Si vapor on fines, $\text{mol}/\text{cm}^2\text{s}$
r_{DL}	- rate of molecular diffusion of Si vapor to seed particles, $\text{mol}/\text{cm}^2\text{s}$
r_{DH}	- rate of homogeneous decomposition of SiH_4 , $\text{mol}/\text{cm}^3\text{s}$
r_{HN}	- rate of homogeneous nucleation, $\text{mol}/\text{cm}^3\text{s}$
r_{HT}	- rate of heterogeneous CVD of SiH_4 , $\text{mol}/\text{cm}^2\text{s}$
R_g	- gas constant, $8.31441 \text{ J}/\text{mol K}$
R_L	- radius of seed particles, cm
$R_G(v)$	- rate of fine particle growth from heterogeneous CVD growth and Si molecular bombardment, cm^3/s
S	- supersaturation ratio, P_{Si}/P_{Si}^o
t	- time scale, s
T, T_e	- temperature of the interstitial gas, K
T_D	- temperature of distributor, K
T_w	- temperature of vessel wall, K
u_{mf}	- superficial fluid velocity at minimum fluidizing conditions, cm/s
v, v_F	- volume of fine particles, cm^3
v_L	- volume of seed particles, cm^3
v^*	- critical volume of fine generated from homogeneous nucleation, cm^3
V_I	- total volume of interstitial gas, cm^3

Greek Symbols

α_c	- condensation coefficient
$\alpha(v, v_L)$	- scavenging coefficient, s^{-1}
$\beta(v, \tilde{v}), \beta_0$	- coagulation coefficient, cm^3/s
$\delta(v-v^*)$	- Delta function, cm^{-3}
ϵ_{mf}	- void fraction in a bed at minimum fluidizing conditions
μ	- viscosity of gas, $g/cm\ s$
ρ_{Si}	- density of silicon, g/cm^3
$\bar{\sigma}$	- rate constant of fine particle growth, cm/s
$\bar{\sigma}$	- specific surface free energy, J/cm^2
ϕ_s	- sphericity of a particle

REFERENCES

1. Duduković, M. P., "Reactor Models for CVD of Silicon", The Science of Silicon Material Preparation Workshop, Phoenix, Arizona, August 1982, JPL Publication 83-13, 199-226 (1983).
2. Hsu, G., R. Hogle, N. Rohatgi and A. Morrison, "Fines in Fluidized Bed Silane Pyrolysis", J. Electrochem. Society 131 (3), 660 (1984).
3. Rohatgi, N. and G. Hsu, "silicon Production in a Fluidized Bed Reactor: A Parametric Study", JPL Report No. 5101-129, October (1983).
4. Grace, J. R., "An Evaluation of Models for Fluidized-Bed Reactors", AIChE Symp. Series 67 No. 116, 159-167 (1971).
5. Grace, J. R., "Generalized Models for Isothermal Fluidized Bed Reactors", Recent Advances in the Engineering Analysis of Chemically Reacting Systems, (Doraiswamy, L. K., ed.) Ch. 13, Wiley Eastern, New Delhi (1984).
6. Yates, J. G., Fundamentals of Fluidized Bed Chemical Processes, Butterworths, London (1983).
7. Kunii, D. and O. Levenspiel, Fluidization Engineering, Wiley, New York (1969).
8. Fane, A. G. and C. Y. Wen, "Fluidized Bed Reactors", Handbook of Multi-phase Systems (Hetsroni, G., ed.), Hemisphere, Washington, D.C. (1983).
9. Coltrin, M. E., R. L. Kee, and J. A. Miller, "A Mathematical Model of the Coupled Fluid Mechanics and Chemical Kinetics in a Chemical Vapor Deposition Reactor", J. Electrochem. Soc., 131(2), 425 (1984).
10. Neudorfl, P., Jodhan, A. and O. P. Strausz, "Mechanism of the Thermal Decomposition of Monosilane", J. Phys. Chem., 84(3), 328 (1980).
11. Hogness, T. R., T. L. Wilson and W. C. Johnson, J. Am. Chem. Soc., 58, 108 (1936).
12. Purnell, J. H. and Walsh, R., Proc. Royal Soc., London, 293, 543-561 (1966).
13. Ring, M. A. and O'Neal, H. E., "Kinetics and Mechanism of Silane Decomposition", Proceedings of the Flat Plate Solar Array Project Workshop on the Science of Silicon Material Preparation, DOE/JPL-1012-81, pp. 63-75 (1983).
14. Iya, S. K. Flagella, R. N. and F. S. DiPaolo, "Heterogeneous Decomposition of Silane in a Fixed Bed Reactor", J. Electrochem. Soc. 129(7), 1531 (1982).
15. Abraham, F. F., Homogeneous Nucleation Theory, Academic Press, N.Y. (1974).

16. Hinds, W. C., Aerosol Technology: Properties, Behavior, and Measurement of Airborne Particles, Wiley, N.Y. (1982).
17. Friedlander, S. K., Smoke, Dust and Haze: Fundamentals of Aerosol Behavior, Wiley, N.Y., (1977).
18. Doganoglu, Y., V. Jog, K. V. Thambimuthu, and R. Clift, "Removal of Fine Particulates From Gases in Fluidized Beds", *Trans. I. Chem. E.*, Vol. 56, pp. 239-248 (1978).
19. Peters, M. H., L. S. Fan, and T. L. Sweeney, "Simulation of Particulate Removal in Gas-Solid Fluidized Beds", *AIChE J.*, Vol. 28, No. 1, pp. 39-49 (1982).
20. Wen, C. Y. and R. F. Hashinger, "Elutriation of Solid Particles From a Dense Phase Fluidized Bed", *AIChE J.*, 6, 220 (1960).
21. Wender, L. and G. T. Cooper, "Heat Transfer Between Fluidized-solids Beds and Boundary Surfaces", *AIChE J.*, 4, 15 (1958).
22. Yang, W. C. and D. L. Keairns, "Estimating the Jet Penetration Depth of Multiple Vertical Grid Jets", *I&EC Fundamentals*, 18, 317 (1979).
23. Weimer, A. W. and D. E. Clough, "The Influence of Jetting-Emulsion Mass and Heat Interchange in A Fluidized Bed Coal Gasifier", *AIChE Symp. Series* 205 (No. 77), 51 (1981).
24. Duduković, M. P. Ramachandran, P. A., and S. Lai, "Modeling of Fluidized-Bed Reactors for Manufacture of Silicon from Silane", *JPL Final Technical Report, DOE/JPL-956737-85/7*, September 30, 1985.

DISCUSSION

LORD: Have you looked at the characteristics of an ideal grid design for suppressing fines?

DUDUKOVIC: No.

LORD: Can you give any indications of the direction which you should go, based on your model?

DUDUKOVIC: Well, I am hesitant to speculate on that, because grid design was not part of my expertise when we started on this project. Now, after we have finished the study, we are convinced that it has a determining effect. First, we would like to crystallize our ideas as to how we should do an experimental study. Since it is very difficult for us to run a silicon system, we would use a mock system to determine the exchange coefficients and then, when we are sure that we are on the right path, we could go further.

FLAGAN: Is it true that you neglected the diffusional resistance between the gas and the large particles that were growing?

DUDUKOVIC: That is correct. The diffusional resistance is small compared to the chemical vapor deposition growth rate, and so the major resistance (i.e., the rate limiting step) is growth by chemical vapor deposition.

FLAGAN: Is that true throughout the entire range of conditions that you've looked at?

DUDUKOVIC: It seems that way.

SILICON PRODUCTION IN AN AEROSOL REACTOR

Jin Jwang Wu and Richard C. Flagan
Division of Engineering and Applied Science
California Institute of Technology
Pasadena, CA 91125

INTRODUCTION

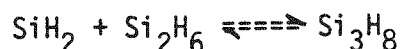
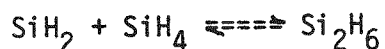
The production of bulk solar-grade silicon by homogeneous gas-phase pyrolysis of silane has been the subject of a number of investigations, beginning with work at Union Carbide Corporation (1) and at the Jet Propulsion Laboratory.(2) While very high efficiencies of conversion of silane to silicon were achieved in those early studies, the silicon powder generated consisted of low density agglomerates of submicron particles. This powder was difficult to collect and melt. Moreover, the product purity was inadequate for the intended use.

In 1980, a study of the factors limiting particle growth in the so-called free space reactor was undertaken. This work has led to an improved understanding of the fundamental processes involved in the formation of low vapor pressure particles by gas phase chemical reactions, and, as a result of this understanding, to the development of a new type of aerosol reactor for the processing of high purity materials. The focus of recent work under this program has been on elucidating the operating regimes in which particles can be grown to large enough size to facilitate separation of the product from the gas. In this paper we summarize the major developments of this program.

LIMITATIONS OF THE FREE SPACE REACTOR

The Union Carbide reactor was called a "free space" reactor because the silane decomposition reactions are carried out in the volume of the reactor rather than on a substrate as in the conventional Siemens process for producing polycrystalline silicon. The choice of silane as a reactant rather than a chlorosilane allows complete conversion of the silane to silicon in a single pass through the reactor.

The reaction kinetics of silane pyrolysis are not completely understood. The initial steps in the reaction sequence are thought to be the reactions first hypothesized by Purnell and Walsh (3), i.e.,



The rate of silane disappearance of silane was found to be

$$\frac{d[\text{SiH}_4]}{dt} = -k_1[\text{SiH}_4]^{3/2} ; \quad k_1 = 10^{14} \exp(-30000/T) (\text{M}^3/\text{Kmol})^{1/2} \text{sec}^{-1}$$

Ring and coworkers (4) suggest that these experiments were in the pressure fall-off regime of the dissociation reaction, Since the free-space reactor experiments have been conducted at atmospheric pressure, the kinetic expression of Purnell and Walsh provide a reasonable approximation to the rate of silane disappearance. The subsequent reactions leading to the production of condensible products are not understood. From the large activation energy of the initial pyrolysis reaction, it appears reasonable to assume that this is the rate limiting step in the formation of silicon by silane pyrolysis.

To achieve complete conversion of silane to silicon in a reactor of reasonable size, the Union Carbide reactor was operated at a temperature of about 1200 K. At this temperature, the characteristic time for the silane pyrolysis reaction on the order of microseconds, so the pyrolysis should be complete as soon as the reactant is heated. Assuming that vapor phase silicon is produced in this mechanism, this rapid reaction would lead to extremely high levels of supersaturation and, consequently, the homogeneous nucleation of large numbers of very small particles. With condensation taking place quickly, the only mechanism by which these nuclei can grow is by coagulation. Assuming residence times on the order of several seconds, particle growth by Brownian coagulation is limited to the production of particles smaller than one micron in diameter. Enhancement of the coagulation rate by turbulence is difficult because of the large drag to inertia ratio of these small particles. Thus, the free-space reactor is limited to the production of a powder comprised of submicron particles.

THE AEROSOL REACTOR

These results suggest immediately an alternate approach to the growth of large particles by direct gas phase chemical reactions in a flow reactor. It is clear that the growth of particles to supermicron sizes by coagulation is not feasible in reasonable residence times. If, however, a small number of particles could be grown by vapor deposition it should be possible to produce the desired large particles within a residence time of a few seconds. The size to which this small number of particles could be grown is determined by a simple mass balance. Assuming all particles grow to the same size, the volume of the final particle is simply the total volume of condensed phase products of gas phase reactions divided by the number of particle on which these products are deposited.

The problem with this approach is that the products of the silane pyrolysis reactions nucleate readily due to their low vapor equilibrium vapor pressures. If such nucleation takes place, large numbers of small particles are again generated and

the growth of the initial particles to the desired size is prevented. There exists a limiting rate of production of condensible species below which nucleation is suppressed and above which significant new particle formation occurs. This rate is determined by the rate at which the products of reaction diffuse to the surfaces of the growing particles. If that diffusion is sufficiently fast, the condensible species are not allowed to accumulate to the point that nucleation is inevitable.

The procedure for the growth of large refractory particles in an aerosol reactor is, therefore:

- (1) Generate seed particles by some means such as the homogeneous nucleation of the products of reaction of a small amount of the precursor gas.
- (2) Dilute the seed particles with sufficient precursor to allow them to be grown to the desired volume by vapor deposition.
- (3) React the precursor at a rate that is, at all times, kept slow enough that the diffusion of reaction products to the seed particles keeps significant supersaturation from developing.

To determine the limiting reaction rate, it is necessary to understand the process of homogeneous nucleation in the presence of growing aerosol particles. The classical theory of homogeneous nucleation(5) treats the formation of particles in a homogeneous system. Vapor diffusion to growing particles creates localized inhomogeneities around the particles. The depletion of vapor in these regions suppresses nucleation locally. If the number concentration is sufficiently high relative to the rate at which condensible species are generated, nucleation can be suppressed. This problem has been examined theoretically, beginning with the use of an artificial construct, the "clearance volume" which is a measure of the ability of an isolated particle to inhibit nucleation but which is not rigorously valid in the limit of complete suppression of nucleation.(6,7) We have recently developed a "cell model" which is more rigorously applicable to the problem at hand, the complete suppression of nucleation. (8)

These models of the influence of growing aerosol particles on the rate of homogeneous nucleation are based on the classical theory of homogeneous nucleation. The low vapor pressures of the reaction products with which we are dealing make important assumptions of the classical theory questionable, notably the assumption that a quasi-steady-state population of molecular clusters is established before the onset of significant nucleation. According to the classical theory, the smallest thermodynamically stable cluster size has diameter d^* , where

$$d^* = \frac{4\sigma v_m}{kT \ln S}$$

and σ is the surface tension, v_m is the molecular volume, and S is the saturation ratio. For silicon in the silane pyrolysis aerosol reactor, we estimate that the number of molecules in the critical cluster, g , is less than 10. At this small size the use of the surface tension of the bulk material is clearly questionable. Moreover, an examination of the kinetics of nucleation indicates that the assumption of a quasi-steady cluster distribution is inappropriate. We have, therefore, recently developed a kinetic model to describe more accurately the nucleation process in the aerosol reactor.

REACTOR DESIGN AND EVALUATION

Two aerosol reactor systems have been constructed in our efforts to grow large silicon particles by silane pyrolysis and to understand the fundamental processes that limit aerosol reactor operation. The first reactor consisted of two stages: (i) a seed generator in which a small amount of silane was pyrolyzed to generate seed particles by homogeneous nucleation; and (ii) a growth reactor in which the seed particles were grown by rate-controlled silane pyrolysis. This system is illustrated in Figure 1. To achieve acceptable velocities and residence times with the small amounts of silane used in these experiments, nitrogen was added to the flows as a diluent.

Between the two reactor stages, the primary silane flow was added to the seed aerosol and thoroughly mixed using a series of static mixers. Very efficient mixing is essential to the operation of the aerosol reactor since small inhomogeneities could allow nucleation to occur in localized regions of the growth reactor and interfere with particle growth. The growth reactor consisted of a 9 mm i.d. quartz tube that was heated in five separately controlled zones. The temperature was increased along the length of the reactor by control of the separate heating zones, providing a temperature profile of

$$T = 755K (1 + 2.74 m^{-1})^{\frac{1}{2}} \quad (+ 10 K)$$

The low initial temperature allowed for slow particle growth until the particles reached a size such that they became efficient vapor scavengers and could suppress nucleation at higher reaction rates. The high temperatures at the end of the process assured complete decomposition of the silane.

The silicon aerosols produced in these experiments were characterized using an electrical aerosol analyzer to determine the size distribution of submicron particles, TSI Model 3030, a condensation nuclei counter to determine the total number concentration, Environment One, and optical particle counters to

determine the size distribution of particles in the 0.15 to 6 micron range, Royco Model 226, and in the 0.5 to 40 micron range, Particle Measurement Systems classical scattering probe. With these instruments it was shown that 0.1 micron seed particles could be grown to mass median diameters on the order of 6 to 10 microns, (8) as illustrated in Fig. 2.

To gain better control over the seed conditions in studies designed to elucidate the operating domain over which seed particles can be successfully grown, and to resolve questions about the density of the product particles, the larger three-stage reactor shown in Figure 3 was constructed. As in the original reactor, seed particles are generated in the first stage by homogeneous nucleation of the reaction products from the pyrolysis of a small amount of silane. The second stage is used to increase the size of the seed particles up to 2 microns. It consists of a 10 mm i.d., 350 mm long quartz tube that is heated in four separately controlled zones. The temperature is ramped along the length of this reactor to accelerate the reaction as the seed particles grow as in the original growth stage. The third stage grows these enlarged seeds to their final size in a 12 mm i.d., 850 mm long quartz tube. This reactor stage is heated in 5 separate zones. The first three zones are 50 mm long and are separated by 10 mm insulation to facilitate precise temperature control. These are followed by zones of 300 and 150 mm length that are heated by Lindbar silicon carbide heating elements. These heaters allow high temperature operation toward the end of the residence time in the reactor, making it possible to heat the aerosol to the melting point of silicon (1685 K) so the volume of silicon contained in individual particles can be determined unambiguously.

EXPERIMENTAL RESULTS

Several types of experiments have been conducted to characterize the reactor. In the following discussion, we focus on the behavior of the primary growth stage of the reactor. The first two stages are used merely as a controllable source of seed particles. Figure 4 shows typical size distributions of the seed aerosol after dilution at the exit of the second stage, after passing through the static mixers, i.e., at the entrance to the primary reactor stage, and at the end of the primary reactor without silane added for growth. The shift in the size distribution as the aerosol passes through the static mixers is due primarily to seed particle losses within the mixers (about 10 percent of the aerosol mass). The seed aerosol passes through the growth stage with little change in the size distribution due either to diffusional losses on the reactor wall or to coagulation. Thus, changes that occur when silane is added to the seed aerosol can be attributed to the results of silane decomposition.

To map the operating domain in which the seed particles

could be successfully grown to large size, a series of experiments were performed with the temperature profile along the growth reactor wall fixed as illustrated in Figure 5. With this temperature profile, nucleation could be fully suppressed when 0.6 liters/min. of 1 percent silane in nitrogen was introduced into the reactor with 1 micron seed particles in a concentration of 2×10^6 particles/cc. The size and number concentration of seed particles was then varied to determine the sensitivity of nucleation control to the seed aerosol characteristics at otherwise constant reactor operating conditions.

The resultant operating map for this flow rate, temperature profile, and silane concentration is shown in Fig. 6. Two outcomes were possible in these experiments: (i) complete suppression of nucleation in which case the seed particles grew as indicated by the connected solid points; and (ii) runaway nucleation leading to a large increase in the number concentration and a corresponding decrease in the mean particle size. The latter experiments are indicated by open points. These results clearly demonstrate the sharp transition from one operating mode to the other. Also shown are theoretical predictions of the separation between the two operating modes. The solid line corresponds to the increase in the number concentration by a factor of two. The dashed line corresponds to the locus of conditions that lead to one half of the aerosol mass appearing as fine new particles.

A more direct illustration of the onset of nucleation is a series of experiments conducted with a fixed temperature profile and seed aerosol, but variable silane concentration. Figure 7 shows the result of such an experiment with a seed concentration of 10^5 /cc, and a mean seed particle size of 0.7 micron. As the silane concentration was increased to 3 percent, the number concentration increased by less than a factor of two. Further increasing the silane concentration to 3.5 percent resulted in an increase in the number concentration of four orders of magnitude.

The results of a similar series of experiments are plotted on a mass distribution basis (as determined from optical sizing data) in Fig. 8. The mass median size increases rapidly to a silane concentration of 3.2 percent. Increasing the silane concentration beyond 4.9 percent does not appreciably enhance the size of the particles since the additional silicon increases the size of the large number of silicon nuclei only slightly and does not contribute to the growth of the seed particles.

PARTICLE CHARACTERISTICS

A scanning electron microscope photographs of the particles grown with a low final temperature in the growth reactor is shown in Fig. 9. The particle appears to be an agglomerate of approximately 0.1 micron spheres. The BET surface area of the collected powder was found to be $20.3 \text{ m}^2/\text{gm}$, indicating that this

structure is uniform throughout the particle volume. The diffusivities of particles of that size are, however, so low that the observed growth of the seed particles and the small increase in the number concentration cannot be attributed to coagulation of these particles with the seeds. Instead, the structure of the particles must reflect the results of partial sintering of a low density particle which initially had a much finer structure.

This sintering can be accelerated by increasing the temperature in the final zone of the primary reactor. The reactor was designed so that this could be done without significantly altering the temperature profile in the upstream regions where the silane decomposition and particle growth take place. Figure 10 shows the effect of processing the grown particles to temperatures of 1523 K and 1673 K. The particles have densified appreciably during this heat treatment due to sintering.

Samples of the powders were also examined for crystallinity using X-ray diffraction. The spectra for samples treated in the reactor to three different temperatures are shown in Fig. 11. The material that was heated to no more than 973 K is clearly amorphous, but as the final processing temperature is increased the material clearly becomes crystalline.

One important concern with such powders is the possible contamination of the large surface area with oxide or, due to the nitrogen diluent used in the experiments, nitride layers. Infrared absorption spectroscopy was used to look for such contamination. Powder samples were collected under nitrogen and pressed into KBr pellets in a glove box under a nitrogen atmosphere. No silicon oxide or silicon nitride absorption was observed in the infrared spectra.

CONCLUSIONS

An aerosol reactor system has been developed in which large particles of silicon can be grown by silane pyrolysis. To grow particles to sizes larger than one micron, vapor deposition must be used to grow a relatively small number of seed particles. To maintain that small seed concentration requires that homogeneous nucleation be suppressed. This is achieved by limiting the rate of gas phase chemical reactions such that the condensable products of gas phase chemical reactions diffuse to the surfaces of the seed particles as rapidly as they are produced. This prevents high degrees of supersaturation and runaway nucleation during the growth process.

The dividing line between runaway nucleation and successful growth of the seed particles is very sharp. In one experiment, a 17 percent increase in the silane concentration resulted in an increase in the number concentration at the reactor outlet of 4 orders of magnitude. Thus, if the reactor is operated near the

maximum feasible growth rate, small excursions in operating conditions can have catastrophic results.

If the peak temperature in the reactor is kept low, the particles have a fine structure, appearing to be agglomerates of very small particles. Calculations of particle growth kinetics clearly indicate that this structure is not the result of coagulation of particles the size of the fine structure. Instead, the structure results from partial sintering of particles that initially had a much finer structure. Heating the particles to higher temperatures for times on the order of one second are sufficient to fuse the particles, eliminating the structure observed in the low temperature aerosol. In practical applications of this technology, that would be useful since the densified particles would be easier to separate from the gas and to process.

Particles on the order of 10 microns have been grown repeatedly with the present aerosol reactor. Particles approaching 100 microns in size have been grown on numerous occasions, although deposition on the reactor walls became a problem under those conditions. The nucleation controlled aerosol reactor is, therefore, a suitable system for the production of powders that can readily be separated from the gas by aerodynamic means.

The process is not limited to silane decomposition. As long as the reaction kinetics are well enough understood that the rate can be limited to control nucleation, other reaction systems can be applied in the nucleation controlled aerosol reactor. For silicon processing, halo-silanes might have important advantages since the etching reaction, e.g., the reaction of HCl with solid Si, reduce the potential for supersaturation and nucleation. Powders of controlled size particles of other materials should also be attainable in aerosol reactors by applying mechanisms that are commonly used for chemical vapor deposition.

ACKNOWLEDGEMENTS

This research has been supported by the Jet Propulsion Laboratory's Flat Plate Solar Array Project which is, in turn, supported by the Department of Energy.

REFERENCES

- (1) J. R. Lay and S. K. Iya, Proc. 15th IEEE Photovoltaic Specialists Conf., pp. 565-568 (1981).
- (2) H. Levin, Proc. Symp. Materials and New Processing Technologies for Photovoltaics, The Electrical Society (1980).
- (3) J. H. Purnell and R. Walsh, Proc. Roy. Soc. 293: 543-561 (1966).

- (4) C. G. Newman, H. E. O'Neal, M. A. Ring, F. Leska, and C. Shipley, *Int. J. Chem. Kin.* 11: 1167-1182 (1979).
- (5) G. S. Springer, *Adv. Heat Transf.* (R. F. Irvine and J. P. Hartnett, Eds.) 14: 281-346 (1978).
- (6) A. J. Pesthy, R. C. Flagan, and J. H. Seinfeld, *J. Colloid Interface Sci.* 82: 465-479 (1981).
- (7) M. K. Alam and R. C. Flagan, *J. Colloid Interface Sci.* 97: 232-246 (1984).
- (8) M. K. Alam and R. C. Flagan, "Controlled Nucleation Aerosol Reactors: Production of Bulk Silicon," *Aerosol Sci. Technol.* (in press).
- (9) J. E. Stern, J. J. Wu, R. C. Flagan, and J. H. Seinfeld, "Effect of Spatial Inhomogeneities on the Role of Homogeneous Nucleation in Systems with Aerosol Particles," *J. Colloid Interface Sci.* (in press).

FIGURE CAPTIONS

- Figure 1. Schematic of the two-stage aerosol reactor of Alam and Flagan. (8)
- Figure 2. Particle size distribution of the silicon aerosol produced in the two stage reactor experiments of Alam and Flagan. (8)
- Figure 3. Schematic of the present three-stage aerosol reactor.
- Figure 4. Size distribution of the seed particles used in the three stage reactor experiments.
- Figure 5. Measured wall temperature profile on the growth stage of the three stage reactor.
- Figure 6. Map of operating conditions that led to successful growth of seed particles (initial and final sizes and concentrations are indicated by connected solid points) and those experiments that resulted in runaway nucleation (open points).
- Figure 7. Variation of final number concentration with percent silane in the feed gas for fixed temperature profile, flows, and seed aerosol.
- Figure 8. Mass distributions measured with three stage reactor for various silane concentrations.
- Figure 9. SEM photograph of the product particles generated with a maximum reactor temperature of 973K.
- Figure 10. SEM photographs of product particles following post-growth processing at elevated temperatures for approximately one second. (a) 1523 K; (b) 1673 K.
- Figure 11. X-ray diffraction patterns for the silicon powders processed at various peak temperatures.

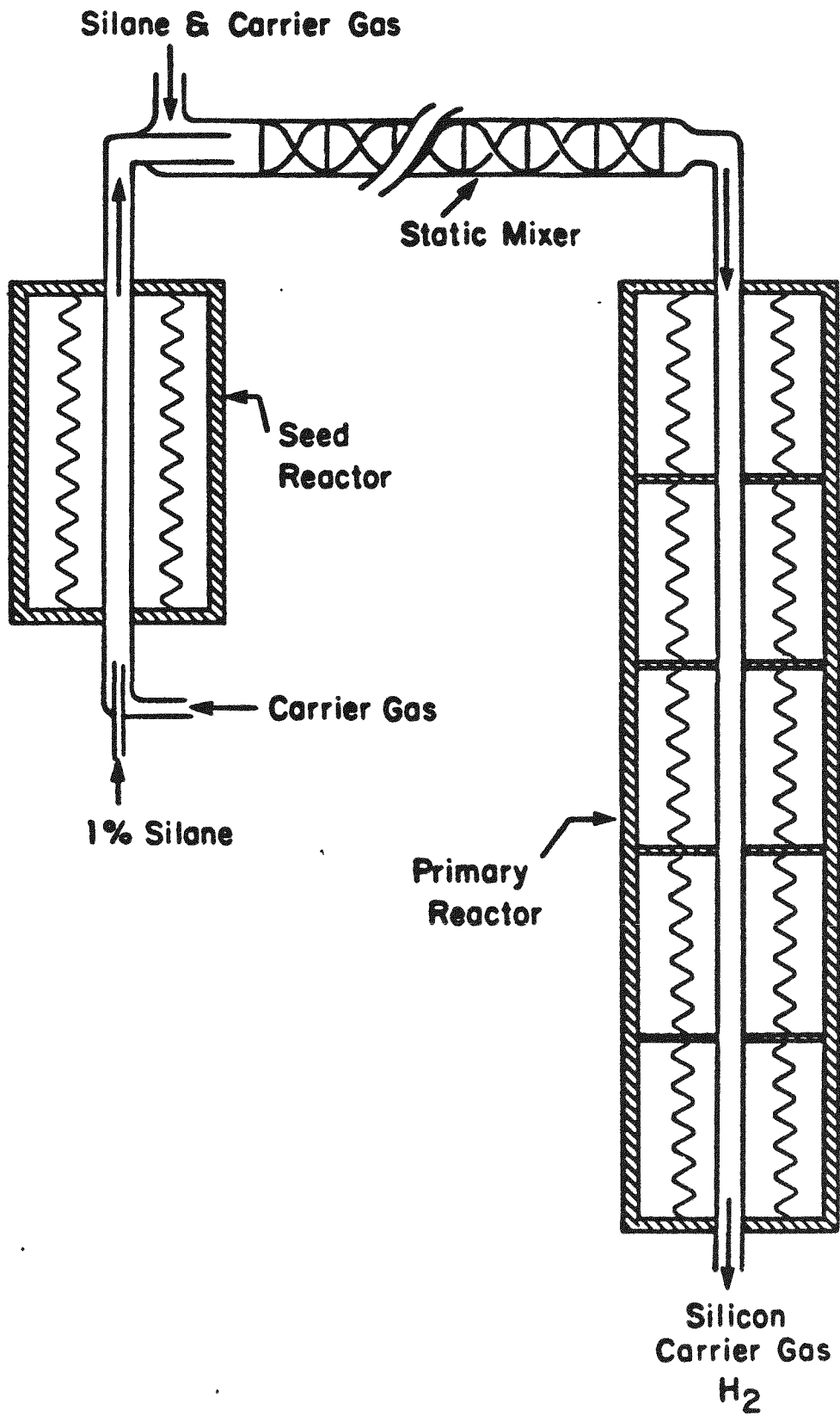


FIG. 1

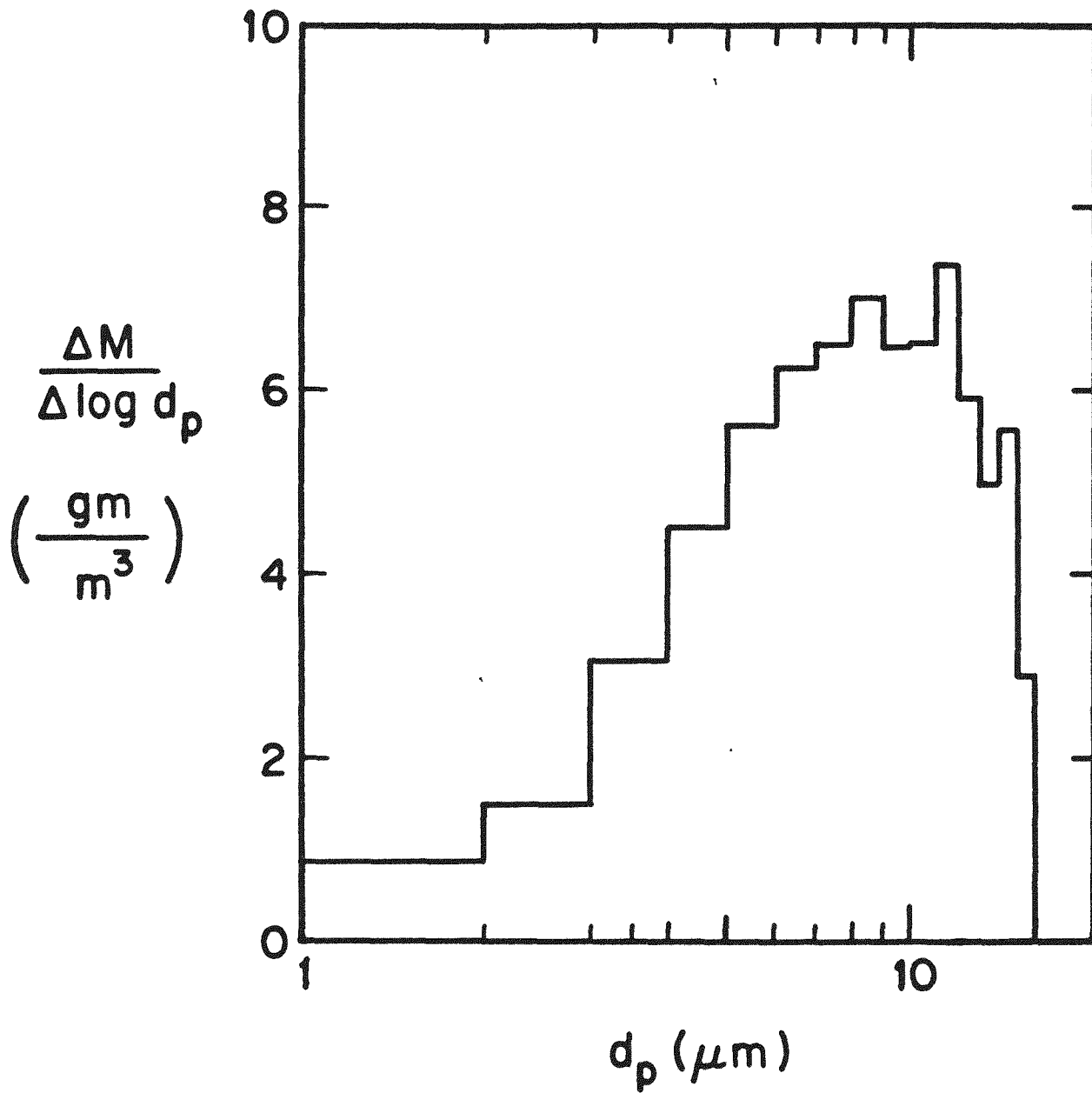


FIG. 2

vaccum and aerosol measuring port

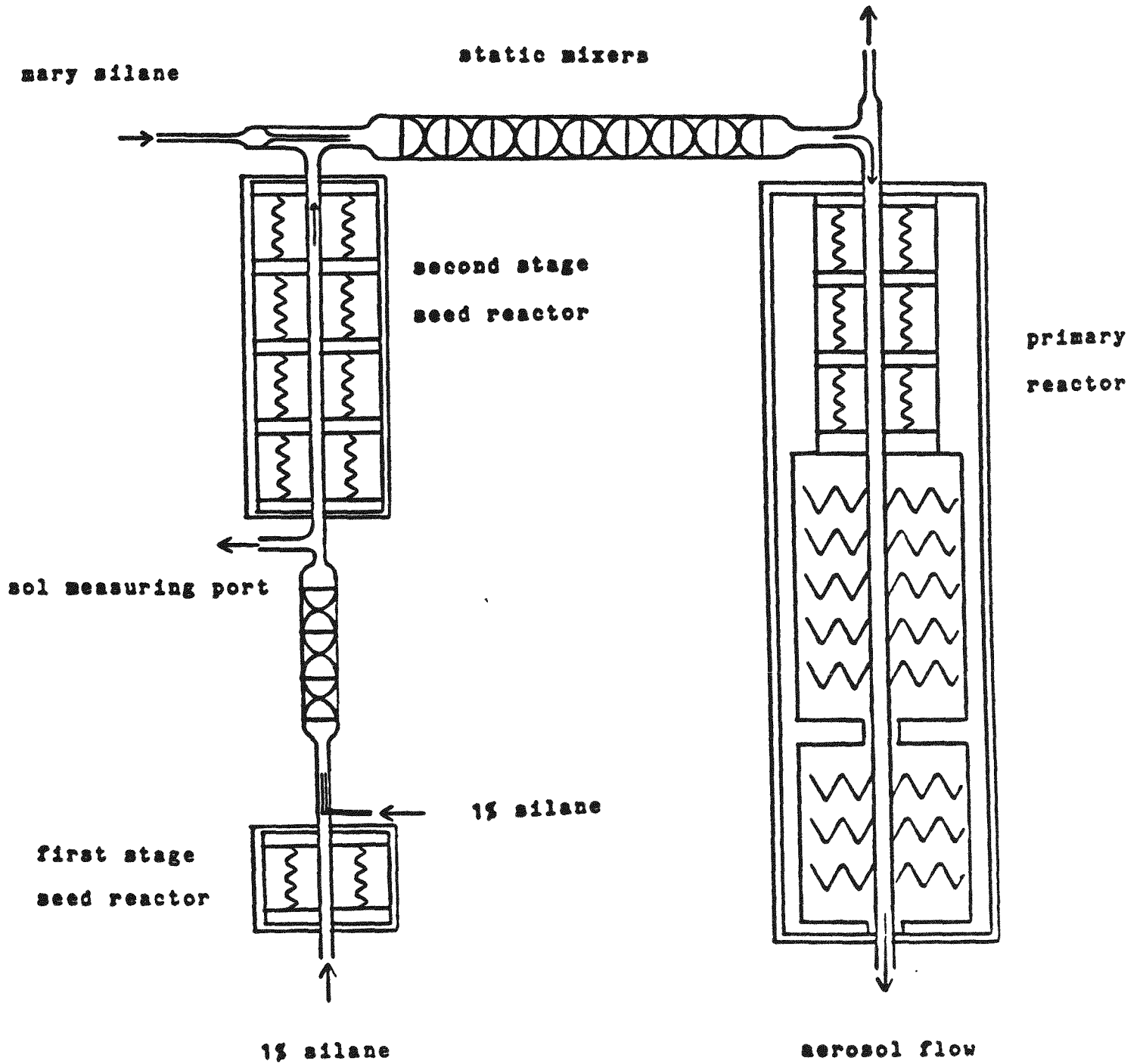


Figure 3. Schematic of the present three-stage aerosol reactor.

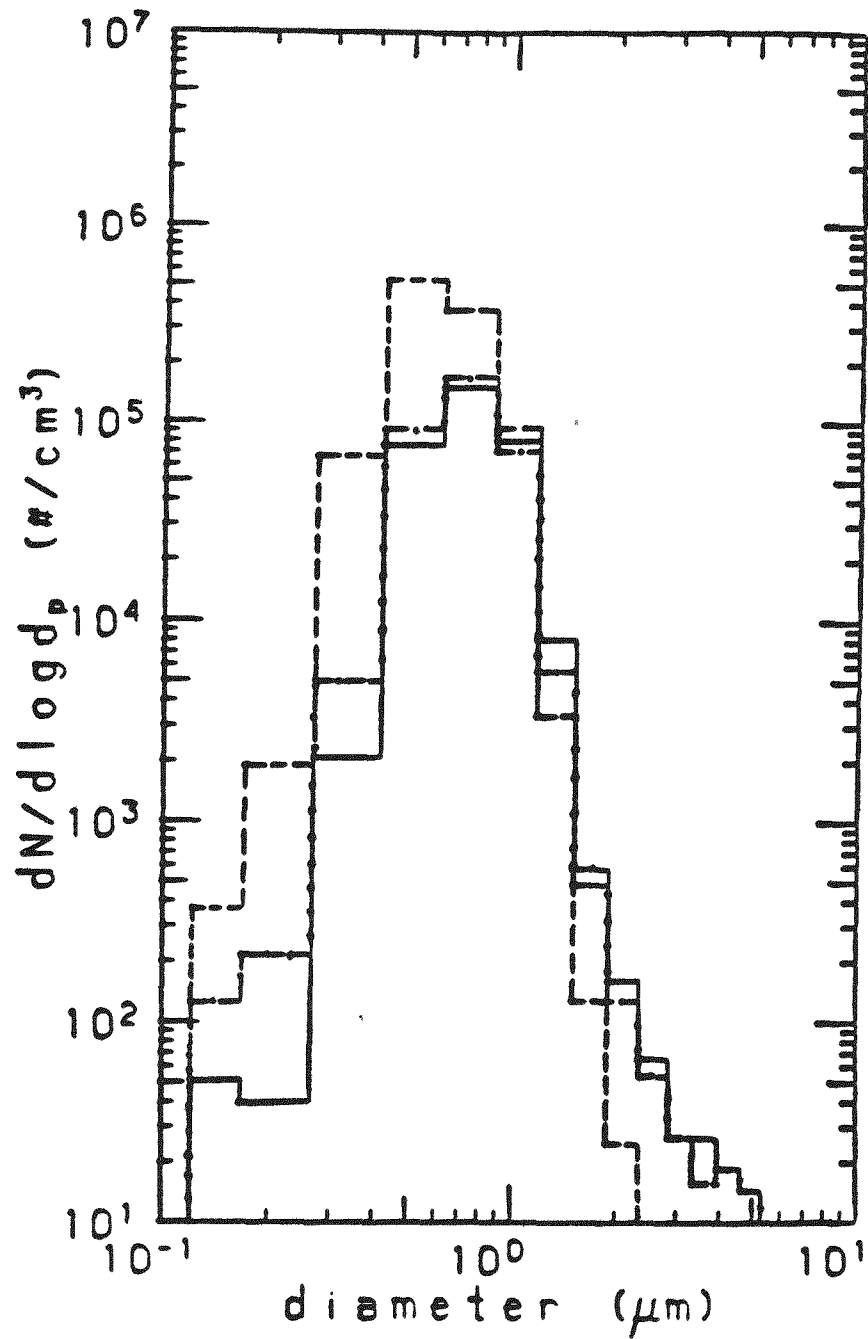


figure 4. aerosol samples monitored by ROYCO OPC
 ----- aerosol from the exit of the seed growth reactor
 aerosol from the entrance of the primary reactor
 ————— aerosol from the end of the primary reactor

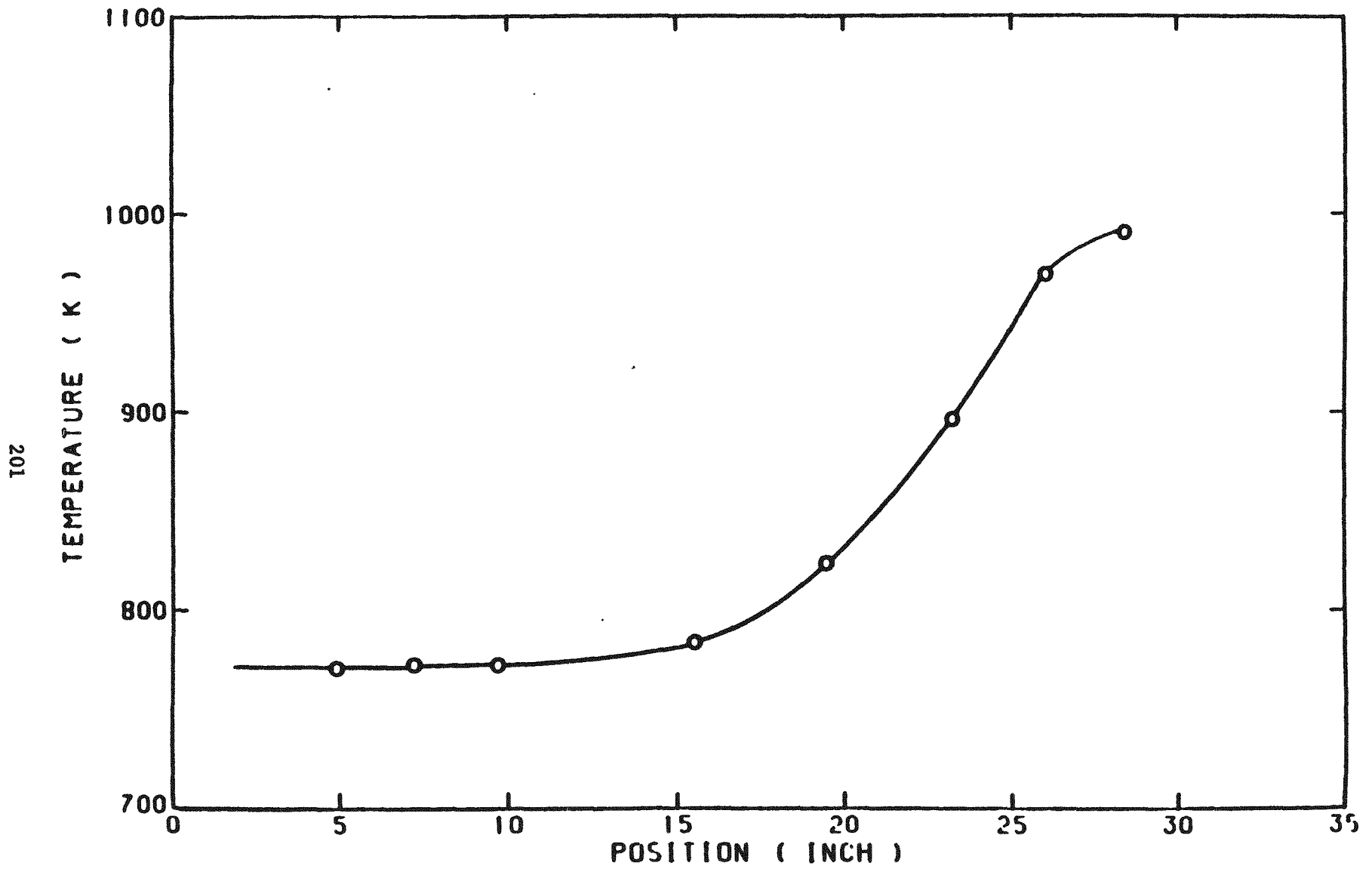


Figure 5. Measured wall temperature profile on the growth stage of the three-stage reactor.

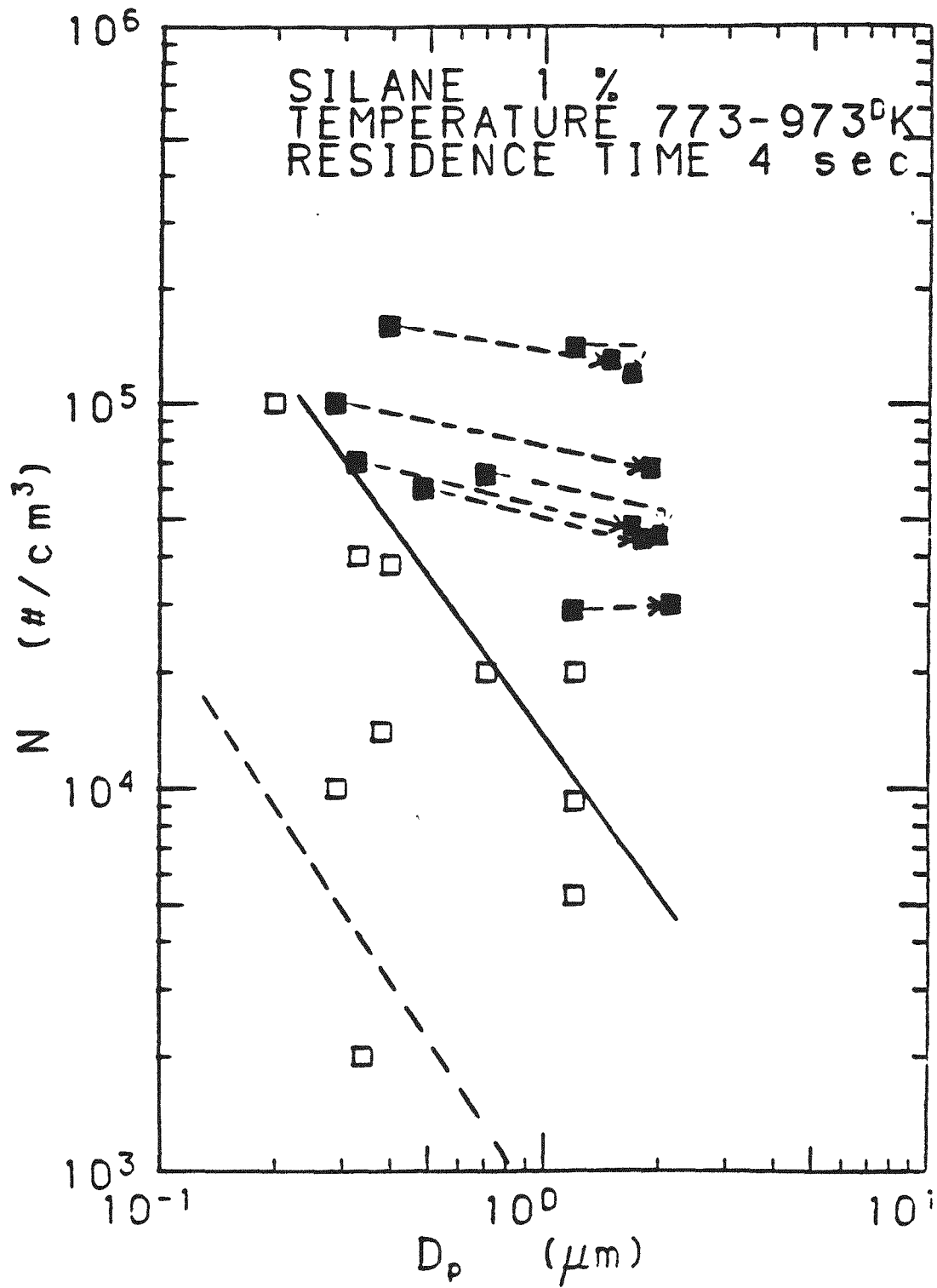


Figure 6. Map of operating conditions that led to successful growth of seed particles (initial and final sizes and concentrations are indicated by connected solid points) and those experiments that resulted in runaway nucleation (open points).

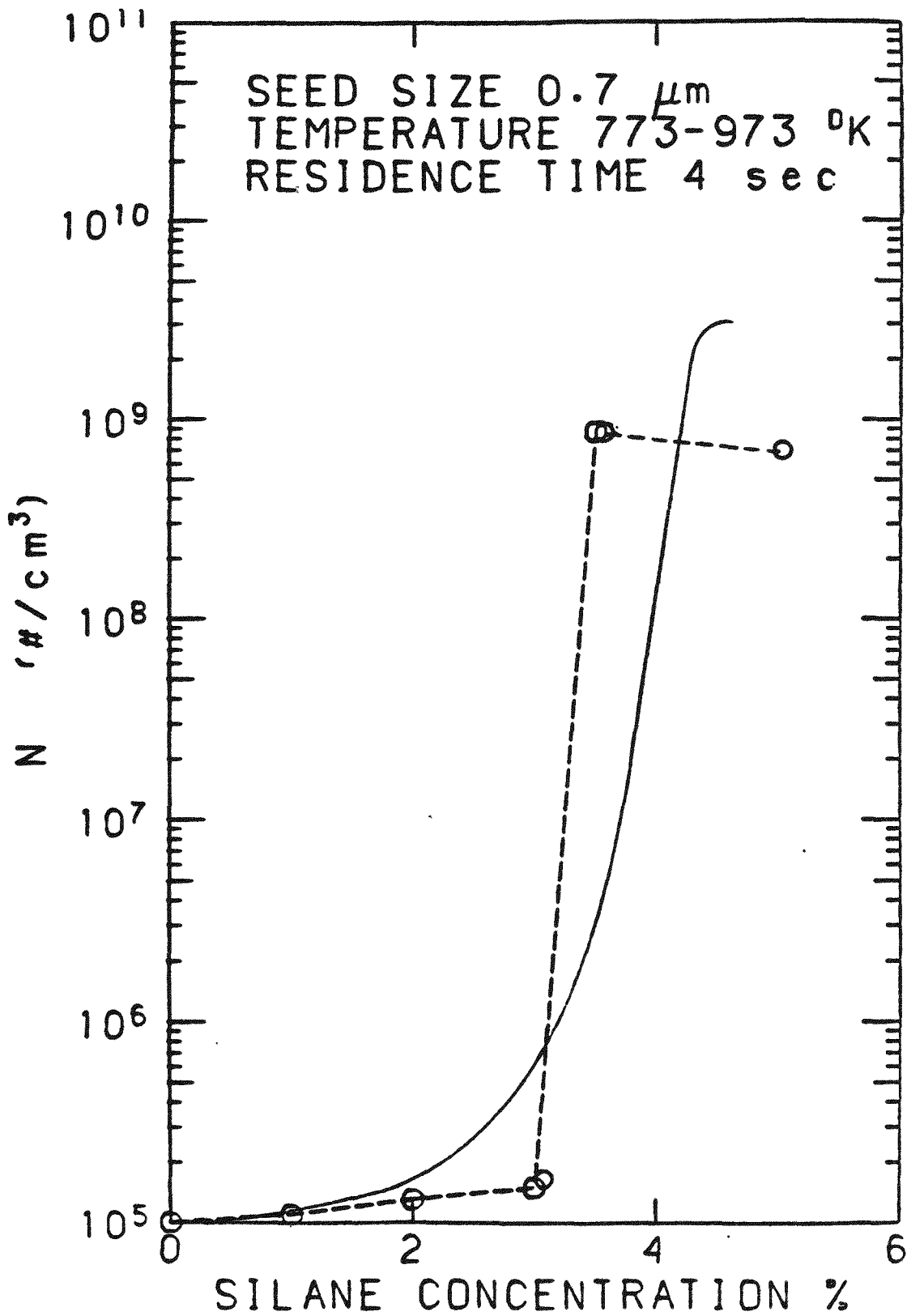


Figure 7. Variation of final number concentration with percent silane in the feed gas for fixed temperature profile, flows, and seed aerosol.

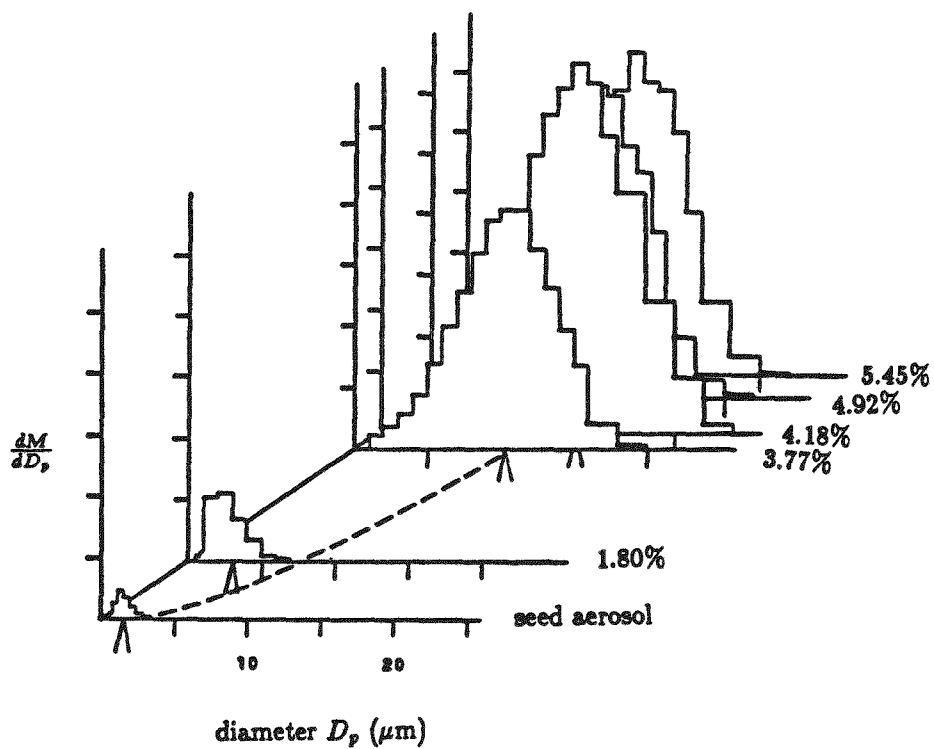


figure 8 seed aerosol growth by increasing primary silane concentration (seed particles were monitored by ROYCO OPC and CNC, particle growth was measured by CSPC)

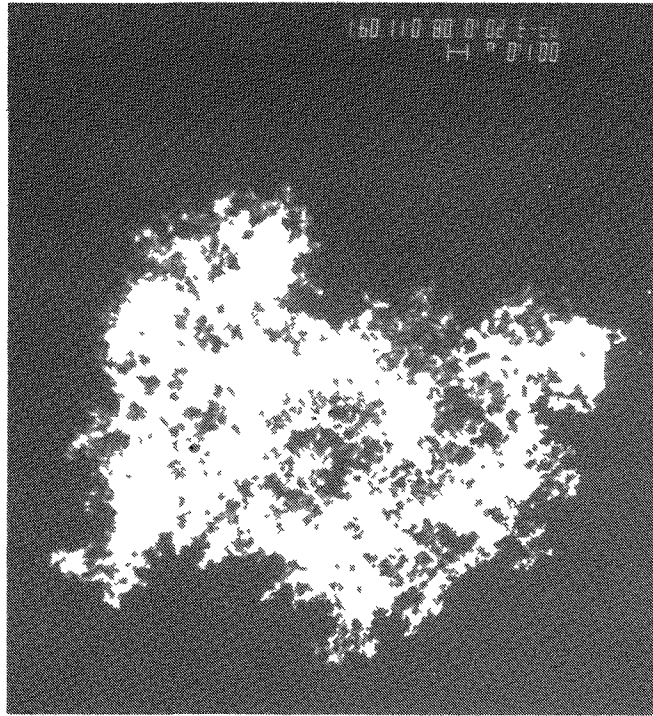


Figure 9. SEM photograph of the product particles generated with a maximum reactor temperature of 973 K.

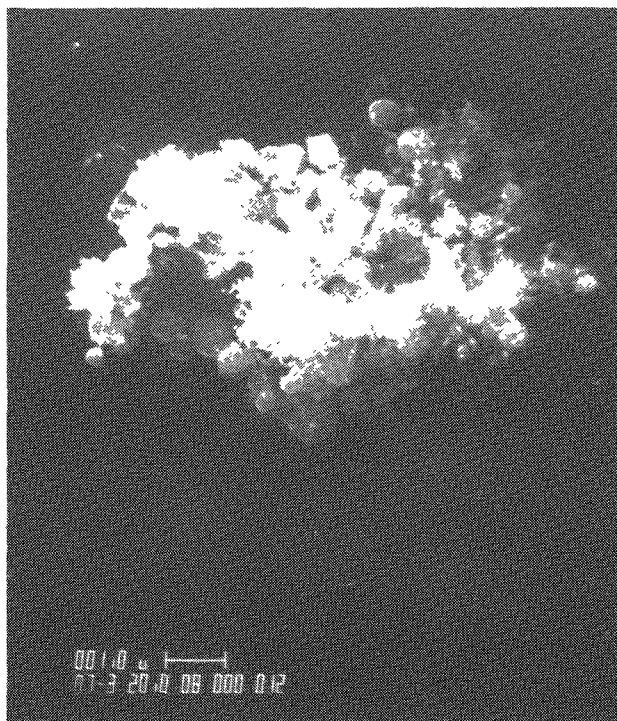


Figure 10a. SEM photograph of product particle following post-growth processing at elevated temperature (1523K) for approximately one second.

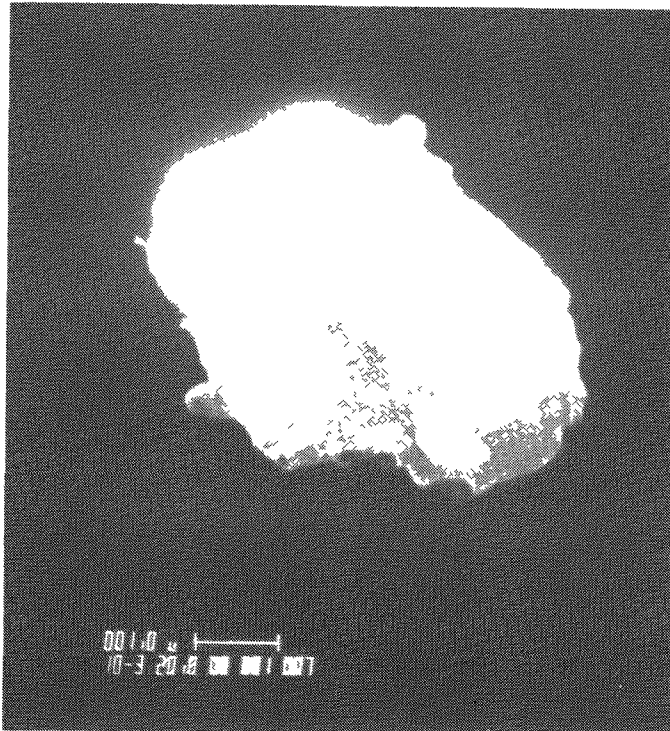


Figure 10b. SEM photograph of product particle following post-growth processing at elevated temperature (1673K) for approximately one second.

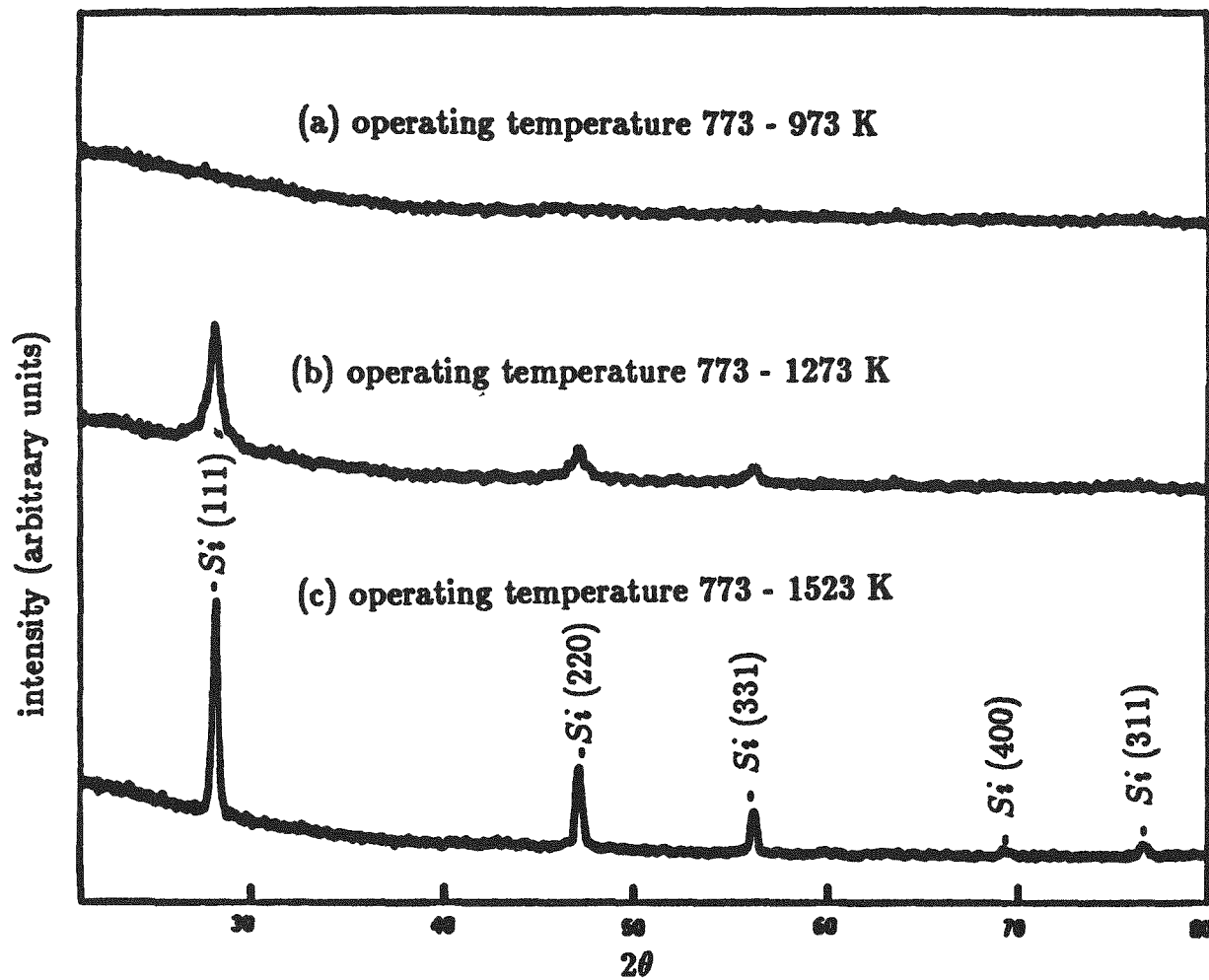


figure 11. structure of silicon particles with different operating temperature ranges
Copper $K\alpha$ X - ray diffraction patterns

DISCUSSION

LORD: What is the diameter reduction you get when the particles are densified?

FLAGAN: It has been a factor of about 3 to 4.

LORD: Does that mean that the size is reduced from 10 μm to about 2 μm ?

FLAGAN: We have also produced dense 10 μm particles.

LORD: Is 10 μm size the largest dense particles you have produced?

FLAGAN: We have produced dense particles of 100 μm , although not for extended periods of time. The reactor plugs very quickly at that point due to the very slow flow in our small-scale reactor.

LORD: Just to follow up on the plugging, did you find out that the particles go to the wall?

FLAGAN: They go to the wall at the exit of the hot zone, but not in the hot zone itself.

AULICH: What is your hydrogen content of your submicron-fine particles?

FLAGAN: I do not have that number. Our focus has been on the characterization of the particle formation process itself, and we simply don't have those data.

SESSION IV

PROCESS DEVELOPMENTS, INTERNATIONAL

R. Lutwack, Chairman



PROCESSES AND PROCESS DEVELOPMENTS IN JAPAN

Toshio Noda
Osaka Titanium Co., Ltd.
Amagasaki, Hyogo, Japan

MOVE TO DEVELOPMENT OF LOW-COST POLYSILICON IN JAPAN

The commercialization of solar power generation necessitates the development of a new, low-cost manufacturing method of silicon suitable for solar cells. To this end, commissioned by the Sunshine Projects Promotion Headquarters in MITI, a special work group was formed in the Japan Electrical Manufacturers Association in 1978, and it inaugurated a variety of research programs as part of Sunshine Project.

The Group investigated the manufacturing methods of semiconductor grade silicon (SEG-Si) and the development of solar grade silicon (SOG-Si) in foreign countries. They concluded that the most efficient method of developing such materials was the hydrogen reduction process of trichlorosilane (TCS), using a fluidized-bed reactor (FBR). The reasons were three: TCS had been proved in a number of studies to be an appropriate material for this purpose; the budget was insufficient to test several processes simultaneously; the hydrogen reduction process seemed to have high feasibility for practical application as revealed by studies conducted thus far.

This process was viewed as meeting the following conditions:

- a. The process is suited to mass production, an essential point for future development.
- b. The process reduces manufacturing costs to a greater extent than conventional SEG-Si manufacturing processes.

The low-cost manufacture of polysilicon requires cost reductions of raw materials, energy, labor, and capital.

Carefully reviewing these conditions, the work group reached the following conclusions:

- a. Polysilicon manufacture should be based on the hydrogen reduction of TCS process. The chlorosilane hydrogen reduction process is the optimum method of obtaining higher-purity SOG-Si, has previously been studied as the SEG-Si manufacturing process, and has already been used in practical manufacture.

Fig. 1 compares the thermodynamic characteristics of hydrogen reduction of silicon tetrachloride (STC), TCS and dichlorosilane (DCS). The results for silicon yields suggest that the use of TCS is more advantageous than STC and in turn the use of DCS is more advantageous than TCS. The conclusion was that TCS, which is already widely used, should

be studied further in the project and that the use of DCS is not yet practical for industrial mass production.

- b. STC, a by-product of the manufacture of polysilicon from TCS, should be recycled into TCS via hydrogenation. The process step of recycling STC to prepare TCS removes the limitation of having to locate the silicon manufacturing process near a plant for producing silicon compounds from the STC by-product.
- c. The FBR process should be adopted. The Siemens process for manufacturing SEG-Si is considered to have the disadvantages of high thermal use and low production rate, which increase manufacturing costs. The FBR process is expected to improve these shortcomings.

The overall conclusion was that a development program should be based on the TCS-FBR process and the experimental program should be conducted in test facilities capable of producing 10 tons of silicon granules a year.

DEVELOPMENT OF LOW-COST SILICON MANUFACTURING TECHNOLOGY

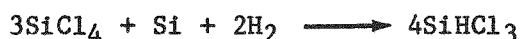
In October 1980, the New Energy Development Organization (NEDO) was established to play a pivotal role in the promotion of new energy development. It was decided that one of its plans should focus on the development of a crystal silicon solar cell. The plan, requiring the development of low-cost silicon as a starting material for solar cells, adopted the conclusions proposed by the work group mentioned above.

NEDO divided the present process (the NEDO process) into two parts, commissioning the part for TCS manufacture to Osaka Titanium and the other for silicon granule manufacture to Shin-etsu Chemical. The respective assignments are shown in Fig. 2.

1. Development of Low-Cost TCS Manufacturing Technology

The two key points in this development project are as follows:

- a. To produce TCS from hydrogen, metallurgical grade silicon (MG-Si) and STC (a bulk by-product of the hydrogen reduction of TCS) as expressed in the equation:



- b. To purify, at the lowest cost possible, the resulting TCS to a grade necessary and sufficient for use in solar cells.

1.1. Testing with small experimental apparatus

From 1980 to 1981 a number of tests were conducted to determine the conversion potential of STC to TCS using a small experimental fixed-bed reactor and a 10 cm-diameter FBR.

The fixed-bed reactor was used to measure the reaction temperature, the gas chemical composition, the residence time requirement and the catalyst effectiveness. The results were then checked using the fluidized-bed reactor which was also used to measure the effects of pressure.

1.2 Operation of TCS 200 T/Y experimental apparatus

Based on the test results obtained using the experimental reactors, further tests were undertaken beginning in October 1982, using the 200 tons/year test manufacturing apparatus shown in Tables 1 and 2, and Fig. 3. (1)

In this facility, TCS is evaporated in a steam-heated evaporator, mixed with hydrogen, heated to 650 to 700°C by a heater at the bottom of the reactor, and released into the fluidized-bed reactor filled with MG-Si seed particles. The fluidized-bed temperature is maintained at 500 to 600°C by the sensible heat of the gas.

The gas discharged from the reactor top is composed of 75 to 77% STC, 23 to 25% TCS and 0.5% DCS. (3) The gas is then cooled to -35°C, condensed and recovered. The condensate is transferred to the distillation plant where the STC is removed in the first column, low-boiling point impurities in the second column, and high-boiling point impurities in the third column; the purified product is TCS.

The operational results, shown in Table 3, indicate that with all targets achieved, the present manufacturing process can produce TCS at the rate of 200 tons/year. (4)

An analysis of TCS obtained via this process produced the results listed in Tables 4 and 5. (7) Analytical samples were prepared by hydrogen-reducing TCS and float-zoning the resultant silicon rods. The samples thus obtained were then measured for electrical resistance to estimate the donor and acceptor concentrations. TCS was analyzed by atomic absorption measurements to determine its metallic impurities.

2. Development of TCS Hydrogen Reduction Technology

The goal of the project is to achieve a reduction of energy-use and improved productivity, both essential for low-cost silicon manufacture, by replacing the Siemens bell jar with a FBR.

2.1. Testing with small experimental apparatus

In 1981, an experimental apparatus of 0.5 ton/year capacity was developed to study the basic structure of the FBR. Tests conducted until the following year revealed the following results: (8), (9)

- a. Quartz tubes used for FBRs ruptured during experimental runs due to silicon deposits on the tube interior. Therefore, SiC-Si tubes (prepared by sintering a SiC-Si mixture) with a thermal expansion coefficient nearly equal to that of silicon were substituted.

- b. It was found that the silicon deposits could be removed by exposure to a HCl-SiCl₄ mixture at high temperature.
- c. The problem of the clogging of the gas injection nozzle by silicon deposits was alleviated by developing and installing a water-cooled bottom plate.
- d. The reactor power consumption was approximately 30 kwh/kg of Si; the diameter of the product granules was 0.8 to 1.5 mm; and the product quality was indicated by measurements of the conversion efficiency of solar cells prepared from 3" diameter Czochralski single crystals grown from the FBR granules; these values ranged from 10 to 12%.
- e. A number of methods were tested for the preparation of silicon seed particles. These included crushing and the use of high frequency plasma for melting and spraying. Crushing using a roll-crusher was found to be the most appropriate method.

2.2. Operation of 10 tons/year experimental FBR apparatus

This apparatus has been undergoing improvement since its completion in August 1982, and continues to be used in test operations. Table 6 lists the major apparatus dimensions and reaction conditions. (6) Table 7 summarizes the operational results for fiscal 1984. (5)

Two of the conventional problems associated with the FBR were alleviated. Clogging of the bed was eliminated by the improvements of the fluidizing conditions and of the bottom plate shape, while silicon deposition on the walls was decreased by improving the reaction temperature control technique.

The most serious problem in the present project was the rupture of FBR tubes. Based upon the findings obtained from the tests with the small experimental apparatus, an attempt was made to use SiC-Si material. It was found, however, that the silicon in the SiC-Si reacted with the HCl gas, thus causing a deterioration of the tube (a problem known as "overcleaning"). As a consequence, the tube became permeable, allowing the diffusion of impurities through microscopic pores.

Accordingly, another attempt was made to use a tube that had been CVD-coated with SiC on the tube interior. Although this basically solved the problem, fragility due to a difference in the thermal expansion coefficients of the CVD layer and the SiC-Si substrate remained unavoidable. This problem is considered to be the most formidable obstacle to enlarging the apparatus.

With regard to seed production, two procedures were attempted based upon the experimental results: crushing high-purity silicon using a roll crusher and then screening the resulting material using a quartz sieve in clean nitrogen gas.

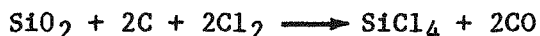
The process flow and the material-product balance are shown in Fig. 4. (8) The yield was approximately 70% and the roll wear was approximately 1 g per kg of crushed material.

The target quality of product silicon granules in the present project was P-30 or N-10 ohm-cm in specific resistance, and 10 μ sec. in lifetime, as measured in the Cz crystal. However, the results showed specific resistance of between N-10 and 20 ohm-cm and a lifetime of between 10 and 30 μ sec. Chemical composition analyses of the product granules are shown in Table 8. (5)

It was proved that the silicon granules obtained in this project could be used to achieve 12.7% conversion efficiency in polycrystalline solar cells, demonstrating that the granules have satisfactory quality as SOG-Si.

OTHER PROCESSES

NEDO has inaugurated two new development projects for SOG-Si manufacturing technology. One, called "TCS manufacturing technology by quenching", commissioned to Denki Kagaku Kogyo; this new method uses silica produced in Japan, whereas the NEDO process and other conventional processes use imported MG-Si to manufacture TCS. TCS is manufactured via the following two steps. This process is undergoing testing using a 4 kg/h apparatus.



The other project underway at Nippon Sheet Glass aims to produce low-cost SOG-Si using low-grade silica sand, found in abundance in Japan. In this method, silica sand is purified into high-grade silica, which is then carbon-reduced in an arc furnace to produce SOG-Si. Since silica is purified in the form of water glass, the process is called the "water glass method".

As shown in the Fig. 5 flowchart, the starting material is silica sand, a material used in sheet glass, containing 96 to 97% SiO_2 . (10) The sand is physically purified into nearly 99.9% purity silica, mixed with an alkali oxide source, such as sodium carbonate, melted in an autoclave and turned into water glass. Water glass thus obtained is subjected to acid treatment to form silica deposits. The resulting silica, washed with acid and water, is of high purity. Table 9 indicates changes in impurity levels of the silica sand before and after physical purification. (6) Table 10 compares the analytical results of silica purity in physically purified silica and water glass silica currently on the market. (10)

Purification testing is being conducted using a 10 kg SiO_2 /day apparatus. Testing is also underway to characterize the carbon-reduction of silica using a small arc furnace (55 KVA), an improved version of the conventional arc reduction.

FUTURE STRATEGIES

Fig. 6 shows the changes in the price of marketed solar cell modules and the future target of the Sunshine Project. The figure indicates that after the module cost is reduced to 500 yen/wp (\$2.30/wp), these modules will begin to sell as dispersed-type PV generation system (primarily in place of diesel

generators). This will be the first step toward the wide use of the solar power system as a general-purpose power supply. Subsequently, it is anticipated that further cost-cuts will result from the mass production effect. As a consequence, many efforts are underway to establish low-cost technologies for polysilicon production and high efficiency solar cell fabrication with the goal of a solar cell module price below 500 yen/wp (\$2.30/wp) by the early 1990's.

Currently a plan is being reviewed to construct and conduct test operation of a pilot plant based on the TCS-hydrogen reduction FBR technology to produce silicon granules. This would be done with the support of NEDO and the Sunshine Project Promotion Headquarters.

In this plan the pilot plant would be of a 80 to 100 tons/year silicon granule production capacity, its construction would begin in 1987, and the operation results would be reported in 1990. A successful demonstration would be a major step toward the commercialization of this process.

The FBR tubes to be used in this development will be of 40 to 60 cm diameter and the production capacity per reactor will be 40 to 50 tons/year.

The cost target in manufacturing silicon granules in this plant is set at 6000 to 8000 yen/kg (\$27.90 to \$37.20). To achieve this target, the following technical goals will have to be realized.

- a. Development of a large-diameter FBR capable of sustaining long-term, continuous operation.
- b. Demonstration of the fully-closed system connecting the TCS production and hydrogen reduction processes. (Research on each process step is under way independently.)
- c. Establishment of the optimum operational conditions and the automatic control technology for a large scale plant.

Especially important among these is the development of large-diameter, high-reliability FBR tubes. This will be a key step in scaling up the present process. For this purpose, it is essential to select the most appropriate material for the tubes. The estimate of the polysilicon manufacturing cost for a 1000 MT/year plant based on this process is 4300 yen/kg (\$20./kg).

In the water glass method, expected as the next-generation SOG-Si manufacturing method following the TCS-hydrogen reduction method, the cost target is set at 2000 to 3000 yen/kg (\$9.30 to \$14.00). By 1986 the development project will have finished evaluating the results thus far and will have decided upon future strategies.

The mass utilization of solar cells is about to occur. It is anticipated that the projects mentioned above will serve to establish the low-cost silicon manufacturing process, thus contributing to the cost reduction of solar cells.

ACKNOWLEDGEMENTS

Before concluding this report, we would like to thank the Sunshine Project Promotion Headquarters, NEDO, Shin-etsu Chemical and Nippon Sheet Glass for giving us advice and the relevant data.

We also want to express our gratitude not only to JPL but also to other organizations all over the world for their discussions of the developments of low-cost polysilicon processes.

LITERATURE

1. Sunshine Project Promotion Headquarters: Japan's Sunshine Project, Summary of Solar Energy R&D Program, (1983), 50
2. *ibid.*, 54
3. Proceedings of NEDO Photovoltaic Symposium 1983, (1983), 181 (Japanese)
4. NEDO: Annual Report of Researches in 1984, (1985), 213 (Japanese)
5. *ibid.*, 230
6. *ibid.*, 226
7. NEDO: Annual Report of Researches in 1983, (1984), 215 (Japanese)
8. Sunshine Project Promotion Headquarters: Annual Report of Sunshine Project in 1982, (1983), 214 (Japanese)
9. NEDO: Second Proceedings of NEDO Activities, (1982), 135 (Japanese)
10. Nippon Sheet Glass and NEDO: 20th Intersociety Energy Conversion Engineering Conference, (1985)

Table 1. Experimental TCS Manufacturing Equipment

<u>Hydrogenation reactor</u>		
Reactor type		Fluidized-bed
Inner diameter	(cm)	25
Reactor Height	(cm)	500
<u>Running conditions</u>		
Bed depth	(cm)	300
Feed gas molar ratio ($H_2/SiCl_4$)		1.5 to 3.0
Hydrogenation temp.	($^{\circ}C$)	550
Hydrogenation pressure (kg/cm^2G)		7.5 to 8.0
Catalyzer		CuCl

Table 2. Experimental TCS Purification Equipment

<u>First distillation column</u>		
Column inner diameter (cm)		40
Column height	(cm)	910
Distillation stage		25
<u>Second distillation column</u>		
Column inner diameter (cm)		40
Column height	(cm)	1,640
Distillation stage		50
<u>Third distillation column</u>		
Column inner diameter (cm)		40
Column height	(cm)	1,640
Distillation stage		50

Table 3. TCS Manufacturing Operation Results

<u>Item</u>		<u>Targets</u>	<u>Results</u>
<u>Conversion</u>			
Conversion ratio	(mol%)	28.0	28.6 max
Production rate	(kg/Hr)	28.5	31.7
Power consumption	(kwh/kg.TCS)	2.7	*2.7
H ₂ consumption	(Nm ³ /kg.TCS)	0.11	0.094
MG-Si consumption	(kg/kg.TCS)	0.06	0.058
<u>Distillation</u>			
Steam consumption	(kg/kg.TCS)	8.0	5.6
Production rate	(kg/Hr)	28.5	31.7

* includes distillation

Table 4. TCS Quality

<u>Lot</u>	<u>One-pass FZ in Ar</u>			<u>Eight-pass FZ in Vac</u>		<u>Donor Concentration Nd (ppba)</u>
	<u>Specific resistivity (ohm-cm)</u>	<u> Nd-Na (ppba)</u>	<u>Lifetime (μ-sec)</u>	<u>Specific resistivity (ohm-cm)</u>	<u>Boron (ppba)</u>	
1	N- 151	0.64	80	P-1100	0.26	0.90
2	N- 255	0.38	100	P-3170	0.09	0.47
3	N- 258	0.37	130	P- 620	0.46	0.83
4	N- 172	0.56	80	P-1190	0.24	0.80
5	N- 150	0.64	70	P-3560	0.08	0.72
6	N- 250	0.38	25	P- 470	0.61	0.99
7	N- 150	0.64	50	P- 890	0.32	0.96
8	N- 327	0.29	60	P- 520	0.55	0.84

Table 5. Metal Impurities in TCS

Lot	(ppba)						
	Ti	Al	Fe	Ni	Cr	Cu	V
1	<20	<0.4	50	<0.2	0.3	<1	<5
2	<20	<0.4	130	0.7	0.3	<1	<5
3	<20	2	28	<0.2	0.5	<1	<5
4	<20	<0.4	210	<0.2	1.0	<1	<5
5	<20	<0.4	53	<0.2	0.9	<1	<5
6	<20	<0.4	15	<0.2	1.5	<1	<5
7	<20	0.5	11	1.1	3.7	<1	<5
8	<20	1.3	12	<0.2	0.7	<1	<5

Table 6. Basic Specifications with Capacity of 10 Tons/Year

Items	Planned Specification
Reactor type	Fluidized bed
Reactor inner diameter (m)	0.21
Reactor height (m)	2.5
Fluidized bed height (m)	1.1 to 1.2
Feed gas, SiHCl ₃ /H ₂	40/60
Reaction temp. (°C)	1,000 to 1,100
Heating system	External, SiC heater
Si yield (%)	about 20
Power consumption (kwh/kg.Si)	30
Si seed diameter (mm)	0.25 to 0.5
Grown silicon diameter (mm)	0.8 to 1.5
Off-gas (CS and H ₂)	Recovered and recycled

Table 7. Silicon Granule Manufacturing Results
(1984)

<u>Items</u>		<u>Targets</u>	<u>Results</u>	
			<u>Overall*</u>	<u>Best**</u>
Total Reaction time	(Hr)	-	4,377	632
Manufactured Si	(kg)	-	8,349	1,504.7
TCS concentration	(%)	-	36.5	42.3
Power consumption	(kwh/kg.Si)	30	28.32	21.30
TCS consumption	(kg/kg.Si)	20	18.72	18.94
Si yield	(%)	20	18.3	21.5

* yearly performance

** best performance

Table 8. Analysis of Si Granule

<u>Lot</u>	<u>Sample</u>	<u>Fe</u>	<u>Cu</u>	<u>Al</u>	<u>Cr</u>	<u>Mn</u>	<u>Mg</u>
A	17	288.8	23.8	90.9	74.4	2.1	50.3
B	11	204.1	37.7	41.4	5.5	nd	20.5
C	27	241.9	76.9	nd	51.7	0.9	38.9
D	17	182.1	45.9	nd	16.5	nd	36.1
E	29	244.5	15.9	nd	2.9	nd	51.5

nd: not detected.

Table 9.

Analysis of Silica Sand for Sheet Glass and Physical Purification Product

	Impurities (ppm W)								SiO ₂ (%)
	Al ₂ O ₃	Fe ₂ O ₃	TiO ₂	CaO	MgO	ZrO ₂	Na ₂ O	K ₂ O	
silica sand for sheet glass	19,000	1,500	642	277	364	20	947	10,480	96.7
physical purifi- cation product	270	40	70	30	9	3	20	20	99.9

Table 10. Impurity Level of Starting Material and Purified Silica

Impurities	(ppm)			
	Starting material		Purified silica	
	A	B	A	B
B	--	--	<1	<1
Na	--	--	0.9	1.0
Al	5,200	457	<3.5	<3.8
P	--	--	<1	<1
Ca	27	38	0.8	0.5
Ti	98	36	0.9	0.6
Fe	330	68	<0.5	<0.5
Zr	31	<7	<0.6	<0.6

A: water glass (whose impurity level was calculated in terms of silica.)

B: upgraded silica after physical purification

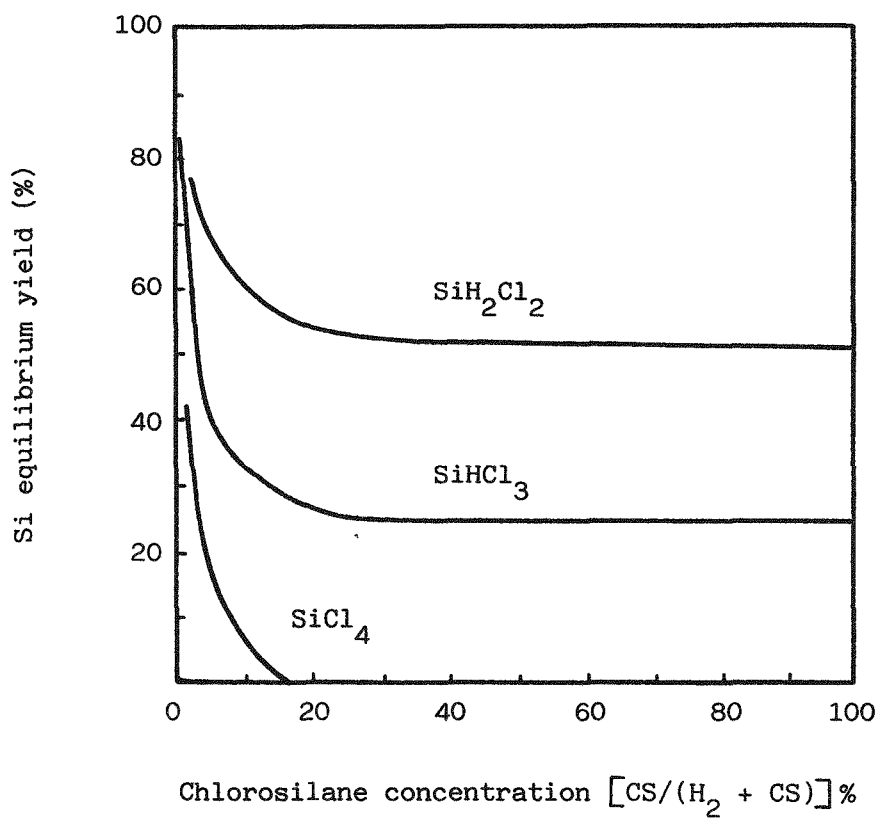


Fig. 1. Chlorosilane Concentration and Si Equilibrium Yield

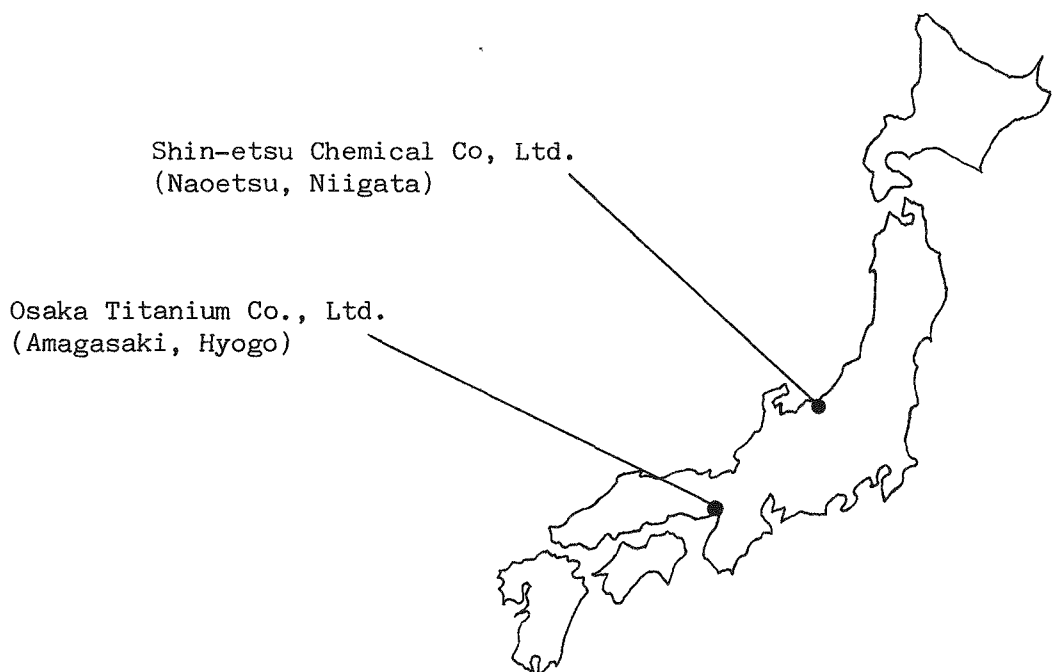
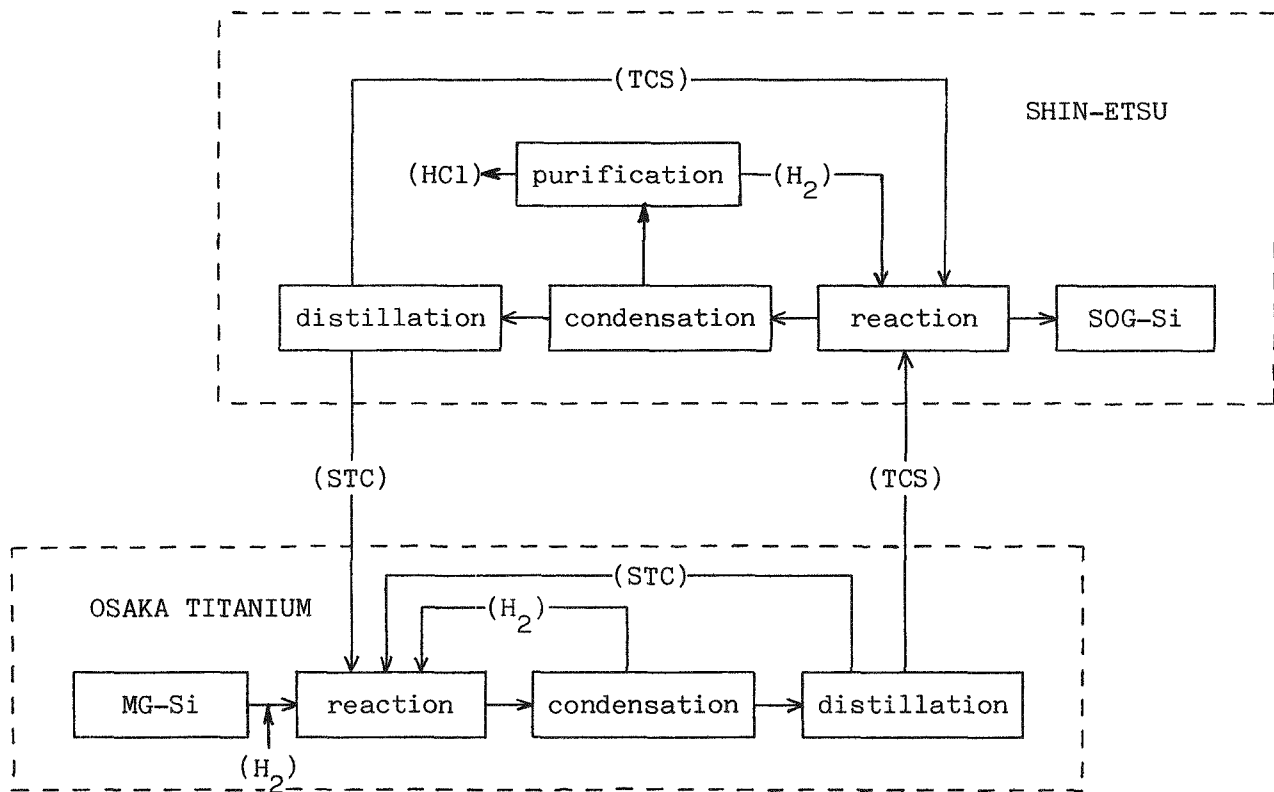


Fig. 2. Allotted Task of Low-Cost Si Manufacturing Technique Development

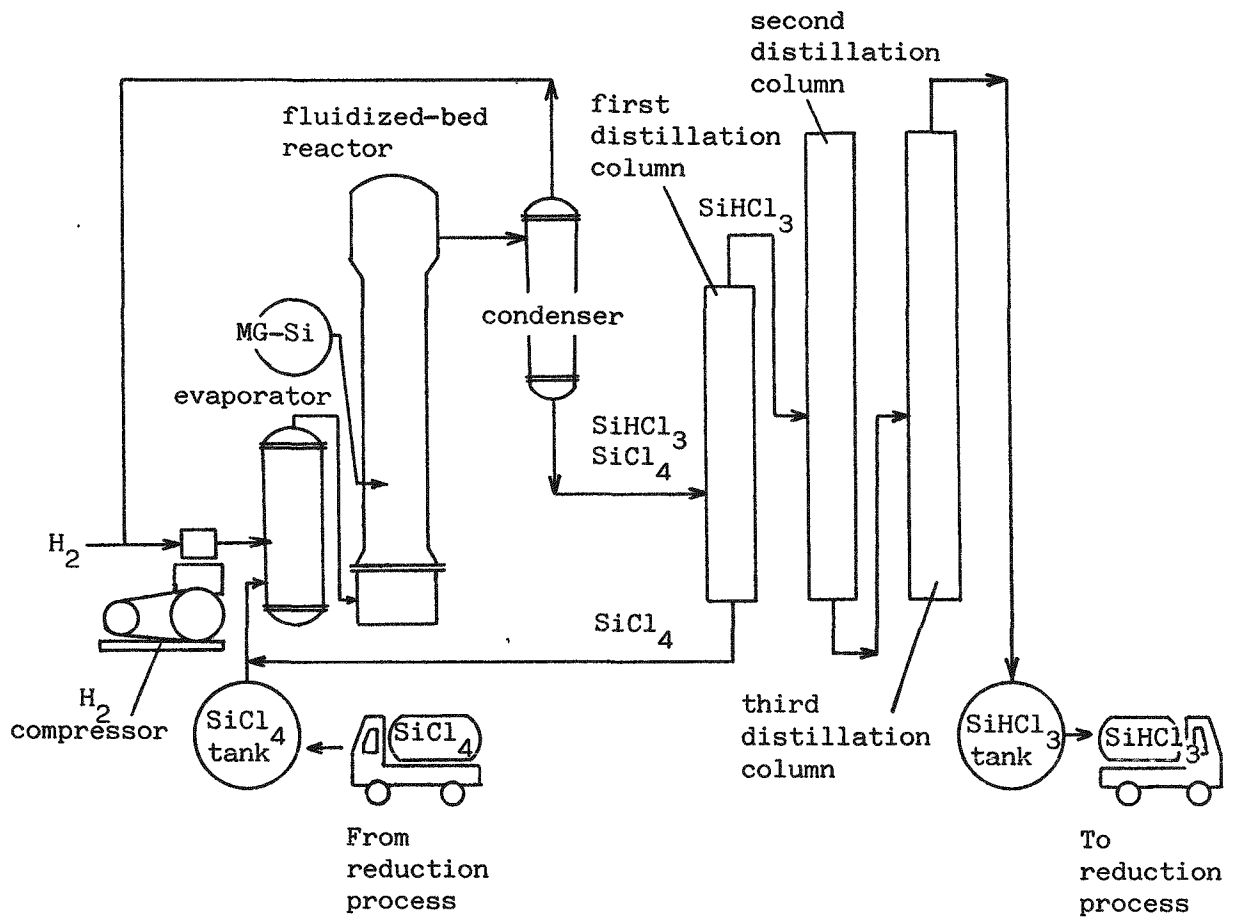


Fig. 3. Experimental TCS Manufacturing Equipment

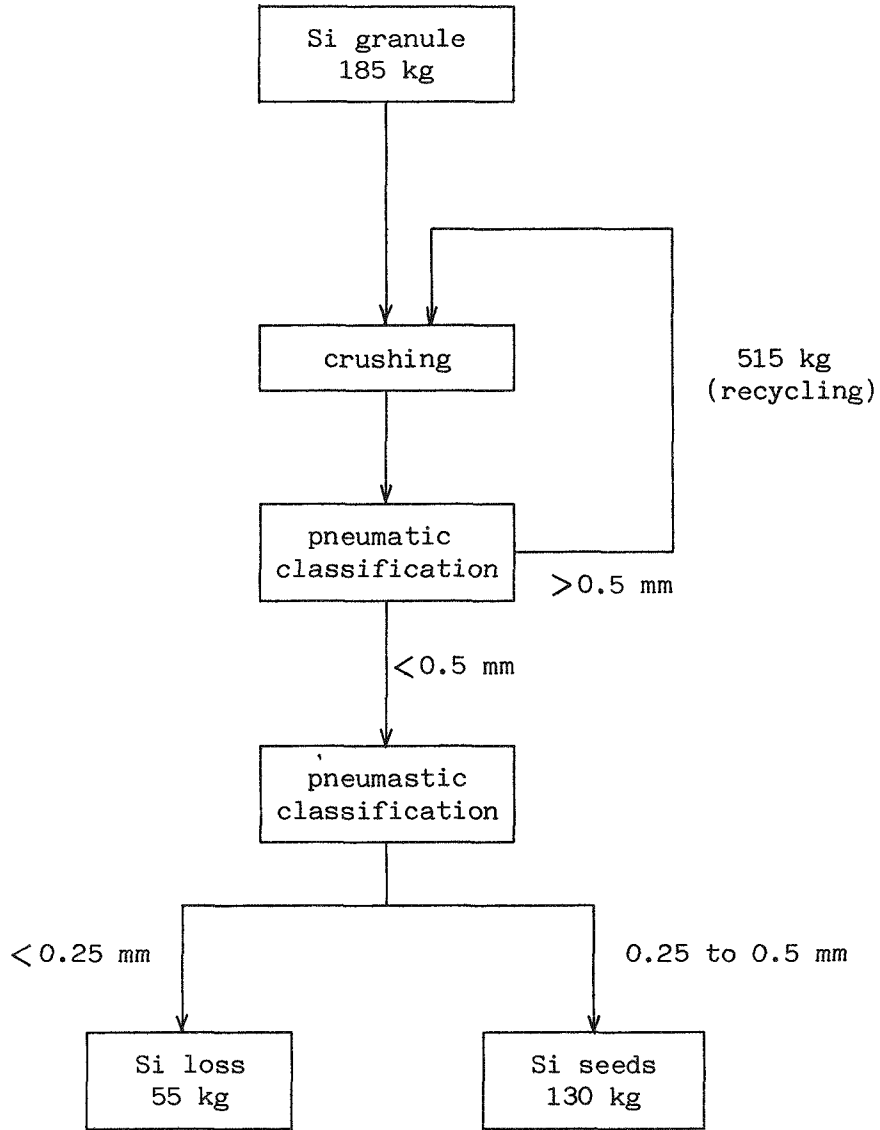


Fig. 4. Material Balance in Seed Preparation

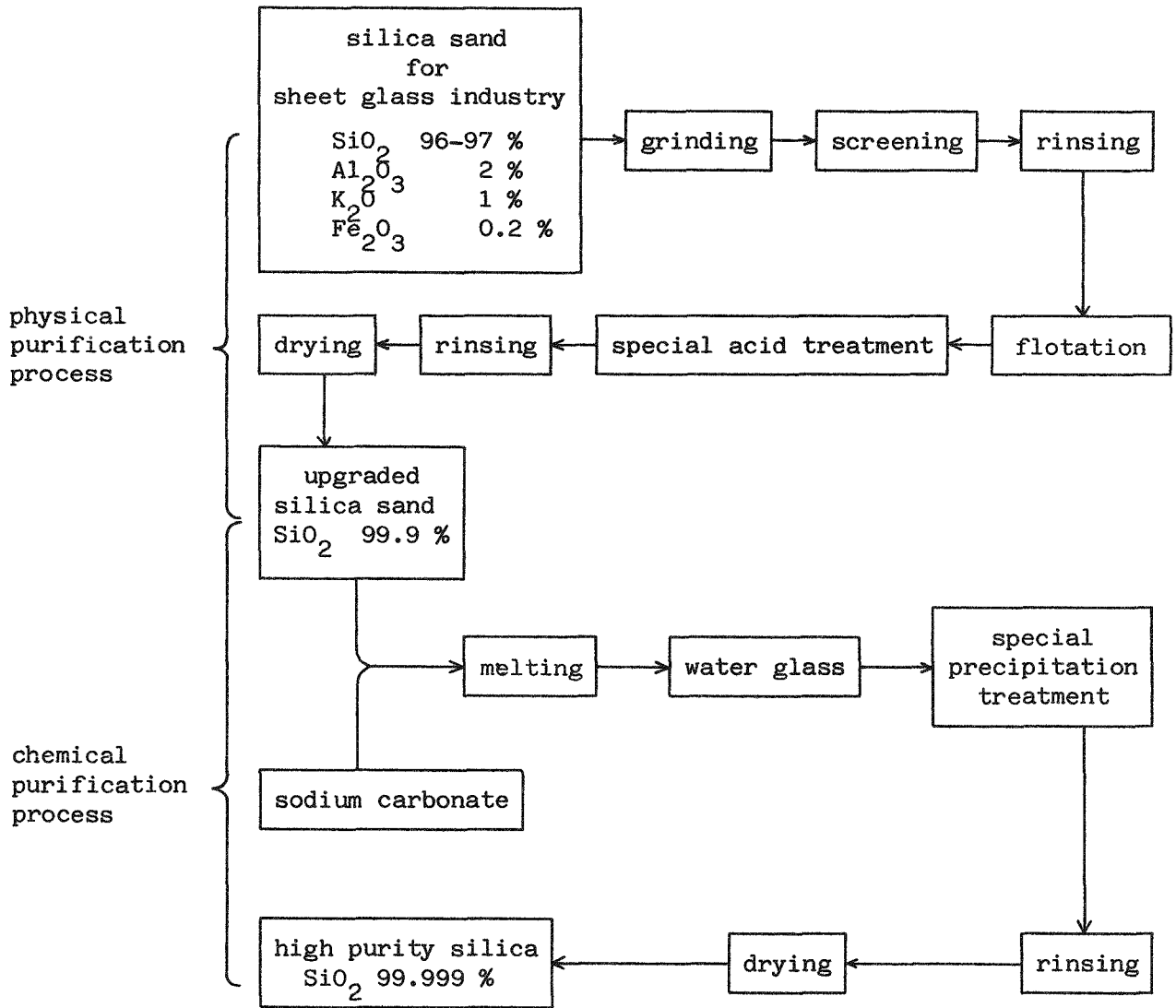


Fig. 5. Water Glass Method

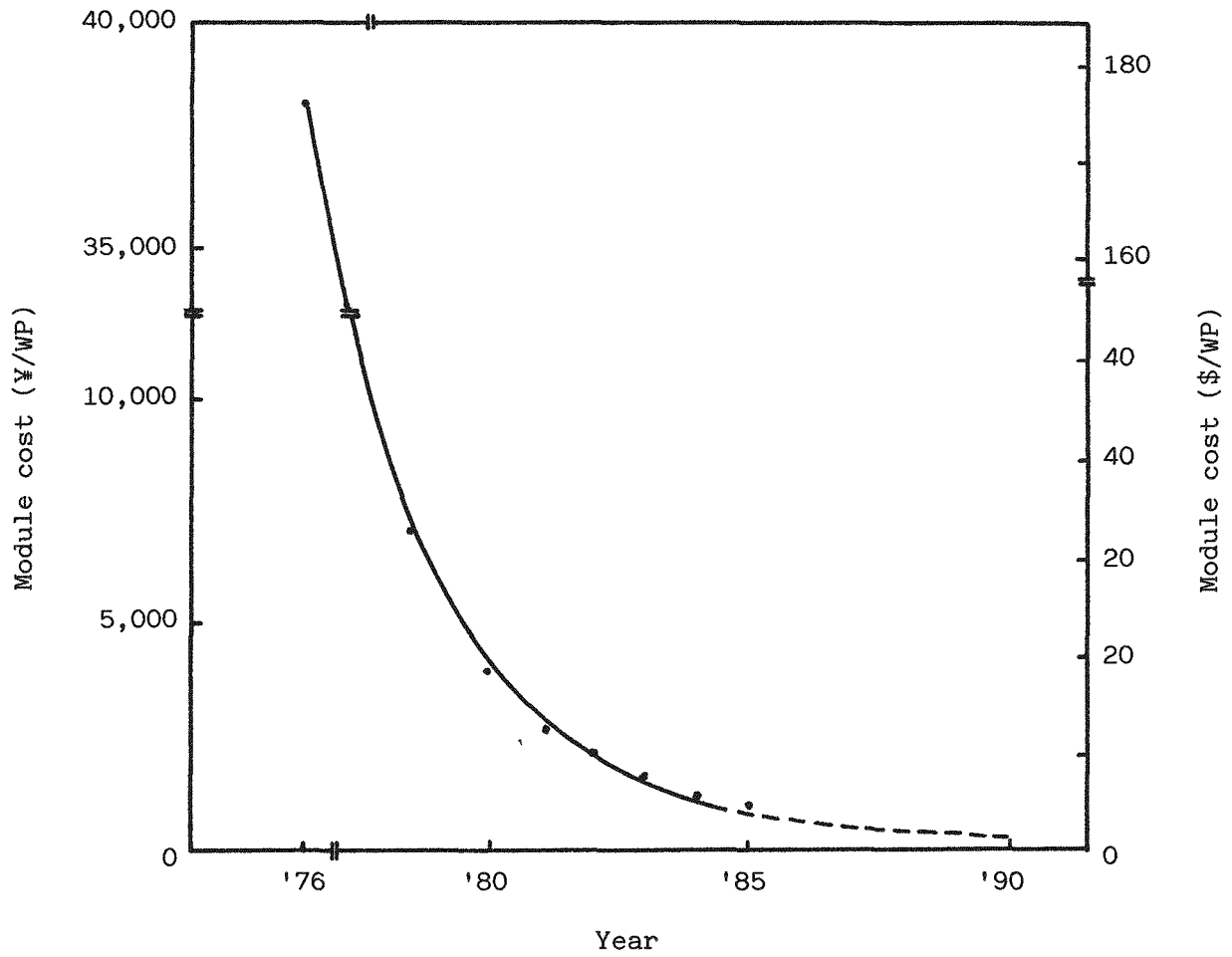


Fig. 6. Cost of Solar Cell Modules

(exchange rate : ¥215/\$)

DISCUSSION

HSU: What is the purity of your solar-grade silicon?

NODA: That is described in detail in the paper, so please refer to the paper.

LEIPOLD: Do you know what limits the purity of the fluidized-bed reactor product? Is it the trichlorosilane gas, the seed, or the reactor?

NODA: The product purity is determined by the composition and quality of the reactor tube.

LORD: How much carbon is there in the material?

NODA: Which material do you mean? Do you refer to the granules? We are achieving NEDO's target. Therefore, in that respect, we have not encountered any major problems in the quality of granules.

LORD: Approximately how much carbon is there in the crystals after you pull them?

NODA: We had a slight problem in carbon concentration, but the problem has been solved. The target for cell efficiency was initially set for 12%. When we try to drive up to 14%, we may encounter some problems, but at least the present efficiency target has been met.

LORD: Do you think it's possible to use this process to produce electronic-grade silicon?

NODA: My understanding is that everyone here has a strong interest to see our process applied to produce electronic-grade material. We would like to see that happen too.

AULICH: Did I understand you correctly that you are planning to produce 100 tons of these granules in 1990? And if the production is satisfactory, you will then decide on a 1000-ton plant? Is that correct?

NODA: The initial target was for 1000 tons. However, the Japanese government is also encountering deficits, so the project has been scaled down to 500 MT, and it may come down further to a smaller size. However, a 100 MT plant has been committed for 1990.

PROCESSES AND PROCESS DEVELOPMENT IN TAIWAN

H.L. Hwang

Department of Electrical Engineering

National Tsing Hua University

Hsin-chu, Taiwan, 300, R.O.C.

ABSTRACT

Silicon material research in ROC parallels its development in electronic industry. This paper gives a brief outline of the historical development in ROC silicon material research. Emphasis is placed on the recent Silane Project managed by the National Science Council, ROC, including project objectives, task forces and recent accomplishments. An introduction is also given to industrialization of the key technologies developed in this project.

INTRODUCTION

For a land of such limited resources, R.O.C. in Taiwan has been ranked as one the highest in population density and in economic developments in the past 20 years or so.

It is an intriguing question as to how this island will develop in the future, especially in the electronics and solar industries. It could set an example for other developing countries.

A Silane Project managed by National Science Council, R.O.C. was initiated in 1981 with the objective to develop key technologies in solar cell and semiconductor Si materials. This project emphasizes coordination among institutions and an overall management plan for various phases of the developments.

Taiwan has a fair amount of high quality quartzite deposits; the Mining Institute of Industry Technology Research Institute (ITRI) is responsible for the mining deposit survey. This organization is also responsible for the crude - and solar-Si production by the reduction/leaching techniques.

The Applied Chemistry Division of Chung-shan Institute of Science and Technology has developed the technologies for the production and pyrolysis of the silanes (SiHCl_3 , SiH_2Cl_2 and SiH_4). Pilot production operation is scheduled and will be carried out by the Institute of Chemical Engineering of ITRI.

The Nuclear Instrumentation Division of INER (Institute of Nuclear Energy Research) is responsible for the Chemical Vapor Deposition (CVD) processes, and for photovoltaic solar cell and module fabrication. A group from the Mechanical Research Laboratories is currently engaged in the development of a LPCVD industrial system for epitaxial Si production.

Polycrystalline Si production by gas assisted solidification has been developed at the Tsing-Hua University, and solar modules made from this material will be installed in the Yu-Shan National Park Electricity Development Project.

Amorphous Si solar cell prepared by glow-discharge has been successfully developed for consumer electronics by the Energy Research Laboratory of ITRI. Pilot production technology is under development.

A strong five-team characterization group has been assembled in Tsing Hua University to support the analysis of silane and Si materials by chemical, defect, electrical and surface measurements; particular emphasis is given to the correlations among these analyses.

This project has also promoted the joint venture of a 10 MW ribbon Si solar cell production in Taiwan. The goal is to develop the key technologies for silicon materials and to establish the foundation for prospective semiconductor Si materials and solar cell industries by 1990.

HISTORICAL

Table 1 depicts a brief historical outline of semiconductor silicon development in Taiwan.

In view of the increasing world-wide demand for ultra-pure silicon, a project was initiated in 1971 at the Department of Mechanical Engineering, National Taiwan University, by the late Prof. T.H. Loh to investigate high-purity silicon-manufacturing processes [1,2]. This work was terminated after the death of Prof. Loh. The activity in high-purity silicon production was soon resumed by the National Science Council (formerly National Research Council) by granting a joint project to the Chemistry and Physics Departments of National Tsing Hua University (NTHU) for studying the techniques for the chemical purification of silicon [3-5] and for single crystal silicon growth. Unfortunately, these efforts were not continued, either due to the limitations of material characterization capability or to a shift in research funding priority.

At almost the same time, the Electronic Research and Service Organization (ERSO) was established in the Industrial Technology Research Institute (ITRI) with the objective of developing IC technology. The establishment of ERSO in ITRI signified a temporal shift in interest from silicon material research to device-related research and development. An ion implanter was provided to the Physics Department of NTHU in 1976.

Tatung Co. was the first industrial establishment to initiate silicon material research by setting up an electronic R&D division in 1977. In 1978 semiconductor silicon wafers from single crystals prepared by the Floating Zone process were on the market for testing. In 1981 the Sino-American Silicon Product Incorporation was established to produce silicon wafers by the Czochralski Process. Currently, these two companies supply a large portion of Si wafers for the local diode--and transistor--industry; more than 70% of the world-wide production of diodes is in Taiwan. In 1981, an interdisciplinary project for the application of silane was initiated by the National Science Council, ROC, with the aim of developing silicon technology in Taiwan.

It is apparent as outlined in Table 1 that silicon material research in Taiwan blew in two waves. The first one was in the early 1970s and the second around the turn of 1980. The description of our recent advances in silicon material research will focus on the Silane Project.

SILANE PROJECT

A distinct feature of this project is its organization and management. The overall program of the project is shown in Fig. 1.

The first phase of the project (1981-1985) will end this year. To date, this project has accomplished the following objectives: (1) a complete survey of the quartzite deposits in eastern, central and northern Taiwan; (2) production of metallurgical-grade silicon (MG-Si), upgraded MG-Si (UMG-Si) and solar-grade Si (SoG-Si); (3) production and purification of SiHCl_3 as in the Siemens Process and production of SiHCl_3 , SiH_2Cl_2 , and SiH_4 by the Chung-Shan Inst. of Science and Technology (CSIST) process; (4) production of 4" diameter multicrystalline Si (Poly-Si) wafers by Gas-Assisted-Solidification (GAS); (5) development of chemical vapor deposition (CVD) technology for silicon epitaxial layer growth; and (6) establishment of the capabilities for chemical (ppb level), structural, electrical, and surface analyses. The second phase (1985-1988) of this project is aimed at the development of pilot production technologies.

1. Production and Chemical Upgrading of Metallurgical-grade Silicon [6]

A detailed survey of high purity siliceous raw materials in Taiwan indicated that the four major types of silica deposits - vein quartz, quartzite, metamorphosed chert and sandstone - are economically feasible for silicon production [7]. MG-Si has been produced from vein quartz using an in-house designed batch-type single electrode submerged arc furnace. The MG-Si thus produced was shown to have an average grade of better than 98% silicon content.

Direct chemical upgrading of MG-Si was performed using a two-stage acid leaching/magnetic separation.

After the two-stage acid leaching, the contents of boron and phosphorus were both below 2 ppmw and the total impurity was below 90 ppmw level, but the C content was still not yet acceptable.

The technique of directional solidification to obtain further purification was investigated, and solar-grade Si has been produced (Table 2).

In addition to melting experiments for MG-Si production, silicon recovery in powder form by reduction of a fluosilicate with an organic reductant has also been tried. Preliminary results from a number of exploratory experiments were encouraging.

2. Silane Production/Pyrolysis

Trichlorosilane has been synthesized by chlorination of MG-Si with anhydrous HCl gas in a 34 mm x 60 cm reactor heated with a tube furnace. Reaction conditions, such as temperature, HCl feed rate, Si particle size and Si packing-weight, have been optimized and a routine GC method for analysis of $\text{SiH}_x\text{Cl}_{4-x}$ ($x = 0-4$) was established. Crude SiHCl_3 was then purified with both multifractional distillation and chemical methods. A comparison of trace impurities in a commercially available SiHCl_3 and those from the project is shown in Table 3. The analytical results indicate the B and P contents in the purified SiHCl_3 are laboratory environment-sensitive.

Moreover, the hydrogenation reaction of SiCl_4 and the disproportionation reactions of SiHCl_3 and SiH_2Cl_2 at "normal" pressure with special treated resin (not A-21) as catalyst were studied at CSIST. The gas-solid reaction was shown to be the dominant feature. Good product yields have been achieved for both reactions. The SiH_2Cl_2 and SiHCl_3 products were used for epitaxial growth in an in-house developed CVD system (vide infra). Diodes and transistors having good performance characteristics were made from these epi-layers with high production yields. A 2" diameter fluidized bed reactor (FBR) was constructed for the pyrolysis of SiH_4 , and ~400 to 500 μm grains have been obtained. However, contamination from the reaction wall is still a problem.

3. Growth of Epitaxial Layer by Chemical Vapor Deposition [9]

A versatile horizontal CVD system was designed and constructed for silicon epitaxial layer growth. Silicon epi-layers have been successfully grown from this system by hydrogen reduction of SiH_2Cl_2 and SiHCl_3 (prepared by the Silane Group). Material characterization and production yields of planar diodes and small signal transistors made from these epi-wafers (Table 4) show that the epi-wafers are industry-applicable. Gettering processes, such as high dose back surface oxygen ion implantation and a mechanical damage followed by heat treatment, have been experimentally used to obtain further improvements in the crystallographic perfection of the epi-layers. Conditions for epi-layer growth on gettered, front surface denuded substrates have been shown to significantly decrease microdefect density.

4. Poly-Si Production [10]

Poly-Si ingots have been produced by a self-designed GAS system. The GAS process is intended to be a low cost process for producing material for solar cells.

SoG-Si was cast in silicon nitride coated quartz crucibles by forced freezing initiated by means of a cold finger located at the bottom of the crucible. Both the heating temperature and the gas flow to the cold finger are microprocessor-controlled. Poly-Si crystals with large elongated grains have been successfully produced. An etched wafer and a solar cell fabricated from a poly-Si crystal are shown in Fig. 2. Analytical results and electrical properties measured on various areas of a wafer cut from one of the poly-Si ingots grown by this GAS system are shown in Tables 5 and 6.

The detailed kinetics of the grain growth have been studied by varying (1) the cooling gas, (2) the heating cycles of the crucibles, (3) the maximum He flow rate, and (4) the He flow/time profile.

5. Fabrication of Amorphous Si Solar Cells [11]

The project is currently endeavoring to develop a glow-discharge CVD process for fabricating amorphous silicon-hydrogen (a-Si:H) solar cells. a-Si:H solar cells with efficiency of 4% for consumer products have been routinely produced.

In-depth studies of the stability of a-Si:H have been carried out. When films are subjected to prolonged illumination, it was found from FT-IR that distinct transitions could occur among various bonds and from EPR that dangling bonds could be produced. A model based on bond-breaking of the three-center bonds was proposed (Fig. 3). [12]

6. Material Characterization

The analytical methods for the determination of trace impurities in both silane and elemental silicon at about ppb levels have been established by two laboratories (NTHU and INER). The methods employed include ICP, DCP, NAA, FAAS and UV/VIS.

Analytical methodology to fulfil the specific requirements of rapidity, sensitivity and depth profile for better characterization of silicon materials is being studied further in the present study. The main accomplishments are: (1) establishment of the ICP-AES technique for achieving fast, reliable and sensitive determinations of over 20 elements in silicon and silane samples by optimally combining various instrumental parameters (optical system, RF power, Ar-gas flow, etc.) with a chemical pretreatment step; (2) development of pretreatment techniques for the concentration of various trace impurities in dichloro- and trichloro-silanes by adding adducting materials (such as Lewis

acids or bases) to react with B, P and As in the samples. This is followed by sensitive instrumental determination. B, P, As and some metallic impurities can be effectively determined down to 10^{-9} g/g; (3) development of methods for the determination of impurity and dopant concentrations (B, P and As) in silicon semiconductor as a function of depth. The method established is based on the anodic oxidation of the silicon sample followed by sensitive instrumental determination of the dissolved oxide layer; the results are then compared with those from physical evaluations; and (4) preliminary study of the determination of carbon in silicon materials by a chemical analytical method. The method consists of steps for converting the carbon in the dissolved silicon materials into carbon dioxide followed by the quantitative determination by conductometry.

Defect and electrical characterization for semiconductor silicon has been routinely carried out following the ASTM Standards. A reflection Lang X-ray topography camera has recently been built and a SEM laboratory for surface characterization was set up.

A TEM/cross-section technique was developed. Improvement of a SEM to run in the EBIC mode was done to determine the carrier lifetimes (Fig. 4). A MOS C-V method was also used to determine the carrier lifetimes of poly-Si crystals.

A major project has been carried out using TEM and SEM for the study of microstructures and defects; the emphasis was placed on type, quantity, and characteristics. The electrical characteristics, including resistivities, mobilities and lifetimes, have been determined. A coordinated study, including chemical, structural, electrical, and surface characterization on poly-Si crystals grown by GAS, has been under way. A numerical scheme employing non-parametric statistics was developed to investigate correlations among them. Effects on sample pretreatments, as well as of gettering processes, on changes of defect characteristics have been studied. Results indicated that there are correlations between the oxygen content and the carrier lifetime.

7. Economic Analysis [13]

Cost and benefit analyses have been carried out based on a preliminary process design for production plants of 1,000 ton/year capacity for the conventional polysilicon process and the U.C.C. process. A power law scaling factor and a sizing model were used to estimate the capital investment. The results indicate that the order of importance of specific cost parameters influencing product cost is plant investment, utilities, raw materials and labor for conventional polysilicon process; the order for the

U.C.C. process is utilities, plant investment, raw materials and labor (Fig. 5). The conclusion is that the plant site should be chosen where the cost of utilities and raw materials are the lowest.

8. Application Project

In 1985, an application project using PV modules made from poly-Si and ribbon Si solar cells was formulated to help in the promotion of local PV industry. A total 2.6 MW electricity is needed for the Yu-shan National Park at specified sites. System experience of ERL of ITRI will be directly applicable to this project.

REFERENCES

- [1] T.H. Loh, Material Science 2, 109 [1970]
- [2] T.H. Loh, *ibid*, 4, 177 [1972]
- [3] C.C. Chen, M.M. Chang, F.R. Shu and C.S. Liu, J. Chinese Inst. Chem. Eng. 5, 93 [1974]
- [4] M.M. Change, C.C. Chen, C.S. Liu and C.T. Chang, *ibid* 5, 99 [1974]
- [5] C.C. Chen, M.M. Chang, F.R. Shu and C.S. Liu, *ibid*, 5, 107 [1974]
- [6] T.N. Lung, J.K. Huang, P.Y. Shen, "Chemical Upgrading of Metallurgicalgrade Silicon" presented at Semiannual Review Meeting on Application of Silanes [1984]
- [7] T.N. Lung and P.Y. Shen, Tech. Report No. 191, "Investigation and evaluation of quartz deposits in eastern and central Taiwan", Mining Research and Service Organization ITRI [1982]
- [8] C.L. Chiou, Y.G. Hsen and T.L. Hwang, Annual Report on "Preparation and Purification Studies of Silanes" [1984]
- [9] S.S. Jao, D.S. Lee, C.Y. Juen and S.J. Chung, Annual Report on "Characterization and Evaluation of Electronic-grade Chlorosilane" [1983]
- [10] C.Y. Sun, H.R. Lo, H.L. Hwang, C.H. Chu, and L.R. Hwang, "Growth of Silicon Crystals for Solr Cells" presented at Semiannual Review Meeting on Application of Silanes [1984]

- [11] H. Yeh and C.S. Hong, "The Study and Fabrication of Amorphous Si Solar Cells" presented at Semiannual Review Meeting on Application of Silanes [1984]
- [12] C.S. Hong, K.S. Teng, K.C. Hsu, W.J. Jon, H.Y. Ueng, S.C. Lee and H.L. Hwang, Proc. of IEEE Photovoltaic Spec. Conf. Las Vegas, 1985.
- [13] H. Long, "Economic Evaluation of Polysilicon Technologies" in Proceedings of 1st ROC-ROSA Workshop on Silanes, Hsin-chu, Taiwan [1983]

Table 1. A Brief Historical Outline of Semiconductor Silicon-related R&D in Taiwan, ROC.

Year	Institution or Organization	Interest
1966	Semiconductor Research Center, National Chiao Tung Univ.	IC and Semiconductor research
1971	Dept. of Mechanical Engineering National Taiwan Hua Univ.	High-purity Silicon- manufacturing Process development
1973	Chemistry Department National Tsing Hua Univ.	Chemical purification of Silicon Project
1973	Physics Department National Tsing Hua Univ.	Single crystal silicon growth project
1974	Electronic Research and Service Organization, Industrial Technology Research Institute	IC technology development
1976	Physics Department National Tsing Hua Univ.	Ion implantation
1978	Electronic R&D Division Tatung Co.	Semiconductor silicon wafer production (FZ)
1981	Sino-American Silicon Product Incorporation	Semiconductor silicon wafer production (CZ)
1981	National Science Council	Application of Silane Project.
1983	Four companies start-up in Hsin-chu Science Park	VLSI

Table 2 Analytical data of SoG-Si produced by chemical leaching/GAS methods

Sample Element	Metallurgical Grade Si	Ultimate Metallurgical Grade Si			Solar Grade Si	
		1st Leaching	2nd Leaching	Analytical Method	Grown by G.A.S.	Analytical Method
Al	6300ppm	250ppm	130ppm	NAA, ICP	< 6ppb	NAA
Fe	2800ppm	32ppm	2.5ppm	ICP	< 4ppb	NAA
Ca	2100ppm	13ppm	7.4ppm	ICP	<98ppb	NAA
Cr	140ppm	1.6ppm		ICP	< 6ppb	NAA
Co	77ppm			ICP	< 1ppb	NAA
Mn	0.5ppm	0.5ppm		ICP	< 1ppb	NAA
Cu	37ppm			ICP	< 1ppb	NAA
B	25ppm	19ppm	19ppm	ICP	<81ppb	ICP
P	23ppm	16ppm	16ppm	UV/VIS	<36ppb	UV/VIS
As	18ppm	10ppm		Polarography	<14ppb	NAA

- *1. Starting material MG-Si from Elkem a/s, Norway
2. 1st stage leaching: HF (12%)+HCl (9%), 80° C, ambient condition, 1hr.
2nd stage leaching: HF (12%)+HCl (9%)+C₂H₂O₄ (10%), 150 C, under pressure, 1hr.
3. Crystal Growth: GAS (Gas Assisted Solidification)
4. Product: Solar-Grade Silicon, Polycrystalline Si ingot.

Table 3. A comparison of trace impurities (in ppb) in trichlorosilane (TCS) Prepared by Silane Group and that from commercial source.

Sample*	P	Al	Mn	Fe	Zn	Ag	Cu	Mg
Commercial	<1.2	156	<2	59	27	<1	<37	35
TCS-1	20	10	<20	31	<16	<10	<12	33
TCS-2	15	194	<9	44	<9	<4	<4	30

* TCS-1 and TCS-2 represent trichlorosilane from two different runs.

Table 4. A comparison of characteristics and product yields (%) of small signal transistors (2N3906) fabricated from commercial epi-wafer and epi layer grown from commercial TCS and TCS-2 from Silane Group*.

Characteristics	A	B	C
$BV_{EBO} > 5.5$ V (at $I_{EBO} = 10$ A)	94%	84%	83%
$BV_{CBO} > 44$ V (at $I_{CBO} = 10$ μ A)	75	56	35
$I_{CBO} > 10$ nA (at $V_{CB} = 30$ V)	76	52	49
$BV_{CEO} > 44$ V (at $I_{CEO} = 1$ mA)	80	65	34
HFE > 80 (at $V_{CE} = 1$ V, $I_C = 10$ mA)	96	92	88

* A, from commercial epi-wafer; B, epi layer prepared from commercial TCS; C, epi layer prepared from TCS-2 (Table 3).

Table 5. Analytical Results of a poly-Si wafer prepared from ingot grown by GAS method*.

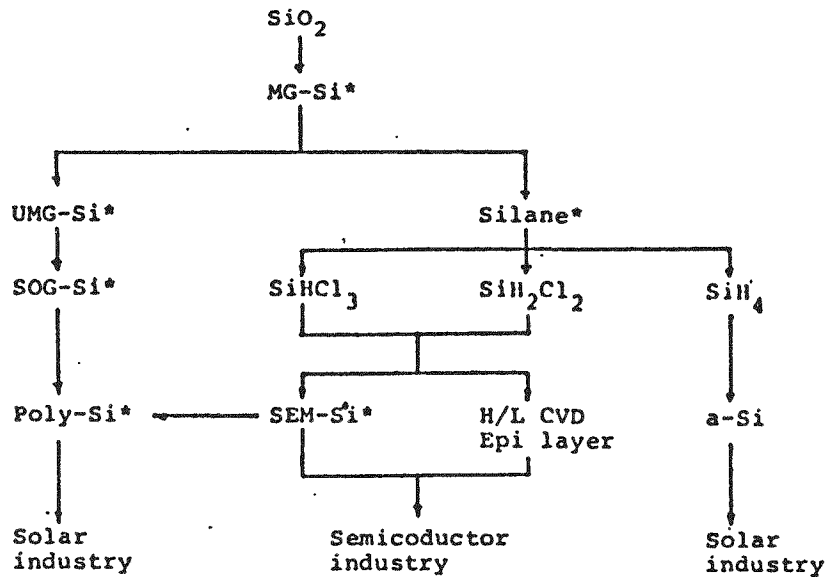
Element	S	33	33̄	13̄	13̄	32	34̄	12̄	14̄
B (ppb)	0.5	-	-	-	-	<2	<2	<2	<2
P	0.4	-	-	-	-	<14	<14	<14	<14
Ca	3.7	350	160	200	60	71	567	97	157
Mg	0.5	210	30	70	14	6	82	10	7
Fe (ppm)	0.9	0.3	0.9	1.0	1.0	7	7	14	7
Al	1.9	-	-	-	-	<21	<21	35	<21

* S represents source material and numericals designate areas of the wafer. Results of 33 - 13̄ from NTHU group and those of 32 - 14̄ from INER. -, no results due to sample loss.

Table 6. Electrical characterization of a poly-Si wafer prepared from ingot grown by GAS method*

Properties	23	23	23	23
Thickness (μm)	687	686	684	678
Hall mobility ($\text{cm}^2/\text{V}\cdot\text{sec}$)	96.6	79.8	142	100
Hall resistivity ($\Omega\text{-cm}$)	2.42	3.08	1.34	2.03
Carrier conc. ($10^{16}/\text{cm}^3$)	2.7	2.5	3.2	3.0
Diffusion length (μm)	6	2	4	6
Carrier lifetime (μs)	0.33	0.45	0.4	0.48
Carbon (10^{17} atom/ cm^3)	1.51	0.91	1.62	0.67
Oxygen (10^{17} atom/ cm^3)	2.15	0.80	0.56	-

* Samples given in numerical represent area code on the wafer.



* Subject to material characterization such as
 chemical analysis
 structure characterization
 electrical characterization
 surface characterization
 economic analysis

Fig. 1. Over-all Program of Application of Silane Project.

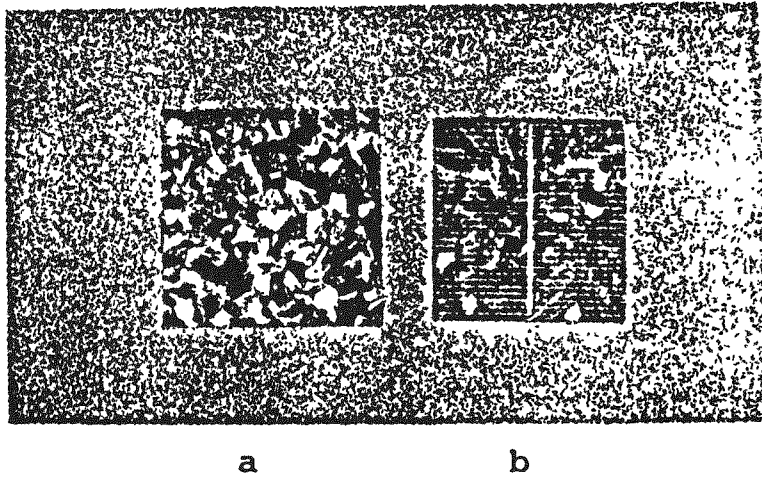


Fig.2. Photographs of a polished GAS Poly-Si wafer (a) and a solar cell fabricated from the wafer (b).

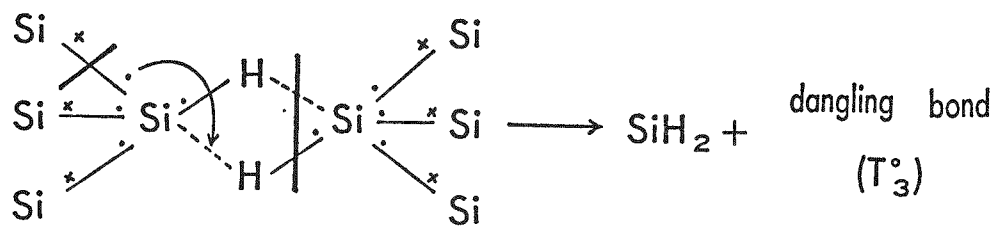


Fig 3. A proposed model to interpret bond change in a-Si:H film

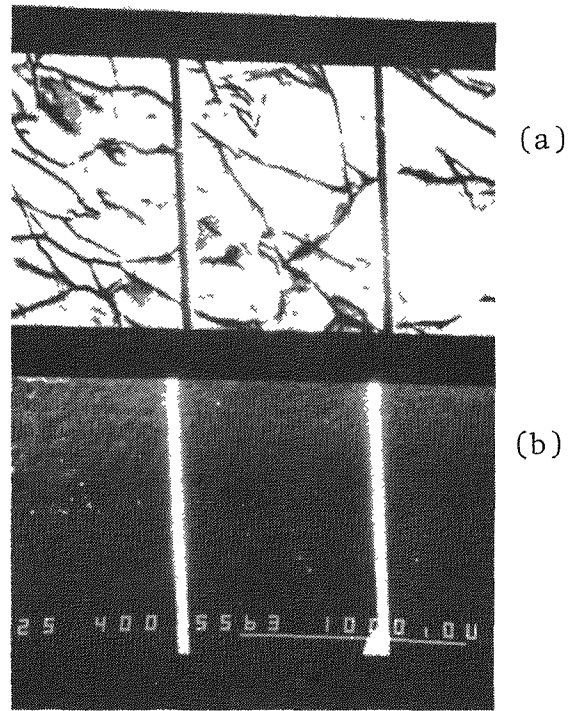


Fig. 4(a) EBIC
(b) SEM photograph of a GAS grown Poly:Si solar cell

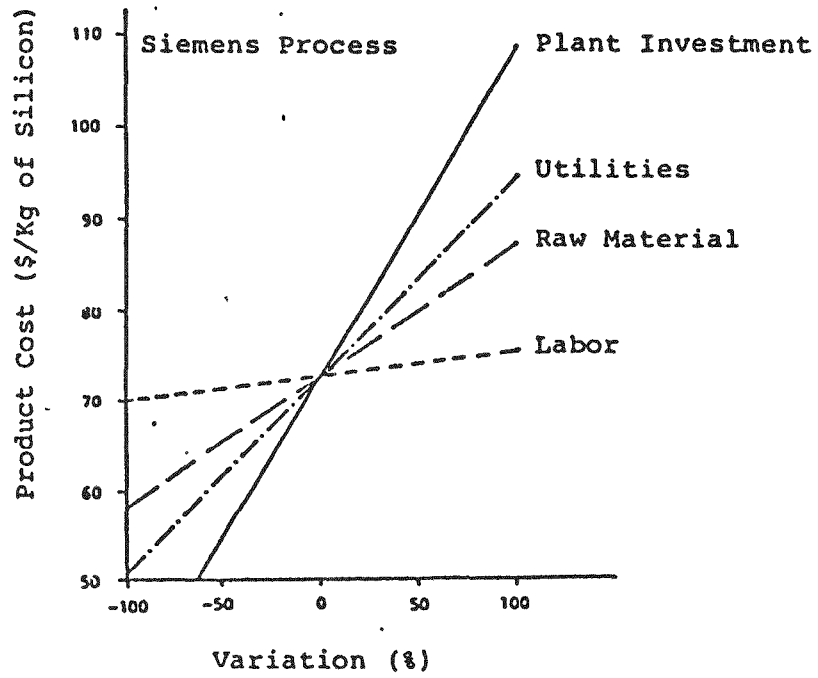
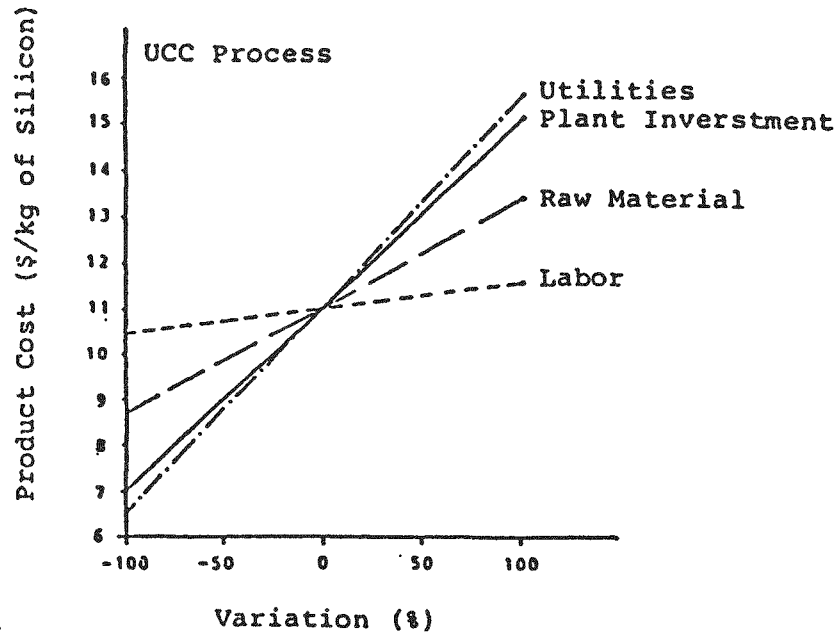


Fig. 5. Cost sensitivity: product cost vs variation.

DISCUSSION

MAYCOCK: I know that there has been a preliminary announcement that Westinghouse is a venture partner in ribbon production. Do you have a venture partner in amorphous silicon yet?

HWANG: We are developing our own technology and we would also like to use our own technology. Because we are not now in the same technical position as the United States, Japan, or West Germany, we welcome joint ventures also.

MAYCOCK: Who made the amorphous-silicon cell? Was it a laboratory product?

HWANG: It was from the laboratory.

AULICH: Would you comment on the fact that your cost projection on the silicon produced by the modified Union Carbide process is only about \$11/kg while the Union Carbide calculations show about \$25/kg?

HWANG: I mentioned that the calculation would not be accurate because the data we obtained do not cover the parameters necessary for an accurate calculation. Also, I believe that the cost advantage of production in Taiwan must be taken into account.

REFINING OF METALLURGICAL-GRADE SILICON

J. Dietl
Heliotronic GmbH
D-8263 Burghausen, Postfach 1129, Germany

ABSTRACT

A basic requirement of large-scale solar cell fabrication is to provide low-cost base material. Unconventional refining of metallurgical-grade silicon represents one of the most promising ways of silicon meltstock processing. The refining concept is based on an optimized combination of metallurgical treatments. Commercially available crude silicon, in this sequence, requires a first pyrometallurgical step by slagging, or, alternatively, solvent extraction by aluminum. After grinding and leaching, "high purity" quality is gained as an advanced stage of refinement. To reach solar-grade quality a final pyrometallurgical step is needed: liquid-gas extraction.

INTRODUCTION

Different possibilities can be seen in the field of low-cost silicon meltstock processing for large-scale solar cell fabrication. Processing routes via the refinement of metallurgical-grade silicon seem to offer best chances of producing solar-grade silicon at costs of lowest possible levels. The present paper follows the steps of previous reviews (see e.g. references 1-4) concentrating mainly on a material concept of an optimized sequence of metallurgical refining steps.

The target of any economy-oriented program can be seen here in a 10 % minimum AM1 conversion efficiency based on a 10 x 10 cm² multicrystalline silicon solar cell (5). Its concept has to consider comparably strong reduction of costs in every subtechnology such as material refining, crystallization, and ingot slicing as well. The final systems balanced against each other, then, would allow optimum economical conditions.

SOLAR-GRADE SPECIFICATION

It has been widely discussed, that the term "solar-grade" should be used only as a rather vague material specification. "Solar-grade" characterizes a category of silicon quality which, though less pure than electronic-grade silicon, can nevertheless be used for solar cell fabrication. Often the term "solar-grade"

does not sufficiently distinguish between chemical, crystallographic or device-related properties. In this paper this expression is primarily confined to the impurity situation of the silicon meltstock.

Fig. 1 illustrates various categories of silicon quality, covering about eight orders of magnitude from metallurgical-grade silicon to hyperpure silicon. The solar-grade or better the terrestrial solar-grade (TSG) quality range - to emphasize the real low-cost character of this product - should be seen as an approach assessing the chemical properties of the starting material modified by the influence of crystallization process and cell technology. The solar cell allows for reduced purity in general, but, as indicated by the dotted range in Fig. 1, demands hyperpure quality in terms of recombination-active elements. The introduction of terms such as "high purity 1" (HP1) or "high purity 2" (HP2) is a rather arbitrary way of defining certain intermediate quality stages of refining.

Impurities in silicon affect the efficiency of solar cells in a variety of ways. At high impurity concentrations crystal growth can be perturbed by inclusions, precipitates, or defects which may finally cause structural breakdown. Semiconductor properties are influenced by electrically active impurities which reduce the minority carrier lifetime. The objective of the wellknown Westinghouse project (6) has been to determine threshold values for a lot of impurity elements. This basic investigation revealed the detrimental influence of transition metals in particular. In order to understand the specific behavior and interaction of certain elements typical impurities have to be pursued by trace analysis on their way through the different refining stages. Profound analytical characterization of starting materials, intermediate qualities, and final products has to be seen as an indispensable task in the framework of solar-grade silicon development.

METALLURGICAL ROUTES TO SOLAR-GRADE SILICON

One of the most evident ideas, namely to win solar-grade silicon by typical metallurgical techniques, has attracted increasing attention. Three economically feasible routes for preparing solar-grade silicon meltstock are shown in Fig. 2. This schematic flow-diagram indicates the currently most-discussed processing sequences leading from different quartz qualities via intermediate purity stages to silicon of TSG-quality.

Two of these routes utilize the carbothermic reduction of quartz. Whereas route A proceeds from the low-purity arc furnace product - which will be discussed more in detail later on - route C is based on an impurity-improved technique from the very beginning. This alternative way, investigated for the first time at Dow-Corning (7) and continued by Elkem/Exxon (8), is not to refine metallurgical-grade silicon but to rather use raw materials of higher purity. Siemens (9) is developing a process in which quartz sand is purified using a combined glass melting/fiber leaching treatment, and carbon black is upgraded by leaching with hot hydrochloric acid. A specially designed arc furnace system is demanded to preserve the much higher degree of purity from where solar-grade quality can be reached by final purification procedures, e.g. by controlled solidification.

The aluminothermic reduction of quartz at comparatively low temperatures - as indicated by route B in Fig. 2 - represents another promising way to produce solar-grade silicon. A suitable technical process on this basis, being under investigation at Heliotronic (10), requires two liquid and immiscible phases - represented by an AlSi alloy and a flux system - acting as solvents for the reduction products Si and Al_2O_3 . In Fig. 3 a schematic flow-diagram indicates the regeneration cycle of the flux system combined with the recovery of Al and the recrystallization of Si in form of platelets which acts as a very effective integrated refining treatment. After separation of the Si-platelets the remaining Al level has to be removed by a final pyrometallurgical purification step to achieve solar-grade meltstock quality.

REFINING OF MG-SILICON

The production of metallurgical-grade silicon in electric arc furnaces is a technically well established large-scale process. The nominal capacity of all existing furnaces in the Western World is known to be between 600.000 and 650.000 tons per year (11). In the carbothermic reduction process impurities from SiO_2 , carbon mixtures, electrodes and other auxiliary materials contaminate the crude silicon to an amount of one to two percents. In Table 1 metallurgical-grade silicon products from different suppliers are characterized by impurity analysis.

Table 1: Concentration of impurities (ppmw) in MG-Si from different suppliers

Element	MG-Si I	MG-Si II	MG-Si III
Mn	260	500	50
Cr	25	20	50
Cu	25	50	20
Ni	110	30	10
Fe	3800	3500	5000
Al	1600	2400	2500
Ca	2700	2200	500
Mg	60	50	70
Ti	150	250	150
B	10	20	15
P	40	30	20

The predominant impurities Fe, Al and Ca are typically present in the range of some 1000 ppmw. Among the impurities below 100 ppmw the doping elements B and P can be seen. Another unavoidable impurity which is found in MG-Si in excess of saturation limits is carbon - mainly precipitated as SiC particles - in the concentration range between 100 and 1000 ppmw.

These impurity concentrations are far above the levels allowed for solar-grade meltstock. Nevertheless, the low cost of the metallurgical-grade product makes the refining by likewise economical metallurgical techniques increasingly attractive. Basic hydrometallurgical and pyrometallurgical refining procedures with special purification effects with regard to certain impurities and element groups are given by

- Solid-liquid extraction (acid leaching)
- Liquid-liquid extraction (slagging)
- Liquid-gas extraction (gas blowing and evaporation)
- Solvent extraction (recrystallization from Al solution)

Practice-oriented approaches have been started at several places to reveal the potentiality of these extractive processes. Optimization of the refining sequence is inseparably combined with economic aspects but also with the conditions of subsequent crystallization and device processing.

LIQUID-LIQUID EXTRACTION

Liquid-liquid extraction as one of the pyrometallurgical processes is applied to remove impurities from MG-Si in the molten state. Successful utilization requires a slag system that has a higher chemical affinity to certain impurities than silicon. The slag melt should be immiscible with molten silicon, which means that besides being chemically stable in contact with molten silicon it does not contaminate the silicon too much or dissolve major amounts of elemental silicon. Slags based on alkaline earth metal silicates have been found to fulfill these criteria.

To optimize the purification effect by slagging the high temperature chemistry of liquid-liquid extraction has to be investigated. As the elemental impurities are reduced or oxidized at the liquid silicon-slag interface, first order thermodynamic predictions can be made on the basis of their oxidative/reductive behavior. Elements forming oxides of higher stability than SiO_2 are expected to get oxidized and slagged. This has proven to be valid for elements like Ca, Mg and Al. On the other hand, elements like Fe, Cr and Mn, which form oxides of lower stability than SiO_2 , get transferred into the silicon melt.

In Fig. 4 a schematic drawing of the liquid-liquid extraction process is given. In a carbon ladle liquid-liquid contact between CaSiO_3 and MG-Si is established using the electroslag procedure as a more or less convenient heating technique. After realizing equilibrium extraction conditions by appropriate choice of extraction duration and temperature preredefined P1-Si quality is obtained. Insertations in Fig. 4 comparing the situation of impurities in MG-Si and P1-Si demonstrate the purification effect by slagging in the case of Al and the non-metal contaminants B and C.

The carbon level is lowered due to the reaction of dissolved carbon and SiC particles with the silicate slag forming volatile CO. Despite intensive contact of the molten silicon-slag system with the carbon ladle, carbon concentrations below detection limits of combustion analysis in the range of 50 ppm are attainable by appropriate control of the kinetics of opposing chemical and physical phenomena.

Following the above stated rule with regard to B no purification by liquid-liquid extraction is expected, as its free energy value of oxide formation is somewhat below that of silicon. To understand the opposite experimental finding a more careful analysis has to take into account second order thermodynamic effects. Accordingly, the observed transference of B into the slag phase becomes understandable by special bonding conditions of boronoxide in the silicate phase. The potentiality to remove B makes the liquid-liquid extraction process an important step of the metallurgical refining sequence.

In Fig. 5 B concentrations of pyrometallurgically refined MG-Si are plotted versus resistivity values of multicrystalline samples. The observed dependence fits well in the correlation of ASTM standard F 723-82. B concentrations reaching levels below 1 ppma correspond to resistivity values up to nearly $0,5 \Omega \cdot \text{cm}$, p-type. Doping levels in Si for solar application currently are settled in the $0,5 - 5 \Omega \cdot \text{cm}$ range. They may experience, for primary economic reasons, a slide towards even lower resistivity values, as soon as modified cell concepts will be optimized.

SOLID-LIQUID EXTRACTION

The formation of impurity precipitates in polycrystalline low-grade silicon is a precondition of solid-liquid extraction known as acid leaching. The formation of precipitates in form of silicides, oxides, silicates or metal eutectics is enhanced by both low segregation coefficient and low solid solubility. A striking correlation is very helpful in the field of hydrometallurgical meltstock processing: The lower the permissible level of the impurity element in question, the lower the segregation coefficient and, thus, the more effective the purification.

During solidification of low-grade Si such as the above mentioned Pl-Si, impurities with low segregation coefficients and concentrations exceeding solid solubility accumulate mainly along grain boundaries of the polycrystalline material. For effective refining, the silicon has to be milled in order to set second phase inclusions free for subsequent attack by acid mixtures. In Fig. 6 a flow-chart of the hydrometallurgical refining process is given. Lumps of Pl-Si are crushed by a sequence of jaw and roll crushers and finally pulverized in a vibration mill. Milling under wet conditions allows a hydrocyclone to be used to classify the milled product.

Extensive experimental work has been done in optimizing particle size of the pulverized Si, type, mixture and concentration of acids as well as temperature and duration of the leaching procedure (12). Fig. 7 demonstrates the effect of particle size on the purification of Pl-Si powder in the treatment with aqueous solutions of hydrochloric acid and hydrofluoric acid. The experimental data cover a range from 10 to 150 μm of average particle size. Fe, Ca and Ti stand for the leaching behavior of certain groups of metal impurities in Pl-Si. The effectiveness of hydrometallurgical refining is improved by grinding the silicon down to a particle size well below the average grain diameter of the polycrystalline material. In the case of extremely fine milling, the improvement in purification, however, has to be balanced against the increasing difficulty of handling and melting the powder in the subsequent pyrometallurgical process.

The leaching equipment in Fig. 6 consists mainly of a filter-extractor in which the pumpable silicon-acid slurry is leached by appropriate acid mixtures followed by rinsing and drying operations. Starting from P1-quality the main impurities Fe and Ca in the range of some 1000 ppma are eliminated down to low ppma levels, whereas in the case of nearly all other metal impurities even sub-ppma levels are attainable. Remaining impurities with unfavourable segregation coefficients such as the doping element P are distributed nearly homogeneously in solid silicon and cannot be selectively attacked by acid leaching.

LIQUID-GAS EXTRACTION

Liquid-gas extraction is another procedure in the field of metallurgical meltstock processing. Blowing reactive gases through molten silicon has been and is currently employed by MG-Si manufacturers for achieving higher material qualities. The conceptual approach is to form impurity compounds which can be slagged or removed by evaporation. The knowledge of both the chemistry of possible high temperature reactions and physical properties such as vapor pressure and solubility of the reaction products in molten Si is a prerequisite of selecting the proper experimental approach. The high reactivity of Si itself, however, limits the effective application of gaseous reactants much more than in the case of steel refinement.

Evaporation of elemental impurities from molten silicon represents a possibly more advantageous performance of liquid-gas extraction. Elements with higher vapor pressure than Si in principle are expected to evaporate from the silicon melt. In Fig. 8 the recovery of elemental impurities in the arc furnace process at temperatures around 1650°C is plotted versus vapor pressure. In fact the recovery has been found to be inversely related to the vapor pressure of the elements in question. This finding shows the possibility to further remove impurity elements such as Al, Ca and especially P.

In Fig. 9 a simplified drawing of the liquid-gas extraction process is given. To enhance the evaporation effect it is advantageous to treat the Si melt to be purified under vacuum conditions. Concentrations of impurities mostly affected by gaseous reactants and/or vacuum treatment are listed before and after liquid-gas extraction in Fig. 9. The obtained HP2-Si quality is characterized by metal concentrations each below 1 ppma, by oxygen below 10 ppma - starting from levels in surface oxide layers in the range of 5000 ppma - and by concentrations of phosphorus as a doping impurity reproducibly reduced to values below 0,5 ppma.

PROCESSING SEQUENCE

To define an optimum sequence of processing steps in the refinement of metallurgical-grade silicon is of central importance in terms of both systematic purification and economical conditions. The final combination of procedures may be different mainly due to special qualities of the starting material but also due to purity requirements of the subsequent crystallization technique. Differences in refining concepts, moreover, may be caused by the commercial availability of auxiliary materials of both adequate quality and dimension. Up to now all the efforts to find auxiliary materials suitable for use in the field of pyrometallurgical purification yielded refractory materials based exclusively on silicon compounds such as silicon oxide, silicon nitride and silicon carbide, respectively. This also applies in principle to carbon as this material in its Si-resistant quality protects itself by forming a dense layer of silicon carbide.

In Fig. 10 the flow-chart of an optimized refining cycle based on metallurgical refining steps is schematically drawn (14). Commercially available metallurgical-grade silicon - of selected quality with regard to certain impurities - in a first step is purified by liquid-liquid extraction. This slagging procedure yields preredefined silicon of the above discussed P1 quality typified by low B and C concentrations. Alternatively to liquid-liquid extraction solvent extraction by recrystallization from Al may be applied.

After grinding and acid leaching in the framework of an optimized hydrometallurgical technique high purity quality HP1-Si is reached. This advanced stage of refinement is characterized by drastically lowered levels of metal impurities. To accomplish Si meltstock of terrestrial solar-grade quality, a second pyrometallurgical step by liquid-gas extraction using reactive gas blowing and/or vacuum treatment is required. Directional solidification for instance carried out in form of multicrystalline ingot casting technique (15) can be considered as the final purification step due to nearly theoretical segregation phenomena. From a different point of view, however, it also represents the first step in crystallization technology.

CONCLUSION

To design a basic low-cost concept of large-scale material production, availability and costs of both starting and auxiliary materials as well as total amount of investment, energy consumption, throughput, and environmental compatibility have to be considered.

Solar-grade silicon at costs in the range of US \$ 5 - \$ 10 will only be realized by utilizing unconventional techniques. The metallurgical way of silicon meltstock processing can meet this target by bringing into action a minimum number of complementary hydro- and pyrometallurgical steps. To transfer the initial advantage of an impurity-optimized starting material to the final goal of large-scale terrestrial solar cell production, crystallization and cutting processes as well as cell technologies of adequate low-cost character are demanded. To reach industrial maturity, technical feasibility as well as economy of the different processes have to be finally investigated via pilot stages of adequate dimensions.

ACKNOWLEDGEMENT

The author would like to thank Prof. Sirtl for many valuable and stimulating discussions. He is also indebted to the Bundesministerium für Forschung und Technologie for supporting this work under Contract 03E-4506-B.

REFERENCES

- (1) L.P. Hunt, Proc. 11th IEEE Photovolt. Spec. Conf., Scottsdale, Az., 259 (1975)
- (2) E. Sirtl, Proc. 2nd E.C. Photovolt. Solar Energy Conf., Berlin, (Reidel Publ. Comp., Dordrecht) 84 (1979)
- (3) S. Pizzini, Solar Energy Mat., 6, 253 (1982)
- (4) J. Dietl, Proc. Symp. Mat. and New Proc. Techn. for Photovoltaics (ECS Inc., Pennington) 52 (1983)
- (5) E. Sirtl, Proc. 3rd E.C. Photovolt. Solar Energy Conf., Cannes (Reidel Publ. Comp., Dordrecht) 236 (1981)
- (6) J.R. Davis et al., Proc. Symp. Mat. and New Proc. Techn. for Photovoltaics (ECS Inc., Pennington) 14 (1982)
- (7) L.P. Hunt, V.D. Dosaj, Proc. 2nd E.C. Photovolt. Solar Energy Conf., Berlin (Reidel Publ. Comp., Dordrecht) 98 (1979)
- (8) J.A. Amick et al., Proc. Symp. Mat. and New Proc. Techn. for Photovoltaics (ECS Inc., Pennington) 67 (1983)
- (9) H.A. Aulich et al., 4th E.C. Photovolt. Solar Energy Conf., Stresa (Reidel Publ. Comp., Dordrecht) 868 (1982)
- (10) J. Dietl et al., US Pat. 4,312,850 (Jan. 26, 1982) assigned to Heliotronic

- (11) H.-P. Jasper, Intern. Ferro Alloy Conf. INFACON, Techn. Session II, Tokyo (1983)
- (12) J. Dietl, Solar Cells, 10, 145 (1983)
- (13) L.P. Hunt et al., Proc. 13th IEEE Photovolt. Spec. Conf., Washington, 333 (1978)
- (14) J. Dietl and M. Wohlschläger, US Pat. 4,304,763 (Dec. 8, 1981) assigned to Wacker
- (15) D. Helmreich, J. Phys. (Paris), Collog. C1, 43, 289 (1982)

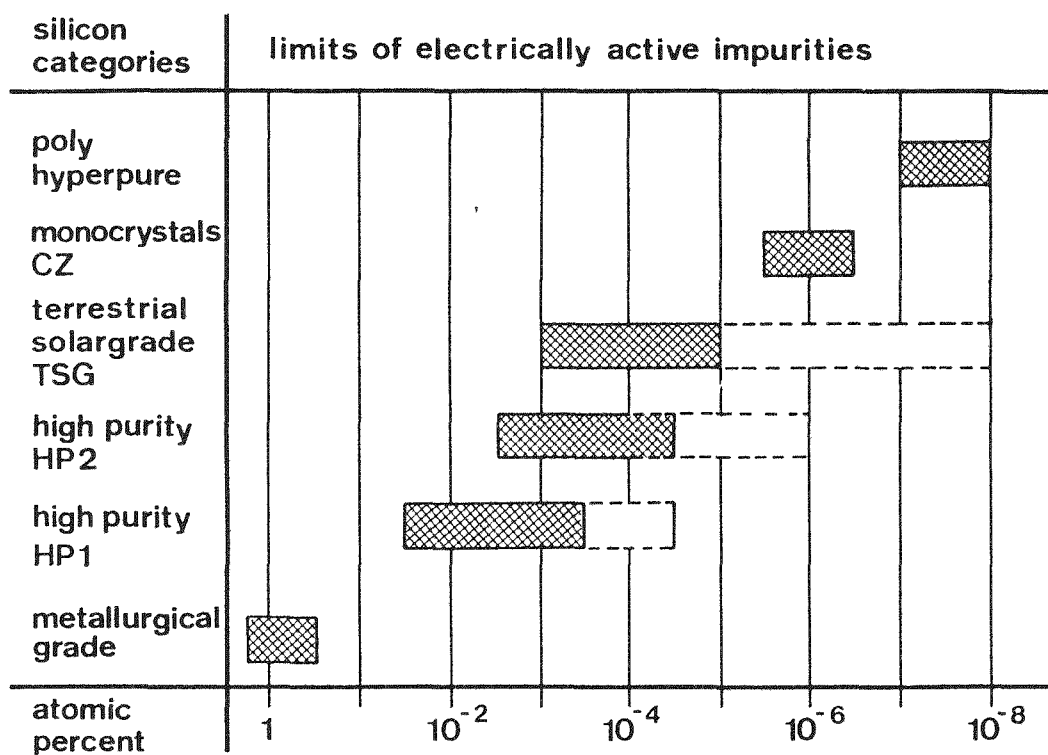


Fig.1. Impurity ranges of different silicon qualities

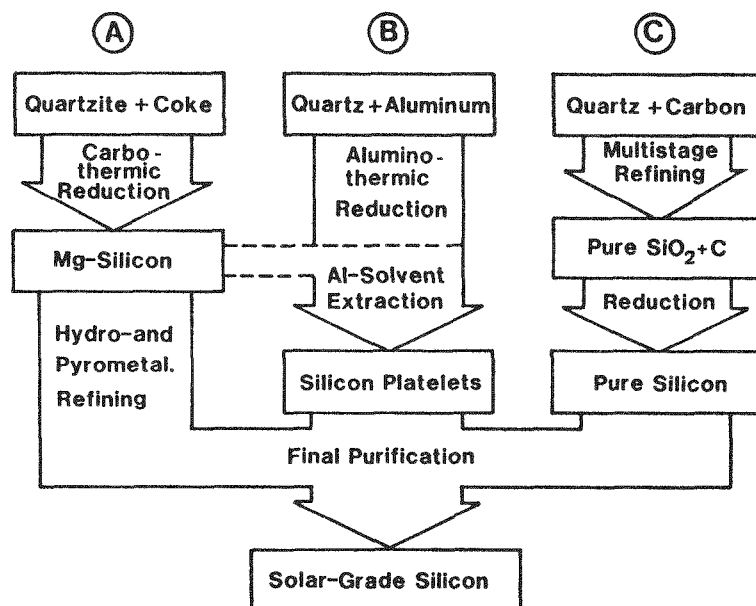


Fig.2. Different approaches to large-scale production of solar-grade silicon

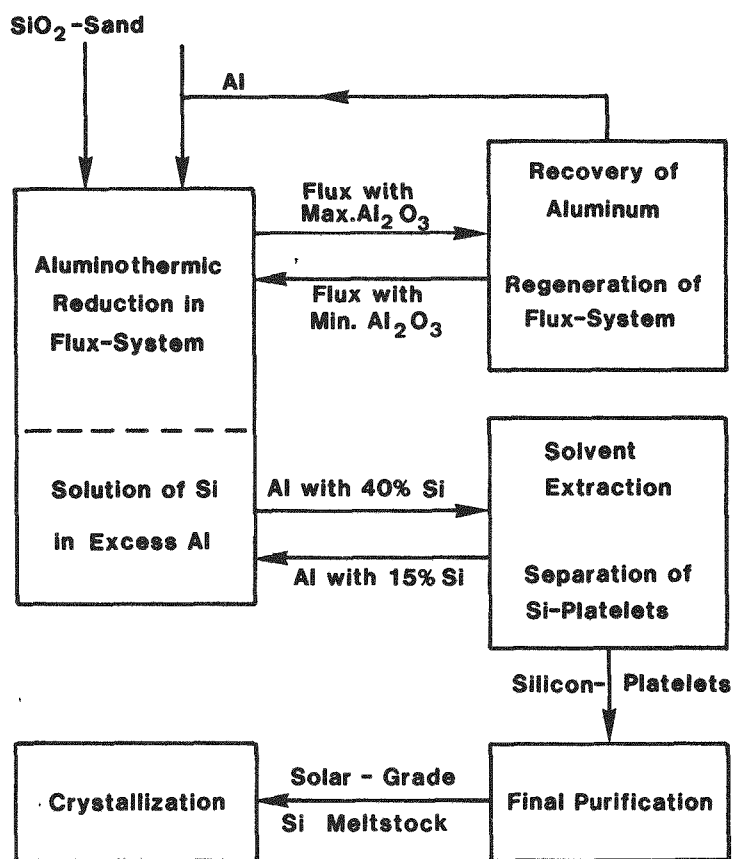


Fig.3. Schematic flow-diagram of aluminothermic production of solar-grade silicon

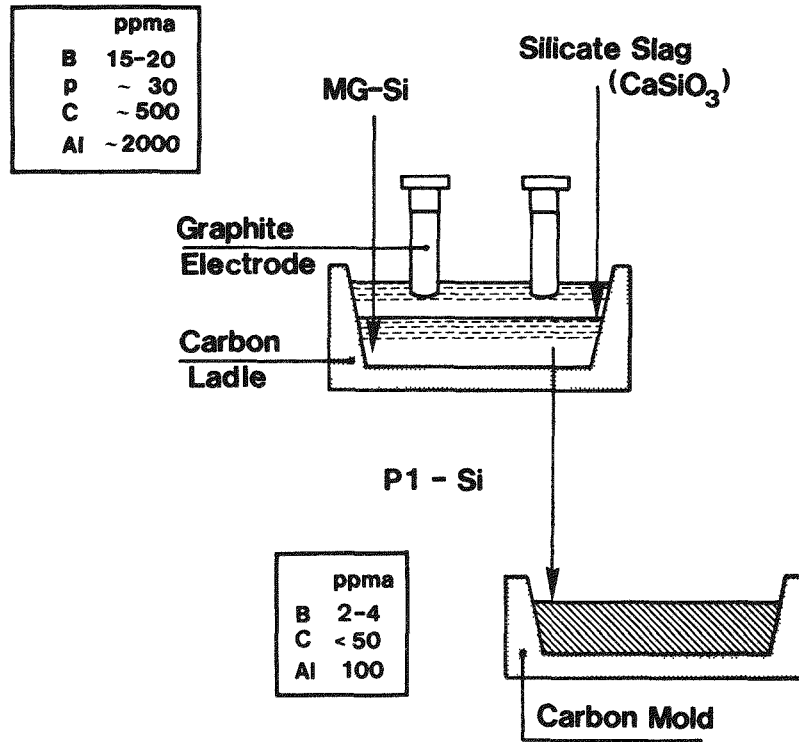


Fig.4. Schematic of the liquid-liquid extraction process yielding preredefined P1-Si

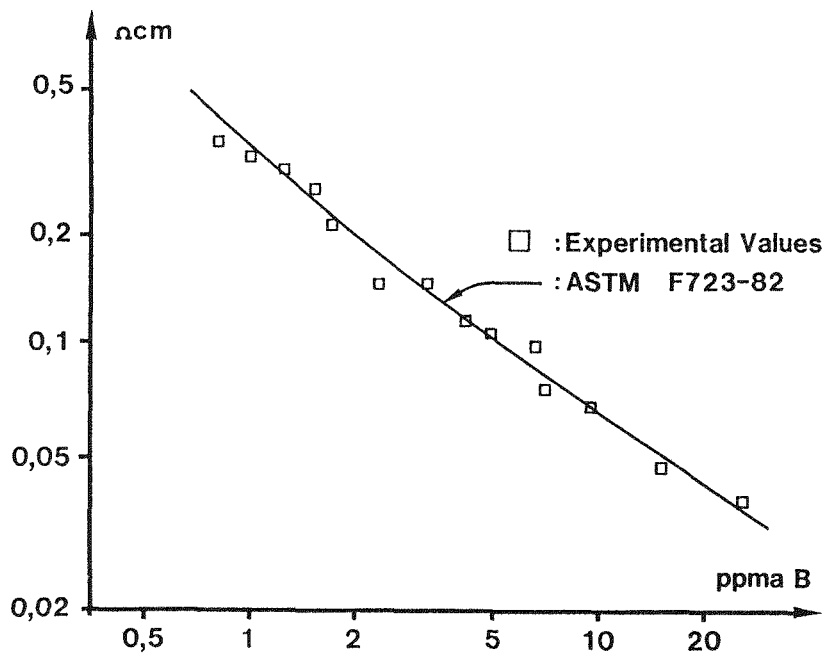


Fig.5. Correlation of boron concentrations with resistivity values in pyrometallurgically refined silicon

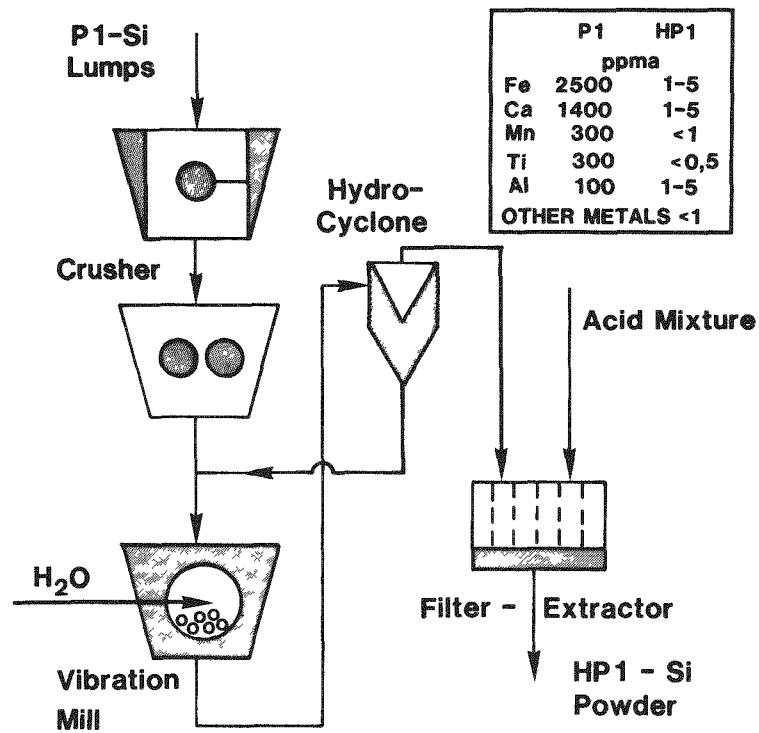


Fig.6. Flow-chart of the hydrometallurgical refining process yielding HP1-Si (high purity 1)

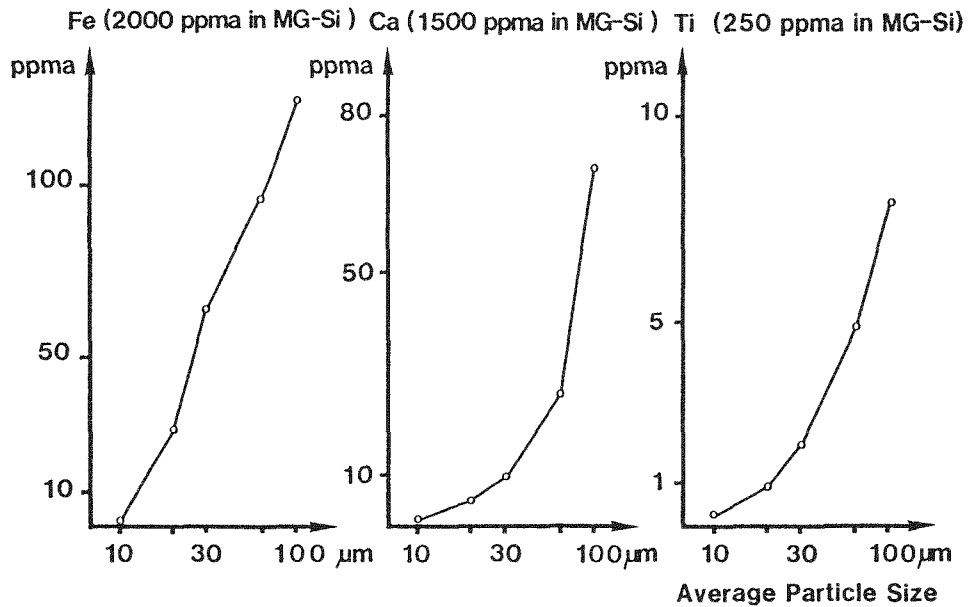


Fig.7. Effect of particle size on the purification of P1-Si powder by leaching with aqueous HCl/HF mixtures

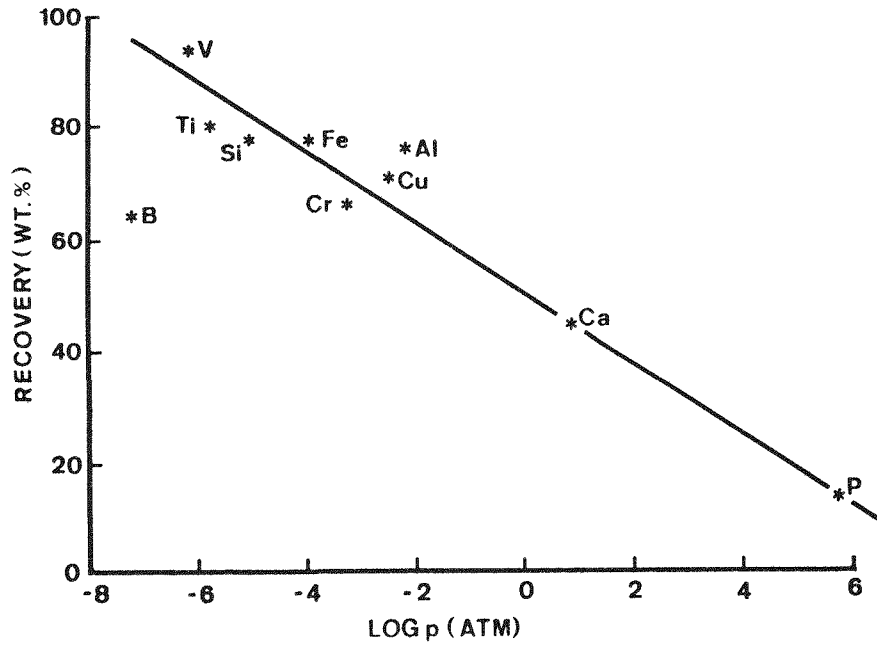


Fig.8. Recovery of impurities in the arc furnace plotted versus elemental vapor pressure (13)

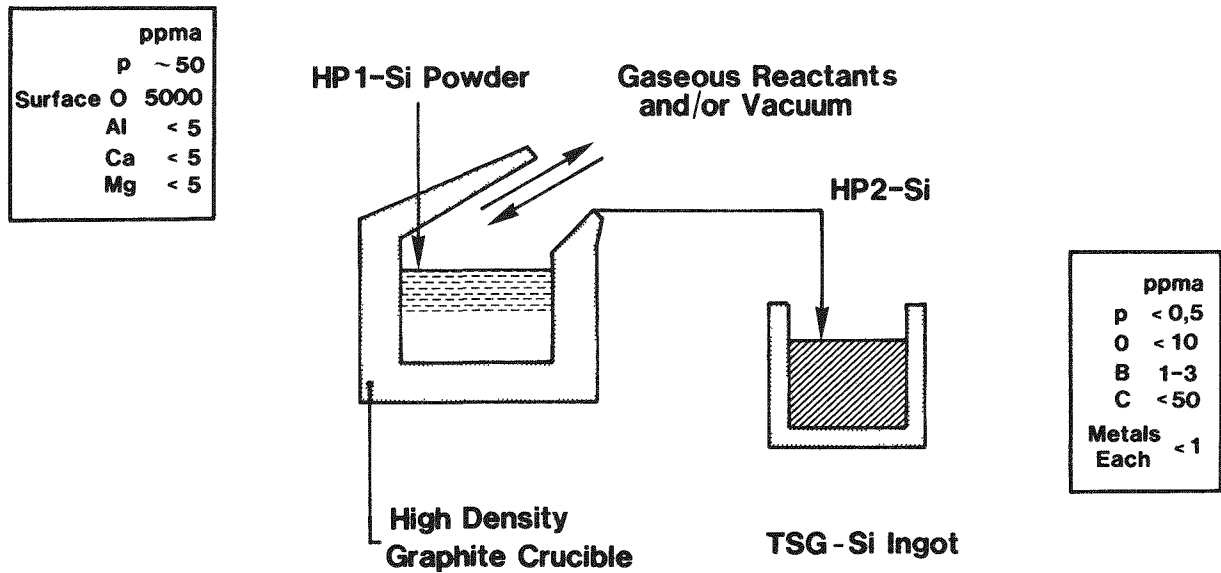


Fig.9. Schematic of the liquid-gas extraction process yielding HP2 (high purity 2) quality

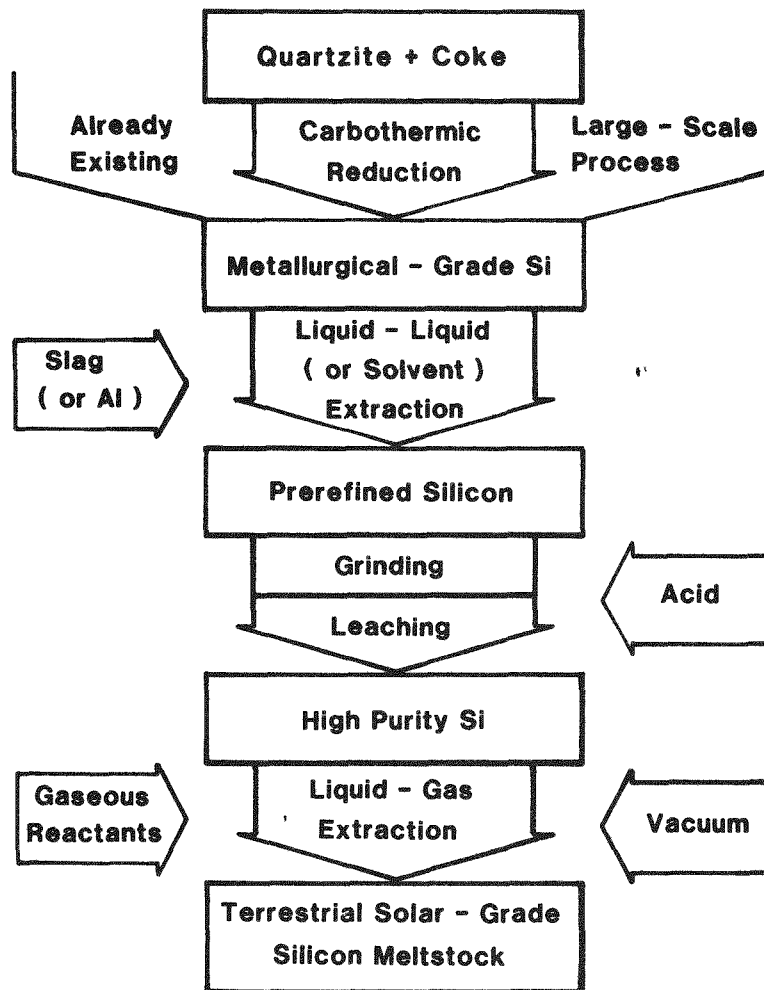


Fig.10. Schematic flow-diagram of the processing sequence for metallurgical refining of MG-Si

DISCUSSION

MAYCOCK: Could you estimate when Wacker could offer a commercial product based on this general research area?

DIETL: More years of basic development remain to be done. In perhaps 3 or 4 years we hope to achieve the state of development that will allow us to make decisions regarding production. The first production of this conventional silicon material will probably be the early 1990s.

RUSTIONI: We worked several years ago in this field. I remember that we had a problem of the formation of foam during the leaching treatment, especially with fine powder present. This was a very difficult problem to solve. We tried to use some surfactant substances in order to decrease this phenomenon. Have you noticed this formation also?

DIETL: In the beginning, we had the same problem. We tried to overcome this problem first by using a very effective classification to remove all of the very fine particles and, secondly, to use a filter extractor in which the worst effects of the foam are decreased.

WRIGHT: We were working on a very similar metallurgical approach in the early days at Solarex. Would you comment on the drop in yield for each step of the process?

DIETL: We have used a pilot two-stage process up to this time. This means batch quantities of about 100 kg in the pyrometallurgical step. We obtain yields ranging from 95 to 98% for those batches, depending on the process being examined.

SOLAR-GRADE SILICON PREPARED BY CARBOTHERMIC REDUCTION OF SILICA

H.A. Aulich, F.-W. Schulze, H.-P. Urbach, A. Lerchenberger
Siemens Research Laboratories, Otto-Hahn-Ring 6, 8000 München 83, W-Germany

Abstract

An advanced carbothermic reduction (ACR) process was developed to produce solar-grade (SG) silicon from high-purity silica and carbon. Preparation of starting materials and operation of the arc-furnace to produce high-purity silicon is described. Solar cells prepared from single crystal SG-Si had efficiencies of up to 12.3%, practically identical to cells made from electronic-grade (EG) silicon. The ACR process is now in the pilot stage for further evaluation.

1. Introduction

Commercial solar cells presently available are manufactured exclusively from high-purity EG-silicon. For large scale application of photovoltaic devices this expensive material must be replaced by inexpensive SG-silicon. Numerous processes are presently under investigation and some have already reached the pilot-stage /1/.

Metallurgical-grade (MG)-silicon is commercially available for ~1\$/kg but its impurity level is much too high to render it suitable for solar cell applications. MG-Si is produced by carbothermic reduction (CR) of quartzite in large arc-furnaces, a process extensively employed world-wide.

The reasons for the CR to succeed as the most economical Si-process are as follows:

- Abundance of inexpensive starting materials (quartzite, coke, charcoal)
- Low energy consumption (~11 KWh/kg Si) and high Si-yield (~85%)
- High throughput (~1000 kg/h)
- Inexpensive process technology
- No toxic by-products are produced

These favourable attributes of the CR-process were the basis of our decision to embark on this method for the production of SG-silicon.

However, to obtain high-purity silicon suitable for solar cell production the commonly employed CR-process must be modified considerably. Fig.1 shows that the high impurity concentration in MG-Si is the result of impure starting materials (mainly carbon) and process technology such as furnace lining, electrodes, poking and tapping equipment.

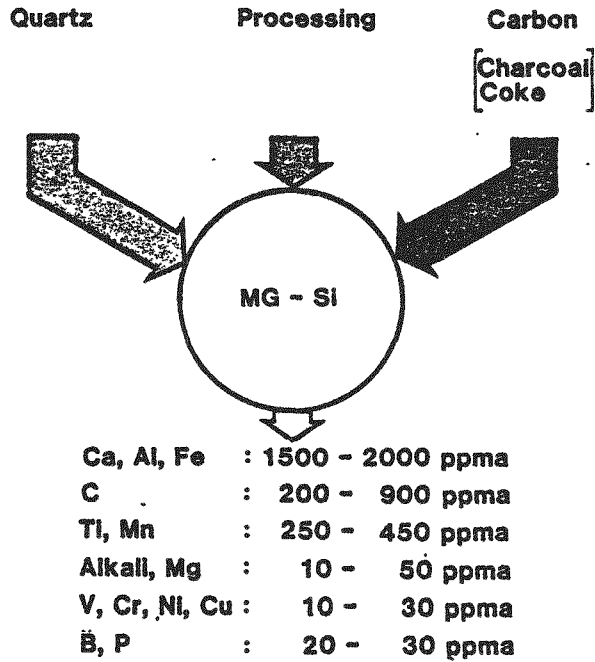


Fig.1 **Origin of impurities in metallurgical(MG)-silicon**

To eliminate these impurities we developed an advanced carbothermic reduction (ACR) process, using high-purity starting materials that are reacted under high-purity conditions in an arc-furnace /2/. A similar approach was first adopted by L.P.Hunt at Dow Corning /3/ and later in a joint Exxon/Elkem research project /4/. In the latter process silicon produced has to be further purified by acid-leaching, a method not employed in our ACR.

By combining economy of production with high-purity conditions the ACR-process has a large potential for meeting cost and purity requirements for SG-silicon production.

2. Preparation of high-purity starting materials

For the ACR high-purity silicondioxide and high-purity carbon are employed. To meet the cost goal these materials should be inexpensive and abundently available. In addition, since impurities present in the starting materials will be incorporated into the silicon produced, it is extremely important to avoid those impurities difficult to remove from silicon by the subsequent crystallization process for sheet production /1/. In particular, the concentration of impurities such as boron and phosphorous with a large distribution coefficient of 0.8 and 0.2 resp. should be below 0.2 ppmw.

a) High-purity silica

The requirements mentioned above leave only a small number of silica sources to be considered for the ACR.

High-purity quartz mined from various deposits located in Brazil, the USA or Canada is too expensive and because it is a natural product, it is likely to vary in purity.

Synthetic silica produced in large quantities by flame hydrolysis from silicon tetrachloride contains several ppm of B and P and is too expensive as well. An inexpensive material is the silica produced from waterglass. However, because of its high impurity content it can not be employed for the ACR.

Since neither natural quartz nor synthetic silica meet our specifications we developed a process in which inexpensive quartz sand is purified using a combined glass melting/fiber leaching (FL)-process /5/.

The quartz sand we use is mined from deposits in Germany and contains a high concentration of impurities such as Al, Fe, Ti etc. To remove these impurities incorporated in the bulk material, the sand is fused with glass forming oxides such as sodium oxide and calcium oxide to form a multicomponent glass. The glass melt is converted into fibers or granules to obtain a product with a large surface area. Treatment with hot HCL leaches out all metal oxides and impurities and high-purity silica is obtained as a result (Tab.1). Basically, the glass forming oxides merely serve as an acid-soluble solvent for the impurities present in the quartz sand.

Impurities	SiO ₂ FL-Process (ppmw)
B	< 0,2 Δ NW
P	< 2 Δ NW
Na	< 0,1
Mg	< 0,1
Ca	< 0,1
Al	< 6
Fe	< 0,1
Ti	< 0,1
Zr	< 1
V,Cr,Mn,Co, Ni,Cu	< 0,1
Nb,Mo,Ta,W	< 0,1

Tab. 1 Impurity content of FL-SiO₂

b) High-purity carbon

The carbon materials commonly used for producing MG-Si such as coal, coke and charcoal, have a very high impurity content and can not be employed in the ACR. High-purity materials such as graphite can not be used either since their reactivity is too low to obtain silicon with high yield.

Carbon of sufficient reactivity is commercially available in the form of various carbon blacks. These materials are produced on an industrial scale by thermal decomposition of C-H-compounds. A commonly applied method uses crude

oil as a starting material which is burned in an oxygen lean flame; the hot gas mixture containing the carbon black particles is subsequently quenched by water spraying.

The material produced usually has an impurity content of several hundred ppm, too high to be used directly for the ACR.

Carbon blacks much higher in purity can be obtained by decomposing acetylene or natural gas, but the high price renders this product unsuitable for our process.

To obtain high-purity carbon from inexpensive carbon black we treat commercially available products with hot HCl-solution to leach out harmful impurities. The purity of the material produced is comparable to the high-purity silica.

3. Granulation of silica and carbon

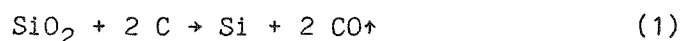
In an MG-Si producing furnace starting materials are commonly employed as chunks up to 10 cm in size. In our process, the silica and carbon prepared are finely powdered materials and must therefore be granulated before being used in the arc-furnace. This may be achieved by briquetting or by pelletizing with the aid of special binders. Regardless of the method employed, no impurities should be introduced by this process and granules produced must exhibit the following properties:

- High mechanical integrity up to temperatures of $\sim 700^{\circ}\text{C}$ to prevent premature disintegration and loss of material
- High reactivity to insure high silicon yield
- Optimal grain size for smooth furnace operation
- Sufficient electrical conductivity to obtain proper temperature distribution in the region of the electrodes.

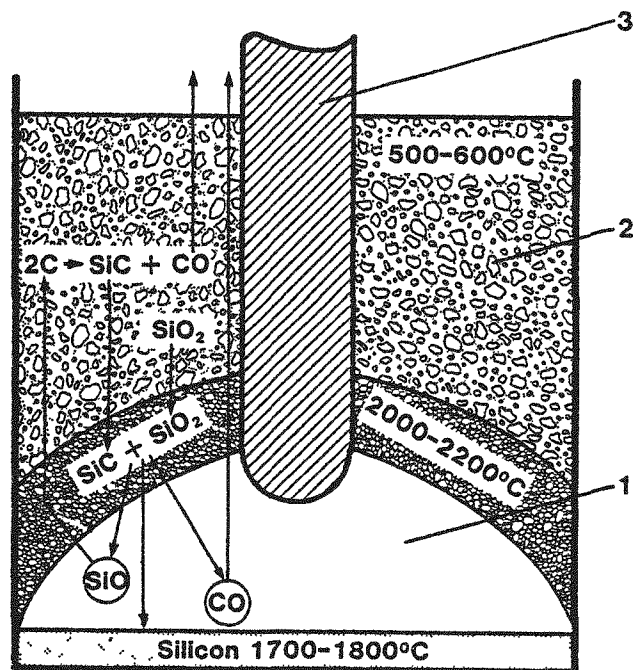
The granules may either contain only one component or may be composed of a SiO_2/C -mixture. Recently SiO_2/C -briquetts were successfully employed in large industrial furnaces resulting in lower energy consumption and higher Si-yield when compared to the conventional charge. In our experiments both pellets and briquetts were successfully tested; as a binder a phenol resin was used.

4. Carbothermic reduction of silica

The production of silicon in an arc-furnace may be described by the overall reaction



The simplicity of this reaction is deceptive, however, for the various reactions actually taking place in an arc-furnace are much more complex. In the high temperature zone in the region of the arc a large number of reactions are thermodynamically feasible between the principle species SiO_2 , SiO , Si , SiC , C and CO /6/. Although a quantitative description of these reactions is not possible at present, a comparatively simple model can be used to describe the processes occurring in the furnace (Fig.2).



Temperatur distribution in an arc furnace and simplified reaction model.

Fig. 2
1 Cavity (filled with SiO and CO),
2 Charge (SiO₂ and C),
3 Electrode

In the region of the arc at a temperature of more than 2000°C SiO₂ and SiC react to form volatile products (SiO, CO) and liquid silicon. This reaction leads to the formation of a cavity (1) filled with SiO- and CO-gas. Rising SiO-gas reacts with carbon to form SiC which, together with the SiO₂ travels into the hot zone, replacing the material that has already been reacted to liquid silicon. Fig. 2 shows that this reaction occurs primarily at the cavity wall, with liquid silicon accumulating at the bottom of the furnace. The CO-gas formed as a by-product rises through the reaction mixture and reacts with atmospheric oxygen to CO₂ at the surface.

To test our high-purity starting materials and to determine conditions necessary for SG-Si production a 70 kW single-electrode reduction furnace was set up (Fig.3).

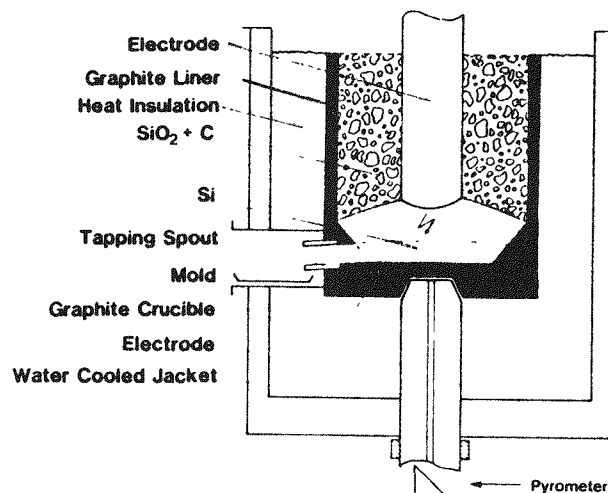


Fig. 3 Schematic of the 70 KW-Reduction furnace

All parts that come into contact with the starting materials and the silicon produced are made of high-purity graphite, including the electrode which supplies about 10% of the carbon necessary for the reduction. To monitor the temperature near the reaction zone, a hole was drilled through the lower electrode and the temperature measured at the bottom of the graphite crucible using a pyrometer.

Carrying out reduction experiments with various SiO_2 -sources and acid-leached carbon black pellets, silicon of p-type was obtained in every case (Tab.2). The production rate was $\sim 2\text{kg/h}$, and the silicon was tapped continuously or every 1 to 2 hours.

Impurity	Quartz (1)	Selected Silica (2)	Synthetic Silica (3)	FL- SiO_2 (4)	Purified Carbon (5)
B	≈ 1	< 1	$< 0,01$	$< 0,5$	$< 0,1$
P	$< 0,5$	$< 0,5$	$< 0,1$	$< 0,5$	$< 0,5$
Al	30	15-20	$< 0,5$	< 10	< 1
Transition Elements	≈ 20	< 20	< 1	< 5	< 5

Tab. 2 Impurity content of SiO_2 -sources and acid-leached carbon

To determine the limit of the carbothermic reduction process with respect to the purity of the silicon produced an experiment was carried out using synthetic SiO_2 of the highest purity commercially available (Tab.2 Nr.3) and leached carbon pellets. High-purity silicon with a B-concentration below 10^{16}a/cm^3 (SIMS-measurement) was produced, the highest purity ever obtained in this process [7]. This shows that under suitable conditions the ACR process can be carried out under high-purity conditions so that purity of starting materials can be maintained.

On account of the promising results obtained in the preparation of starting materials and small scale reduction, a 550 kVA furnace was built for pilot production of SG-Si. This 3-electrode furnace has an inside diameter of 1.2m and a capacity for filling it with 1.2t of silica and carbon /2/. The electrode arrangement and the electronics for furnace operation are similar to those commonly used in large industrial furnaces. All parts of the furnace that come into contact with raw materials or liquid silicon are made from high-purity graphite to prevent contamination of the silicon produced. Using specially selected silica and carbon black briquettes silicon was produced at a rate of ~15kg/h. This furnace will be used to estimate the overall cost of our SG-Si process.

5. Processing of silicon

At 1750°C, the temperature liquid silicon leaves the furnace, about 500ppmw of carbon may be dissolved in the silicon melt /8/. In addition solid SiC-particles may also be present. Upon solidification carbon will precipitate and numerous SiC-particles may be detected. When using this material as feedstock for Czochralski-growth, at temperatures of 1420°C only 25-30ppmw carbon will dissolve the remainder being solid SiC-particles floating in the melt preventing single crystal growth. Consequently, to obtain first generation single crystal rods the carbon content of the silicon produced has to be reduced down to values below 25-30ppmw.

In principle, this can be achieved by physical or chemical methods:

- Physical methods

Si-samples obtained from the furnace usually contain SiC-particles 10-20µm in size. Remelting this material in a crucible and holding the temperature close to the melting point SiC-particles will grow and, due to its larger density compared to the melt, sink to the bottom of the crucible. The supernatant melt may be removed and used for crystal growth. SiC-particles may also be removed by passing the melt through a suitable filter made from an inert material such as SiO₂ or SiC. Finally, by collecting the liquid silicon from the furnace in suitable moulds and carrying out a simple directional solidification carbon and SiC-particles can also be segregated effectively.

- Chemical methods

These techniques rely on the reaction of carbon and SiC with oxidizing agents, i.e. $\text{SiC} + 2 \text{SiO}_2 \rightarrow 3 \text{SiO} + \text{CO}$ (2). Whether this reaction is feasible is determined by thermodynamics. Neglecting the influence of the silicon melt, the vapor pressure of CO at a temperature of 1500°C is ≈0,15 Torr and ≈1 Torr at 1600°C ($P_{\text{SiO}} = 3 P_{\text{CO}}$). Removing CO continuously by pumping or by working under flowing inert gas, reaction (2) is shifted to the right resulting in a reduced carbon content.

Using metallurgical silicon with a high carbon content as well as our own SG-Si and employing methods discussed above silicon was produced that could be converted into single crystal rods using one Cz-pull only. More work is necessary to determine the most economical technique to remove carbon.

6. Solar cell preparation

Silicon obtained by our ACR-process was converted into single crystal material using Cz-technique. Second generation ingots having a diameter of 100mm and 125mm and free of dislocations were sliced using ID-saw. Wafers obtained having a resistivity of 0,5 - 0,4 Ωcm and diffusion length of $\sim 50\mu\text{m}$ (SPV-method) were converted into solar cells using conventional technique /7,9/. Best values obtained (AM1) were 11.1% for 100mm \emptyset cells.

Similar results were obtained when comparing cells made from EG-Si (0.5 Ωcm).

The cells (5cm x 5cm) made from SG-Si and EG-Si (1.9 Ωcm) having an improved grid structure had the following cell parameter: $\eta = 12.2\%$ (EG-Si = 13.0); $I_{\text{SC}} = 690\text{mA}$ (720mA); $V_{\text{OC}} = 596\text{ mV}$ (593mV); $\text{FF} = 74.3$ (76.0). In our opinion, the lower values for SG-Si cells are mainly due to the higher B-concentration of SG-Si ($5 \times 10^{16}\text{cm}^{-3}$) as compared to EG-Si ($7 \times 10^{15}\text{cm}^{-3}$).

In general, for Cz-material solar cell efficiency and diffusion length decrease for B-concentration $> 5 \times 10^{16}\text{cm}^{-3}$ and little difference is observed between SG-Si and EG-Si of the same resistivity /10/. Similar findings were reported by Amick et al. /4/.

To produce solar cells of higher efficiency the B-concentration of our SG-Si should be lowered to $\sim 2-3 \times 10^{16}\text{cm}^{-3}$.

This was demonstrated by using high-purity silica (Nr.3 in Tab.2) and leached carbon pellets in our ACR process. Silicon obtained was converted into a 3" single crystal by Cz-technique rod.

Solar cells with conventional grid structure obtained from wafers (p-type 1 $\Omega\cdot\text{cm}$) had an efficiency of 12.3%, $I_{\text{SC}} = 283\text{mAcm}^{-2}$, $V_{\text{OC}} = 593\text{mV}$ and $\text{FF} = 74\%$, identical to the reference cell made from EG-Si (1 Ωcm).

7. Conclusions

Using our ACR-process silicon was obtained that could be converted into solar cells having an efficiency of up to 12.2%. Carbon and SiC-particles were successfully removed from the tapped silicon using simple separation methods to obtain a feedstock suitable for single crystals growth.

The process is now in the pilot stage to estimate cost of SG-Si production.

Acknowledgements

The authors are indebted to Dr. H. Pink for carrying out chemical analysis of starting materials and silicon, and to Mr. Münzer for cell preparation. This work was supported by the Bundesministerium für Forschung und Technologie.

References

- /1/ Aulich, H.A.:
Proc. 17th IEEE Photovoltaic Spec. Conf., May 1984, Kissimee, USA, p. 390
- /2/ Aulich, H.A.; Dietze, W.; Eisenrith, K.-H.; Schäfer, J.; Schulze, F.-W.;
Urbach, H.-P.:
4th E.C. Photovoltaic Solar Energy Conf., May 10-14, 1982, Stresa, Italy,
p. 868
- /3/ Hunt, L.P.; Dosaj, V.D.:
Proc. 2nd Photovoltaic Solar Energy Conf., April 23-26, 1979, p. 98
- /4/ Amick, J.A.; Dismukes, J.P.; Francis, R.W.; Hunt, L.P.; Ravishankar, P.S.;
Schneider, M.; Matthei, K.; Sylvain, R.; Larsen, K.; Schei, A.:
Electrochem. Soc. 132 (1985), p. 339
- /5/ Aulich, H.A.; Eisenrith, K.-H.; Urbach, H.-P.:
J. Mater Sci. 19 (1984), p. 1710
- /6/ Aulich, H.A.; Eisenrith, K.-H.; Schulze, F.-W.; Urbach, H.-P.:
6th E.C. Photovoltaic Solar Energy Conf., April 15-19, London, U.K., p.951
- /7/ Schulze, F.-W.; Fenzl, H.J.; Geim, K.; Hecht, H.-D.; Aulich, H.A.:
17th IEEE Photovoltaic Spec. Conf., May 1984, Kissimee, USA, p. 584
- /8/ Scace, R.J.; Slack, G.A.:
J. Chem. Phys. 30 (1959), p. 1551
- /9/ Claeys, D.E.; Hecht, H.D.; Münzer, K.A.:
6th E.C. Photovoltaic Solar Energy Conf., April 15-19, 1985, London, U.K.,
p. 1021
- /10/ Aulich, H.A.; Cammerer, F.; Fenzl, F.J.; Schulze, F.-W.:
1st Int. Photovoltaic Science and Engineering Conf., Kobe, Japan, 1984, p.777

DISCUSSION

MAYCOCK: Is the pre-chemical purification step also scaled up to the pilot plant level?

AULICH: We are in the process of doing that. In other words, we are setting up pilot plant level production for high-purity silica.

SCHMID: It seems that you have achieved some very impressive results with respect to getting the impurities like boron, phosphorus, and others down to low levels. The one situation that you did mention was the presence of silicon carbide, which is involved in the reaction. You mentioned a number of ways of reducing the silicon-carbide concentration. What do you believe is the most feasible way of doing this on a production scale?

AULICH: I believe a good way would be to use an inexpensive directional solidification process in which the ingot quality with respect to mechanical properties and its use for slicing, and so on, are not the primary objectives. That is, the procedure is used simply as a separation method. We know that this procedure works, but it must also be low cost because if this process is expensive, it is prohibitive. We have two possibilities now, and we are evaluating the economics of these processes.

CALLAGHAN: What are the schedules for the completion of the economic analysis of the pilot plant scale operation and for the installation of large-scale production that would provide \$10/kg silicon?

AULICH: We intend to evaluate the pilot plant operation in the next few years and, within this time frame, we will produce silicon, solar cells, and modules. Thus, we will evaluate the whole process from the starting material to the finished module. This decision for building a larger furnace should be reached in the next 3 years or so.

KOINUMA: I fear that the fiber purification of silica is poor in productivity, and I wonder if your process is really practical.

AULICH: Why do you think the productivity is poor?

KOINUMA: Because the amount of fiber is small.

AULICH: Oh, no. There is no problem in producing hundreds of thousands of tons of glass fiber. This is an established technology which is used in the building industry and, as I showed, leaching is done within a few minutes. Therefore, enormous amounts of high-purity silica can be produced with the correct technology. It is no problem.

SCHWUTTKE: I find it very surprising and rewarding that your baseline process gives you the same solar-cell efficiency as the use of boron-doped semiconductor-grade silicon of the same resistivity. This is very encouraging. I would like to propose that it would be worthwhile to use this type of material as a substrate for epitaxial deposition for integrated circuits.

AULICH: Yes, we have done this. The results are quite good.

SCHWUTTKE: I would assume so.

WRIGHT: What was the base resistivity of the material used for the high efficiency cells?

AULICH: The cells prepared by our process had a resistivity of about 0.5 to 0.6 ohm-cm, and this was compared with 0.5 to 0.6 ohm-cm Czochralski material.

WRIGHT: I assume you use a carbon plug in the furnace tapping operation. How did you remove the carbon plug without introducing metal contaminants?

AULICH: We used the conventional technique. In the industrial process, an arc is produced between a graphite rod and the closure point. The temperature becomes high enough to melt the solidified silicon and molten silicon runs out. To produce high-purity silicon, the graphite rod must be of high purity. Of course, this can be done and it is our procedure.

RUSTIONI: We also have used similar electrode techniques for tapping the furnace. You mentioned a system for obtaining amorphous silica from fluosilicic acid, but this process is not expensive because a byproduct of the industrial production of phosphoric acid can be used. The process involves the precipitation of the sodium salt of fluosilicic acid. Can you comment on this?

AULICH: We looked at this process very carefully because fluosilicic acid is relatively inexpensive. The sodium salt can be produced without any problem, but there are a large number of problems involved in the decomposition step to produce silicon tetrafluoride. If this reaction is not carried out correctly, some compounds of boron and other elements remain in the silicon tetrafluoride, and other separation methods must be used. We looked at the large-scale production of silicon dioxide using this process, and we concluded that the environmental hazards using the fluorine compounds are very severe, at least in Germany. That makes the processing cost very high. On the other hand, there are no such problems melting glass and leaching with hydrogen chloride. Almost all the technology for leaching is available from the chemical industry. We concluded that it was much better to use our approach than to use silicon tetrafluoride.

RUSTIONI: What is the temperature used for the production of the glass fibers?

AULICH: It is the conventional glass-melting process. The temperature used is about 1300 to 1400°C. Window glass is produced in the same way. We don't spin the fibers. We melt and let the melt run into water producing the glass fibers.

RUSTIONI: During the purification of carbon black, you first prepared the pellets or briquettes and then the leaching was done. Do the pellets or the briquettes remain intact during the process?

AULICH: It is important that they remain intact because if it is not done correctly, the product is a high-surface area carbon black which has to be filtered and this is a cumbersome procedure. We make pellets that remain intact during the leaching process and after leaching they are, of course, much purer.

RUSTIONI: After leaching, are you obliged to dry the pellets before feeding the arc furnace?

AULICH: Some drying must be done, but it doesn't have to be super dry.

RUSTIONI: Do you use three-electrode, three-phase in the pilot plant?

AULICH: It's a three-electrode, three-phase furnace.

MAYCOCK: When do you think this process will be commercial?

AULICH: As in my answer to Dr. Callaghan, we will develop this process in the next few years and also evaluate the economics. During this time, we will use the product silicon for our own purposes. In a few years, based on the evaluation as a technically sound, economic process, the decision will be made concerning large-scale production by us or licensing the process. I can't tell you exactly when this will occur, but it will take a few years.

A METALLURGICAL ROUTE TO SOLAR-GRADE SILICON

Anders Schei
Elkem a/s, R&D Center
Kristiansand S , Norway

ABSTRACT

The aim of the process is to produce a silicon for crystallization into ingots that can be sliced to wafers for processing into photovoltaic cells. The specifications of the product are:

		Present	Potential
B	ppmw	< 1	< 1
P	"	< 1	< 1
C	"	< 50(?)	< 1
Ca	"	< 10	< 10
Al	"	< 10	< 0.1
Other metals	"	< 10	< 0.001

If the potential purity can be realized, the silicon will also be applicable for ribbon pulling techniques where the purification during crystallization is negligible.

The process consists of several steps: Selection and purification of raw materials, carbothermic reduction of silica, ladle treatment, casting, crushing, leaching and remelting. The leaching step is crucial for high purity, and the obtainable purity is determined by the solidification before leaching. The most difficult specifications to fulfil are the low contents of boron, phosphorus and carbon. Boron and phosphorus can be excluded from the raw materials, but the carbothermic reduction will unavoidably saturate the silicon with carbon at high temperature. During cooling carbon will precipitate as silicon carbide crystals, which will be very harmful in solar cells.

The cost of this solar silicon will depend strongly on the scale of production. It is as yet premature to give exact figures, but with a scale of some thousand tons per year, the cost will be only a few times the cost of ordinary metallurgical silicon.

INTRODUCTION

The carbothermic process is potentially the cheapest process for silicon production, but the purity of the typical metallurgical silicon is far below the specifications of a solar silicon for use in a Bridgman or similar crystallization.

	Metallurgical grade Typical content	Solar grade Tentative specifications
B	30 ppmw	1 ppmw
P	50 "	0.3 "
C	250 "	No SiC precipitate
Metals	6000 "	10 ppmw

The problem is then to improve the metallurgical process to give the solar grade silicon. This paper describes one solution to this problem. A more detailed description, including references to several other approaches, is given elsewhere [1]. The work was done by Exxon Research and Engineering Company and Elkem a/s in a joint project on low cost silicon for solar cells. The project was partly based on a research programme run at Dow Corning by Hunt and Dosaj [2].

SURVEY OF THE CARBOTHERMIC PROCESS

A complete carbothermic route to solar silicon is sketched in Figure 1. The smelting step has an overall reaction



The detailed reaction mechanism is, however, more complex. The recovery of the impurities is high, and one can as a first approximation assume that all the impurities in the raw materials will be recovered in the silicon.

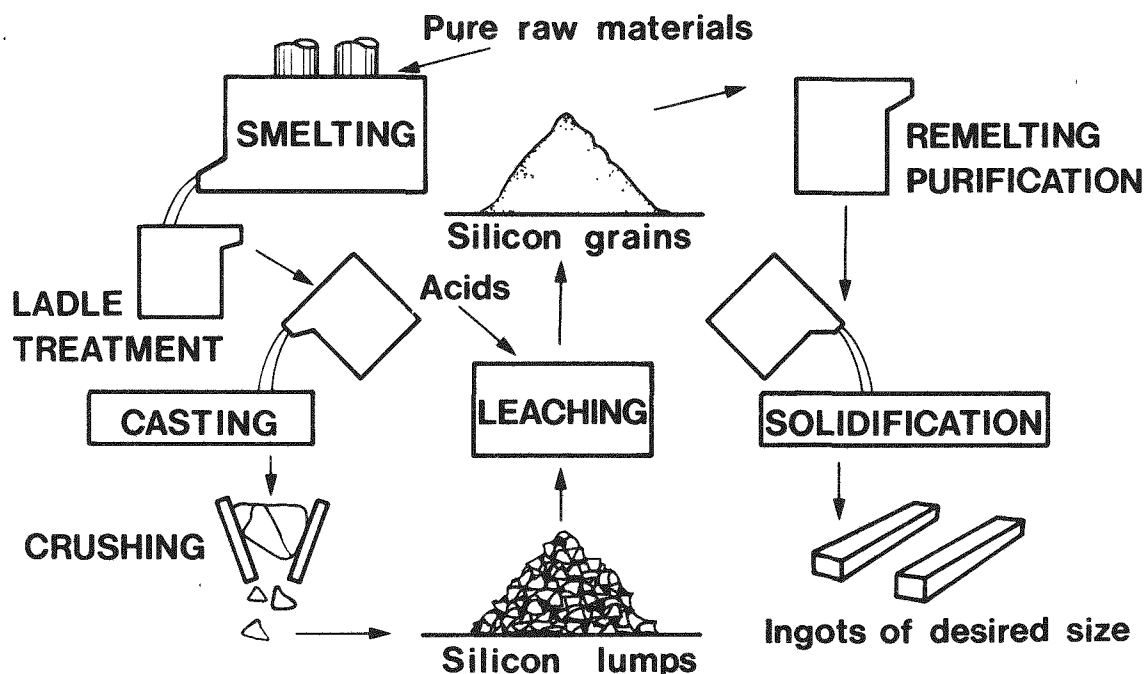
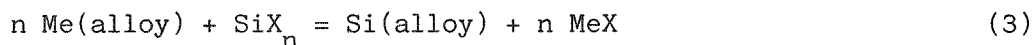


Figure 1.
Survey of the carbothermic route to metallurgical silicon

The molten silicon from the smelting furnace can be purified in the ladle. Separate impurity phases, as silicates and silicon carbide, will partly stick to the lining of the ladle, and some can be removed in a filtering step. Impurities (Me) dissolved in the molten silicon can be attacked by a purifying agent (X):



This exchange type of reaction limits the possibilities of ladle purification to elements less noble than silicon, that is in practice to aluminium and calcium. Important impurities like iron and titanium cannot be removed significantly. A thorough discussion of the refining of molten silicon has recently been given by Tuset [3].

The molten silicon is cast and crushed to lumps, which are leached in acids. If the silicon contains sufficient calcium (or other suitable elements), the lumps will disintegrate to millimeter-sized silicon grains, while most of the impurities are dissolved. The grains are remelted and solidified to crystal-line ingots for slicing to wafers.

Boron and phosphorus are, as will be seen later, only weakly removed by this process. Therefore, it is essential to have a low boron and phosphorus content in the raw materials.

In this process the leaching step is crucial for obtaining a less than 10 ppmw content of the metallic impurities. Alternatively one could have started with extremely pure or purified raw materials, but a smelting furnace operation adding less than 10 ppmw metallic impurities, will probably be rather difficult and more expensive than leaching.

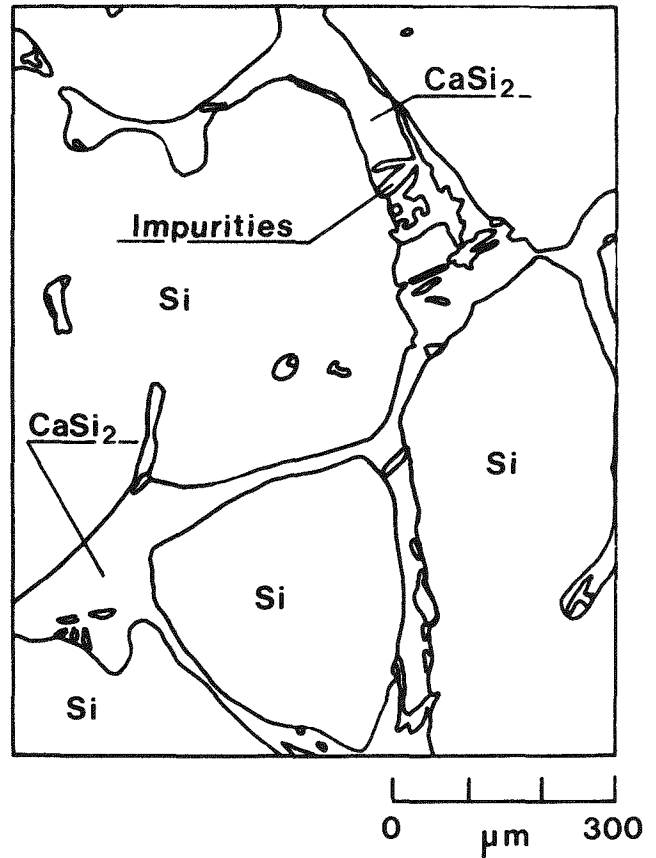
THE LEACHING STEP

The Elkem leaching process

Elkem has developed a modification of the general leaching process that makes it suitable for production of high purity silicon [4]. Silicon containing a few per cent calcium is cast, cooled slowly and then crushed into lumps around 5 cm in size. The lumps are treated with an aqueous mixture of hydrochloric acid with ferric chloride and disintegrate giving fairly pure silicon crystals of a size below 2 mm. These crystals are then further purified with hydrofluoric acid in combination with some oxidizing agent.

Chemical interpretation of the leaching

The leaching can be understood from the microstructure of the leaching alloy. A scanning electron micrograph is shown in Figure 2. Fairly large silicon crystals are separated by the phase calcium disilicide, CaSi_2 . Other impurities are concentrated as small grains within the calcium disilicide phase.



Photograph: A. G. Forwald

Figure 2.

Scanning electron micrograph of the leaching alloy. The micrograph gives an indication of the chemical composition: The darker a phase, the lower the mean atomic mass. The amounts and compositions of the impurity phases are strongly dependent upon the composition of the leaching alloy. In the present sample compositions close to the following formulas were found: FeSi_2 , AlSiCa , FeAlSiCa , $\text{FeSi}(\text{Ti},\text{V})$.

This structure should be expected from the phase diagrams of the systems Ca-Si and Ca-Si-Me (Figure 3). When an alloy A of silicon, calcium and a small amount of a third element Me is cooled, fairly pure silicon crystals are precipitated, and the composition of the melt changes along the crystallization path AE. At E the phase calcium disilicide starts precipitating eutectically together with the silicon phase, and with further cooling more solid precipitates until the alloy is completely solidified at a eutectic or peritectic point. In a technical process Me is replaced by a mixture of several elements, corresponding to a multicomponent phase diagram. The behaviour will still be analogous to the simpler three component system discussed above, and the type of alloy structure shown in Figure 2 will be formed. A condition for this crystallization sequence is a sufficiently high calcium content in the leaching alloy. Then all the impurity phases will occur within the calcium disilicide phase.

When the alloy is treated with hydrochloric acid and ferric chloride, the calcium disilicide reacts and swells. The lumps of calcium-containing silicon

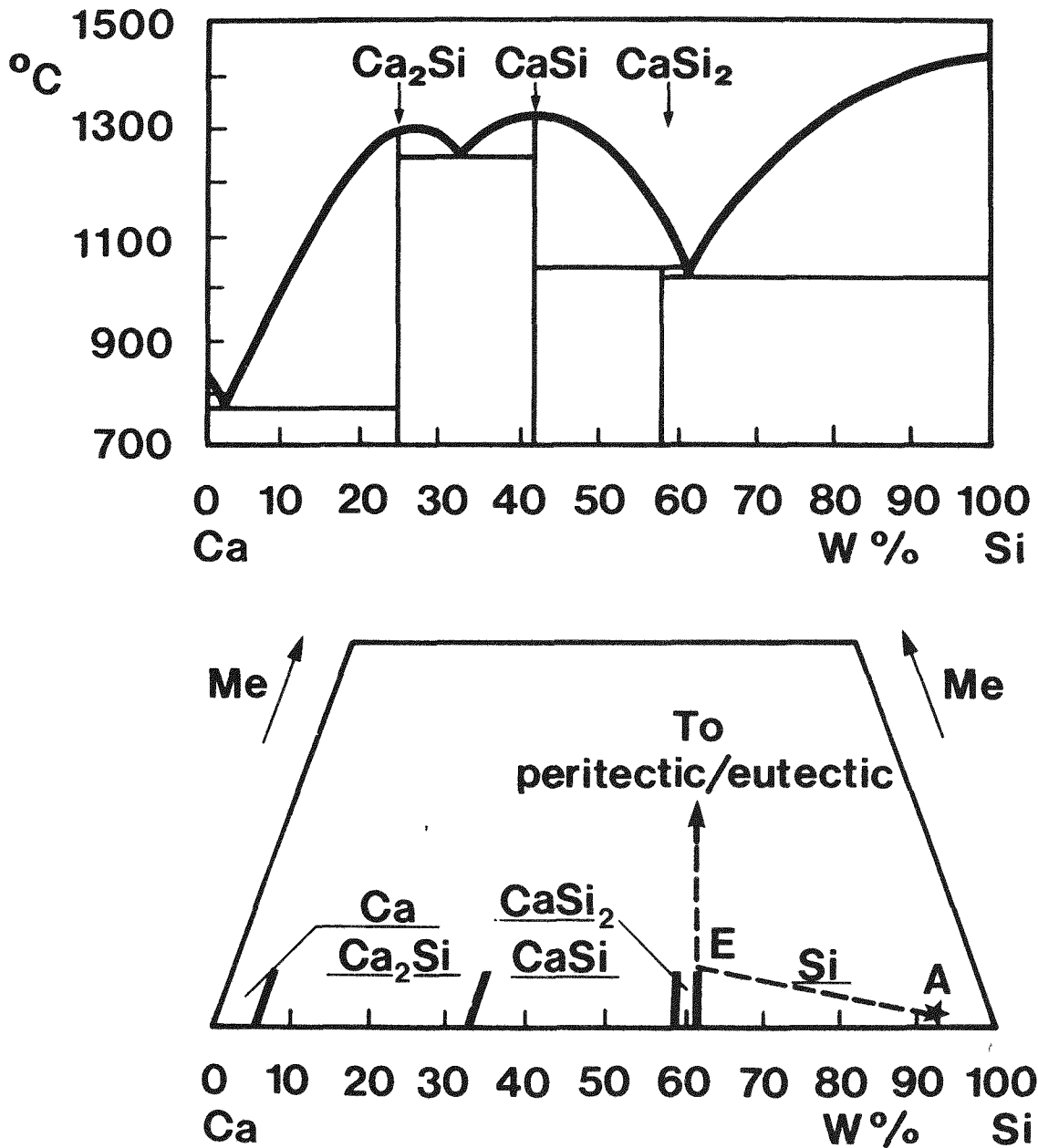
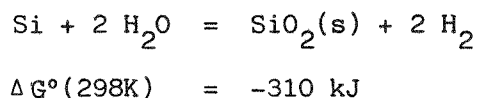


Figure 3.
 The phase diagram for the system Ca-Si [5] and Ca-Si-Me (Me - an impurity element, e.g. Fe, Al, Ti).

break up exposing new surfaces of calcium disilicide for attack. This leaves free, fairly pure silicon crystals and a fine-grained silicon-containing substance that is easily removed by washing. Some small impurity crystals attached to the surface of the silicon grains, are removed by hydrofluoric acid treatment.

The leaching is based upon the fact that silicon is insoluble in acids, while the impurity phases are soluble. The insolubility of silicon must have kinetic reasons, since a thermochemical calculation indicates that silicon should be readily soluble:



The impurity phases dissolve irreversibly. This is important from a practical point of view, since rather impure chemicals can be used for leaching.

The leaching treatment will remove only impurities that occur as accessible separate phases. After leaching, the silicon will contain two types of impurities:

- o Impurities in solid solution in the silicon crystals
- o Impurity-containing particles engulfed in the silicon crystals

The trapped impurity particles are separate phases that will occur rather erratically in the silicon crystals. The impurities in solid solution, in contrast, result from a fairly well-defined distribution between two phases, and they should be expected to behave quite regularly.

Theoretical expectations

The aim of this theoretical discussion is to establish an ideal model for use as an indication of the potential of the process and as a scale for the evaluation of the practical results. The model is based on the classical theory of solidification [6]. This theory is rather crude and cannot be expected to give better than an order-of-magnitude agreement with experiment.

During solidification an element Me will be distributed between the silicon crystals and the melt. This distribution is described fairly well by the equation

$$\frac{c}{c_1} = k \quad (4)$$

where c and c_1 are the Me content of solid and respectively liquid silicon in contact and k is the distribution coefficient. This k is fairly constant for low contents of most elements in silicon. An equilibrium value k_0 can in principle be read from the phase diagram Me-Si, but the observed value will also depend on the kinetic conditions during solidification. Some examples of k_0 values are given in Table 1. All the elements, except possibly oxygen, have a distribution coefficient less than 1, that is, second elements will be rejected from the crystal and concentrate in the melt. These k_0 values have been determined in the pure system Me-Si. In the leaching alloy the added calcium will change the conditions. The situation is rather complicated with several effects that can influence the value of k . Considering these uncertainties, the k_0 values are accepted as reasonable first estimates for the most favourable k values that can be expected in industrial solidification of the leaching alloy.

Table 1.

Equilibrium values k_0 of the distribution coefficient for some elements in silicon [7].

Me	k_0	Me	k_0	Me	k_0
Al ¹⁾	$2 \cdot 10^{-3}$	Cu	$4 \cdot 10^{-4}$	O ¹⁾	1.4
As	0.3	Fe	$8 \cdot 10^{-6}$	P	0.35
Au	$2 \cdot 10^{-5}$	Ge	0.33	S	10^{-5}
B	0.8	Mg	$2 \cdot 10^{-3}$	Sn	$2 \cdot 10^{-2}$
C	$8 \cdot 10^{-2}$	Mn	10^{-5}	Ta	10^{-7}
Co	$8 \cdot 10^{-6}$	Na	$2 \cdot 10^{-3}$	Ti	10^{-5}
Cr	10^{-5}	Ni	10^{-4}	V	10^{-5}

1) Newer values: $k = 0.03$ for Al [8], $k = 0.25$ for O [9]

It is then assumed that the overall solidification of the leaching alloy is described by the wellknown solidification equation

$$c = k c_0 (1-g)^{k-1} \quad (5)$$

where

c_0 is the overall concentration of Me in the leaching alloy
 g is the solidified part of the total amount of leaching alloy

This equation is based upon three assumptions:

- o There is no diffusion in the solid
- o There is complete mixing in the liquid
- o The equation $k = c/c_1$ is true with constant k

These assumptions are believed to be fairly true for reasonable solidification conditions. The mean Me content of the silicon crystals is then

$$\bar{c} = \frac{1}{g} \int_0^g k c_0 (1-g)^{k-1} dg = \frac{c_0}{g} (1-(1-g)^k) \quad (6)$$

For the leaching process it is reasonable to assume that all the silicon crystallized before the coprecipitation of calcium disilicide is recovered, while the remainder of the alloy is lost during leaching. With low Me content, the Ca-Si phase diagram describes the amounts of silicon crystals fairly well (Figure 3). The eutectic calcium content is 39 weight per cent, and if the overall calcium content of the leaching alloy is x weight per cent, the lever rule gives the recovery R of silicon crystals

$$R \cdot x = (1-R) \cdot (39-x)$$

$$R = 1 - 0.0256 x \quad (7)$$

Here the recovery is defined as

$$R = \frac{\text{weight of crystals recovered}}{\text{total weight of leaching alloy}}$$

For the solidification of the leaching alloy, R is equal to g in the solidification equations (5) and (6) just before the start of eutectic crystallization. The mean concentration of the impurity M_e can then be calculated when the content of calcium is known.

The impurity content is calculated as the ratio \bar{c}/kc_0 for several values of k in Figure 4. (This ratio is chosen as an indicator of purification because it gives the mean concentration as a factor times the readily calculable concentration in the first silicon to crystallize). The formulas and the graphs demonstrate some important properties of the leaching operation, as discussed below.

In practical operation one needs a certain amount of the calcium disilicide phase to obtain sufficient disintegration and separation of the crystals. For the high purity silicon one will probably prefer an R value as low as 0.95.

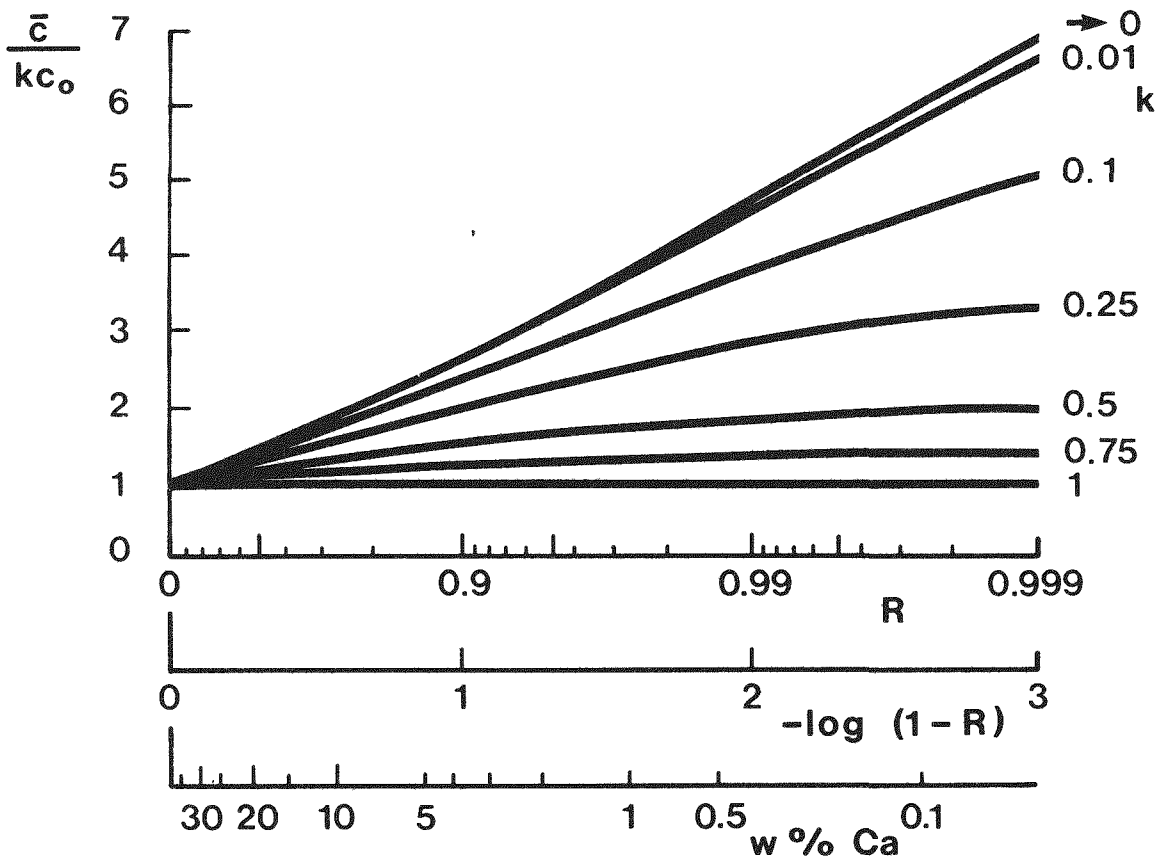


Figure 4.
Mean content \bar{c} of an impurity in silicon crystals.

Figure 4 then shows that $\bar{c}/c_0 \sim 3$ for elements with $k \leq 0.01$, that is, for most impurities. This gives the rule-of-thumb that the mean impurity concentration of the leached silicon is three times the concentration of the first silicon to precipitate. The removal of an impurity with a high distribution coefficient is modest, as shown by a calculation for phosphorus and boron:

$$P: k = 0.35, \quad \bar{c}/c_0 = 0.68$$

$$B: k = 0.80, \quad \bar{c}/c_0 = 0.95$$

For all impurities the concentration in the product is directly proportional to the concentration in the leaching alloy, as shown by equation (6). The impurity content is relatively insensitive to the value of R in the range of practical interest. Thus, if R is increased from 0.9 to 0.99, the ratio \bar{c}/c_0 is less than doubled. Therefore, the value of R , and with that the content of calcium in the leaching alloy, is chosen mainly with the aim of obtaining the correct crystallization sequence and complete disintegration. Also, the moderate sensitivity of \bar{c}/c_0 to R shows that the purifying effect of dissolving the outer layers of the silicon crystals will be moderate. However, impurities attached to the crystal surfaces may justify additional treatment.

Experimental results

The impurities should occur at a concentration less than ten ppmw in the leached solar silicon. With the available analytical equipment it was impossible to obtain reliable determinations in this range. Any result less than about 5 ppmw could indicate that the true value may be close to zero. Therefore only experiments with a rather impure leaching alloy can give results for the testing of the calculations of the previous paragraph, and only the most abundant elements, aluminium and iron, can be considered with some certainty.

The results from one experiment are shown in Table 2. The agreement between measured and calculated values is poor for iron. For aluminium the measured values fall within the area of uncertainty of the distribution coefficient. A conceivable interpretation of the high iron content is that most of the

Table 2.
Experimental and calculated results from leaching experiments

	Impurities, ppmw		
	Fe	Al	Ca
Leaching alloy	3600	3700	29000
Leached product			
Experimental	17	150	200
Calculated			
Old k value } Table 1	0.1	19	
New k value }		300	

iron occurs in inclusions that have been formed by trapping of melt during solidification. This melt, especially towards the end of the solidification, will be quite rich in impurities, and even minute quantities may increase the overall impurity content. For the present experiment it is calculated in Table 3 that an inclusion content of 850 ppm volume can explain the total iron content of the silicon. An inclusion containing 850 ppm volume is rather modest, and the qualitative impression from several micrographs is that this amount of inclusions may well occur in the grains. The contribution of aluminium from the inclusions should be close to the content of iron, but this is small compared to the amount dissolved in silicon. Thus, the content of aluminium has the correct order of magnitude, and the deviation of the iron content may be explained by the occurrence of inclusions. Therefore it is concluded that the classical theory of solidification gives a fairly good description of the impurity content of the silicon crystals.

The minor elements in the leaching alloy, as e.g. titanium, manganese, vanadium and zirconium, will occur with a content of less than 10 ppmw. From the solidification mechanism they are expected to have a content proportional to the iron content in the inclusions. The overall contents of these elements are calculated in Table 4. Because of the inclusions it is impossible to reach the low potential content of the minor elements. Some of these elements are very important when the silicon is intended for crystalline solar cells, especially if the silicon is to be crystallized as ribbons where there is no purification during the crystallization. Preferably, electrically active elements, such as titanium, vanadium and tungsten, should be in the sub-ppb range in the final solar cell.

The effect of leaching on the content of boron and phosphorus is shown in Table 5. The phosphorus removal seems to be slightly better than calculated. That may not be significant, as the range of results is close to the limit of detection of the analytical method. But a high phosphorus removal should not be surprising, since calcium has a strong affinity for phosphorus and might influence the distribution between the two phases.

Table 3.

The iron content of leached silicon interpreted as inclusions.

Leaching alloy	3600 ppmw Fe
Fe content of melt at eutectic: $c_0/(1-R)$	48000 "
Mean Fe content of inclusions, estimated	20000 "
Mean Fe content of crystals with inclusions	17 ppmw Fe
Volume content v of inclusions to explain all the Fe content ($20000 v = 17$) (Density of Si \sim Density of Fe-containing melt)	850 ppmv "

Table 4.
Calculated content of minor impurities of silicon grains

Impurity content(ppmw)	
Leaching alloy	Product
200 ppmw	$(200000 \cdot 17/3600) = 944$ ppbw
100 "	472 "
10 "	47 "
1 "	5 "

Table 5.
Effect of leaching on boron and phosphorus content

Sample	Element	Before leaching	After leaching	
			Experimental	Calculated
A	B ppma	1.8	1.8	1.7
B		2.6	3.1	2.5
C		2.0	2.0	1.9
D		2.1	1.5	2.0
E		2.0	2.0	1.9
F		2.4	2.5	2.3
Mean		2.15	2.15	2.04
A	P ppma	4.2	0.5	2.7
B		2.7	1.3	1.8
C		2.5	1.3	1.6
D		4.2	0.9	2.7
E		4.2	2.0	2.7
F		9.3	4.5	6.0
Mean		4.52	1.75	2.94

Some additional results are given in Table 6. The aluminium content is changed by a factor of slightly below 0.1. According to the rule-of-thumb discussed above, one should expect a factor $k = 0.09$ when the newer value $k = 0.03$ is used. The results are close to the expectation.

Table 6.
Examples of leaching

		Impurities (ppmw)			
		Fe	Al	Ca	Ti
High Al	Before leaching	60	5000	11200	10
	After	4	360	500	1
Medium Al	Before leaching	70	660	7500	10
	After "	3	50	280	1
Low Al	Before leaching	52	140	11000	10
	After "	2	10	280	1

CALCIUM AND CARBON

Calcium and carbon are added voluntarily during the process, but they are impurities in the final product and have to be removed as far as possible. Calcium has a retrograde solubility in silicon with a maximum calcium content of 100 ppmw [10]. The mean concentration of calcium dissolved in the crystal should be less than 100 ppmw, but inclusions can increase this amount strongly. The calcium content may be reduced by remelting the crystals and e.g. treating the melt with chlorine, maybe to about 10 ppmw.

The carbon content is high during production in the submerged arc furnace. The silicon is in contact with silicon carbide and to a lesser extent silica at a temperature around 2000°C. Silicon should therefore be close to saturation at that temperature. When the silicon is cooled, dissolved carbon precipitates as silicon carbide. However, many particles are small and will sink slowly in the melt, and analysis of samples will show a carbon content higher than the true content of the melt after cooling. The analysis of rapidly cooled samples should therefore be quite close to the carbon solubility at the furnace temperature.

The solubility of carbon in molten silicon is poorly established experimentally, as pointed out in a recent review [11]. However, the measurements given the highest credibility in this review, indicate a far too high carbon solubility to fit with the experience from the carbothermic smelting of silicon. Silicon tapped directly from the submerged arc furnace contains 0.1 - 0.2 weight per cent carbon. This is in fairly good agreement with the solubility measurements of Scace and Slack [12], reproduced in Figure 5. The experimental values in this paper fall well on a straight line in a log c versus 1/T diagram, indicating good consistency of the experimental work. Therefore, at present these values are accepted as the most reliable estimate of carbon solubility.

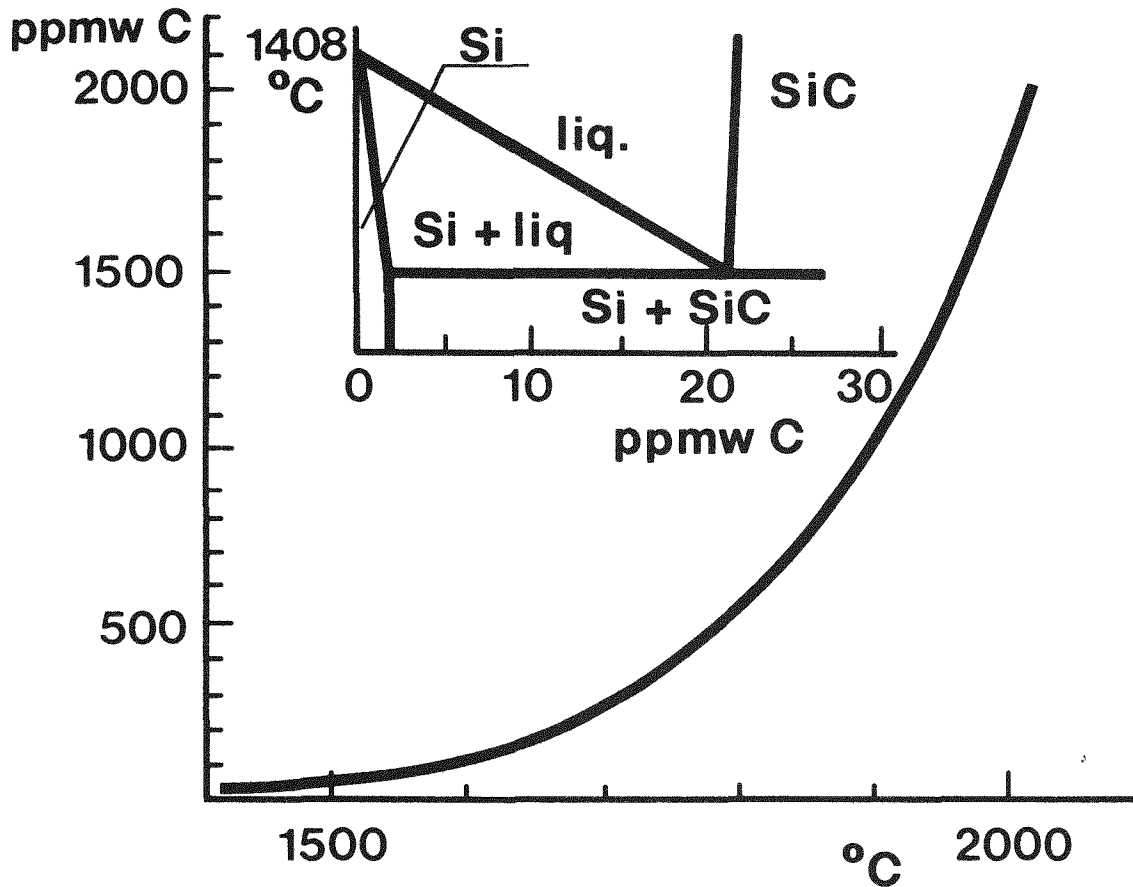


Figure 5.
The solubility of carbon in silicon. (Solubility in liquid silicon from [12], distribution coefficient 0.07 from [13])

The molten silicon cools during and after tapping, and the precipitated silicon carbide is partly trapped by the slag and at the ladle lining during melt treatment. It is difficult to remove all the precipitated silicon carbide, and the cast silicon will as a rule contain more carbon than the value read from the solubility curve at the temperature of the ladle treatment. According to practical experience, the carbon content may be reduced to some 100 ppmw in the ladle. The solubility of carbon in solid silicon near the melting point is around 4 ppmw, and any excess of this value is present as a supersaturated solid solution or as silicon carbide particles in the solidified leaching alloy. This silicon carbide will not be removed by the leaching unless the particles are completely surrounded by the calcium disilicide phase.

In the calculation of the recovery of the leaching process it was assumed that silicon was the only solid phase. Because of the precipitation of silicon carbide during the entire solidification, this assumption is not strictly true. But the amount of carbon is so low that the calculation is not invalidated.

POTENTIAL OF THE PROCESS

As shown above it is possible to estimate the final purity of the product fairly well from a simple theory of the distribution of the impurities during crystallization. Very low impurity contents can be obtained. In principle the product may be improved further by remelting and releaching several times. According to the calculations above, this can give extremely low impurity contents. Exceptions are boron, phosphorus and aluminium, which all have unfavourable distribution coefficients, and calcium, which is added in each remelting. In practical operation, however, the remelting will add impurities, and a steady state will be reached where addition balances removal. More work is necessary to evaluate this possibility.

An important contribution to the overall impurity is melt inclusions in the crystals during solidification. The calculated contents of most metals show strong improvements when the inclusions are avoided. An impurity in a class by itself is calcium, which results from the use of calcium as auxiliary element in each step. In principle calcium could be left out, at least in the last of repeated leachings, but then it would be necessary to grind the leaching alloy finely. This would complicate the aftertreatment of the leached grains, and small, slowly dissolving impurity particles would not be washed away easily.

An estimate of attainable impurity levels is given in Table 7. The intention was to produce a silicon that could be used for solar cells after a crystallization step of the Czochralski or Bridgman type, where the content of metallic impurities and carbon would be strongly reduced. This intention has been fulfilled. The Bridgman-crystallized silicon gave solar cells with an efficiency in the modul up to 13 per cent. This compares favourably with the 14 per cent value typical for high quality production-size Czochralski cells in the photovoltaic industry [14].

Table 7.
Anticipated impurity contents of high purity silicon produced by leaching

Elements	Impurities (ppmw)		
	Present technique	Without inclusions	Repeated leachings
Boron	< 1	< 1	< 1
Phosphorus	< 1	< 1	< 1
Calcium ¹⁾	< 10	< 10	< 10 ⁻³
Aluminium	< 10	< 1	< 10 ⁻³
Metals except calcium and aluminium	< 10	< 10 ⁻³	< 10 ⁻⁶
Carbon	< 50(?)	< 5	< 1

1) Remelting and calcium removal, untreated grains would contain 100 ppmw Ca without inclusions.

If the anticipated impurity contents without inclusions or for repeated leachings can be realized, the silicon can be used even for a ribbon-type wafer production where there is essentially no purification during crystallization.

The purity of the product is determined during the solidification. This purity may not be obtained because of poor leaching, but the potential for purity is set when the alloy is solidified. The leaching process is thus really a purification by crystallization with a purifying efficiency similar to the unidirectional solidification technique, and these two techniques are to be compared. In unidirectional solidification at most a few hundred kilograms can be treated in each batch, and the crystallization parameters are very critical. One has to use a rather low cooling rate to avoid constitutional supercooling, which will seriously decrease the efficiency of the purification. The separation of the pure and the impure fractions requires time-consuming manual work. For the leaching process, in contrast, even rather crude cooling gives fairly good leaching results, and both the solidification and the leaching can be adapted to large scale automated operation.

The cost of the silicon will depend strongly on the scale of the production, especially for the carbothermic step. The cost of the leaching alloy will drop rapidly with the scale up to a few thousand tons per year, and then flatten out. The cost of the leaching procedure will be less dependent on the scale. It is premature to give exact cost information before the details of the procedure have been fixed. It can be claimed, however, that for a production of several thousand tons a year, the cost of production will be only a few times the cost of ordinary metallurgical silicon.

ACKNOWLEDGEMENT

The author acknowledges the support and valuable advice from several persons in Exxon Research and Engineering Company and in Elkem a/s during a joint project on low cost silicon for solar cells. Especially he will mention Dr. L.P. Hunt for extensive work on raw materials, Dr. J.P. Dismukes and Dr. P.S. Ravishankar for informative discussions on crystallization, K. Larsen for experimental work on submerged arc furnace operation with high purity raw materials and G. Halvorsen for experimental data on leaching of calcium-containing silicon alloys.

REFERENCES

- [1] A. Schei "High purity silicon production" in Refining and Alloying of Liquid Aluminium and Ferro-Alloys, Editors T.A. Engh, S. Lyng, and H.A. Øye, Aluminium-Verlag Düsseldorf, 1985, pp. 71-89.
- [2] L.P. Hunt and V.D. Dosaj "Solar silicon via the Dow Corning process" Report DOE/JPL-954559-78/7, 109 pages, 1979.
- [3] J.Kr. Tuset "Principles of silicon refining" in Refining and Alloying of Liquid Aluminium and Ferro-Alloys, Editors T.A. Engh, S. Lyng, and H.A. Øye, Aluminium-Verlag Düsseldorf, 1985, pp.49-69.
- [4] G. Halvorsen "Method for production of pure silicon" US Pat. 4,539,194 (1985), priority 1983.

- [5] E. Schürmann, H. Litterscheid, and P. Fünders "Investigation of the melting equilibria of the phase diagram calcium-silicon" Arch. Eisenhüttenwes. 45 (1974) No. 6 pp. 367-371.
- [6] B. Chalmers "Principles of solidification" Robert E. Krieger Publ. Co. 1977, reprint of original edition 1964.
- [7] D. Morvan, J. Amouroux, and G. Revel "Mise au point d'une technique de fusion de zone sous plasma appliquée à la préparation du silicium photovoltaïque" Revue Phys.Appl. 15 (1980) pp. 1229-1238.
- [8] R.H. Hopkins, J.R. Davies, A. Rohatgi, R.B. Campbell, P.D. Blais, P. Rai-Choudbury, and R.E. Stapleton "Effects of impurities on processing on silicon solar cells" Report DOE/JPL-954331-80/9, Westinghouse R&D Center, 1980.
- [9] W. Lin and D.W. Hill "Oxygen segregation in Czochralski silicon growth" J. Appl. Phys. 54 (1983) No. 2, pp. 1082-1085.
- [10] H. Sigmund "Solubilities of magnesium and calcium in silicon" J. Electrochem. Soc. 129 (1982) pp. 230-234.
- [11] R.W. Olesinski and G.J. Abbaschian "The C-Si (carbon-silicon) system" Bull. Alloy Phase Diagr. 5 (1984) pp. 486-489.
- [12] R.I.Scace and G.A.Slack "Solubility of carbon in silicon and germanium" J. Chem. Phys. 30 (1959) pp. 1551-1555.
- [13] T. Nozaki, Y. Yatsurugi, and N. Akiyama "Concentration and behaviour of carbon in semiconductor silicon" J. Electrochem. Soc. 117 (1970) pp. 1566-1568.
- [14] J.P. Dismukes, J.A. Amick, P.S. Ravishankar, E.E. Ship, L.B. Younghouse, J. Blake, R. Sylvain, G. Halvorsen, K. Larsen, A. Schei "Solar cell performance assessment of Elkem HPMS-silicon" The Electrochemical Society, Proceedings of the Symposium on Materials and New Processing Technologies for Photovoltaics, New Orleans, Oct. 7-12, 1984, in preparation.

DISCUSSION

AULICH: Would you comment on your carbon removal technique and why you believe that repeated leaching will reduce the carbon content?

SCHEI: As you explained in your paper, you have used crystallization to remove carbon. In our experiments, it seems that small silicon-carbide particles are not always engulfed in growing silicon crystals, so we have the hope of removing them and containing them in the calcium disilicide. If we are below the solubility limits, it will be a normal precipitation procedure.

SCHMID: You mentioned in your paper that the silicon carbide concentration was reduced by the ladle treatment. What type of treatment is used?

SCHEI: That's mainly a mechanical procedure. Silicon carbide tends to stick to the slag and the lining of the ladle and, also, if it spends some time in the ladle, the large, heavier particles will sink. The solidification can be improved by blowing with a gas, and we also have the option of filtering.

WRIGHT: At Solarex, we confirmed that a gas extraction technique was very effective in removing silicon carbide. Using a directional solidification technique, we didn't find that particles below 10 μm tended to be within the solidified structure. We weren't growing single crystals, but polysilicon. The silicon carbide particles were actually within the crystal and not at the grain boundaries, and we didn't get a significant reduction in silicon carbide particles by a directional solidification process.

KOINUMA: I would like to ask about the effects of leaching on the boron and phosphorus levels. I think you mentioned that the boron and phosphorus levels were not reduced very much by leaching, but Dr. Aulich mentioned that the levels could be reduced considerably by leaching of the silica. I wonder why there are these differences between the silica and silicon leaching.

SCHEI: Well, these are two completely different processes. I don't know much about the leaching of silica, but it has been well known for many years that crucibles of quartz are made from a boron containing material and the boron is leached out. We do not have the same distribution problems as in that system.

AULICH: I would like to comment on this question. Two different materials are being considered. On the one hand, there is silicon and it is leached. On the other hand, glass fibers are processed. The processes are not the same.

SOLAR SILICON FROM DIRECTIONAL SOLIDIFICATION OF MG SILICON
PRODUCED VIA THE SILICON CARBIDE ROUTE (*)

M. RUSTIONI+(o), D. MARGADONNA+, R. PIRAZZI++,

+ PRAGMA S.p.A. - Via M. Ghetaldi, 64 - Roma - Italy

++SAMIM ABRASIVI S.p.A. - Via Piave, 76 Domodossola - Italy

and

S. PIZZINI

DEPARTMENT OF PHYSICAL CHEMISTRY AND ELECTROCHEMISTRY -
UNIVERSITY OF MILANO, Via Golgi, 19 - Milano - Italy.

ABSTRACT

A novel process of MG silicon production is presented which appears particularly suitable for PV applications.

The MG Silicon is prepared in a 240 KVA, three electrodes submerged arc furnace, starting from high grade quartz and high purity silicon carbide (patent pending). This last has been obtained by reacting in a Acheson type of furnace, high grade sand and carbon black.

The silicon smelted from the arc furnace under very smooth furnace operations has been shown to be sufficiently pure to be directionally solidified to 10-15 Kg, 23cm x 23cm square bricks, after grinding to than > 5 mm grain size and acid leaching, with a material yield larger than 90%.

With a MG silicon feedstock containing about 3 ppmw B, 490 ppmw Fe, 190 ppmw Ti and 170 ppmw Al, blended with 50% of off grade EG silicon to recondact the boron content to a concentration acceptable for solar cells fabrication, the 99% of deep level impurities concentrate in the last 5% of the ingot, which appears structurally perfect in the rest, after the first crystallization, while deep level impurities are close to the detection limits by ICP-ES technique after a second crystallization.

(o) Presente Address: ENICHIMICA, piazza Boldrini 1 -
San Donato Milanese - Italy

(*) Work partially supported by E.N.E.A.

10cmx10cm wafer, sliced from twice crystallized silicon ingots, after sizing showed resistivity in excess of 0.1 ohm cm, diffusion lengths in excess of 40 μ m and PV conversion efficiencies in excess of 6%, when processed like polycrystalline silicon wafers of EG quality.

Quite remarkable of this material is the fact that the OCV values range higher than 540 mV and that no appreciable shorts due to SiC particles could be observed, neither on the top or bottom slices.

It is felt that still considerable improvements of this process could be achieved, such to allow the direct use of MG silicon for solar cells fabrication, when considering that the use of the same raw materials in a direct reduction process got to a MG silicon containing only 2,5 ppmw boron and that still B concentration could be reduced by a suitable control of the residual pollution sources.

1. INTRODUCTION

"Solar grade" silicon is the ultimate product of a process which starts from suitable raw materials and yields wafers which could be directly used for manufacturing > 10% efficient solar cells (1), satisfying at the same time the economic constraints which indicate as the target for a "solar grade" feedstock(*) a figure around or less than 10\$/Kg.

This paper reports comprehensively the results of a research carried out by a team of italian companies which succeeded in approaching very closely the efficiency and economics targets by a process which will be indicated as the HPS process from the names of the companies involved (Heliosil, Pragma and Samim Abrasivi).

This process, which will be discussed in details in the next sections, consist essentially of the following steps:

- The syntesis of high purity SiC from low boron ($B < 0.5$ ppmw) silica sands and carbon black (2).
- The reduction of quartz lumps in an arc furnace using SiC as

(*) We mean as "feedstock" a material which could be directly crystallized to obtain wafers usable for manufacturing PV cells, with a yield larger than 90%.

the reductant (2).

-The purification of the MG silicon obtained in such a manner using a directional solidification technique.

Although the work is still in progress, nevertheless the results appear so encouraging that we strongly believe that the industrial feasibility of MG silicon route has been demonstrated.

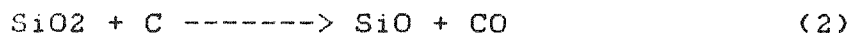
2. GENERAL REMARKS ON HPS PROCESS

Metallurgical silicon is currently manufactured by direct reduction of quartzites with carbon in a submerged electrodes arc-furnaces (DAR process).

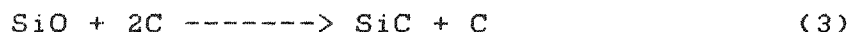
The overall reduction reaction could be described, formally with the following equation:



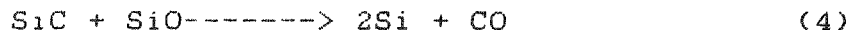
According to the scheme shown in fig. 1, the process actually occurs in a multi-step pattern, with a series of reactions taking place simultaneously at different heights of the furnace, depending on the temperature which rises from the top to the bottom. With reference to fig. 1, one can observe that on the cooler portion of the furnace, where the temperature is lower than 1500degreeC, the thermodynamically most probable reaction is the following one:



while only in the inner and hotter portion of the furnace, thermodynamics favours the reactions:



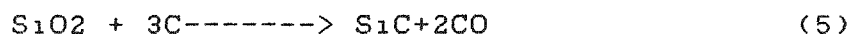
and:



The last one provides silicon from SiC and SiO. It appears that SiC is an intermediate by-product in the direct reduction process of silica and therefore SiC must be considered a primary and unavoidable pollutant of MG silicon, unless being able to control the rate of reactions (3) and (4), which is never the case when operating industrial arc furnaces.

On the other hand, SiC may be directly and efficiently ma-

nufactured using resistance furnaces of the Acheson type (this is in fact the way by which silicon carbide is produced world-wide for the abrasive industry) according to the following equation:



Therefore synthetic SiC is very attractive as the reductant (instead of carbon) of SiO₂ in arc furnace. In this case the overall reduction equation occurs according to:



which involves, apparently the evolution of only 2/3 of moles of CO every mole of silicon produced, which is just 1/3 of the amount of CO evolved in the direct arc furnace reduction process as appears in reaction (1).

The lower amount of gases evolved (which causes the lower amount of heat lost and smoother furnace operation) is not the only advantage of the HPS process in respect to the DAR process. Meanwhile, in fact, also the theoretical electrical energy demand (per mole of SiO₂) is one third, and this should improve the overall electric yield of the HPS process, since the production of SiC in Acheson furnace occurs quite effectively. Actually, in spite of the excess heat needed in the HPS process for bringing the intermediate SiC to the reaction temperature in the arc furnace, after being produced in the Acheson furnace, still the overall electrical yield of the HPS process is comparable with the DAR process, as it appears in Table I and Table II, which will be further commented in the next section. A further advantage of the HPS process arises from the physical requirements of the raw materials used in Acheson furnaces which do not need to be compacted or extruded before feeding them into the arc furnace, as required in DAR process in order to allow a smooth furnace operation.

Finally, the fact that the graphite electrode consumption is reduced of a factor of three in the arc furnace step of the HPS process and that no electrode consumption is involved in the Acheson process, makes contamination of the produced silicon lower.

It must also be considered that high operation temperature (> 2200degreeC) are reached in the inner part of the Acheson furnace. The high temperature gradient makes possible the transfer of impurities from the inner part to the cooler outer zone via gas phase as well solid phase. Therefore, during the synthesis of SiC in the Acheson furnace a significant purification of the reactants and product takes place that results

in well crystallized, transparent SiC platelets in the inner part of the furnace. The purification may also be enhanced carrying out the synthesis of SiC in the presence of NaCl or chlorine gas which allows the formation of volatile halides.

Besides residual metallic impurities (whose amount depends on the the reduction yield of the parent oxides present in quartzites), the MG silicon smelted from the arc furnace always contains carbon in excess over saturation conditions which precipitates as silicon carbide.

Being firmly established in the literature and confirmed by previous experiments that bulk SiC and impurities (except boron and phosphorous) could be removed by crystallization procedures (3-6) quite better than using intermediate slagging or leaching steps, the HPS process is completed by a twice crystallization in a Bridgman furnace, conducted according to a proprietary knowledge (7).

The first cristallization step allows to segregate most impurities (SiC included) in the last 5% of the solidified ingot. This part can be easily separated by sawing and the resulting product is the "solar grade feedstock".

Then, the wafers sliced from ingots grown in Bridgman furnace using "solar grade feedstock" (second step of cristallization) are directly usable for solar cell fabrication.

A schematic flow-diagram of the HPS process is reported in Fig. 3.

3. EXPERIMENTAL

A) Synthesis of high purity SiC

SiC has been prepared starting from high purity silica sand and carbon black. The mechanical mixture of both components has been agglomerated by extrusion or briquetting using sucrose as the binder. By this way, 18000Kg of pellets have been prepared which were allowed to react in the Acheson furnace, whose schematic lay-out is reported in Fig.2. The average impurity content in the pellets is reported in Table I, as determined by ICP-ES techniques after dissolution. In the same table, the impurity content in SiC produced in the middle part of the furnace, is also reported together with the expected impurity contents calculated from the amount of impurities in the raw materials, assuming no impurity losses during the SiC production process. It appears that, with the exception of titanium, the impurity content is lower than that expceted,

indicating a purification effect during reaction of the mixture due, as already discussed, to impurity migration towards the cooler part of the charge. These purification effects are particularly relevant in the case of boron and phosphorus: in both cases a purification factor of the order of ten is obtained.

The silicon carbide obtained by the Acheson process is very brittle and porous. Both factors are very beneficial for the use of SiC in the arc furnace, as brittleness limits intermediate manipulation steps before the final use to one single crushing step in order to reconduct the large SiC blocks to the right size (1 - 20 mm), and porosity enhances the permeation of the gases (CO and SiO) during the arc furnace operation and consequently enhances also the yield of reaction (4).

Crushing, however has been found to seriously affect the purity of SiC (see table I) and therefore the crushing step should be implemented by acid leaching.

B) Arc furnace experiments

Arc furnace experiments have been carried out in a 240 KVA three-phase submerged electrodes arc furnace. A picture of the furnace is shown in fig. 4, while fig. 5 reports a schematic lay-out and table III reports further technical details.

The furnace has been fed with SiC and 20-60 mm quartz "nuts" which have been obtained by grinding, HCl leaching and deionized water rinsing of large natural quartz blocks whose original impurity content is reported in table II.

High purity graphite tools or SiC tools have been used throughout during the furnace operation (smelting, breaking the crusts which form on the surface of the charge and limit the vertical electrode movements as well as the escape of the gases) in order to avoid the silicon pollution caused by the furnace handling.

Fig. 6 reports details of a typical run when the furnace is fed with SiO₂ and SiC. It appears from the energy consumption curve that the furnace operates smoothly and that the specific energy consumption averages 13 Kwhr/Kg after the furnace start-up period, which takes about one day. Smelting operations were carried out every 8 hrs and silicon was poured in an high purity graphite mould.

Sampling of silicon for impurity content analysis was carried out at the beginning, in the middle and at the end of the

smelting operations directly on the molten silicon in order to avoid that segregation affects in the solid ingot during cooling could affect the reliability of the analysis.

Results referring to a typical run (# 10/2) are reported in Table III and compared with a typical DAR run (# 12/6) which was carried out in the same arc furnace few months ago (6,8), before having introduced the routine use of carbon black and SiC runs in furnace operations.

It is worth noting that, in spite of improved furnace operation, still a substantial pollution of the produced silicon is observed.

However, if one compares the deviation factors, calculated as the ratios between the actual and expected values, between the run HPS 10/2 and the run DAR 12/6, one observes that pollution has been definitively reduced for every impurity investigated, except for boron in the run HPS 10/2.

Furthermore, by remarking that grinding of SiC was another source of pollution, one could forecast that leaching of SiC could get a material, under the same furnace operating conditions of run HPS 10/2, containing 40 ppmw Al, 1.6 ppmw B, 340 ppmw Fe, 0.6 ppmw P and 350 ppmw Ti which is still the most harmful impurity present.

Within the possible pollution sources, the construction materials of the furnace and the surrounding atmosphere are the most critical, as they behave like "infinite size" pollution sources.

By no means, therefore, is worthwhile to improve the quality of starting materials before having solved these problems to which we intend to observe the maximum of attention in the next period of time.

C) Purification of MG silicon by directional solidification.

As the material having the impurity content of HPS or DAR silicon reported in Table III could not be directly casted or CZ-pulled for getting ingots useful for solar cells fabrication, one intermediate purification step is needed and the directional solidification process was found to be very effective for this purpose.

The furnace and the crystallization procedures used have been already described (8-10): it operates in the Bri-

dgman-Stockbarger configuration and houses square section crucibles up to a size of 25 x 25 sqcm.

All purification experiments were carried out using quartz crucibles, coated on the inner walls by a thin layer of silicon nitride which avoids the direct contact of liquid silicon with the crucible walls and, therefore, avoids sticking effects with cause the breaking of both crucible and ingot.

In order to avoid spurious effects due to additional impurities introduced into the silicon charge during grinding procedures, which serve to obtain chunks of suitable size for casting, the charge was acid leached with an HF: HCl : H₂O (1:1:4) solution at 60°C, for two hours, rinsed and dried.

The purification experiments reported in this paper have been carried out on material coming from the run HPS10/2, having the impurity content reported in Table III. After grinding, only the fraction having a grain size larger than 2 mm has been used, to facilitate the melting of the charge. The original charge was added of "off grade" EG silicon chunks to adjust the boron content to an equivalent resistivity value of 0.15 ohm cm or more.

From the ingot so obtained, a 1 cm thick slice was sectioned in the middle of the ingot, and then, by further slicing, 112 cubes of 1 cubic cm were obtained, each one was numbered and analysed for impurity content by the ICP-ES technique. Results for sample coming from a vertical row at the periphery of the ingot (nrs. 9, 11, 14, 15) and in the middle (nrs 50, 52, 54, 56,) are reported in table IV (see for reference fig. 7).

One remarks that the impurity content (except B and P) is strongly depressed in more than 90% ingot, while impurities segregate in the last 10% (see impurity content in cube nr. 56 and on the top samples) where also SiC segregates, leaving the remainder substantially free of SiC particles, as observed by visual inspection.

Segregation coefficients calculated from the original impurity content of the MG sample end of the first lowest cubes of each vertical row are also reported in table IV.

Although the segregation coefficients so derived are much higher than ones reported for from pulling, still the values obtained allow a high degree of purification from aluminum, iron and titanium which are the most abundant contaminants.

Obviously, no purification is observed for boron and pho-

sphorus. Unexpected large values are obtained for Ca and Mg: an accidental contamination during analysis procedures is suspected in these cases.

The "solar grade feedstock" was then obtained cutting away from the ingots grown, as above described, the top and the lateral sides. The material was then subjected to a second directional solidification with the same procedures of the first-one. The resulting ingots was analysed in the same way as previously described. Results are shown in Table V.

Also in this case some degree of purification is obtained, although it occurs in lower extent than expected from data of table IV. Since the resistivity measurements described in the next paragraph are in substantial agreement with analytical results, one has to conclude that some contamination occurred during the second solidification step.

D) Physical characterization and solar cells performance of HPS material.

10cm x 10cm x 0.04cm wafers cut from ingots prepared with "solar grade feedstock" as previously described, were subjected to physical and PV test (see table VI for results). All slices examined resulted p-type, with an average resistivity of 0.13 ohm cm, which well compares with the expected one, obtained from the excess acceptor concentration $(N_A - N_D) = 2.4E17/cm^3$ calculated using the experimental values of B, P and Al concentration (see Table IV) and by taking the aluminum 30% ionized.

The diffusion length of the minority carriers, measured using the SPV technique resulted in average larger than $40\mu m$ with top values of $50\mu m$ which is definitely lower than the average L_d values ($> 150\mu m$) measured on "off grade" EG silicon wafers manufactured with the same casting process.

Solar cells, manufactured using the standard Pragma procedures, resulted in average 6,2% efficient while "off grade" E.G. silicon wafers processed in the same batch resulted 9.85% efficient.

As it results from Table VI, not only the low values of short circuit current are responsible of the efficiency measured but also the OCV (540 mV) which is about 60 mV lower than the OCV which could be obtained with a FZ silicon having the same resistivity. The analysis of I-V curve for such solar cells shows that the shunt resistance is lower than one observed on cells manufactured starting from standard material, so

revealing a certain amount of shortage probably due to small particles of SiC which still remain after twice crystallization process.

4. CONCLUSIONS

From the results reported in the different sections of this paper it appears that a definitive progress towards the industrialization of a MG silicon process for solar uses has been obtained in the course of our research program. In our opinion it results that MG silicon is a possible low cost source of solar feedstock. It has been proven infact, that:

- The use of SiC, which could be synthesized in an Acheson furnace at a reasonable grade of purity, improves definitely the arc furnace operations.
- The purity of HPS Si₁, before the first crystallization is significantly close to the expected one and impurity contamination sources were clearly indentified.
- Crystallization of HPS silicon, without any intermediate purification process yields a material capable of getting cell with efficiencies in excess of 8.5% if only the active area is considered.

Therefore, one can forecast that by improving the handling of SiC and by carrying the first crystallization step in the presence of Ca, followed by an acid leaching (according to a process suggested by Schei (11)), our material is already useful for >10% efficient solar cells.

ACKNOWLEDGEMENTS

Authors warmly acknowledge the italian Comitato Nazionale per la Ricerca e lo sviluppo dell' Energia Nucleare e delle Fonti Rinnovabili (E.N.E.A.) for the financial support given to the project on solar grade silicon. They are particularly indebted to G. Gazzola of E.N.E.A. for continuous encouragement. Authors are also indebted to P. Fabris and M. Tomassini for many helpful discussions and to M. Colombo, F. Rota and M.P. Bianchini for technical assistance.

LITERATURE

- (1) S. Pizzini, Solar Energy materials, 6 (1982) 253
- (2) P. Fabris, D. Margadonna, R. Pirazzi, R. Rustioni
It. Pat. n. 23136A/84 (Oct. 1984).
- (3) J.A. Amick, J.P. Dismukes, R.W. Francis, L.P. Hunt, P.S. Ravishankar, M. Schneider, K. Mathei, R. Sylvain, K. Larsen, A. Schei
Proc. Symp. Materials and new process Technology for Photovoltaics.
Proc. Vol. 83-11 (The Electrochem. Soc.) 1983, p. 67.
- (4) J.P. Dismukes, J.A. Amick, P.S. Ravishankar, E.E. Shipp, L.B. Younghouse, J. Blake, R. Sylvain, G. Halvorsen, K. Larsen, A. Schei, Proc. Symp. Materials and new process technologies for Photovoltaic, Proc. Vol. 85 (The Electrochem. Soc.) in press.
- (5) H.A. Aulich, L. Bernewitz, H.J. Fenzl, H. Pink, F.W. Schulze, MRS-Europe, Poly-microcristalline and amorphous semiconductors. Les Editions de Physique (1983) p. 175.
- (6) S.Pizzini, M. Rustioni
Proc. sixth E.C. Photovoltaic Energy Conference
D. Reidel Publ. (1985) p. 875.
- (7) M. Rustioni, R. Pirazzi, M. Tincani, D. Margadonna, S. Pizzini
Proc. Symposium on Materials and new processing tech. for Photovoltaics Proc. Vol. 85 - (The Electrochem. Soc.) in press.
- (8) S. Pizzini, C. Chemelli, M. Gasparini, M. Rustioni
It. Pat. 203501 (April 1984).
- (9) M. Beghi, C. Chemelli, S. Fossati, S. Pizzini, MRS Europe, Poly-microcristalline and amorphous semiconductors. Les Edition de Physique (1984) p. 181.
- (10) C. Chemelli, M. Beghi, S. Fossati, F. Rota, L. Bigoni
Proc. sixth E.C. Photovoltaic Solar Energy Conf. D. Reidel (1985) p. 1036.
- (11) A. Schei. Private communication.

ELEMENT ppmw (§)	SILICA SAND	CARBON BLACK ANIC 550D	PELLETS	SiC (*)	EXPECTED VALUES (°)	DEVIATION FACTORS
Al	132	56	132	21	240	0.09
B	<0.5	<0.5	3	1	9	0.1
Ca	95	8	191	42	290	0.15
Fe	32	24	105	181	315	0.6
Mg	6	9	37	15	60	0.25
P	3	0.8	7	1.6	21	0.08
Ti	60	3	42	110	90	1.2

ACHESON FURNACE DATA

- ELECTRIC CONSUMPTION : 16700 Kw.h
- SiC PRODUCTION : 1500 Kg
- SPECIFIC ENERGY : 11 Kwh/Kg
- REACTION YIELD : 75%

(§) MEASURED BY ICP - ES

(*) MEAN VALUE OF SAMPLES COMING FROM DIFFERENT PARTS OF THE REACTED MATERIAL

(°) TAKING INTO ACCOUNT THE STOICHIOMETRY OF THE PROCESS

TABLE I - SYNTHESIS OF SiC IN ACHESON FURNACE: ANALYTICAL AND ELECTRICAL DATA

	HPS PROCESS (SiO ₂ + SiC) RUN # 5	DAR PROCESS (SiO ₂ + C) RUN # 12
ENERGY CONSUMPTION (Kwh/Kg)	11.9 (+11 required for SiC)	21
ELECTRODES (Kg/Kg)	0.06	0.11
REACTION YIELD	95%	65%
<ul style="list-style-type: none"> • INTERNAL DIAMETER OF THE VESSEL: 1020mm • ELECTRODES DIAMETER: 175mm • LENGHT BETWEEN ELECTRODES: 370mm • MAXIMUM POWER: 240KVA 		

TABLE II - COMPARISON BEETWEN THE ARC FURNACE STEPS OF THE HPS AND DAR PROCESS

ELEMENT ppmw (*)	SiC AFTER GRINDING	QUARTZ	Si HPS RUN # 10/2	Si HPS EXPECTED VALUE (°)	DEVIATION FACTOR HPS	Si DAR RUN # 12/6	Si DAR EXPECTED VALUE (°)	DEVIATION FACTOR DAR
Al	156	31	340	182	1.9	365	168	2.2
B	2.1	<0.5	5.8	3.6	1.6	2	3	0.7
Ca	194	60	153	203	0.8	115	225	0.5
Fe	290	10	986	504	2.0	615	100	6
Mg	45	15	27	48	0.6	14	63	0.2
p	5.6	5.2	6.1	16	0.4	32	34	1
Ti	96	5.2	382	120	3.2	270	2.6	10

(*) MEASURED BY ICP - ES

(°) TAKING INTO ACCOUNT THE STOICHIOMETRY OF THE PROCESS

TABLE III - IMPURITY CONTENT IN Si HPS AND Si DAR OBTAINED STARTING FROM SIMILAR RAW MATERIALS IN THE SAME ARC FURNACE

ELEMENT ppmw	FEED - STOCK (*)	CUBE n°									\bar{C}_s
		9	11	13	15	50	52	54	56	TOP	C1
Al	170	6.6	8.8	6.4	7.5	4.9	5.3	7.0	275	>5000	0.04
B	2.9	2.8	2.9	2.5	2.8	2.6	2.7	3.0	3.1	8.7	1
Ca	77	126	84	212	40	183	314	171	330	>1500	?
Fe	490	3.7	5.6	6.2	4.8	1.8	1	1	640	>6000	0.006
Mg	14	34	28	32	15	12	23	19	31	250	?
P	3	3.8	6	10	5.2	5.3	7.1	10	16	300	1
Ti	190	< 1	< 1	< 1	< 1	< 1	< 1	< 1	240	>1500	<0.005

(*) - HALF OF THE VALUES REPORTED IN TABLE III

TABLE IV - IMPURITIES DISTRIBUTION MEASURED IN THE INGOT W 271
(FEEDSTOCK: # 10/2 50% AND Si EG 50%)

ELEMENT ppmw	CUBE n°					
	14	16	18	43	45	47
Al	1.5	3.0	3.0	5.1	6.5	2.0
B	2.5	2.8	4.1	2.4	2.9	3.1
Ca	27	47	66	250	250	28
Fe	1	1	3.0	4.7	4.5	2.6
Mg	21	16	26	80	62	13
P	2.1	2.5	4.0	7.5	5.6	6.5
Ti	<1	<1	<1	<1	<1	<1

TABLE V - IMPURITIES DISTRIBUTION IN THE INGOT W 273
GROWN USING INGOT W 271 AS FEEDSTOCK

TABLE VI - PHOTOVOLTAIC PROPERTIES OF SOLAR GRADE SILICON PRODUCED
BY HPS PROCESS.

WAFERS FROM INGOT n° W 273

WAFER SIZES:	10cm x 10cm x 0.04cm
TYPE:	P
RESISTIVITY:	$\bar{\rho} = 0.13 \Omega \times \text{cm}$
DIFFUSION LENGHT:	$\bar{L}_D = 40 \mu\text{m}$ (best value = 50 μm)
CONVERSION EFFICIENCY:	$\bar{\eta} = 6.2\%$ (100mW/cm ² , 25°C)
BEST VALUE of η =	$I_{sc} \times V_{oc} \times FF =$ $= 1.83 \text{ Amp} \times 0.549\text{V} \times 0.69$ $= 6.9\%$
ACTIVE AREA EFFICIENCY:	$\eta_a = \frac{6.9}{0.8} = 8.6\%$
RELATIVE EFFICIENCY:	$\eta/\eta_0 = 6.9/9.85 = 0.77$
TOTAL NUMBER OF MEASURED CELLS =	43

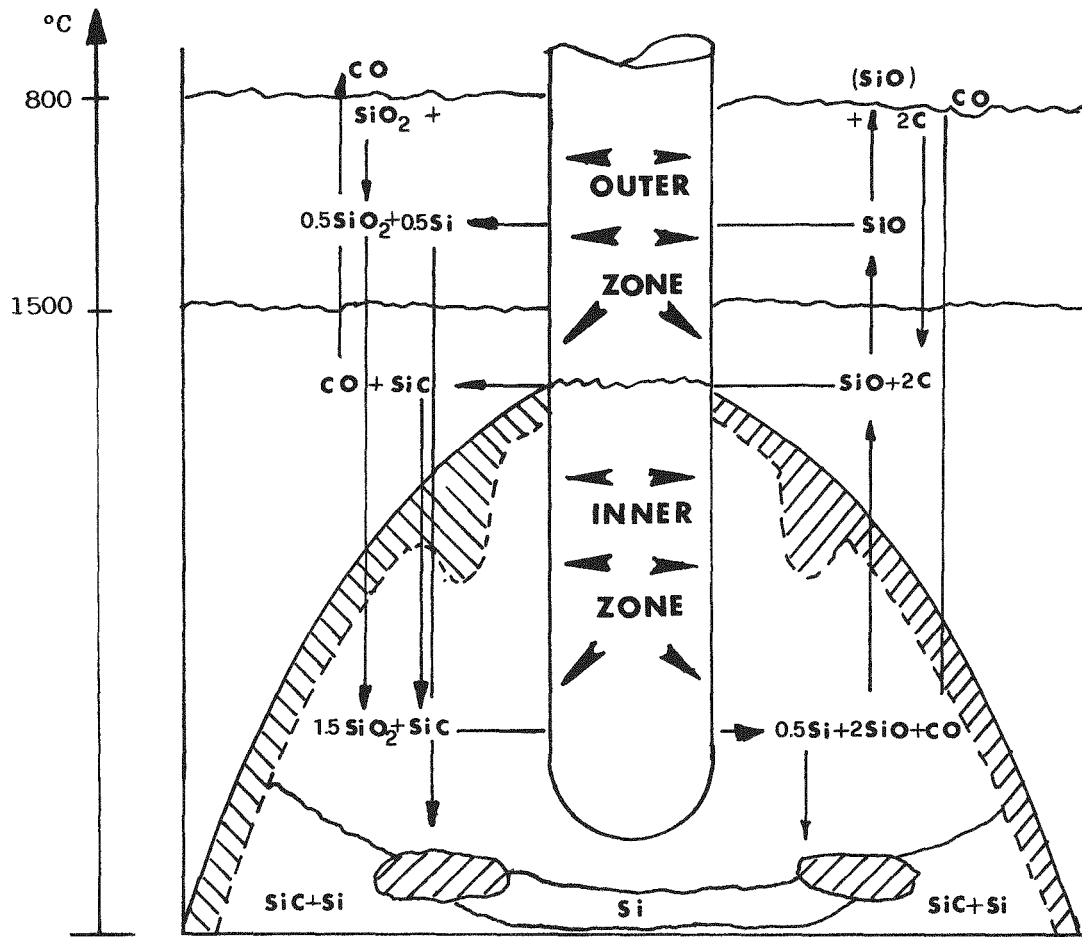
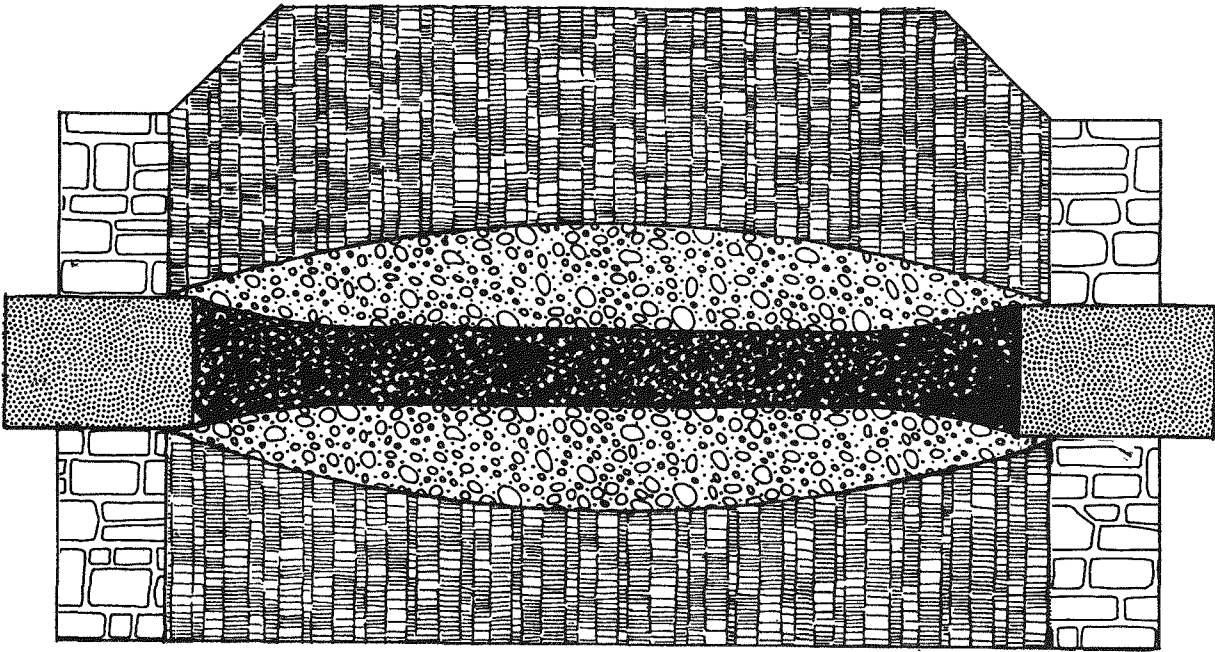


FIGURE n. 1 - SCHEME OF REACTIONS OCCURING INSIDE THE ARC FURNACE



	EXTRUDED PELLETS
	BRIQUETTES
	GRAPHITE
	ELECTRODES
	FURNACES WALLS

FIGURE n. 2 - VERTICAL SECTION OF THE ACHESON
FURNACE USED FOR THE SiC SYNTHESIS

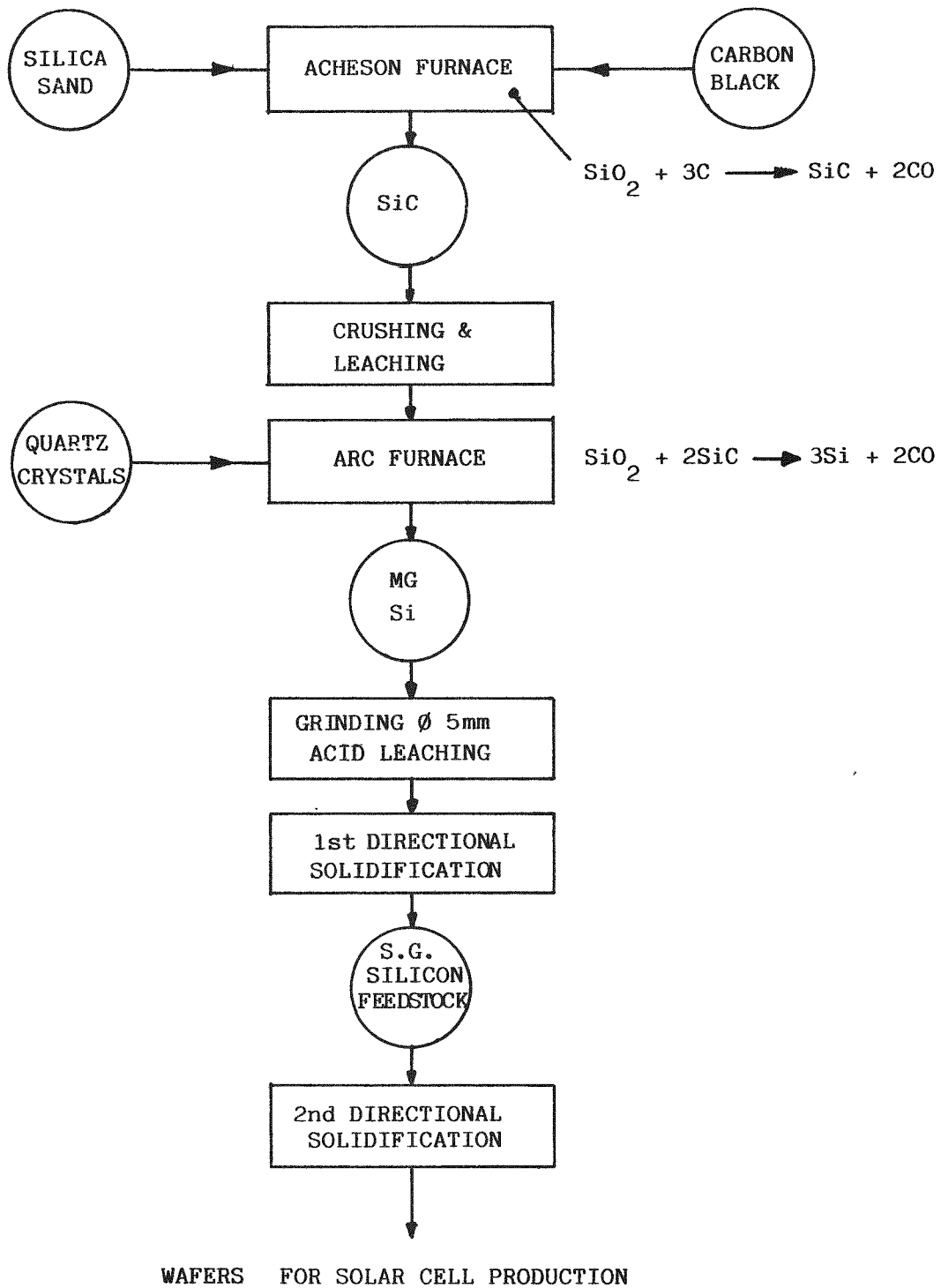


FIGURE n. 3 - SCHEMATIC FLOW CHART FOR THE HPS PROCESS

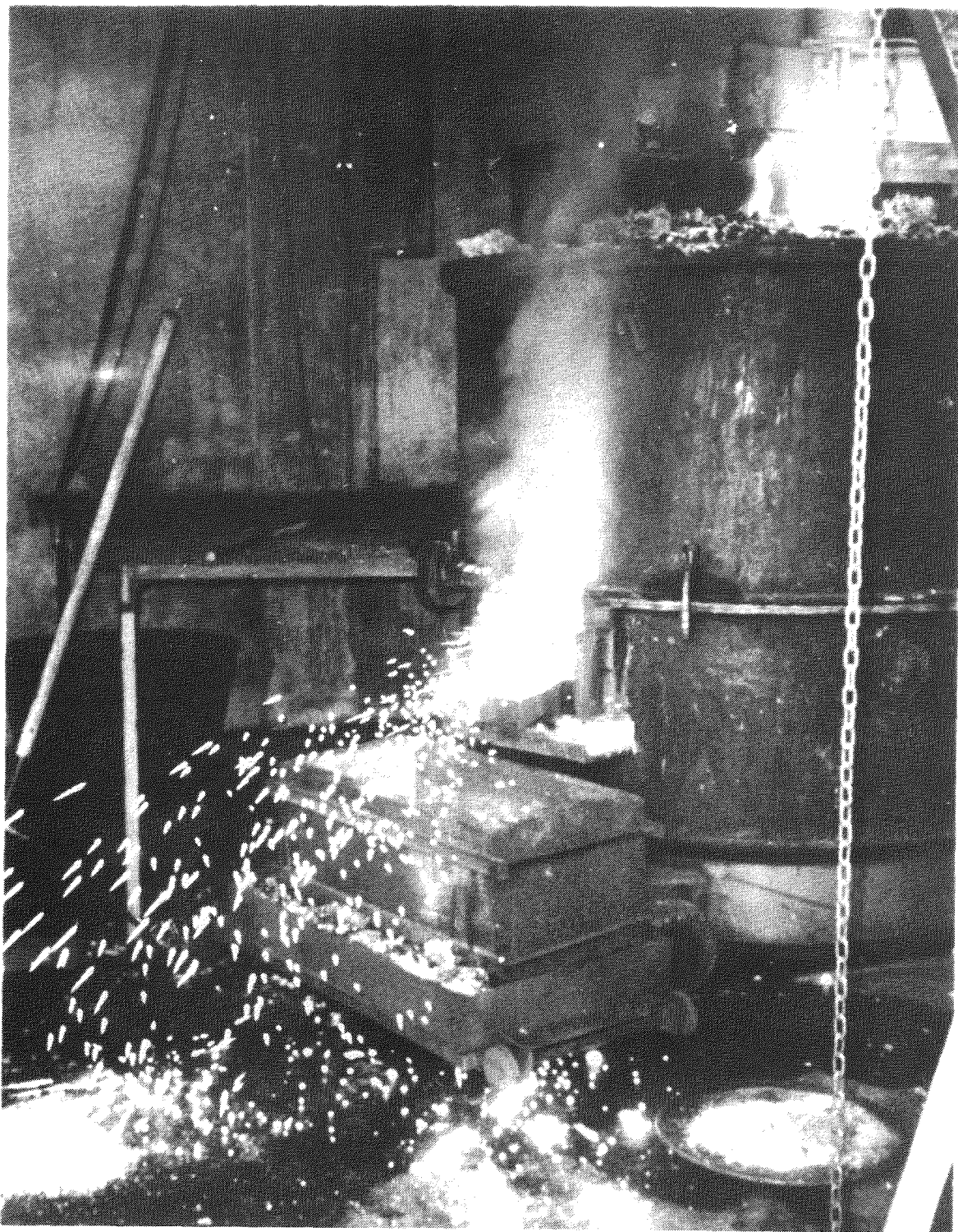
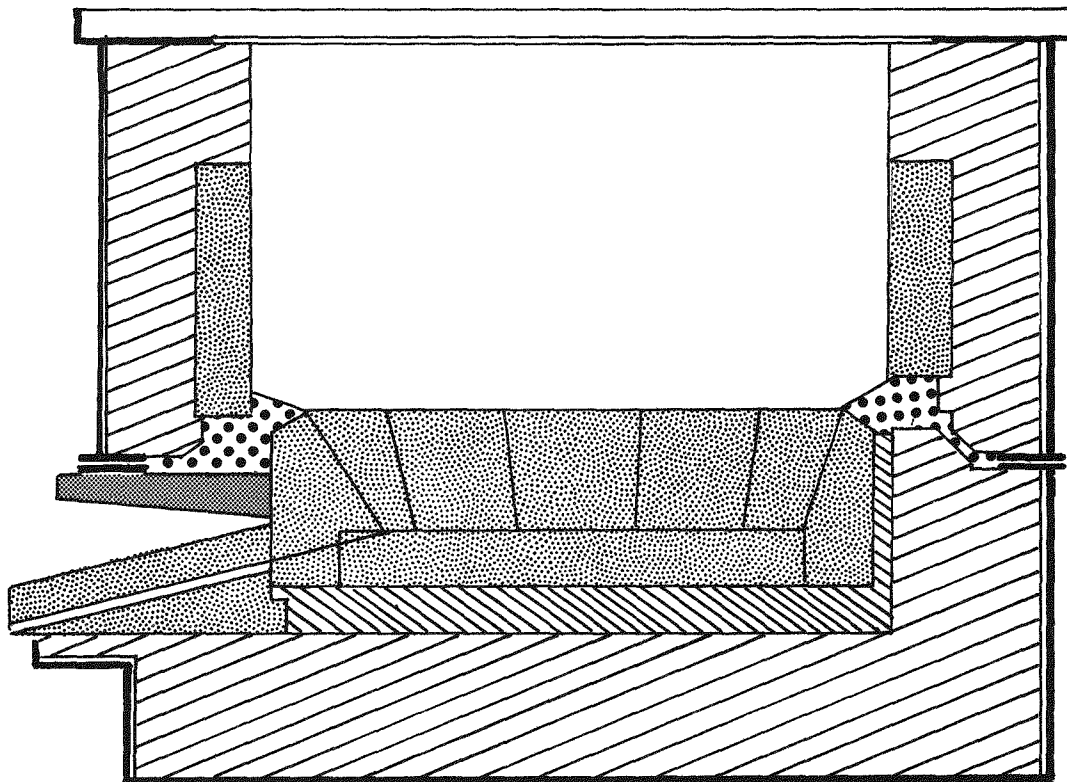


FIGURE n. 4 - Picture of the arc furnace during the smelting of silicon



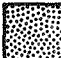




	GRAPHITE
	ALUMINA FIREBRICKS
	SILICA SAND
	ELECTRODE PASTE
	SiC

FIGURE n. 5 - SCHEMATIC VIEW OF THE ARC-
FURNACE USED FOR Si-METAL
SMELTING EXPERIMENTS

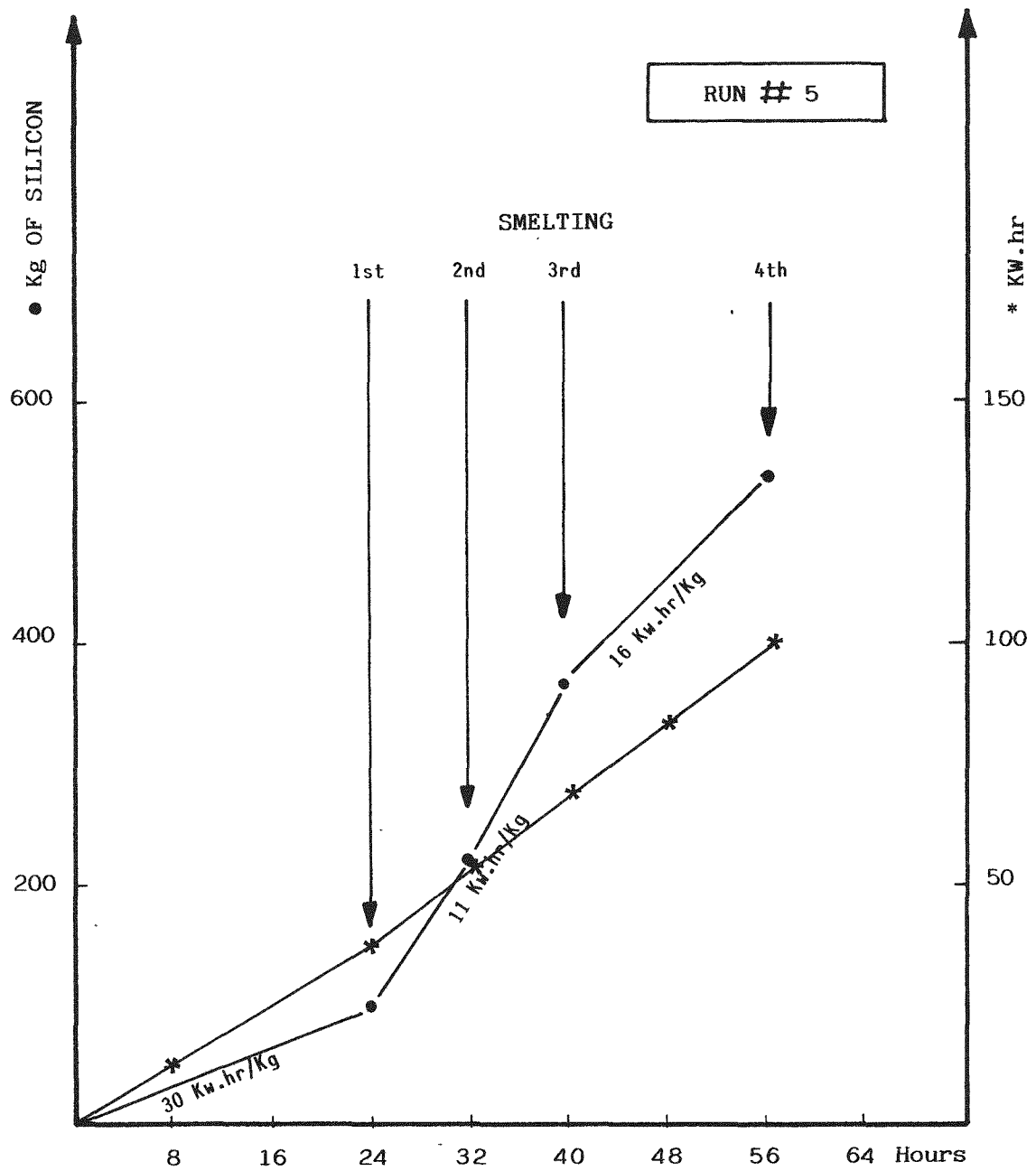


FIGURE n. 6 - SILICON METAL PRODUCTION IN 240 KVA ARC FURNACE UNDER CONTINUOUS OPERATION CONDITIONS IN HPS PROCESS

8	16	21	29	40	48	56	64	72	80	88	96	104	112
7	15	23	31	39	47	55	63	71	79	87	95	103	111
6	14	22	30	38	46	54	62	70	78	86	94	102	110
5	13	21	29	37	45	53	61	69	77	85	93	101	109
4	12	20	28	36	44	52	60	68	76	84	92	100	108
3	11	19	27	35	43	51	59	67	75	83	91	99	107
2	10	18	26	34	42	50	58	66	74	82	90	98	106
1	9	17	25	33	41	49	57	65	73	81	89	97	105

FIGURE n. 7 - VERTICAL SECTION OF THE INGOT W 271 GROWN FROM HPS 10/2. NUMBERED CUBES SUBJECTED TO CHEMICAL ANALYSIS REPORTED IN TABLE IV ARE SHOWN

DISCUSSION

AULICH: Do you feel that by eliminating impurities from the environment that you can obtain a material with low enough boron and phosphorus to make good solar cells without the addition of electronic-grade silicon?

RUSTIONI: We hope so, because we can demonstrate that in some cases the boron concentration is only 2 ppmw. In the run that I described, we could operate the arc furnace for 5 or 6 days, and we obtained 1 MT of this kind of metallurgical silicon with 2 ppm boron. But this is not sufficient, and we must improve to get < 1 ppmw boron. This is a real problem.

LUTWACK: Did you obtain cell efficiency data from baseline cells manufactured from semiconductor-grade silicon so that you could compare the cell data obtained for cells manufactured from your silicon?

RUSTIONI: Yes. The baseline cells made from electronic-grade silicon had efficiencies of 9 to 10%.

LUTWACK: Then the comparison is 6% with about 9%?

RUSTIONI: Yes, and it's not so bad. Now, Pragma is improving the quality of production.

WRIGHT: Using carbon black as the primary carbon source in the arc furnace operation, you ran 5 to 6 days before shutting down. On a much larger scale, say 1000 MT/year (which was what the Solarex plant was capable of producing), the use of carbon black as the primary source will tend to clog the furnace, so you will be forced to use a different carbon source. Then, the decrease in quality of the carbon product with an increase in the productivity of the arc furnace needs to be looked at so that there will be a dilution factor. The tradeoffs of each particular type of submerged arc furnace operation should be investigated.

RUSTIONI: It's possible to change the quality of the quartz lumps used in the carbothermic reduction with silicon carbide. Instead of using single-crystal quartz from Venezuela, we can use very high-purity quartzite. Silicon carbide and quartz powder can be leached, and briquettes can be prepared from silicon carbide and silica to improve the arc furnace operation. Of course, the cost of this type of processing must be considered.

MAYCOCK: I assume that the cell efficiencies you gave were for cells without anti-reflection coatings.

RUSTIONI: That's correct.

SESSION V

PROCESS DEVELOPMENTS IN THE USA

A. Briglio, Chairman



CHARACTERIZATION OF SOLAR-GRADE SILICON
PRODUCED BY THE SiF_4 -Na PROCESS

by

A. Sanjurjo, K. M. Sancier, R. M. Emerson and S. C. Leach
SRI International, Menlo Park, California 94025

J. Minahan
Spectrolab, Sylmar, California 91342

ABSTRACT

We have developed a process for producing low-cost solar grade silicon by the reaction between SiF_4 gas and sodium metal. In this paper we present results of the characterization of the silicon. These results include (a) impurity levels, (b) electronic properties of the silicon after crystal growth, and (c) the performance of solar photovoltaic cells fabricated from wafers of the single crystals. The efficiency of the solar cells fabricated from semiconductor silicon and SiF_4 -Na silicon was the same.

PRODUCTION AND ANALYSIS OF SILICON

Since the SiF_4 -Na process has been described previously,^{1,2} it will only be outlined briefly in this section.

The SiF_4 -Na process for producing silicon is shown schematically in Figure 1. Briefly, it consists of three major steps: production of SiF_4 , production of Si, and recovery of silicon. For the production of SiF_4 , NaF is added to an aqueous solution of H_2SiF_6 (a waste product of

the phosphate industry) to precipitate crystalline, nonhygroscopic, Na_2SiF_6 . The Na_2SiF_6 is filtered, dried, and thermally decomposed to form SiF_4 gas. The remaining solid residue of NaF is recycled to the precipitation step.

To produce silicon, the SiF_4 gas and sodium are fed continuously to a reactor where they react exothermically to form silicon crystallites dispersed in a matrix of NaF. The silicon is recovered from the product by one of two methods: (a) aqueous leaching of NaF followed by filtration and drying, or (b) melting of both phases to form two immiscible liquids that can be discharged separately. The results presented in this paper pertain only to leached separated silicon.

For convenience we used commercial SiF_4 gas as the source of silicon. We also used commercial sodium without any purification. In most of the production runs, the sodium was fed to a batch reactor as small, solid pieces. In two runs, the sodium was fed as a liquid.

The reactor was operated as follows. For solid sodium feed, the sodium pieces were located in a plastic hopper and fed continuously to the reactor by means of a screw feeder. For liquid sodium feed, the sodium was stored in a stainless steel melter and fed continuously to the reactor by a back pressure of argon gas. The pressure of SiF_4 in the reactor was kept approximately constant at 1 atm by means of a pressure regulator. The temperature of the reactor walls was kept at or above 600°C by means of external heating tapes. This operating temperature was selected to minimize the formation of the byproduct, Na_2SiF_6 , by the reaction between SiF_4 and NaF. The reactor vessel was made of Inconel 600 which contained a nickel liner, which in turn was lined with a graphite sheet (Grafoil, Union Carbide Corp.). In a production run we could produce as much as 10 kg of products containing approximately 1.4 kg of silicon and no unreacted sodium. The average production rate was about 0.5 kg of silicon per hour.

During the silicon recovery process, the products from each run were first separated mechanically from the Grafoil liner, crushed to particles smaller than 1 cm in diameter and loaded into the leaching

tanks. Deionized water was used to dissolve the NaF, and H₂SO₄ was added to the initial leach steps to retard silicon oxidation. The slurry of products in the aqueous media was stirred, allowed to settle, and filtered. The leaching process was continued until the fluoride ion concentration was below 10⁻⁴ M. At that point, silicon powder ranging in size from 1 micron to 1 mm was recovered by vacuum-filtration and dried in a vacuum oven. The recovery yield of silicon powder was typically around 90% with yields as high as 95%. Table 1 shows typical impurities of 14 batches of silicon powder. We used two different SSMS systems, one for Runs A to J, and a second one for runs K to N. High quality semiconductor polycrystalline silicon (10⁴ ohm-centimeters) was used to establish the limit of detection of each of the two SSMS systems used for analysis. The operational detection level is shown for each SSMS system in Table 1.

MELT CONSOLIDATION AND CRYSTAL GROWTH

Silicon powder samples were melted in a quartz crucible (7-cm i.d., 13-cm high) under an argon atmosphere. A film of slag was present on the ingots after melt-consolidation. The slag was removed by mechanical grinding and/or by chemical etching in HF or HNO₃-HF mixtures.

Silicon was grown into single crystals by the Czochralski method. A total of eight single crystals were grown from approximately 2 kg of silicon recovered from the melt consolidation steps. Typically 50% to 70% of the melt was pulled as a single crystal. Crystal 6 was grown from remains from the previous crystal growths. All were single crystal except No. 2 which became polycrystalline at 30% growth. The first seven crystals were oriented in the <1,1,1> direction, and the last crystal was oriented in the <1,0,0> direction. The SSMS analysis of two crystals of silicon are shown in columns 2 and 3 of Table 2. The last column shows the SSMS readings for high quality Monsanto semiconductor silicon (10⁴ ohm-cm) which was reported to have impurities in the sub-ppm w. level. This high purity silicon was used to determine the limit of detection of the SSMS system. Analysis of carbon and oxygen were made by infrared absorption spectroscopy.

ELECTRONIC CHARACTERIZATION

The electronic characterization of the single crystal wafers produced from the leach-recovered silicon was performed by several techniques and by several laboratories. A summary of the results of resistivity, mobility, and carrier concentration is shown in Table 3.

We measured the resistivity of the wafers from each of the eight single crystals with a four-point probe. For some samples, we used contactless, capacitive probes to verify the values obtained by the four-point probe. Because the agreement among the values obtained by the different techniques was good, only values obtained with the four-point probe are reported in Table 3.

The type of silicon was determined mainly by thermoelectric measurements. The results indicated that all crystals were p-type as shown in Table 3. We checked the results for crystal 1 by making a Si-electrolyte interface and studying its photodiode behavior; the photocurrent measurements confirmed that all crystals were strongly p-type.

We measured the mobility of the carriers in the silicon by using the Hall technique, and the results are shown in Table 3.

Carrier concentration was estimated by making a silicon wafer electrode in an electrolytic solution and studying the capacity that could be developed in the silicon by applying a potential across the silicon/electrolyte interface. The silicon wafer was polished and etched to diminish the density of surface states due to mechanical damage. Thus, the capacitance measured was essentially equal to the capacitance in the bulk (space charge region) of the semiconductor.

The voltage dependence of the space-charge capacitance of the semiconductor at the electrolyte/semiconductor interface was plotted according to the Mott-Schottky relationship for a p-type semiconductor

$$1/C^2 = \frac{2}{qN_A \epsilon \epsilon_0} (-V + V_{fb} - kT/q)$$

In this equation, q is the charge of the electron, N_A is the acceptor density, C and C_0 are the dielectric constants in the semiconductor and in vacuum, respectively, V is the applied potential, and V_{fb} is the flatband potential. From the sign of the slope of this equation, we can determine the conductivity type of the material. We confirmed in this way that our silicon is a p-type semiconductor. From the magnitude of the slope, we calculated N_A , the acceptor density, to be 3.9×10^{-16} reciprocal centimeters for a wafer from crystal 1. The carrier concentrations for all other crystals were obtained from resistivity and mobility values determined by the standard Hall technique.

The carrier lifetime (τ) was determined with a Loe instrument from photocapacitance decay curves. In this technique a Xe laser pulse hits the surface of the wafer and produces an increase in electron-hole pairs that immediately start to recombine to reestablish equilibrium. The temporary increment in carrier concentration results in an increase in conductivity that can be detected by the change in intensity of the reflection of microwaves on the silicon wafer. The lifetime was determined by following the decay in conductivity with time after the light pulse. The silicon wafers were used as-cut, without any polishing to diminish surface states. Therefore, the measured lifetime values reported here may be smaller than that of intrinsic bulk lifetimes.

Another technique for measuring very low concentrations of impurities is deep level transient spectroscopy. Measurements were performed in this technique on wafers from crystal 1 by Dr. P. Claus et al. of the University of Ghent in Belgium. There were no detectable traces of transition metal contamination.

SOLAR CELL FABRICATION AND CHARACTERIZATION

The following procedure was used to prepare the silicon wafer for fabrication as solar cells and subsequent characterization of the cells. A number of 2-inch diameter control wafers of high quality semiconductor silicon (1-3 ohm-cm) were included with the fabrication lot. Wafers were cleaned and then etched to a thickness of ~ 0.025 cm. This was expected to remove mechanical damage that might have arisen from slicing the wafers. Following rigorous surface cleaning, the wafers were placed in a quartz boat and inserted into a clean quartz tube within a furnace at 825°C . The wafers were subjected to a 5-minute warmup in a nitrogen/oxygen atmosphere; to phosphorous deposition for 3 minutes in a mixture of nitrogen, oxygen, and phosphine; and to a 5-minute "drive" in nitrogen.

After removing the wafers from the diffusion furnace, resistivity (V/I) measurements were made using a four-point probe.

The front of the wafers were masked with ink, dried, and then etched in a 60:40 solution of HNO_3 :HF for 5-8 seconds to remove the n^+ type layer from the base. A dicing saw was used to cut the wafers into 2-cm squares. All cells were cleaned, and then mounted in evaporation masks and metallized, front and back, with an electron gun evaporation system. Titanium, palladium, and silver were deposited, in that order, on the front of the wafers with layer thicknesses of 800A, 400A, and $\sim 50,000\text{A}$, respectively. Aluminum, titanium, palladium, and silver were deposited in that order on the back of the wafers. The 2 cm x 2 cm metallized solar cells were then mounted in masks and placed in an electron beam evaporator. Dual anti-reflecting films of TiO_2 and Al_2O_3 were deposited on the front surface. Wafer edges were then etched, after masking front and back, to remove any inadvertently-deposited metals from the cell edges. The contact metallization system used on each cell occupied 0.172 cm^2 of the cell front area. Each of the 20 grid lines were 0.0033 cm in width, while the ohmic bars and contact tables occupied 0.032 cm^2 . Front metallization thickness was approximately 0.0006 cm.

The solar cells were characterized as follows. Illuminated I-V measurements were made using a Spectrolab X-25 Solar Simulator. Spectral response was measured using a 14 segment filter wheel assembly. Measurements of resistivity, V/I, and dark current were made using conventional volt meters and power supplies. The maximum power point was measured from the I-V curve using standard power curves. Fill factor, FF and efficiency, EFF were calculated using

$$EFF = \frac{P_{\max}(\text{mW})}{135.3 \text{ mW/cm}^2 \times 4 \text{ cm}^2}$$

$$FF = \frac{I_{\max} \times V_{\max}}{I_{\text{sc}} \times V_{\text{oc}}}$$

The results of the characterization of the solar cells are shown in Table 4 for the open circuit potential (VOC), short circuit current (ISC), maximum power (PMX), fill factor (FF), and efficiency (EFF) at AMO. In the last column is shown the value of the efficiency at AML which was calculated by multiplying the value of AMO by the factor 1.14 (10). The SiF₄-Na cells examined were made from wafers cut from four crystals: 3, 5, 7, and 8, with the slice number (starting from the seed end) following the hyphen. The eight cells made from semiconductor silicon are indicated by a prefix C. The low efficiency of cell 7-11 resulted from a shunting problem that occurred during manufacture.

The overall results indicate that solar cells made from SiF₄-Na silicon have efficiencies equal to those made from semiconductor grade silicon in the same batch.

DISCUSSION

It is possible presently to use the impurity content in silicon to predict the suitability of polycrystalline silicon for the manufacture of single crystal solar cells. The work by Hill at Monsanto⁴ and of

Hopkins et al.⁵ and Davis et al.⁶ at Westinghouse resulted in the establishment of maximum levels that can be permitted for each impurity in silicon without affecting the efficiency of solar cell manufactured from that silicon. The work done by Pizzini⁷ and Galluzi et al.⁸, among others, has also started to establish the same type of levels for polycrystalline silicon solar cells. These definitions cannot be taken as absolute guidelines as pointed out by the authors above because the efficiency of the solar cells also depends on the type of crystal growth and the cell manufacturing process. Nevertheless, these impurity values (such as in Table 5) can be used as general guidelines. Therefore, the first test of the suitability of our silicon for solar cell manufacture was to analyze it. Because the maximum allowable impurity levels in solar grade silicon (Sol-Si), as established by the authors mentioned above, are roughly at the low ppm w. level, only techniques such as Spark Source Mass Spectrometry (SSMS) can be used. Even when using the SSMS technique, some precautions have to be taken in order to obtain reliable analyses. Some of the typical sources of error in the SSMS values include common sampling errors, inhomogeneity of the sample, and SSMS system background shifts or contamination. We determined first the limits of detection of the SSMS systems by analyzing very high purity Monsanto polycrystalline semiconductor silicon (10,000 ohm cm). We use these readings to define the limit of detection for each impurity. We also determine the reliability of the readings by analyzing the same sample in different days. We concluded that the reproducibility of the readings was not perfect, but most of the readings for each impurity were within a factor of 2 from the average. This finding is similar to that reported by Hunt et al.⁹ The sampling errors and inhomogeneity of the sample were less of a problem. In our case, the silicon is in the form of powder with an average particle size of 100 microns. The samples were taken using normal sampling techniques and we believe, therefore, that they were representative of each batch.

Taking the preceding remarks into account, we can interpret the values in Table 1 (runs I to J) as indicating that all the silicon batches were very pure and they all had similar composition. This

result is of great industrial importance because it gives assurances that the purity of silicon produced by the SiF_4 -Na process will be constant. In addition, because the readings were so close to the limit of detection, we suspected that the silicon might be purer than those readings indicate. In effect, when a different SSMS system (System 2 in Table 1, runs K to L) with higher sensitivity was used, the readings for some of the impurities were lower, although the silicon had been produced in basically the same conditions as before. In particular, Ti readings were a few ppm.w in System 1, but they were below 200 ppb.w in batches analyzed with System 2. Phosphorous readings were also lower with System 2. Later, we determined that all the silicon is strongly p-type, without any sign of compensation and has a resistivity of 0.3 to 5 ohm cm which indicate P levels much lower than those indicated by the SSMS readings. In Table 5, we compare the readings in System 2 with the definition of solar grade as proposed by Hopkins et al. It is clear that the SiF_4 -Na silicon is much purer than required for solar cell manufacture. The only possible exception is Na, but as we describe below, this impurity can be removed almost completely.

The melt consolidation and crystal growth step result, as expected, in great purification, as can be seen by comparing the values in Tables 1 and 2. The level of Na, which is typically at the 10^2 ppm w level in the silicon powder, is below detection limit in the polycrystalline ingot and, naturally, in the final silicon crystal. In independent mass spectrometric studies we have observed that Na in silicon starts vaporizing at 600°C and the volatilization becomes very fast at temperatures above 1000°C . The low initial levels of the transition metals in the silicon powder, combined with the normal purification during crystal growth, should result in values at the sub ppb w levels. In effect, Deep Level Transient Spectroscopy studies of the silicon wafers from crystal 2 did not show any indication of the existence of transition metals. The limit of detection for this technique ranges from 10^{12} to 10^{14} atoms per cm^3 . Therefore, the readings for the transition metals in Table 2 for crystals 1 and 2 are again indicative of the limit of detection of the SSMS system. These

readings and those for the semiconductor silicon also illustrate the typical variability of the limit of detection of the SSMS system for three extra pure but different samples.

The variations in the values of the electronic parameters are not well understood yet (more studies are in progress), but they were well within the range expected for crystals grown from different melts, obtained from the mixture of powders from different production batches. When the crystals were grown from exactly the same melt as was the case for crystals 3 and 4, their characteristics were reasonably similar. Crystal 6 was grown from remains of previous crystal growths. Its higher resistivity and lower mobility may be due to high content of C.

The photovoltaic behavior of the silicon was studied in several laboratories, and solar cells were manufactured in experimental and in industrial lines. The results were consistently indicative of high performance indistinguishable from that of cells made from semiconductor silicon. Although all crystals (except No. 2) were investigated, only the results of crystals 3, 5, 7 and 8 are shown here. The efficiency values were determined in AMO conditions. Based on results obtained at Spectrolab¹¹ and elsewhere, we know that the efficiency at AMI can be estimated by multiplying the AMO efficiency by a factor which ranges in value from 1.14 to 1.18. Taking the conservative approach, we used the 1.14 value in this work to estimate the AMI values shown in Table 4.

A comparison of control cell and experimental cell efficiencies would indicate that the better lifetime to be found in the semiconductor silicon has resulted in a somewhat better short circuit current characteristic, especially in the case of the lower resistivity material. This shortcoming is balanced however by the higher open circuit voltage that one expects from lower resistivity base material. Efficiency can be enhanced by means of front surface texturing [(100) only] and by introduction of a back surface field on the higher resistivity material. A back surface field effect will be more obvious on higher lifetime material. Some examples of these effects are shown in Table 6.

CONCLUSIONS

Silicon produced from commercial SiF_4 and Na is more than pure enough to be used in the fabrication of solar cells of high efficiency. All the results obtained--chemical analysis, electronic parameters, cell efficiencies--demonstrate clearly the high quality of the SiF_4 -Na silicon.

The fact that the quality of the silicon was consistently high in all batches indicates clearly that the process can be scaled up with confidence to the industrial scale. This process produces silicon of much higher purity than any of the processes developed for solar cell manufacture based on the direct purification of metallurgical grade silicon, and at a projected cost much lower than the projected costs for halosilane-based processes. Therefore, it holds great promise for decreasing the overall cost of silicon solar cells.

ACKNOWLEDGEMENTS

We wish to thank Dr. W. Allred of Crystal Specialties, Inc. and Mr. R. May of Aerojet General Corp. for growing the single crystal. We also wish to thank our colleagues, Drs. P. Jorgensen and D. Hildenbrand and Mr. J. Harsch, for their advice and support of the program, as well as Dr. Marc Madou for this electronic characterization, and Messrs. George Craig and Mike Gusman for their technical support. We also wish to express gratitude to our colleagues Dr. G. Marchetti of Enichimica; Drs. G. Missoni, G. Sironi, F. Galluzzi and E. Scaffè of Eniricerche (Italy) for their advice and comments.

REFERENCES

1. A. Sanjurjo et al., J. Electrochem. Soc. 128(1), 79 (1981).
2. A. Sanjurjo and K. Sancier, "Silicon Material Preparation and Economical Wafering Methods," R. Lutwack and A. Morrison, E. Noyes, Publishers, New Jersey, U.S.A. (1984).
3. Marc Madou, "Bulk and Surface Characterization of Silicon," Surface Science, Vol. 108, pp. 135-152 (1981).
4. D. E. Hill et al. Final Report, "Determination of a Definition of Solar Grade Silicon," ERDA/JPL RA54-338-76 (1976).
5. R. Hopkins et al., Final Report, "Effect of Impurities and Processing on Silicon Solar Cells," DOE/JPL 954-331-81/14 (1982).
6. S. R. Davis et al., IEEE Trans. of Elect. Devices, ED-27, 677 (1980).
7. S. Pizzini et al., "Materials and New Processing Technologies for Photovoltaics," Ed. J. Amick, V. Kapur. S. Dietl, Proc. J. Elect. Soc. 83(11), 200-220 (1983).
8. F. Galluzi et al., Extend. Abst., J. Electrochem. Soc. 84(2), Abst. No. 340 (1984).
9. L. Hunt et al, Extend. Abst., J. Electrochem. Soc.
10. G. F. J. Garlick, Private Communication.
11. J. A. Minahan et al., "Solar Cells Fabricated with Unconventional Silicon Materials", Proceedings IEEE 15th Photovoltaic Specialists Conference, Orlando, FL. (1981) p. 608.

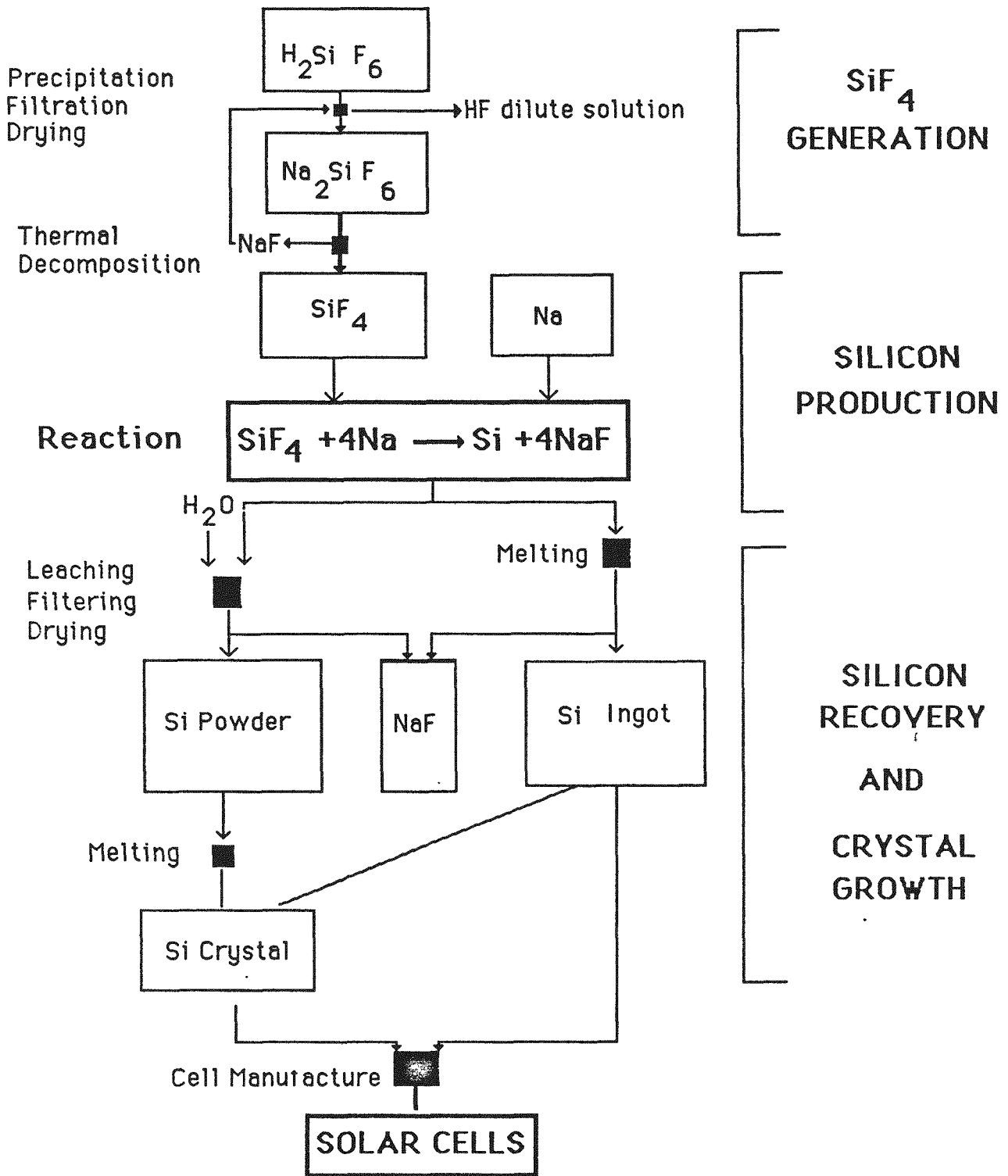


FIGURE 1. Schematic of the SiF₄ - Na Process

Table 1
SPARK SOURCE MASS SPECTROMETRY ANALYSES OF LEACH-RECOVERED Si POWDER (ppm, w.)

Impurity	SSMS SYSTEM 1											SSMS SYSTEM 2				Limit of Detection
	A	B	C	D	E	F	G	H	I	J	K	L	M	N		
B	0.2	0.1	<0.1	0.2	<0.1	0.1	<0.1	<1	<0.1	<0.1	<0.1	0.2	0.2	0.04	0.02	0.02
Al	0.8	0.4	0.4	2	0.4	3	1	0.1	0.3	0.2	0.4	2	0.2	0.1	0.1	0.2
P	1	2	2	4	0.7	0.2	0.1	1	1	0.6	0.3	0.2	0.1	0.05	0.03	0.05
As	0.6	2	2	0.3	4	1	1	2	3	1	<0.3	<0.3	<0.3	<0.3	<0.3	<0.03
Ti	3	1	1	2	6	2	0.3	7	4	4	0.2	<0.2	<0.2	<0.2	<0.2	<0.08
Zr	<0.1	0.1	<0.3	<0.4	0.5	<0.3	0.1	0.3	0.4	0.7	<0.3	<0.3	<0.3	<0.3	<0.3	<0.1
V	<0.1	0.1	<0.1	0.1	0.1	<0.1	<0.1	0.1	<0.1	<0.1	<0.3	<0.2	<0.2	<0.2	<0.2	<0.08
Pa	0.4	--	<0.1	0.8	<0.1	<0.1	<0.1	<0.1	<0.1	<0.1	<0.3	<0.7	<0.7	<0.7	<0.7	<0.2
Cr	1	4	4	<6	<1	2	3	11	11	13	<0.3	0.7	<0.4	<0.4	<0.4	0.1
Mo	<0.6	1	1	2	0.9	1	0.7	1	1	0.7	<0.3	<0.3	<0.3	<0.3	<0.3	<0.1
W	<0.1	--	<0.1	<0.1	<0.1	<0.1	<0.1	<0.1	<0.1	<0.1	<0.3	<0.7	<0.7	<0.7	<0.7	0.2
Mn	0.3	0.1	<0.1	0.1	0.7	0.7	0.1	0.5	0.2	0.1	<0.3	0.1	0.04	0.04	0.04	0.05
Fe	--	--	--	--	--	--	--	--	--	--	<0.3	<2	<2	<2	<2	<0.4
Co	--	--	--	--	--	--	--	--	--	--	0.5	<0.2	<0.2	<0.2	<0.2	0.1
Ni	--	--	--	--	--	--	--	--	--	--	4	<0.4	<0.4	<0.4	<0.4	<0.2
Cu	0.9	--	0.9	0.5	2	1	0.7	3	2	0.8	0.2	0.5	0.07	0.05	0.03	0.2
Zn	4	--	3	1	1	6	0.7	0.9	1	1	15	<0.2	<0.2	<0.2	<0.2	<0.3
Na	<160	230	<230	<370	<480	<330	<160	<340	160	<390	9	<300	<100	3	2	1
K	17	--	14	9	23	36	96	4	20	12	0.1	3	3	0.8	0.8	1
Mg	3	9	9	6	2	14	3	6	2	3	<0.3	2	<1	<1	<1	0.1
Ca											0.1		15	3	3	1
Ba	<0.5	--	<0.4	4	<5	0.3	<1	1	<0.1	<0.1	--	<0.5	<0.5	<0.5	<0.5	<0.5
S	5	2	2	3	20	7	7	3	5	21	--	<0.1	<0.1	<0.1	<0.1	--

Table 2
 SSMS ANALYSIS OF SRI SILICON CRYSTALS AND SEMICONDUCTOR REFERENCE
 (ppmw)

Impurity	SRI Si CRYSTAL		Semiconductor
	1	2	Si
B	0.02	0.08	0.02
Al	0.3	0.2	0.2
P	0.03	0.1	0.05
As	< 0.03	< 0.05	< 0.03
Ti	< 0.08	< 0.1	< 0.08
Zr	< 0.1	< 0.1	< 0.1
V	< 0.08	< 0.1	< 0.008
Ta	< 0.3	--	< 0.2
Cr	< 0.08	0.04	0.1
Mo	< 0.2	--	< 0.1
W			< 0.2
Mn	0.02	--	0.05
Fe	< 0.4	2	< 0.4
Co	< 0.2	< 0.2	< 0.1
Ni	< 0.2	< 0.2	< 0.2
Cu	0.2	0.02	0.2
Zn		< 0.08	< 0.3
Na			1
K	--	--	1
Mg	0.05	0.05	0.1
Ca	0.07	0.1	1
Ba	--	--	< 0.5
C	6-10	5*	1*
O	12	10*	10*

*Infrared Absorption Nicolet Spectrometer

Table 3
CRYSTALLOGRAPHIC AND ELECTRONIC PARAMETERS

Parameter	Crystal							
	1	2	3	4	5	6	7	8
Orientation	<111>	<111>	<111>	<111>	<111>	<111>	<111>	<100>
Resistivity ρ (Ω cm) _i	0.5 ± 0.05	2	0.6 ± 0.2	0.65 ± 0.05	0.6 ± 0.1	1.3 ± 0.05	2 ± 0.2	0.35 ± 0.05
Type	P	P	P	P	P	P	P	P
Mobility ($\text{cm}^2/\text{V s}$) _i	310-320	--	--	278	215	-82	184	203-303
Carrier concentration (atoms/ cm^3)	3.9×10^{16}	--	--	3.6×10^{16}	4.8×10^{16}	7.5×10^{16}	2.25×10^{16}	$9.9-5.7 \times 10^{16}$
Carrier lifetime (μs)	5-14	3.						
Diffusion Length			120-150	80-130	100-110	100-130	100-150	120-150

Table 4
SOLAR CELL CHARACTERISTICS

		VOC (MV)	ISC ^a (MA)	PMX (MW)	CFF	EFF(AM0) %	EFF(AM1) ^b %
	C-3	603	150	67.9	.750	12.5	14.3
	C-17a	592	154	72.9	.799	13.5	15.4
	C-17b	591	155	72.0	.786	13.3	15.2
Control Cells (Semi- Si)	C-18a	591	153	69.7	.771	12.9	14.7
	C-18b	589	155	69.4	.761	12.9	14.6
	C-19	585	153	71.5	.799	13.2	15.0
	C-20a	591	154	71.6	.787	13.2	15.0
	C-20b	586	153	66.7	.744	12.3	14.0
	3-B	615	153	73.4	.780	13.6	15.5
	5-30	600	145	67.0	.770	12.4	14.1
	5-24	596	148	67.0	.759	12.4	14.1
	5-85	607	149	71.4	.789	13.2	15.1
Sample Cells (SRI-Si)	5-12	608	149	71.0	.784	13.1	14.9
	5-42	608	150	72.1	.790	13.3	15.2
	7-11	222	143	15.4	.485	2.8	--
	7-63	585	153	67.7	.757	12.5	14.3
	7-57	576	152	67.6	.770	12.5	14.3
	8-26	615	150	67.7	.734	12.5	14.3

^a2 x 2 cm cells.

^bEFF(AM1) estimated from AM0. Multiplying factor 1.14.

Table 5
 IMPURITY THRESHOLD LEVELS FOR SOLAR GRADE Si
 VERSUS
 IMPURITY LEVELS IN Si PRODUCED BY THE SiF₄-Na PROCESS

Element	<u>Impurity Threshold Levels</u>		
	100% Max Efficiency ^(a)	90% Max Efficiency ^(b)	Si from SiF ₄ -Na
Al	0.4	0.7	0.1-0.2
Ti	0.9	4.5	< 0.2
Zr	10.5	325	< 0.3
V	0.6	4	< 0.2
Ta	--	90	
Cr	16	133	< 0.4-0.7
Mo	--	65	< 0.3
W	--	1000	< 0.7
Mn	16	150	0.04-0.1
Fe	32	372	< 2
Co	10	194	< 0.2
Ni	17	--	< 0.4
Cu	280	4500	0.03-0.5

(a) Maximum impurity level allowed in polycrystalline silicon feedstock that does not result in degradation of single crystal solar cells manufactured from that silicon.

(b) Impurity level that results in single crystal cells with only efficiencies of 90% of those produced with ultrapure semiconductor Si.

Table 6
EFFECTS ON CELL EFFICIENCY OF BACK SURFACE FIELD, AND TEXTURE

<u>Cell No.</u>	<u>V_{oc}</u>	<u>I_{sc}</u>	<u>FF</u>	<u>η(AMO)</u>	<u>Projected η(AMO)</u>
C-1**	585	173	.639	12.0	15.0
C-5a*	612	164	.779	14.4	14.8
3-B	615	153	.780	13.6	13.9
C-17a	592	154	.779	13.5	13.5
7-10*	593	159	.655	11.4	13.9
7-63	585	153	.757	12.5	13.2
8-28*	602	150	.692	11.5	13.3
8-26	615	150	.734	12.5	13.6

*Back surface field.

**Back surface field, front textured cell.

Note: The projected efficiency at AMO is the efficiency that cell would have had if its fill factor were .799, the value for Cell C-17a.

DISCUSSION

SCHWUTTKKE: I congratulate you on your semiconductor-grade silicon. I assume that you have used this material to make solar cells. What kind of cell efficiency did you obtain using this type of material?

SANJURJO: You mean the last material? No, we haven't.

SCHWUTTKKE: Oh, that's too bad.

SANJURJO: Well, I think so, but basically our program has been switched to preparing semiconductor-grade silicon.

SCHWUTTKKE: I think it would be extremely interesting to determine cell efficiencies using this material.

SANJURJO: Every time we made solar cells with the previous material, we had the possibility of getting even higher efficiencies and we were limited by several things. One was the saw damage, which was not properly etched. There were some problems in the fabrication itself so that when we tried to use back-surface fields, we had very scattered data with shunting of several of the cells, including the control cells. Therefore, we were limited to a certain extent. We could have probably obtained high efficiency for both the semiconductor-grade and solar-grade cells. One thing that we would like to do is to get the highest purity material we can, and try to make the best solar cells and then compare it with our product.

SCHWUTTKKE: Looking at the cell data of the Spectrolab labs and cells from your solar-grade material, the efficiencies are very similar. Are the areas for the cells the same?

SANJURJO: The same. All of these cells were 2 x 2 cm cells, and they were co-processed and intermixed.

SCHWUTTKKE: Did Spectrolab use a standard baseline process or a high-efficiency process?

SANJURJO: For their level, I think it was a standard process.

SCHWUTTKKE: Do the cells have a back-surface field?

SANJURJO: No. The cells were without back-surface field. Then we tried with the back-surface field. The particular batch used had several short-circuited cells. The aluminum somehow got through on both batches of the semiconductor grade and on our material. I have some information in the paper regarding the effect of back-surface fields. The major effect was probably in the semiconductor silicon cells which had a diffusion length of about 180 μm and higher. Our best cells were about 150 to 180 μm , and some of the others were 100 to 150 μm .

SCHWUTTKE: What was the cell thickness: 150 or 200 μm ?

SANJURJO: We used 300 to 500 μm . The cells were made not only by Spectrolab, but also by two other laboratories, one of which used an industrial-cell fabrication line. The efficiencies of the reference semiconductor cells were always the same, but the cells from the industrial line had lower efficiencies. The nominal average for both semiconductor and our cells was 12.5% AM1.

LEIPOLD: I noticed that the open-circuit voltage for the cells made from your material was higher. Were they the same base resistivities? Do you have an explanation?

SANJURJO: There was a slight difference. Our cells had higher open circuit voltage, and the semiconductor cells had higher short-circuit current. There is some information relative to this in the paper, but more work is needed to characterize the material. We felt that the crystals were very good for the first attempt, but better crystals are required. We were limited by the crystals and by the processing of the wafers to a point that we did not make any determination with respect to any other differences. The differences are probably due to the crystal growth rather than the material.

A SILANE-BASED POLYSILICON PROCESS

Paul E. Grayson
Eagle-Picher Industries, Inc.
Miami, OK.

James Jaffe
Allied Corporation
Morristown, N.J.

INTRODUCTION:

Commencing in early 1981, a joint development program to pilot demonstrate a silane based polysilicon process was constructed at Eagle-Picher Laboratories in Miami, Oklahoma. The pilot plant included technologies contributed by Allied Corporation of Morristown, New Jersey, Eagle-Picher Industries of Miami, Oklahoma, and G. A. Technologies, Inc. of San Diego, California. The described process as piloted included the synthesis of crude silane gas, ultra purification of the gas, and then direct pyrolysis to product silicon. Features of the process provided for direct continuous operation from process feed to final product, without the requirement to store intermediates or ever convert the silane to a liquid phase. Semiconductor quality product as analyzed internally, and confirmed by independent laboratories, was demonstrated by the first integrated operation of the plant.

The project organizational responsibilities were as shown in Figure 1. The pilot plant described by this paper was constructed by the engineering and technical staff of the participating companies in residence at the Miami, Oklahoma site. The results of the first integrated operation of the plant as evaluated by Monsanto, are as shown in Figure 2.

The process development, although considered by all participants to be technically and financially very successful was abandoned in late 1982 for business reasons unrelated to this project.

ALLIED PROCESS:

In early 1980 Allied was considering making fumed silica from by-product fluosilicic acid on a large scale. Fluosilicic acid is formed in a phosphoric acid plant when the silicon tetrafluoride from the main rock digester is scrubbed. Large quantities of fluosilicic acid are available and much more could be made available if a market existed. Phosphate rock contains about 3.5% fluorine and about 30 - 50% of that fluorine can be recovered as fluosilicic acid.

The silicon tetrafluoride is produced from fluosilicic acid by reaction with strong sulfuric acid, which acts as a dehydrating agent.



The hydrofluoric acid can be further reacted by the addition of silicon dioxide



Allied looked at possible routes to photovoltaic silicon and decided to pursue two paths. The first was the use of high temperature plasma to react to the silicon tetrafluoride with hydrogen.



This route was considered the most desirable since Allied is the largest merchant producer of hydrofluoric acid in the U.S. No by-product would be produced.

A contract was let with Columbia University, who had an operating thermal plasma, to develop feasibility. The plasma process could not get greater than 5% yields of silicon, as it was not possible to quench the reactor products before most of the fine silicon recombined with the HF.

Concurrently, the reaction of sodium hydride with silicon tetrafluoride was investigated at Allied's Morristown, New Jersey laboratories.



A process was discovered that gave high yields of silane at moderate conditions. The silane was of high purity, as could best be determined by standard analytical procedures.

This process is covered by U.S. Patent No. 4,374,111 dated February 15, 1983.

With silane, it was apparent that purification could be effected by many methods and a literature search revealed that considerable work had been done. Allied decided that the immediate future of silicon lay in semiconductor grade, although it would be desirable to have a process that could produce silicon cheap enough to compete in the photovoltaic market. Allied made plans to pursue the necessary research to purify silane, produced from SiF_4 , and the subsequent decomposition of the purified silane into semiconductor grade silicon.

At about this time, Allied was approached by Eagle-Picher to investigate the possibility of a joint venture to produce semiconductor silicon. Eagle-Picher had a process to purify silane and had also contacted General Atomic, who were in position to develop a process for the decomposition of the purified silane.

In a surprisingly short period of time, the three-party venture was approved and an agreement reached on a joint pilot plant to produce 1 kg. per hour of semiconductor silicon. The pilot was built at Eagle-Pichers'

Miami, Oklahoma facility. Allied's facility included two units. Photographs of the units are in Figure 3 and 4.

The first unit produced silicon tetrafluoride from purchased fluosilicic acid. Figure 5 shows how this was accomplished.

Fine sand was added to the fluosilicic acid which was then sent to a silicon tetrafluoride reactor. The sulfuric acid was fed to the top of the reactor and product SiF_4 was compressed to 300 psig for storage. The outgoing waste sulfuric acid was practically free of fluorides and was sent to waste disposal.

Yields were almost stoichiometric and the purity level of the SiF_4 was very high. Capacity of the small unit that was built exceeded design by more than 200%.

In a commercial plant the fluosilicic acid would come from an adjacent plant or tank car and the sulfuric acid would be returned to the fluosilicic acid producer or other user.

In Figure 6, the proposed commercial silane operation is shown. Hydrogen returned from the silane decomposer plus make up hydrogen is reacted with sodium to form sodium hydride. This reaction is done in mineral oil.

The sodium hydride slurry in mineral oil is fed to the silane reactor where it reacts with silicon tetrafluoride to form silane gas. The solvent used is a commercially available high boiling material, like diphenyl ether. The reactor runs at about 250°C and slightly above atmospheric pressure. Yields on sodium hydride and silicon tetrafluoride were demonstrated to be greater than 90% in the pilot plant. It is believed that with optimization this could be raised somewhat.

The silane produced was of good quality, with small impurity levels. Design capacity was exceeded and the reliability of the process was demonstrated.

PURIFICATION PROCESS:

The process developed by Eagle-Picher for silane purification was motivated by the low cost photovoltaic project being conducted by JPL at that time. A number of years earlier Eagle-Picher had looked at the feasibility of separating the isotopes of boron by the technique of large scale preparative gas chromatography (LSGC), but had abandoned the concept in favor of liquid exchange. With the advent of the JPL project, the prospect that large quantities of photovoltaic grade silane might be available led to the investigation of the method as a means to ultra purify the gas to the extent of semiconductor quality. Further, to do so very safely and economically, thus establishing the possibility of a competing process to Siemens, which had put Eagle-Picher out of the silicon business some 25 years earlier.

Gas Chromatography (GC) is widely employed as an analytical tool to separate components of a volatile mixture. The several components are then characterized, both qualitatively and quantitatively, with one of a wide variety of detectors. The heart of such an instrument is the chromatographic column. Figure 7 shows the action of such a column. The column consists of a length of stainless steel pipe packed with particles of very uniform size and composition. An inert gas, called the carrier, passes through the column. The mixture to be separated is introduced as a small batch, or injection, into one end of the column. In Figure 7, the sample is composed of three components represented by squares, triangles, and circles. As the mixture is pushed through the column by the flowing carrier, the various components interact differently and so percolate through the column at differing rates. If the operator has been clever about selection of the particles with which the column has been packed and the values of the various operational parameters, the components of the mixture will be separated by the time they exit, or elute, from the end of the column. As the mixture percolates through the column, the molecules become mixed with carrier gas and the concentration of the component in the carrier gas assumes a near-Gaussian distribution.

Figure 8 is a block diagram of the large scale GC (LSGC) used for the purification of silane gas. Carrier gas is supplied to the column through standard regulators and flowmeters. Silane pulses are periodically admitted into the column by a computer operated valve. At the end of the column is a hot wire detector which registers the passage of any gas with a thermal conductivity different than that of the hydrogen carrier gas. Immediately following the detector is the gas flow system is a switching valve that routes the GC effluent to one of several lines. In our silane system, there were two such lines: a waste line going to a flare and a pure line going to the silane collection system. In normal LSGC useage, the components of interest are separated from the carrier gas in a condensor at this point. In our system, we were interested in retrieving only a hydrogen mix of the silane, so the condensor was eliminated. Carrier gas is recycled through a cleaning system consisting of carbon scrubbers, molecular sieve traps, and catalytic deoxygenators. The switching of all valves is done on a timed basis. A dedicated valve sequencer module is used for this purpose. The system employed in the effort described in this paper was a commercial unit heavily modified for use with mixtures of silane and hydrogen, and shown in Figure 9.

Nearly 60 different column packing materials were tested for silane use. A set of gas mixtures composed of silane, hydrogen, argon, oxygen, nitrogen, carbon dioxide, water, diborane, arsine, phosphine, silicon tetrafluoride, and the various chlorosilanes were used for this testing. (No one mixture contained all of the various samples). The concentration of the sample gases ranged from 30 ppm to 2% in either silane, hydrogen, or helium. Best success was obtained with a porous polymer, Poropak. A composite chromatogram of these materials is shown as Figure 10. Two one meter sections 80 mm in diameter were packed with this material. The separation was done at essentially room temperature and typical throughputs of 1200 grams per hour were obtained at the optimum operational parameters. Eagle-Picher has a patent pending on the system as described.

The purified silane/hydrogen mixture was compressed into specially cleaned carbon steel holding containers. A two-stage triple stainless steel diaphragm compressor was used for this compression, and is shown in Figure 11. A surge tank between the LSGC and the compressor was found necessary.

The measurement of the purity of the silane proved to be as difficult a technical problem as the purification itself. The silane was converted to silicon and the resulting silicon was used to grow Czochralski crystals of comparable purity to those obtained from Siemens material. The various impurities present could be attributed to either the pure silane, the conversion process, or the crystal growth. This leads to a great deal of uncertainty to the quality of the silane as purified by LSGC. The assumption appears justified that the silane is equal to or surpassing conventional Siemens polysilicon.

The silane was also characterized by analytical gas chromatography. Work done in our laboratories utilized the hot wire detector and the flame ionization detector. The hot wire detector is sensitive down to about 10 ppm, depending on the identity of the impurity. No impurities were found in the purified silane with this detector. The flame ionization detector proved useless for the analysis of the silane, even when the silane itself was routed around the detector to prevent silicon oxide formation on the internals of the detector. In addition to the work done in our laboratory, samples of the purified gas were sent to an outside laboratory for GC/MS analysis. Again, no impurities were detected, even when concentrations were used.

The silane was further characterized by growing epitaxial films of silicon from the gas and subjecting the films to spreading resistance profiling. The substrates used were low boron antimony doped silicon wafers. The antimony doping was used to demark the interface between the substrate and the film. Antimony was used because it was felt that less diffusion into the growing film would occur than with other dopants. Growth of films was done in our laboratory and also contracted to SDI, a manufacturer of electronic devices. All of the films were profiled for net carrier concentration at Solecon Laboratories by the spreading resistance technique. A bevel was ground on the films, then the film was profiled by stepping the probe at regular intervals down the bevel. A resulting profile is shown as Figure 12. Nearly all of the films tested showed carrier concentrations in the range of 10^{12} , with about a 50% variation. This was true for two different feedstock materials of assumed differing starting impurity composition. These profiles indicate that all films are either of very high purity or nearly perfectly compensated.

The work described in this paper indicates that silane gas may be purified by the technique of LSGC. The purity of the silane is enhanced beyond the limits of commonly used analytical tools. Epitaxial films indicate the gas may be of very high purity. Direct analytical methods need development to confirm this indication.

The method for pyrolysis piloted by General Atomic Technologies will not be discussed in this paper at their request.

The economics of producing semiconductor quality silicon by the combined process is as shown in Figure 13.

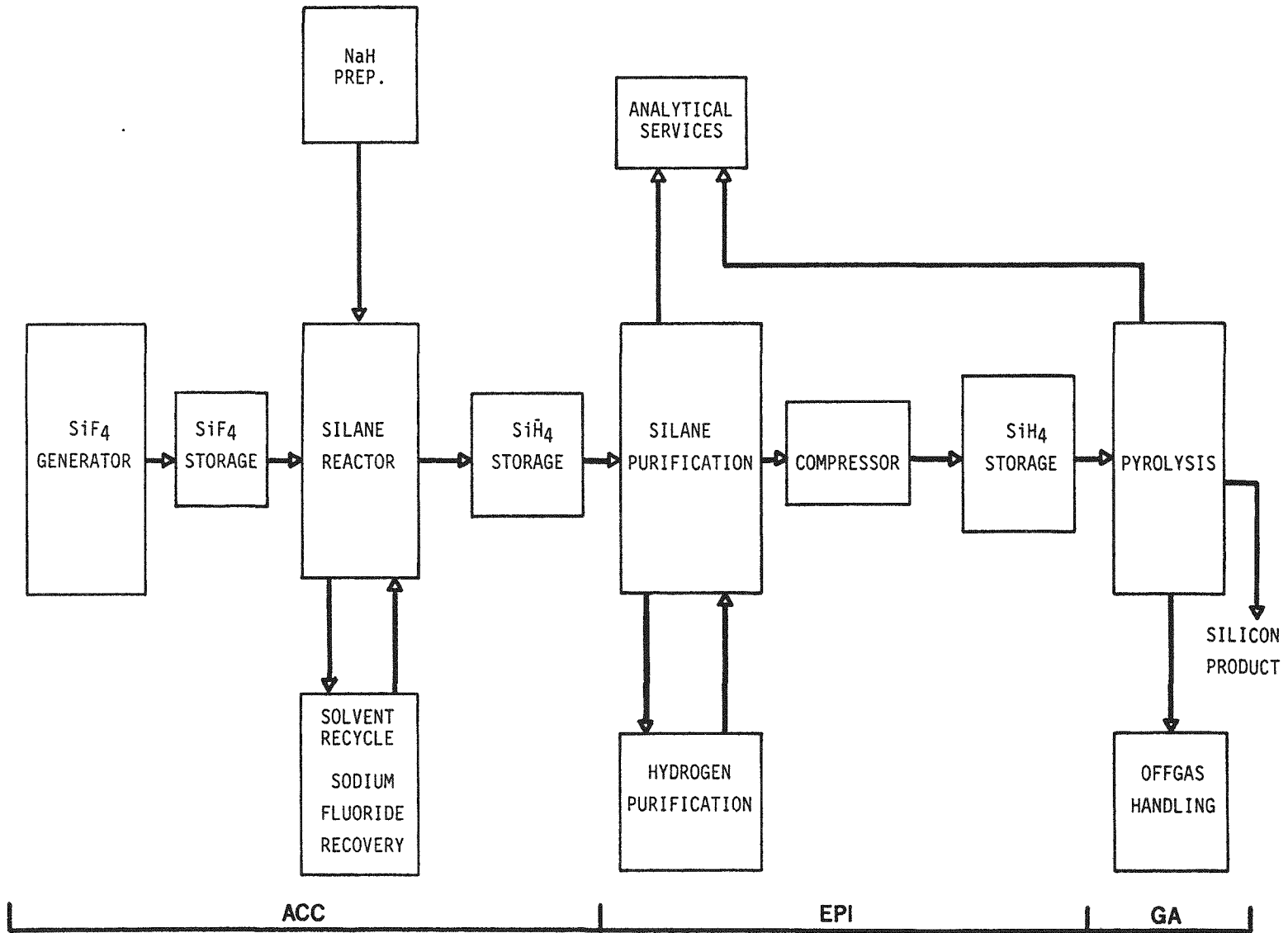


FIGURE 1
PROJECT ORGANIZATION

EAGLE-PICHER POLYSILICON - CRYSTAL EVALUATION

	#PULLS FOR "Z-D"	RESISTIVITY (ohm cm)	CONDUCTIVITY TYPE	P-L ANALYSIS (ppba)				CARBON (ppma)	LIFETIME (μ secs)
				B	P	Al	As		
E-P 1 *	1	2000	P	1.2	1.1	0.1	0.04	4.8	300 +
E-P 2 *	2	2500	P	1.5	1.4	0.2	0.09	2.6	300 +
TYPICAL SIEMENS	1 or 2	200 to 5000	90% N	0.3 to 1.0	0.5 to 1.5	AS ABOVE	AS ABOVE	<0.3	300 +

* CRYSTALS: ~ 2 INCH DIAMETER X 6 INCHES LONG.

FIGURE 2
FIRST PILOT PRODUCTION

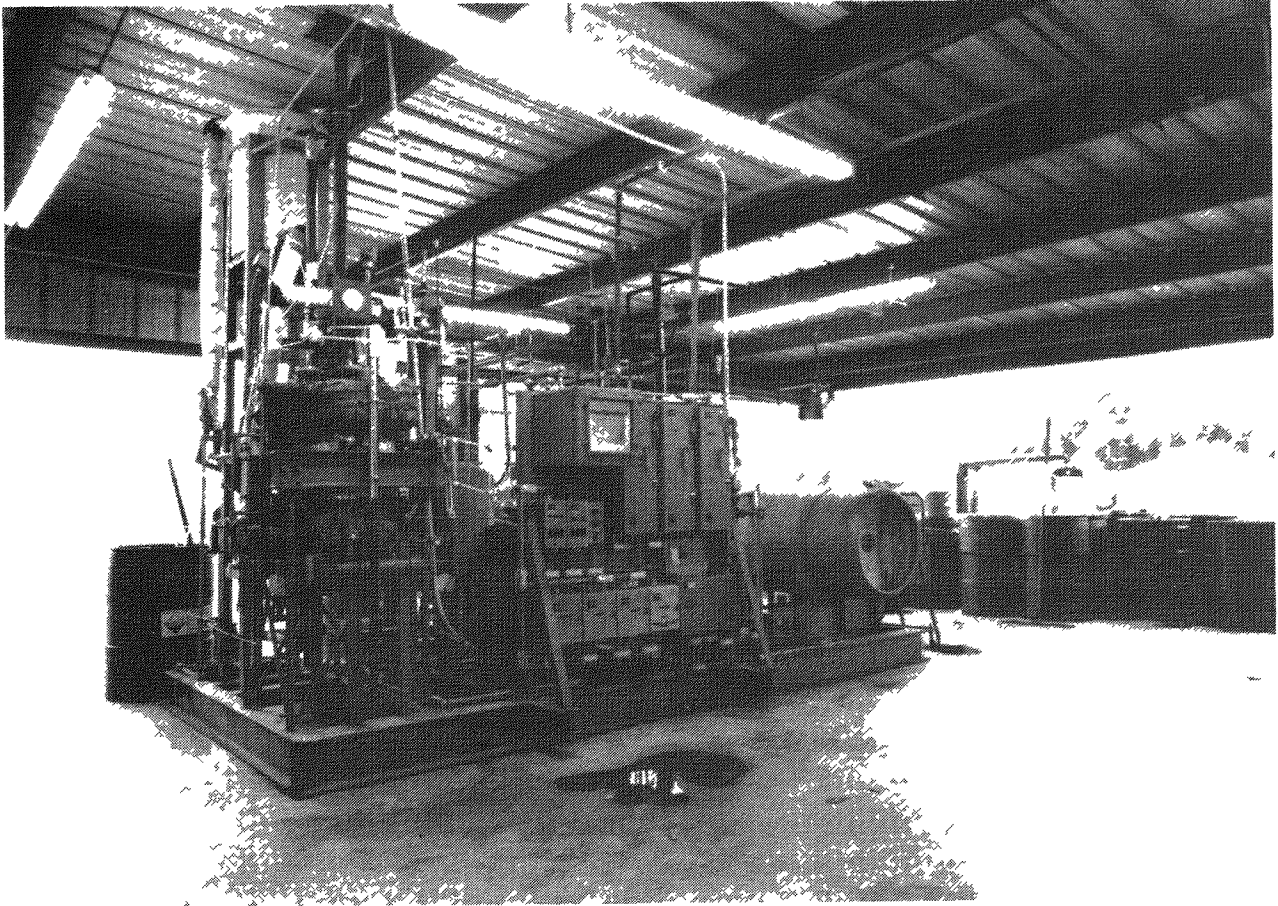


Figure 3

Pilot Plant SiF_4 Generator Skid

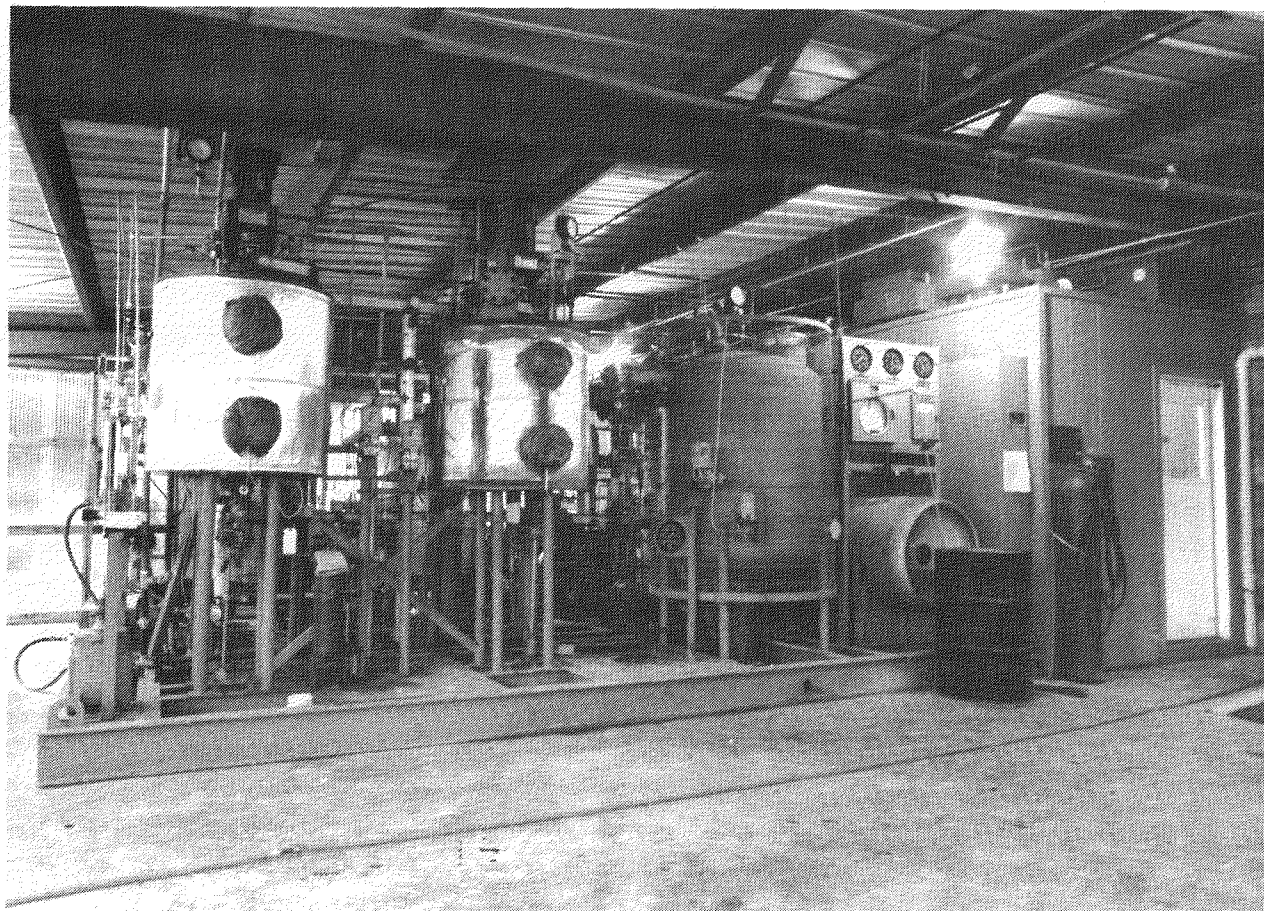


Figure 4
Pilot Plant SiH₄ Generator Skid

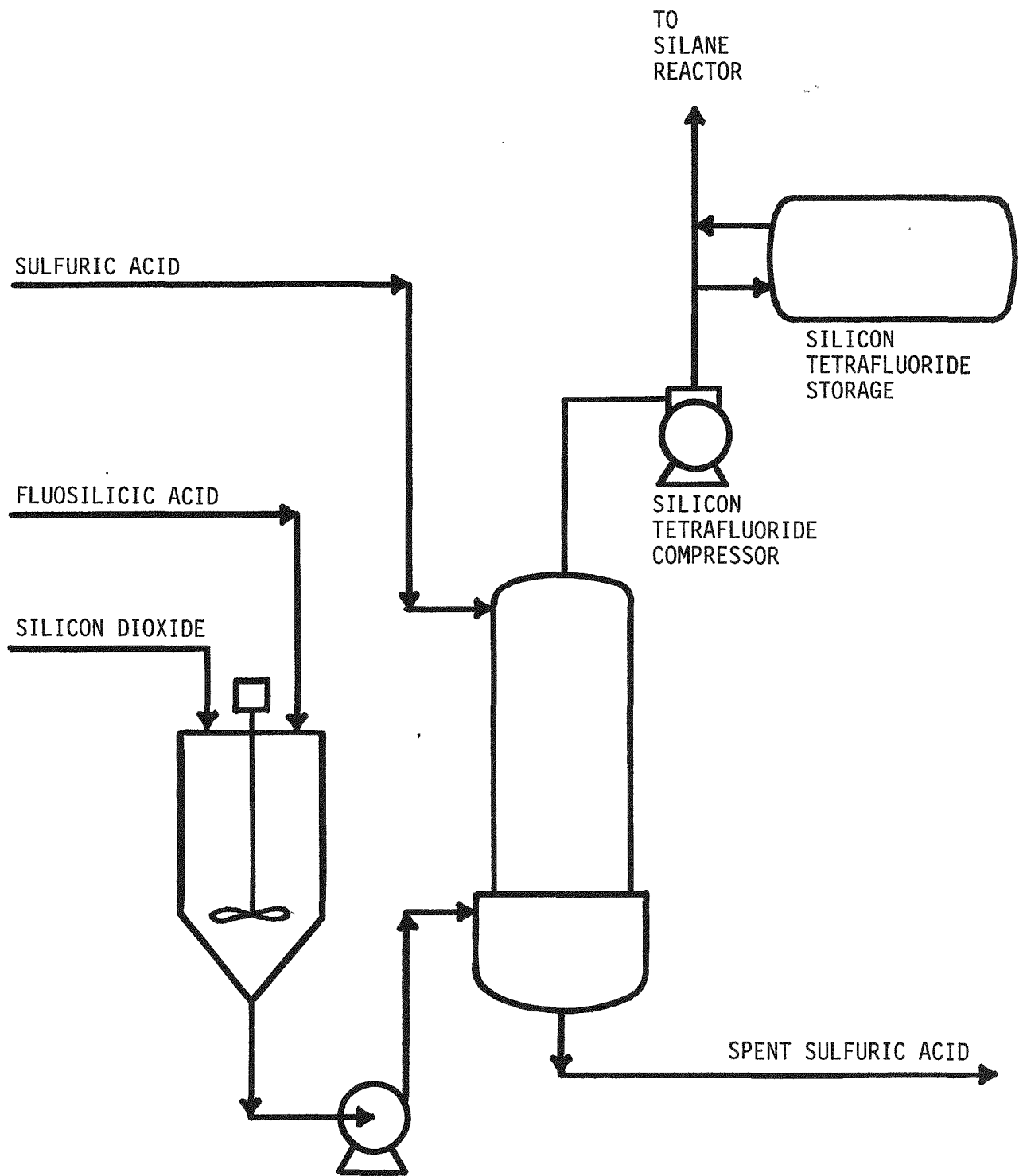


FIGURE 5
SiF₄ PROCESS

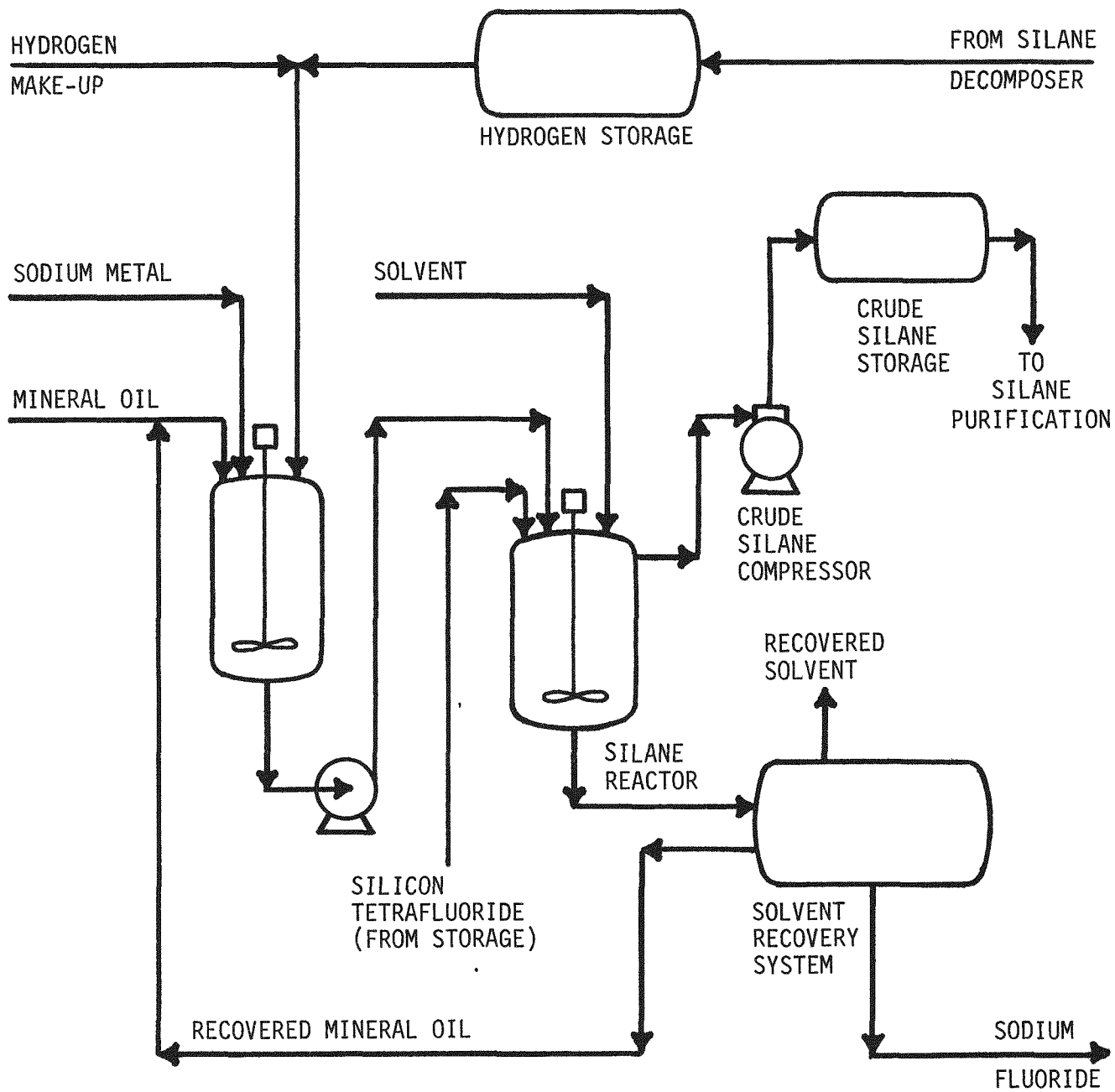


FIGURE 6
 SiH_4 PROCESS

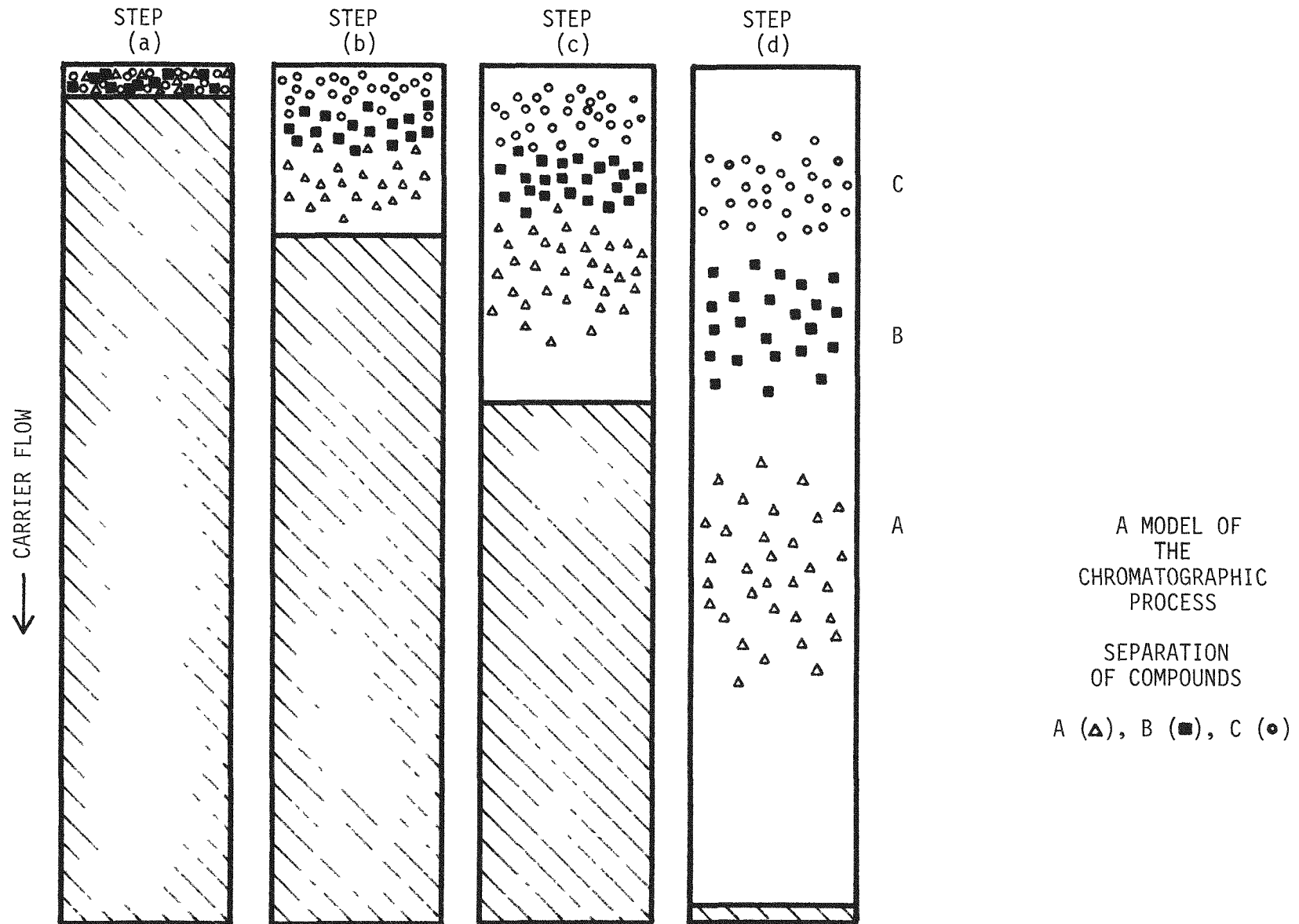


FIGURE 7

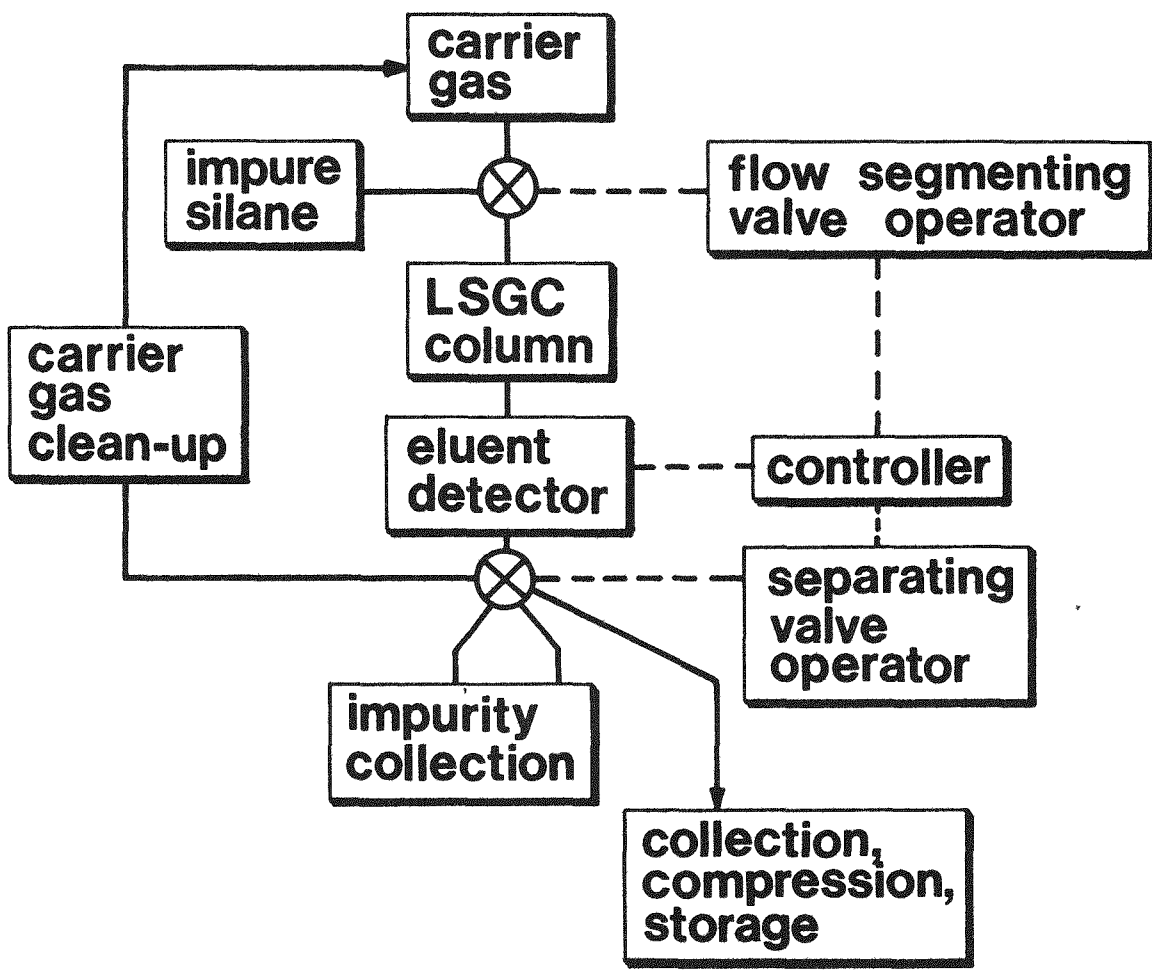


FIGURE 8
 LSGC PURIFICATION PROCESS FLOW

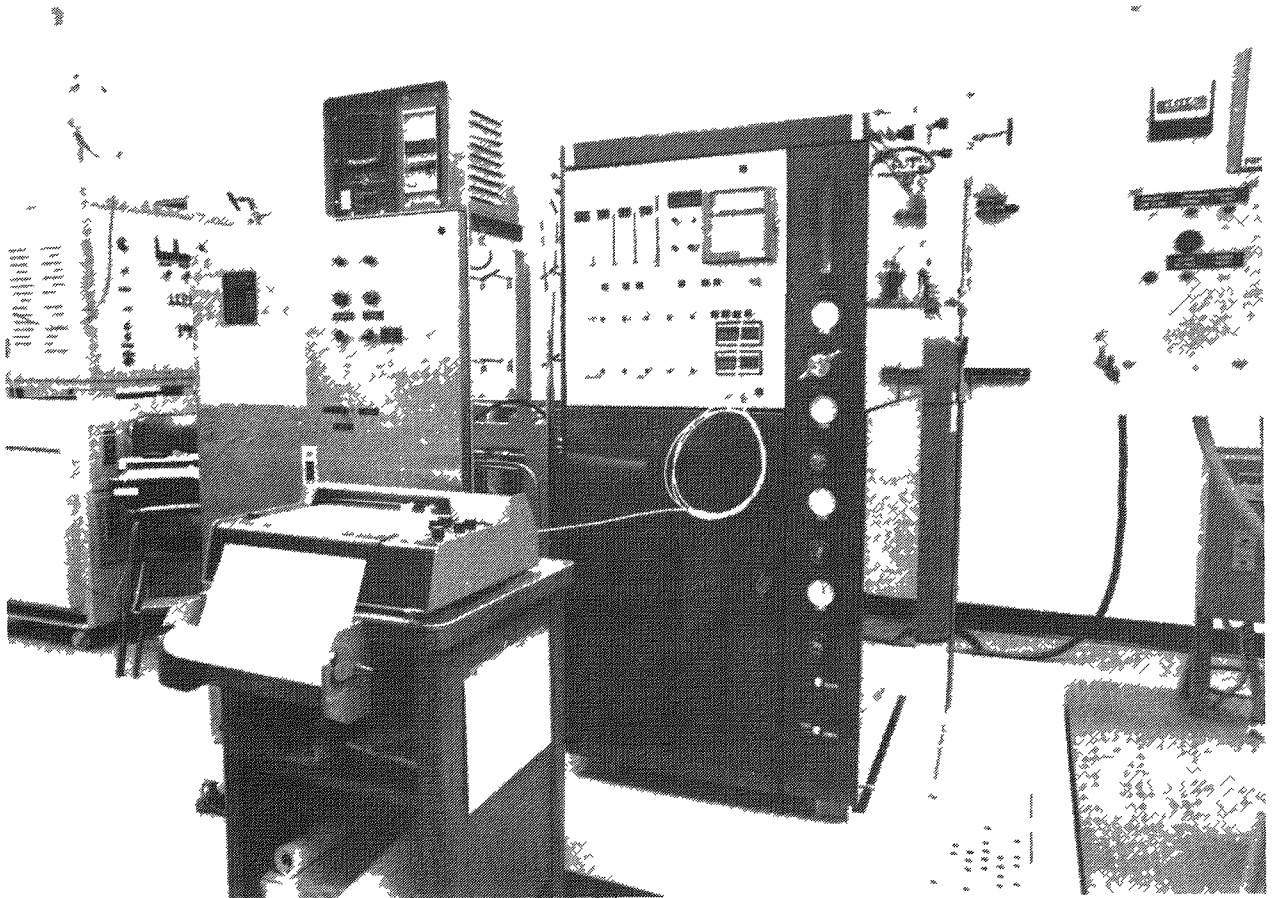


Figure 9
LSGC Pilot Plant

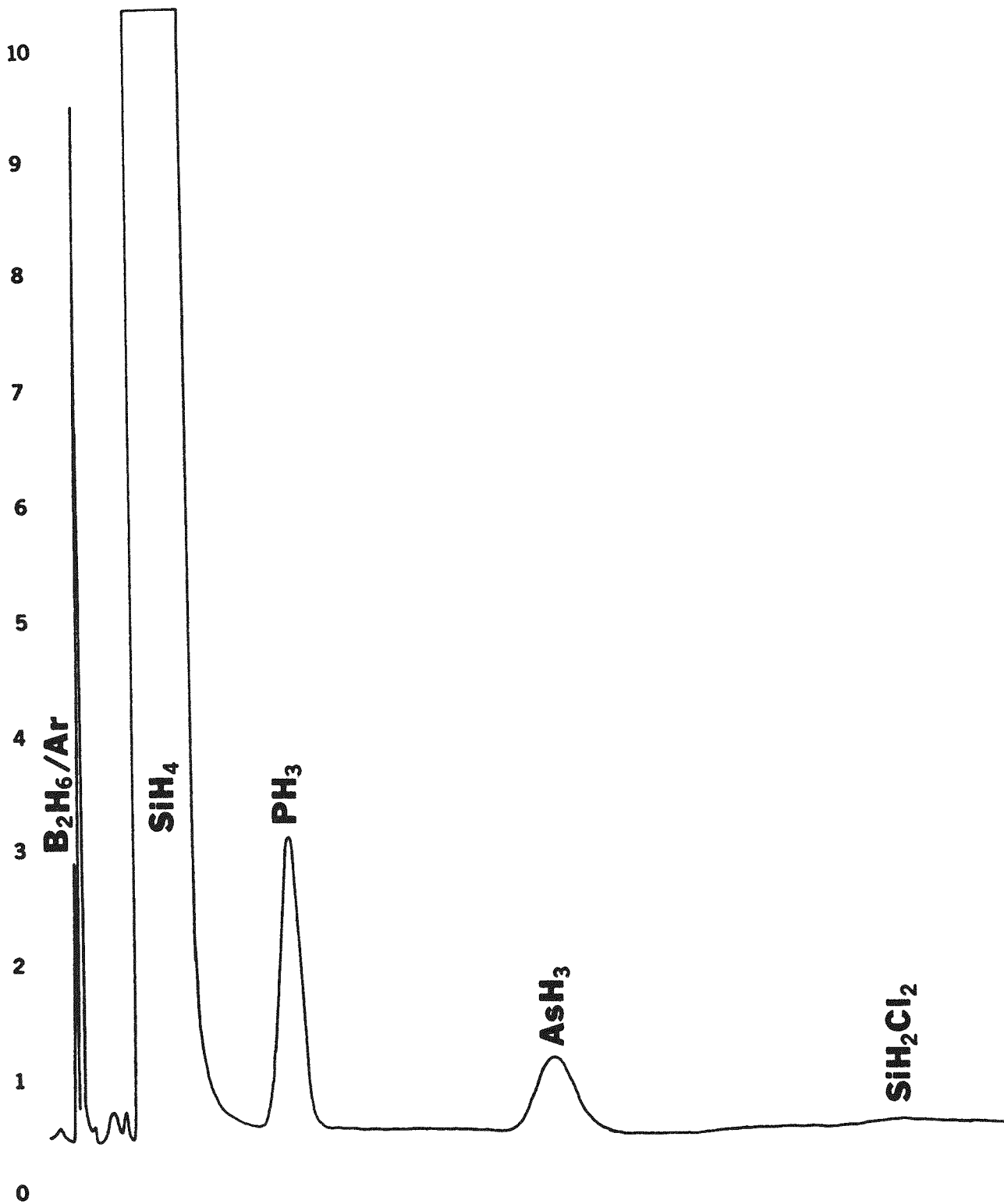


FIGURE 10
TYPICAL G. C. IMPURITY PROFILE

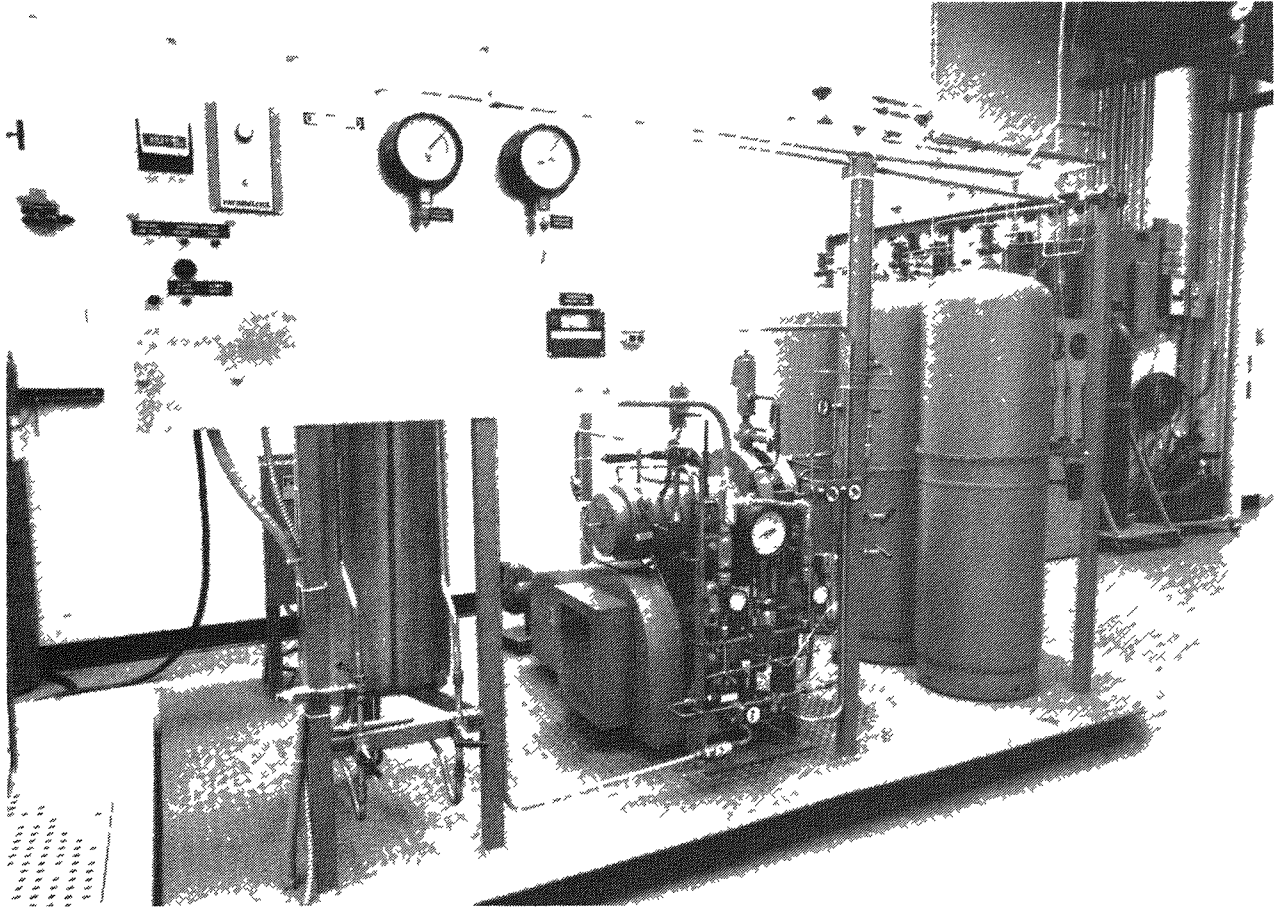


Figure 11
Picture of Compressor

SPREADING RESISTANCE ANALYSIS

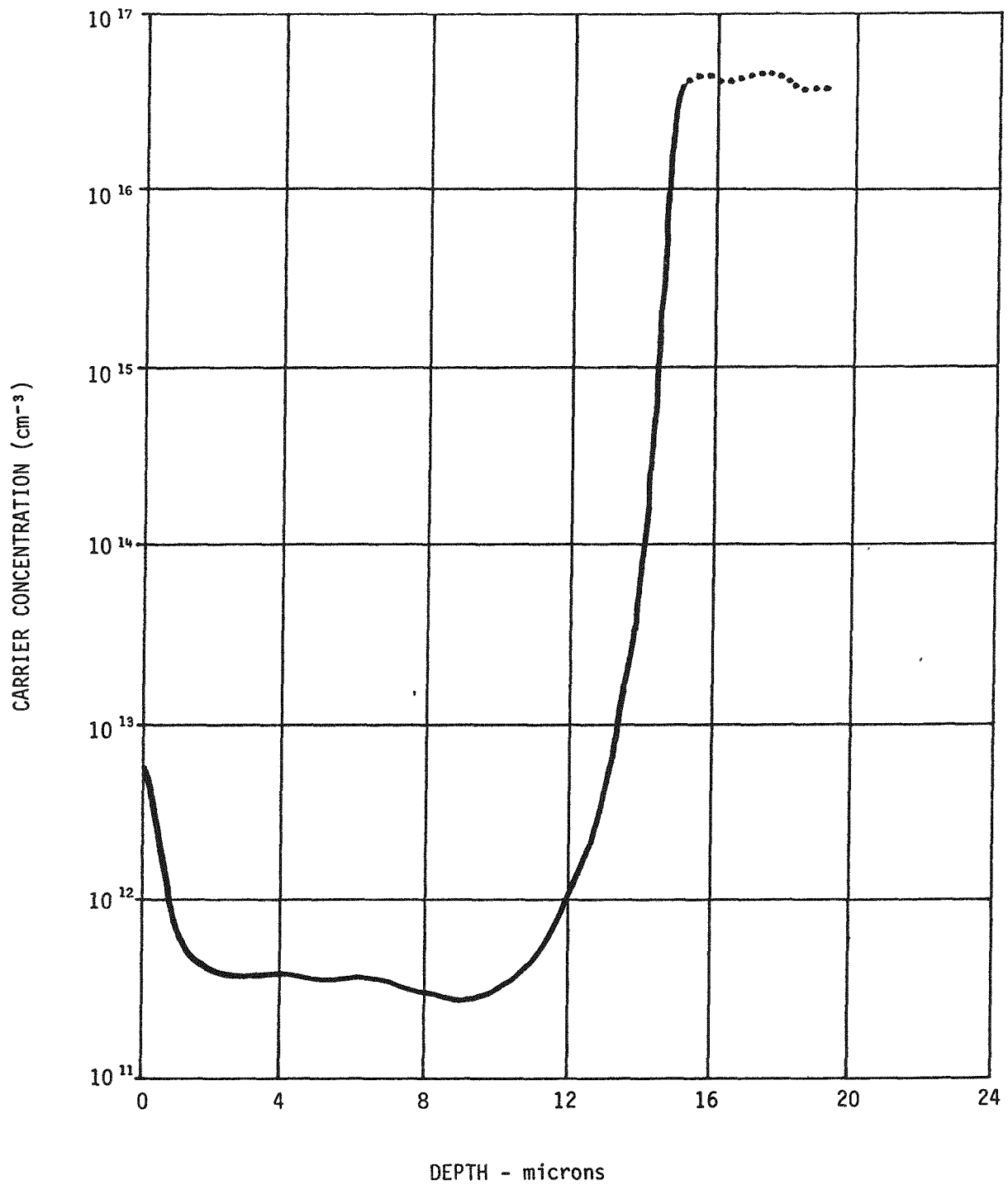


FIGURE 12
ANALYSIS OF EPI-SILICON FILM
GROWN FROM LSGC PURIFIED SILANE

CAPITAL AND MANUFACTURING COST ESTIMATES

FOR

POLYSILICON FACILITY

BASIS

- o Capacity 1000 Metric TPY
- o Grass roots facility
- o Based on SiH_4 from SiF_4 via Allied's process
- o Involves purification of SiH_4 and decomposition to polysilicon
- o 1983 Dollars

CAPITAL

Fixed capital is estimated at \$40MM which includes:

\$5MM for the SiF_4 facility;

\$10MM to produce crude SiH_4 , and

\$10MM for off-sites

Of the total of \$40MM, 15% is engineering/project management and 10% is contingency.

MANUFACTURING COST

Raw Materials	\$8.25/Kg Si
Productive Labor & Supervision	1.25
Depreciation (10% of Capital)	4.00
Maintenance (5% of Capital)	2.00
Taxes (1.5% of Capital)	0.60
Utilities	1.50
Plant Administration	0.50
Test & Inspection	0.45
Miscellaneous	<u>1.00</u>
TOTAL	\$19.55/Kg Si

FIGURE 13

DISCUSSION

HSU: What throughput was demonstrated for the large-scale gas chromatographic unit for the silane portion?

GRAYSON: It was a 1200 gm/h throughput for the GC column we had.

SILICON PURIFICATION USING A Cu-Si ALLOY SOURCE

R. C. Powell, P. Tejedor, and J. M. Olson
Solar Energy Research Institute
Golden, CO 80401

ABSTRACT

Production of 99.9999% pure silicon from 98% pure metallurgical-grade silicon by a vapor-transport filtration process (VTF) is described. The VTF process is a cold-wall version of an HCl chemical vapor transport technique using a Si:Cu₃Si alloy as the silicon source. The concentration, origin, and behavior of the various impurities involved in the process were determined by chemically analyzing alloys of different purity, the slag formed during the alloying process, and the purified silicon. Atomic absorption, emission spectrometry, inductively coupled plasma, spark source mass spectrometry, and secondary ion mass spectrometry were used for these analyses. The influence of the Cl/H ratio and the deposition temperature on the transport rate was also investigated.

INTRODUCTION

A large fraction of the cost of a silicon solar cell can be attributed to the cost of the high-purity silicon feedstock or polysilicon. The silicon feedstock problem is likely to persist in the near future since the price of polysilicon appears to be driven by the supply and demand cycles of the electronics industry, the needs of which are not totally compatible with that of the photovoltaics industry.

In 1981, Olson and Carleton (1) invented a process for purifying silicon that combined the silicon filtration properties of Cu₃Si with a molten salt electrorefining process. This process produced a 99.9995 a/o pure silicon capable of yielding solar cells with an efficiency of 12.2% relative to a baseline of 11.9% (2). Later, Olson and Powell developed a vapor transport technique (3-4) that not only lacks the practical problems associated with the molten salt electrolyte but is more efficient and easier to implement on a production scale. The vapor-transport filtration (VTF) process for purifying metallurgical-grade silicon is based on the chemistry of the Si:Cl:H system and combines the filtration properties of Cu₃Si with the chemical selectivity of a closed-cycle HCl vapor transport process to produce 99.9999% pure silicon. Vapor transport processes are covered in the monograph by Schäfer (5) and hot filament processes for purifying metals were first described by van Arkel and de Boer in 1925 (6). In equilibrium, the temperature and Cl/H ratio determine the silicon solubility in the gas phase for the Si:Cl:H system (7-9). For a given Cl/H ratio, thermal conditions can be established such that silicon will be transported in a closed system in the direction of increasing temperature. Conversely, HCl will transport copper (and certain other impurities) in the opposite direction, precluding the accumulation of copper at the filament (5).

The overall purification is a result of at least four mechanisms: 1) diffusional trapping of impurities in the Cu-Si alloy by slow, solid state diffusion; 2) segregation by the differential action of the HCl chemical vapor transport reactions for the various metal impurities; 3) gettering of impurities by a $\text{Cu}_2\text{O}:\text{SiO}_2$ slag during the Cu-Si alloying stage; and 4) condensation of metal impurity chlorides on the water-cooled baseplate of the reactor during the vapor-transport stage of the process.

In the following we first briefly describe the apparatus and its operation. The remainder of the paper is devoted to a discussion of the characteristics of the refined silicon including its purity, electronic properties, deposition rate, and morphology. Furthermore, we will attempt to quantify the relative importance of the various mechanisms responsible for the purification efficiency.

EXPERIMENTAL

A schematic of the experimental reactor is shown in Figure 1. The reactor consists of a hot silicon filament surrounded by a battery of Si: Cu_3Si composite alloys. The composite alloys are cast from a hypereutectic solution of metallurgical-grade silicon (mg-Si) and copper to form a two-phase system consisting of a primary silicon phase embedded in a Cu_3Si matrix. The alloys are approximately $5 \times 5 \times 1 \text{ cm}^3$.

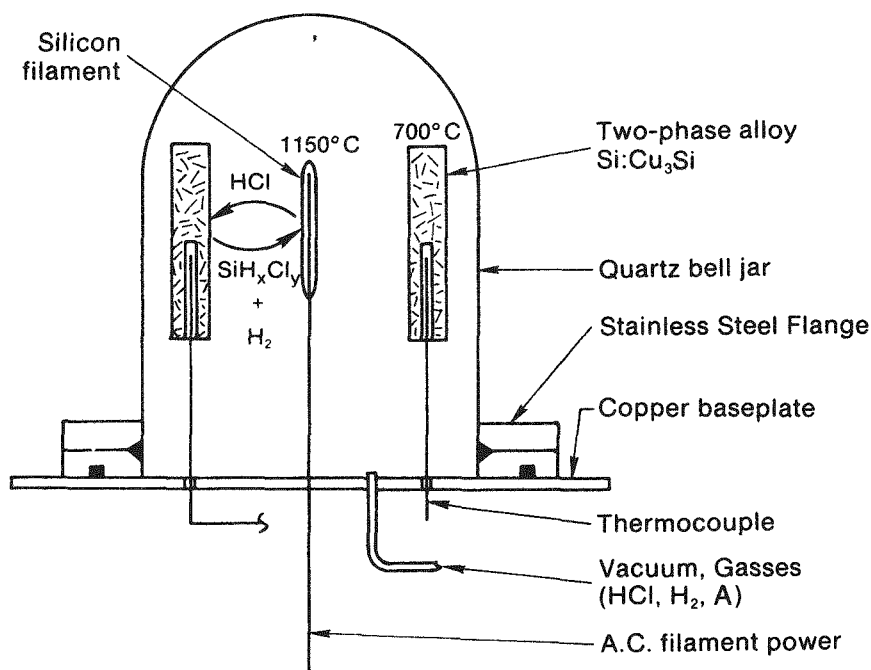
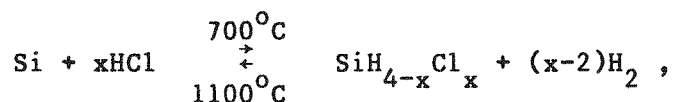


Figure 1. Schematic diagram of the experimental VTF reactor.

Inconel-sheathed thermocouples within embedded graphite wells support the alloys. Graphite fixtures, connected to copper power feedthroughs, support and conduct current to the filament. The filament, made of high-purity Poco® DFP-1 graphite sheet, is clamped between two graphite pieces with graphite screws. A 1.5-liter quartz bell jar encloses the primary components and seals to a copper baseplate by means of a stainless steel flange and Viton O-rings. Both the stainless steel flange and the copper power feedthroughs are water-cooled. Before every run, the reactor is evacuated by means of a turbomolecular pump and outgassed until the pressure is ~30 mtorr. After evacuation, the free space of the reactor is backfilled to atmospheric pressure with a mixture of HCl and H₂. These initial proportions determine the Cl/H ratio. An optical pyrometer is used to measure the filament temperature.

Radiation from the resistively heated filament passively heats the alloys. With the silicon filament at 1100°C and the composite alloy at 700°C, silicon is transported from the alloy to the filament by the following nominal transport reaction:



where $x = 2, 3,$ and/or 4 . The HCl reacts with the Si-Cu alloy to form a mixture of chlorosilanes and hydrogen. These reactants are then transported to the hot silicon filament by a combination of diffusion and convection where they back-react, depositing silicon on the filament and releasing HCl to continue the process. The general process is traditionally called chemical vapor transport (CVT) and is a well-known technique (5).

The deposition of silicon causes the electrical conductance of the filament to change. Since it is very easy to monitor these changes continuously, we have a convenient way to indirectly monitor the filament growth (4,10). If silicon is deposited uniformly on a filament of length L , width W , and thickness X , then the conductance is given by

$$C = \sigma WX/L ,$$

where σ is the electrical conductivity of the deposited silicon. This conductivity depends on the doping, the temperature, and the grain structure of the deposited silicon. However, if these factors remain relatively constant, the increase in conductance with time is directly related to the increase in filament thickness and hence filament mass m . Thus,

$$\frac{dC}{dt} = \frac{\sigma}{\rho L^2} \frac{dm}{dt} ,$$

where ρ is the mass density of silicon.

As silicon is removed from the surface of the alloy, it must be replenished by the outdiffusion of silicon from the bulk of the two-phase alloy. From the Phase Rule we can show that the outdiffusion silicon must result in a decrease in the concentration of primary silicon particles and the formation of a single-phase (Cu₃Si) depletion layer that grows with time. The run is terminated after the composite alloy has been depleted of its primary silicon.

For convenience, we use a graphite starter filament, which is much easier to ohmically heat than silicon. Therefore, for chemical and electrical analysis, the silicon must be stripped from the graphite filament. Chemical analysis of the refined silicon is made by spark source mass spectrometry on bulk samples cut from lapped sections. The alloys during various stages of the process and the slag formed during the alloying step are analyzed by inductively coupled plasma atomic absorption (ICP) and standard emission spectroscopy. Resistivity measurements are made on lapped, polycrystalline samples and also on single-crystal samples grown by the Czochralski technique from the refined polycrystalline material.

RESULTS AND DISCUSSION

Purity

The alloying process plays an important role in the overall purification. Since the silicon and the copper are alloyed in an open-air furnace with a graphite crucible, a slag of SiO_2 and Cu_2O is formed on the surface of the molten alloy. This slag getters many impurities associated with the metallurgical-grade silicon, resulting in an alloy substantially purer than the starting materials. Table 1 compares the purity of a series of alloys made under different alloying conditions of time t and temperature T . In all cases, the alloys were soaked for 90 and 150 min at temperatures between 1060° and 1300°C for a Cu-Si alloy with an initial metallurgical-grade silicon concentration of 20 w/o. The data indicate that the purity of the alloy generally increases with soaking temperature and decreases with soaking time. The eutectic temperature of the $\text{Cu}_2\text{O}:\text{SiO}_2$ slag is 1060°C , which explains the rather poor results observed at the 1060°C soaking temperature. At higher temperatures the slag is in the liquid state and at still higher temperatures it becomes less viscous, conditions necessary for efficient gettering. Also, the silicon content of the alloy, compared with the initial proportion, is an inverse function of soaking temperature.

Table 1. Effects of casting conditions on alloy purity

T_{soak} (C)	t_{soak} (min)	Cu (%w)	Si (%w)	Al (ppm)	Cr (ppm)	Fe (ppm)	Mn (ppm)	Ti (ppm)	V (ppm)
1060	90	73.37	25.64	3797	<5	559	30	<70	151
1060	150	76.76	21.31	14953	<5	1220	35	<70	469
1200	90	80.00	19.85	686	<5	181	14	<70	5
1200	150	80.43	19.46	775	5	265	19	<70	5
1300	90	81.35	18.59	512	<9	178	39	190	5

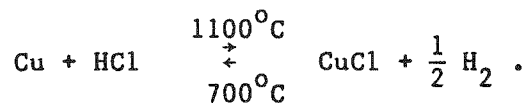
To track the impurities throughout the process, we analyzed by spark source mass spectroscopy, emission spectrometry, and inductively coupled plasma 1) the metallurgical-grade silicon used to form the Cu-Si alloy source, 2) the Cu₂O:SiO₂ slag, 3) a Cu-Si alloy with ~25 w/o Si and soaked at a temperature of 1200°C, 4) the Cu-Si alloy after the VTF process, and 5) the VTF-refined silicon. The results are shown in Table 2. The data indicate that a significant fraction of the impurities in the mg-Si are gettered by the Cu₂O:SiO₂ slag during the alloy-forming process. In particular, the slag is efficient at getting Al and Ca. At this point, any further segregation of the impurities must be associated with the VTF process, including the condensation, diffusional trapping, and vapor transport mechanisms. The purity of the alloy is essentially unchanged by the action of the VTF process.

Table 2. Typical impurity concentrations (ppm) in mg-Si in the slag, the Cu/mg-Si alloy before and after the VTF process, and the refined Si.*

Impurity	mg-Si	Slag	Alloy before VTF	Alloy after VTF	Refined Si
(ppm)					
Al	1400	1800	50	<10	<0.1
B	<10	<10	<10	<10	0.5
Ba	20	30	<10	<10	<0.02
Ca	235	365	<10	<10	0.07
Cr	185	95	55	55	<0.05
Cu	---	---	~8.7x10 ⁵	---	0.12-0.15
Fe	3150	1200	720	690	<0.08
Mg	15	25	<10	<10	0.12
Mn	755	325	155	60	0.05
Mo	<10	<10	<10	<10	0.03
Ni	30	30	<10	<10	0.14-0.57
P	<10	105	45	<10	0.15-1.8
Ti	260	105	45	40	<0.06
V	195	105	40	30	<0.05
Zr	195	70	10	10	<0.04

*mg-Si = metallurgical-grade silicon

Some segregation of impurities is likely to occur in most vapor transport systems of this type. This segregation is determined by the enthalpy change of the relevant transport reaction. Exothermic reactions, like those involving HCl and Si, transport the solid to the hot filament. Endothermic reactions and physical vapor transport tend to accumulate the deposit at the coolest point in the system (see Figure 2). For example, the HCl transport reaction for copper is probably the following endothermic reaction (5):



The net effect is to transport copper from the "hot" filament to the "cold" alloy source, essentially precluding the accumulation of copper at the filament. But for impurities like B and Al, the segregation (due to the CVT process) should be negligible (4). If these impurities exist at the surface of the alloy, the HCl should transport them to the hot silicon filament.

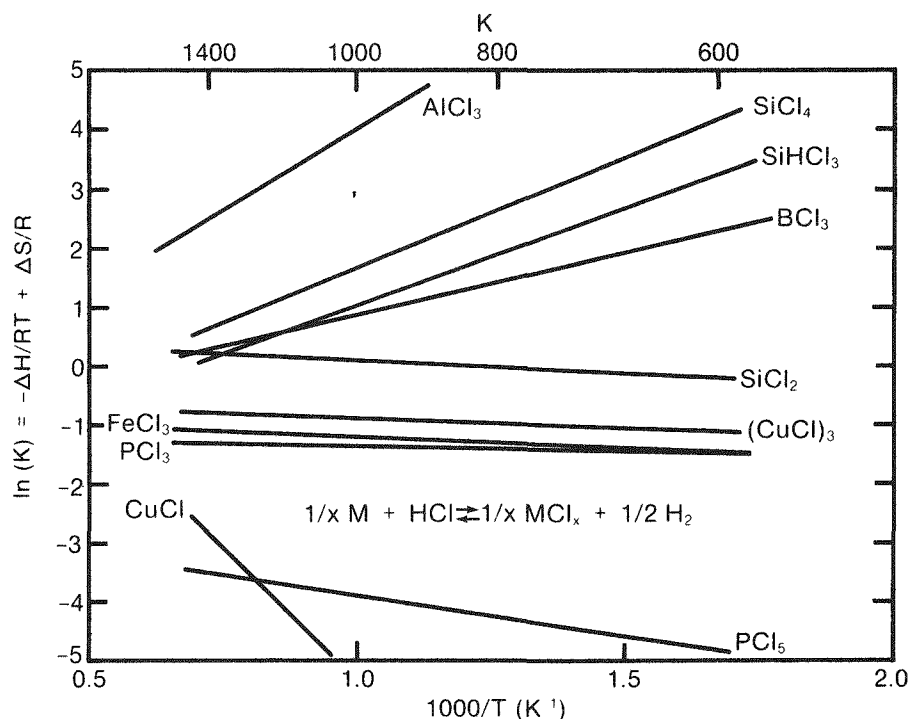


Figure 2. Calculated equilibrium constants for various HCl transport reactions possible as a function of inverse temperature. Exothermic reactions have a positive slope and are expected to transport up the temperature gradient.

The use of a composite Si:Cu₃Si source, however, greatly enhances the segregation of these impurities by limiting the rate at which they can be extracted from the bulk of the source. As a result of the rapid cooling during casting, the impurities originating from either the metallurgical silicon, the copper source, or the alloying crucible are presumably distributed more or less uniformly throughout the alloy (although there may be some enrichment of impurities in the interior). The effective diffusion of silicon in Cu₃Si at 700°C is rapid ($D_{Si} > 10^{-5}$ cm²/s), while the diffusion of other metal impurities like B, P, Al, and Ti is much slower (2,4,12). Hence, the transport gas HCl, capable of acting only on the surface of the alloy, can extract or transport only silicon at any reasonable rate, leaving behind impurities that otherwise might have been transported to the hot filament. The net effect is that all impurities, independent of their thermochemical properties, are efficiently segregated. The copper concentration in the refined silicon is never larger than 0.1 ppma, illustrating the purification efficiency of the HCl vapor transport process for elements that react endothermically with HCl. Boron is typically less than 0.2 ppma. Boron, aluminum, titanium and phosphorus should be diffusionally trapped within the bulk of the n-Cu₃Si matrix. These, plus other elements such as Fe, Ti, and Mn, are also segregated during the casting step by slagging processes. Compared with the results for the other elements, the residual phosphorus concentration is anomalously high. This residual P concentration could be intrinsic to the process or could be a function of the purity of the reactor/process environment. Finally, the carbon concentration varies from <10 ppma to >100 ppma. This again seems to be a function of reactor purity, since C should not be transported by HCl.

The serendipitous purification mechanism is the condensation of impurity chlorides on the cooled baseplate. Although it is not possible to quantitatively determine the fraction of impurities removed by this mechanism, Al, K, and Mn have been chemically identified. Furthermore, it is not clear whether or not much of this condensate accumulates during cooling of the reactor. In addition, a powdered residue originating on the surface of the alloys accumulates on the baseplate. This residue contains Fe, Al, Ca, Mg, Ti, V, Ni, Mn, and B (4).

To determine the background or baseline for the overall process, a number of different silicon sources were substituted for the mg-Si:Cu alloy source. Alloys made from electronic-grade Si (eg-Si) were considerably purer than alloys made from mg-Si; almost every impurity was below the 10-ppm level. However, the purity of the Si derived from these alloys was essentially the same as that derived from those alloys made with mg-Si. Moreover, deposits made using a pure eg-Si or a mg-Si source were also of similar purity.

Semiconductor Characteristics

The refined silicon material is typically n-type with a resistivity of 0.1-1 ohm-cm. After recrystallization, this material is still n-type with a resistivity of 0.08 ohm-cm. This correlates well with the relative concentration of P and B usually measured by chemical analysis in this material. The Hall mobility is 520 cm²/Vs with a carrier concentration of 1.5×10^{17} cm⁻³.

To determine the photovoltaic quality of the VTF-refined silicon, a single crystal with (111) orientation was grown from 75 g of the VTF material using the Czochralski crystal-growth technique. This 75 g was the product of four separate purification runs. Wafers from the middle of the boule along with 0.2 ohm-cm

wafers from Monsanto and wafers from a grown control boule were simultaneously processed into solar cells. The junctions were formed from a boron spin-on diffusion source with a 30-min drive-in at 906°C. The front and back contacts were of the TiPdAg type with no antireflection coating. The average, total area (0.1 cm²) efficiency for four cells was 9.6%, with a high of 9.8%. The 9.8% cell had an open-circuit voltage (V_{oc}) of 622 mV, a short-circuit current density (J_{sc}) of 19.6 mA/cm², and a fill factor (FF) of 0.81. The control cells had an average efficiency of 9.6%; no cell had a V_{oc} greater than 604 mV. These results are a good indication that this VTF-refined silicon is of solar-grade quality.

Growth Morphology

The morphological stability of the silicon filament is an important process parameter. If the growth morphology of the silicon filament becomes dendritic, the purification efficiency and yield of the process can decrease. This growth morphology is affected by several parameters including temperature, pressure, reactor purity, and growth rate. At filament temperatures much less than 900°C, the growth morphology becomes dendritic. (At temperatures much greater than 1300°C, the growth rate approaches zero.) Good product morphology is favored by initial gas pressures ($P_H + P_{HCl}$) greater than 400-500 torr. Furthermore, oxygen and/or water vapor appear to adversely affect the product morphology.

Deposits on graphite are polycrystalline with a semicolumnar grain structure and a [110] fiber texture. Near the silicon-graphite interface, the grain size is typically on the order of 1-10 μ m, and increases with distance from the graphite-silicon interface.

Purification Rate

The purification rate is an important economic parameter. In principle, it is a function of several variables including temperature, pressure, Cl/H, alloy composition and the surface areas of the filament and alloy sources. Under normal operating conditions, however, the purification rate is limited by the rate of diffusion of silicon from the bulk to the surface of the alloy and is therefore most affected by the alloy temperature and surface area.

To study the transport rate, we carried out a series of runs at deposition temperatures of 1050° to 1300°C and with Cl/H ratios between 0.3 and 1.0 at atmospheric pressure. The transport rate was measured using both a time-average method and the real-time, *in situ* method described previously. The time-average transport rate was obtained by dividing the mass deposited by the total run time. Under optimum growth conditions using the Cu-Si alloy, the conductance increases as $t^{1/2}$. Thus, the deposition rate decreases as $t^{-1/2}$. In Figure 3, the filament conductance is plotted as a function of $t^{1/2}$ for a series of runs carried out at four different Cl/H ratios and a filament temperature of 1160°C. We observe a linear behavior in all cases in which good deposits are made at times that extend over ~20 hours. This time dependence suggests a diffusional limitation that cannot be attributed to gas-phase diffusion. Therefore, the purification rate must be limited by the diffusion rate of silicon from the bulk to the surface of the alloy. Although the transport rate values plotted were determined by the time-average method, they agree with the real-time measures since the total run time was held constant.

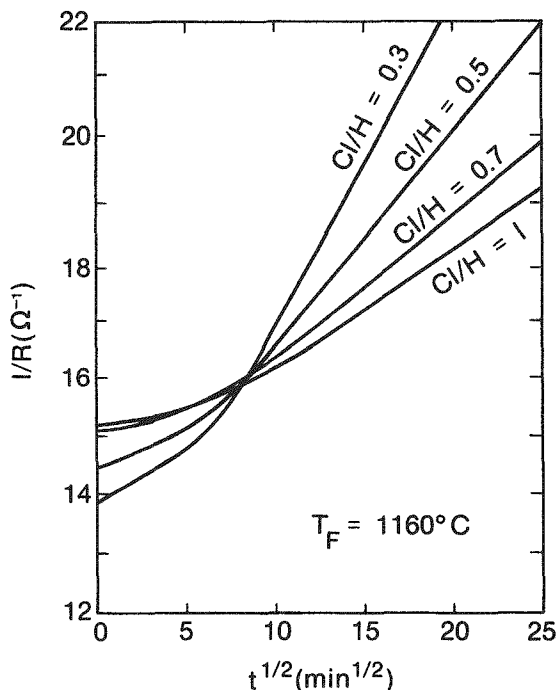


Figure 3. Real-time plot of the filament conductance as a function of $t^{1/2}$ for four different Cl/H ratios.

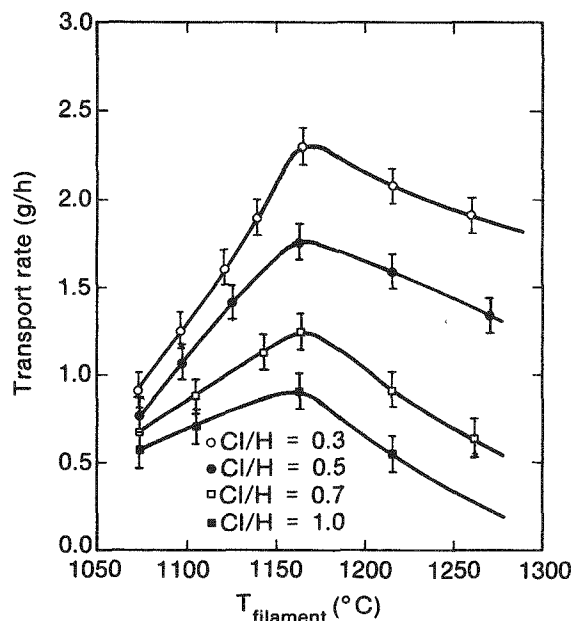


Figure 4. Average-time transport rate as a function of the filament temperature for Cl/H = 0.3 to 1.0.

For any given Cl/H ratio, we observe that the transport rate exhibits an asymmetric maximum around 1160°C (see Figure 4). Since the alloy temperature scales with the filament temperature, the increase in rate with increasing filament temperature below the maximum is attributed to the increased diffusivity of Si within the alloy. However, the gas-phase solubility of Si near the alloy decreases with increasing temperature (7). This tends to decrease the rate since the surface concentration of Si in the alloy presumably is an inverse function of the local gas-phase solubility. Furthermore, the gas-phase solubility passes through a minimum with increasing temperature. Thus, the difference in gas-phase solubility between the alloy and the filament, which drives the gas-phase transport, passes through a maximum and then decreases to zero with increasing temperature for a given temperature difference between alloy and filament. This is observed experimentally at very high temperatures where no deposition occurs. Thus, at low temperatures the rate is controlled by Si diffusion in the alloy and is fairly insensitive to Cl/H. At higher temperatures the rate passes through a maximum due to the competing effects of larger diffusivity within the alloy but lower driving forces for both diffusion through the alloy depletion layer and for gas-phase transport. At very high temperatures, gas-phase transport controls the rate. In fact, the driving force for gas-phase diffusion, which is sensitive to Cl/H, inverts and no deposition occurs.

The optimum Cl/H ratio appears to be near 0.3. At lower values the deposits can become dendritic, and of course as Cl/H approaches zero so does the rate. At higher values of Cl/H, the relative concentration of SiCl_2 increases. Since the formation reaction of HCl with Si to form SiCl_2 is endothermic, this reaction

tends to transport Si from the filament to the alloy. Thus, at higher Cl/H we expect the transport rate to diminish. A growth rate as high as 2.3 g/h has been achieved for Cl/H = 0.3 and deposition temperatures of 1160°C.

SUMMARY

The vapor-transport filtration (VTF) process permits the production of 99.9999% pure silicon from metallurgical-grade silicon, which is suitable for solar cells. The purification efficiency is attributed to four mechanisms: gettering of impurities during casting of the alloy, the chemical selectivity of the HCl vapor-transport process, the unusual filtration properties of Cu₃Si, and the condensation of impurities in the form of chlorides on the cold walls and baseplate of the reactor. Optimum growth rates occur at deposition temperatures around 1160°C and a Cl/H ratio of 0.3.

The VTF technique is a closed-cycle process that is adaptable to small- or large-scale operations requiring only a small volume of HCl and H₂ and Si:Cu₃Si composite alloys as inputs. There are no large volumes of waste gas to recycle or dispose of, and the spent copper alloy can easily be recycled by means of common metallurgical processes.

ACKNOWLEDGMENTS

The authors would like to thank T. F. Ciszek for growing the single crystals, T. Schuyler for the cell processing, and C. Osterwald for the cell measurements. This work was supported by the U.S. Department of Energy under contract no. DE-AC02-83CH10093 and by the Instituto de Electronica de Comunicaciones (C.S.I.C), Madrid, Spain.

References

1. Olson, J.M., and K.L. Carleton, "A Semipermeable Anode for Silicon Electrorefining," J. Electrochem. Soc., Vol. 128, No. 12, Dec. 1981, pp. 2698-2699.
2. Olson, J.M., "Silicon Electrorefining and the Transport Properties of Cu₃Si," Proc. of the Fourth Symposium on Materials and New Processing Technologies for Photovoltaics, Vol. 83-11, edited by J.A. Amick, V.K. Kapur, and J. Dietl, Pennington, NJ: Electrochem. Soc., 1983, pp. 119-131.
3. Olson, J.M., and R.C. Powell, "A Vapor Transport Filtration Technique for Purifying Silicon," 17th IEEE Photovoltaics Specialists Conf., New York, NY, IEEE, 1984, pp. 1143-1145.
4. Powell, R.C., 1984, Silicon Purification Using Chemical Vapor Transport From a Copper-Silicon Alloy Source, M.S. Thesis, Golden, CO: Colorado School of Mines.
5. Schäfer, Harald, Chemical Transport Reactions, New York, NY: Academic Press, 1964, pp. 30-114.
6. van Arkel, A.E., and J.H. de Boer, "Darstellung von reinem Titanium-, Zirkonium-, Hafnium- und Thoriummetall," Z. anorg. u. allgen. Chem., Vol. 148, 1925, pp. 345-350.

7. Bloem, J., Y.S. Oei, H.H.C. de Moor, J.H.L. Hanssen, and L.J. Giling, "Near Equilibrium Growth of Silicon by CVD. I. The Si-Cl-H System," J. Cryst. Growth, Vol. 57, Nos. 1-3, Dec. 1983, pp. 399-405.
9. Hunt, L.P., and E. Sirtl, "A Thorough Thermodynamic Evaluation of the Silicon-Hydrogen-Chlorine System," J. Electrochem. Soc., Vol. 119, No. 12, Dec. 1972, pp. 1741-1745.
10. Lever, R.F., "The Equilibrium Behavior of the Silicon-Hydrogen-Chlorine System," IBM J. Res. Develop., Vol. 8, Sept. 1964, pp. 460-465.
11. Rolsten, R.F., Iodide Metals and Metal Iodides, New York: John Wiley & Sons, 1961, pp. 273-292.
12. Kibbler, A., R.C. Powell, and J. M. Olson, to be published.

FORUM: POLYSILICON PROCESS TECHNOLOGY

H. Aulich, Chairman

LUTWACK: The intent of this Forum is to provide the opportunity to exchange information, to present critiques of the work reported or of other work, to ask additional questions of the speakers, and to offer additional comments which may have occurred to you as a consequence of having additional time for consideration of the earlier presentations. Feel free to participate in all of these ways. Dr. Aulich will act as the Chairman of this Forum.

AULICH: I hope that the Workshop attendees will participate in lively discussions. First, I will present a short summary of what has transpired so far and maybe raise some questions. I invite everyone to participate during my discussion.

We learned from Dr. Hopkins that in order to have a good feedstock for solar cells, we have to have low impurity concentrations in the feed-stock. We can tolerate a few parts per million of some elements that have very low distribution coefficients. He also pointed out that gettering will work only for fast diffusers (such as copper or nickel) and that, in principle, impurities such as titanium and molybdenum cannot be removed once they are in the wafer. We then heard that solar cells from high-purity silicon had been prepared with efficiencies of about 20% and that it's possible, in principle, to even achieve an efficiency of around 25%. For multi-crystalline materials, we learned that H₂-passivation should drastically improve the efficiencies of solar cells made from this material. In an economic study, it was shown that polysilicon using the CVD process, and there are a number of CVD processes being used now or at least under consideration, will end up with a material price varying between \$25 and \$40/kg. From Union Carbide, we heard that the silane process works well using the Komatsu technology, but this process is too expensive for solar cell applications. The silane fluidized-bed reactor, which is under development now, must be used. It has been shown that high-purity material can be produced, but the question remains regarding the solar cell efficiencies which can be obtained using this material.

There were also a number of papers showing that the basic understanding of the silane fluidized-bed reactor system and also of particle formation exists. In the work of Osaka Titanium and Shin-Etsu, the trichlorosilane fluidized-bed reactor system was demonstrated. It works, and the production capacity is now about 10 MT/year. More development for that process is needed, particularly with the kind of reactor walls that can be used, like silicon carbide or quartz, and in 1990 this process should yield about 110 MT of silicon for solar cell applications. In Taiwan, a process development is underway for the reduction of silica and then the leaching of metallurgical-grade silicon that could be used for solar cell applications. The Wacker process uses hydro- and pyro-metallurgical purification steps to purify metallurgical-grade silicon to the low parts per million level. At the present time, this process yields charges of about 100 kg. The Siemens advanced carbothermic reduction process was shown to yield silicon which was fabricated in solar cells of about 10% efficiency; it is presently in the pilot plant scale production. The Elkem research work shows that silica reduction and leaching of the silicon seems to work and yields a material with resistivity of about 0.2

to 0.3 ohm-cm, and this basic research done by Exxon and Elkem should now be transferred to a pilot plant scale. It was reported that Pragma has a very similar approach except that silicon carbide is used in place of carbon for the reduction step. Then there is a step for the leaching of the product silicon. If this product is diluted with electronic-grade silicon, solar cells with efficiencies of around 6% or maybe 7% have been made; this value is about 70% of cells made from electronic-grade silicon. At SRI, the silicon tetrafluoride-sodium process works. The silicon has been processed into single crystals which have a quality comparable to electronic-grade silicon crystals. At SERI, the copper silicide vapor transport purification yields a material from which quite decent solar cells were made.

Basically, we have heard about two routes to low-cost silicon. One is the chemical vapor deposition (CVD) method which is followed in Japan and the United States. It gives a material that has a high purity. It's usable for Czochralski crystals and for casting. Its use for sheet production remains to be demonstrated, but I have some doubts (this is my personal opinion) that this material will be low cost. It seems to me that these are competing processes for electronic-grade silicon, and I'm not sure that this is what the photovoltaic industry is waiting for. Then, there are the metallurgical or non-CVD processes, which are primarily being developed in Europe. This route yields silicon which contains a number of impurities in the parts per million range. Consequently, this silicon is considerably lower in purity than the products of the CVD processes. It can be used for solar cells using the Czochralski and casting methods. It remains to be seen whether it is usable for sheet processes. The interesting thing is that the costs of these processes should be below \$10/kg, and this is exactly what is needed for the solar cell photovoltaic industry. The Forum is now open for discussion of the technologies being pursued in these two routes or any other subject of interest.

SCHWUTTKE: We started out 12 years ago with the objective of low-cost silicon, and I believe that maybe this was the wrong emphasis, although it was dictated by the time. Why are we still riding the same horse of low-cost silicon today? Do we really need to push for low-cost silicon as we did 10 years ago? I feel that a tremendous amount of technology has been generated over the last few years which did not exist at the start of the program. In this respect, I believe the photovoltaic program has been one of the greatest successes, and I'm pleased that I was allowed to participate for over 12 years. Now, what do we know today that we did not realize 12 years ago? I think that most of us now believe that the road to success is in the high-performance, single-crystal solar cell. Looking at the paper given by Professor Sah in which he showed that, in contrast to what Dr. Aulich said, the theoretical efficiency of a high-performance silicon solar cell is 22% and not 25%. Now, how can a 22% efficient cell be obtained? Professor Sah pointed out that the first thing to be done is to get rid of the traps in the base of the cell. That means that high performance silicon is needed. Therefore, why worry about cost if high performance silicon is not available? I hope that we will discuss this point in more detail. Another point is that no one has produced a solar cell better than 20%, to my knowledge. In fact, the best cell ever

produced was made by Green and it was, as I remember, 19.1%.

AULICH: In the IEEE Conference here in Las Vegas, he showed a cell with an efficiency of about 25%.

SCHWUTKE: This is late news I was not aware of. However, most likely, it is for a single cell and has not been achieved in production. Maybe then, Professor Sah will have to recalculate the theoretical value for cell efficiency. However, we should discuss whether the driving force is still low cost or will it be high performance. Will low cost be a consequence of obtaining high performance cells?

SANJURJO: The SRI process does not belong to either the CVD process category or to the other category of yours. Where does it fit in your two categories?

AULICH: I didn't pick out any specific processes, but the SRI process probably will fit into the non-CVD category.

NODA: Another important field of amorphous silicon seems to have been forgotten. In Japan, the recent NEDO plan includes amorphous-silicon flat-plate solar cell research together with the polysilicon project. Previously, the amorphous silicon studies had been separated from the low-cost polysilicon project. However, recently the development of amorphous silicon has progressed very rapidly. Starting with this year, the two are competing, like contestants in a small wrestling circle. Thus, the amorphous-silicon project and the low-cost polysilicon project are to compete on equal terms in this arena. Amorphous silicon is a very important competitor for low-cost polysilicon technology. Consequently, this additional factor of amorphous silicon should be discussed here along with our discussion of low-cost polysilicon.

AULICH: I agree with you. I did not discuss amorphous silicon because this conference was mainly about crystalline silicon, but you are absolutely right that amorphous silicon and, really, thin-film technology in general is a very strong competitor in the photovoltaic area. If I may give my personal opinion, it is precisely because the low-cost polysilicon material is not available that a large number of activities in the thin-film area were started. If a low-cost material becomes available, or if the Siemens-type silicon is not too expensive, I think the activities in the amorphous silicon field would not be as large as they are now. I also agree with you that the discussion of cost should include the consideration of amorphous silicon, but I'm not sure that this is the correct time to discuss amorphous silicon. At the IEEE Conference last week, there were a number of excellent contributions regarding not only amorphous silicon, but of thin-film technology in general. I think we must be very careful in our considerations of low-cost silicon for solar cells.

LORD: Regarding the questions of high purity and low cost for the CVD processes, the high-purity processing has been well developed due to the semiconductor silicon market. However, with the successful development of the fluidized-bed reactor processes, there will be an increasing tendency

in the electronic-grade market to go to continuous crystal pulling. Monsanto and other companies have already been involved in looking at this, and it's very attractive. Hence, that puts an additional strain on the purity requirement for the fluidized-bed reactor polysilicon. In continuous Czochralski growth, the same segregation benefits are not available as with batch Czochralski, so there will be a tendency to produce even higher purity polysilicon from CVD processes. That should help, to some degree, the sheet manufacturers who also have very low segregation coefficients. This is one reason that non-CVD silicon producers will have a problem of acceptance in the sheet silicon market because there has been a reliance on the segregation coefficients of the Czochralski system. I think the sheet is a major factor in low cost due to the kerf loss and manufacturing cost of wafering. Cost is, of course, a matter of plant size. The fluidized-bed reactors are far more sensitive to plant size than are the Siemens reactors because the fluidized-bed reactors are much cheaper than the Siemens reactors. Therefore, a 3000 or 4000 MT plant with fluidized-bed reactors will have a considerably lower product cost than a 1000 MT fluidized-bed plant. The other factor that drives low cost is, of course, greed and with the current market price of silicon being high and the production cost of fluidized-bed process being so low, there will be a great temptation to overbuild. I think you will see Union Carbide proposals for 3000 MT plants, and the photovoltaic market may have access to a lot of distressed silicon from companies which built too many plants to satisfy the electronic silicon market.

AULICH: I would like to comment on this. I feel that if the photovoltaic industry is going to make it, it cannot live off the semiconductor-grade silicon. I think it will be a single industry which will have to have its own source of polysilicon. We did not answer the question of Professor Schwuttke whether we need high purity silicon. I invite you to discuss this question.

CALLAGHAN: In Bob Aster's presentation yesterday he gave the driving force of the DOE program in terms of energy price. If we are going to pursue competitive energy prices with other technologies in this country, then the mass of silicon and the silicon price that can be paid, given certain technologies for converting silicon into sheets, cells, and modules, are fairly well prescribed, as he presented. If the price is relaxed, then the silicon cost constraint can be relaxed. That's what is in the DOE Program. There is valid criticism that there are many more markets other than bulk power and competitive energy price at which point, given the various applications, one could mediate the cost one could afford to pay for the polysilicon. I think we have to work it backwards in that way before we can answer the question, "what do we need to pay," in terms of what do we want to do with it. With respect to amorphous silicon, I believe that amorphous silicon-technology was developed based on consumer product activity and proliferated mainly in Japan and was nearly independent of photovoltaic activity in this country. Whether amorphous silicon will be competitive with silicon in the near term, i.e., within a 10-year period, remains to be seen.

McCORMICK: I think using dollars/kilogram is the wrong approach. It should

be dollars/watt and, therefore, the efficiency factor must be used in the computation. I agree with Dr. Schwuttke and Professor Sah because a 20% cell probably allows the use of \$40/kg polysilicon rather than \$10/kg for a 10% cell. It's not a linear relationship. The second thing that I've seen as a supplier of polysilicon is that originally, in discussions with the photovoltaic industry, the statement is that there should be no worry or concern about polysilicon purity as long as it's cheap. That holds until the producer supplies the first 1 or 2 MT of material, and then the photovoltaic company responds by asking for purer poly. I think that, at present, the photovoltaic requirements are almost equivalent to those of the semiconductor-grade level. The difference between what a major solar cell manufacturer uses today and what the semiconductor industry uses today is not tremendously significant.

SCHWUTTKE: Let me amplify this point. For years I have been bothered by the definition of solar-grade silicon. When I was a young physicist, whatever we threw in the wastebasket was solar grade and could be used to make 8% efficient cells. We called this solar grade. Somehow, this has always meant low quality. Actually, a solar cell is an extremely sophisticated device. It needs the finest material we can produce, and if we use the term solar-grade in the context of silicon material for solar cells, it doesn't have meaning for me. Really, in this context, what is needed is a statement of the desired cell efficiency to specify the silicon material. We should forget about solar grade. Finally, everyone will want the highest efficiency and then there won't be any solar grade. It'll just be good silicon.

LUTWACK: I remember that in the early discussions that culminated in the 1973 Cherry Hill Conference, the pricing of the silicon, the sheet, the cells, and the array was based on dollars/watt of the array and not on a value of \$10/kg silicon. The concept of the use of the words solar grade, as far as I can remember, started with a report from a major semiconductor company under contract to the NSF in which one of the primary conclusions was that there was no way of promoting the photovoltaic industry for terrestrial applications using semiconductor-grade silicon. It was simply too expensive. Therefore, a conclusion was that a process for producing less pure silicon had to be developed, and the less pure material was labeled solar-grade silicon.

AULICH: I would like to comment on Dr. Schwuttke's remarks. We have a very pure material available. It is produced by the Siemens CVD process, but this material is not low cost, it is high-cost material. If it is used with the present technology involving Czochralski crystal growth and wafer slicing, the end product photovoltaic module has a peak watt price of about \$5. If this situation is to be the final situation, I think there is no hope for the photovoltaic industry. The use of float-zone material to secure higher efficiencies, which you mentioned, would drive up the cost of the photovoltaic modules considerably. In Europe, we believe that there are photovoltaic applications other than for the utilities. If the cost can be reduced considerably, the consumer will not ask what the peak watt cost is, but he will buy a module. If the cell efficiency is around 9% and the module is good enough for his purpose, the consumer will buy

it; so we should not look only at the use of high-efficiency cells for utility applications. There are a large number of applications. I don't understand how the cost of photovoltaic modules can be decreased by using electronic-grade silicon or using float-zone or Czochralski technologies. An inexpensive starting material is needed. The name for it is unimportant. This material must be convertible into a sheet-like form at a high-drawing velocity and then into cells and modules. The ultimate price must be about \$2/peak watt or even less. Otherwise, as Dr. Noda pointed out, amorphous-silicon or thin-film technology is a serious competitor. I see no future for the photovoltaic industry using electronic-grade silicon along with the other processes being used for the semiconductor industry purposes.

SANJURJO: I am happy to have heard these remarks, because I think that the SRI process is closer to electronic-grade silicon in purity and also closer to the non-CVD processes in cost.

LORD: It's always tempting to put together a new process especially designed for a particular application, but history has shown that when it is possible to take an existing process, like the Siemens process, and make some relatively small modifications (such as adding a fluidized-bed reactor), there is a great potential for improvement in capital cost, in operating cost, and in utility cost by increasing size and, in some cases, the degree of sophistication of design of the plants. It will always be cheaper, I think, to build a 4000-MT/year CVD process instead of a 2000-MT/year CVD process, and a 1000-MT/year solar process plant. Hence, the non-CVD processes will have to wait until the photovoltaic market has developed to a much larger size than it is now.

AULICH: I agree with you that there is a strong tendency in the conventional semiconductor industry to improve on their process and make slight modifications. This is one of the big problems in photovoltaics. On the one hand, a production plant size using the non-CVD process of about 1000 MT/year is required but, on the other hand, the photovoltaic market is much smaller. Therefore, the question is, what can be done with the silicon that is being produced? This is a chicken and egg problem. If the photovoltaic industry can be supplied with \$10/kg material and useful cells can be made, the material problem can be solved. This discussion is very similar to the one conducted 3 or 4 years ago. It seems to me that this is a frustrating situation. Very little is happening and the photovoltaic industry doesn't know what to do. As a consequence, there is much interest in thin-film technology.

LEIPOLD: With respect to solar-grade silicon, we've heard from a number of people that commercial production is several years away and, therefore, we must wait for them if, in fact, they are suitable. I've heard three or four people say that they are producing 10 to 20 MT of solar-grade silicon a year. Now, those quantities, although small, are capable of providing for a significant fraction of the world's present photovoltaic production. Where is that material going and why isn't it being used? Maybe this question is being asked of the wrong audience. Maybe the solar cell manufacturers should answer the question. Why can't this material be

used? Is it being stored? Is it price? Is product quality the problem preventing use? Don't the photovoltaic manufacturers talk to the producers of so-called high-quality solar-grade silicon, which seems to be consistent with the quality being used for the photovoltaic modules being produced today?

AULICH: One answer I heard this afternoon was that the Osaka Titanium fluidized-bed reactor material is being used for casting and is being evaluated in solar cells and modules within the NEDO program. That is the only 10 MT I know of which is being used to fabricate cells. I don't know of any other process that produces 10 MT of usable material. I mentioned that at Siemens we are at the pilot scale development and have run our furnace several times, and each time we produce a few hundred kilograms, which we evaluate in-house by making solar cells. This is not a material that can be commercially distributed. It isn't ready yet. The time scale seems to be about 3 to 5 years.

WRIGHT: All of the economics described today were based on 1000-MT/year production plants, and the price range was given as about \$20/kg. On a pilot scale of 20 to 100 MT/year, I believe the price would be significantly higher. It probably would be \$40 to \$50/kg, if not higher, and I believe that price is the main factor for keeping this material off the market. Also, the non-CVD processes are being developed by the polycrystalline wafer market companies, which are looking at the concept of using the grain boundaries as a sink for some of the impurities. They believe that they could use a cheaper type material. This is similar to the concept I used at Solarex that we could use a much lower grade quality of material given the fact that we could use the inherent nature of the grain boundaries in a polycrystalline wafer as compared to a single-crystalline wafer grown by the Czochralski process. If we tried to process what we called solar-grade material in a Czochralski grower, the product would be a much lower quality material than that obtained from a Semix or HEM process.

AULICH: This morning we saw some pictures of the Pragma process shown by Dr. Rustioni and, of course, it didn't look like the semiconductor industry. It's very difficult for someone familiar with semiconductor devices to look at these pictures of furnaces with their fires and flames and believe that this processing would be useful as a part of the scheme of processing solar cells. However, you have to realize that low-cost polysilicon processing requires compromises. On one hand, there is the semiconductor industry with very clean processes for its devices. On the other hand, there is the metallurgical industry which uses very dirty, but high-efficiency processes. There has to be something inbetween. The question is, where can the inbetween point be? This is why there are many companies working on the non-CVD processes.

LUTWACK: There are people here who can discuss other technologies such as the fluidized-bed reactor systems for the silane process or for the trichlorosilane process, and I'd like to invite them to give us descriptions.

SCHUMACHER: Looking at the papers that have been presented, all of the cost analyses show that the fluidized-bed reactor process would give the lowest cost product. A number of other papers have shown that the impurity levels in the fluidized-bed reactor product were much higher than are achieved in the filament process. The objective of anyone working with a fluidized-bed reactor process today would be to achieve the same quality level obtained in the filament process, and this can be done, I believe. It's obvious, then, there would be a low-cost method of making high-purity silicon to satisfy the requirements described by Professor Sah. We have announced that we have built a pilot plant, called a PDU, a process demonstration plant which (if everything works properly, and usually they don't for some time after startup) could produce as much as 50 MT/year of whatever quality of material the process is capable of. I think we will continue our development and see what happens.

AULICH: I think that any cost reduction that comes about for high-purity silicon that will be offered to the photovoltaic industry will be gladly accepted. I sometimes have the feeling that the competition among the various electronic-grade silicon processes will not end with a large cost reduction, and that, in a few years, the silicon cost will be about the same as it is today. I fear this will happen. If there is anyone here working in the thin-film field, I would like to hear why they have abandoned or shifted or decided to work in thin-film technology. Apparently, there is no one.

FLAGAN: I'm not representing the thin-film technology. To pick up on the comments made by Ralph (Lutwack), the question can be turned around. The fluidized-bed reactor does look like a promising technology, but there are problems. What are the problems and what are the solutions? How much will achieving the solutions cost? Will they drive the price of the fluidized-bed reactor process to the same level as the Siemens process? The reactor liner is clearly a major problem that has been identified in many laboratories. The fluidization process itself, in particular the nature of the distributor plate, is a problem. Advances have been made there and it seems like that is fairly well under control. What are the other problems and what are the directions that the technology development is likely to go to in order to solve them? These are key questions we could discuss, perhaps providing some feedback to lead to results in a shorter time.

SCHWUTKE: I don't want to comment on the fluidized-bed reactor technology, but I would like to consider the question asked about thin films and amorphous silicon. I will express my opinion based on what I have seen over the last few years. The reason for the emphasis on high-efficiency, flat-plate silicon array is the reliability that is built into that system. It is very difficult for me to see that a thin film, or an amorphous film, can match the reliability of a single-crystalline flat-plate array. A lot of difficult research is required to advance amorphous or thin-film cells to the level of reliability now demonstrated by single-crystalline flat-plate arrays and to reach that level will take a long time. Thin films have a special place in the industry, but I believe they are not suitable for large power systems. There needs to be a lot of good research in the next 10 years to improve the reliability.

AULICH: However, there are many people who think otherwise and the progress in recent years has been impressive. One other thing that happens is that a number of companies are turning away from crystalline silicon. They are moving into amorphous-silicon technology or thin-film technology in general. The reason is that they feel that this kind of technology, regardless of the efficiency factor, can achieve a low cost per peak watt. If this happens, and the time for a crystalline material to be used in the photovoltaic industry becomes longer, industry will be very reluctant to come up with a factory that produces 1000 MT/year of silicon if there is no future in crystalline silicon.

SCHWUTTKE: I have to agree that companies stay in business for only one purpose: to make a profit. A company will jump in quickly to skim off the market, and this has been done with amorphous silicon and with thin-film technology, but this does not exclude the conclusion that research must be done and must be emphasized in order to make progress. We must separate profit from research activities and progress. Profit does not always mean progress in technology and in science. These are two separate issues.

AULICH: I agree with you.

FLAGAN: I agree with your comments also, but there is one thing that really disturbs me in this discussion. Everyone has talked about major power systems. It reminds me of what I heard for years in the synthetic fuels game. Everyone was going to put the oil companies out of business with shale oil, synthetic natural gas, and so on. Those things came into the spotlight for awhile, and then faded from view. They will come back again. The immediate application for photovoltaics is not likely to be in major electric utility installations. It will be in smaller installations. The photovoltaic industry today is certainly not providing hardware for the utilities on a large scale, but rather are providing for specialty applications. Emphasis on producing a material which is only usable for installations by large-scale utilities is a very narrow view that will, in fact, limit progress because it will prevent development and hinder the momentum necessary to carry on for the long term rather than be shut down by a quirk in funding.

SCHWUTTKE: I think we are in agreement. Our society is money oriented and profit driven. The ideal solution to the problem would be a large government program that funds the production of small photovoltaic units and gives them away to underdeveloped countries. I think that this would be the greatest contribution the United States could make for the under-developed countries. There would be a tremendous feedback. It would be an ideal situation because such units are desperately needed, and these countries don't have the money to pay for the units.

AULICH: I agree that this would be an ideal situation but, unfortunately, reality is different. It is extremely important for the photovoltaic industry to find applications for photovoltaic modules now, and there are a number of applications. If the cost of photovoltaic modules drops down, it doesn't have to drop by a factor of 10, there will be more and more applications at the existing prices. This is what is necessary. There will be no sharp jumps, but it will be a slow, continuous development, which is needed by the photovoltaic industry.

LORD: I can't help responding to the statement about giving photovoltaic panels away to poor, undeveloped countries because that's what they need. I believe that the French did, in fact, do that and gave away solar-powered systems that ran water pumps on the edge of the Sahel desert in the mid-1970s. These were very useful, pulling a lot of water out of the ground. This encouraged the nomads to gather around the well and to build up their cattle herds. However, these photovoltaic systems were not maintained and fell into disrepair. The huge numbers of cattle were a major contribution to the Sahel famine in the late 1970s. So before we push our problems of excess solar-cell capacity, we should look carefully at what we do for the poor, undeveloped countries.

AULICH: I'd like to correct you. They were not photovoltaic-driven hot water pumps. They were conventional diesel-powered water pumps. There were very few photovoltaic pumps.

SCHWUTTKE: What they needed was a 25- to 30-year reliability.

LUTWACK: I would like to ask Professor Flagan to comment on the application of the theory and experimental information about nucleation that he has obtained to what he has learned about the operation conditions of the fluidized-bed reactor in the silane system, and whether he sees great technical problems in the application of the silane fluidized-bed reactor.

FLAGAN: I don't understand all of the things going on in a fluidized-bed reactor. I look at the structure of the particles coming out of our silane pyrolysis flow reactor, and it is a very low-density material. The product particles from the fluidized-bed reactor are a high-density material, on the other hand. The basic chemistry and physics of the particle growth of the fluidized-bed reactor are not obvious. A better understanding is necessary in order to apply nucleation theory to the fluidized-bed reactor-silane system. There are major differences between the fluidized-bed reactor and the flow reactor. In the fluidized-bed reactor, there are boundary layers around the large particles in the bed, and the effects of the bed particles are not felt outside the boundary layer. One can apply the basic theory which we have developed to those interstitial regions without major approximations. To describe the whole bed will require a major theoretical development. I'm not sure that this is a limiting factor or even a major consideration in the development of the fluidized-bed reactor. It looks like the technology is well advanced provided the technology problems of seed particles, of reactor liners, and basic materials can be solved. I don't see a major problem.

AULICH: From your research, can you comment on any problems that would arise on increasing the fluidized-bed reactor size, assuming a large reactor size would be advantageous so that 50 or 60 reactors would not be necessary for a 1000 MT/year plant? How large a reactor is feasible or desirable?

FLAGAN: Which type of reactor do you mean?

AULICH: The fluidized-bed reactor.

FLAGAN: I'm not an expert on fluidized-bed reactors. I must leave the answer to your question to those who are.

LUTWACK: Professor Flagan, companies have been successful, to a large extent, in the operation of fluidized-bed reactors using trichlorosilane as the feedstock. Would you comment on the differences between the use of trichlorosilane and silane in a fluidized-bed reactor?

FLAGAN: A discussion of this point began in 1980 when I participated in a workshop dealing with the problems experienced by Union Carbide and JPL in their experiments with the silane-free space reactor. The following question was raised: In the free-space reactor, there is a problem with homogeneous nucleation, i.e., with the formation of large numbers of very small particles. The control of this fine particle formation and the production of larger particles were desirable (usable either as seed particles for the fluidized-bed reactor, or alternatively usable directly as feed for a crystal puller crucible). Both of these uses are feasible if large enough particles can be made. The fluidized-bed reactor requires particles of perhaps 100 μm , and the other process could use smaller particles. The silane system was chosen for a variety of reasons. A question that I asked at that early workshop was, "why use silane?" If a flow reactor is to be used and the objective is to grow large particles, it is desirable that homogeneous nucleation be minimized. To do this, the extent of supersaturation that can possibly take place in a reactor must be minimized. The first step of the silane system is an irreversible reaction; maybe it's not strictly irreversible, but at these temperatures it can be treated as irreversible. With that type of reaction, super-saturation builds up very quickly and that, in fact, leads to the very large number of small particles in the free-space reactor. On the other hand, if a halosilane is used, the decomposition reaction is not irreversible, and the reverse reaction of etching of the silicon can occur. The result would be an equilibrium vapor pressure of silicon species, the supersaturation would be lower, and the problem of controlling nucleation would be greatly reduced. No one has yet gone that route to my knowledge. Although I have seen papers, I haven't seen data from experiments to produce usable-sized particles from such a reactor. However, it seems that by choosing a more reversible chemical system, control requirements would be eased and there would be a better chance to produce larger particles. However, from my point of view, the silane system was the best one for my studies because by investigating the most difficult system first, we learned a tremendous amount about homogeneous nucleation. Now we can apply that knowledge to simpler systems.

AULICH: After learning so much about the silane system, would you like to turn to the trichlorosilane system now?

FLAGAN: Perhaps. I have not done the full analysis on that system. The use of a reaction which has the possibility of etching would probably result in denser particles because the higher surface energy will lead to some vaporization and recondensation from the flocs that we now see. Second, the tendency to nucleate will decrease.

AULICH: Dr. Noda, in your paper, you presented the work from Osaka Titanium and Shin-Etsu, but you also mentioned other processes underway such as production of silicon tetrachloride by a silica, carbon, and chlorine reaction as well as the process being developed by Nippon Sheet Glass for the carbothermic reduction of high-purity silica. Does this mean that NEDO is not very confident that your process will achieve the cost goal? Why are other processes being developed?

NODA: I think that NEDO has confidence in the NEDO process. The descriptions of many low-cost polysilicon processes were given today in this workshop. NEDO has also evaluated the different means of using the Japanese resources, and this evaluation has resulted in a change of the NEDO position in processing. Therefore, NEDO has expanded its project plan from 10 to 100 MT and then to 1000 MT/year. I want to emphasize that in Japan, as I have already mentioned, the research in the amorphous-silicon field is very important and is well supported. Not only has there been activity for using amorphous silicon for calculators and watches, but recently also in the field of solar-power generators. Many are involved in these research programs. This year, NEDO included in the NEDO plan the development of two methods. One of these is the conventional low-cost polysilicon production by the NEDO process and the other is the amorphous-silicon method. Many think there is a definite possibility for the successful development of amorphous silicon for solar cells within 10 or 15 years. However, in the interval before that happens, solar cells must be manufactured and, therefore, it is necessary to develop another polysilicon production method to bridge this time period. Each of these methods has an equal opportunity for success, and they will complement each other in many areas in the future. As Professor Schwuttke said, some solar-cell areas require crystalline silicon and other solar-cell areas may require another type of solar-grade silicon. The methods of producing these types of silicon can coexist. This is the current opinion in Japan.

KOINUMA: I would like to add some comments on this question. As far as I know, NEDO considers the fluidized-bed reactor process for producing solar-grade silicon as the method for producing the raw material for solar photovoltaic cells until the year 2000. Then, NEDO believes the non-CVD type of process may be feasible for the long term for producing a type of silicon material. NEDO believes that in the field of fluidized-bed reactor technology, Japan is already leading JPL and UCC in the production of high-purity silicon. However, Japan has not paid much attention to the non-CVD type of process so far. Recently, a new idea for the production of silicon by a non-CVD process was proposed in Japan. That's the reason that NEDO supports such a process. The process will be evaluated at the end of next year to determine if it should have continued support.

SCHWUTTKE: I would like to consider the subject of the impurity carbon in silicon. I have noticed a great deal of concern repeatedly at this meeting, but I haven't obtained from anyone a precise definition of the anticipated effects of carbon in silicon and what are the actual effects. I would like to summarize my experience dealing with carbon in silicon. If carbon is present substitutionally in silicon, it will contract the lattice. The silicon lattice can take up a fairly large amount of

carbon. In fact, in our experiments at IBM with silicon doped with carbon, we had driven up the carbon concentration to $5 \times 10^{18}/\text{cc}$ and maintained zero defect 4-in.-diameter crystals and found that the minority carrier lifetime distribution was better for carbon-doped silicon than for silicon with low carbon. We explained this result simply by a lattice contraction which drives the large-size impurities out of the lattice. Whenever the carbon concentration was made higher, say above $5 \times 10^{18}/\text{cc}$, silicon matrix breakdown occurs locally through silicon-carbide formation. Many do not appreciate that this local breakdown occurs. My experience in ribbon growth using carbon dies confirms that the carbon concentration can be at a high level (for instance, $5 \times 10^{18}/\text{cc}$) without causing any negative influence on single-crystal silicon, even in the presence of oxygen, by the way.

AULICH: What would happen with respect to the doping concentration? We observed, for example, that when we grow Czochralski crystals, if the boron concentration is greater than 5×10^{16} , the diffusion length decreases dramatically, and there are no impurities in this electronic-grade material. This is a mystery. Others found the same behavior, and no one has offered an explanation for this. Do you have any experience with this?

SCHWUTTKE: Are you referring to Czochralski or float-zone material? I have never observed this effect in boron-doped Czochralski material. As a matter of fact, our experiments were conducted with 10 to 20 ohm-cm, boron-doped material. It may be different with your material at your concentrations.

AULICH: The high-efficiency solar cells of Green were obtained on float-zone material of about 0.2 ohm-cm. If we would have done exactly the same with Czochralski material, the solar-cell efficiency would be very low.

SCHWUTTKE: I want to emphasize that our investigations were with integrated circuits and MOS devices, and the minority carrier lifetime I measured was generation lifetime. There is obviously a difference between recombination and generation lifetimes but, in general, I would like to repeat that we did not observe any negative effects for integrated devices. What was your doping concentration of the drop in the minority carrier lifetime?

AULICH: Around 10^{17} .

SCHWUTTKE: A concentration of 10^{17} is equivalent to less than 1 ohm-cm. I have no experience with such material.

AULICH: This is one of the important factors to be considered for low-cost silicon by a metallurgical process; i.e., that there are given boron and phosphorus concentrations and if these are not at levels to give 0.4 or 0.5 ohm-cm, then the solar cells will be very low efficiency. No matter how pure the silicon is with respect to molybdenum, titanium, and so on, this doping level has to be reached.

I have one other question, and it is directed to Union Carbide. Up to now, the photovoltaic industry seems to live on so-called off-grade scrap solar-grade material from many sources. The photovoltaic industry needs more low-cost material to expand. Will there be more of this scrap material available to the photovoltaic industry after Union Carbide reaches large-scale production of, for instance, 1200 MT/year, using the silane-Komatsu process?

IYA: I'm not sure I can answer that question. It's our intention not to produce any off-grade polysilicon. We would like to make everything on specification.

AULICH: Well, my question is not answered.

BRIGLIO: I don't feel that I feel nearly as hopeless about the use of fluidized-bed reactors to get high purity and run for long times. I think that the solution is the liner. I'd like to ask Union Carbide if in their longest run, which I think was 66 h with a liner, whether the liner broke on cooldown. I think if there are long durations (continuous operation for perhaps several months), then maybe liner breakage will not be a big problem. I think that some of the liner problems in the past were because of liner support design and I think those have been solved, and if now there are very long runs without cooldowns, I'm hopeful it will not be a problem.

IYA: I believe the question pertains to whether the quartz liner will break on cooldown. In our experience with the runs of 40, 50, 60 h duration, the liners cracked during the cooldown cycle because of thermal stresses. The answer to this problem is not to interrupt the run after short times, but rather to use runs of 2 or 3 weeks or longer and make a lot of product and then throw away the used liner and install a new liner. Another approach would be to use a liner, such as a polysilicon liner, which we will test under our program.

SESSION VI

POLYSILICON MARKET AND FORECASTS

M. Prince, Chairman

Semiconductor Market

Remo Pellin
Industrial Consultant
Charlotte, North Carolina

Electronic grade polycrystalline silicon is the basic raw material of the electronic industry and will remain the most important semiconductor material for the rest of this century. The technology of manufacture of silicon devices has advanced rapidly and the physics of the material, silicon, will allow this technology to continue to improve rapidly. Since 1975 the computational power of silicon devices has increased by a factor of a thousand for a price increase of only a factor of six. During the next ten years a similar 1000 fold increase in the computational power of silicon devices for a price increase of only a factor of six will again take place. Other materials will be used in the manufacture of electronic devices but such devices will only be supplementary to the silicon electronics that exists today.

Forecasting the amount of polycrystalline silicon that will be used in future years is not a simple task. Obviously the amount of polycrystalline silicon used will correlate with the number of silicon devices manufactured and the number of silicon devices manufactured will correlate with the value of electronic equipment produced. In this paper a forecast of polycrystalline silicon usage will be constructed based on forecasts of the production of electronic equipment and silicon electronic devices.

The electronic industry, the silicon device industry, and the polycrystalline silicon industry are a truly worldwide phenomenon. The same electronic equipment is used everywhere. The same electronic devices are used everywhere. The same silicon wafers are used in all parts of the world. The same quality polycrystalline silicon is used everywhere. The value of all these products is high versus their weight and therefore can be shipped anywhere cheaply. This electronic industry is truly worldwide in every respect and in this paper world wide data only is used.

In Figure 1 the free world consumption of electronic equipment in real dollars is plotted for the years 1974 - 1990. The market is further broken down for the four electronic categories, data processing equipment, industrial equipment, consumer goods, and communication gear. In 1974 less than one hundred billion dollars worth of electronic goods were used. In 1985 it is expected that a half trillion dollars worth of goods will be sold. It is forecasted that by 1990 the electronic market will pass a trillion dollars.

In Figure 2 the free world consumption of electronic equipment is compared with the free world consumption of silicon electronic devices. Between 1974 and 1984 the average value of silicon devices consumed was 9% of the value of electronic equipment manufactured. During 1985 the price of the average silicon device has decreased by 18%.⁽¹⁾ This has caused the percentage value of silicon devices versus electronic equipment to decrease to 8%. This value is

forecasted to continue for some years. Figure 2 explains this phenomena. Bookings for silicon devices have dropped substantially. Bookings for computers are still increasing. As competitive as is the personal computer market, the silicon device industry is even more predatory and it is believed the price decreases in silicon devices are permanent.

Regardless of sales decreases in the silicon device industry during 1985 the market is still elastic and will continue to grow at an average of 25% per year.(2) The growth will not however be constant. The years 1971, 1974, 1981 and 1985 were all recession years for this industry. The years 1970, 1973, 1979 and 1984 were boom years. The market will fluctuate similarly in future years.

In Table #1 the history of silicon electronic device usage by device category is presented for the years 1974 - 1984. This Table shows the growth of silicon integrated circuits dramatically. In Table #2 a forecast is made of future use of silicon devices. Basically these Tables show that the consumption of silicon devices will grow from \$5,750,000,000 in 1974 to \$80,300,000,000 in 1990.

Table #3 shows the companies who manufacture silicon electronic devices and their sales over the years 1977 - 1985. The growth of the Japanese Companies. NEC, Hitachi, and Toshiba is phenomenal. This Table shows estimates of silicon device manufacture by IBM, Western Electric and General Motors who sell no devices to the outsideworld but only use such devices internally. Actual sales of silicon electronic devices for the years 1983 and 1984 are shown in Table #4.

Between 1960 and 1982 one figure of merit in the silicon electronic device industry was remarkably constant: Worldwide, silicon device companies manufactured \$18 worth of silicon devices per square inch of polished silicon wafer used over all these years. The value of devices manufactured per square inch of silicon varies with device and with the time cycle of the device. The price of silicon polished wafers varies with the device manufactured. Nevertheless during the years 1960 - 1982 the average value of devices manufactured per square inch of silicon wafer was \$18. In 1983 a slight decline in this figure of merit was noticed and the decline continued in 1984 and 1985 and is expected to decline in future years as the industry matures.

Table #5 makes use of this figure of merit to construct a forecast of silicon material usage. The Table is enormously complex but has proved quite accurate and useful during the past ten years. Column 2 shows silicon electronic device usage. Column 3 shows the above discussed figure of merit to determine the value of silicon wafers required. By 1990 it is expected that the figure of merit will increase to \$23 of silicon device sales per square inch of silicon wafer used. Column 4 shows the dollar value of silicon polished wafers used during any given year. Column 5 shows the average price per square inch of polished wafer. Column 6 shows the number of square inches of silicon polished wafers used. Column 7 shows the average diameter of silicon crystal used during any given year. Column 8 shows the average number of grams of polycrystalline silicon required to manufacture one square inch of polished silicon wafer. Column 9 shows the number of metric tons of specification crystal required to manufacture the annual need of silicon wafers. Column 10 shows the

requirement of electronic grade polycrystalline silicon in any given year.

A large number of assumptions were made in putting this forecast together.

1. Prior to 1983 the following yields at each silicon material process step were standard practise.

1. Crystal Growth	- 60%	5. Lapping	- 97%
2. Crystal Grinding	- 98%	6. Etching	- 97%
3. Crystal Slicing	- 93%	7. Polishing	- 93%
4. Wafer Beveling	- 97%		

By 1983, the crystal growth yield was no longer exact. Japanese silicon device manufacturers began requiring tighter silicon crystal parameters and drove this yield in Japan below 50%.

2. The progression to larger and larger diameter wafers, but insistence upon equivalent wafer flatness forced wafers to be manufactured thicker and thus require more polycrystalline silicon per square inch.
3. Silicon Device manufacturers use a great many test wafers during device processing. Test wafers have similar specifications to product wafers but produce no devices. Test wafers are not included in Table 5.
4. It is assumed that much averaging occurs. When a new silicon materials plant comes on line, yields are poor for a time. When new devices come on line, the yield of good devices is poor for a time. As knowledge increases, the yields of wafers and devices increase.
5. New plants and new devices are seldom brought on line in recession years. This makes boom years boomier and recession years gloomier for silicon material manufacturers.
6. A considerable time lag occurs between the manufacture of polycrystalline silicon and the sale of a silicon device manufactured from it. In Table 5 it is assumed that 3 months occur between the manufacture of polycrystalline silicon and the sale of the polished wafer and that an additional 3 months occurs between the sale of the polished wafer and the device manufactured from it.
7. Silicon materials people live on a learning curve and get better and better at their jobs. It is assumed that wafer specifications get tighter and tighter as transistor density increases and that the tug of war between improving efficiency of wafer manufacture and tighter specifications is a standoff.
8. The dollars referred to in Table 5 are real dollars at time of use.
9. The manufacturing technology of silicon wafers and devices has been

continuously modified for 25 years but never significantly changed. It is assumed this situation will continue.

10. It is assumed that between 1985 and 1990 much of the growth in silicon electronic devices will take place in CMOS Integrated Circuits. This change is traumatic to the silicon wafer industry since the sale of polished wafers will be replaced by the sale of epitaxial wafers. In Table 5 the sale of epitaxial wafers is not delineated. Only the sale of polished wafers as substrates for epitaxial wafers is considered. It is expected that the overall increased yield of devices from epitaxial wafers will exactly compensate for the yield loss in going from a polished wafer to an epitaxial wafer.
11. Implicit in Table 5 is a major change in the silicon materials market. The merchant vendors of silicon polished wafers have won the battle with internal manufacturers. In the future most wafers will be manufactured by merchant vendors such as Wacker, Monsanto, SEH and Osaka.

The companies listed in Table 4 are the customers for silicon polished wafers and will purchase wafers in correlation with their sales of silicon devices. The thirty companies listed will purchase at least 80% of all silicon wafers sold.

In Table 6, a history is presented of silicon wafer manufacturers for the years 1977 - 1984 and in Table 7 a forecast is made of who will manufacture wafers in the future. The all other category grows large toward the end of the 1980s. The companies listed below have announced plans to enter the polished silicon wafer business in the near future and will compete with the 21 companies listed in Table 7 for a forecasted three billion dollar business in 1990.

1. Rhone Poulenc - France (3)
2. J.C. Schumacher - USA (4)
3. Toya Soda Mfg. Co. - Japan (5)
4. Showa Denko K.K. - Japan (6)
5. Kawasaki Steel Corp. - Japan (7)
6. Nippon Steel - Japan (8)
7. Korea Electronic Materials - Korea
8. Lucky Gold Star - Korea

The manufacture of polished silicon wafers requires electronic grade polycrystalline silicon of exceptional purity and more than 90% of all polycrystalline silicon is sold on a long term contract basis. Some 5% of electronic grade polycrystalline silicon is sold on the spot market. The remaining 5% of polycrystalline silicon produced, does not meet the stringent specifications and is sold as an off grade product. Table 8 shows the price history of polycrystalline silicon. Contract pricing has been remarkably constant. The pricing on the spot market has been volatile and shows the results of panics in 1970, 1973, 1980 and 1984 when annual usage exceeded annual capacity to produce and inventories were depleted.

A history of polycrystalline silicon manufacturing capacity is shown in Table 9. A Forecast of future capacity is shown in Table 10. Capacity stays close to demand. All companies except Texas Instruments, Komatsu Electronic Metals and Union Carbide use the Siemens Process, decomposing trichlorosilane to elemental silicon of a rod form. Texas Instruments decomposes trichlorosilane on silicon particles in a fluidized bed. Komatsu manufactures silane by hydrolyzing a magnesium silicide alloy and decomposes the silane to silicon in a rod form. Union Carbide catalytically converts silicon tetrachloride to silane which is then decomposed to elemental silicon in a rod form.

A number of new companies have announced plans to manufacture polycrystalline silicon in the near future.

1. Ethyl Corporation - USA
2. Great Lakes Chemical Corporation - USA
3. J.C. Schumacher Co. - USA
4. Nippon Kokan KK - Japan

The Ethyl Corporation(9) will decompose silane on silicon seed particles in a fluidized bed. The Great Lakes Chemical Corporation will use an advanced Siemens Process. J.C. Schumacher will decompose tribromosilane to elemental silicon on seed particles in a fluidized bed. Nippon Kokan will use Siemens Process Technology obtained from the General Electric Company.

Crystal growth people prefer the fluidized bed product spherical pellet polycrystalline silicon because it pours easily. The use of this product allows crystal growers to fill crucibles more completely and thus get greater throughput from equipment. Further, this product would allow the development of semi-continuous crystal growers. Unfortunately, up to this time, the requisite purity in polycrystalline silicon has been difficult to attain.

The Siemens Process is only generically named. All companies practise widely different technologies which result in rather different types of products and widely ranging costs. Purity, however has never been a problem when the Siemens Process is used.

Bibliography

1. In-Stat - Electronic News October 7, 1985
2. Loring Wirbel - Electronic News September 30, 1985
3. Electronic News June 25, 1984
4. Electronic News September 30, 1985
5. Electronic News July 8, 1985
6. Electronic News October 21, 1985
7. Electronic News August 5, 1985
8. Electronic News June 17, 1985
9. Electronic News October 21, 1985

Table 1
A History of Free World Silicon Device Usage
By Product And In Millions of Dollars

<u>Device Type</u>	<u>1974</u>	<u>1975</u>	<u>1976</u>	<u>1977</u>	<u>1978</u>	<u>1979</u>	<u>1980</u>	<u>1981</u>	<u>1982</u>	<u>1983</u>	<u>1984</u>
<u>Total Silicon Devices</u>	5750	5170	6545	8610	9905	11,900	14,120	15,100	16,460	20,822	30,124
<u>Total Discrete Devices</u>	2895	2350	2801	3010	3280	3460	3720	3700	3770	4522	5724
Thyristors	232	180	241	292	319	353	361	335	351	410	530
Power Rectifiers	482	398	504	570	618	670	690	473	453	530	690
Power Transistors	526	425	540	610	653	669	707	676	665	800	1110
Zener Diodes	139	100	135	148	158	203	206	171	175	210	300
Small Signal Transistors	874	638	803	853	881	988	1026	1038	1026	1200	1575
Solar Cells	10	10	13	15	22	27	38	44	56	77	85
Other Devices	632	599	665	562	629	809	692	943	1044	1302	1434
<u>Total ICs</u>	2855	2820	3744	5600	6625	8440	10,400	11,400	12,690	16,300	24,400
Bipolar ICs	979	782	905	1301	1487	1775	2119	2402	2690	3300	5200
Linear ICs	651	601	1004	1216	1373	1724	1993	1920	2501	2850	4300
Microprocessors	41	97	154	318	508	774	1159	1402	1769	2150	3900
MOS ICs	880	937	1229	2037	2412	3457	4488	4791	5118	6800	9800
Special Circuits	304	403	452	728	845	710	641	685	612	1200	1200

Table 2

A Forecast of Free World Silicon Device UsageBy Product And In Millions of Dollars

<u>Device Type</u>	<u>1984</u>	<u>1985</u>	<u>1986</u>	<u>1987</u>	<u>1988</u>	<u>1989</u>	<u>1990</u>
<u>Total Silicon Devices</u>	30124	25000	29000	38000	50000	65000	80300
<u>Total Discrete Devices</u>	5724	5500	6000	6700	7400	8200	9000
Thyristors	530	510	560	575	655	745	800
Power Rectifiers	690	660	730	730	830	940	
Power Transistors	1110	1050	1150	1465	1730	2040	2500
Zener Diodes	300	290	310	325	370	444	490
Small Signal Transistors	1575	1500	1650	1675	1875	2075	2250
Solar Cells	85	90	100	115	125	140	160
Other Devices	1434	1400	1500	1815	1815	1816	1800
<u>Total ICs</u>	24400	19500	23000	31300	42600	56800	71300
Bipolar Digital ICs	5200	4100	5000	6700	7900	8400	9000
Linear ICs	4300	4100	4100	5100	6600	7000	7200
MOS Logic ICs	3700	2800	3300	4700	5900	6200	6400
MOS Memory ICs	5400	3500	4600	6500	8100	9000	10000
CMOS ICs	3400	3700	4600	6400	12000	24000	36000
Special Circuits	1200	1300	1400	1900	2000	2200	2700

Table 3

Silicon Device Manufacture
By Company And In Millions of Dollars

<u>Company</u>	<u>1977</u>	<u>1978</u>	<u>1979</u>	<u>1980</u>	<u>1981</u>	<u>1982</u>	<u>1983</u>	<u>1984</u>	<u>1985</u>
Texas Instruments Inc.	772	945	1210	1410	1400	1500	1595	2446	1850
Motorola Inc.	572	718	920	1135	1350	1650	1497	2224	1670
IBM*	550	625	750	940	980	1040	1200	1700	1700
Western Electric*	520	600	700	800	880	980	1080	1400	1400
General Motors*	400	430	480	550	500	550	600	900	900
National Semiconductor	300	420	620	780	750	780	894	1245	900
Nippon Electric Corp.	363	555	780	970	1050	1180	1435	2207	1900
Hitachi Ltd.	271	455	728	900	980	1080	1294	2156	1800
Toshiba	253	381	495	645	700	800	1021	1545	1400
Fujitsu	89	124	240	391	430	470	704	1078	900
Matsushita	192	254	270	283	330	390	610	905	800
Mitsubishi Electric	100	140	190	253	300	370	445	705	600
Fairchild	323	379	470	520	530	530	460	658	500
Siemens	250	292	410	460	440	450	510	620	600
RCA	206	236	270	300	290	280	297	404	300
Intel Corp.	200	300	430	680	700	720	770	1190	1000
Mostek Corp.	71	105	210	290	270	270	315	470	200
Advanced Micro Devices	82	132	208	270	270	300	477	922	600
Phillips	533	622	780	895	885	950	910	1265	1100
Tokyo Sanyo Electric	80	99	140	174	190	205	330	492	400
Oki Electric	80	90	100	113	130	170	221	315	250
Sharp Corp.	300	295	290	291	240	200	265	376	300
Sony Corp.	-	-	-	5	10	40	70	110	110
American Microsystems Inc.	82	132	140	145	145	155	162	173	160
All Others	2083	1676	1049	880	1350	1400	3660	4618	3660
Total	8610	9905	11900	14120	15100	16460	20822	30124	25000

*Estimated

Table 4

**SEMICONDUCTOR SALES—WORLD WIDE
U.S.—EUROPEAN—JAPANESE MANUFACTURERS
DOLLARS IN MILLIONS**

	Annual Sales		Percent Change
	1983	1984	1984
1. Texas Instruments	\$1595	\$2446	+53.4
2. Motorola	1497	2224	+48.6
3. NEC	1435	2207	+53.8
4. Hitachi	1294	2156	+60.0
5. Toshiba	1021	1545	+51.3
6. National	894	1245	+39.3
7. Intel	770	1190	+54.5
8. Fujitsu	704	1076	+53.1
9. AMD	477	922	+93.3
10. Matsushita	610	905	+48.4
11. Signetics	435	720	+65.5
12. Mitsubishi	445	705	+58.4
13. Fairchild	400	656	+43.0
14. Philips	475	545	+14.7
15. Sanyo	330	492	+49.1
16. Mostek	315	470	+49.2
17. Siemens	335	452	+34.9
18. RCA	297	404	+36.0
19. Sharp	265	376	+41.9
20. SGS-ATES	230	335	+45.7
21. OKI	221	315	+42.5
22. General Instrument	283	287	+ 1.4
23. General Electric	204	282	+38.2
24. Thomson CSF	190	275	+44.7
25. Harris	180	268	+48.9
26. ITT	195	255	+30.8
27. Analog Devices	140	219	+56.4
28. Monolithic Memories	121	200	+65.3
29. AMI	162	173	+ 6.8
30. International Rect.	94	124	+31.9
TOTAL Top 30	\$15674	\$23470	+49.7
Percent of Total Semi Industry	88.2%	90.4%	
TOTAL Semi Industry	\$17767	\$25956	+46.1

Table 5

A Free World Forecast of Silicon Material UsageBasis - Millions of Dollars & Millions of Square Inches

Year	Silicon Device Usage \$	% Material Value	Silicon Wafer Value \$	Average Value Per Sq. Inch \$	Silicon Wafers Square Inches	Average Crystal Diameter Inches	Grams of Polysilicon Per Square Inch of Wafer	Single Crystal Metric Tons	Polysilicon Metric Tons
1974	5,750	4.17	234	0.75	312	2.8	2.79	522	871
1975	5,170	4.17	230	0.75	307	2.9	3.00	533	921
1976	6,545	4.17	294	0.75	392	3.0	2.99	702	1170
1977	8,610	4.17	373	0.75	497	3.0	2.66	796	1326
1978	9,905	4.17	430	0.75	573	3.2	2.91	1001	1668
1979	11,900	4.17	519	0.77	674	3.5	3.10	1289	2148
1980	14,120	4.17	599	0.80	749	3.7	3.09	1387	2312
1981	15,100	4.17	644	0.82	785	3.9	3.27	1515	2568
1982	16,460	4.17	714	0.85	840	4.1	3.68	1793	3092
1983	20,822	4.15	963	0.90	1070	4.3	4.31	2718	4853
1984	30,124	4.10	1164	0.90	1293	4.4	4.43	3090	5617
1985	25,000	4.05	1053	0.88	1197	4.6	4.41	3039	5525
1986	29,000	4.00	1252	0.88	1423	4.8	4.47	3781	6875
1987	38,000	3.95	1620	0.86	1884	5.0	4.44	4957	9013
1988	50,000	3.90	2098	0.85	2468	5.2	4.50	5647	11620
1989	65,000	3.80	2485	0.85	2924	5.4	4.60	7860	14292
1990	80,300	3.70	3108	0.85	3657	5.6	4.70	9936	18067

Table 6

Free World Manufacture of Silicon Polished WafersIn Millions of Square Inches

<u>Company</u>	<u>1977</u>	<u>1978</u>	<u>1979</u>	<u>1980</u>	<u>1981</u>	<u>1982</u>	<u>1983</u>	<u>1984</u>
1. Wacker Chemetronic Gmbh	96	110	119	133	131	122	160	205
2. Monsanto Company	96	110	119	133	131	120	151	195
3. Texas Instruments Co.	46	52	60	65	65	63	65	80
4. Osaka Titanium*	50	42	60	63	66	90	145	195
5. Motorola Inc.	23	31	41	45	47	41	41	41
6. Shen Etsu Handotoi	22	33	48	54	74	122	165	190
7. Siltec Corp.	22	28	31	32	34	30	40	50
8. IBM	19	21	31	36	37	32	30	30
9. General Motors	21	24	25	26	26	25	25	25
10. Dynamit Nobel	14	21	25	29	34	54	65	65
11. Western Electric	12	16	19	23	28	25	25	25
12. Fairchild C. & I. Co.	10	16	19	21	21	19	20	22
13. Komatsu Electronic Metals	11	13	15	14	23	25	44	55
14. Philips	5	5	6	6	8	7	7	7
15. Ametek Inc.	-	-	-	3	3	3	3	3
16. Crysteco Inc.	4	4	3	3	6	6	7	11
17. Pennsilco	4	4	5	6	6	7	7	11
18. Cincinnati Milacron Inc.	-	-	-	2	5	5	8	11
19. Topsil (Denmark)	5	5	5	5	5	5	5	5
20. All Others	37	38	43	44	41	49	57	67
Annual Usage	<u>497</u>	<u>573</u>	<u>674</u>	<u>749</u>	<u>785</u>	<u>840</u>	<u>1070</u>	<u>1293</u>

*Includes Production By Japan Silicon Company, Toshiba and Hitachi

Table 7

A Forecast of Free World Manufacture of Silicon Polished WafersIn Millions of Square Inches

<u>Company</u>	<u>1985</u>	<u>1986</u>	<u>1987</u>	<u>1988</u>	<u>1989</u>	<u>1990</u>
1. Wacker Chemetronic Gmbh	180	200	250	320	360	450
2. Monsanto Company	175	180	210	260	300	380
3. Texas Instruments Inc.	80	80	80	80	80	80
4. Osaka Titanium	75	120	175	240	300	400
5. Motorola	40	40	40	40	40	40
6. Shen Etsu Handotai	190	230	300	400	500	700
7. Siltec Corp.	50	60	70	80	105	125
8. IBM	30	30	30	30	30	30
9. General Motors	25	25	25	25	25	25
10. Dynamit Nobel	60	70	90	120	150	180
11. Western Electric	25	25	25	25	25	25
12. Komatsu Electronic Metals	60	60	100	140	160	200
13. Philips	7	7	7	7	7	7
14. Crysteco Inc.	10	14	14	18	25	30
15. Pennsilco	10	14	18	22	25	30
16. Cincinnati Milacron	11	14	18	22	32	40
17. Topsil (Denmark)	5	5	5	5	5	5
18. Japan Silicon Co.	85	130	180	250	300	380
19. Toshiba	21	27	40	45	45	45
20. Hitachi	20	27	40	45	45	45
21. Virginia Semiconductors	6	6	6	6	6	6
22. All Others	27	59	161	288	312	422
Total	1197	1423	1884	2468	2924	3745

Table 8

Polycrystalline Silicon Pricing RangeDollars/Kilogram

<u>Year</u>	<u>Prime Grade Contract</u>	<u>Prime Grade Spot Market</u>	<u>Off Grade Spot Market</u>
1970	40-52	40-60	10-50
1971	40-50	40-50	10-30
1972	45-55	45-50	10-30
1973	50-60	50-80	Product Not Available
1974	55-65	55-80	20-50
1975	50-60	50-60	25-35
1976	45-65	45-55	25-35
1977	40-65	40-65	20-40
1978	45-60	40-60	20-40
1979	45-60	40-100	20-60
1980	45-85	75-125	25-100
1981	55-80	51-85	25-50
1982	50-80	38-70	20-35
1983	40-60	45-70	20-50
1984	43-60	50-110	Product Not Available
1985	43-60	40-60	20-35

Table 9
World Capacity to Manufacture
Prime Semiconductor Grade Polycrystalline Silicon

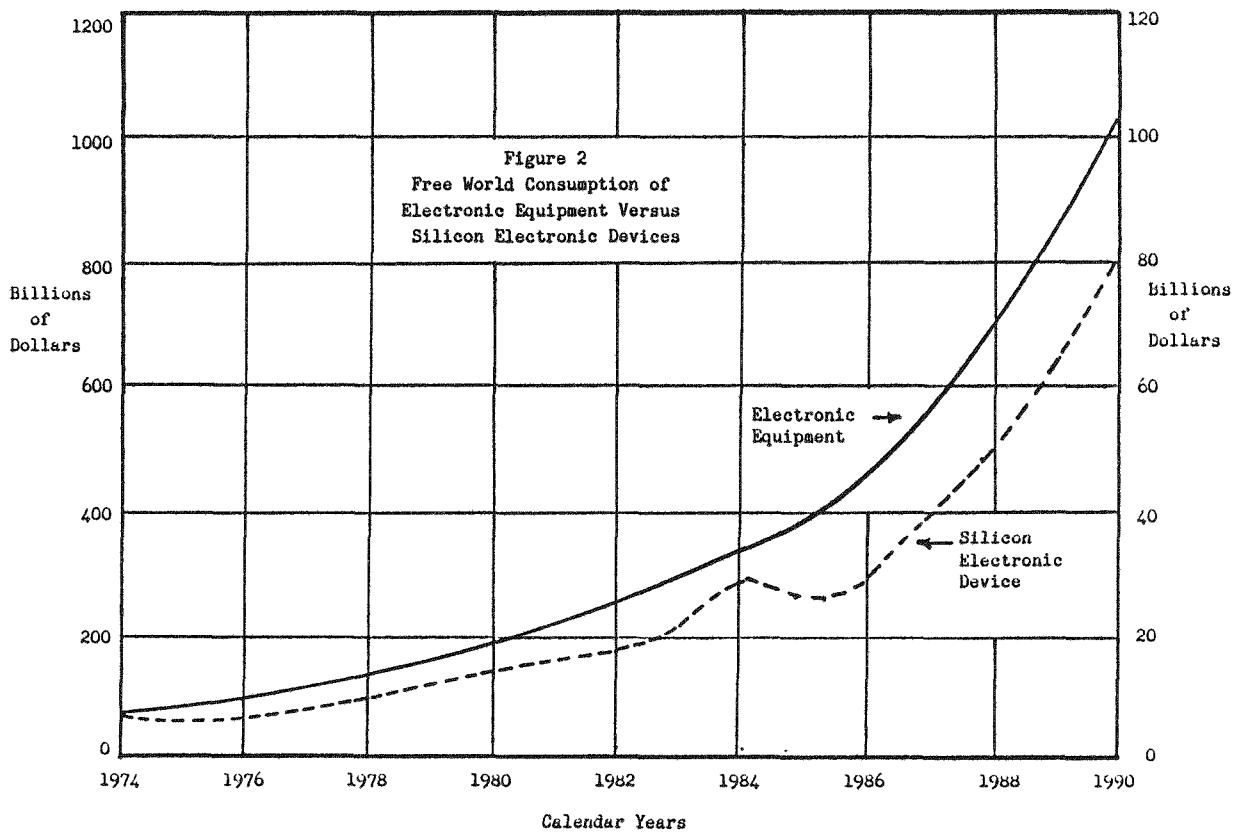
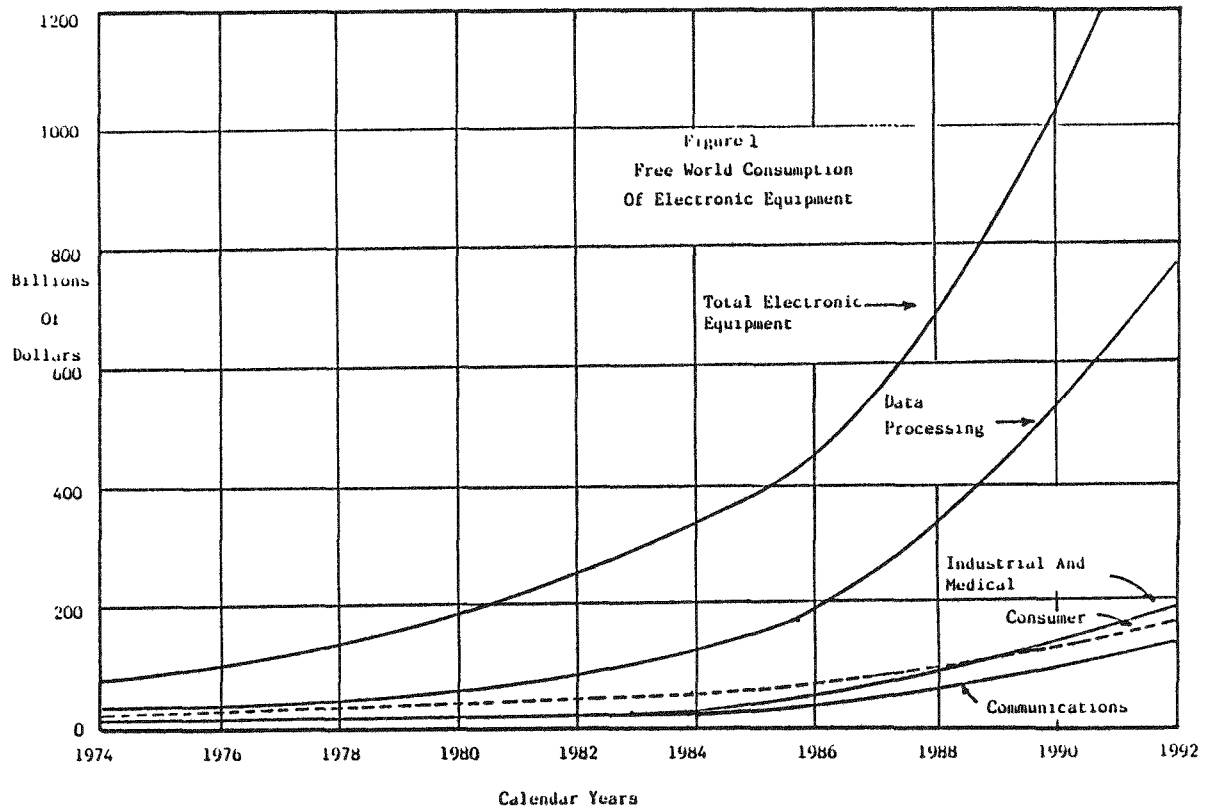
	<u>Company</u>	<u>In Metric Tons</u>							
		<u>1977</u>	<u>1978</u>	<u>1979</u>	<u>1980</u>	<u>1981</u>	<u>1982</u>	<u>1983</u>	<u>1984</u>
1.	Wacker Chemetronic GmbH	700	700	700	1200	1400	1800	2000	2000
2.	Hemlock Semiconductor Inc.	500	500	600	700	900	1000	1000	1000
3.	Osaka Titanium Mfg. Co.*	150	150	200	400	400	450	450	640
4.	Texas Instruments Inc.	175	175	200	250	300	350	350	350
5.	Dynamit Nobel	150	175	190	220	300	350	400	400
6.	Monsanto Company	175	190	200	210	230	230	230	230
7.	Motorola Inc.	100	100	100	100	100	100	100	100
8.	Great Western (GE)	-	10	50	100	200	200	200	200
9.	Shen-Etsu Handotai	100	100	100	100	100	100	140	160
10.	Komatsu Electronic Metals	30	30	30	60	60	60	60	60
11.	Topsil	15	15	20	20	20	20	20	20
12.	Union Carbide Corp.	-	-	-	-	-	10	100	100
13.	Peoples Republic of China	100	100	150	200	200	200	200	200
14.	Russia	200	200	200	200	200	400	400	600
	Annual Capacity	<u>2395</u>	<u>2445</u>	<u>2740</u>	<u>3760</u>	<u>4410</u>	<u>5270</u>	<u>5650</u>	<u>6060</u>

*Includes Production of Polycrystalline Silicon by Hi Silicon Co. and Tokuyama Soda Company as well as by Osaka Titanium.

Table 10
Free World Capacity To Manufacture
Electronic Grade Polycrystalline Silicon

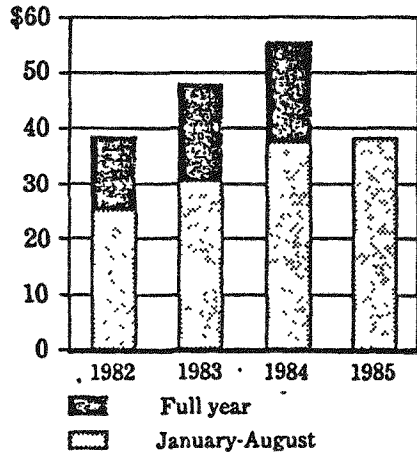
		<u>In Metric Tons</u>					
<u>Company</u>	<u>1985</u>	<u>1986</u>	<u>1987</u>	<u>1988</u>	<u>1989</u>	<u>1990</u>	
1. Wacker Chemetronic							
a. Burghausen	2400	2800	2800	2800	2800	2800	
b. Portland	-	-	200	500	1000	1000	
2. Hemlock Semiconductor Inc.	1000	1400	2000	2400	2700	3000	
3. Osaka Titanium Mfg. Co.	200	400	600	800	1500	2000	
4. Hi Silicon*	800	1100	1100	1600	1800	2000	
5. Texas Instruments Inc.	300	300	-	-	-	-	
6. Dynamit Nobel	600	800	800	800	800	800	
7. Monsanto Company	230	-	-	-	-	-	
8. Motorola Inc.	100	100	-	-	-	-	
9. General Electric	200	200	200	200	200	200	
10. Shen Etsu Handotai	160	160	-	-	-	-	
11. Komatsu Electronic Metals	60	60	-	-	-	-	
12. Topsil	20	20	20	20	20	20	
13. Union Carbide	500	1200	2000	3000	4000	5000	
14. Tokuyama Soda Co.	200	400	600	800	1000	1000	
15. Other New Manufacturers	-	200		2000	3000	3000	
Annual Capacity	<u>6770</u>	<u>9140</u>	<u>11320</u>	<u>14900</u>	<u>17820</u>	<u>20820</u>	

*Includes Output of Japan Silicon and Mitsubishi Silicon



Sales in the Computer Industry

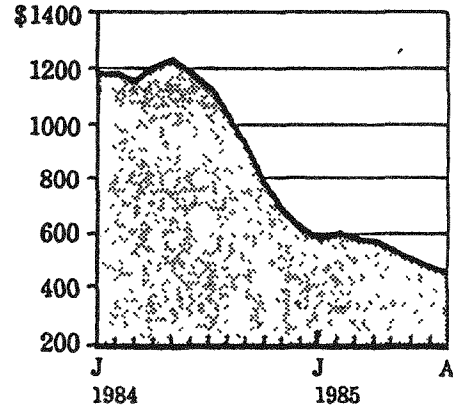
Seasonally adjusted orders
for U.S.-made computers
(Billions of dollars)



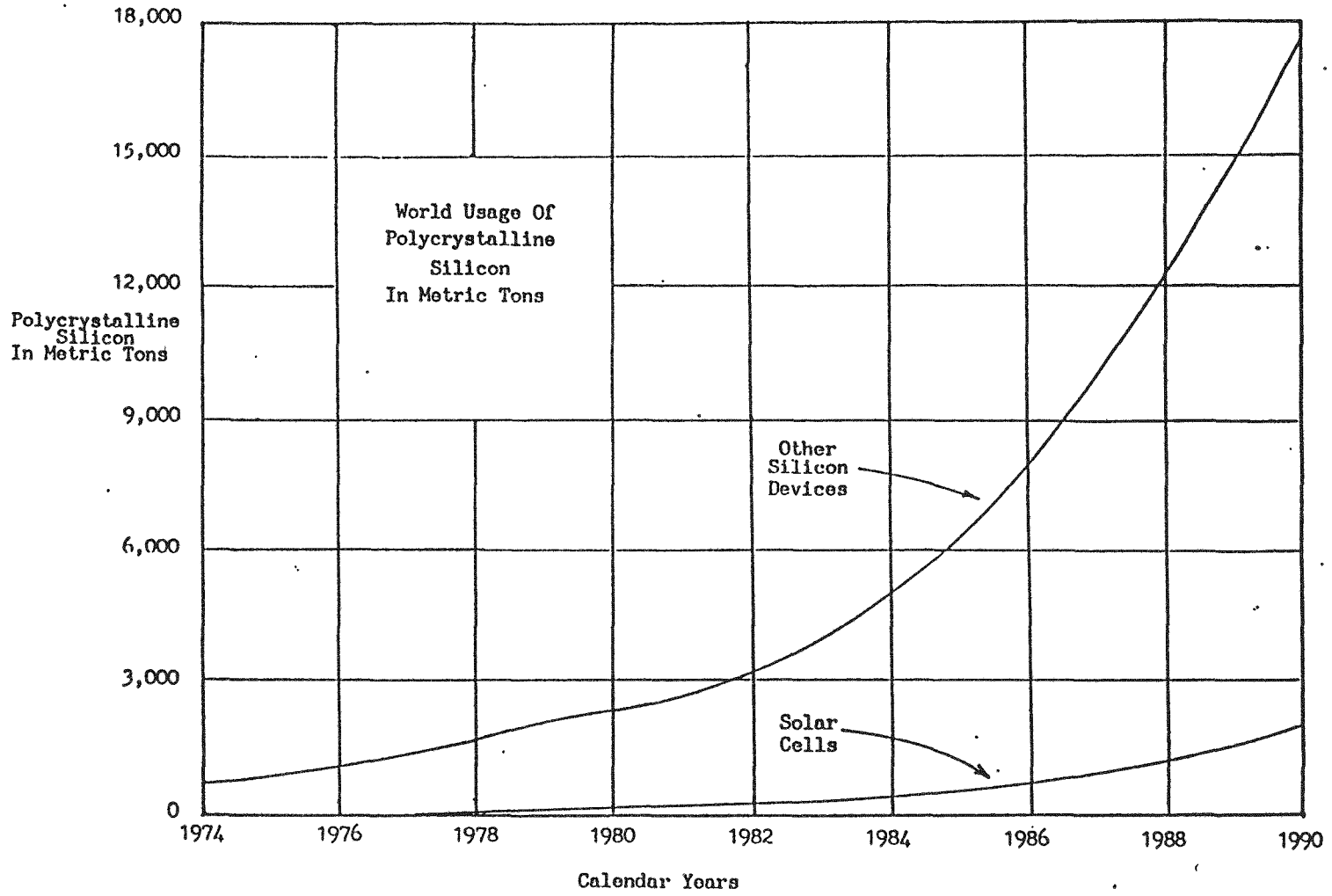
Source: Bureau of the Census, U.S. Commerce Dept.

FIGURE 3

Three-month moving average of U.S.
monthly semiconductor orders
(Millions of dollars)



Source: Semiconductor Industry Association,
San Jose, Calif.



DISCUSSION

HWANG: Can you predict what the growth rate of the epitaxial silicon market will be?

PELLIN: I showed the numbers for CMOS, and I feel that epitaxy will take over in CMOS. Perhaps by 1990, half of all of the CMOS and NMOS devices will be made on epitaxial wafers. It's slower than was expected. Epitaxial wafers are still high priced, but they are also a high profit item.

SCHUMACHER: What is the principle source material for making epitaxial layers?

PELLIN: It really depends on the thickness of the layer. For instance, if the required layer is only 1 or 2 μm thick, silane is always used. For somewhat thicker layers, trichlorosilane is used. Silicon tetrachloride is used for the thickest layers. Trichlorosilane will be used for 95% of all epitaxial wafers in the future.

SCHWUTTKE: I really enjoyed your presentation, and I believe that the photovoltaic industry must recognize that it is the tail of the dog, and the tail is not going to wag the dog, which is the semiconductor industry. I tried to make this point before. Your numbers made this conclusion very clear.

PELLIN: I would like to discuss a number of comments you have made at this workshop. The silicon solar cell is an extremely complex device and anyone who believes that a good silicon solar cell can be made with anything but the best silicon, I think, is wrong. The silicon costs so little and if the best polysilicon can be made for \$20/kg (and I think it can be made for \$15/kg), why use anything else?

PATTEN: Given your statement that the quality of the Texas Instruments' polysilicon is electronic grade now and given the statement that the process is available for licensing, what is your estimate of the cost compared with what it would have to be for photovoltaic industry to make ready economic use of that process?

PELLIN: I would like to digress a little. I don't think that it's necessary to go to the fluidized-bed reactor technology to get the lowest cost. I think that all that is basically needed is to find ways, even in the Siemens process, to lower costs. However, to answer your question directly, I'm absolutely convinced that with complete recycling of by-products and, perhaps, a better material usage in the fluidized-bed reactor than Texas Instruments has, the process cost is easily \$10/kg in today's dollars. I emphasize that this is a cost number.

MCCORMICK: We at Hemlock Semiconductor obviously also plot silicon price as a function of time and cumulative volume to develop a learning curve for the industry. The data from the 1970s is really badly distorted because a 110% inflation rate occurred between 1975 and 1985. If the plot is made in constant dollars, the industry has been on about a 75% learning curve

from the early 1960s when sizable plants based on Siemens technology were built. I think your conclusion that there are many advances in technology, described in patents, to indicate that the trend will continue. Starting with the 1975 economics, the conclusion would be that polysilicon can be bought today for the equivalent of maybe \$25/kg in 1975 dollars and, using the Pellin projections, the estimates for the 1990s give a \$10 to \$15/kg price for top-quality material in 1975 dollars. Obviously, the price would not be that in current dollars.

LORD: I would like to consider the question of how the semiconductor industry can get a cheap price for silicon even if it can be manufactured cheaply. The marginal cost in plant capacity in these processes, particularly in fluidized-bed reactor processes, is relatively small. It's relatively cheap to go from 1000 MT to 1200 MT or 1500 MT, or whatever the appropriate range might be. The problem is selling that material without cutting the price for the first 1000 MT. I suggest that if the photovoltaic people want high-quality silicon on a regular basis, they should go back to the oil companies that now own them and suggest that they look at joint ventures. In a joint venture, a percentage of the product is taken. I'm sure many companies would be willing to do this on the basis of a guarantee of no resale to the electronic industry. On this basis, the \$20/kg price would probably be obtained and that is what is really needed.

PELLIN: I agree that scale is a primary factor in the polysilicon business. However, in 1990 when there will be a requirement for about 20,000 MT, the demand is so large that a situation of diminishing returns may occur. A 5000 MT/year plant is a huge plant. In the case of fluidized-bed reactor processes, the reactors may have to be 6 to 10 ft in diameter.

AULICH: I am somewhat surprised. Ten years ago, the DOE project was started with the objective of obtaining inexpensive solar-grade polysilicon. A large number of new processes were studied. Now you are saying, after 10 years of this program, that modifications of the Siemens process or a modification of the Texas Instruments process will yield \$10/kg. I'm puzzled.

PELLIN: You're talking price. I was using cost numbers.

AULICH: Yesterday we learned about studies showing that the economics of the fluidized-bed reactor process and the other electronic processes would be about \$20 to \$40 for silicon. If the Texas Instruments process yields at \$10/kg, it's really not necessary to develop any other process to make solar-grade or any other inexpensive silicon. Silicon, at \$10/kg, is the goal of many of these developments for solar-grade or inexpensive silicon. I don't believe it.

PELLIN: Well, we've gotten into our first disagreement.

SILICON REQUIREMENTS OF THE PHOTOVOLTAIC SOLAR CELL MARKET

Paul D. Maycock
PV Energy Systems, Inc.
PO Box 290, Casanova, VA 22017
703-788-9626

ABSTRACT

The terrestrial photovoltaic module market is summarized for 1983 through 1985 and a module shipment forecast developed for 1990 and 1995. The PV module shipments for each major cell material option: single crystal silicon, polycrystal cast silicon, silicon sheet, silicon concentrator cells, amorphous silicon and other materials, is forecast. A silicon consumption factor (kilograms used per kilowatt) for the present product and for each cell option is shown. The reduction in silicon usage as processes are improved, and efficiencies increase are forecast to 1995 for each option. Given the market, the technology mix, and the silicon usage forecast, an aggregate silicon consumption estimate will be made for a "high" case (U.S. tax credits extended), and a "low" case (U.S. tax credits terminate).

THE PV MODULE MARKET TO 1995

In 1984 the world shipments of flat plate PV modules were about 22 MW. Of this 22 MW, 14.8 MW were "thick crystal" - single or polycrystal - silicon, 7 MW were made with amorphous silicon thin films. Figures One and Two show the 1983-84 module markets and the technology mix.

We have attempted to forecast the PV markets to 1995. The role of the extension and expansion of the U.S. tax credits was considered. Figure Three shows our forecast for the world PV market to 1995 with and without the tax credit extension. If the tax credits are extended, we can see a 975 MW market in 1995 at an average module price of \$2/Wp. If the tax credits are not extended, the PV module market can grow to 310 MW at an average module price of \$3/Wp.

FIGURE ONE

WORLD PV MODULE SHIPMENTS

	1983		1984	
	<u>MW SHIPPED</u>	<u>PERCENT</u>	<u>MW SHIPPED</u>	<u>PERCENT</u>
UNITED STATES	13.1	60.4	11.7	46.8
JAPAN	5.0	23.0	8.9	35.6
EUROPE	3.3	15.2	3.6	14.4
OTHER	0.3	1.4	0.8	3.2
TOTAL	21.7 MW	100%	25.0MW	100%

FIGURE TWO

WORLD PV MODULE SHIPMENTS BY MODULE TYPE

	1983		1984	
	<u>MW SHIPPED</u>	<u>PERCENT</u>	<u>MW SHIPPED</u>	<u>PERCENT</u>
SINGLE CRYSTAL FLAT PLATE	10.9	50.2	10.8	43.2
AMORPHOUS	3.1	14.3	6.95	27.8
POLYCRYSTAL	3.1	14.3	3.95	15.8
SINGLE CRYSTAL CONCENTRATORS	4.5	20.7	3.1	12.4
RIBBON	0.1	0.5	0.2	0.8
TOTAL	21.7 MW	100%	25.0 MW	100%

FIGURE THREE: **WORLDWIDE MODULE SALES**
(Factory Prices - 1985 \$)

	<u>1983</u>	<u>1984</u>	<u>1985</u>	<u>1986</u>	<u>1988</u>	<u>1990</u>	<u>1995</u>
MWp	22	22	26	60(1) 35(2)	150 50	300 * 107 *	975 * 310 *
\$/Wp	8	7	6.50	5(1) 6(2)	4 5	3 4.50	2 3
\$(M)	176	155	170	300(1) 210(2)	600 250	900 480	1950 930

(1) U.S. Tax Credits Extended to 1989

(2) U.S. Tax Credits Expire after 1985

* Includes Japanese Grid-Connected PV Powered Houses

PV CELL TECHNOLOGY TO 1995

In either market scenario, we see two major changes in the technology of the modules. Virtually all PV product will be silicon-based with low (less than 5%) penetration by cadmium telluride, gallium arsenide, and II-VI compounds. The first change is the cost per Watt to manufacture the silicon-based product, and the second is the performance increase in the thick crystal, and silicon-based concentrator modules. Figure Four summarizes the technology forecast that we used in preparing the market forecast.

The "profitable prices" in Figure Four are developed using a production cost model that assumes automation, increasing yields, increasing efficiencies, and ten year warranties. The single crystal forecast is virtually certain, the ribbon and sheet forecasts are 70-80% likely, and the amorphous silicon forecast is 60-70% likely.

FIGURE FOUR

SUMMARY OF TECHNOLOGY/ COST FOR KEY SILICON-BASED OPTIONS (1984 \$)

	1985	1990	1995
● SINGLE CRYSTAL SILICON			
- Module Efficiency (%)	11	15	16
- Profitable Price (\$/Wp)	6.50	4-5	3
● CONCENTRATORS			
- Module Efficiency (%)	14	17	20
- Profitable Price (\$/Wp)	5-6	3.30-4.00	2.50
● RIBBON / SHEET			
- Module Efficiency (%)	10	11	14
- Profitable Price (\$/Wp)	7.50	3.30	2-3
● CAST INGOT			
- Module Efficiency (%)	11	13	15
- Profitable Price (\$/Wp)	7.00	3.50	3.00
● AMORPHOUS SILICON			
- Module Efficiency (%)	5	8	10
- Profitable Price (\$/Wp)	5.00-6.50	2-3	1.66-2.50
● AVERAGE MODULE PRICE (\$/Wp)	6.50	3.50	2.50

IMPACT ON SILICON USAGE

The dominant cost in today's product is the cost of silicon. These forecasts all involve major reductions in the amount (grams/Watt) of silicon consumed because the industry will:

- eliminate kerf loss;
- increase cell efficiency;
- increase product yield;
- use thinner slices;

or go to micron thick films deposited from silanes.

PRESENT CONSUMPTION OF SILICON

The production of single or polycrystal modules using .015 inch thick cells consume .035 to .045 inches of silicon per slice. If the module is ten percent efficient, then we need about 100 square cm of cell area per Watt or about 25 grams per Watt consumed. This is 25 metric tons per megawatt. In 1985 we will produce about 15 MW of "thick crystal" product. This means we consumed about 375 metric tons of silicon.

In our technology forecast, we attributed almost all cost reduction, around 70%, to silicon cost reduction. Of the thick crystal options, we see the trends in silicon usage shown in the table below.

Thick Crystal Silicon

	<u>1985</u>	<u>Grams/Watt</u>	<u>1995</u>
Single Crystal	20		10
Cast Ingot	25		12
Ribbon/Sheet	25		8
Single Crystal Concentrator Cells	5		1

HOW MUCH SILICON IN 1995?

We can only bracket the silicon consumption requirements for 1995. The primary issue is the degree of penetration of the amorphous silicon and the concentrator into the thick crystal arena.

HIGH SCENARIO FOR SILICON CONSUMPTION: 1995

If we assume amorphous silicon grows to 40 percent of the 1995 market, then the following scenario holds.

MW Shipped: 975
Percent Thick Crystal: 60
MW Thick Crystal: 585
Grams Per Watt: 10
Metric Tons: 5850

Clearly to grow from about 400 tons in 1985 to nearly 6000 tons in 1998 is a major barrier to the progress of PV. This "high" scenario assumes dramatic market growth, U.S. tax credit extension, and slow penetration by amorphous silicon.

LOW SCENARIO FOR SILICON CONSUMPTION: 1995

If we assume that the tax credits are not extended, and that amorphous silicon gains 70 percent of the PV market by 1995, then the following "low" scenario applies.

MW Shipped: 310
Percent Thick Crystal: 30
MW Thick Crystal: 93
Grams Per Watt: 12
Metric Tons: 1116

The growth from about 375 tons of silicon to 1100 in 1995 can be easily assimilated by the industry. This will be especially true if the Wacker/Japanese silicon ventures result in a true "solar" grade material (SILSO) that is available at a reasonable cost (\$20-30/kg) independent of the silicon demand by the semiconductor device industry. We are not aware of any U.S. effort that will result in low cost poly for PV. This is understandable as virtually all U.S. PV R&D is now focused on amorphous silicon cell technology. Investment in silicon production capacity for PV will be delayed until the role of ribbon, cast ingot and amorphous silicon is clear.

If amorphous silicon becomes the "material of choice" for PV, then pure silanes will be the issue. Our present analysis indicates that present silane capacity plans are more than adequate to respond to the amorphous silicon demand at very profitable prices to the material producer. Because silicon cost is not the driver for amorphous silicon PV, we do not see the pressures on silane price that we see in polycrystal for PV.

SUMMARY

It is risky to forecast silicon consumption for PV ten years ahead. This forecast proposes two scenarios. The "high" scenario with low penetration for amorphous silicon, tax credit extension and major cost reductions lead to nearly

6000 tons of silicon per year used by the PV industry. This is as large as today's semiconductor industry consumption in a good year. The "low" scenario with no tax credits, high amorphous silicon penetration, moderate cost reduction leads to a silicon demand for PV of 1100 tons per year by 1995. At this moment, October 1985, we feel the "low", no tax credit extension scenario is more likely to occur.

DISCUSSION

McCORMICK: If I compare your data on demand and usage with the data of Pellin on scrap, either from poly or from single crystal, there is no demand for additional solar-grade silicon.

MAYCOCK: That's right. If we take the premise that scrap is available, as it is now at \$20 or lower, and take Pellin's data that there is continued growth in the semiconductor industry and in the ratio of scrap, which may go up even higher, there is 3000 MT of scrap available in 1995, and that's the highest we would need. I think we should be very careful. Those of you who are in the electronic semiconductor-grade business have that business to defend. If I were Siemens and I believed that I could purify and make solar-grade silicon that allowed the casting people to make 14% cells, and I believed that there was a 3000 MT opportunity and that I could sell it at \$15, then I could wipe out the scrap market and I could make an industry. There are some business scenarios allowing entrance, but the price would have to be lower than scrap and a quality equivalent to that of scrap. There is a very narrow window. A lot of people don't realize that. In my opinion, ARCO Solar, which is the leading purchaser of scrap in the United States, has a cost below \$24/kg.

McCORMICK: The exception is that there is no bottom on scrap price, particularly if the scrap comes from the single-crystal area such as the material coming from tang ends of ingots. That's where Pellin showed 10%. This scrap will be dumped at very low prices.

MAYCOCK: The other market, which is what one of the small companies (Solec International) is based on, buys scrap slices and etches off the integrated circuit information and puts aluminum on it and makes solar cells. Their silicon cost per slice is one third of that of ARCO Solar.

McCORMICK: Was the price shown in your data, comparing the different technologies, the module price or the installed price?

MAYCOCK: Those were only module prices.

McCORMICK: What is the impact of efficiency on driving those different technologies if one compares installed versus module prices?

MAYCOCK: I ended up with approximately a 60% higher efficiency for single-crystal cells than for amorphous-silicon cells, and it was 16% versus 10%. At those prices of \$3/watt for module and \$2/watt for the amorphous silicon, the area-related cost for remote fixed installation is about a \$1/watt higher for amorphous silicon, and therefore it's a wash. They both come in at about \$5/watt installed system in that time frame.

SCHWUTTKE: You may not realize how serious the scrap situation can be if a price war would start. I remember when IBM at Fishkill was paying for scrap to be removed and only when a demand started did IBM go into business selling the scrap.

MAYCOCK: There's another scenario and that is if one is dependent on scrap, then one is dependent on random events. If one wants to have a serious photovoltaic business, then one may have to produce his own silicon and that may be using whatever process is needed to obtain the estimated necessary price. I'm sure that the Siemens strategy is that because we know everything about the Siemens process, then we know that we had better have a photovoltaic material that works well and a dependable supply. There are some situations in the scrap market that get wild. The scrap market is very big.

LEIPOLD: I think that the point to be made about the scrap market was given clearly in Pellin's data showing that the scrap prices clearly tracked the spot market prices. This means that the photovoltaic manufacturer is affected by the spot market which, I believe, is an unacceptable position.

MAYCOCK: Pellin also showed that the contract price for scrap was very low all the way through. His bottom line was low. His escalations were very high. Those who have a contract for scrap, like ARCO Solar, are not affected.

SANJURJO: The bottom line is that if we want to produce a solar-grade material, we have to compete with the \$10 to \$20/kg, or whatever, scrap material on the market.

MAYCOCK: Well, about \$20. I don't know of any \$10 prices now.

SANJURJO: Again, I want to make the same point which I made yesterday. SRI has a process that produces a material having 4 to 10 ppb of boron, and I remind everyone that the estimated cost of this process is \$13 to \$15/kg.

MAYCOCK: If that's cost, the price would have to be \$20, so you don't have anything.

SANJURJO: With 25% return on investment, the price would be \$18 to \$20. The difference is that this process would be in the market with a constant supply of material of a constant quality and characteristics. There would not be a dependency, such as the case you just mentioned in which scrap wafers are bought and used. Yes, the material is much cheaper, but the cost of labor to sort and process that material is much higher.

MAYCOCK: I think that those of us who are forecasting the market, don't see a market at this time that gets out of the scrap domain. If we had a market that was twice the scrap domain, then we would have to have new technologies and new low-cost processes and that's what the market was when we began the DOE program. The DOE program had an amplitude of ten times these levels in terms of its objectives and, therefore, there wasn't enough scrap, and Pellin was telling us that there wasn't enough silicon. Remember that we had a crisis in 1974 and, when we were planning the program, we actually had to give presentations to the DOE saying there wouldn't be enough silicon under any circumstances, not only scrap, to provide for the photovoltaic industry. That's what started the silicon initiative. Now it's quite a different story. We are told that the

amount of scrap is more than enough to cover our present market forecasts. If there is a doubling of the price of oil, it will be a different story.

NODA: I agree with the comment of Dr. McCormick. The conclusion from my own calculations is that, under normal conditions, the scrap from the semiconductor industry is about 10%. This result corresponds to Dr. Pellin's data which show that, in 1990, the overall consumption of polysilicon will be 18,000 MT, and solar use will be 2000 MT. Perhaps, as Dr. McCormick said, we have enough polysilicon material for solar use and do not need to hurry up in installing new capacity for solar use, although the effort for a more economical process should continue. According to the forecast by Mr. Maycock, we have been very busy making scrap and now we can, perhaps, take a vacation for 5 years.

FORUM: POLYSILICON MARKETS

J. Lorenz, Chairman

LORENZ: We would like this Forum to be an opportunity for expressions of opinion, especially if they are different from what the speakers have said. It's also an opportunity to ask questions of the speakers.

LORD: I would like to comment on the question of scrap material. I wonder if there will be a place for a non-CVD or a nonelectronic-grade process. Let me mention a technology driver that has a lot of impact on scrap, i.e., the development of continuous crystal pulling. Monsanto has done a lot of work in this area and has stated that they have been successful. Others, such as Hamco, have been working on it. It's probably reasonable to assume the technology will be available by 1990 and, perhaps, before that. With continuous crystal pulling, a much longer crystal can be grown. Far less of the material is in the seed and tang ends. Also, if it is done correctly, far more of the material is on specification, and the indications are that if all the problems are solved, there will be less wafer rejection. There could be a major driving force to reduce scrap. This would indicate the potential for a non-CVD process to enter the market. However, if the technology is successful, the amount of polysilicon required would be reduced. There might be a surplus of polysilicon capacity at that time, which would again foreclose the opportunity for a solar-grade product. This depends on how people who forecast the market for CVD applications foresee the developments in these other technology areas. I advise following the development of continuous crystal pulling and the actual building of polysilicon production plants, rather than the announcements of plans to build plants.

PELLIN: I've been in this industry a long time and there has been continual change. I don't believe that future changes will differ greatly from changes in the past. Basically, we now make wafers having particular properties which are sold to the device makers. The device makers would like the range of material properties to be tightened considerably. I don't think that less polysilicon will be used, but rather the parameters will be tightened on the wafers and, as a consequence, somewhat the same kind of situation as today will continue for at least the next 5 years. The main change will be the tighter requirements on wafer properties. This is already seen, obviously, in the example of the Japanese device companies going full steam ahead. It's a tug-of-war between improving product and cost.

LORENZ: I concur with Remo's (Pellin) comments and also note that, from his data, it can be seen that over the last 4 or 5 years there have been at least five companies which have looked at polysilicon and, for various reasons, have chosen not to enter into production. Furthermore, I would like to emphasize that, as Remo said, any of the polysilicon expansion that occurs will be based on the semiconductor industry. There is no other way that the management of a chemical company would be convinced that there is a market for 2000 MT of polysilicon in 1995.

WRIGHT: As a former Solarex employee, I was also involved in looking at various types of scrap material available on the market. Hopefully, in the near future, with increases in polysilicon production, the quality of the scrap will go up as well. The Solarex product was highly dependent on

the type of scrap from the individual source, and there were seven to twelve different scrap dealers (i.e., different sources of scrap). Occasionally, we had large deliveries that just produced garbage. This caused executive decisions to enter into our own production of material just to control the material to be used. A company which depends on the scrap market must have a long-term contract with a high-quality dealer to have a satisfactory arrangement. The user depends on the quality of the scrap. Having just one batch of unsatisfactory material which slips through the quality control (and often a plant's quality control is not really capable) will result in large money penalties. Some of the processes discussed at this meeting have some merit based solely on the reasoning that the manufacturer feels assured.

LORENZ: I would like to make an additional comment on that. The polysilicon producers today (Wacker, Hemlock, Union Carbide, and Osaka Titanium) are chemical companies. Two-tier pricing is quite commonly used in the chemical industry. Later, maybe Jim McCormick, Remo Pellin, or someone else will comment on the use of two-tier pricing as a possibility if the scrap improves and all the production is good.

SANJURJO: I would like to emphasize again, and it has been our experience as well, that there are problems of extra costs if polysilicon bought from different sources is used.

HWANG: I would like to comment from our experience in Taiwan. About 5 years ago, we in Taiwan were manufacturing solar cells for watches. We had a large fraction of the world's solar cell production for watches. We used wafers, but the Japanese introduction of the use of amorphous silicon forced us to stop production. I would also like to ask a question of Mr. Maycock. Disregarding the definition of solar-grade silicon, do you believe that a situation with a solar-grade silicon cost of \$10/kg and a module efficiency of 10% can survive?

MAYCOCK: I think I said that module efficiencies had to be 15% in 1995 for cast poly, and it has to be based on a low-cost solar-grade material in the \$10/kg range. The answer is that, generally speaking, if 15% can be obtained from \$20/kg material, then the \$10 material is not a bargain at all. It's something like \$5/kg per efficiency point in the cost of material.

SANJURJO: I would like to remind you that the manufacture of solar cells is not solely dependent on the polysilicon material quality. The cell manufacturing process must be fitted to the material used. That means that the crystal growth and all the steps of the cell processing must be well understood. When plants use materials from different sources, there are continual problems, such as in the etching step to remove the surface damage, in the use of various process temperatures, and in the diffusion methods. All of these process steps are important factors in achieving a reasonable efficiency. It makes a difference of one or two efficiency points and, therefore, has a very important effect on the cost. I think that this has to be taken into account in the consideration of the use of scrap silicon.

WRIGHT: I would like to expand on that comment. In looking at various scrap materials, there is no guarantee by the manufacturer of the scrap. The material is accepted on an "as is" basis. The reason for declaring the material to be scrap is not given, whether it is high-oxygen content or high-carbon content. Occasionally, we used to get material with high boron concentration. Suddenly, the feed stock may drop from several hundred ohm-centimeters resistivity material down to perhaps 50 ohm-cm. I have seen wide fluctuations. In doping to a specific resistivity for the base material, it is unrealistic to treat the incoming material as equivalent. The wide fluctuations in base resistivity have a tremendous effect on the resultant solar cells that were manufactured. Vertical integration must be considered. The basis for productivity and profit should not be dependent on the scrap market, especially if one is considering plants of the 25 MW size.

LORENZ: I think that those comments emphasize what Dr. Schwuttke and Dr. Pellin said earlier. The cell manufacturer should use the best quality of material he can to ensure being in the business for a long time.

CLOSING COMMENTS

LUTWACK: This workshop is the last one to be sponsored by FSA dealing with the technology and production of polysilicon. We were made aware in this workshop of the technology advances which have taken place throughout the world during the last eleven years; we were also reminded of the technical and market problems that remain. I want to especially thank the speakers for presenting papers which were informative and thought-provoking. I also want to thank all of you for participating in the discussions and in the forums. I hope that you enjoyed the workshop and derived something of interest from the meeting. Thank you very much for being here.

APPENDIX

PARTICIPANT LIST

LOW-COST POLYSILICON FOR
TERRESTRIAL PHOTOVOLTAIC SOLAR-CELL APPLICATIONS WORKSHOP

ASTER, Robert
JET PROPULSION LABORATORY
4800 Oak Grove Dr., M.S. 506-316
Pasadena, CA 91109
(818) 577-9545

AULICH, Hubert
SIEMENS AG
Corporate Technology Div.
Otto-Hahn-Ring 6
D-8000 Munich 83, WEST GERMANY
(089) 636-44683

BJLANCETTI, Michael
UNION CARBIDE CORP.
1170 Sonora Ct.
Sunnyvale, CA 94086
(408) 733-3500

BOONE, James
ETHYL CORP.
Box 341
Baton Rouge, LA 70810
(504) 359-2454

BOYKIN, R.G.
GREAT LAKES CHEMICAL CORP.
Rt. 7, Box 27
Newport, TN 37821
(615) 623-1878

BRIGLIO, Anthony
JET PROPULSION LABORATORY
4800 Oak Grove Dr., M.S. 238-343
Pasadena, CA 91109
(818) 354-4883

BROWNING, MELVIN F. (Pete)
CONSULTANT
2390 Wickliffe Rd.
Columbus, OH 43221
(614) 457-1244

CALLAGHAN, William T.
JET PROPULSION LABORATORY
4800 Oak Grove Dr., M.S. 502-422
Pasadena, CA 91109
(818) 577-9517

CALZIA, Jacques
RHONE POULENC MINERALE-FINE
Les Miroirs-Defense 3-92400
Courbevoie, FRANCE
(1) 4768 01 50

CARMAN, Justice
J.C. SCHUMACHER CO.
580 Airport Rd.
Oceanside, CA 92054
(619) 433-1663

CHEN, Paul Y.
J.C. SCHUMACHER CO.
580 Airport Rd.
OCEANSIDE, CA 92054
(619) 433-1663

COLEMAN, Michael
SOLAVOLT INTERNATIONAL
P.O. Box 2934
Phoenix, AZ 85062
(602) 231-6455

DIETL, Josef
HELIOTRONIC GMBH
P.O. Box 1129
Burghausen, GERMANY D-8263
(08677) 83 3314

DUDUKOVIC, Milorad
WASHINGTON UNIVERSITY AT ST. LOUIS
Campus Box 1198
St. Louis, MO 63130
(314) 889-6021

EVANS, Gary
ALCAN ALUMINIUM LTD.
Corporate Ventures
1188 Sherbrooke St. W.
Montreal, Quebec, CANADA H3A 3G2
(514) 848-8453

FABRE, Emmanuel
PHOTOWATT INTERNATIONAL SA
131, route de l'empereur
Rueil-Malmaison, FRANCE 92500
(1) 47.08.05.05

FAIRLEY, Kenneth
J.C. SCHMACHER CO.
580 Airport Rd.
Oceanside, CA 92054
(619) 433-1663

FLAGAN, Richard C.
CALIFORNIA INSTITUTE OF TECHNOLOGY
Env. Eng. Sci. & Mech. Eng.
1201 E. California Blvd., M/C 138-78
Pasadena, CA 91125
(818) 356-4383

FLAGELLA, Robert
UNION CARBIDE CORP.
3333 Index St.
Washougal, WA 98617
(206) 835-9830

FUJII, Shigetaka
MITSUI TOATSU CHEMICALS, INC.
2-5 Kasumigaseki 3-Chome
Chiyoda-ku
Tokyo, JAPAN 100
(03) 593-7401

GRAYSON, Paul
EAGLE-PICHER INDUSTRIES, INC.
P.O. Box 1090
200 Ninth Ave.
Miami, OK 74354
(918) 542-1801 ext. 41

HONG, Chum-Sam
ENERGY RESEARCH LABORATORIES, ITRI
195, Sec. 4, Chung Hsin Rd.
Chutung, TAIWAN
(036) 966100-8050

HOPKINS, Richard
WESTINGHOUSE ELECTRIC CORP.
R&D Center
1310 Buelah Rd.
Pittsburgh, PA 15235
(412) 256-1341

HORI, Keiichi
SUMITOMO CORPORATION
11-1, Kandanishikicho 3-chome
Chiyoda-ku
Tokyo, JAPAN 100-91
(03) 296-3191

HSU, George C.
JET PROPULSION LABORATORY
4800 Oak Grove Dr. (125-159)
Pasadena, CA 91109
(818) 577-9628

HSU, Kuo-Chiang
ENERGY RESEARCH LABORATORY, ITRI
195, Sec. 4, Chung, Hsin Road
Chutung, TAIWAN
(036) 966100-8052

HWANG, Huey-Liang
NATIONAL TSING HUA UNIVERSITY
Department of E.E.
Hsin-chu, TAIWAN 300
(035) 715131, X 349

ISHIGURO, Masamichi
OSAKA TITANIUM CO.
950 Elm Ave. Ste. 355
San Bruno, CA 94066
(415) 589-8193

IYA, Sridhar
UNION CARBIDE CORP.
333 Index St.
Washougal, WA 98671
(206) 835-9826

JAFFE, James
ALLIED CORPORATION
Box 1021R
Morristown, NJ 07960
(201) 455-2150

KIM, Jonathan J.
SOHIO ENGINEERED MATERIALS CO.
Box 832
Niagara Falls, NY 14302
(716) 278-2378

KOIE, Yasukuki
TOYO SODA USA, INC.
1700 Water Pl.
Atlanta, GA 30339
(404) 956-1100

KOINUMA, Hideomi
UNIVERSITY OF TOKYO
Hongo, Bunkyo-ku
Tokyo, JAPAN 113
(03) 812-2111, ex. 7203

KOLIWAD, Kris
JET PROPULSION LABORATORY
4800 Oak Grove Dr., M.S. 122-123
Pasadena, CA 91109
(818) 354-5197

KOPPEL, Lewis
SOHIO ENGINEERED MATERIALS CO.
345 Third St.
Niagara Falls, NY 14301
(716) 278-6084

KUNII, Daizo
YOKOHAMA NATIONAL UNIVERSITY
Chemical Engineering Dept.
156 Tokiwadai, Hotogaya-ku
Yokohama, Kanagawa, JAPAN 660
(045) 335-1451

LAGENDIJU, Andre
J.C. SCHUMACHER CO.
580 Airport Rd.
Oceanside, CA 92054
(619) 433-1663

LEIPOLD, Martin H.
JET PROPULSION LABORATORY
4800 Oak Grove Dr., M.S. 122-123
Pasadena, CA 91109
(818) 354-3931

LEVITCH, Roy
SOLAVOLT INTERNATIONAL
3646 E. Atlantic Ave.
Phoenix, AZ 85040
(602) 231-6422

LIM, John C.
ABLE CHEMICAL TECHNOLOGY CORP.
3250 Wilshire Blvd., Suite 808
Los Angeles, CA 90010
(213) 381-3616

LORD, Steven M.
SML Associates
157 Rancho Santa Fe Rd.
Olivenhain, CA 92024
(619) 942-1594

LORENZ, James H.
CONSULTANT
5331 E. Poinsettia Dr.
Scottsdale, AZ 85254
(602) 952-0343

LUTWACK, Ralph
JET PROPULSION LABORATORY
4800 Oak Grove Dr., M.S. 238-343
Pasadena, CA 91109
(818) 354-7648

MATTHEWS, David
STEARNS-CATALYTIC
P.O. Box 5777
Denver, CO 80217
(303) 692-3796

MAYCOCK, Paul D.
PHOTOVOLTAIC ENERGY SYSTEMS
P.O. Box 290
Casanova, VA 22017
(703) 788-9626

MUI, Jeffrey Y.P.
SOLARELECTRONICS, INC.
21 Rita Lane
P.O. Box 141
Bellingham, MA 02019
(617) 966-1234

MULLER, Frederick
CABOT CORP.
P.O. Box 188
Tuscola, IL 61953
(217) 253-3370

McCORMICK, James
HEMLOCK SEMICONDUCTOR CORP.
12334 Geddes Rd.
Hemlock, MI 48626
(517) 642-5201

NODA, Toshio
OSAKA TITANIUM CO., LTD.
One Higashihama-cho
Amagasaki, Hyogo, JAPAN 660
(06) 411-1121

PATTON, Harold R.
MONSANTO ELECTRONICS MATERIALS CO.
800 N. Lindberg Blvd.
St. Louis, MO 63167
(314) 694-3166

PELLIN, Ramo
INDUSTRIAL CONSULTANT
7200 Old Oak Lane
Charlotte, NC 28212
(704) 545-9964

PHILLIPS, Mary
JET PROPULSION LABORATORY
4800 Oak Grove Dr.
M.S. 502-422
Pasadena, CA 91109
(818) 577-9096

POWELL, Rick
SOLAR ENERGY RESEARCH INSTITUTE
1617 Cole Blvd.
Golden, CO 80401
(303) 231-1774

PRINCE, Morton
U.S. DEPARTMENT OF ENERGY
1000 Independence Ave., S.W.
Washington, D.C. 20585
(202) 252-1725

RAEUBER, Armin
FRAUNHOFER-INSTITUTE FUR
SOLARE ENERGIESYSTEME
Oltmahsstr. 22
D7800 Frieberg Bundesrepublik
DEUTSCHLAND

RAGHAVAN, Narasimha S.
ALCAN INTERNATIONAL LTD.
Kingston Laboratories
Kingston, Ontario, CANADA K7L 4Z4
(613) 549-4500

RHINE, Bruce
J.C. SCHUMACHER CO.
580 Airport Rd.
Oceanside, CA 92054
(619) 433-1663

ROGERS, Leo
POLYCRYSTALLINE SILICON TECHNOLOGY CORP.
1819 S. Dobson Rd., Ste. 107
Mesa, AZ 85202
(602) 897-2222

ROHATGI, Naresh
JET PROPULSION LABORATORY
4800 Oak Grove Dr., M.S. 125-112
Pasadena, CA 91109
(818) 354-3073

RUSTIONI, Massimo
ENICHIMICA
20097 San Donato Milanese
Milano, ITALY
(02) 520-32375

SAH, C. Tang
C.T. SAH ASSOCIATES
403 Pond Ridge Lane
Urbana, IL 61801
(217) 384-5210

SANJURJO, Angel
SRI INTERNATIONAL
333 Ravenswood Ave.
Menlo Park, CA 94025
(415) 859-5215

SCHEI, Anders
ELKEM A/S, R&D CENTER
P.O. Box 40
4620 Vagsbygd, NORWAY
47-42-72000

SCHMID, Fred
CRYSTAL SYSTEMS, INC.
35 Congress St.
Salem, MA 01970
(617) 745-0088

SCHUMACHER, Joseph C.
J.C. SCHUMACHER CO.
580 Airport Rd.
Oceanside, CA 92054
(619) 433-1663

SCHWUTTKE, Guenter H.
GHS CORP.
8162 E. Del Pico
Scottsdale, AZ 85258
(602) 951-0422

SEIDEL, Thomas E.
J.C. SCHUMACHER CO.
580 Airport Rd.
Oceanside, CA 92054
(619) 433-1663

SHAW, Bill C.
12301 E. 48th Ter.
Independence, MO 64055
(816) 251-5006

SHIMIZU, Yasuhiro
OSAKA TITANIUM CO., LTD.
One Higashihama-cho
Amagasaki, Hyogo, JAPAN 660
(06) 411-1171

SIVILOTTI, Olivo
ALCAN INTERNATIONAL, LTD.
P.O. Box 8400
Kingston, Ontario, CANADA K7L 4Z4
(514) 848-8040

TENG, Kau-Shen
ENERGY RESEARCH LABS, ITRI
195, Sec. 4, Chung-Hsin Rd.
Chutung, HSINCHU, TAIWAN
(036) 966100, X8052

TIERNEY, Paul
MONSANTO CO.
800 N. Lindbergh Blvd., M.S. F2WB
St. Louis, MO 63167
(314) 694-3844

TOPEL, Bruno
HELIODINAMICA
Rodovia Raposo Tavares KM 41
06730 Vargem Grande Paulista
Sao Paulo, BRAZIL
(011) 493-3888

TUSTIN, David
JET PROPULSION LABORATORY
4800 Oak Grove Dr., M.S. 502-422
Pasadena, CA 91109
(818) 577-9597

WINEGARANER, Richard M.
STRATEGIES UNLIMITED
201 San Antonio Circle
Suite 205
Mountain View, CA 94040
(415) 941-3438

WRIGHT, Lloyd F.
J.C. SCHUMACHER CO.
580 Airport Rd.
Oceanside, CA 92054
(619) 433-1663

WRIGHT, Steve R.
RESEARCH TRIANGLE INSTITUTE
P.O. Box 12194
Research Triangle Park, NC 27709
(919) 541-6316

YAWS, Carl
LAMAR UNIVERSITY
P.O. Box 10053
Beaumont, TX 77710
(409) 880-8784

SESSION I

POLYSILICON MATERIAL REQUIREMENTS

J. McCormick, Chairman

DO NOT MICROFILM
COVER

SESSION II

ECONOMICS

R. Pellin, Chairman

**DO NOT MICROFILM
COVER**

SESSION III

PROCESS DEVELOPMENTS IN THE USA

P. Maycock, Chairman

DO NOT MICROFILM
COVER

SESSION IV

PROCESS DEVELOPMENTS, INTERNATIONAL

R. Lutwack, Chairman

COVER

SESSION V

PROCESS DEVELOPMENTS IN THE USA

A. Briglio, Chairman

**DO NOT MICROFILM
COVER**

SESSION VI

POLYSILICON MARKET AND FORECASTS

M. Prince, Chairman

2001
COVER